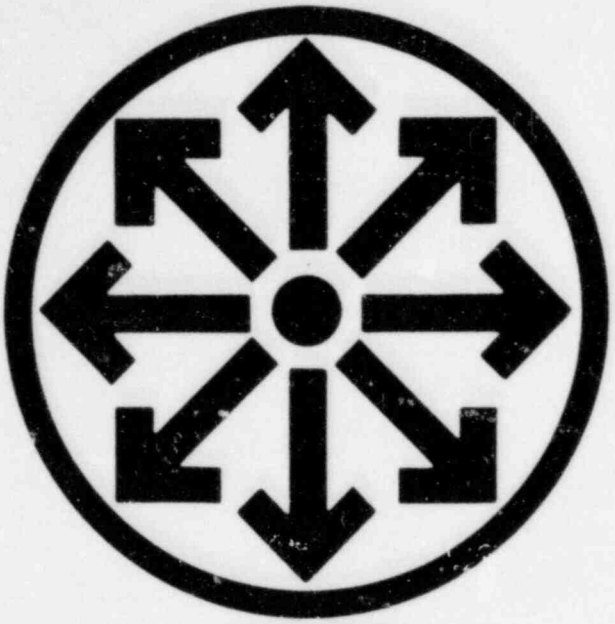

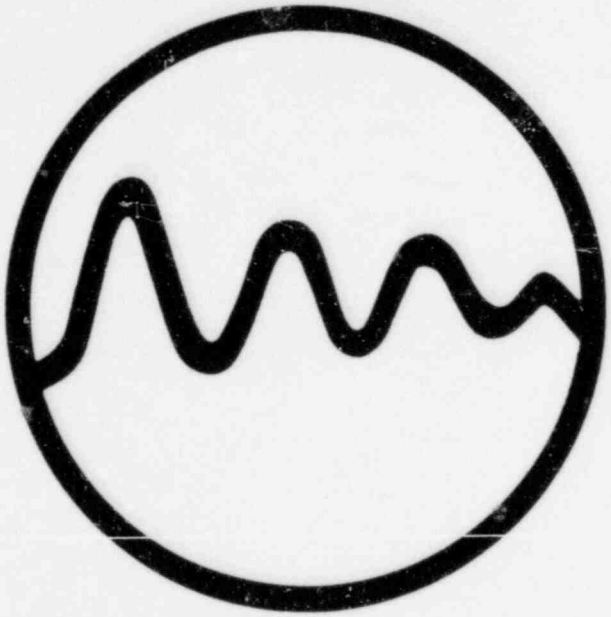

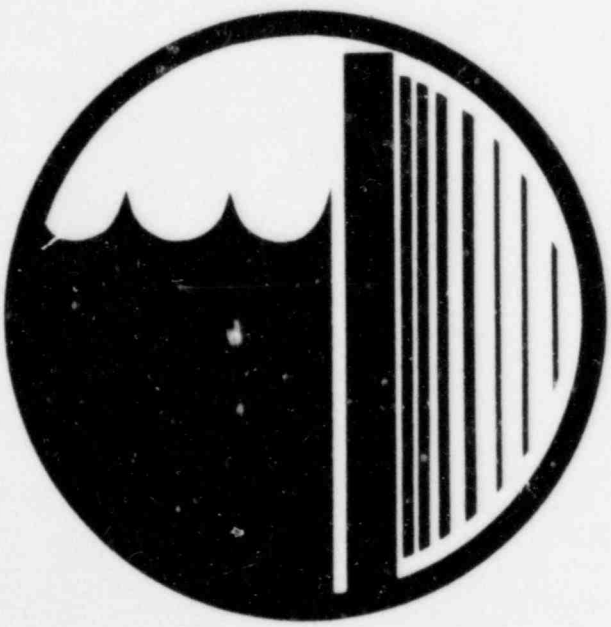

AN APPROACH TO CHUGGING

$(\Box^2 p = -4\pi q)$

ASSESSMENT OF
RHR STEAM DISCHARGE
CONDENSATION OSCILLATION IN
MARK III CONTAINMENTS

SAN FRANCISCO POWER DIVISION
NUCLEAR ENGINEERING STAFF

BECHTEL

MARCH 1984

AN APPROACH TO CHUGGING
($\Box^2 p = -4\pi q$)

ASSESSMENT OF RHR STEAM DISCHARGE CONDENSATION OSCILLATION IN MARK III CONTAINMENTS

PRINCIPAL INVESTIGATORS

G. K. ASHLEY II

T. S. LEONG

PREPARED FOR
THE MARK III CONTAINMENT
ISSUES OWNERS GROUP

JOB 16031

CONTENTS

FIGURES

TABLES

1 INTRODUCTION

This report is an assessment of the effect of condensation oscillation resulting from steam discharge through the residual heat removal (RHR) heat exchanger relief valve discharge lines into the Mark III pressure suppression pool. This assessment was made at the request of the Mark III Containment Issues Owners' Group (CIOG)* in response to a concern raised by Mr. John Humphrey, a former lead systems engineer at the General Electric Company. Mr. Humphrey's concern related to whether or not all loads that could be produced by steam discharge through these relief valves had been adequately considered.

The assessment was completed by using a derivative of the acoustic chugging model developed by Bechtel for the Mark II chugging program[1] to estimate the pressure field produced by RHR condensation oscillation. The suppression pool boundary pressures and forces on a submerged structure produced by RHR condensation oscillation were compared with loads resulting from safety relief valve (SRV) discharges. This comparison affirmed the CIOG's initial assessment that the effects of condensation oscillation at the RHR heat exchanger relief valve discharge line exit are bounded by other design controlling loads.

This report contains, first, a short description of Mr. Humphrey's concern about RHR steam discharge induced condensation oscillation. This is followed by a technical description of the acoustic chugging model and its verification. Next, RHR condensation oscillation source development is given. Finally, an assessment is made of the effect of this phenomenon on the CIOG members' Mark III containments and submerged structures.

---

* The Mark III Containment Issues Owners Group (CIOG) consists of Grand Gulf Nuclear Station (GGNS), Perry Nuclear Power Plant (PNPP), River Bend Station (RBS), and Clinton Power Station (CPS)

2 HUMPHREY CONCERNS

Mr. John Humphrey was the containment lead systems engineer for General Electric Company. Upon leaving General Electric, he identified a number of questions related to the Mark III containment design.[2] One of these concerns related to potential condensation oscillation loads which could be produced by steam discharges through the RHR heat exchanger relief valves.[3]

During steady state operation of the RHR system in the steam condensing mode, steam from the reactor pressure vessel is condensed in the RHR heat exchanger. The pressure of the steam at the inlet to the heat exchanger is regulated by a pressure control valve. Relief valves are provided on the heat exchanger to accommodate postulated failure of the pressure control valve.

If the pressure control valve fails open, the safety relief valves on the heat exchanger will be actuated. The mass flux which would be discharged through the relief valve discharge line exit is sufficiently high that condensation oscillation might be expected. Mr. Humphrey's concern related to the lack of a final load definition for these potential condensation oscillation loads.

The Mark III CIOG initially stated that any condensation loads produced by steam discharge through the RHR heat exchanger relief valves would be less than the loads produced by other design controlling phenomena.[4] The Nuclear Regulatory Commission (NRC) requested[5] the CIOG to provide supplemental, confirmatory analyses which would quantify the potential RHR condensation oscillation loads in order to demonstrate that other load definitions bound the RHR condensation oscillation loads.

3 THE ACOUSTIC MODEL FOR UNSTABLE STEAM CONDENSATION

The unsteady condensation of steam discharging into a water-filled tank is usually referred to as chugging and/or condensation oscillation. The precise meaning of these terms varies, but they are almost always used to describe the shape of the time-history of the resulting pressure field. In the domestic boiling water reactor industry, the term "chugging" has come to mean a series of impulsive condensation events. Each event or "chug" generates a pressure field similar in appearance to that produced by the collapse of an isolated steam bubble or void. The term "condensation oscillation" refers to steam condensation that gives a "sinusoidal" pressure field. Often during unstable steam condensation, chugs may occur randomly with condensation oscillation.

Chugging and condensation oscillation can each be viewed as a three-part phenomenon composed of (1) a source, (2) a pressure field, and (3) a fluid-structure interaction. The source is the result of an acceleration of the steam-water interface created by the condensation of the steam discharging into the water-filled tank. This acceleration can either be the result of a catastrophic collapse of a detached steam bubble, the movement of the interface in the vicinity of the vent discharging the steam, or a combination of the two. This acceleration of the interface produces a pressure field that propagates the effects of the source to the pool boundary. Finally, the interaction between the fluid and the tank results in the acceleration of the fluid-tank boundary to create an additional pressure field. This interaction has come to be known as fluid-structure interaction (FSI). The total pressure field is the combination of the field produced by direct action of the source plus the field produced by the subsequent motion of the tank boundary.

It should be pointed out that the role played by steam condensation is to create an accelerating interface which could just as well be accomplished by mechanical means such as the breaking of an evacuated glass sphere or by the discharge of air into a tank.

3.1 EMPIRICAL CONDENSATION SOURCE

The pressure excursions caused by chugging or condensation oscillation are the result of intermittent steam condensation occurring at the exit of a vent through which steam discharges into a tank or suppression pool. This condensation is controlled principally by the vent steam mass flux, air content in that flux, impurities in the water, and the temperature difference across the steam-water interface. When conditions are such that stable condensation is not possible, the sequence as shown in Fig. 1 begins:[6]

(1) The water in the vent is isolated, which allows a layer of saturated water to form at the interface which, in turn, reduces the rate of condensation.

(2) The reduced condensation rate allows the drywell pressure to increase; the interface is thus pushed out of the vent back into the pool. The layer of saturated water protects the interface while it is inside the vent.

(3) As the steam-water interface emerges into the pool, local turbulence destroys the protective boundary layer of saturated water and the interface comes in contact with the colder pool. A "burst" of condensation follows.

(4) The steam flow through the vent is not sufficient to supply the rapid condensation. The drywell is depressurized and water again reenters the vent to repeat the cycle.

As shown in Fig. 1, the steam-water interface motion undergoes a volume acceleration that is the source of the accompanying pressure field. This source is dependent on several factors, some of which are highly random. As a result, the nature of the source is also random. For example, if local conditions permit the steam-water interface to extend sufficiently far into the pool, and if the ensuing condensation in this steam bubble is rapid enough, a void will result which will impulsively collapse, exciting

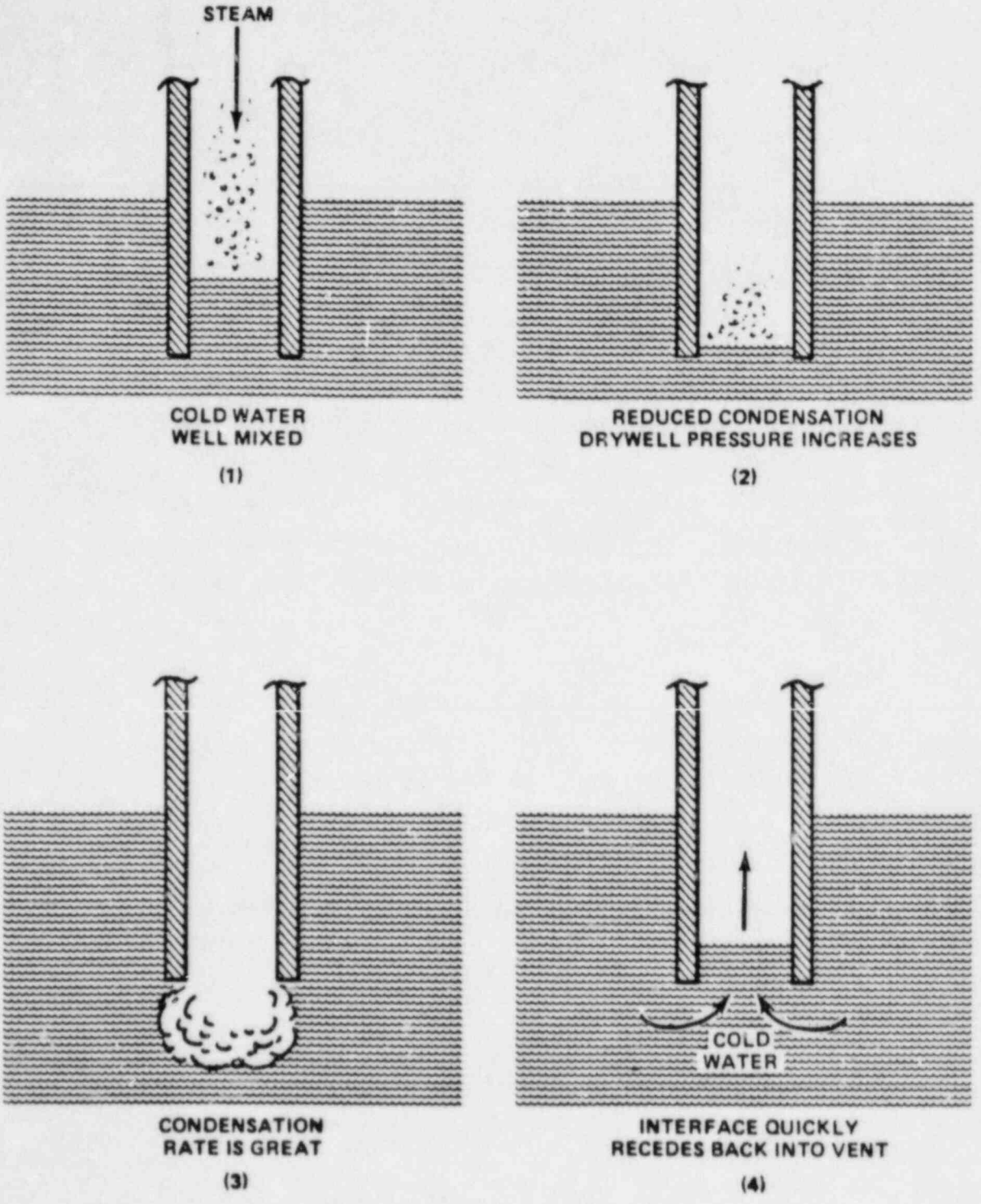

Figure 1 The Observed Sequence of Events During Unstable Condensation

G1004058-01

the pool acoustic modes (chugging) as shown in Fig. 2. In addition, there might be multiple smaller condensation events which will cause the interface to execute sinusoidal motion (condensation oscillation).

To develop a completely analytical description of unstable condensation, it is obvious that an analytical model of interface collapse is required. A model of steam-bubble collapse has been developed by Florscheutz and Chao.[7] This model treats the mechanics of the collapse under spherically symmetrical conditions to ascertain the relative importance of the dominant mechanisms controlling the collapse: liquid inertia and heat transfer. Florscheutz and Chao conclude that when the collapse is inertia controlled, collapse rates are high and increase as the collapse proceeds. In contrast, when the collapse is heat-transfer controlled, collapse rates are low and decrease as the collapse proceeds. An integral component of the Florscheutz and Chao model is the use of a calculational result obtained by Plesset and Zwick.[8] In their article on bubble dynamics and cavitation, Plesset and Prosperetti[9] express doubts as to the applicability of this result to collapsing steam bubbles. In their opinion, no entirely satisfactory theoretical results are available for the modeling of steam bubble collapse under conditions in which thermal effects play a significant role.

Because of the disagreement between notable workers in this field and because the conditions at the vent exit that affect condensation are random, the condensation source is best obtained in an empirical manner from relevant test data. To extract an empirical source for either chugging or condensation oscillation, a transfer function for the relevant test tank geometry is used to relate the measured pressure to the source. This is expressed mathematically in the following manner:

$$p(\vec{x}|\omega) = H(\vec{x}|\vec{x}_o|\omega)\ S(\vec{x}_o|\omega)\ . \qquad (1)$$

The component of the pressure Fourier transform at a frequency $\omega/2\pi$ observed at a location in the test tank given by the vector $\vec{x}$ is represented by $p(\vec{x}|\omega)$. The similar component of the condensation source, which is at a location $\vec{x}_o$, is given by $S(\vec{x}_o|\omega)$. The transfer function $H(\vec{x}|\vec{x}_o|\omega)$ depends on parameters such as bulk average fluid density, sonic speed, tank

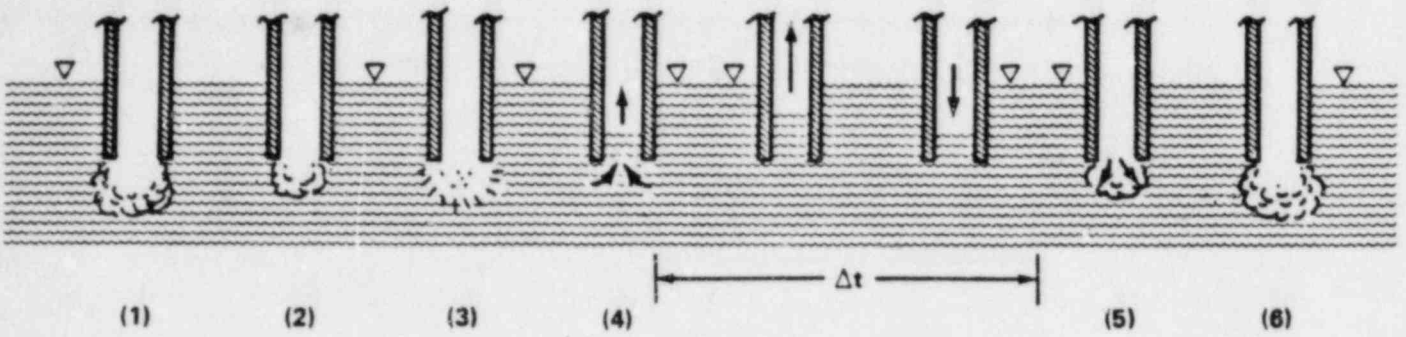

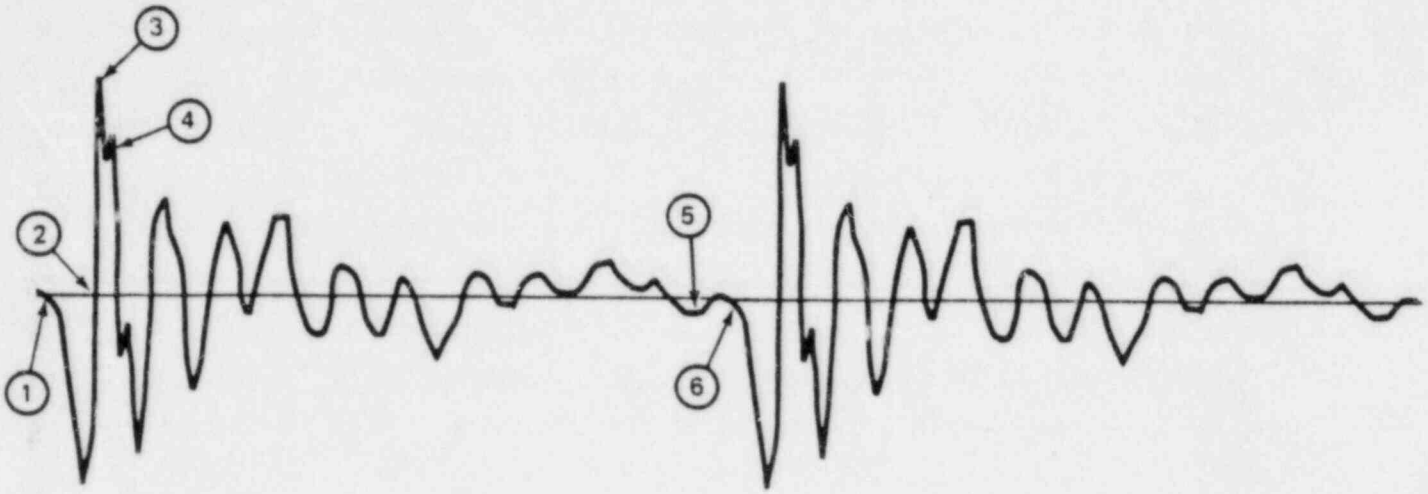

(1) THE CONDENSATION PROCESS BEGINS, THE BUBBLE BEGINS TO COLLAPSE, AND THE PRESSURE DECREASES.

(2) THE WATER MASS FLOWING INTO THE SPACE PREVIOUSLY OCCUPIED BY THE BUBBLE IS DECELERATED SO THAT THE PRESSURE RISES AGAIN.

(3) THE BUBBLE VANISHES. IN SOME CASES, THIS COLLAPSE OCCURS OUTSIDE THE DISCHARGE PIPE SO THAT A PRESSURE SPIKE IS PRODUCED.

(4) THE WATER ENTERS THE VENT; THE PRESSURE IN THE DRYWELL REACHES ITS MINIMUM AT THAT INSTANT.

(4)–(5) THE VESSEL EXECUTES A DAMPED OSCILLATION.

(6) THE NEW BUBBLE REACHES ITS MAXIMUM EXPANSION.

Figure 2 Schematic Representation of a Chugging Sequence

geometry, structural response frequency, and damping. Since both $p(\vec{x}|\omega)$ and $H(\vec{x}|\vec{x}_o|\omega)$ are known, the source $S(\vec{x}_o|\omega)$ is obtained from Eq. (1) by the simple complex division

$$S(\vec{x}_o|\omega) = p(\vec{x}|\omega)/H(\vec{x}|\vec{x}_o|\omega) \tag{2}$$

Note that the source function given by Eq. (2) is purely empirical: it is the function that, when acted on by the transfer function for the test tank, yields the measured pressure.

Although an empirically derived source may be unpalatable to the purist, it offers several advantages. First, any theoretical source would, of a necessity, be based on one of the several theoretical models of steam bubble collapse. As good as these models may be, they all contain assumptions and parameters such as heat transfer coefficients, the validity of which are not well known beforehand, and thus would have to be obtained from some prototypical test data. This is also true for the "semiempirical source" used by the Mark II Owners Group in their assessment of the impact of chugging on containment design.[10] Although nothing is wrong with using either a theoretical or a semiempirical source, each would require a confirmation by comparison with test data for validity. Second, a much more exact source--one which yields a better reproduction of the measured pressure--can be obtained using the empirical approach than either the theoretical or semiempirical source. Finally, the third advantage is that a source obtained via Eq. (2) is quite easy to obtain at a minimum computer cost.

3.2 TRANSFER FUNCTION

The transfer function $H(\vec{x}|\vec{x}_o|\omega)$ is so called because of the special mathematical relationship it bears with the pressure field $p(\vec{x}|\omega)$ and the source $S(\vec{x}_o|\omega)$ in Eq. (1). Physically, however, the transfer function is the pressure field due to an impulsive unit source, i.e., a delta function, located at $\vec{x}_o$. The total field is then the summation of the fields from all the elementary sources plus the fields generated by the motion of the boundary surface. This unit-source pressure field, which is often termed a

Green's function, is relatively easy to obtain from the equations governing the motion of the fluid. If certain reasonable standard assumptions are made, an analytical expression for this pressure field, or Green's function, can be derived as demonstrated below.

3.2.1 Fluid Equations of Motion

The state of a fluid is completely determined once we specify the fluid velocity $\vec{u}$ and any two of the thermodynamic properties pertaining to the fluid as functions of space and time. Hence, the motions of a fluid medium are governed by four equations.[11] The first equation is a continuity equation expressing the conservation of mass:

$$\frac{\partial \rho}{\partial t} + \nabla \cdot (\rho \vec{u}) = 0 \ . \tag{3}$$

The second equation is a force equation expressing the conservation of momentum,

$$\rho \frac{\partial \vec{u}}{\partial t} = - \rho \ (\vec{u} \cdot \nabla) \ \vec{u} - \nabla \left[P + \rho \phi - \left(\eta + \frac{4}{3} \mu \right) \nabla \cdot \vec{u} \right] - \mu \nabla \times \nabla \times \vec{u}, \tag{4}$$

where μ and η are the coefficients of shear and bulk viscosity, and ϕ is a potential energy caused by a force per unit mass. The third equation is a heat exchange equation expressing the conservation of energy written in terms of specific entropy,

$$\rho T \frac{\partial s}{\partial t} = - \rho T \ \vec{u} \cdot \nabla s + \nabla \cdot (\kappa \nabla T) + \tilde{\tau} : \nabla \vec{u} \ , \tag{5}$$

where $\tilde{\tau}$ is the viscous-stress tensor and κ the thermal conductivity. The last equation is the equation of state for the fluid

$$P = P(\rho, s) \ , \tag{6}$$

where we have chosen the fluid density ρ and specific entropy s as the independent variables.

The above four equations form the governing set of equations for the fluid. The implicit assumption has been made that the fluid properties (bulk modulus, viscosity, thermal conductivity) are everywhere constant. To obtain a unique solution for a particular fluid geometry, we need to impose some boundary conditions. Normally we require that the fluid pressure equal its equilibrium value P_o at a free surface and that the fluid cannot penetrate a solid surface. Since these solid surfaces are formed by structures that are seldom perfectly rigid, a fluid-structure interaction must be considered. This is accomplished by simply requiring the normal component of fluid velocity to equal the structure velocity at the fluid-structure interface. Thus, we must augment the governing set of fluid equations with the equation of motion for the structure represented symbolically as

$$M \frac{dy^2}{dt^2} + L^{(N)} y = P \ , \tag{7}$$

where y is the displacement of the boundary, $L^{(N)}$ is a space operator of order N describing the local structural restraining force at the boundary, and M is the local mass of the boundary per unit area.

Upon inspection, it is readily apparent that analytical solutions to the above set of coupled nonlinear partial differential equations would be such a formidable task that such solutions would be rare. Therefore, in general we rely on numerical techniques in the form of finite-difference or finite-element computer programs. Numerical solutions are in principle quite adequate. However, in practice they do not contain all the physical insight to which one is accustomed from analytical solutions. It will be shown that if certain assumptions are made, this set of equations will collapse to a single equation of acoustic fluid motion that will have a straightforward analytic solution. If these assumptions can be justified, we will obtain the physical insight and at the same time maintain an adequate representation of the pressure field.

3.2.2 Assumptions and their Justifications

The theory of sound deals with systematic motions of a fluid relative to an equilibrium state. Such perturbations of state can be described by

incremental or acoustic variables, and approximate equations governing them can be obtained by linearizing the general equations of motion given above. These results, as well as higher order approximations, can be derived in an orderly way by invoking a modified perturbation analysis.[12,13] This consists of replacing the dependent variables appearing in Eqs. (3) through (7) with the sum of their equilibrium or zero-order values and their first- and second-order variational components and then forming the separate equations that must be satisfied by the variables of each order. The resulting first-order equations, with the assumption of isentropic behavior of the fluid, yield the scalar wave equation of classical acoustics which has analytic solutions. The second-order equations, however, have no general solution but are useful for making approximations and investigating some second-order phenomena that cannot be predicted by the first-order equations alone. If an analytic solution is sought, some rationale must be given to show that the second-order effects can safely be neglected.

Thus, we proceed in the same spirit as the modified perturbation analysis except we explicitly make three a priori assumptions: (1) the fluid motion is isentropic, (2) the change in the fluid pressure is proportional to the change in the fluid density, and (3) the velocity of the fluid particles is small compared with the velocity of sound. In addition, we also implicitly assume average values for the fluid properties and that the fluid is at rest. To justify these assumptions, we first separate the fluid pressure and density into an equilibrium value P_o, ρ_o plus a small acoustic part P, δ:

$$P = P_o + p \qquad \rho = \rho_o + \delta, \tag{8}$$

and then proceed as follows:

(1) Isentropic Fluid Motion

We write the general equation of heat transfer expressing the conservation of energy (Eq. (5)) in the following form:

$$\rho T \frac{ds}{dt} = \rho T \left(\frac{\partial s}{\partial t} + \vec{u}\cdot\nabla s\right) = \nabla\cdot(\kappa\nabla T) + \tilde{\tau}:\nabla\vec{u} \ . \tag{9}$$

For reversible adiabatic or isentropic fluid motion, the above equation vanishes. To be able to approximate the fluid as an isentropic fluid, we must show that thermal conductivity and viscosity are unimportant, i.e., the fluid is ideal. The left-hand side of Eq. (9) is the quantity of heat gained per unit volume per unit time at the expense of the mechanical energy of a sound wave. Therefore, the sound wave is damped out in time. This subject is treated extensively in the literature[14-17] whereby one can calculate the rate of acoustic energy loss to be so slight as to warrant the neglect of viscosity and thermal conduction. Therefore, to a good approximation, the fluid may be considered as ideal, i.e., the effects of viscosity and thermal conductivity can be neglected. Hence, $ds/dt = 0$ and the fluid is said to be isentropic.

(2) First-Order Equation of State

Since the fluid is isentropic, the equation of state is a function of the fluid density only and can obviously be expanded in a Taylor series in the term δ/ρ_o (called the "condensation"):

$$P = P_o + A\left(\frac{\delta}{\rho_o}\right) + \frac{B}{2!}\left(\frac{\delta}{\rho_o}\right)^2 + \frac{C}{3!}\left(\frac{\delta}{\rho_o}\right)^3 + \ldots , \qquad (10)$$

where $A = \rho_o c^2$ since $(dP/d\rho)_s \equiv c^2$. By application of thermodynamic formulae for the isentropic derivatives of the pressure with respect to density, the ratios B/A and C/A can be computed.[18] For water, the numerical values for these ratios are $B/A < 6$ and $C/A < 39$ where $P_o < 24.5$ MPa (3553 psia) and $T = 30°C$ (86°F). Keeping only the linear term in Eq. (11), we write

$$p = A\left(\frac{\delta}{\rho_o}\right) = c^2 \delta . \qquad (11)$$

If this first-order equation of state is used instead of the Taylor series expansion, it can be quickly shown that an error in P of no more than 1% is made when the condensation δ/ρ_o is less than 0.0032. A condensation this large would produce an acoustic pressure p in excess of 73 atm (7.4 MPa or 1073 psi) -- far larger than any condensation event possible in a Mark III containment.

(3) Linear Equation of Motion ($u << c$)

Since the assumption of isentropic fluid motion is tantamount to neglecting fluid viscosity and thermal conductivity, the equation of motion (Eq. (4)) reduces to Euler's equation,

$$\frac{\partial \vec{u}}{\partial t} + (\vec{u} \cdot \nabla)\,\vec{u} = -\frac{1}{\rho}\nabla P \ . \tag{12}$$

We now explore under what conditions it is justified to omit the nonlinear term $(\vec{u} \cdot \nabla)\vec{u}$ compared with the other two terms. We are interested in the relative order of magnitude of the terms of Eq. (12) in connection with the propagation of sound waves. If we introduce for the characteristic time and length over which the sound wave changes appreciably the period T and the length λ of the wave, $\partial/\partial t \sim 1/T$ and $\nabla \sim 1/\lambda$, then to obtain the relative orders of magnitude of the different terms, we use the property of plane waves that $p = \rho c u$. The relative orders of magnitude of the terms in Eq. (12) are thus: 1, u/c, 1. The condition, then, that the fluid equation of motion be linear is $u << c$.

3.2.3 Acoustic Wave Equation

The above assumptions when applied to the mass, momentum, and energy conservation equations and to the equation of state yield two linear equations of motion for the fluid:

$$c_o^2 \frac{\partial p}{\partial t} + \rho_o \nabla \cdot \vec{u} = 0 \tag{13}$$

$$\rho_o \frac{\partial \vec{u}}{\partial t} + \nabla p = 0 \ . \tag{14}$$

Eq. (13) is the equation of conservation of mass where Assumption 2 has been used to eliminate the fluid density. Assumption 3 linearizes the momentum conservation and, together with Assumption 1, gives Eq. (14) as the expression for the conservation of momentum. Finally, Assumption 1 alone eliminates the energy conservation equation.

The above two equations of motion can be combined by eliminating the velocity between them, resulting in the linear acoustic wave equation:

$$\Box^2 p(\vec{x},t) \equiv \{\nabla^2 - \frac{1}{c_o^2}\frac{\partial^2}{\partial t^2}\}\, p(\vec{x},t) = 0, \tag{15}$$

where $\Box^2 \equiv \nabla^2 - c_o^{-2}\,\partial^2/\partial t^2$ is the d'Alembertian operator. Eq. (15) is a homogeneous linear wave equation describing regions of space not containing any sources of acoustic energy. However, a source must be present to generate any acoustic disturbance. If the source is external to the region of interest, it can be taken into account by introducing time dependent boundary conditions. For a source internal to the region of interest, the hydrodynamic equations can be modified to include source terms. There are many possible types of sources, but only two will be considered here:

(1) If mass is being injected into the space at a rate per unit volume $Q(\vec{r},t)$, the linearized equation of continuity becomes

$$c_o^2 \frac{\partial p}{\partial t} + \rho_o \nabla\cdot\vec{u} = Q(\vec{r},t)\ . \tag{13a}$$

This $Q(\vec{r},t)$ is generated by any closed surface that changes volume.

(2) If there are body forces present in the fluid, then a body force per unit volume $\vec{F}(\vec{r},t)$ must be included in Euler's equation. The linearized equation of motion then becomes

$$\rho_o \frac{\partial \vec{u}}{\partial t} + \nabla p = \vec{F}(\vec{r},t)\ . \tag{14a}$$

An example of this kind of force is that produced by a body that oscillates back and forth without any change in volume.

If these two modifications are combined with the linearized equation of state, an inhomogeneous wave equation is obtained

$$\Box^2 p = \nabla^2 p - \frac{1}{c^2}\frac{\partial^2 p}{\partial t^2} = -\frac{\partial Q}{\partial t} + \nabla\cdot\vec{F}\ . \tag{15a}$$

Unsteady condensation has source terms of the first type. Defining a source density q, Eq. (15a) in the absence of body forces, i.e., $\vec{F} = 0$, becomes

$$\Box^2 p(\vec{x},t) = -4\pi q(\vec{x},t) \ . \tag{16}$$

For a single point source located at $\vec{x}_o$, the source density is given by

$$q(\vec{x},t) = \rho\delta(\vec{x} - \vec{x}_o)\ S(t) \ , \tag{17}$$

where $\delta(\vec{x} - \vec{x}_o)$ is the Dirae delta function.[19]

3.2.4 Solution of the Acoustic Wave Equation

A Fourier transformation to the frequency domain yields a straightforward solution of the linear acoustic equation. Thus, Eq. (16) becomes

$$\{\nabla^2 - (\tfrac{\omega}{c})^2\}\ p(\vec{x}|\omega) = -4\pi q(\vec{x}|\omega) \ , \tag{18}$$

where the Fourier transform of $p(\vec{x},t)$ is defined[20] by

$$p(\vec{x}|\omega) = \frac{1}{2\pi}\int_{-\infty}^{\infty} p(\vec{x},t)\ e^{+i\omega t}dt \ , \tag{19}$$

with a similar definition for the source density function.

The complete solution[21] of Eq. (18) in terms of Green's function is

$$p(\vec{x}|\omega) = \int dy^3\ G(\vec{x}|\vec{y}|\omega)\ q(\vec{y}|\omega)$$

$$+ \frac{1}{4\pi}\oint dy^2\ \{G(\vec{x}|\vec{y}|\omega)\ \frac{\partial}{\partial n}\ p(\vec{y}|\omega) - p(\vec{y}|\omega)\frac{\partial}{\partial n}\ G(\vec{x}|\vec{y}|\omega)\} \ , \tag{20}$$

which is an equation for the spatial factor of the pressure field at frequency $\omega/2\pi$ within and on the surface bounding the fluid in terms of a volume integral of the source density $q(\vec{y}|\omega)$ over the bounded volume and a surface integral of the boundary values of $p(\vec{y}|\omega)$ and its outward-pointed

normal gradient $\partial p/\partial n$ over the boundary surface. The first integral on the right of Eq. (20), the volume integral, is the contribution of the total pressure field from the action of the source density while the second integral, the surface integral, is the contribution from the motion of the boundaries that is induced by the source density.

For flexible containment boundaries,[22] the condition satisfied by the pressure field is

$$\frac{\partial}{\partial n} p(\vec{x}_s|\omega) = i\left(\frac{\omega}{c}\right) \beta(\vec{x}_s|\omega)\ p(\vec{x}_s|\omega) \ , \tag{21}$$

where $\beta(\vec{x}_s|\omega)$ is the specific acoustic admittance of the boundary surface at $\vec{x}_s$ on the surface. Note that Eq. (21) is of the form of a general homogeneous boundary condition and for $\beta \to 0$ the pressure field is that for a rigid boundary containment.

The Green's function $G(\vec{x}|\vec{y}|\omega)$ is defined as that function which satisfies

$$\{\nabla^2 + \left(\frac{\omega}{c}\right)^2\}\ G(\vec{x}|\vec{y}|\omega) = -4\pi\delta(\vec{x} - \vec{y}) \tag{22}$$

and is subject to the same boundary condition as the pressure (Eq. (21)). Thus, the component of the pressure field with frequency $\omega/2\pi$ at a location $\vec{x}$ (Eq. (20)) becomes

$$p(\vec{x}|\omega) = \int dy^3\ G(\vec{x}|\vec{y}|\omega)\ q(\vec{y}|\omega) \ . \tag{23}$$

Note that the surface integral in Eq. (20) vanishes because the Green's function $G(\vec{x}|\vec{y}|\omega)$ satisfies the same boundary condition as the pressure field (Eq. (21)) and hence is a flexible boundary Green's function.

3.2.4.1 Flexible-Boundary Eigenfunction Expansion

The flexible boundary Green's function $G(\vec{x}|\vec{y}|\omega)$ can be expanded in a series of flexible boundary eigenfunctions $\Psi_N(\vec{x}|\omega)$:

$$G(\vec{x}|\vec{y}|\omega) = \sum_N a_N \Psi_N(\vec{x}|\omega) \ , \tag{24}$$

where the eigenfunctions are solutions of the eigenvalue equation

$$\{\nabla^2 + K_N^2\}\ \Psi_N(\vec{x}|\omega) = 0\ , \tag{25}$$

subject to the same boundary condition as the pressure field (Eq. (21)):

$$\frac{\partial}{\partial n}\ \Psi_N(\vec{x}_s|\omega) = i(\frac{\omega}{c})\ \beta(\vec{x}_s|\omega)\ \Psi_N(\vec{x}_s|\omega)\ . \tag{26}$$

This boundary condition will guarantee that Eq. (23) follows from Eq. (20) and also that $G(\vec{x}|\vec{y}|\omega)$ satisfies the same condition as the pressure field.

If any portion of the boundary has a real component of $\beta(\vec{x}_s|\omega)$, the acoustic conductance which is nonzero, the eigenvalue $K_N = K_N(\omega)$ will be complex with negative imaginary parts. The index N stands for a trio of quantum numbers as required for a three-dimensional standing wave. At the Nth resonance, the Nth mode of the pressure field predominates, having an amplitude inversely proportional to the imaginary component of $K_N(\omega)$ for that frequency. Suppose a root of the equation $cK_N(\omega) = \omega$ is equal to $\omega_N - i\lambda_N$, with ω_N and λ_N positive quantities. Because of the symmetry of $\beta(x_s|\omega)$ about the imaginary ω axis, there will also be a root at $-\omega_N - i\lambda_N$, so that the two roots of the equation $cK_N(\omega) = \omega$ are

$$\omega = \pm\omega_N - i\lambda_N = cK_N(\pm\omega_N - i\lambda_N)\ . \tag{27}$$

Combining Eqs. (22), (24), and (25) yields

$$\sum_N \{-K_N^2 + (\frac{\omega}{c})^2\}\ a_N\Psi_N(\vec{x}|\omega) = -4\pi\delta(\vec{x} - \vec{y})\ . \tag{28}$$

Since the flexible boundary eigenfunctions are orthonormal,

$$\langle\Psi_M|\Psi_N\rangle \equiv \int dx^3\Psi_M^*(\vec{x}|\omega)\ \Psi(\vec{x}|\omega) = \delta_{MN}\ , \tag{29}$$

where $\Psi_N^*(\vec{x}|\omega)$ is the complex conjugate flexible boundary eigenfunction. Multiplication of Eq. (28) on the left by $\Psi_M^*(\vec{x}|\omega)$ and using Eq. (29) yields a_N of Eq. (24) and thus

$$G(\vec{x}|\vec{y}|\omega) = 4\pi c^2 \sum_N \frac{\Psi_N^*(\vec{y}|\omega)\ \Psi_N(\vec{x}|\omega)}{\{(cK_N)^2 - \omega^2\}} \ . \tag{30}$$

Hence, the flexible boundary pressure field given by Eq. (23) due to the source density given by Eq. (17), i.e., a point source, is

$$p(\vec{x}|\omega) = 4\pi\rho c^2 \sum_N \frac{\Psi_N^*(\vec{x}_o|\omega)\ \Psi_N(\vec{x}|\omega)}{\{(cK_N)^2 - \omega^2\}}\ S(\vec{x}_o|\omega) \ , \tag{31}$$

where $\vec{x}_o$ is the source location. Note that $S(\vec{x}_o|\omega)$ is in fact independent of the location $\vec{x}_o$; this notation is understood to differentiate between different sources at different locations.

The form of Eq. (31) suggests that the pressure field can be expressed in terms of a transfer function operating on the source:

$$p(\vec{x}|\omega) = H(\vec{x}|\vec{x}_o|\omega)\ S(\vec{x}_o|\omega) \ , \tag{32}$$

where the transfer function is given by Eq. (31)

$$H(\vec{x}|\vec{x}_c|\omega) = 4\pi\rho c^2 \sum_N \frac{\Psi_N^*(\vec{x}|\omega)\Psi_N(\vec{x}|\omega)}{\{\omega_N^2 - (\omega + i\lambda_N)^2\}} \ . \tag{33}$$

Note that the denominator in Eq. (33) is the same as Eq. (31) since the roots of the equation $\omega = cK_N(\omega)$ are $\pm\omega - i\lambda_N$. By inspection, both Eqs. (31) and (33) have poles at $\omega = \pm\omega_N - i\lambda_N$.

For multiple sources, each with a specific location x_ν and start time t_ν, the source density becomes

$$q(\vec{x},t) = \sum_\nu \rho\delta(\vec{x} - \vec{x}_\nu)\ S(t + t_\nu) \ . \tag{34}$$

Using the properties of Fourier transforms, the pressure field for multiple point sources can be expressed as (Eq. (32))

$$p(\vec{x}|\omega) = \sum_\nu H(\vec{x}\ \vec{x}_\nu|\omega)\ e^{-i\omega t_\nu}\ S(\vec{x}_\nu|\omega) \ . \tag{35}$$

3.2.4.2 Rigid Boundary Eigenfunction Expansion

Although Eqs. (31), (32), and (33) determine the pressure field inside a containment with flexible boundaries for a specified point source, it is necessary to know the flexible boundary eigenfunctions $\Psi(\vec{x}|\omega)$ and the eigenvalue $K_N(\omega)$ to evaluate these equations. An alternative would be to expand the Green's function in terms of rigid boundary eigenfunctions $\phi_N(\vec{x})$, which are defined as solutions of

$$\{\nabla^2 + k_N^2\}\ \phi_N(\vec{x}) = 0 \tag{36}$$

subject to the boundary condition

$$\frac{\partial}{\partial n}\ \phi_N(\vec{x}_s) = 0\ , \tag{37}$$

For simple geometries, i.e., cylindrical and annuler solutions to Eq. (36) subject to the boundary condition expressed by Eq. (37) are readily obtainable. Thus, expansion of the Green's function in terms of these eigenfunctions yields

$$G_\phi(\vec{x}|\vec{y}|\omega) = 4\pi c^2 \sum_N \frac{\phi_N^*(\vec{y})\ \phi_N(\vec{x})}{(cK_N)^2 - \omega^2}\ . \tag{38}$$

Hence, the pressure field is given by the combination of Eqs. (20), (21), (37), and (38)

$$p(\vec{x}|\omega) = \int dy^3\ G_\phi(\vec{x}|\vec{y}|\omega)\ q(\vec{y}|\omega) + i\ \frac{\omega/c}{4\pi} \oint dy_s^2\ G_\phi(\vec{x}|\vec{y}_s|\omega)\ \beta(\vec{y}_s|\omega)\ . \tag{39}$$

Note that in this form the pressure field exhibits the nature of a superposition of a field due to a source density in a rigid boundary containment plus a field due to the acceleration of the boundary. This then is the mathematical expression for the fluid-structure interaction.

Although Eqs. (23) and (39) describe the same pressure field in a containment with flexible boundaries, each form has its own advantages: the rigid boundary eigenfunctions $\phi_N(\vec{x})$ are generally easier to obtain than the

flexible boundary eigenfunctions $\Psi_N(\vec{x}|\omega)$, but Eq. (39) is an integral equation which is more difficult to solve than is Eq. (23).

3.2.4.3 First Order Perturbation Expansion

The flexible boundary eigenfunctions $\Psi_N(\vec{x}|\omega)$ can be expressed in terms of rigid boundary eigenfunctions $\phi_N(\vec{x})$ by noting that the pressure field given by Eq. (31) can be written as

$$p(\vec{x}|\omega) = \sum_N b_N \Psi_N(\vec{x}|\omega) \ . \tag{40}$$

In the absence of sources, the combination of Eqs. (39) and (40) yields an integral equation for $\Psi_N(\vec{x}|\omega)$:

$$\Psi_N(\vec{x}|\omega) = i \frac{\omega/c}{4\pi} \oint dy_s^2 \, G_\phi(\vec{x}|\vec{y}_s|\omega) \, \beta(\vec{y}_s|\omega) \, \Psi_N(\vec{y}_s|\omega) \ , \tag{41}$$

where again N represents a tric of quantum numbers and the subscript s indicates that the integral is to be evaluated at the containment boundary. If the rigid boundary eigenfunction expansion of the Green's function (Eq. (22)) is substituted into the above, the result is

$$\Psi_N(\vec{x}|\omega) = i\omega c \sum_\ell \phi_\ell(\vec{x}) \frac{1}{(\omega_\ell^o)^2 - \omega^2} \oint dy_s^2 \, \phi_\ell^*(\vec{y}_s) \, \beta(\vec{y}_s|\omega) \, \Psi_N(\vec{y}_s|\omega) \ , \tag{42}$$

which is an expression of the form

$$\Psi_N(\vec{x}|\omega) = \sum_\ell c_\ell \phi_\ell(\vec{x}) \tag{43}$$

and where $\omega_\ell^o \equiv ck_\ell$.

Since Eqs. (25), (36), and (42) are all homogeneous in the functions $\Psi_N(\vec{x}|\omega)$ and/or $\phi_N(\vec{x})$, a convenient normalization of the flexible boundary eigenfunction $\Psi_N(\vec{x}|\omega)$ can be chosen. Therefore, we choose

$$\langle \phi_N(\vec{x}) | \Psi_N(\vec{x}|\omega) \rangle \equiv \int dx^3 \phi_N^*(\vec{x}) \, \Psi_N(\vec{x}|\omega) = 1 \ , \tag{44}$$

where N denotes some specified eigenfunction of Eq. (36). Comparison with Eq. (42) yields the equivalent condition $c_N = 1$ for one particular N. This choice of normalization requires that

$$(\omega_N^o)^2 - \omega^2 = i\omega c \oint dy_s^2 \; \phi_N^*(\vec{y}_s) \; \beta(\vec{y}_s|\omega) \; \Psi_N(\vec{y}_s|\omega) \; . \tag{45}$$

The series given by Eq. (42) then becomes

$$\Psi_N(\vec{x}|\omega) = \phi_N(\vec{x}) + i\omega c \sum_{\ell \neq N} \frac{\phi_1(\vec{x})}{(\omega_\ell^o)^2 - \omega^2} \oint dy_s^2 \; \phi_\ell^*(\vec{y}_s) \; \beta(\vec{y}_s|\omega) \; \Psi_N(\vec{y}_s|\omega) \; . \tag{46}$$

It is obvious now that when $\beta \to 0$ (rigid boundaries), then $\Psi_N \to \phi_N$ and $\omega_N \to \omega_N^o$. Note the sum in Eq. (46) runs over all ℓ except for the value $\ell = N$.

The relations given by Eqs. (45) and (46) are exact, for they involve no approximations apart from the assumption that $\Psi_N(\vec{x}|\omega)$ contains some nonzero component of the particular eigenfunction $\phi_N(\vec{x})$ in the expansion Eq. (43); otherwise, it is not possible to impose the normalization condition Eq. (44). The expression for the flexible boundary eigenfunctions given by Eq. (46) shows that the effect of the flexible boundary is to "mix" or couple the rigid boundary eigenfunctions.

For relatively stiff boundaries, i.e., a small acoustic admittance β, Eqs. (46) and (45) can be solved via a perturbation expansion. To first order in β:

$$\Psi(\vec{x}|\omega) \cong \phi(\vec{x}) + i\omega c \sum_{\ell \neq N} \phi_\ell(\vec{x}) \{(\omega^o)^2 - \omega^2\} \oint dy^2 \; \phi_\ell(y_s) \; \beta(y_s|\omega) \; \phi_N(y_s) \tag{47}$$

and

$$\omega^2 \cong (\omega_N^o)^2 - i\omega c \oint dy_s^2 \; \phi_N^*(\vec{y}_s) \; \beta(\vec{y}_s|\omega) \; \phi_N(\vec{y}_s) \; . \tag{48}$$

Hence, to a first approximation the change in the eigenfrequency $\omega = cK_N(\omega)$ caused by the fact that $\beta \neq 0$ is proportional to the average value of $i\beta$ over the boundaries, weighted by ϕ_N^2 so that the boundary areas, where the Nth standing wave or field component is large, is emphasized.

When $\beta(\vec{y}_s|\omega)$ is nearly uniform or constant, because of the orthoganality of the $\phi_\ell(\vec{x})$, it follows that

$$\Psi_N(\vec{x}|\omega) \cong \phi_N(\vec{x}) \ , \tag{49}$$

and, remembering Eq. (27),

$$(\omega_N - i\lambda_N)^2 \cong (\omega_N^o)^2 - i(\omega_N - i\lambda_N)\, c\beta(\omega_N - i\lambda_N) \oint dy_s^2\, \phi_N^*(\vec{y}_s)\, \phi_N(\vec{y}_s) \ , \tag{50}$$

where $\beta(\vec{y}_s|\omega) \cong \beta(\omega)$ and $\omega = cK(\omega) = \pm\omega_N - i\lambda_N$. Note that for simplicity only the complex eigenfrequency $+\omega_N - i\lambda_N$ is used in Eq. (48), but the eigenfrequency $-\omega_N - i\lambda_N$ yields a result similar to Eq. (50), leading to identical conclusions.

3.2.4.4 Locally Reactive Boundary

Suppose the containment walls are locally reacting* so that to a good approximation we can assign a specific acoustic admittance

---

*The acoustic pressure acts on the surface of the structure and tends to make it move. If any fluid motion normal to the surface is possible, there will be wave motion in the material forming the surface. The motion of the surface at one point will be related to motion at another point of the surface by the wave motion inside the material as well as by the incident and reflected pressure waves. If the various parts of the surface are not strongly coupled together and we can consider that the motion, normal to the surface, of one portion of the surface is dependent only on the acoustic pressure incident on that portion and independent of the motion of any other part of the area, then we say that surface is one of <u>local reaction</u>.

$\beta(\omega,\vec{x}_s) = \rho c\, u_n/p$, where u_n is the normal velocity magnitude at the boundary, to each point $\vec{x}_s$ on the wall surface for each frequency $\omega\ 2\pi$.

If the containment boundary can be approximated by a simple harmonic oscillator, then the specific acoustic admittance is given by

$$\beta(\vec{y}_s|\omega) \cong \beta(\omega) = \rho c\{R + iM(\frac{\omega_s^2}{\omega} - \omega)\}^{-1} \tag{51}$$

where

$$M \equiv \rho_s h_s = \text{effective mass per unit area}$$

$$R \equiv 2\zeta M\omega_s = \text{mechanical resistance}$$

$$M\omega_s^2 = \text{effective wall stiffness}$$

and M, R, and ω_s^2 are considered to be constant. Thus, $\beta(\omega)$ is a couplex quantity, the inverse of which is the specific impedance of the boundary surface. The real part of β is called the conductance ξ and the imaginary part the susceptance s:

$$\beta(\omega) \equiv \xi(\omega) - i\sigma(\omega)\ . \tag{52}$$

In general, both ξ and σ are also functions of location on the boundary surface $\vec{y}_s$. However, by taking advantage of the symmetry of the containment, β can be taken to be independent of location over large regions of the boundary surface.

Eq. (21) gives the impression that $\xi << \sigma$; thus, making the assumption that

$$R^2\omega_N^2 << M^2\ (\omega_s^2 - \omega_N^2)^2 \tag{53}$$

yields for the specific acoustic admittance

$$\beta \cong \frac{\rho c}{\rho_s h_s}\{2\zeta\ \omega_s(\frac{\omega_s^2}{\omega_N} - \omega_N)^{-2} - i(\frac{\omega_s^2}{\omega_N} - \omega_N)^{-1}\}\ . \tag{54}$$

Substitution of Eq. (54) into Eq. (50) eventually will yield

$$\omega_N^4 - \{(\omega_N^o)^2 + \omega_s^2(1 + \rho c^2 \delta)\}\ \omega_N^2 + (\omega_N^o)^2\ \omega_s^2 \cong 0 \tag{55}$$

and

$$\lambda_N \cong \zeta\ \rho c^2 \delta\ \frac{\omega_s^3\ \omega_N^2}{(\omega_s^2 - \omega_N^2)^2}\ \{1 + \frac{1}{2}\ \rho c^2\ \delta(\frac{\omega_s^2}{\omega_s^2 - \omega_N^2})\}^{-1}\ , \tag{56}$$

where

$$\delta \equiv (\rho_s h_s \omega_s^2)^{-1} \oint \phi_N^2(\vec{y}_s)\ dy_s^2\ . \tag{57}$$

The surface integral of Eq. (57) has units of m^{-1} and is to within a numerical factor equal to 2/L where L is the water depth. Experience suggests[23,24] that the value of the fluid damping factor ζ for a welded steel structure of 0.045 is reasonable. For the Mark III containment, the value of ζ that will be used is set by regulatory guide.[25]

The volume flexibility is defined as the increase in the containment volume per unit of applied pressure and is thus simply given by $V\delta$. Two special cases are worth discussion: first, a right circular cylinderical tank with separate specific acoustic admittance functions for the circular wall and baseplate and, second, an annular tank with a single average specific acoustic admittance function. For the cylindrical tank, we assume that $\omega_s^2 >> (\omega_N^o)^2$. Starting with Eq. (48) and taking into account different flexibilities for the base plate and the cylindrical walls we obtain

$$\omega_N \cong \omega_N^o\ \{1 + 2\ \frac{\rho c^2}{\rho_s}\ (\frac{1/L}{h_b \omega_b^2} + \frac{1/a}{h_w \omega_w^2})\}^{-1/2}\ , \tag{58}$$

where h_b, ω_b is the baseplate thickness and eigenfrequency and h_w, ω_w is the wall thickness and eigenfrequency. For an annular tank assuming $\omega_s^2 >> (\omega_N^o)^2$ Eq. (55) reduces to

$$\omega_N \cong \omega_N^o\ (1 + \rho c^2 \delta)^{-1/2}\ . \tag{59}$$

This provides a simple way in which to estimate the consequence of FSI for Mark II and Mark III containments via the volume distensibility δ.

Note that the rigid wall eigenfrequencies ω_N^o area to first order shifted by a constant amount independent of frequency. The rigid wall fundamental frequency (N = 0) is given by $\omega_o^o = \pi c/2L$. Eq. (59) is thus tantamount to an apparent reduction in the sonic speed. That such reduction exists for acoustic signals traveling in flexible wall enclosures is well known.[26-30]

We have thus succeeded in obtaining a solution to the acoustic wave equation with flexible boundaries in terms of the specific acoustic admittance $\beta(\vec{x}_s|\omega)$. If the functional dependence of $\beta(\vec{x}_s|\omega)$ on frequency $\omega/2\pi$ and wall location $\vec{x}_s$ is known, we can completely determine the total pressure field which includes the effects of the fluid-structure interaction. The structural response would then be calculated using a structural model without the fluid ("dry containment") and applying the total pressure field to the boundary. All that is required is that $(\vec{x}_s|\omega)$ be small to permit a perturbation series expansion of Eq. (46). This is not an unreasonable expectation for containments with fairly stiff boundaries. In summary, we see that[31,32] the fluid-structure interaction effects are threefold:

(1) Reduction in the rigid wall eigenfrequencies ω_N^o shown by Eq. (45).

(2) Mixing of the rigid wall normal modes as shown by Eq. (46).

(3) Damping of the free vibrations of the standing waves as given in Eq. (50).

Two computer programs, IWEGS and IWEGS/MARS, have been written to evaluate the solution of Eq. (16) via Eqs. (33) through (35). IWEGS (Inhomogeneous Wave Equation Green's Function Solution) is used in cylinderical containments for source evaluation while IWEGS/MARS (Multivent Annular Solution) is used in annular geometries.

It is noteworthy to mention that this method of describing the response of a fluid in a cavity with flexible walls to a source or sources is that which has been used successfully by physicists and engineers active in the field of acoustics for over three decades.

4 VALIDATION OF THE ACOUSTIC CHUGGING MODEL

To verify that the acoustic fluid-structure interaction methodology correctly gives the flexible wall eigenfrequency ω_N, we shall compare the ω_N as computed from Eq. (48) with that computed by other methods and with experimental results:

4.1 EIGENFREQUENCY COMPARISON

(1) Consider a right circular cylindrical tank with rigid walls and a flexible base plate filled with water to a depth L as shown in Fig. 3. For low frequencies, the acoustic motion is in one dimension only and the fluid-structure problem is exactly soluble yielding the following expression for the coupled eigenfrequencies:[33]

$$\tan\left(\frac{\omega_N L}{c}\right) = \frac{\rho_s h_s}{\rho c}\left(\frac{\omega_s^2}{\omega_N} - \omega_N\right) , \tag{60}$$

where ρ_s is the density of the base plate, h_s the thickness, and ω_s the eigenfrequency with no fluid present. Table 1 compares the eigenfrequencies from Eqs. (55) and (60).

(2) In order to determine the coupled fluid-structure eigenfrequency of the test tank used in the Mark II Owners Group chugging program, the General Electric Company commissioned the Anamet 4T bell jar and impact tests.[34] The average coupled fundamental eigenfrequency (N = 0) for these tests was $\omega_o/2\pi$ = 33.4 ± 1.6 Hz. The average water depth was L = 6.25 m (20.5 ft). Using the observed base plate eigenfrequency ω_b = 1185.6 s^{-1} and assuming a water temperature of 18.3°C (65°F) for which the acoustic speed in air-free water at one atmosphere is c = 1478 m/s (4849 fps), Eq. (58) gives $\omega_o/2\pi$ = 34.0 Hz.

(3) The fundamental eigenfrequency in the 4T was calculated using the NASTRAN[35,36] computer program to be 23.8 ± 0.1 Hz. Since the 4T NASTRAN model had a "simply supported" base plate, ω_s = 674.1 s^{-1} and Eq. (58) gives $\omega_o/2\pi$ = 23.2 Hz (see Table 2).

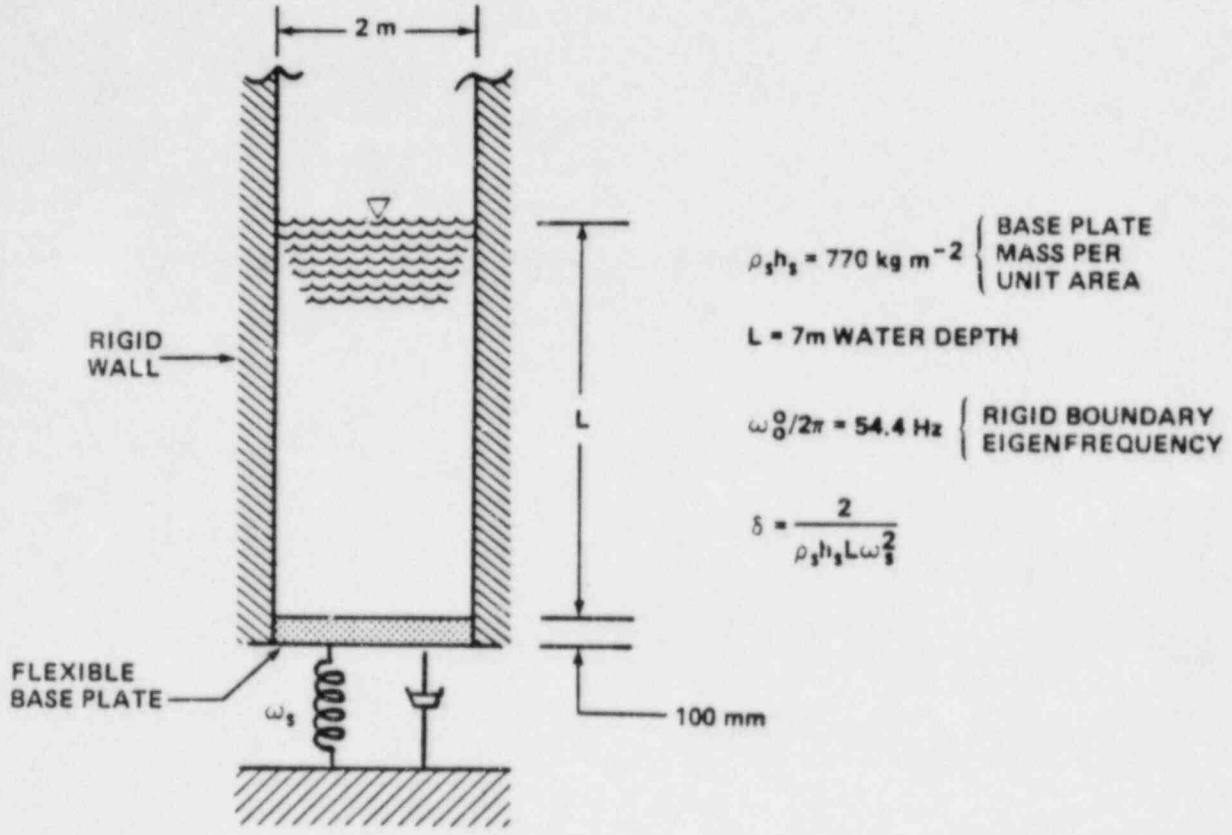

EIGENFREQUENCY ω_N COUPLED SOLUTION:

$$\text{TAN}\left(\frac{\omega_N L}{c}\right) = \frac{\rho_s h_s}{\rho c}\left\{\frac{\omega_s^2}{\omega_N} - \omega_N\right\}$$

FIRST-ORDER PERTURBATION:

$$\omega_N^4 - \left\{\left(\omega_N^o\right)^2 + \omega_s^2\left(1 + \rho c^2 \delta\right)\right\}\omega_N^2 + \left(\omega_N^o\right)^2 \omega_s^2 = 0$$

Figure 3 Eigenfrequency for a Cylindrical Containment With a Flexible Base

Table 1

COMPARISON OF COUPLED AND FIRST ORDER PERTURBATION SOLUTION EIGENFREQUENCIES FOR A CYLINDRICAL CONTAINMENT WITH VARIOUS BASE FLEXIBILITIES

Representation Containment	Flexibility $\rho c^2 \delta$	Eigenfrequency Coupled $\omega_N/2\pi$	Eigenfrequency Perturbation $\omega_N^*/2\pi$	Percent Error
GKM II-M	0.345	46.3	46.7	0.9
SSES/LGS (MK II)	0.673	40.7	41.6	2.2
RIVER BEND	0.705	40.3	41.2	2.2
PERRY	0.756	39.(	40.6	2.5
GKM I	1.12	35.4	36.7	3.7
JAERI	1.216	34.5	35.8	3.8
4T/4TCO	2.196	27.9	29.5	5.7
GRAND GULF	2.635	26.0	27.6	6.2
CLINTON	2.863	25.1	26.9	6.4

(4) To verify the first order perturbation solution for the fluid-structure interaction eigenfrequency for a Mark II type suppression pool, use of the NASTRAN computer program was again made. The NASTRAN model of the Limerick-Susquehanna containment used is shown in Fig. 4. The volume flexibility $V\delta$ of the containment was determined to be $V\delta = 1.061 \times 10^{-3}$ m^3/kPa (0.252 ft^3/psi). It was computed from the Mark II boundary pressures resulting from an actuation of the safety relief valves (SRV). This boundary pressure has its principal frequency in the range 7 through 12 Hz. This value for $V\delta$ is the sum of separate volume flexibilities for the basemat, wall, and pedestal. The volume of water is $V = 3504.8$ m^3. Thus, $\delta = 302.7 \times 10^{-12}$ m^2/N (2.09×10^{-6}/psi). The water density ρ and sonic speed c used in the NASTRAN model as 1000 kg/m^3 and 1036 m/s. The computed rigid wall fundamental frequency for a triangular impulse was $\omega_o^o/2 = 37$ Hz, while for flexible walls it was $\omega_o/2\pi = 32$ Hz. Using Eq. (55) $\omega_o/2\pi = 32.1$ Hz, which compares quite well with 32 Hz.

Thus, we conclude from these comparisons that the flexible wall solution of the acoustic wave equation is capable of predicting the eigenfrequency ω_o to within 6.5%.

4.2 MODE SHAPE COMPARISON

The verification of the assumption that $\beta(\omega,\vec{r}_s)$ is sufficiently uniform such that $\phi_N(\vec{r})$ is a good approximation to $\Psi_N(\omega,\vec{r})$ for the Nth vibrational mode is accomplished by comparing the mode shape of the pressure response obtained during the Anamet tests with that computed by the flexible-wall acoustic theory. This comparison can easily be affected using the acoustic transfer function $H(\vec{x}|\vec{x}_o\omega)$ in which $\Psi_N(\omega,\vec{r}) \equiv \phi_N(\vec{x})$:

$$H(\vec{x}|\vec{x}_o|\omega) = 4\pi c^2\rho \sum_N \phi_N^*(\vec{x}_o)\phi_N(\vec{x})[(\omega_N^2 + \lambda_N^2 - \omega^2)^2 - 4\omega^2\lambda_N^2]^{-1/2}\, e^{i\theta_N} \qquad (61)$$

with

$$\theta_N = \tan^{-1}[2\omega\lambda_N(\omega_N^2 + \lambda_N^2 - \omega^2)^{-1}] \; . \qquad (62)$$

Table 2

NOMINAL 4T STRUCTURE AND FLUID PROPERTIES USED IN THE VERIFICATION OF THE ACOUSTIC FLUID-STRUCTURE INTERACTION METHODOLOGY

a = 1.0668 m (3.5 ft) = tank radius

L = 7.0104 m (23 ft) = nominal water depth

= 6.2484 m (20.5 ft) = water depth for Anamet test

h_b = 101.6 mm (4 in) = base plate thickness

h_w = 15.875 mm (5/8 in) = wall thickness

ω_b = 1185.6 S^{-1} = base plate vibrational frequency *

= 1373.6 S^{-1} **

= 674.1 S^{-1} ***

ω_w = 4913.8 S^{-1} = wall vibration frequency

ρ_s = 7700 kgm^{-3} (470.7 lbm ft^{-3}) = steel density

Y = 195 GPa (28.3 Mpsi) = steel eleastic modulus

μ = 0.28 = Poisson's ratio for steel

ρ = 1000 kgm^{-3} (62.4 lbm ft^{-3}) = water density

c = 1036 m/s (3400 fps) = acoustic speed

---

* Observed in Anamet 4T FSI study

** $\omega_b = \frac{1}{a}\left[\frac{Y}{\rho_s}(1-\mu^2)^{-1}\right]^{1/2}$ (clamped plate)

*** $\omega_b = (4.99)\frac{h_b}{a^2}\left[\frac{Y}{12\rho_s}(1-\mu^2)^{-1}\right]^{1/2}$ (simply supported plate)

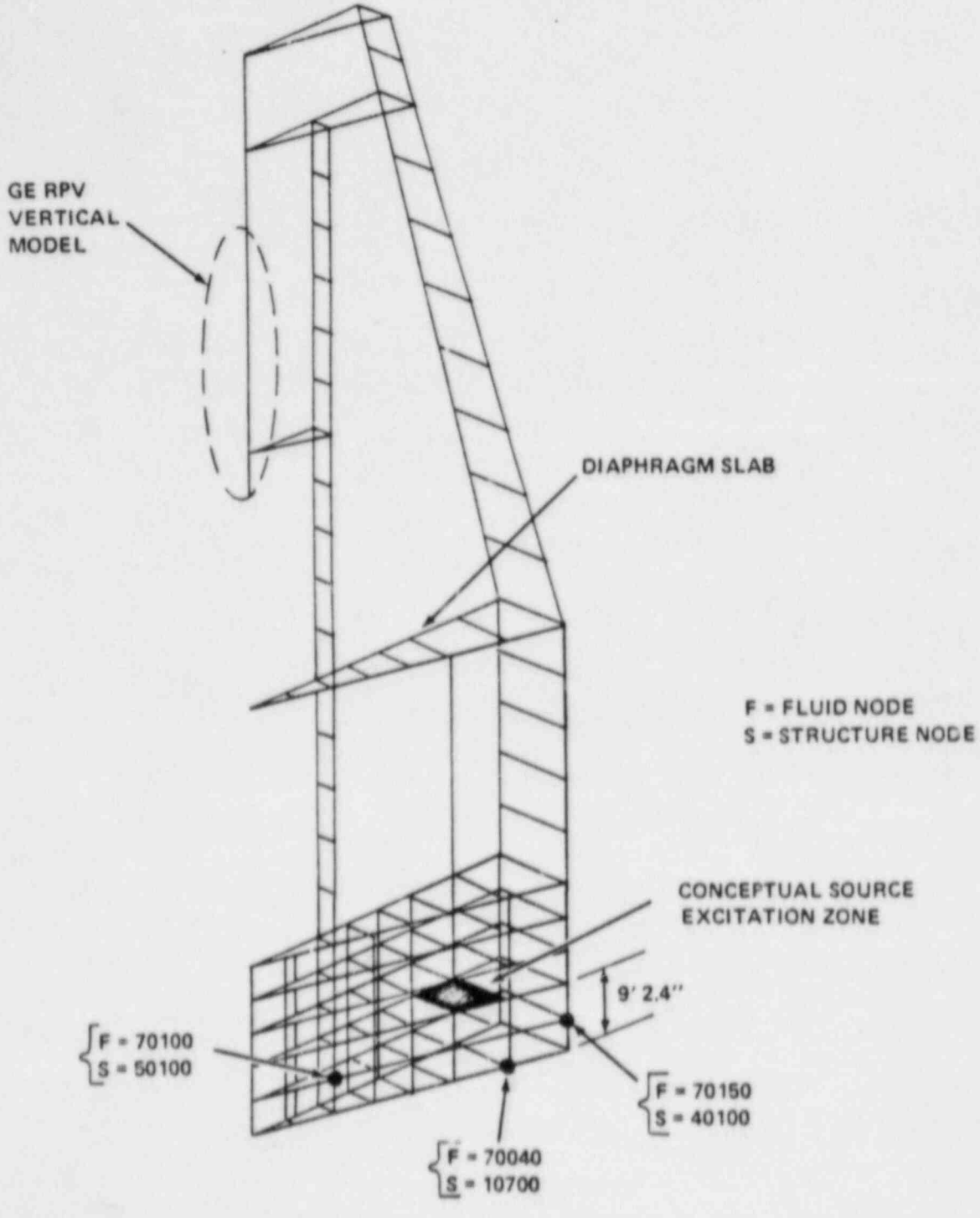

Figure 4 Mark II Soil-Interacted Fluid-Interacted RPV-Associated Containment NASTRAN Model

G1004058-04

The solution of Eq. (36), subject to the boundary condition of Eq. (37), yields for the rigid boundary cylindrical containment eigenfunctions

$$\phi_N(\vec{x}) \equiv \phi_{\ell mn}(r,\theta,z) = A_{\ell mn}\, J_m(\pi\alpha_{mn}\frac{r}{a}) \begin{matrix}\sin\\ \cos\end{matrix} (m\theta)\, \cos\left[(\ell+\tfrac{1}{2})\tfrac{\pi}{L}\, z\right] , \qquad (63)$$

where the normalization constant $A_{\ell mn}$ is determined from the condition $\langle\phi_N|\phi_N\rangle = 1$ and is given by

$$A_{\ell mn} = \{\frac{\pi a^2 L}{4}\}\,(1+\delta_{om})\,[1-(\frac{m}{\pi\alpha_{mn}})^2]\,J_m^2\,(\pi\alpha_{mn})\}^{1/2} . \qquad (64)$$

The eigenvalue α_{mn} is defined by the boundary condition $J_m'(\pi\alpha_{mn}) = 0$, where the prime indicates the derivative of J_m with respect to its argument.

Upon inspection of Eq. (33), it is immediately obvious that $H(\vec{x}|\vec{x}_o|\omega) = \rho G_\phi(\vec{x}|\vec{x}_o|\omega)$ for the case where $\Psi_N = \phi_N$.

To demonstrate the effect of fluid-structure interaction, we compare $H(\vec{x}|\vec{x}_o|\omega)$ in Fig. 5 for both a rigid wall and flexible wall 4T. The flexible wall case corresponds to a sonic speed c = 701 m/s and a fluid damping factor $\zeta = 0.045$. Note that an effect of wall flexibility is to <u>increase</u> the spectral density of the pressure in some frequency ranges. We also see that the 4T responds ("rings out") primarily in the fundamental mode N = 0 for an impulsive source. Thus, under our assumption that $\beta(\omega,\vec{r}_s)$ is uniform, the fundamental mode is described by $\Psi_o(\vec{r})$ $\phi_o(\vec{r})$ and depends on z as $\cos(\pi z/2L)$ as is seen from Eq. (63). The comparison between the mode shape obtained from the Anamet test results and $\cos(\pi z/2L)$ is shown in Fig. 6.

We have thus been able to solve the acoustic wave equation in geometries with flexible walls. It is significant that these solutions are no more complex than the rigid wall solutions provided certain assumptions hold. These assumptions circumscribe the fluid-structure interaction which is described by the specific acoustic admittance $\beta(\vec{x}_s|\omega)$ or, equivalently, by δ and ζ. Specifically:

(1) $\beta(\vec{x}_s|\omega)$ must be sufficiently small that Eqs. (47) and (48) are valid;

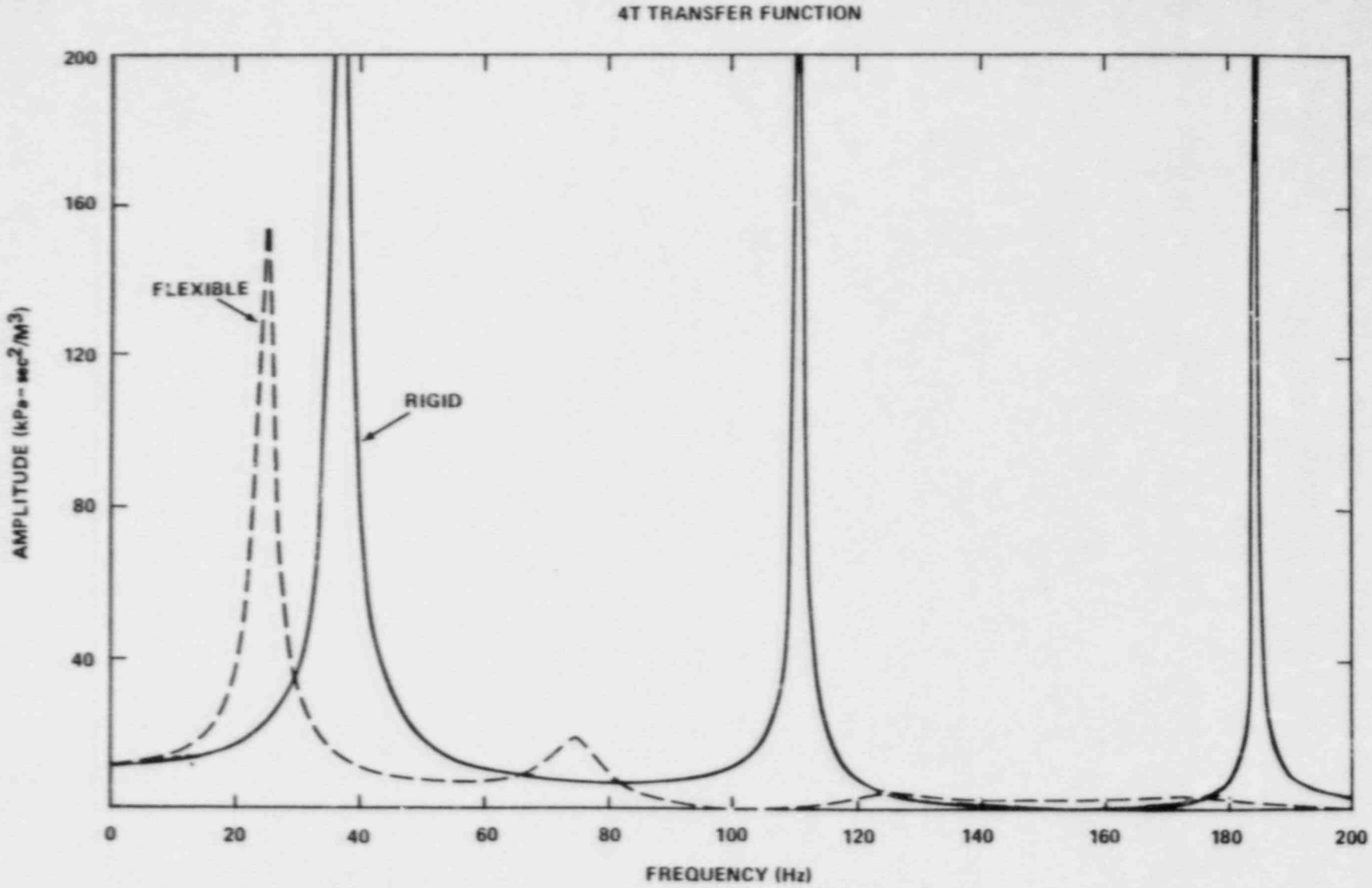

Figure 5 Transfer Function $H(\vec{x}\,|\,\vec{x}_o|\omega)$ at Bottom-Center in 4T

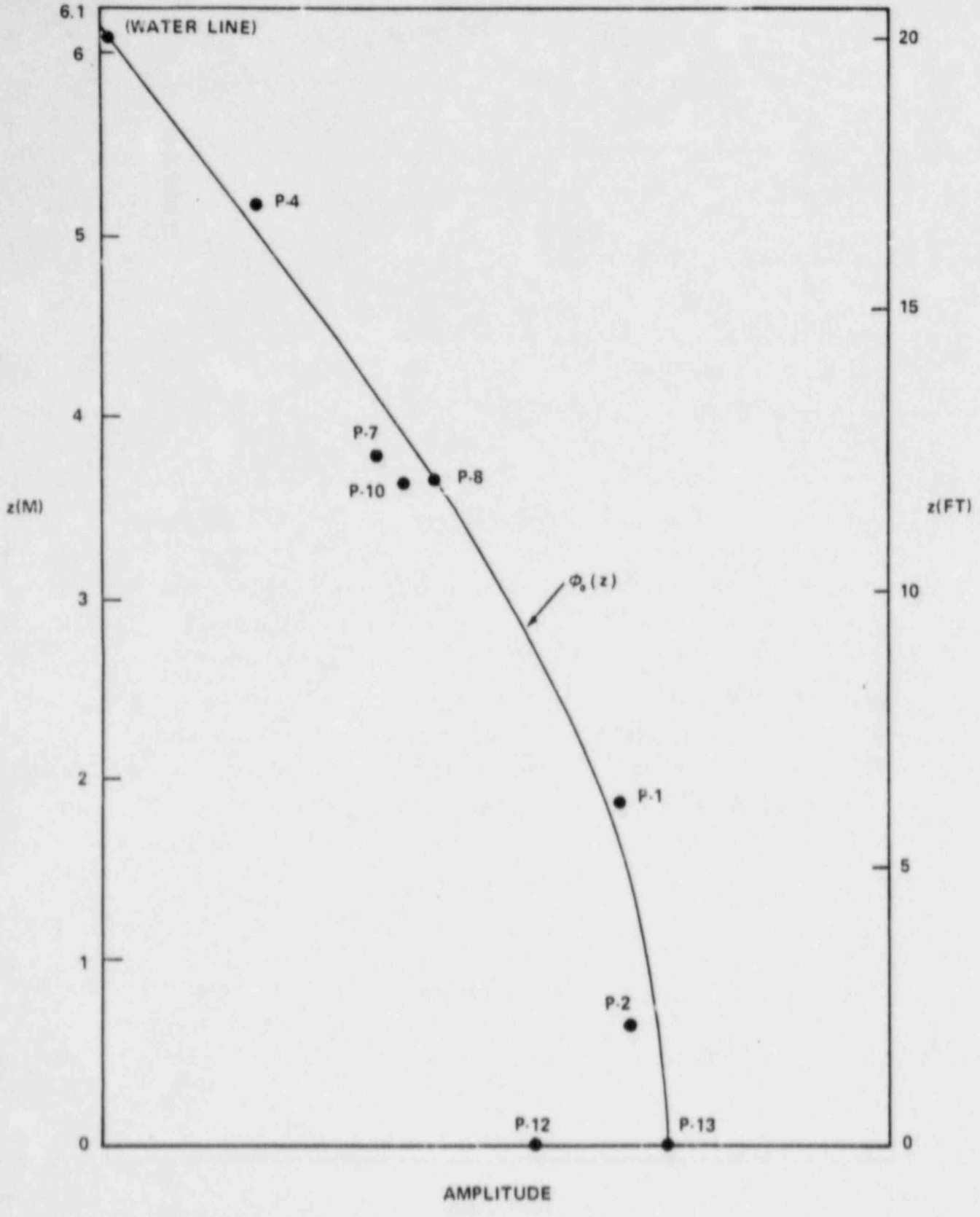

Figure 6 Normalized Mode Shape for 30 Hz as Estimated from Anamet Bottle Test No. 1 as a Function of Elevation. The Points P-1 Through P-12 Are the RMS Pressure Amplitudes at Various Locations in the 4T.

G1004058-06

(2) $\beta(\vec{x}_s|\omega)$ must be sufficiently uniform that the surface integral of Eq. (47) may be neglected so that $\Psi(\vec{x}|\omega) \cong \phi_N(\vec{r})$;

(3) the boundary must be locally reactive with an acoustic admittance given by Eq. (51).

4.3 PRESSURE RESPONSE COMPARISON

Essentially, we have reduced the description of the fluid-structure interaction to specification of the parameters δ and ζ which control the shift in eigenfrequency and the amount of damping. To provide further verification of this method of treating fluid-structure interaction, we compare the predictions of flexible wall acoustic theory with the results of a flexible wall NASTRAN calculation for our 4T model. Both IWEGS and NASTRAN used the same chug source shown in Table 3. For use in the NASTRAN computer program, however, the source had to be converted from a volume acceleration to a linear acceleration. This conversion was accomplished by a multiplication constant which was obtained by requiring the peak pressures calculated by IWEGS and NASTRAN to agree in a rigid wall 4T. The speed of sound was chosen to be c = 1036 m/s (3400 fps). Values for the various constants for the 4T geometry are found in Table 2. Since the NASTRAN model treats the base plate as simply supported, we set $\omega_b = 647.1^{-1}$. NASTRAN used a structural damping of 0.045 which was manifest as a fluid damping factor of $\zeta = 0.03$. The comparison of the IWEGS and NASTRAN results is shown in Fig. 7.

To conclude this section, we show in Figs. 8 through 12 some examples of the ability of the acoustic methodology to adequately represent both chugging and condensation oscillation events by comparison with 4T chugging test data.

Table 3

CHUGGING SOURCE PARAMETERS (GE125) USED IN COMPARISON OF IWEGS AND NASTRAN IN 4T

$$S(t) = - A_o \Lambda\left(\frac{2t}{\tau} - 1\right) + \sum_{i=1} A_i \sin(\omega_i t)$$

i	A_i (m^3/s^2)*	$\omega_i/2\pi$ (H_z)
0	5.2	(τ = 36 ms)
1	0.73	5.0
2	0.43	12.6
3	0.13	20.9
4	0.10	28.7
5	0.23	39.1
6	0.48	45.6
7	1.30	56.1
8	0.29	63.9

* To convert the source strengths A_i which are in terms of volume accelerations (m^3/s^2) to linear accelerations (in/s^2) suitable for NASTRAN $A_i \rightarrow (16760)A_i$

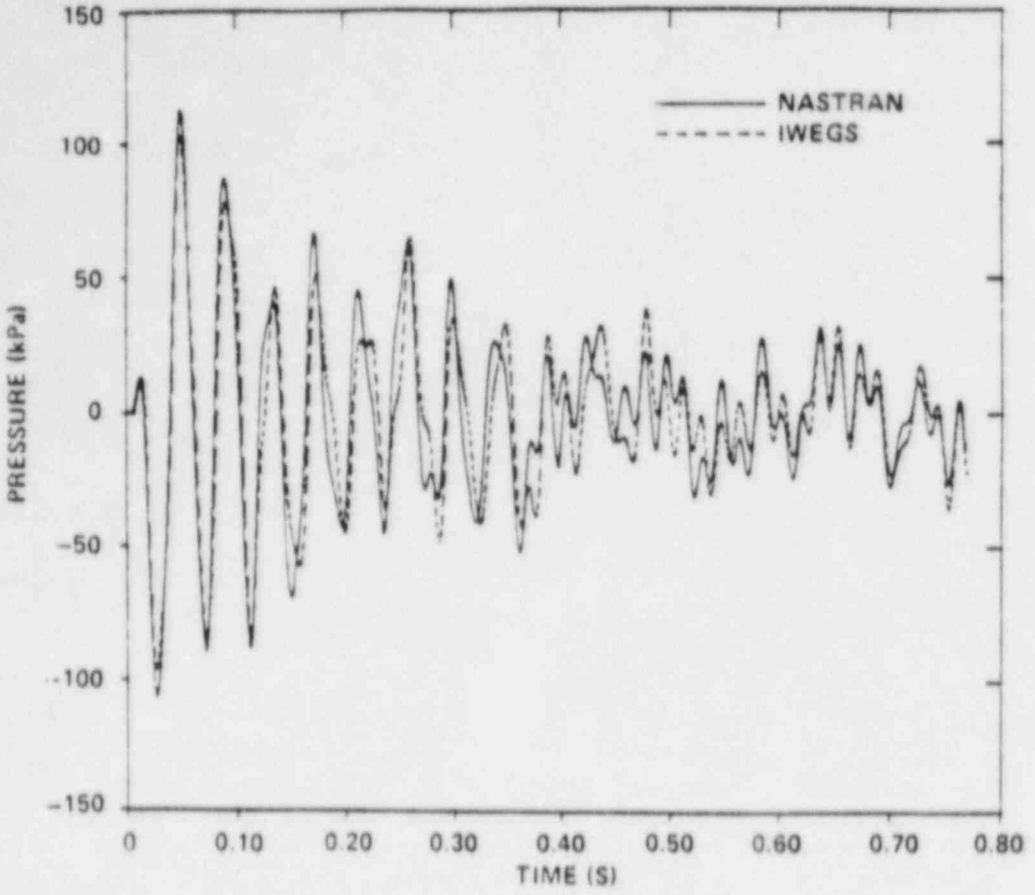

(a) PRESSURE

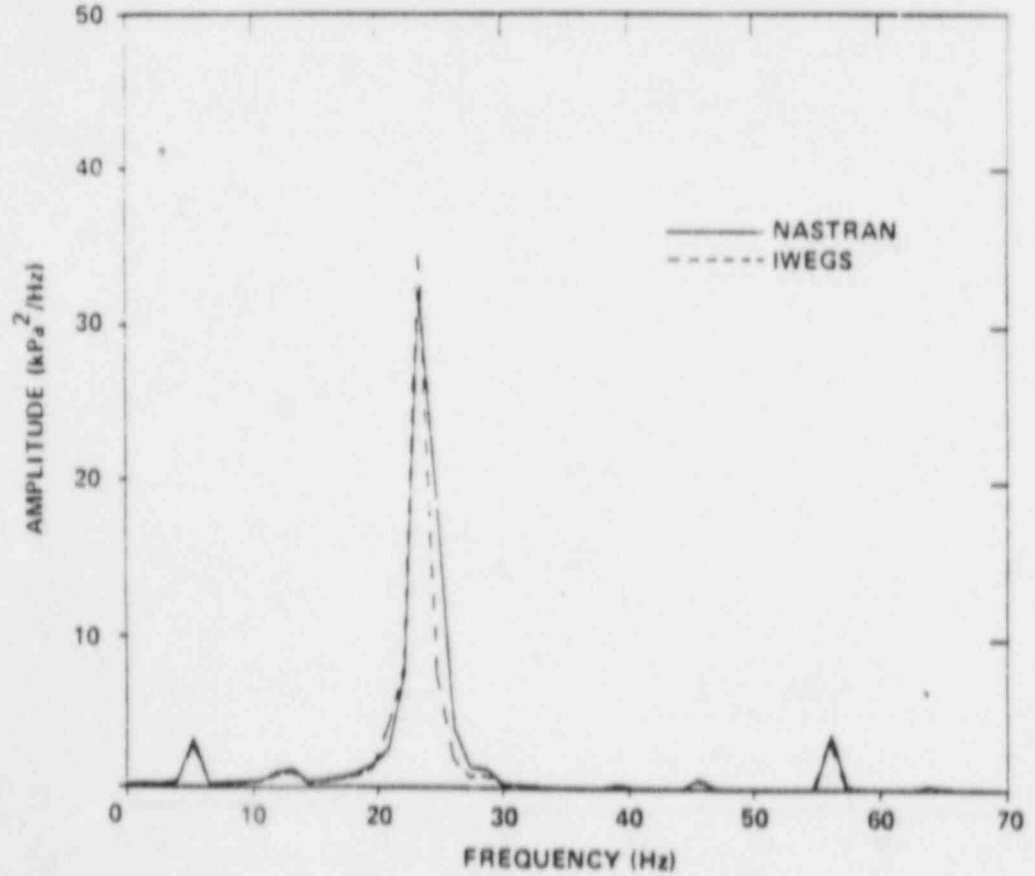

(b) SPECTRAL DENSITY

Figure 7 Comparison of IWEGS and NASTRAN in a Flexible Wall 4T

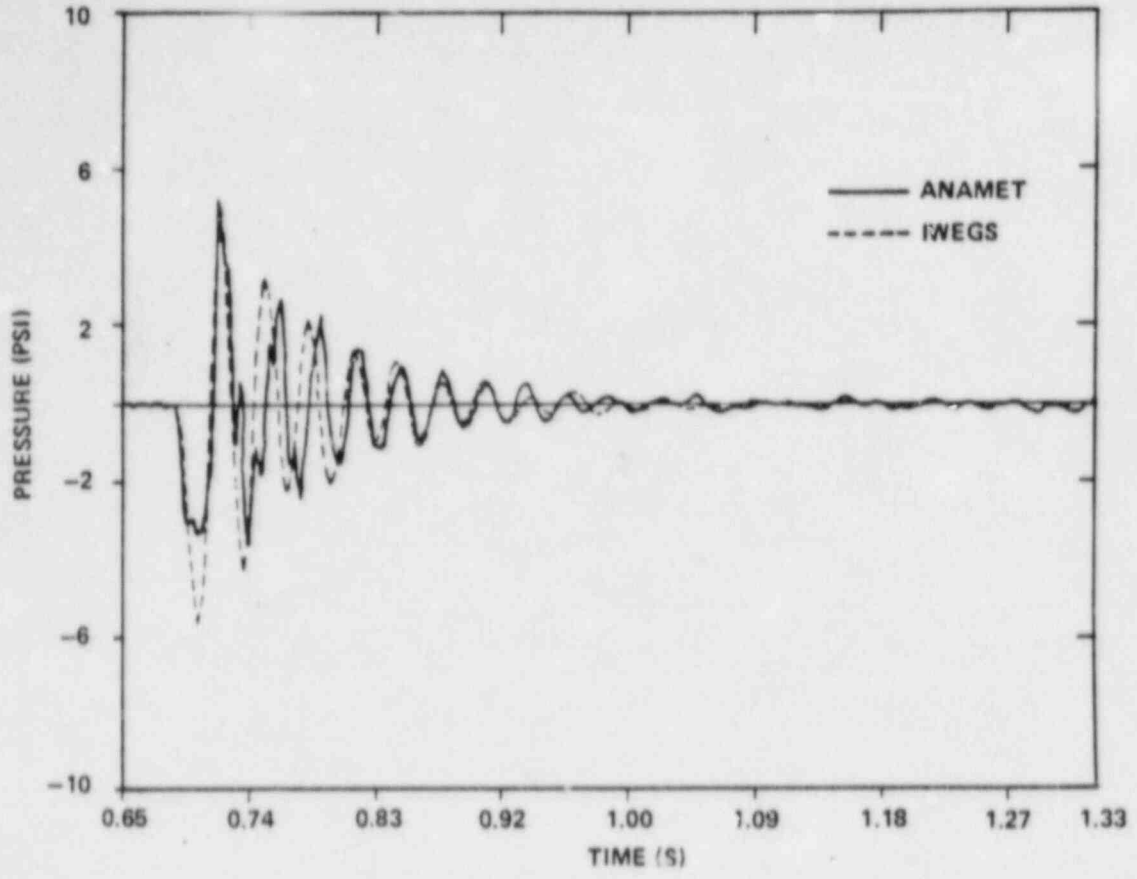

(a) PRESSURE TIME-HISTORIES

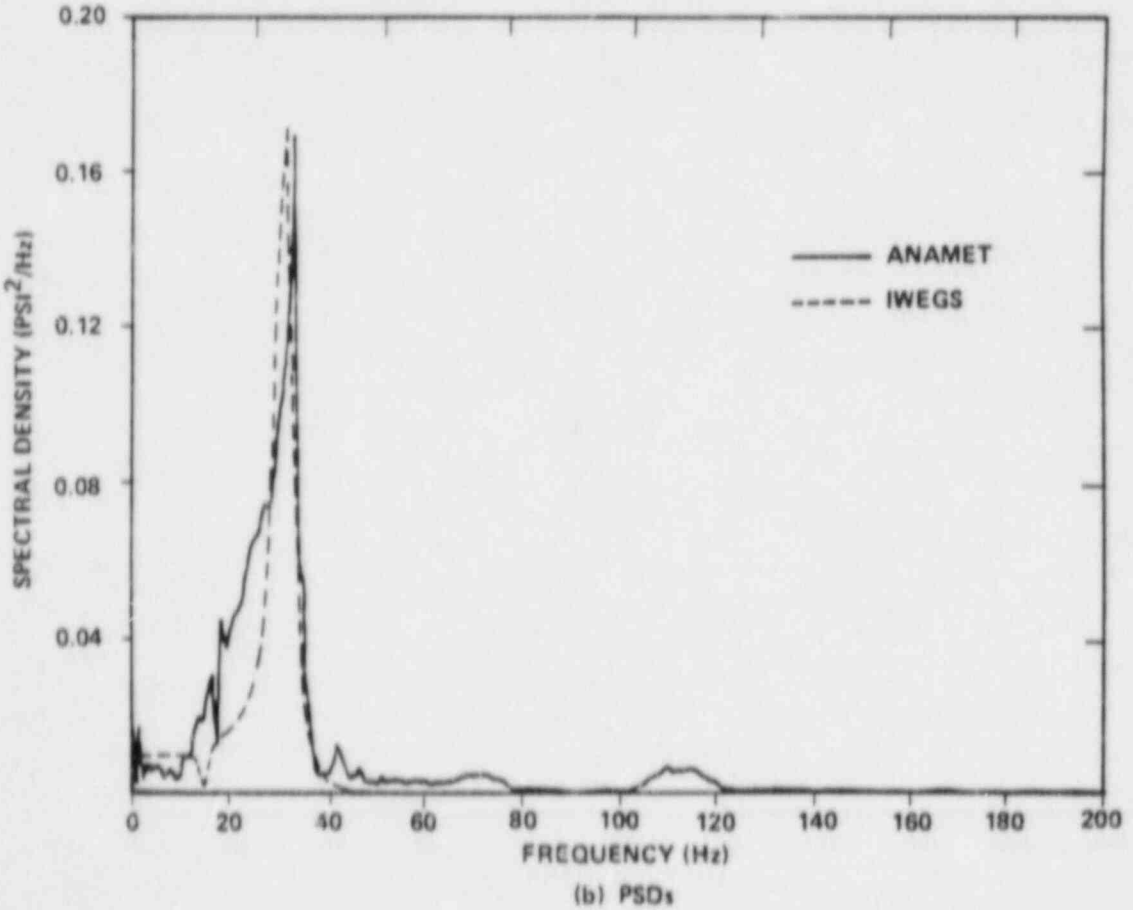

(b) PSDs

Figure 8 Comparison With Anamet Bell Jar Test No. 8

G1004058-08

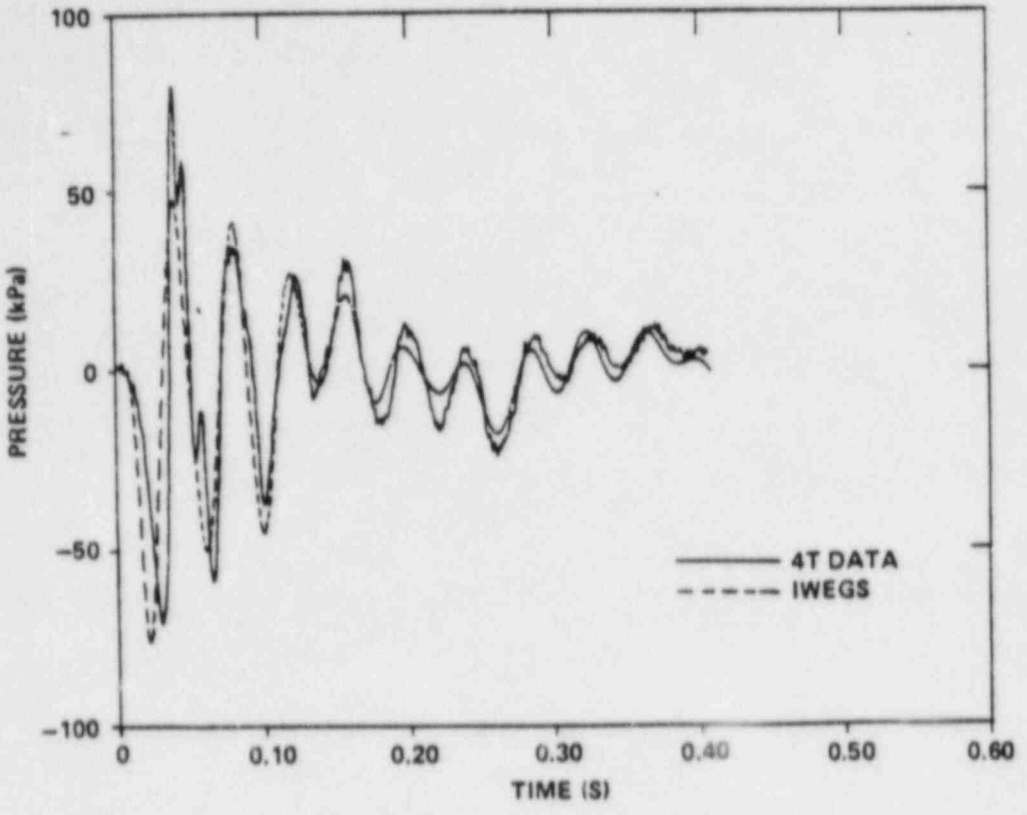

(a) PRESSURE TIME-HISTORIES

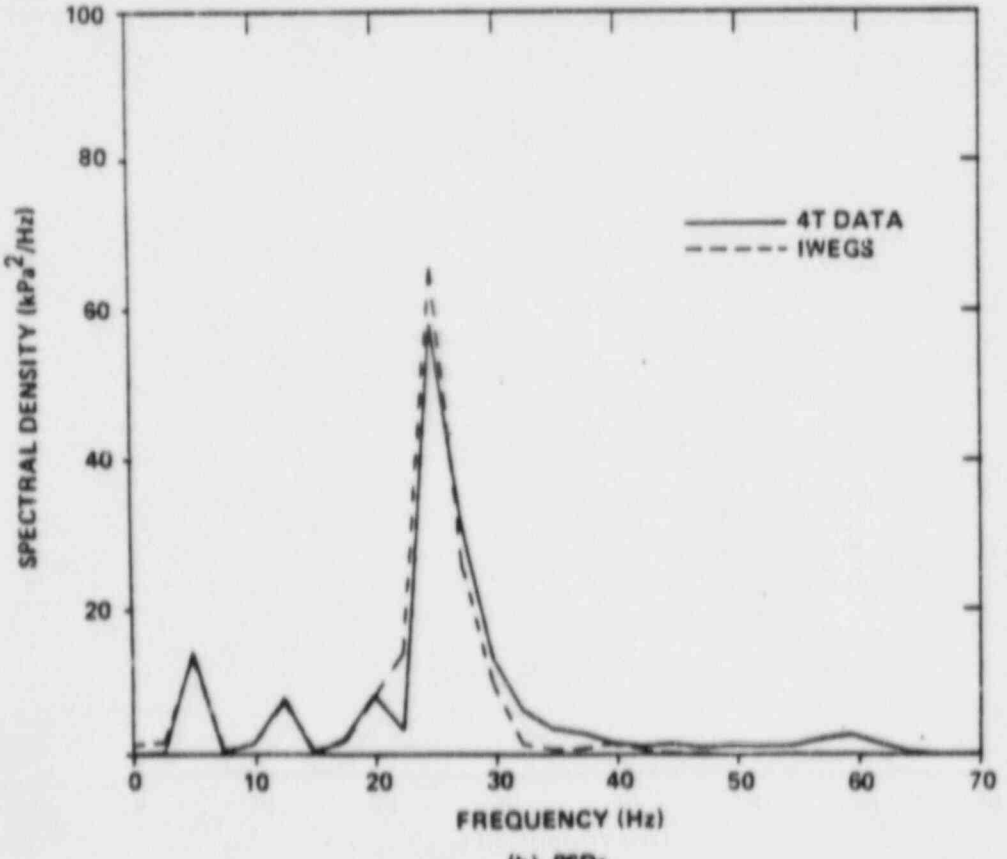

(b) PSDs

Figure 9 Comparison With Data — Chug #30

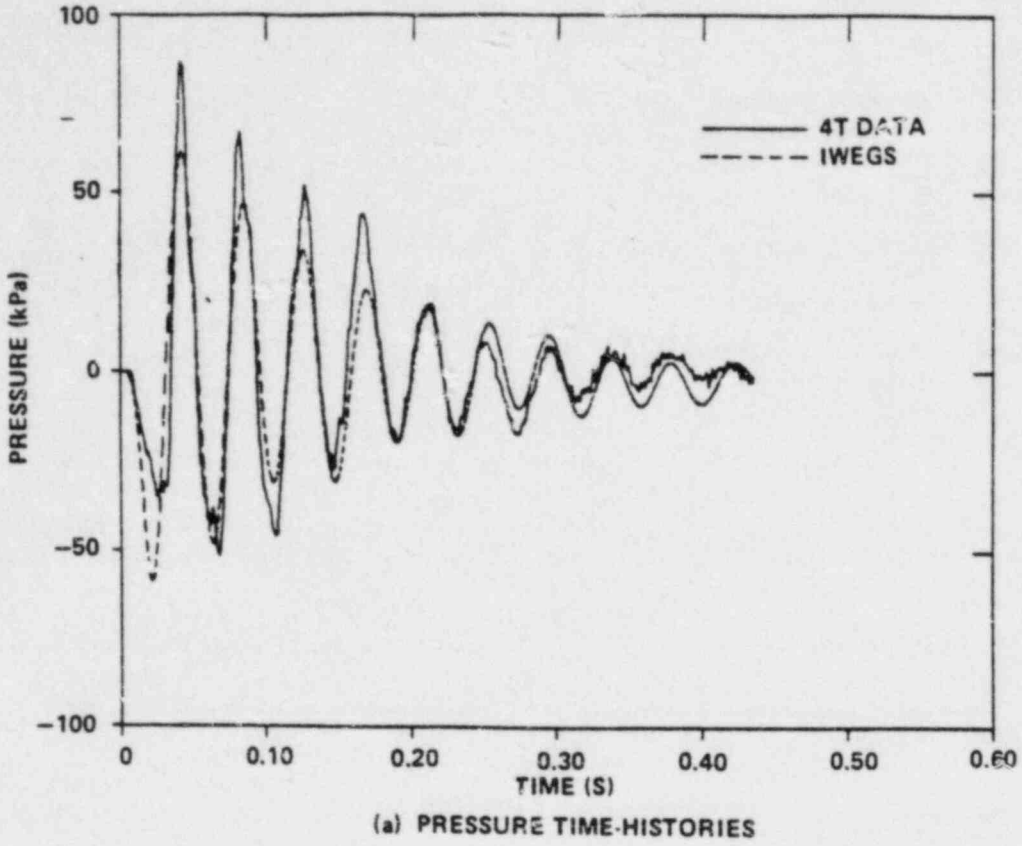

(a) PRESSURE TIME-HISTORIES

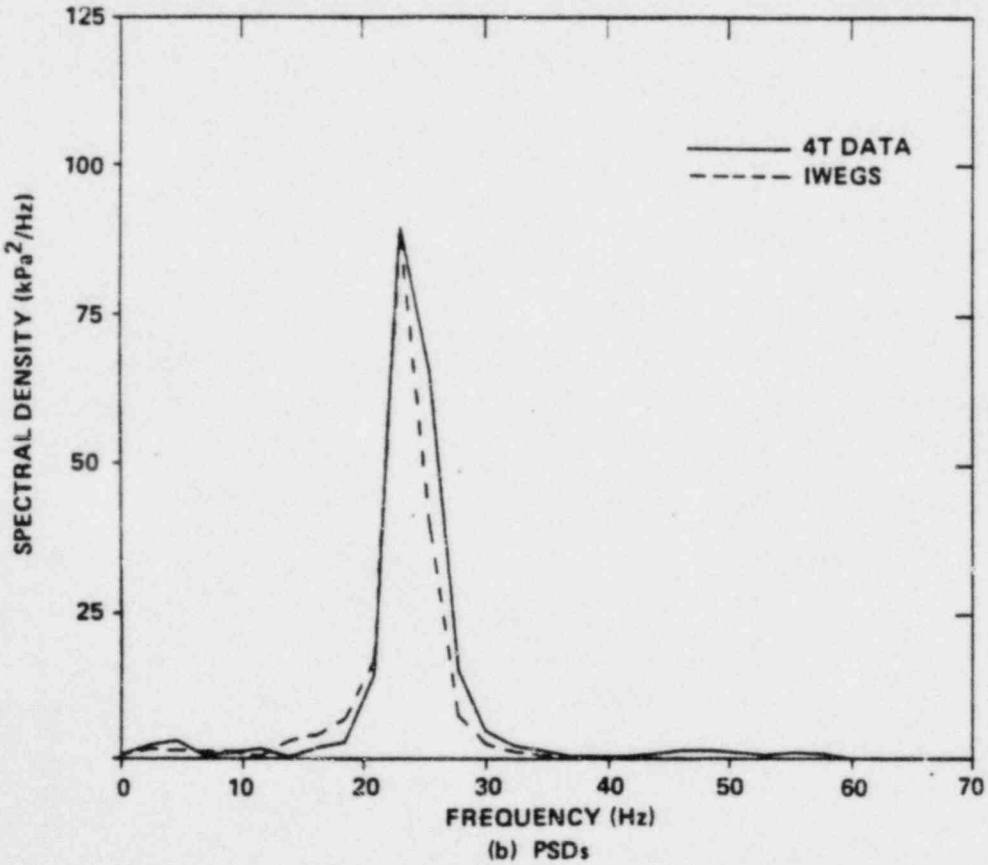

(b) PSDs

Figure 10 Comparison With Data — Chug #71

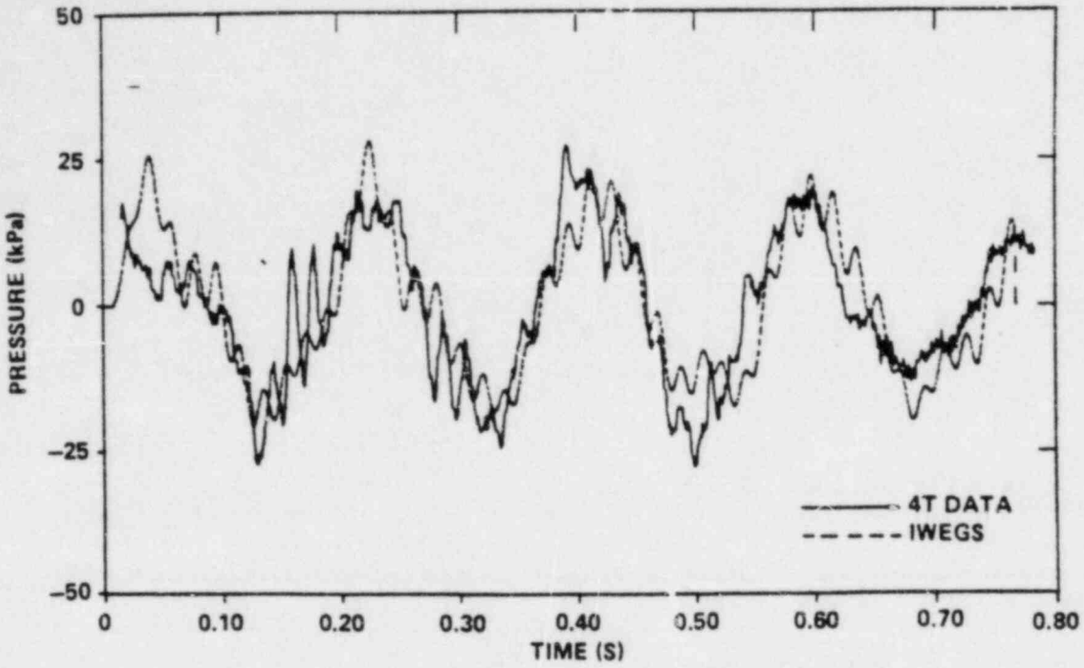

(a) PRESSURE TIME-HISTORIES

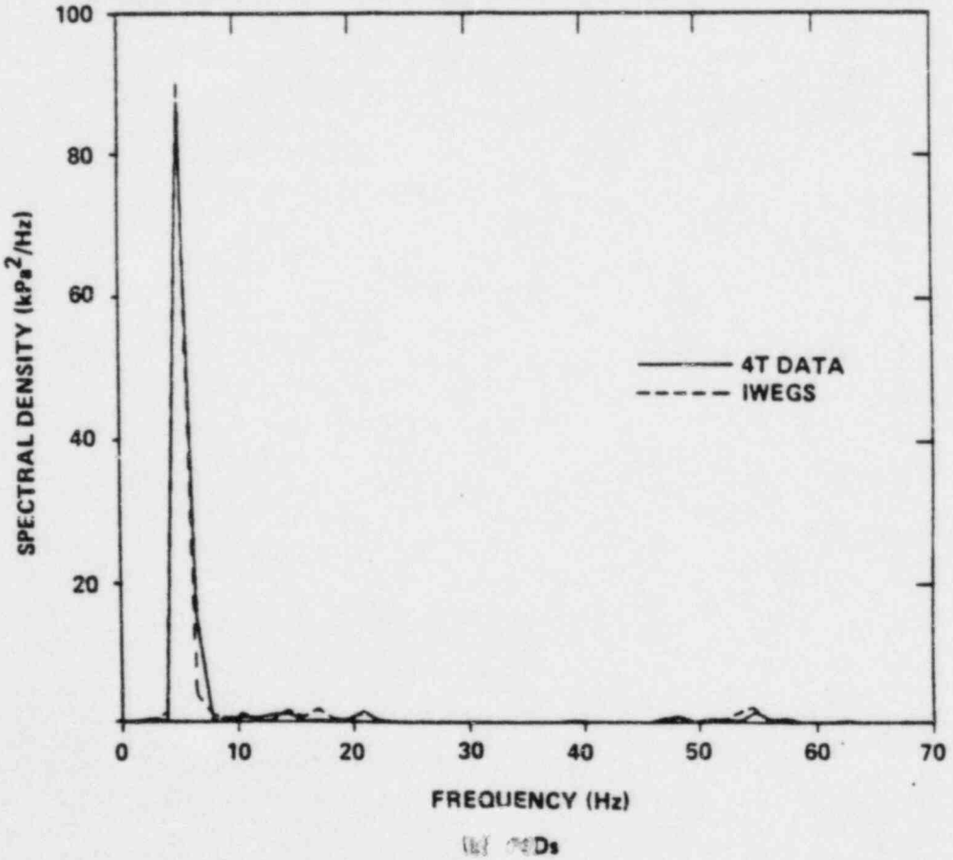

(b) PSDs

Figure 11 Comparison With Data — Chug #11

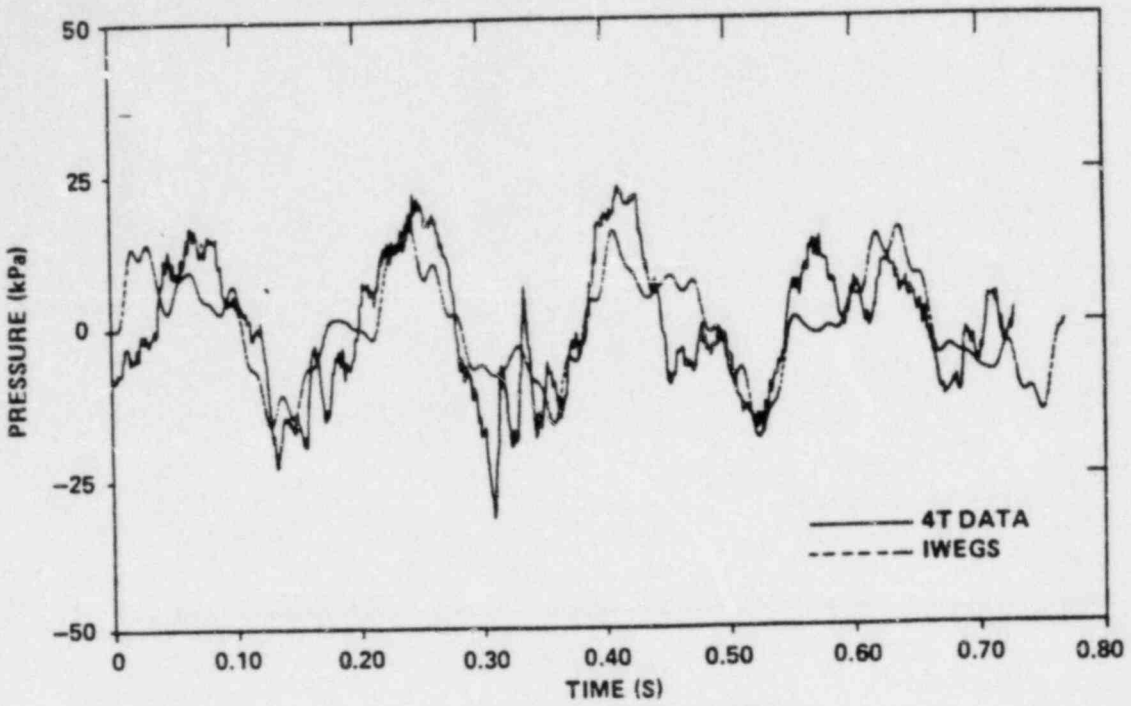

(a) PRESSURE TIME-HISTORIES

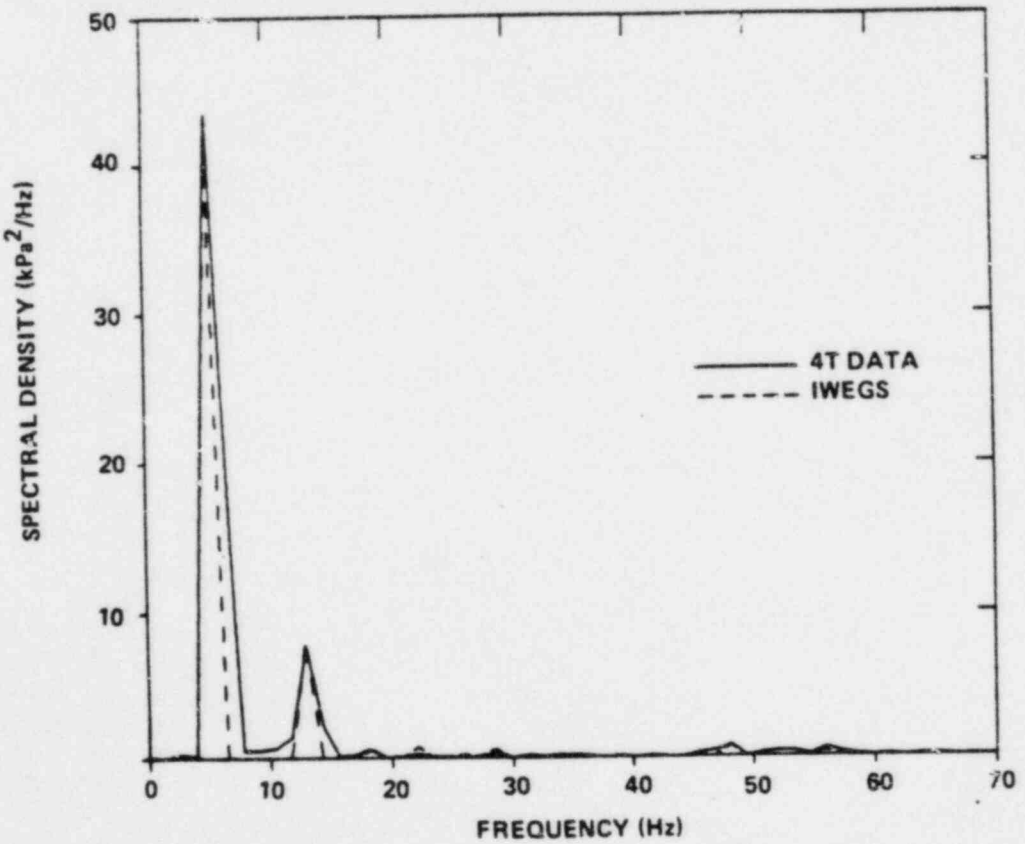

(b) PSDs

Figure 12 Comparison With Data — Chug #57

5 MARK III ASSESSMENT FOR RHR CONDENSATION OSCILLATION

In the previous section the acoustic methodology for unstable condensation (chugging and/or condensation oscillation) in containments with flexible boundaries was described in some detail. Also, it was demonstrated that this methodology is capable of generating pressure responses that compare quite well with experimental data. In this section the CIOG Mark III containments will be assessed for the effects of RHR induced condensation oscillation. This assessment will be made as follows. First, a pressure trace will be selected from some relevant test data and an RHR condensation oscillation source will be extracted. This source will then be used to compute pressures at the containment boundary as well as forces on the submerged structure closest to the RHR discharge point. These boundary pressures and submerged structure forces will be compared with those resulting from safety relief valve discharge (SRV).

The Mark III design was used for the containments of the Grand Gulf Nuclear Station (GGNS), Perry Nuclear Power Plant (PNPP), River Bend Station (RBS), and the Clinton Power Station (CPS). A typical Mark III containment (GGNS) is shown in Fig. 13.

In Table 4 a comparison is made among the CIOG member containment geometries, RHR mass fluxes, and boundary flexibilities. Although the containment geometries and mass fluxes are similar, the boundary flexibilities are dissimilar. Hence we shall conduct a unique assessment for each CIOG member containments. From the results, conclusions will be drawn for the CIOG as a whole. In addition, a submerged structure load on a cylindrical object will be computed for each CIOG member containment.

5.1 RHR CONDENSATION OSCILLATION SOURCE

As explained above, the generation of a source function S(t) due to unstable condensation resulting from RHR steam discharge into the Mark III suppression pool is best done empirically. Therefore, it is necessary to have some pressure response data in a known geometry that is believed to be representative of the actual RHR source expected to occur in a Mark III

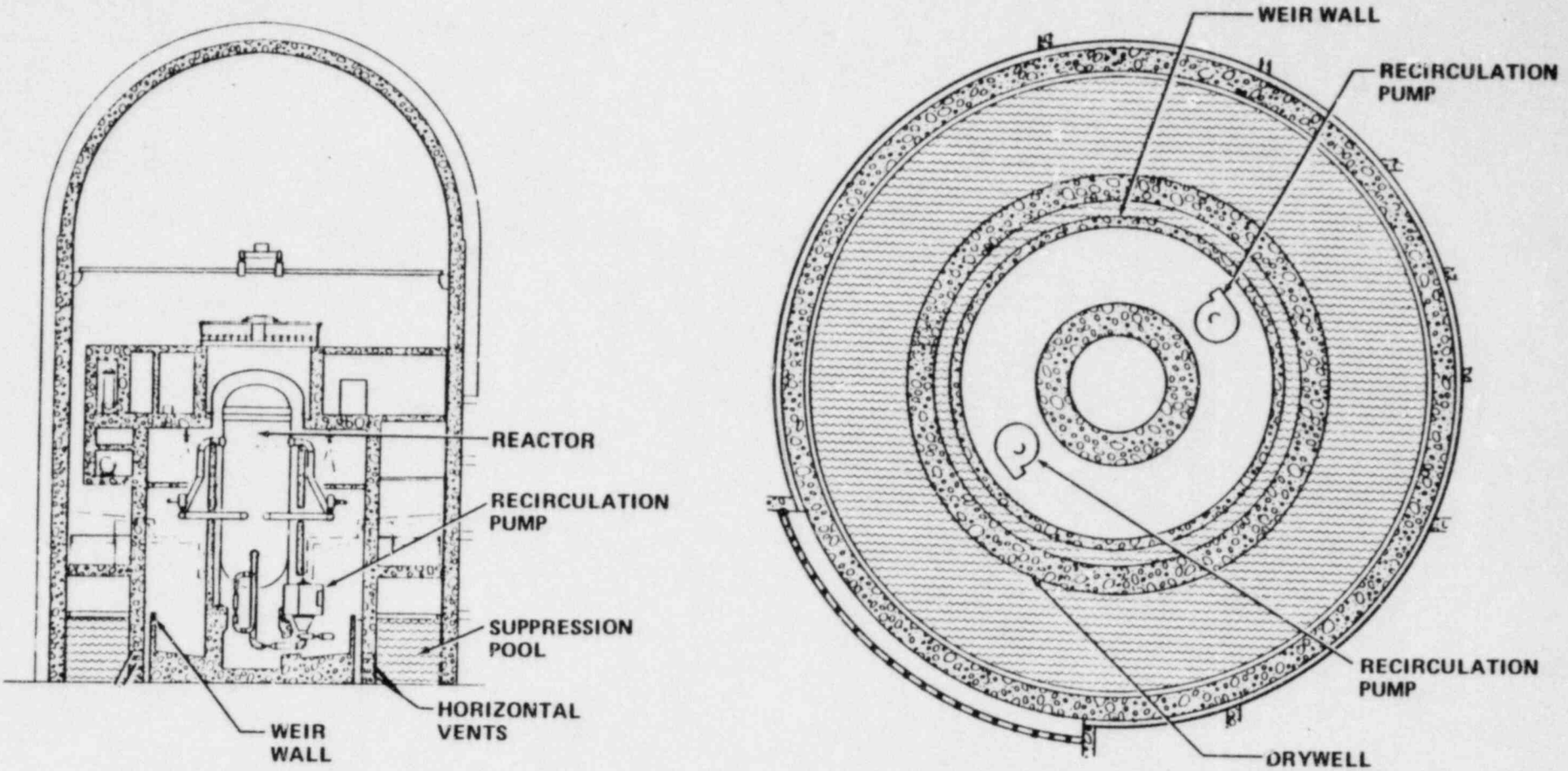

Figure 13 Typical Mark III Containment

G1004058-13

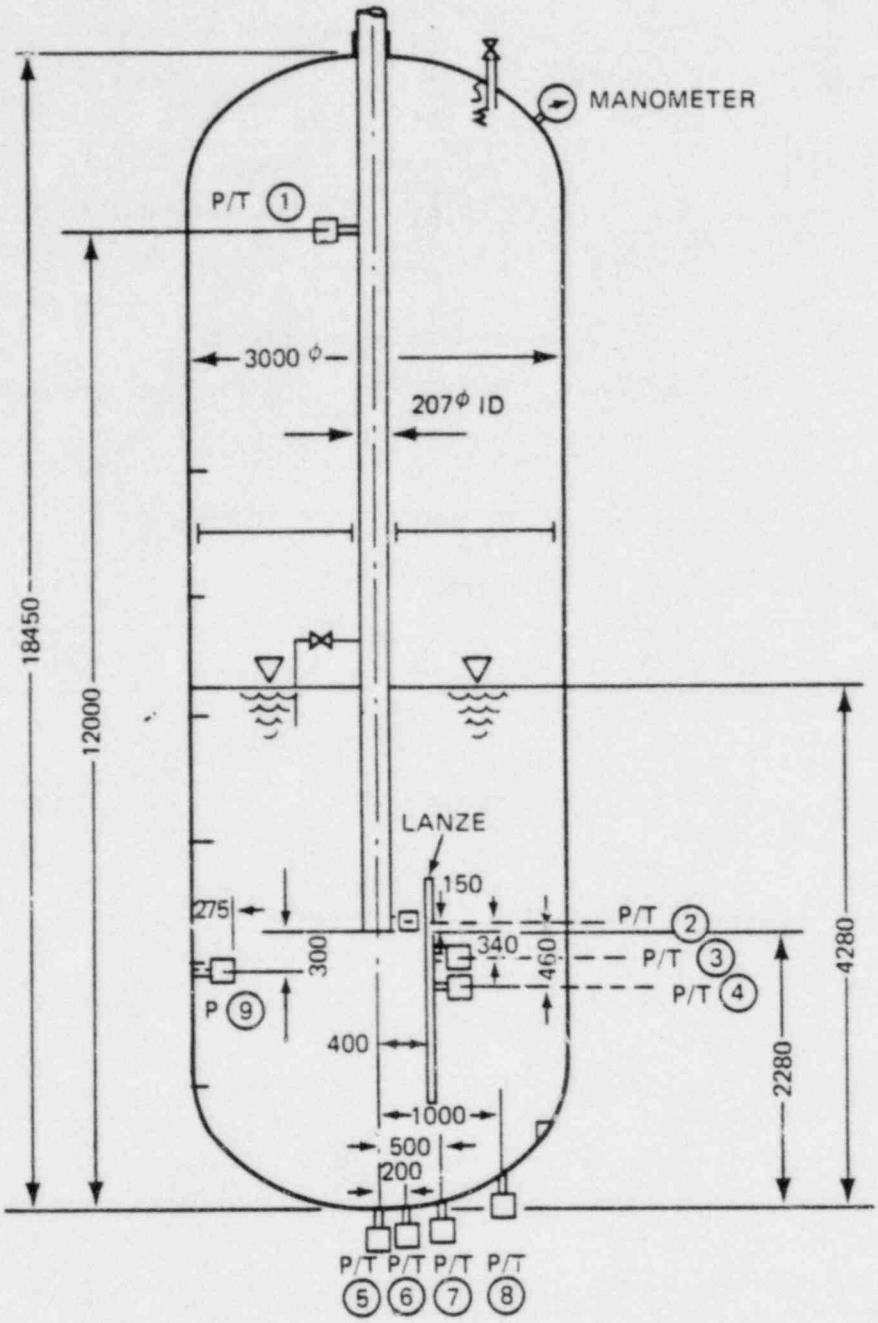

Figure 14 RHR CC Test Facility Schematic Showing Pressure Measurement Locations (all dimensions are in mm)

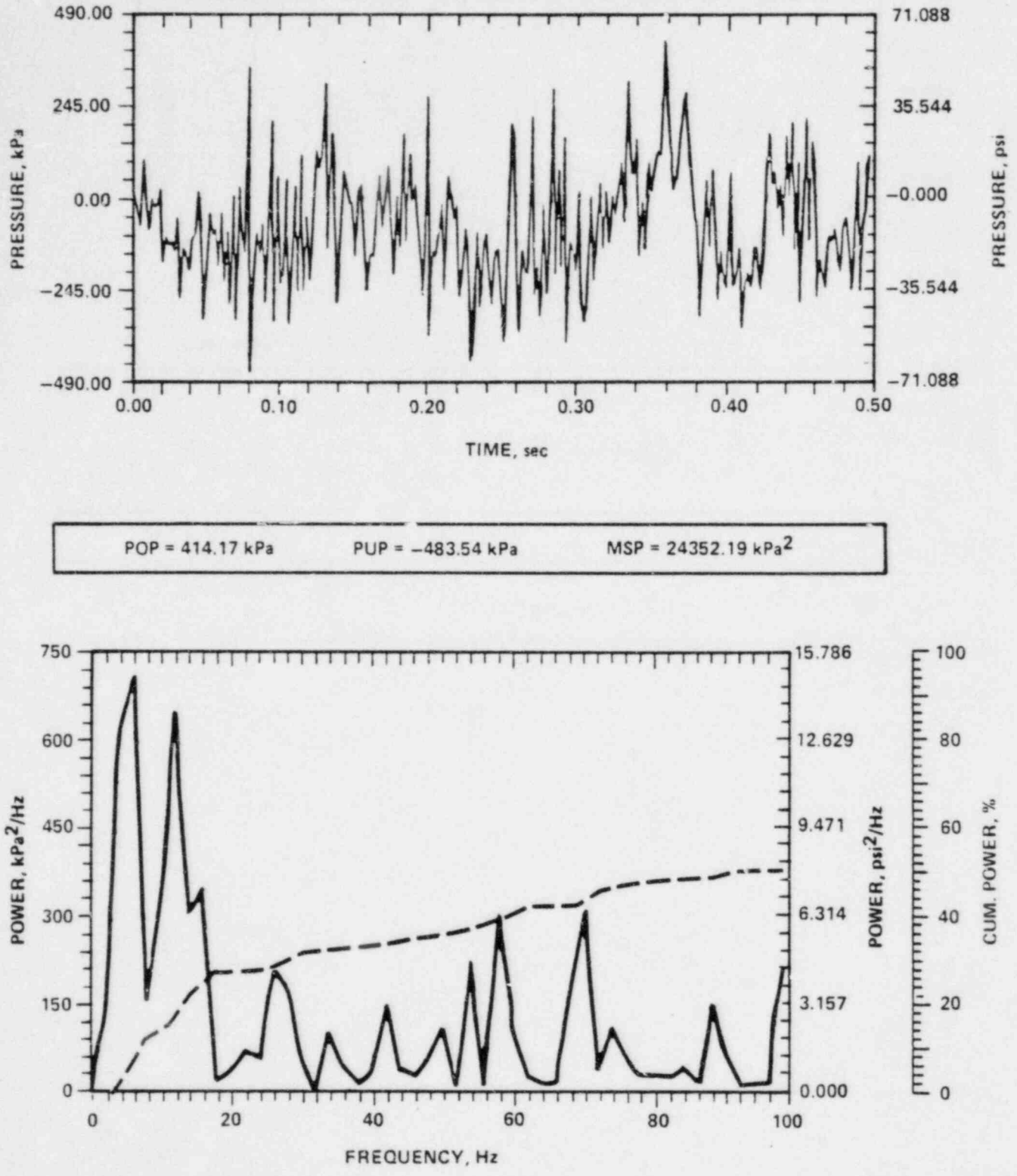

Figure 15 RHR Condensation Oscillation
Selected Pressure Trace Provided to Bechtel
by General Electric

Table 4

COMPARISON OF CIOG MARK III PARAMETERS
FOR RHR CONDENSATION OSCILLATION

	Suppression Pool Geometry			RHR Mass Flux	Distance To Closest Submerged Structure	Containment Flexibility
	a (ft)	b (ft)	L (ft)	(lbm/ft^2-s)	(in.)	$\rho c^2 w$
Grand Gulf	62	41.5	18.833	140	39.6	2.635
Perry	60	41.5	18.500	190	12	0.756
River Bend	60	39.5	20.000	92	60	0.705
Clinton	62	39.500	19.417	198	43.4	2.863

suppression pool. To this end, the General Electric Company examined test data from some steam condensation experiments conducted by their overseas licensee. These experiments were performed in a cylindrical tank shown schematically in Fig. 14. From the resulting pressure responses from these experiments, General Electric selected one that was considered to be representative of an actual RHR source. This determination was primarily based on the value of the RHR steam mass flux. The selected pressure time-history was measured by sensor P/T5 which is located at the bottom center of the test tank $\vec{x}_5 = (0,0,0)$. This pressure trace was normalized to a maximum positive pressure of 413.7 kPa (60 psid). This maximum positive pressure was the largest value observed in the tests for a bulk pool temperature corresponding to that expected in Mark III. Information concerning the source pressure trace was transmitted to the Bechtel Power Corporation for Mark III assessment and is contained in Appendix A. This pressure time-history and its power spectral density (PSD) is shown in Fig. 15.

Given the selected pressure trace $p(\vec{x}_5,t)$ and the test tank geometry, the source function $S(t)$ is extracted. First it is necessary to create a transfer function $H(\vec{x}_5|\vec{x}_o|\omega)$ for the test tank. From Fig. 14, it is seen that the tank geometry is almost right circular cylindrical. Approximating the tank geometry by a right circular cylinder will not only facilitate the computations but will yield a conservative source strength (magnitude). That such is the case can be seen as follows. The volume of a right circular cylindrical tank with the same radius a and maximum water depth L will be greater than the actual test tank. Since the transfer function is proportional to the inverse of the volume, the approximation of the test tank by a right circular cylinder will yield a greater source strength. Although the hemispherical bottom of the test tank will contribute different eigenfrequencies than that for a right circular cylinder, the values of these eigenfrequencies are in excess of 100 Hz. Thus, this difference in geometry will not have a noticeable effect on the frequency content of the source generated using a right circular cylinder. Hence, the transfer function $H(\vec{x}_5|\vec{x}_o|\omega)$ will be constructed assuming a right circular cylinder. The flexibility $\rho c^2 \delta$ was estimated to be 1.12 for the test tank.

Next, the source pressure time-history $p(\vec{x}_5,t)$ shown in Fig. 15 is transformed to the frequency domain, becoming $p(\vec{x}_5|\omega)$. The corresponding source function $S(\vec{x}_o,\omega)$, which is at location $\vec{x}_o$, results from the complex division

$$S(\vec{x}_o|\omega) = \frac{p(\vec{x}_5|\omega)}{H(\vec{x}_5|\vec{x}_o|\omega)} \quad . \tag{65}$$

This source function could be transformed to the time domain, but this is not a necessary step.

During steam condensation experiments conducted by the overseas licensee, the pressure field in the test tank was not measured directly. Rather, the pressure in a small volume connected by an orifice to the test tank was measured (Fig. 14). The drawback of this type of pressure sensor is that the acoustic coupling between the sensor volume and the test tank obscures the high frequency content of the source pressure time-history. The fundamental acoustic eigenfrequency of these pressure sensors is approximately 100 Hz. Even though the true condensation source that produced the selected pressure time-history may not have contained any high frequencies, the impulsive nature of the true source would have acoustically excited the pressure sensor cavity and some response would be observed. Because the exact nature of this masking is not known, it cannot be removed. As a result, the source function $S(\vec{x}_o|\omega)$ generated from Eq. (65) will contain some admixture of high frequency signal which will result in an unknown amount of conservatism. The source should be free of this contamination at frequencies below about 60 Hz.

To obtain a more realistic source, the pressure trace selected by General Electric (Fig. 15) was filtered at 100 Hz, and the frequency content greater than 100 Hz discarded. However, the total mean-square-power was held constant by increasing the strength of the frequency content below 100 Hz. The pressure response calculated from this source at the P/T 5 sensor location in the test tank is shown in Fig. 16.

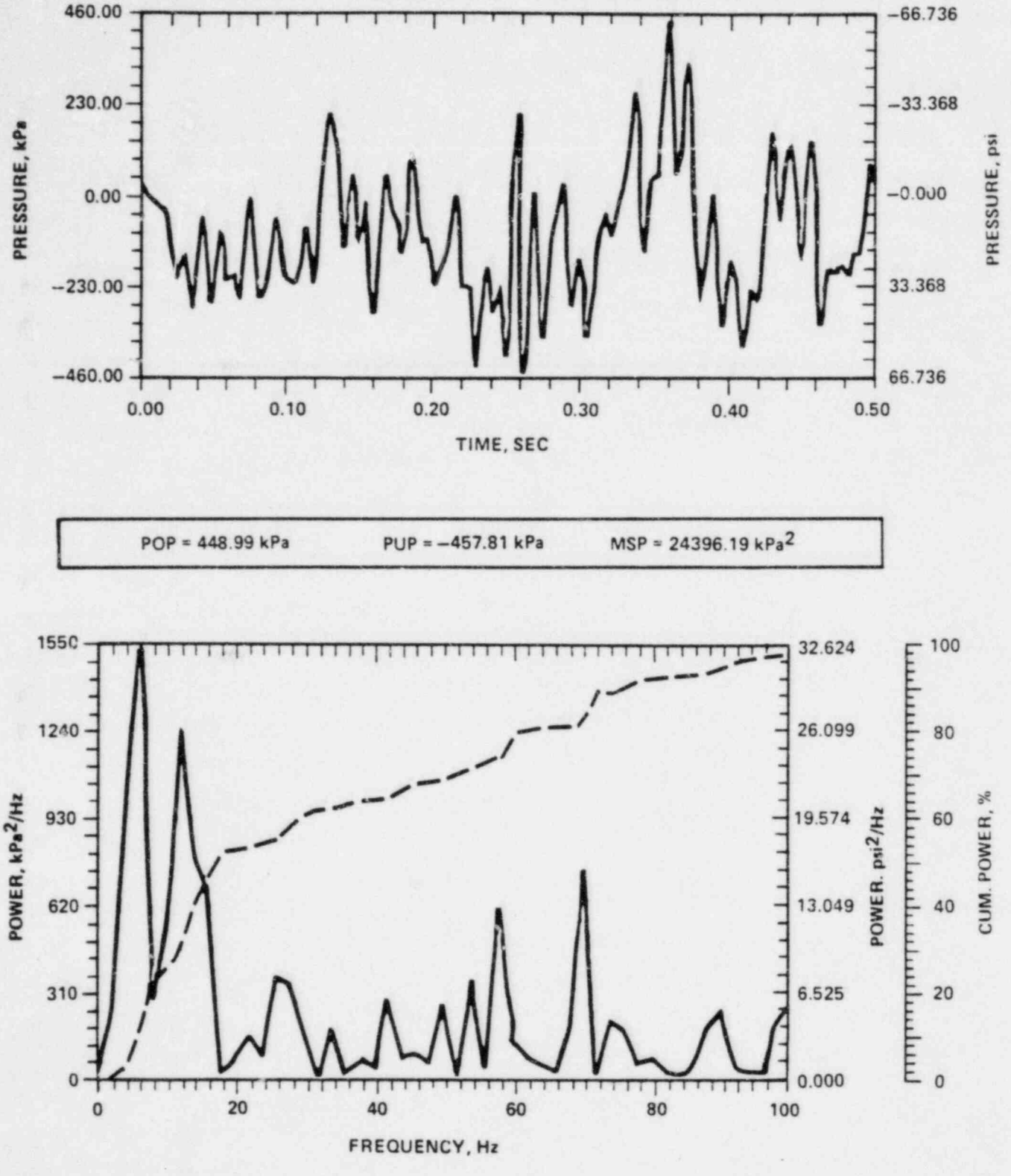

Figure 16 RHR CO Source Pressure Trace at Sensor Location P/T 5

5.2 MARK III EVALUATION

Once a representative source for RHR induced condensation oscillation has been determined, it can be used in the assessment of the Mark III containments for this phenomenon. In order to be able to use a source in a facility other than the one in which it was generated, it must be assumed that all the conditions that determine the nature of the condensation source are the same. Such, of course, will never be exactly true because of the random nature of the condensation process. However, if care is exercised in selection of the pressure time-history used for source generation such that conditions at the vent exits are reasonably similar, then the source from the test facility should be an adequate representation of the true Mark III RHR condensation oscillation source. This "transportability ansatz" will be invoked in the Mark III assessment for RHR induced condensation oscillation.

To assess the Mark III CIOG member containments for RHR condensation oscillation, each containment geometry will be evaluated individually. This is probably the most straightforward approach since, although each containment is geometrically similar, the boundary flexibilities appear to full into two groups: the relatively stiff containment (Perry and River Bend), and the relatively flexible containment, Grand Gulf and Clinton. In order to evaluate each containment geometry, it will be necessary to construct unique Mark III transfer functions. This is easily done using the equations for $H(\vec{x}|\vec{x}_o|\omega)$ for annular geometry along with the unique geometries for each containment given in Table 4.

In order to construct these transfer functions, the sonic speed C in the Mark III containments must be specified. The sonic speed which, together with the density is a measure of the fluid compressibility, is a weak function of pressure and temperature. For pure water at 37.78 C (100°F) and one atmosphere, the sonic speed is 1524 m/s (5000 fps).[37] However, with the addition of air, the sonic speed will change drmatically as can be seen in Fig. 17.[38] The precise amount of air is difficult to estimate without a test, but for large suppression pools the void fraction of air should be in excess of the equilibrium value obtained from Henry's Law.[39]

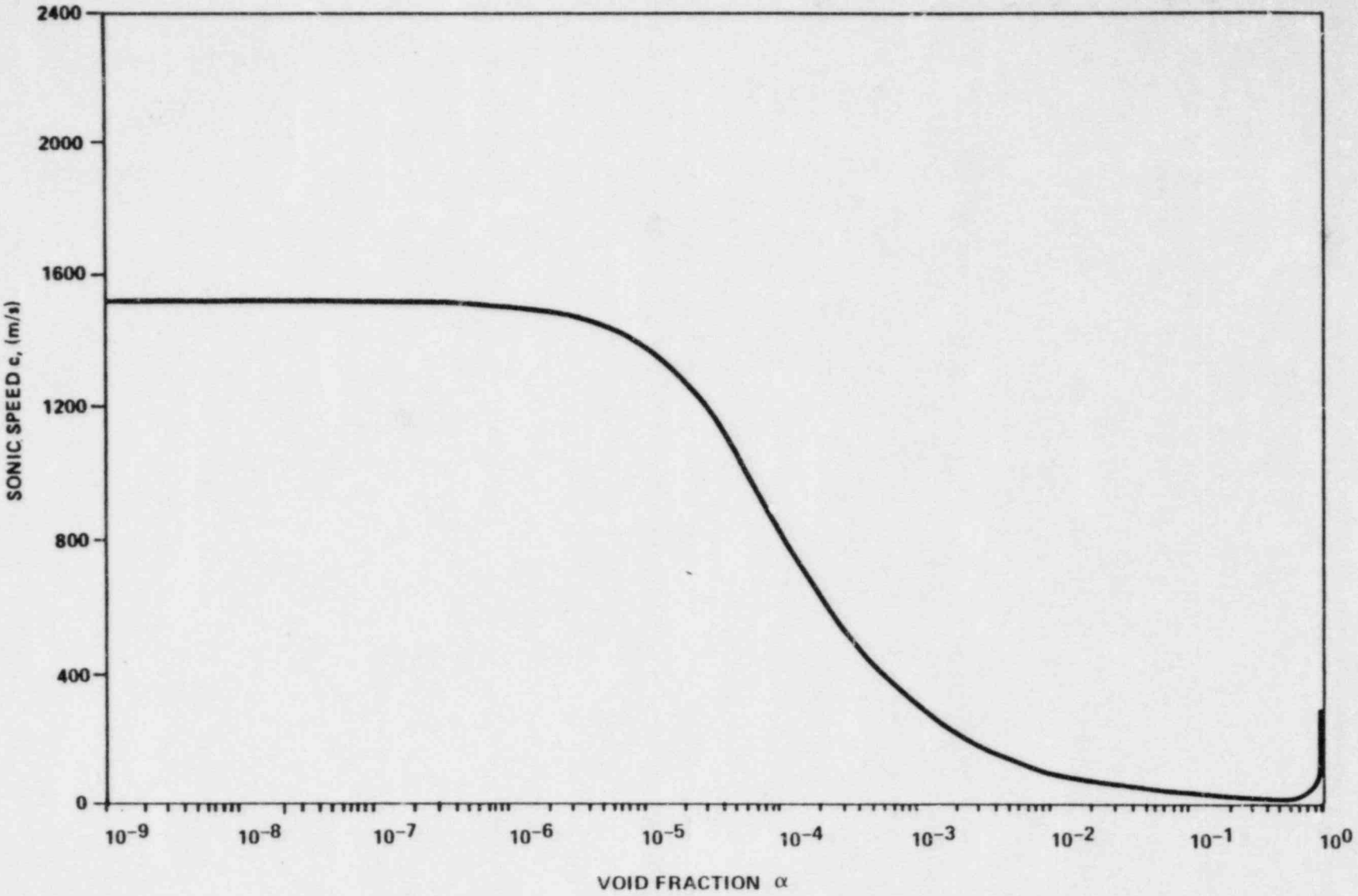

Figure 17 Sonic Speed vs Void Fraction

G1004085-19

For a suppression pool at 100°C (212°F) the void fraction α 9.34×10^{-6} corresponding to a sonic speed c = 1383 m/s (4537 fps) while for a pool at 20°C (68°F), $\alpha = 1.50 \times 10^{-5}$ and c = 1314 m/s (4311 fps). The reason the air void fraction will be greater than the equlibrium value is that the structural boundaries of the suppression pool are not smooth. This non-smooth nature provides myriad locations where air can accumulate. The exact value of the void fraction probably depends upon a multitude of factors, but a typical value would yield a sonic speed of 1067 m/s (3500 fps). Hence, the range of possible sonic speeds for Mark III varies between 1067 m/s and 1383 m/s. We will evaluate the CIOG member containment at two values for the sonic speed: (1) a typical realistic value of 1067 m/s and (2) the maximum possible value of 1524 m/s. We choose to use as the maximum value 1524 m/s instead of the equilibrium value for a boiling pool 1383 m/s in order to forego any discussion of the rate of which dissolved air can form bubbles and increase the compressibility of the water.

Once the Mark III transfer functions have been constructed, the pressure field $p(\vec{x}|\omega)$ can be generated at any desired location $\vec{x}$ via Eq. (66):

$$p(\vec{x}|\omega) = H(\vec{x}|\vec{x}_o|\omega)\ S(\vec{x}_o|\omega), \tag{66}$$

where $\vec{x}_o$ is the location of the RHR condensation oscillation source. This location is taken to be the exit plane of the RHR discharge. In cylindrical coordinates $\vec{x}_o = (r_o, \theta_o, z_o)$. The source location for each geometry was obtained from information supplied by each CIOG member and is given in Table 5.

Table 5

SOURCE LOCATION $\vec{x}_o = (r_o, \theta_o, z_o)$

	r_o	θ_o	z_o
GGNS	18.3642m (60'-3")	28°	4.2164m (13'-10")
PPNP	17.526m (57'-6")	28°	4.2367m (13'-10")
RBS	17.526m (57'-6")	28°	4.2672m (14'-0")
CPS	17.907m (58'-9")	23°	4.5467m (14'-11")

For example, the pressure response for GGNS at the containment wall directly opposte the RHR source is shown in Fig. 18. The location of the pressure response is given in cylindrical coordinates $\vec{x} = (r, \theta, z)$. In this example $(r, \theta, z) = (18.90\ m, 28°, 4.09\ m) = (62\ ft, 28°, 13.42\ ft)$. Pressure responses at other locations for each CIOG containment are given in Appendix B.

To determine the significance of these results, a comparison will be made between the maximum positive pressures due to RHR induced condensation oscillation and SRV actuation at the containment boundaries in the azimuth plane of the RHR discharge. The comparison of RHR and SRV peak pressures for each CIOG member containment is shown in Figs 19, 20, 21, 22. It can be seen that the maximum positive pressure due to a single SRV actuation exceeds that due to RHR condensation oscillation except in a small region on the containment wall adjacent to the RHR discharge, and that the actuation of all 20 SRVs produces a peak positive pressure that exceeds the maximum positive pressure generated by RHR condensation oscillation.

5.3 SUBMERGED STRUCTURE FORCES

In addition to the containment pressures, the magnitudes of the forces produced on submerged structures by both SRV actuation and RHR condensation oscillation were compared. The force exerted on a submerged structure by a fluid in motion is given by

$$\vec{F} = \oint p d\vec{S} \tag{67}$$

where p is the fluid pressure acting on an area increment $d\vec{S} = \hat{n}\, S$, $\hat{n}$ being the inward-pointing normal unit vector at dS. If static pressures are excluded from p, then $\vec{F}$ is the dynamic load due to fluid motion.*

*This treatment of the force on submerged structures neglects contributions due to tangential shear stresses since they are significant only for Reynolds numbers less than unity.40

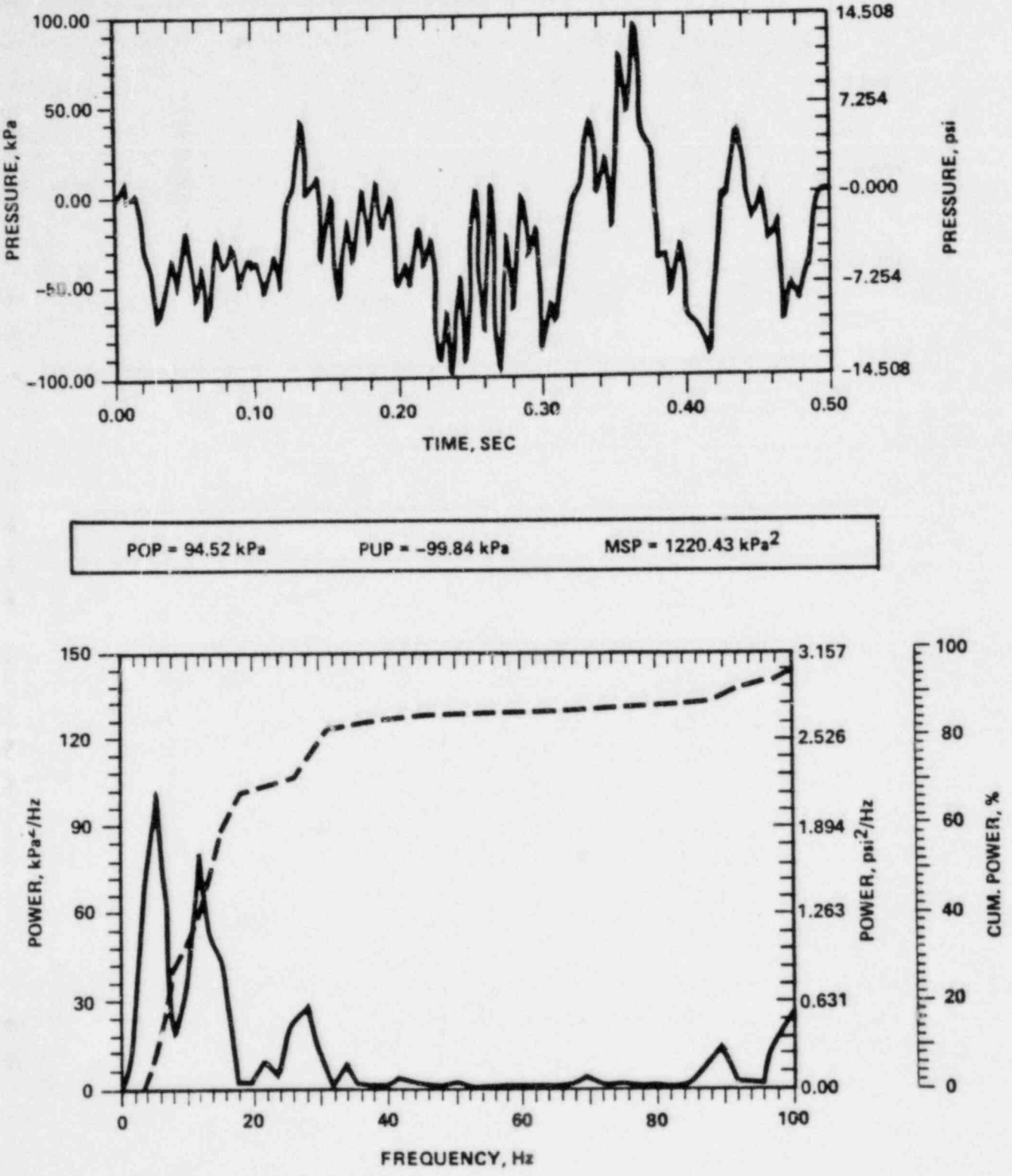

Figure 18 GGNS RHR CO Pressure at (18.9m, 28°, 4.09m)

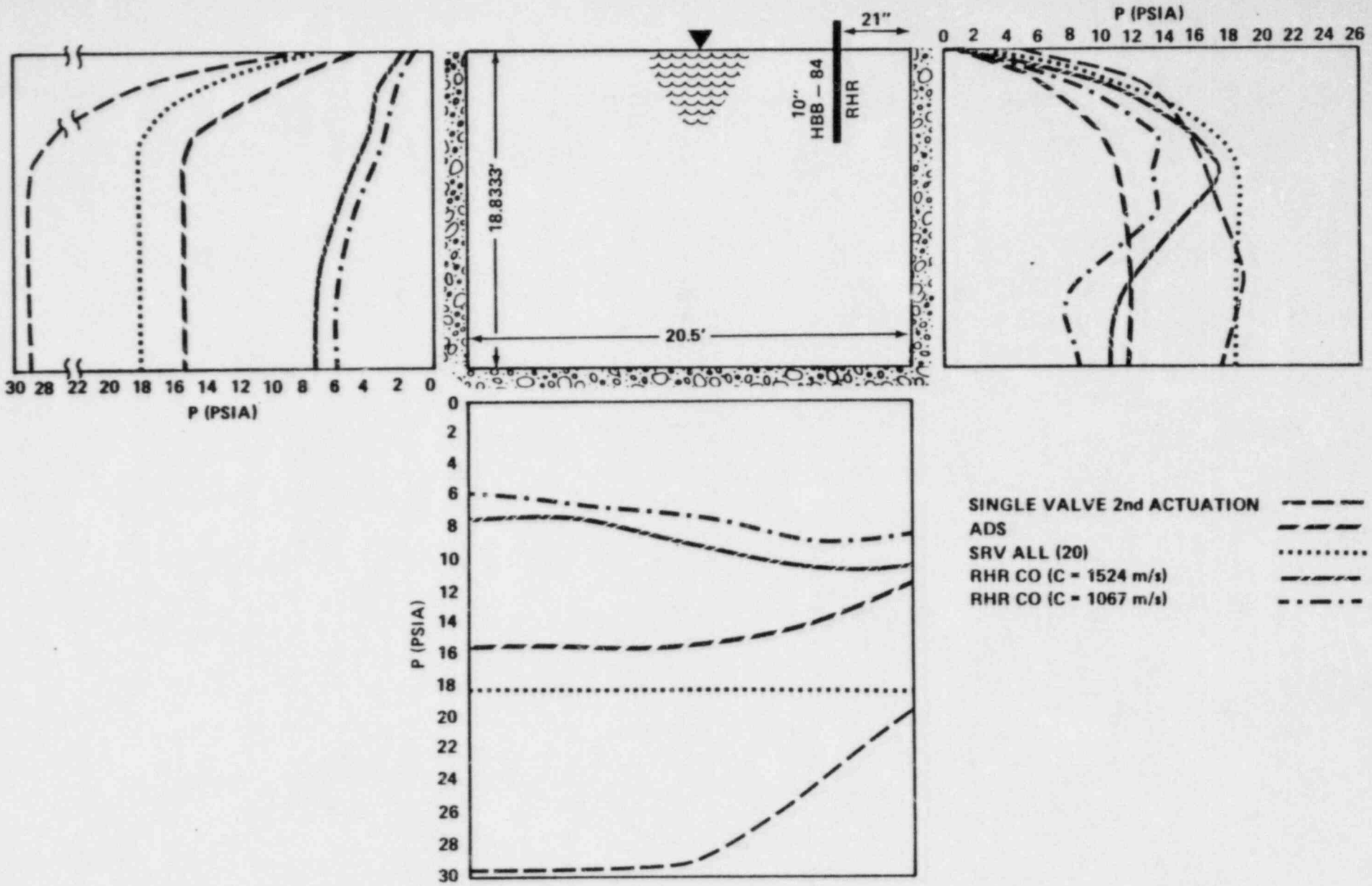

Figure 19 Comparison of GGNS RHR CO and SRV Pressure Distributions at 28° Azimuth Around Suppression Pool Boundaries

G1004085 23

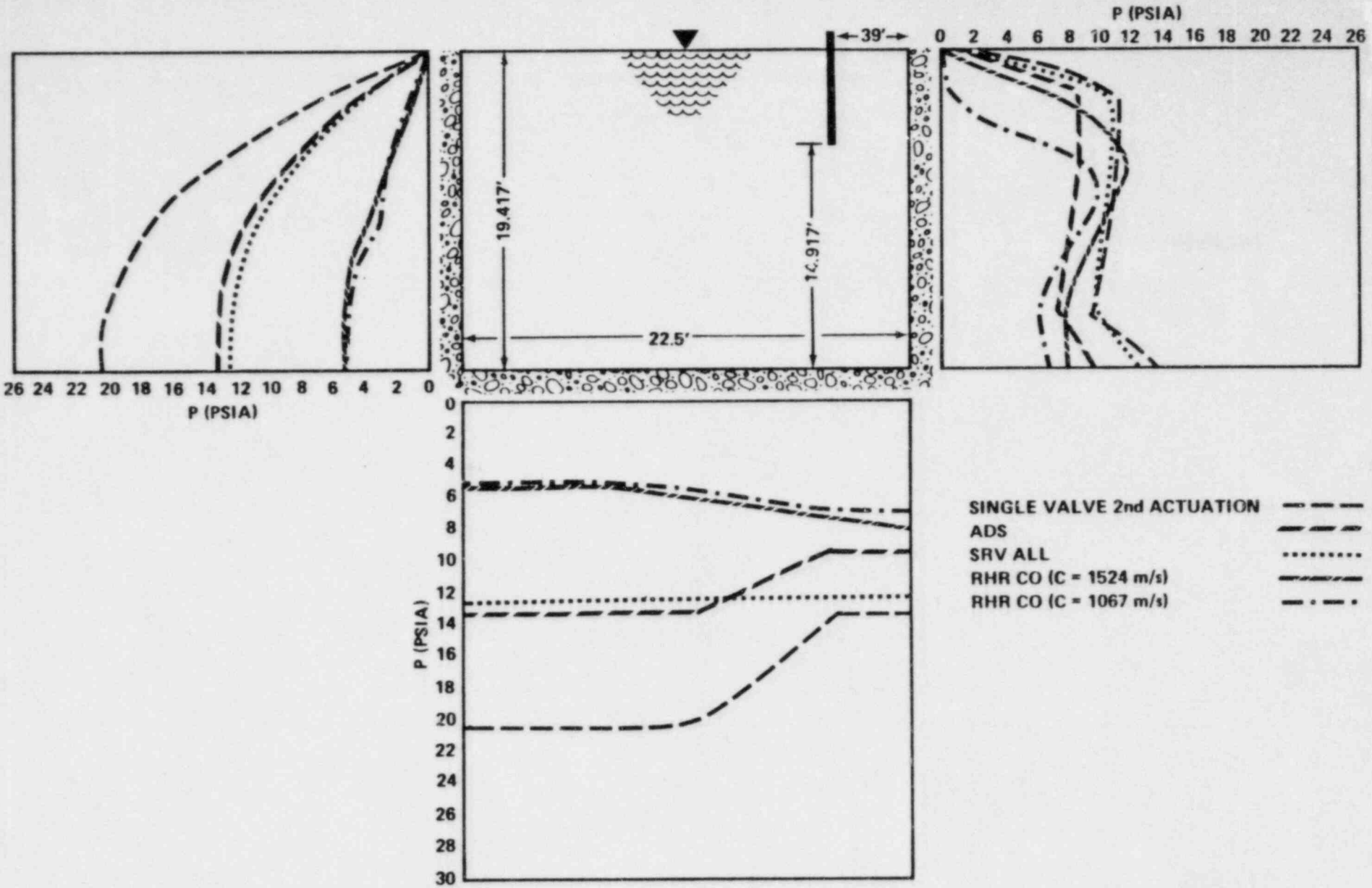

Figure 20 Clinton RHR CO Pressure Distributions at 28° Azimuth Around Suppression Pool

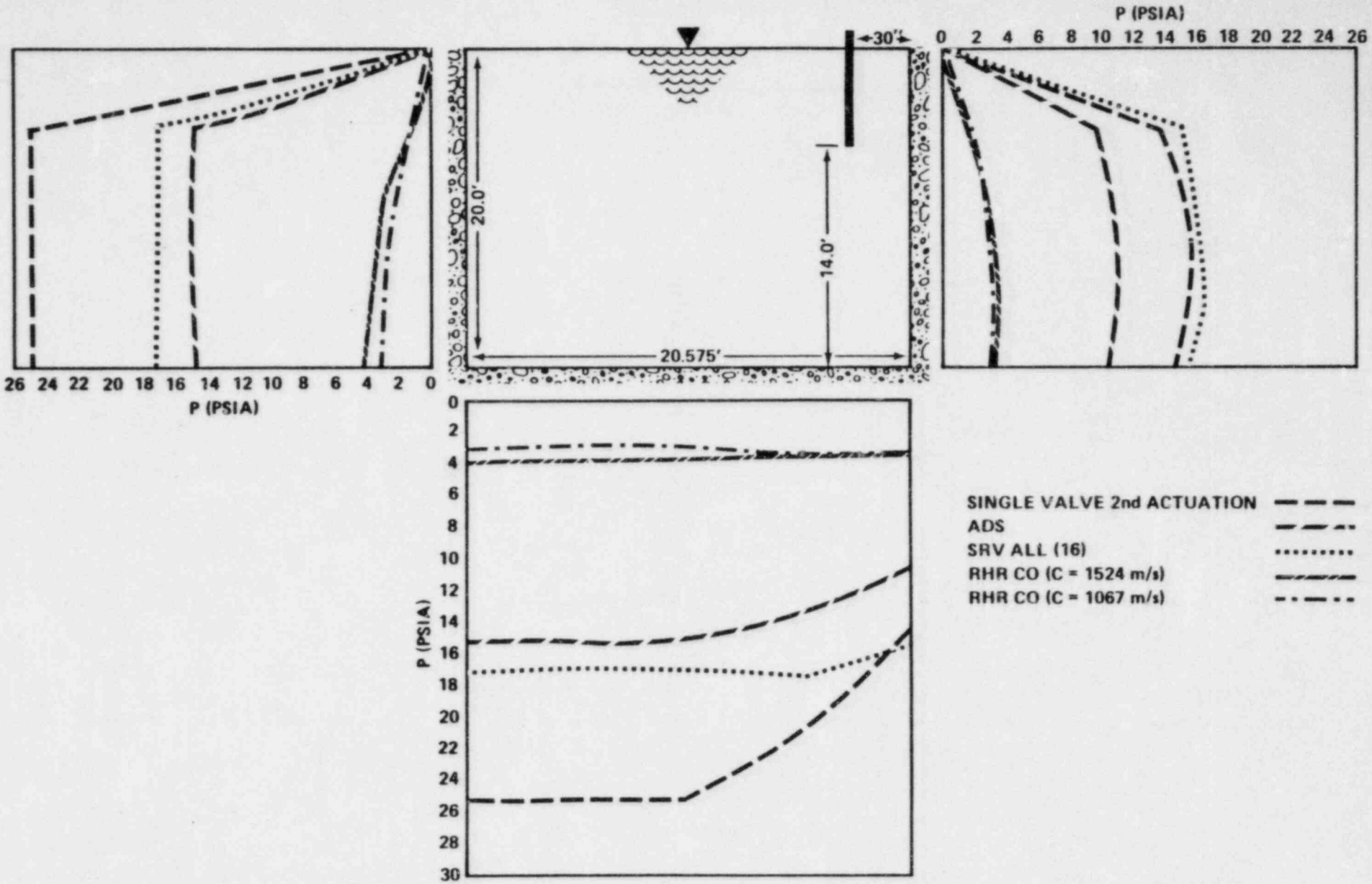

Figure 21 River RHR CO Pressure Distributions at 28° Azimuth Around Suppression Pool Boundaries

G1004085-24

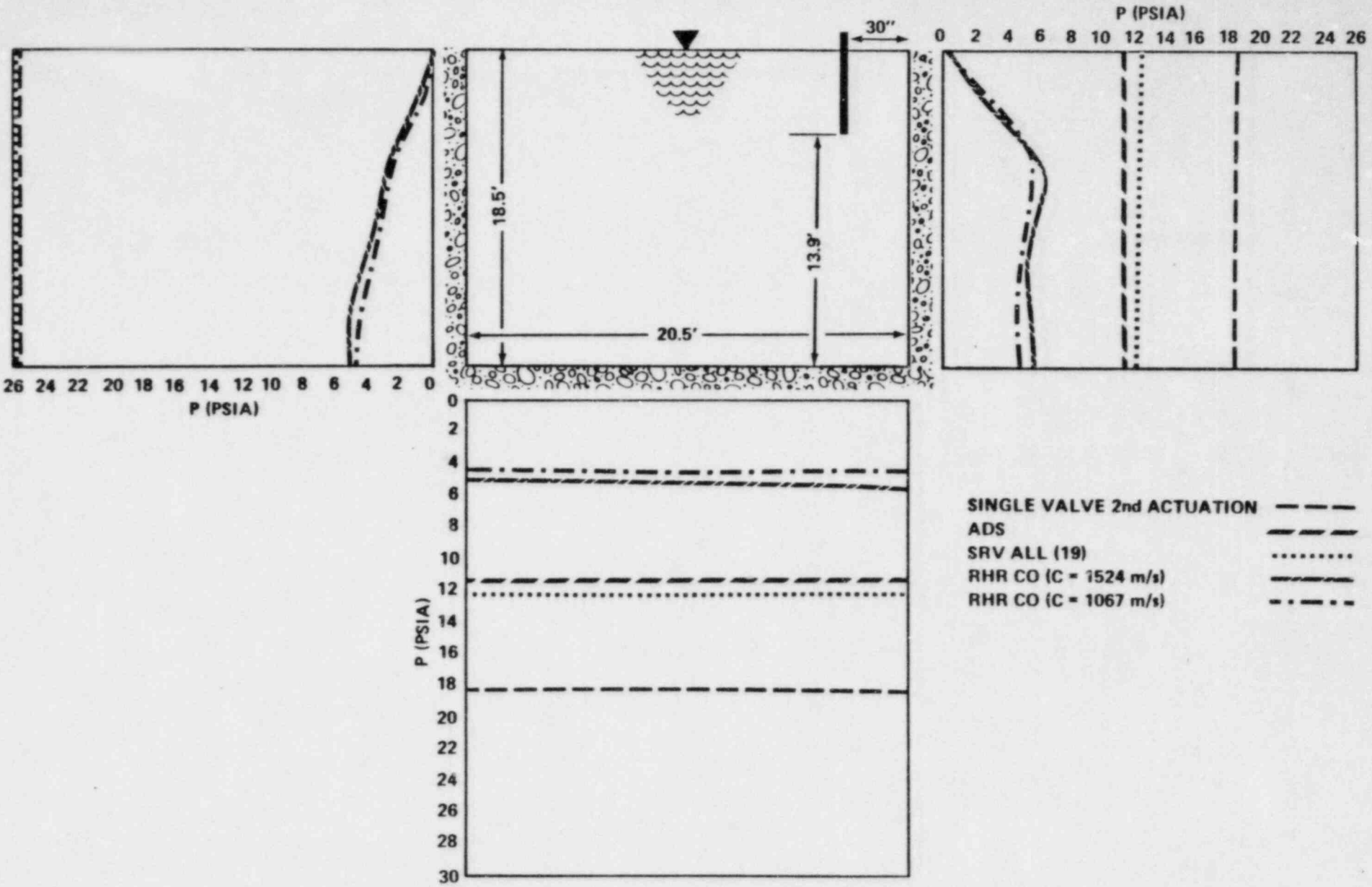

Figure 22 Perry RHR CO Pressure Distributions at 28° Azimuth Around Suppression Pool Boundaries

G1004085-22

For large Reynolds numbers (10^3 - 10^5), the flow field can be divided into an external region and a thin boundary-layer near the structure together with a wake behind it. In the external region potential flow theory (compressible or incompressible) can be used to evaluate the flow field or the pressure field, while in the boundary-layer and wake, the Navier-Stokes equation must be used.[41,42] Therefore, the surface integral in Eq. (67) can be divided into an integral over the surface outside the wake region where the pressure is given by the solution to the linear acoustic wave equation, P_ϕ, and an integral given the surface inside the wake where the pressure is given by P_w.[43] These two integrals can be modified such that the force is given by

$$\vec{F} \oint_S p_\phi d\vec{S} + \oint_{S_w} (p_w - p_\phi) d\vec{S} \ . \tag{68}$$

The second integral in Eq. (68) is performed over the surface adjacent to the wake region, and S_w is all but impossible to evaluate, so we set

$$\oint_{S_w} (p_w - p_\phi) d\vec{S} = \frac{1}{2}\rho C_A A |\vec{U}_\infty| \vec{U}_\infty \tag{69}$$

where $\vec{U}_\infty = \vec{U}_\infty(t)$ is the uniform flow velocity. This is a defining equation for the unsteady drag coefficient C_A which reduces to the steady drag coefficient C_D for $\vec{U}_\infty$ constant in time. Values for C_A are obtained from experiment.

A somewhat limited conclusion[44] drawn from the comparison of the unsteady drag force

$$\vec{F}_D = \frac{1}{2}\rho C_A A |\vec{U}_\infty| \vec{U}_\infty \tag{70}$$

with experimental data is that for cylinders in unidirectional flow acceleration $C_A < 2\ C_D$ where $10^3 < Re < 3 \times 10^5$. In this Reynolds number range, $C_D \simeq 1$.[45]

The expression for the force given by Eq. (68) thus becomes

$$\vec{F} = \oint p_\phi d\vec{S} + \frac{1}{2}\rho C_A A |\vec{U}_\infty| \vec{U}_\infty \tag{71}$$

where the pressure field, p_ϕ, is determined from the acoustic wave equation in conjunction with a set of suitable boundary conditions.

For an inviscid fluid described by potential flow, Euler's equation can be transformed into an expression relating the pressure p_ϕ, the time derivative of the velocity potential $\dot{\phi}$, and the gradient of the velocity potential:[46]

$$p_\phi - \rho\dot{\phi} + \frac{1}{2}\rho(\nabla\phi)^2 = f(t). \tag{72}$$

Here f(t) is an arbitrary function of time which can be set equal to zero without loss of generality. Taking into account d'Alemberts paradox,[47] the integral in Eq. (71) can be written

$$\oint p_\phi d\vec{S} = \rho \oint \dot{\phi} d\vec{S} = \kappa\rho V_S \dot{\vec{U}}_\infty . \tag{73}$$

The acceleration volume $V_A \equiv \kappa V_S$ is equal to the sum of the structure volume V_S, plus the classical hydrodynamic mass[48], M_H, divided by the fluid density. Hence

$$\kappa = 1 + M_H/\rho V_S . \tag{74}$$

Under certain conditions the force acting on the submerged structure given by the integral term in Eq. (71) (which is also known as the acceleration drag force) can be significantly larger than the unsteady drag force given by Eq. (70). Since $\vec{U}_\infty$ is parallel to $\dot{\vec{U}}_\infty$, it thus becomes convenient to express the submerged structure force given by Eq. (71) in the following form,

$$\vec{F} = \left(2 + \frac{C_A AD}{2V_S Sr}\right) \oint p_\phi d\vec{S} , \tag{75}$$

where D is a characteristic dimension of the structure and $Sr \equiv \dot{U}_\infty D/U_\infty^2$ is the Strouhal number.[49] The parameter κ is equal to 2 in Eq. (75) in order to account for the hydrodynamic mass in Eq. (74). Hence Eq. (75) under-

estimates the true submerged structure force. It is obvious that when $Sr >> C_A AD/2V_S$, the submerged structure force is essentially given by the integral of the pressure field p_ϕ over the structure surface S. A cylindrical structure at the closest distance to the RHR source given in Table 4 was used for the comparison.

In order to estimate the load on submerged structures resulting from RHR CO, the tangential and radial forces were computed for a cylindrical structure in each CIOG containment. This structure was oriented such that its axis was parallel with the containment axis and located a distance from the RHR CO source given in Table 4. Table 6 gives the resulting peak forces.

Table 6

RADIAL, TANGENTIAL OR AZIMUTHAL FORCE
ON A SUBMERGED CYLINDRICAL OBJECT

	Force		
	Radial	Tangential	Azimuthal
GGNS	9.0 LBf		160.0 LBf
PPNP	230.0 LBf	180.0 LBf	
RBS	98.4 LBf		103.2 LBf
CPS	160.0 LBf		112.0 LBf

6 CONCLUSIONS

In May 1982, the NRC raised the concern that condensation oscillation loads that might be produced by steam discharges from the RHR heat exchanger relief valves had not been completely defined. The Mark III Containment Issues Owners Group has maintained that the potential RHR condensation oscillation loads can be accommodated by conservatisms in an existing load definition, or that they are bounded by existing load definitions. In response to an NRC request to submit additional supporting information, the Mark III CIOG commited to complete a detailed evaluation of the impact of potential condensation oscillation loads produced by steam discharges from the RHR heat exchanger relief valve.

To carry out this task, Bechtel utilized a derivative of the acoustic chugging model used in the Mark II chugging program that had been reviewed by both the NRC and the Advisory Committee on Reactor Safeguards. This report describes in technical detail both the theoretical model and the verification that the model has the capability of producing boundary pressures that include the effects of the fluid-structure interaction. The paper also shows results that agree well with experimental data and calculations of more elaborate computer programs (NASTRAN).

Using test data supplied Bechtel by the General Electric Company that are representative of the condensation source expected to occur in Mark III from RHR steam discharge, a source function was empirically erected. This source was argued to be conservative with respect to the true RHR condensation oscillation source and was used to generate boundary pressures and submerged structure forces in a typical Mark III containment: Grand Gulf Nuclear Station. These were compared with pressures and forces from SRV actuation with the result that the SRV loads adequately bound the RHR condensation oscillation loads. This study has shown that the potential condensation oscillation loads which could be produced by steam discharge from the RHR heat exchanger relief valves are bounded by the loads which are produced by main steam SRV actuations. Therefore, the RHR condensation oscillation loads can be concluded to have no design significance.

REFERENCES

1. G. K. Ashley II, N. M. Howard, E. Rabin, "Mark III Improved Chugging Methodology," General Electric Co., NEDE-24822-P, May 1980 (Proprietary).

2. Letter to L.F. Dall from John M. Humphrey, May 8, 1982.

3. Memorandum to A. Schwencer and W. Butter Butler from D. Houston and J. Kundrick, 13 May 1982, Docket Nos. 50-416/417.

4. Letter to H. R. Denton from L.F. Dale, 28 May 1982, File L-860, 0/0260, Docket Nos. 50-416/417.

5. Memorandum to Schwencer and Butler.

6. J. M. Healzer, "Single Vent Chugging Model," NEDE-23703-P, General Electric Co., September 1977.

7. L. W. Florscheutz and B. T. Chao, "On the Mechanics of Vapor Bubble Collapse," J Heat Transfer, May 1965, pp 209-220.

8. M. S. Plesset and S. A. Zwick, "A Non-Steady Heat Diffusion Problem with Spherical Symmetry," J Appl Phys, 1952, 23:9.

9. M. S. Plesset and A. Prosperetti, "Bubble Dynamics and Cavitation," Ann Rev Fluid Mech, 1977, 9:145-185.

10. _____, "Generic Chugging Load Definition Report," General Electric Co., NEDE-24302-P, April 1981.

11. P. M. Morse and K. V. Ingard, Theoretical Acoustics, McGraw-Hill (New York, 1968) pp 278-280.

12. D. E. Gray, American Institute of Physics Handbook, 3rd ed., McGraw-Hill (New York, 1972) pp 3-44.

13. Morse and Ingard, op. cit., pp 863-866.

14. Ibid., pp 270-300.

15. L. E. Kinsler and A. R. Frey, Fundamentals of Acoustics, 2nd ed., John Wiley & Sons (New York, 1962) Chapter 9.

16. J. J. Markham, et al, "Absorption of Sound in Fluids," Rev Mod Phys, 1951, Vol 23, No. 4, p 353.

17. L. D. Landau and E. M. Lifshitz, Fluid Mechanics, Pergamon Press (Oxford, 1959) pp 298-304.

18. D. E. Grey, op. cit., p 3 and pp 206-209.

19. John Mathews and R.L. Walker, Mathematical Methods of Physics, W. A. Benjamin, Inc. (New York, 1965) p 97.

20. Morse and Ingard, op. cit., p 28.

21. Ibid., pp 319-322.

22. Ibid., pp 554-563.

23. W. T. Thomson, Vibration Theory and Applications, Prentice-Hall (New York, 1963) p 70.

24. N. M. Newmark and E. Rosenblueth, Fundamentals of Earthquake Engineering, Prentice-Hall, Inc., (New York, 1971) pp 420-423.

25. U.S. Atomic Energy Commission, Directorate of Regulatory Standards, Regulatory Guide 1.61, "Damping Values for Seismic Design of Nuclear Power Plants," October 1973.

26. P. M. Morse, Vibration and Sound, McGraw-Hill (New York, 1948) p 401.

27. P. M. Morse and R. H. Holt, "Sound Waves in Rooms," Rev Mod Phys, 1944, pp 16, 69.

28. Morse and Ingard, op. cit., pp 263-264.

29. E. B. Wylie and V. L. Streeter, Fluid Transients, McGraw-Hill (New York, 1978) pp 3-8, 9-11, 19-29, 140-142.

30. Morse and Ingard, op cit, pp 475-477.

31. Ibid., pp 688-689.

32. J. Lighthill, Waves in Fluids, Cambridge University Press (London, 1978) p 92.

33. _____, "Mark II Containment Supporting Program. Summary of 4T Fluid-Structure Interaction Studies," NEDE-23710-P, General Electric Co., April 1978 (Proprietary).

34. Ibid.

35. _____, "CDC/NASTRAN, Supplementary Documentation, Applications Manual," Revision Q, Control Data Corporation Manual for CDC 6000 Series), September 1976.

36. R. H. MacNeal, "The NASTRAN Theoretical Manual (Level 15.0)," NASA Documentation No. SP-221 (01) (includes Level 15.5 Supplement), December 1972.

37. Gray, op. cit., pp 3-95.

38. G. B. Wallis, One-dimensional Two-phase Flow, McGraw-Hill (New York, 1969) p 265.

39. R.H. Perry, C.H. Chilton, S.D. Kirkpatrick eds., Chemical Engineers' Handbook, 4th ed., McGraw Hill (New York, 1963) pp 3-14.

40. H. Schlichting, Boundary-Layer Theory, 6th ed., McGraw-Hill (New York, 1968) p 104ff.

41. Ibid., p 22.

42. Landau and Lifshitz, op. cit., p 169.

43. F. J. Moody, "Forces on Submerged Structures in Unsteady Flow," Proc. ANS Topical Meeting on Thermal Reactor Safety, July 31-August 4, 1977, Sun Valley, Idaho, pp 3 and 516ff.

44. Ibid., pp 3-592.

45. Schlichting, op. cit., p 17.

46. Landau and Lifshitz, op. cit., p 19.

47. Ibid., p 34.

48. L. M. Milne-Thomson, Theoretical Hydrodynamics, 5th ed., McMillan Press Ltd. (London, 1968) pp 246-247.

49. Schlichting, op. cit., p 32.

GLOSSARY OF SYMBOLS

a	Radius of 4T tank or outer radius of Mark III suppression pool (m)
A	Cross section area (m^2)
b	Inner radius of Mark III suppression pool (m)
c	Acoustic speed (m/s)
D	Diameter of 4T cylindrical tank (m)
$G(\vec{x}\|\vec{y}\|\omega)$	Flexible-boundary general Green's function $G(x\|y\|\omega)$
$G_\phi(\vec{x}\|\vec{y}\|\omega)$	Rigid-boundary Green's function
h	Boundary thickness (m)
$H(\vec{x}\|\vec{x}_o\|\omega)$	Transfer function
$J_m(x)$	Bessel function of order m
$J'_m(x)$	Derivative of Bessel function of order m
$k = \omega/c$	Wave number
$K_n(\omega)$	Flexible-boundary eigenvalue
ℓ	Axial quantum number
L	Water depth (m)
m	Azimuthal quantum number
$M = \rho_s h$	Effective mass per unit area (kg/m^2)
n	Radial quantum number
$N = n,m,\ell$	Quantum number trio
p	Acoustic pressure (P [illegible] kg/m)
P_o	Equilibrium pressure
P	Total pressure
$q(\vec{x},t)$	Source density function
$q(\vec{x}\|\omega)$	Fourier transform of source density function

$R = 2\zeta M\omega_s$	Boundary resistance factor
s	Entropy per unit mass
S	Surface area
$S(t)$	Chug source strength
t	Time
T	Temperature
$\vec{u}$	Acoustic fluid velocity (m/s)
u_n	Acoustic fluid velocity magnitude normal to the boundary surface (m/s)
V	Water volume
$\vec{x} = (r,\theta,z)$	Location of pressure measurement (m)
$\vec{x}_o(r_o,\theta_o,z_o)$	Location of point source (m)
$\vec{y}$	Position vector (m)
Y	Young's (elastic) modulus (Pa)
z	Elevation from origin (m)
z_o	Axial position of source (m)
$z(\omega) = p/u$	Acoustic impe nce
α_{mn}	Characteristic numbers for Bessel functions in cylindrical geometry
$\beta(\vec{x}_s \mid \omega)$	Specific acoustic admittance
δ	Acoustic density change (kg/m^3)
δ	Boundary distensibility (Pa^{-1})
$\delta(x)$	Dirac delta function
δ_{mn}	Kronecker delta symbol
ε_m	Normalization constant
ζ	Structural damping factor
η	Bulk viscosity

Θ_N	Rigid wall wave number
Θ	Azimuth angle
Θ_o	Azimuth angle of source
κ	Thermal conductivity
λ_N	Fluid damping constant
μ	Coefficient of shear viscosity
μ	Poisson's ratio
$\zeta(\vec{x}_s \mid \omega)$	Specific acoustic conductance
$\bar{\zeta}(\omega)$	Spatial average specific acoustic conductance
ρ	Mean fluid density (kg/m^3)
ρ_s	Mean boundary density (kg/m^3)
$\sigma(\vec{x}_s \mid \omega)$	Specific acoustic susceptance
$\bar{\sigma}(\omega)$	Spatial average specific acoustic susceptance
$\tilde{\tau}$	Viscous-stress tensor
τ	Source start time (s)
$\Phi_N(\vec{x})$	Rigid wall eigenfunction
Φ	Potential energy per unit mass
$\Psi_N(\vec{x} \mid \omega)$	Flexible-boundary eigenfunction
ω_N	Flexible-boundary eigenfrequency
$\omega_N^o \equiv ck_n$	Rigid-boundary eigenfrequency
ω_b	4T base plate vibrational frequency
ω_s	Structure vibrational frequency
ω_s	4T shell vibrational frequency
∇	Gradient operator
∇^2	Laplacian operator
$\Box 2$	d'Alembertian operator
$\partial/\partial n$	Normal derivative

APPENDIX A

SPECIFICATION OF RHR CONDENSATION OSCILLATION

March 16, 1983

Dr. Gordon K. Ashley
Bechtel Power Corporation
P. O. Box 3965
San Francisco, CA 94119

Dear Gordon:

Enclosed is the information which General Electric agreed to supply to you during the March 1 meeting of the Mark III Containment Issues Owners Group. The information includes a description of the test facility, the peak pressure on the bottom of the test facility and GE's normalized pressure time history for a sensor on the bottom of the test facility.

This information should be sufficient to allow you to complete development of the condensation oscillation source for steam discharges from the RHR heat exchanger relief valve to the Grand Gulf Nuclear Station suppression pool. You may reference this transmittal letter in your source definition report.

Please note that the information enclosed with this letter is proprietary to General Electric Company and should be handled in accordance with the proprietary information agreement which is in effect between Mississippi Power & Light and Bechtel Power Corporation.

If you require any additional information to complete the development of the condensation oscillation source, please let me know as soon as possible.

Yours very truly,

J D Richardson-/kb

J. D. Richardson
Manager Safety and Licensing
Mississippi Power & Light Company

JDR:kb

RHR SRV CO LOAD DEFINITION

Test data which may be used to develop a representative RHR SRV CO load may be found in Reference 1. A specific normalized pressure time history is given in Table 1. The test configuration is similar to that shown in Figure 4.2-20 of Reference 1, included here as Figure 1. This facility may be modeled as a 10 ft. diameter cylindrical tank. For this application the steam was vented into the water through a straight pipe 8.2 inches in diameter located in the center of the test tank. The pipe exit was located 7.5 ft. above the tank bottom and the submergence was 6.6 ft.

For load definition the maximum positive pressure at the tank bottom center should be set at 60 psid. Radial attenuation from the projection of the pipe centerline on the tank bottom is well represented by $1/(1+r)$ where r is the radial distance. On the tank wall at the elevation of the vent pipe exit, the peak pressure was 13% of the maximum bottom center pressure.

Reference: Fukushima, T. et. a., "Test Results Employed by GE for BWR Containment and Vertical Vent Loads," NEDE-21028, October 1975.

WMD:cal/K031416*
3/14/83

GENERAL ELECTRIC COMPANY
PROPRIETARY INFORMATION

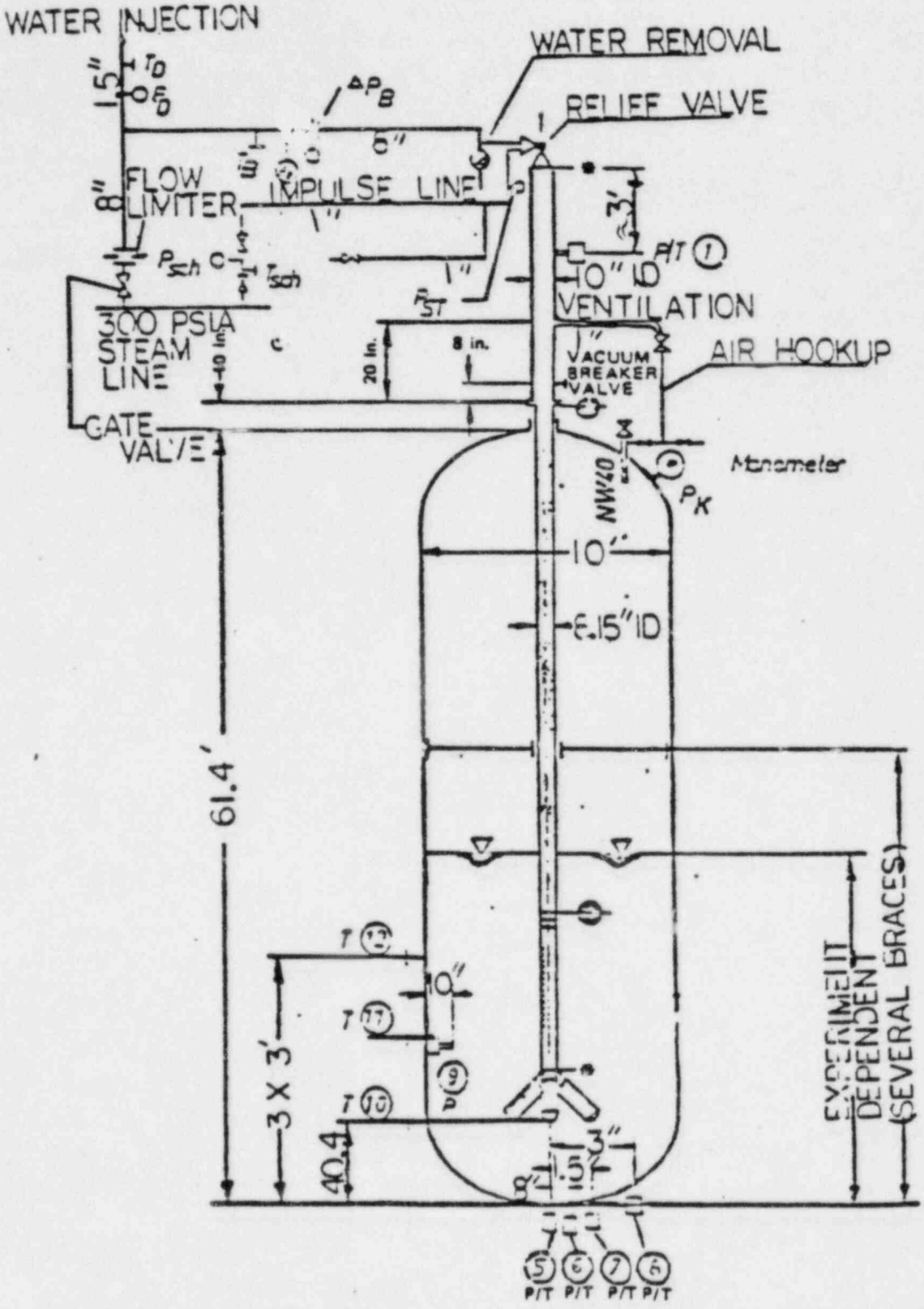

Figure 4.2-20. P&ID for Large-Scale Test Stand

TABLE I

NORMALIZED PRESSURE TIME HISTORY

TEST B, SENSOR P5

Time -sec-	Normalized Pressure
0.001000	0.260
0.003000	-0.396
0.006000	0.257
0.011000	-0.313
0.013000	0.283
0.015000	-0.385
0.017000	0.302
0.020000	-0.408
0.021000	0.
0.023000	-0.498
0.025000	-0.106
0.027000	-0.453
0.030000	-0.121
0.032000	+0.642
0.035000	-0.158
0.037000	-0.558
0.040000	-0.264
0.041000	-0.377
0.045000	0.181
0.048000	-0.781
0.052000	-0.094
0.053000	-0.653
0.055000	0.196
0.057000	-0.608
0.060000	-0.094
0.061000	-0.694
0.065000	-0.068
0.066000	-0.679
0.069000	0.377
0.070000	-0.785
0.073000	0.502
0.075000	-0.947
0.078000	0.842
0.080000	-1.170
0.083000	0.
0.085000	-0.453
0.088000	-0.170
0.090000	-0.672
0.094000	0.498
0.096000	-0.800
0.098000	0.143
0.101000	-0.919
0.105000	0.428
0.106000	-0.915
0.112000	-0.611

0.115000	0.725
0.116000	-0.604
0.118000	-0.106
0.120000	-0.543
0.124000	0.309
0.125000	-0.045
0.127000	0.434
0.129000	0.140
0.130000	0.736
0.132000	-0.328
0.135000	0.785
0.138000	-0.675
0.143000	0.385
0.145000	-0.219
0.147000	0.143
0.150000	-0.381
0.153000	0.260
0.158000	-0.600
0.161000	-0.257
0.163000	-0.491
0.165000	0.321
0.169000	-0.370
0.171000	0.385
0.176000	-0.498
0.179000	0.234
0.180000	-0.328
0.182000	0.419
0.184000	-0.287
0.186000	0.283
0.188000	-0.045
0.190000	0.106
0.196000	-0.634
0.198000	0.649
0.200000	-0.891
0.203000	-0.079
0.205000	-0.694
0.207000	0.234
0.210000	-0.600
0.213000	0.506
0.215000	-0.528
0.217000	0.245
0.220000	-0.642
0.225000	-0.094
0.228000	-1.057
0.232000	-0.230
0.233000	-0.904
0.237000	-0.125
0.242000	-0.694

2

0.115000 0,725

0.252000 -0.181

0.260000	-0.872	0.255000	0.806
0.263000	-0.057		
0.265000	-0.943		
0.268000	0.517		
0.270000	-0.634		
0.271000	-0.283		
0.274000	-0.766		
0.276000	-0.049		
0.279000	-0.913		
0.282000	0.698		
0.284000	-0.506		
0.287000	0.528		
0.288000	-0.460		
0.291000	0.808		
0.292000	-0.743		
0.295000	0.049		
0.297000	-0.732		
0.300000	0.		
0.301000	-0.566		
0.305000	-0.019		
0.305000	-0.894		
0.308000	0.		
0.310000	-0.540		
0.315000	0.245		
0.316000	-0.340		
0.319000	0.230		
0.320000	-0.298		
0.323000	0.143		
0.325000	-0.385		
0.327000	0.415		
0.330000	-0.170		
0.332000	0.747		
0.335000	0.030		
0.338000	0.377		
0.340000	-0.385		
0.341000	0.128		
0.344000	-0.340		
0.347000	0.513		
0.348000	0.		
0.350000	0.223		
0.351000	-0.045		
0.353000	0.634		
0.354000	0.277		
0.356000	1.000		
0.362000	0.045		
0.365000	0.468	0.369000	0.426
0.365000	0.177		
0.368000	0.634		

0.373000	0.019
0.373000	0.226
0.377000	-0.411
0.379000	0.030
0.380000	-0.774
0.384000	0.106
0.385000	-0.577
0.389000	0.426
0.391000	-0.830
0.395000	-0.185
0.397000	-0.928
0.400000	0.125
0.403000	-0.936
0.405000	-0.075
0.408000	-0.849
0.411000	-0.438
0.414000	-0.600
0.417000	-0.200
0.420000	-0.600
0.426000	0.408
0.429000	-0.087
0.430000	0.162
0.432000	-0.083
0.435000	0.158
0.436000	-0.257
0.439000	0.717
0.440000	0.
0.443000	0.721
0.444000	-0.347
0.447000	0.502
0.448000	-0.687
0.452000	0.506
0.453000	-0.604
0.457000	0.672
0.460000	-0.649
0.463000	-0.287
0.465000	-0.747
0.468000	-0.257
0.470000	-0.287
0.473000	-0.170
0.475000	-0.642
0.479000	-0.019
0.484000	-0.611
0.488000	0.223
0.490000	-0.611
0.492000	-0.162
0.493000	-0.226
0.496000	0.264

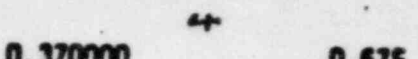

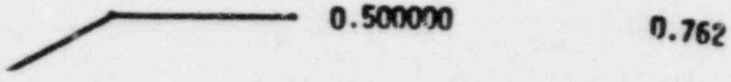

APPENDIX B

PLANT PRESSURE TIME-HISTORIES AND PLANT SUBMERGED STRUCTURES FORCE TIME-HISTORIES WITH C = 1067 m/s

GGNS RHR CO (C=1067)

Output at point (18.90,28.00,3.45)

NAME - LEONG, TAI SENG
DATE - FEB 22, 1984
PROJECT NO. - 15026004

CHECKED _____
DATE _____
CALC NO. - AP-84-

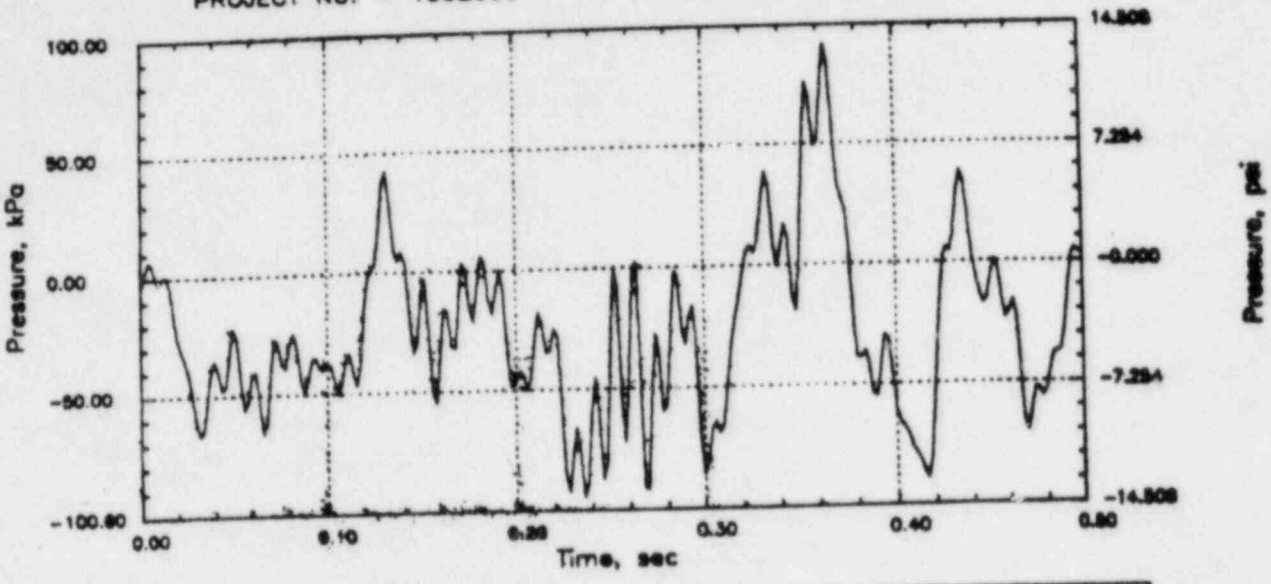

POP = 91.95 kPa PUP = -94.79 kPa MSP = 1178.93 kPa²

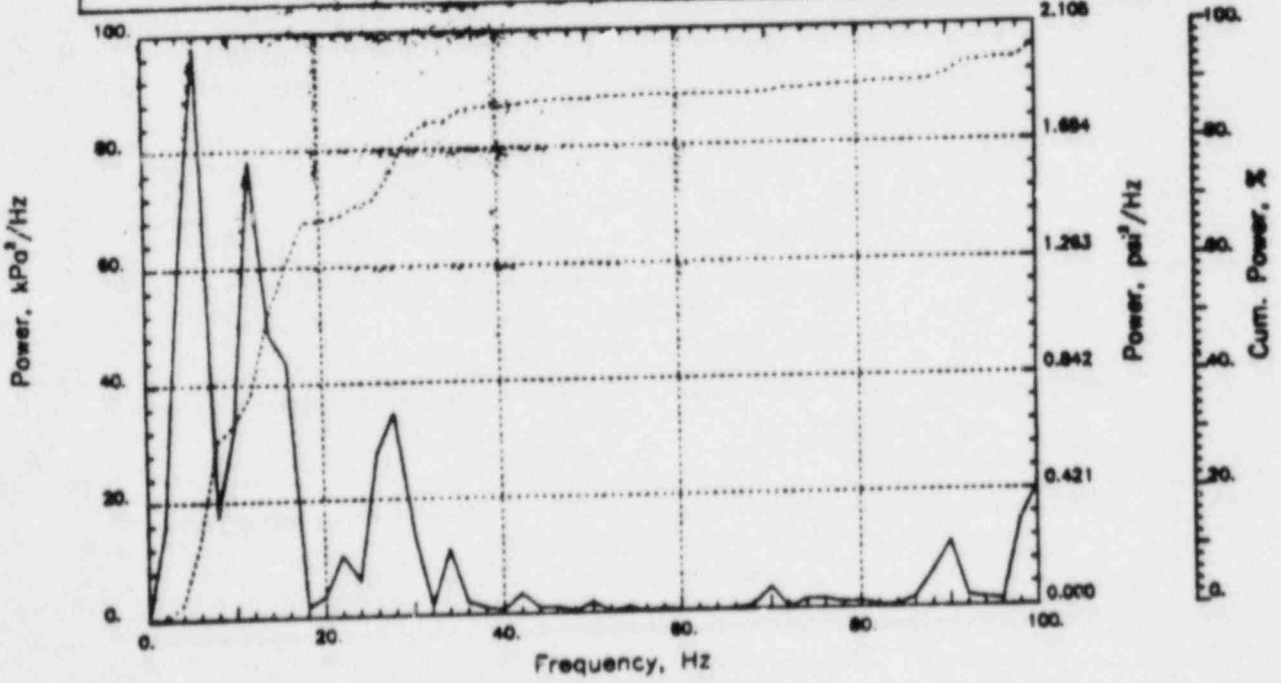

GGNS RHR CO (C=1067)

Output at point (18.90,28.00,2.82)

NAME - LEONG, TAI SENG
DATE - FEB 22, 1984
PROJECT NO. - 15026004

CHECKED _____
DATE _____
CALC NO. - AP-84-

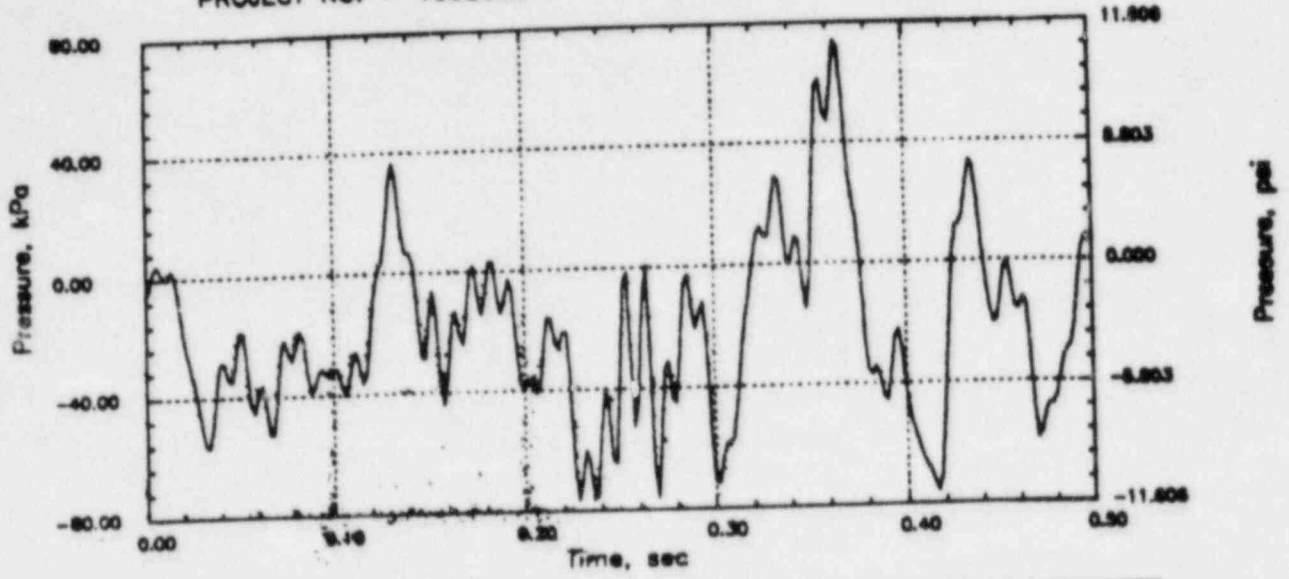

POP = 74.17 kPa PUP = -76.55 kPa MSP = 631.71 kPa²

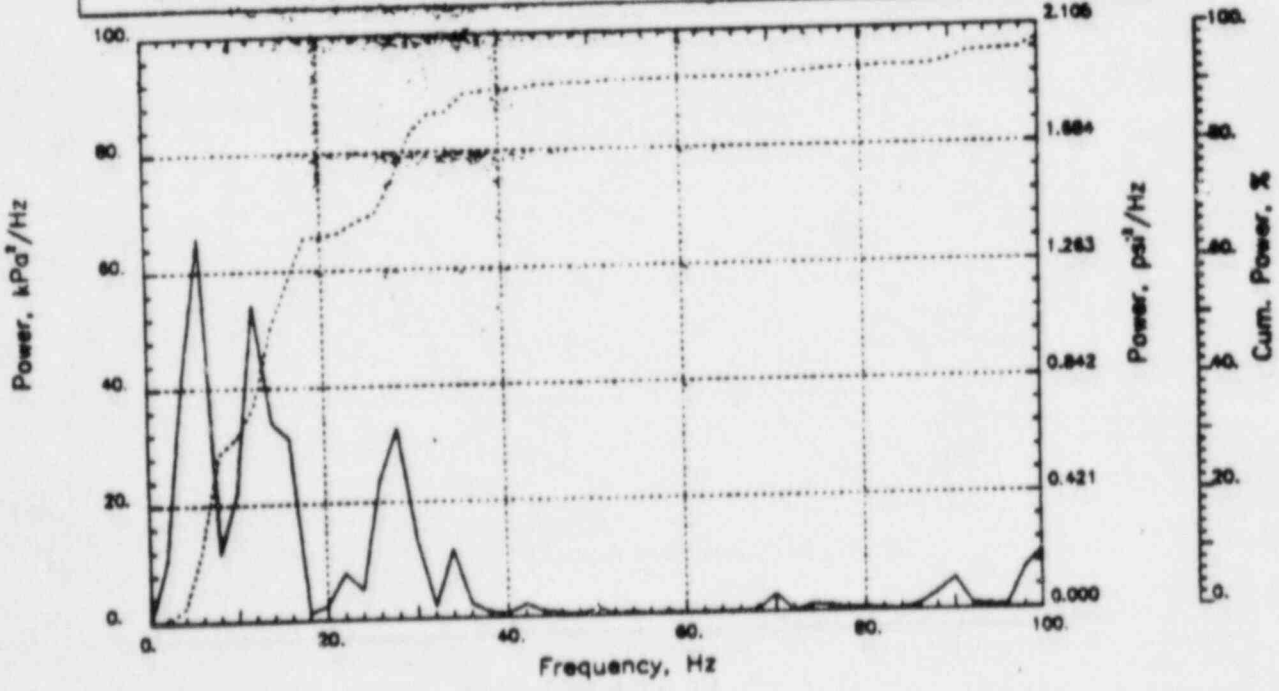

GGNS RHR CO (C=1067)

Output at point (18.90,28.00,2.18)

NAME - LEONG, TAI SENG
DATE - FEB 22, 1984
PROJECT NO. - 15026004

CHECKED _____
DATE _____
CALC NO. - AP-84-

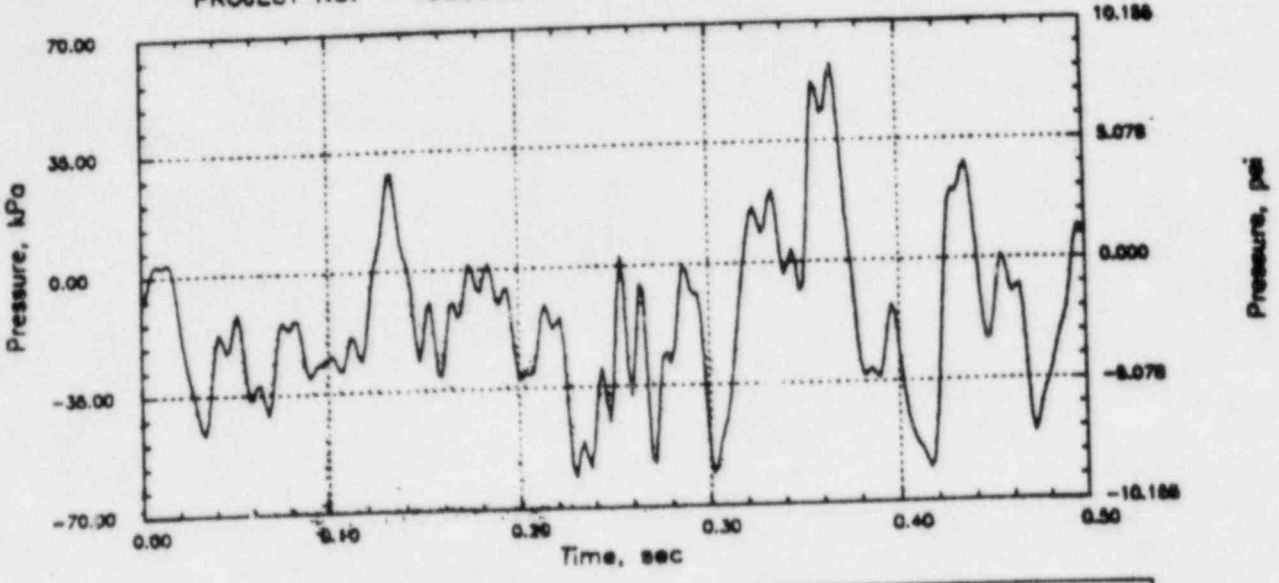

POP = 57.62 kPa PUP = -61.15 kPa MSP = 541.95 kPa²

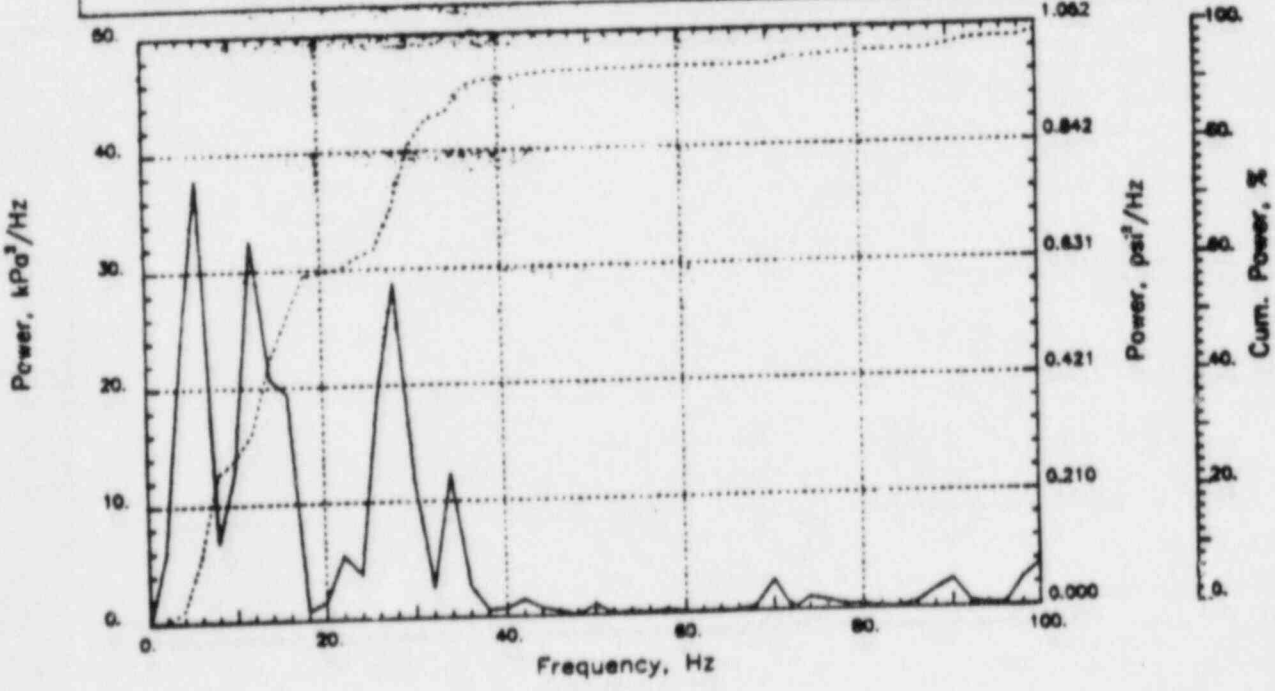

GGNS RHR CO (C=1067)

Output at point (18.90,28.00,1.55)

NAME - LEONG, TAI SENG
DATE - FEB 22, 1984
PROJECT NO. - 15026004

CHECKED _____
DATE _____
CALC NO. - AP-84-

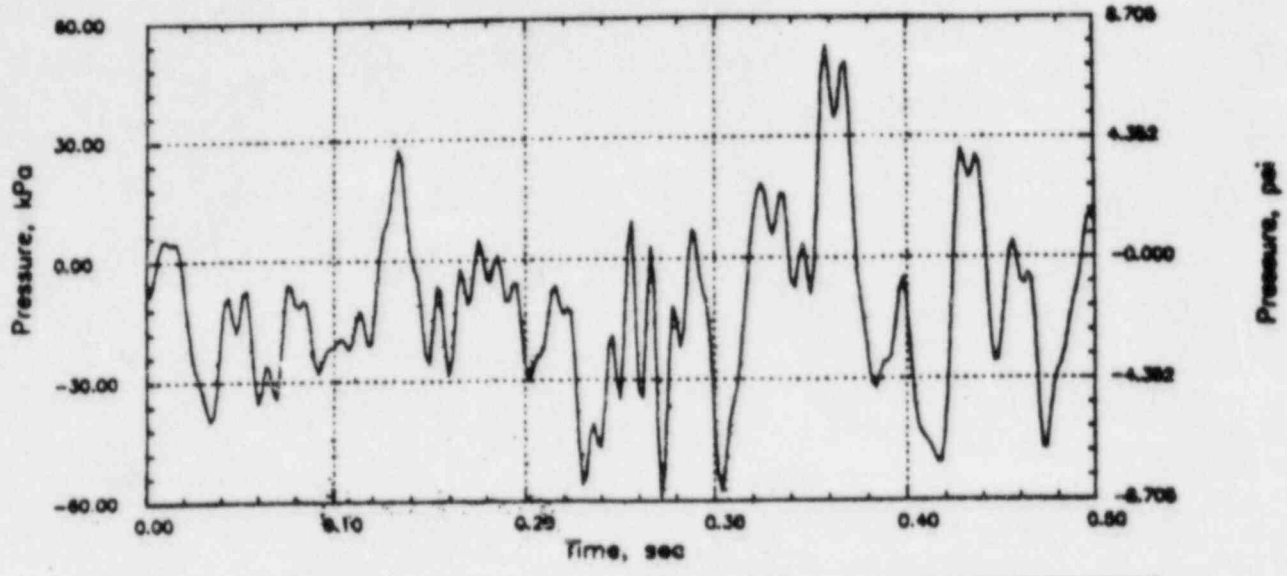

POP = 52.84 kPa PUP = -59.15 kPa MSP = 429.28 kPa²

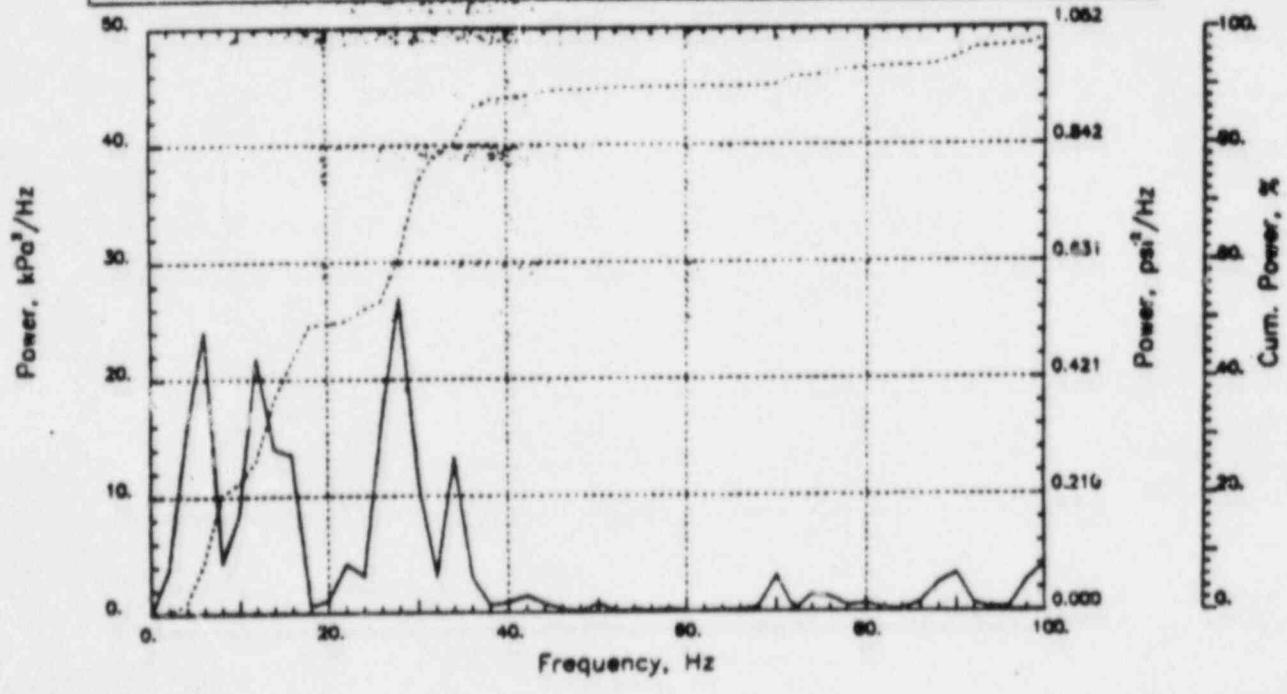

GGNS RHR CO (C=1067)

Output at point (18.90,28.00,0.91)

NAME - LEONG, TAI SENG
DATE - FEB 22, 1984
PROJECT NO. - 15026004

CHECKED _____
DATE _____
CALC NO. - AP-84-

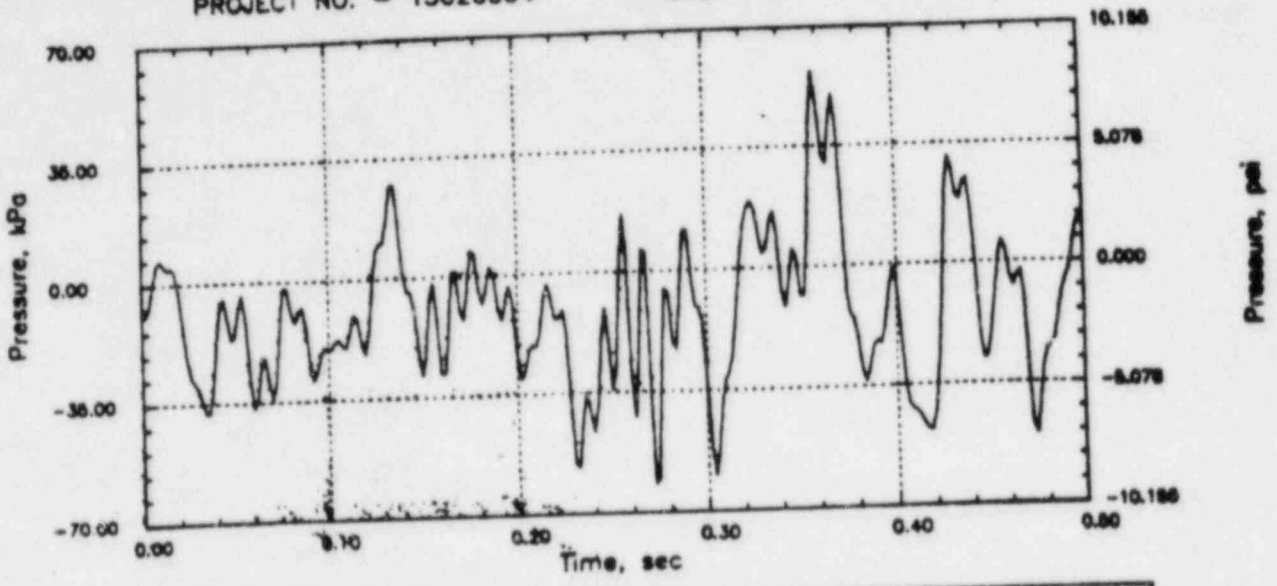

POP = 56.85 kPa PUP = -61.49 kPa MSP = 429.61 kPa²

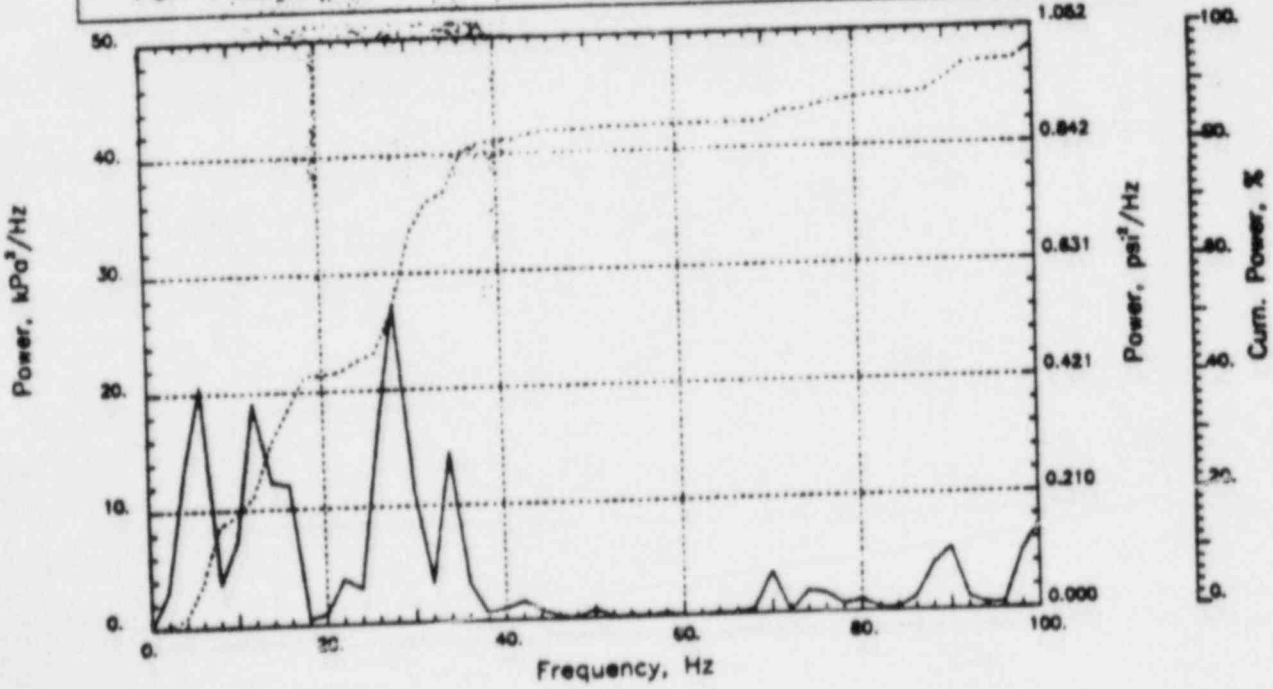

GGNS RHR CO (C=1067)

Output at point (18.90,28.00,0.46)

NAME - LEONG, TAI SENG
DATE - FEB 22, 1984
PROJECT NO. - 15026004

CHECKED _____
DATE _____
CALC NO. - AP-84-

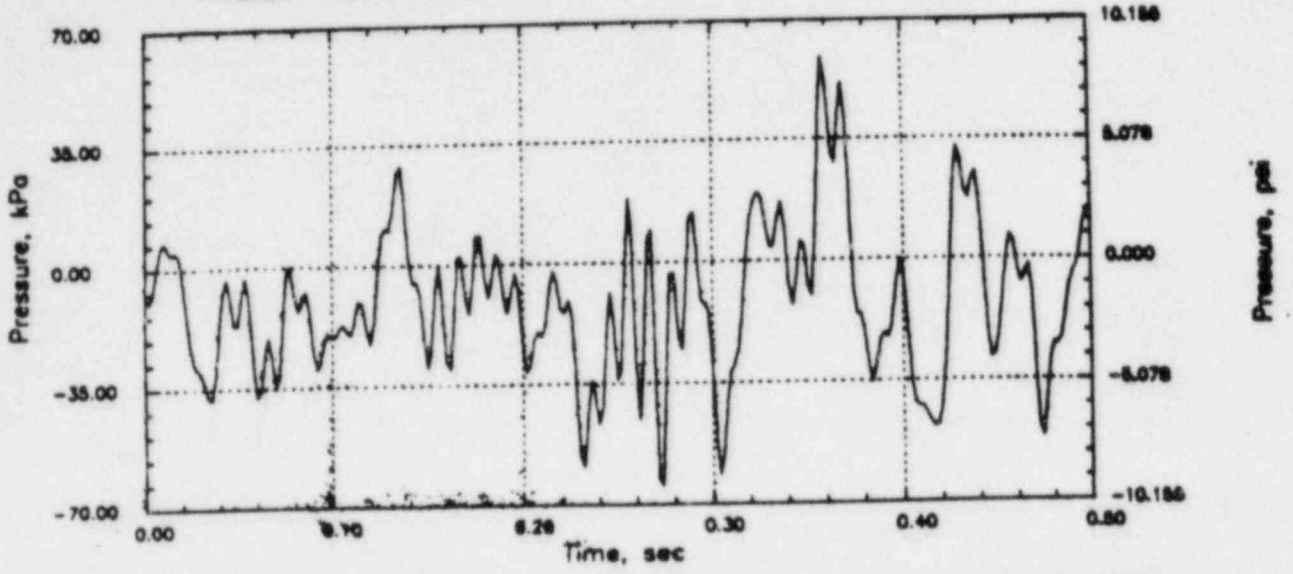

POP = 59.22 kPa PUP = -64.58 kPa MSP = 449.66 kPa²

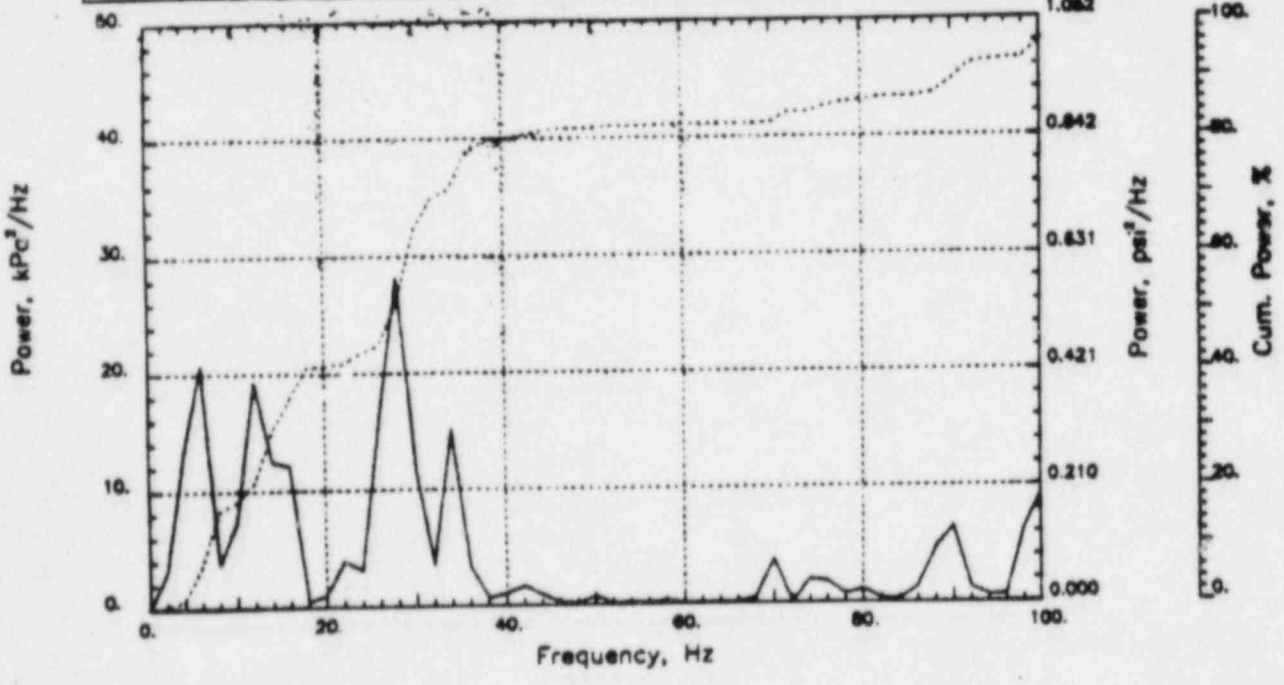

GGNS RHR CO (C=1067)

Output at point (18.90,28.00,0.00)

NAME - LEONG, TAI SENG
DATE - FEB 22, 1984
PROJECT NO. - 15026004

CHECKED _____
DATE _____
CALC NO. - AP-84-

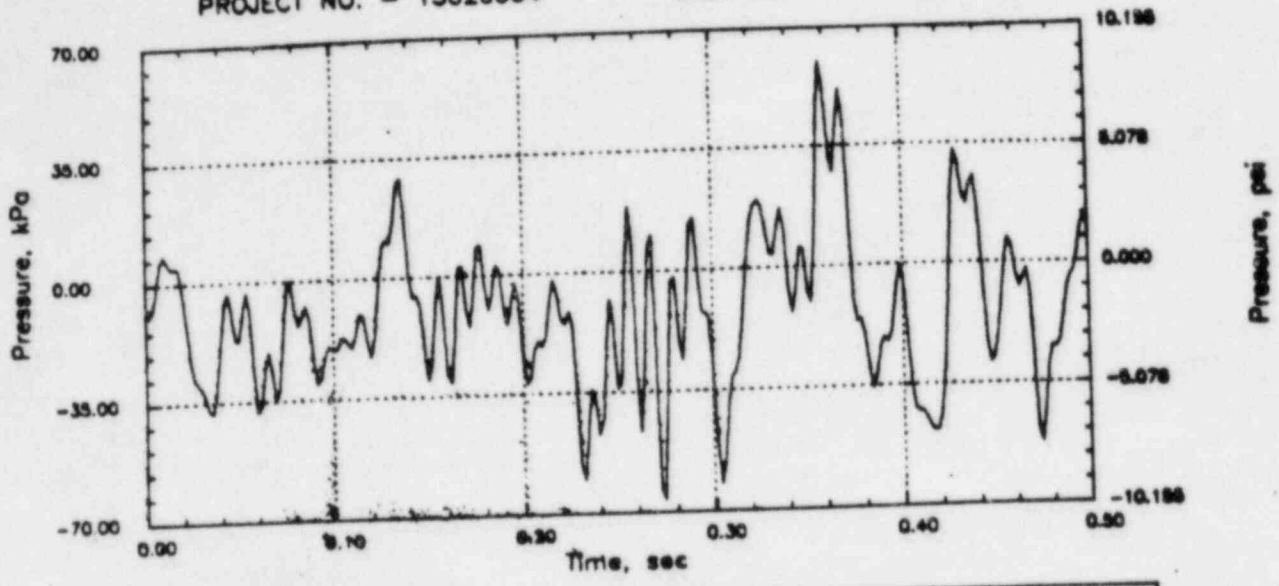

POP = 60.13 kPa PUP = -66.19 kPa MSP = 459.26 kPa²

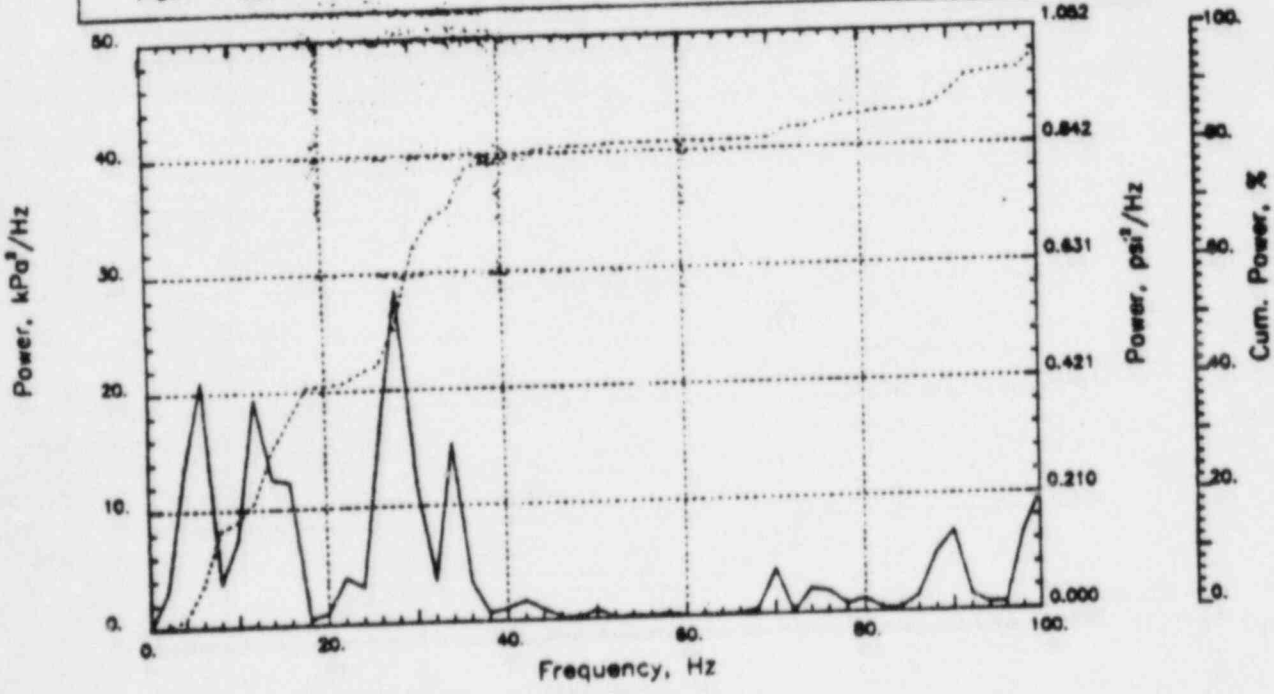

GGNS RHR CO (C=1067)

Output at point (17.34,28.00,0.00)

NAME - LEONG, TAI SENG
DATE - FEB 22, 1984
PROJECT NO. - 15026004

CHECKED _____
DATE _____
CALC NO. - AP-84-

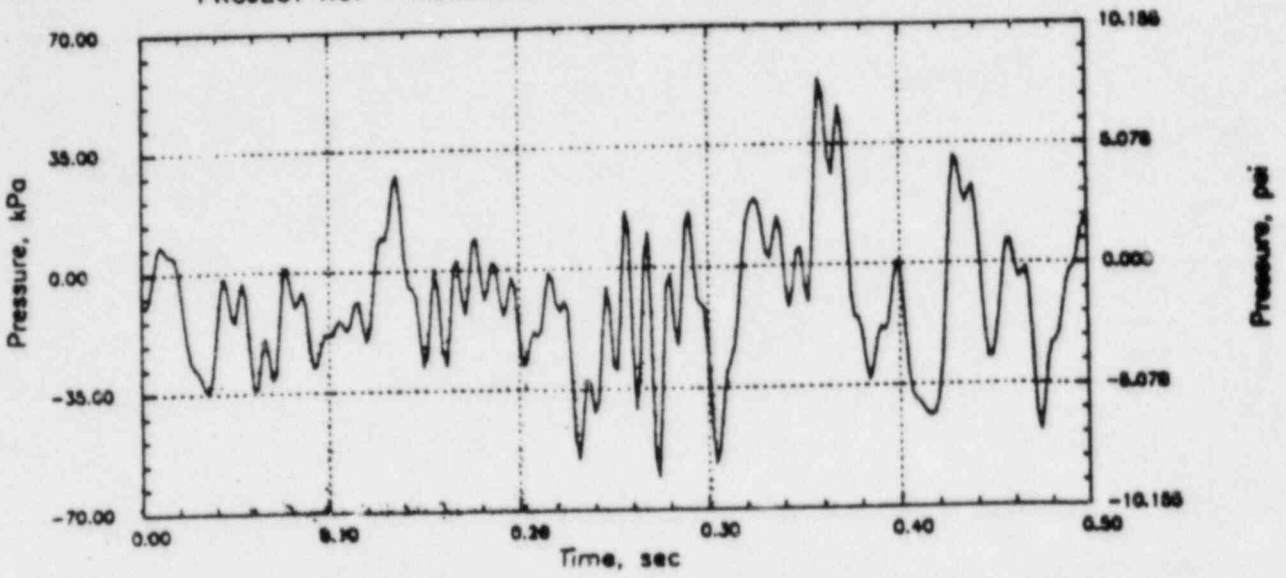

POP = 54.09 kPa PUP = -60.67 kPa MSP = 385.95 kPa²

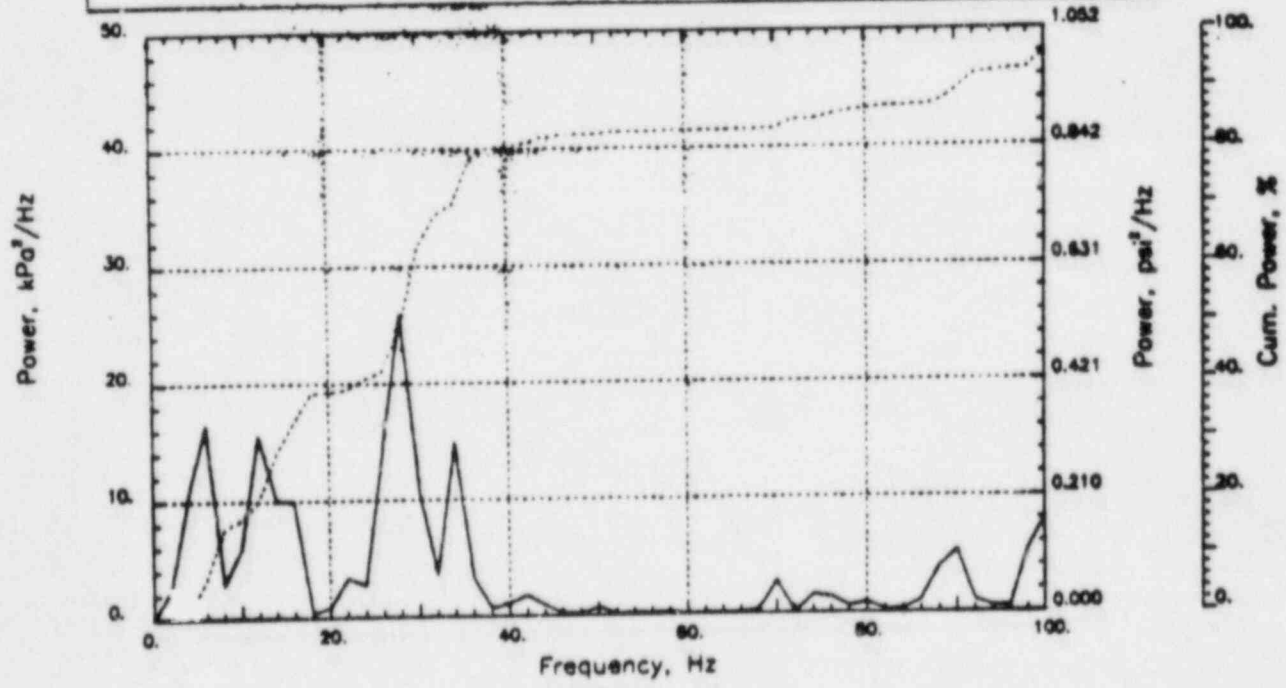

GGNS RHR CO (C=1067)

Output at point (15.77,28.00,0.00)

NAME - LEONG, TAI SENG
DATE - FEB 22, 1984
PROJECT NO. - 15026004

CHECKED _____
DATE _____
CALC NO. - AP-84-

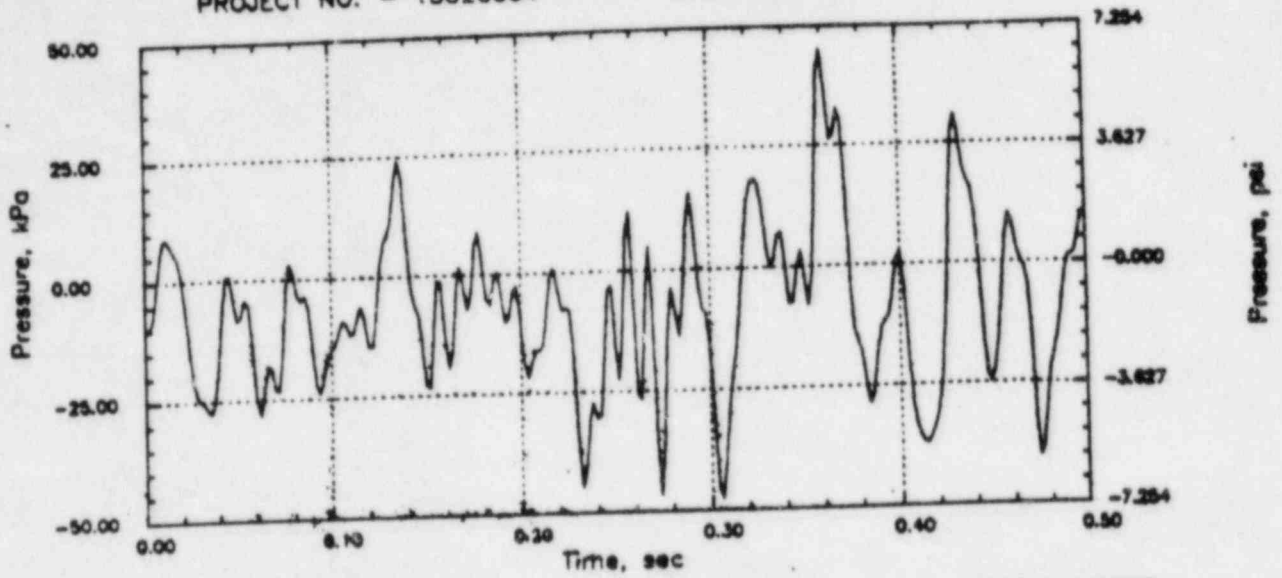

POP = 45.10 kPa PUP = -47.67 kPa MSP = 266.54 kPa²

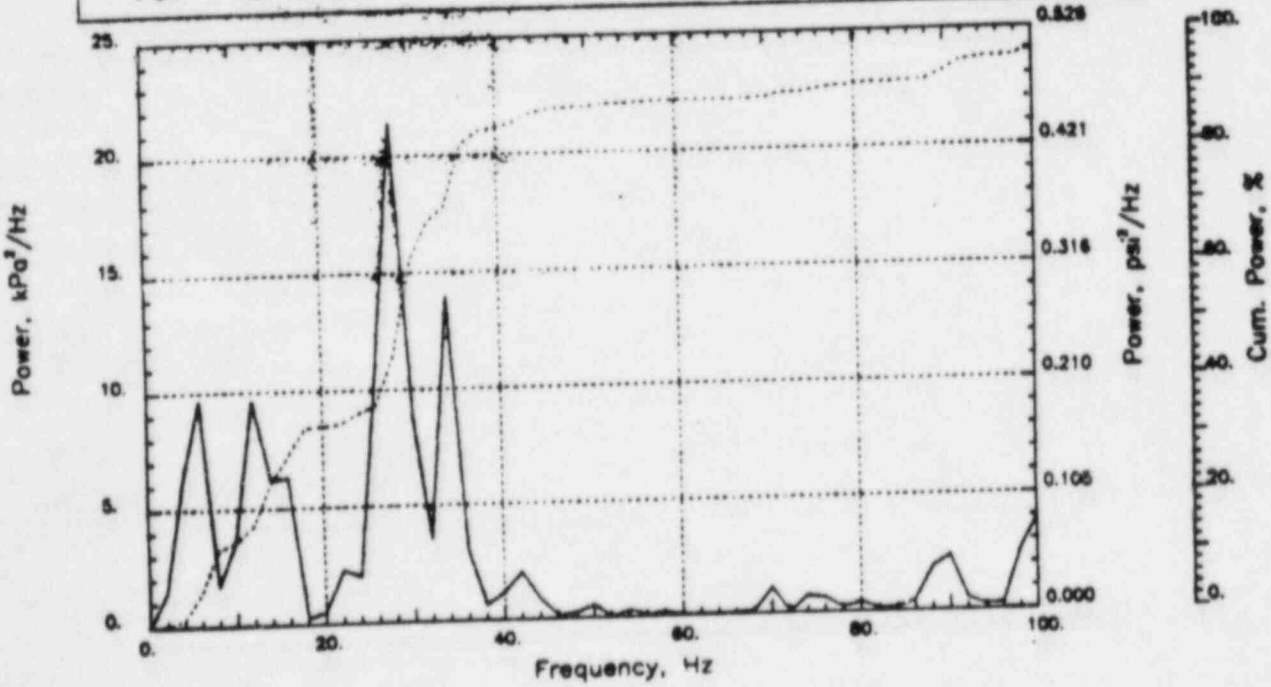

GGNS RHR CO (C=1067)

Output at point (14.21,28.00,0.00)

NAME - LEONG, TAI SENG
DATE - FEB 22, 1984
PROJECT NO. - 15026004

CHECKED _____
DATE _____
CALC NO. - AP-84-

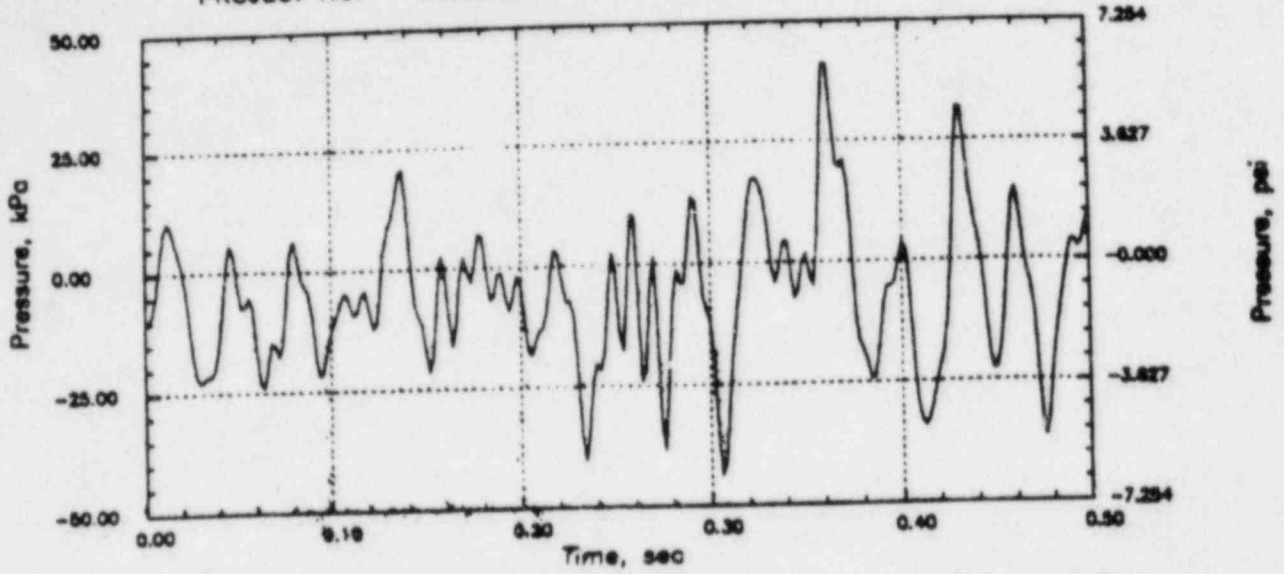

POP = 41.08 kPa PUP = -43.55 kPa MSP = 207.75 kPa²

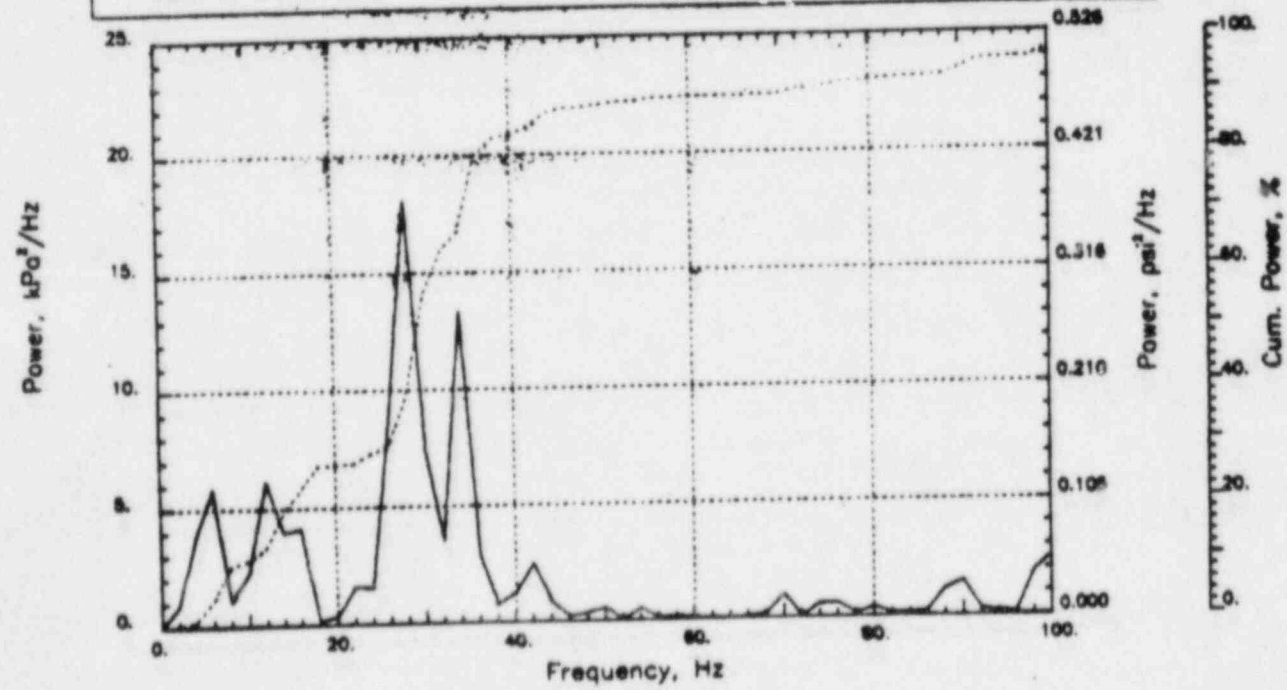

GGNS RHR CO (C=1067)

Output at point (12.65,28.00,0.00)

NAME - LEONG, TAI SENG
DATE - FEB 22, 1984
PROJECT NO. - 15026004

CHECKED _____
DATE _____
CALC NO. - AP-84-

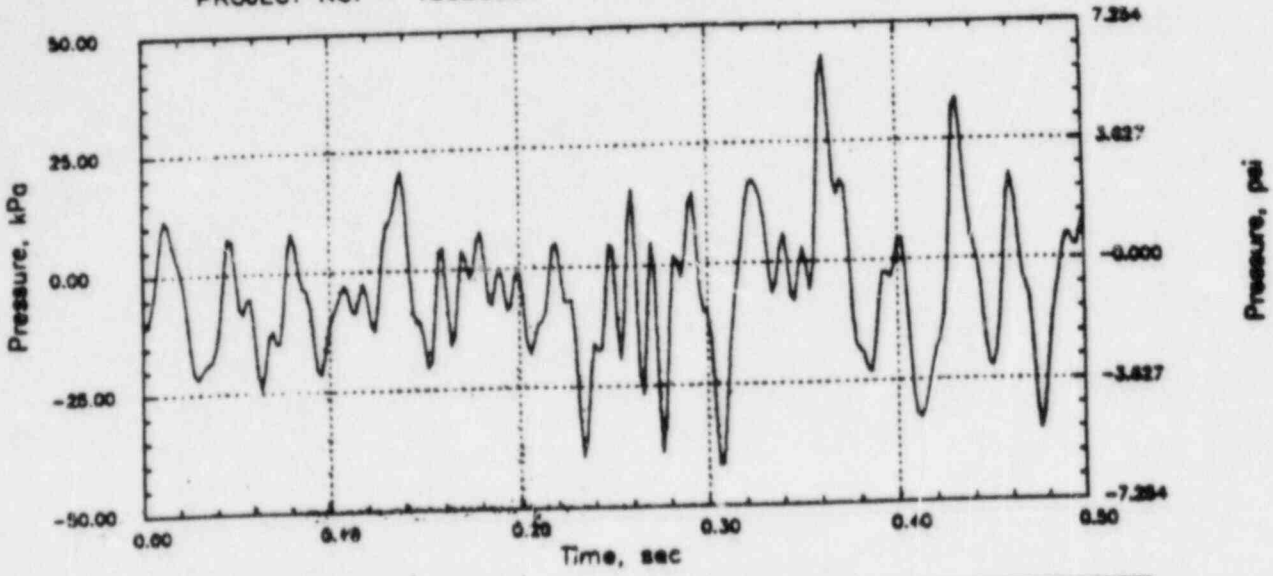

POP = 43.11 kPa PUP = -41.53 kPa MSP = 196.81 kPa²

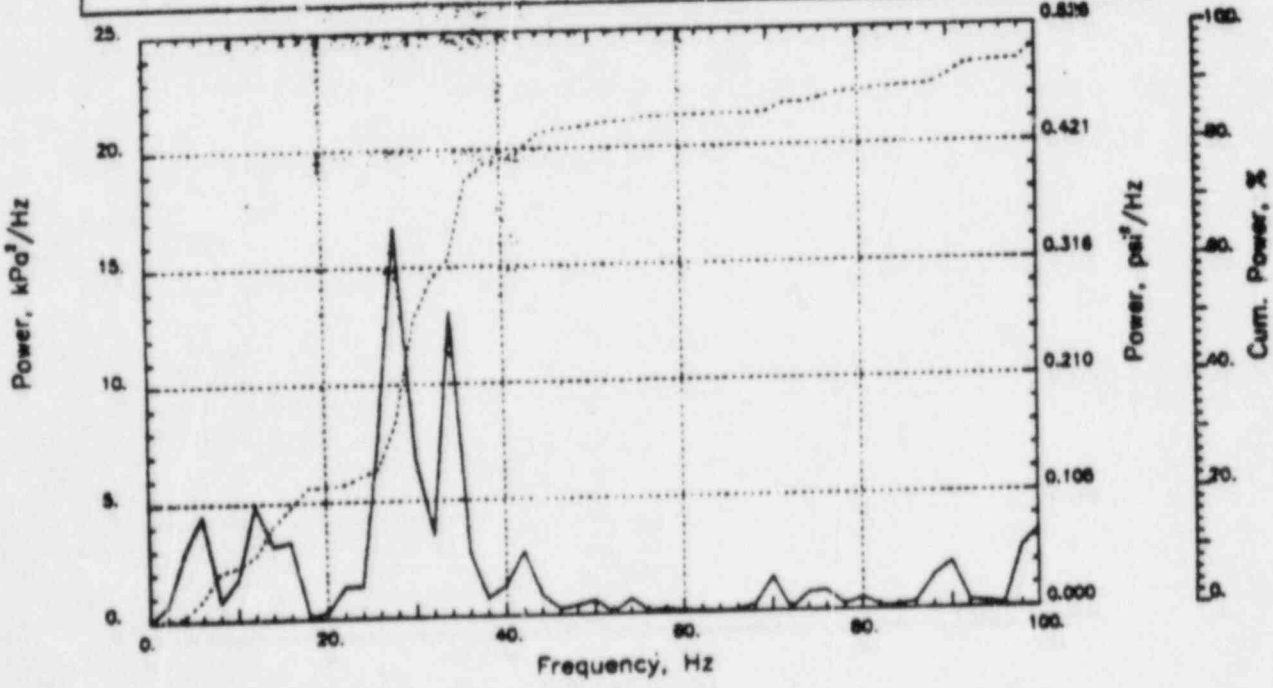

GGNS RHR CO (C=1067)

Output at point (12.65,28.00,0.46)

NAME - LEONG, TAI SENG
DATE - FEB 22, 1984
PROJECT NO. - 15026004

CHECKED _____
DATE _____
CALC NO. - AP-84-

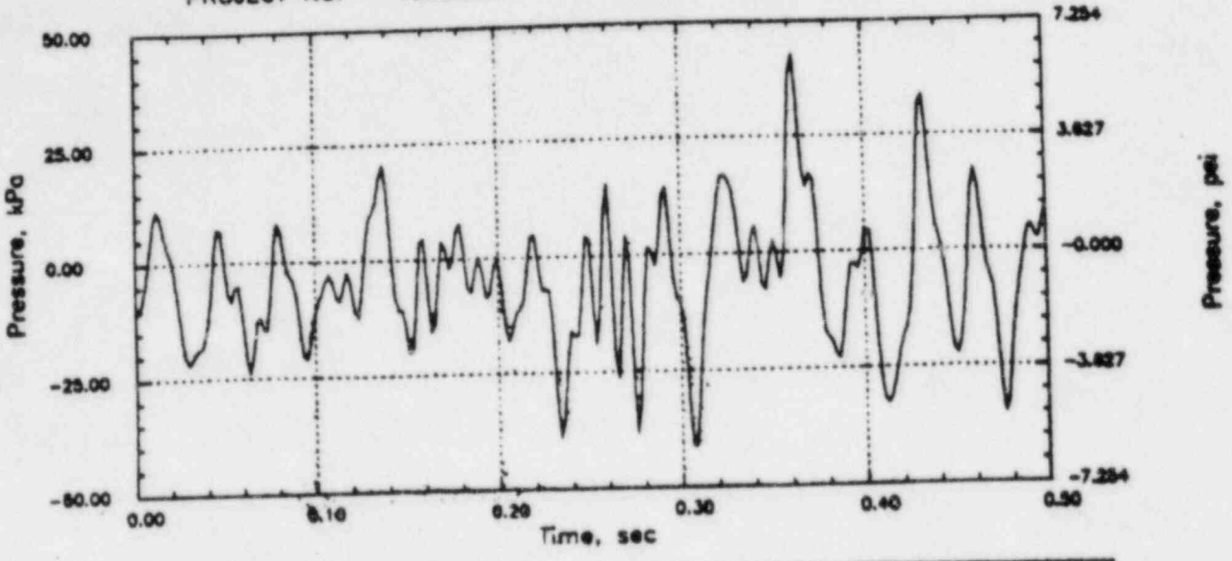

POP = 42.68 kPa PUP = -41.10 kPa MSP = 193.24 kPa²

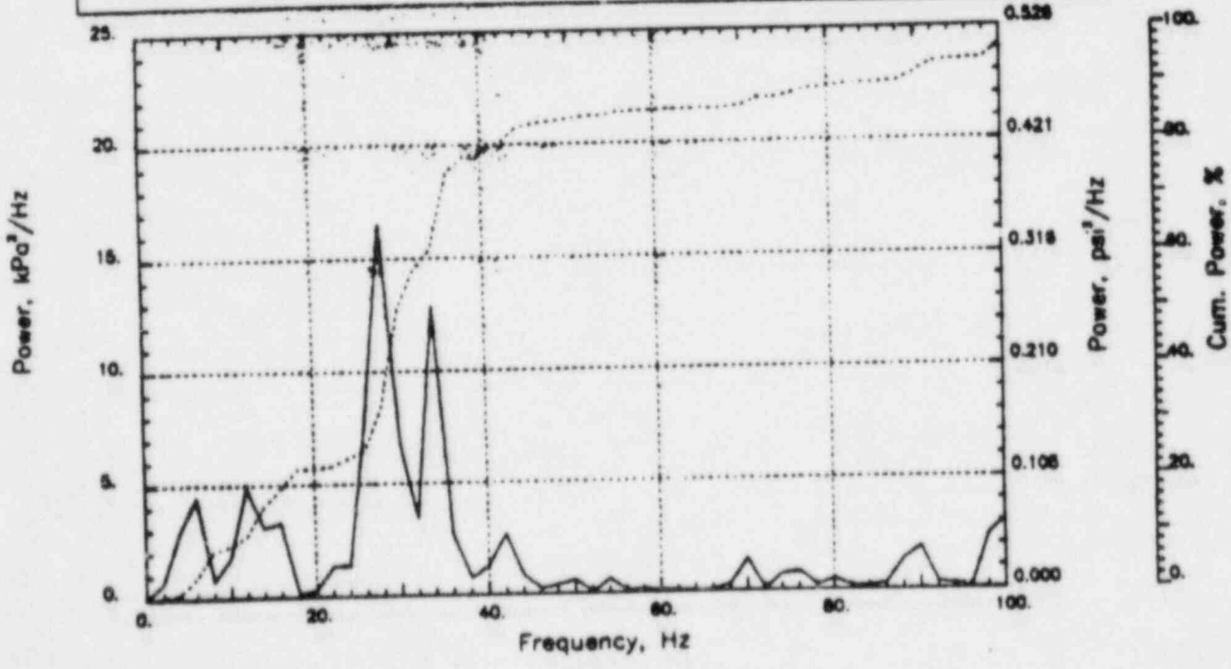

GGNS RHR CO (C=1067)

Output at point (12.65,28.00,0.91)

NAME - LEONG, TAI SENG
DATE - FEB 22, 1984
PROJECT NO. - 15026004

CHECKED _____
DATE _____
CALC NO. - AP-84-

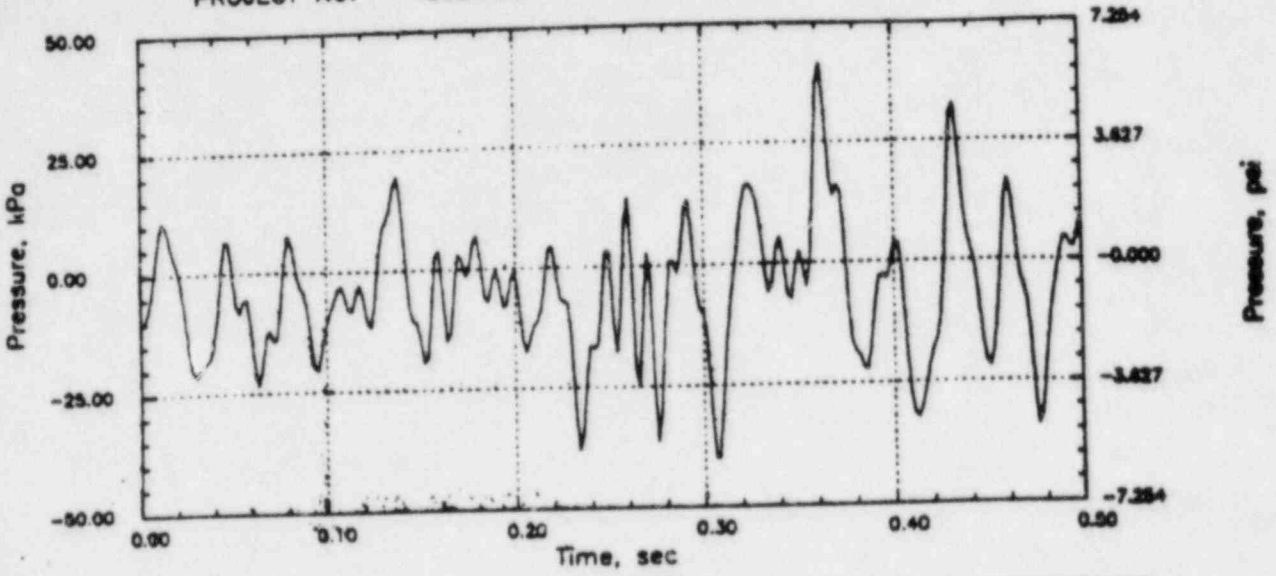

POP = 41.42 kPa PUP = -39.91 kPa MSP = 182.84 kPa²

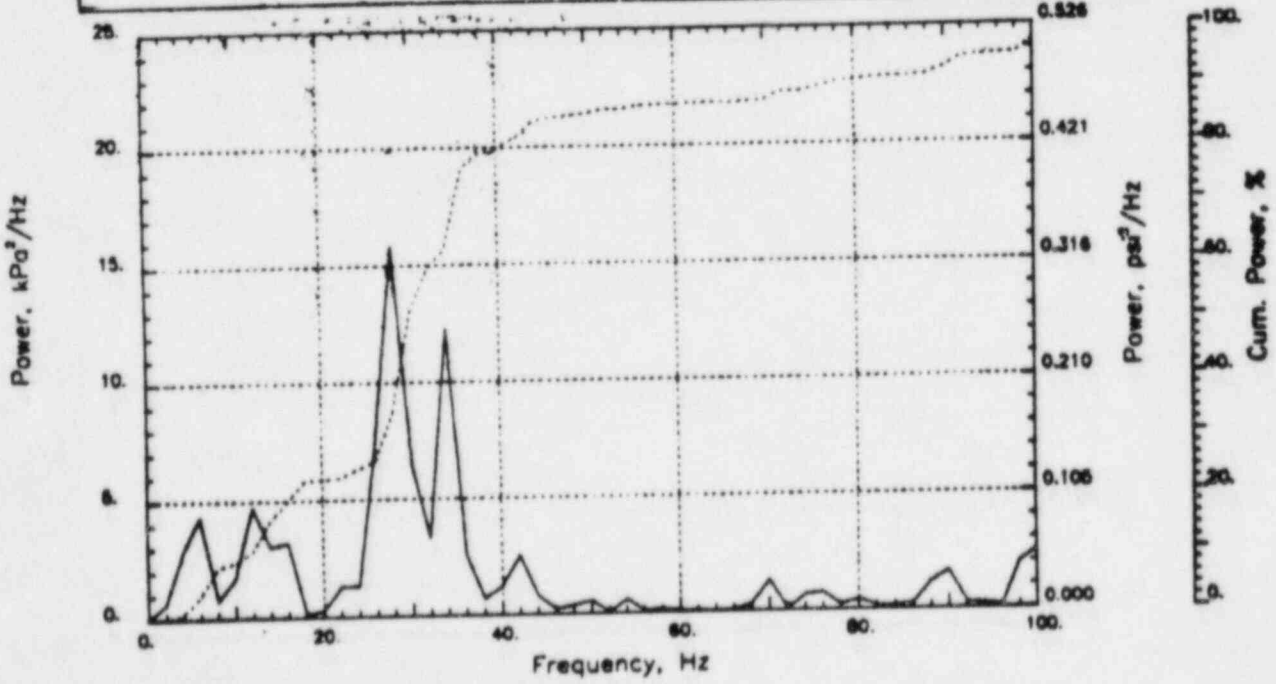

GGNS RHR CO (C=1067)

Output at point (12.65,28.00,1.55)

NAME - LEONG, TAI SENG
DATE - FEB 22, 1984
PROJECT NO. - 15026004

CHECKED _____
DATE _____
CALC NO. - AP-84-

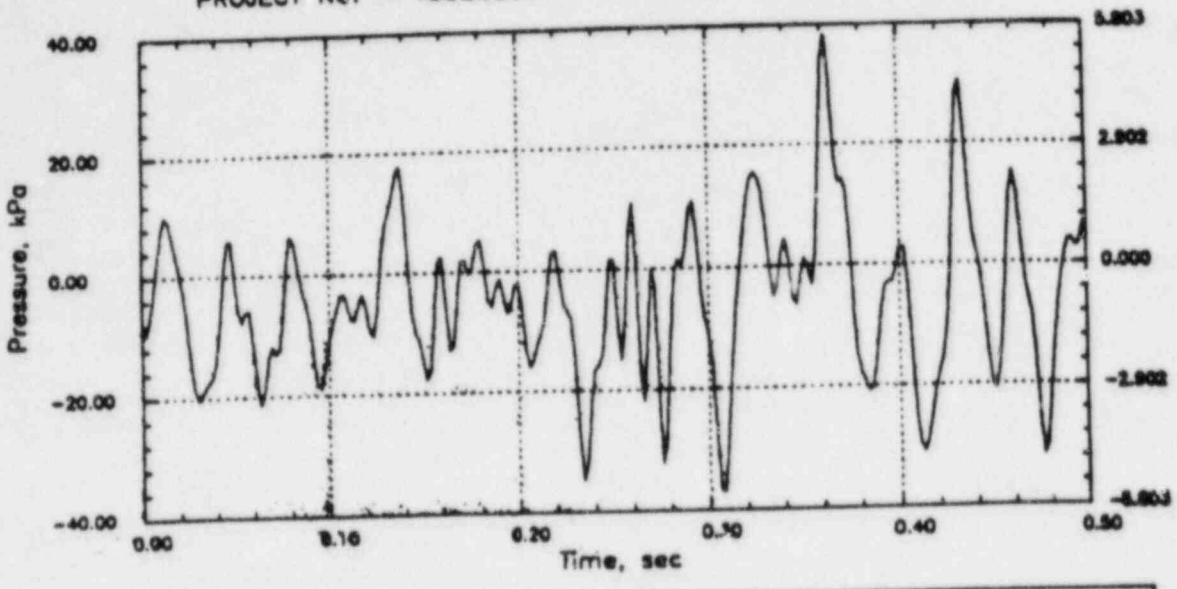

POP = 38.26 kPa PUP = -37.06 kPa MSP = 158.87 kPa²

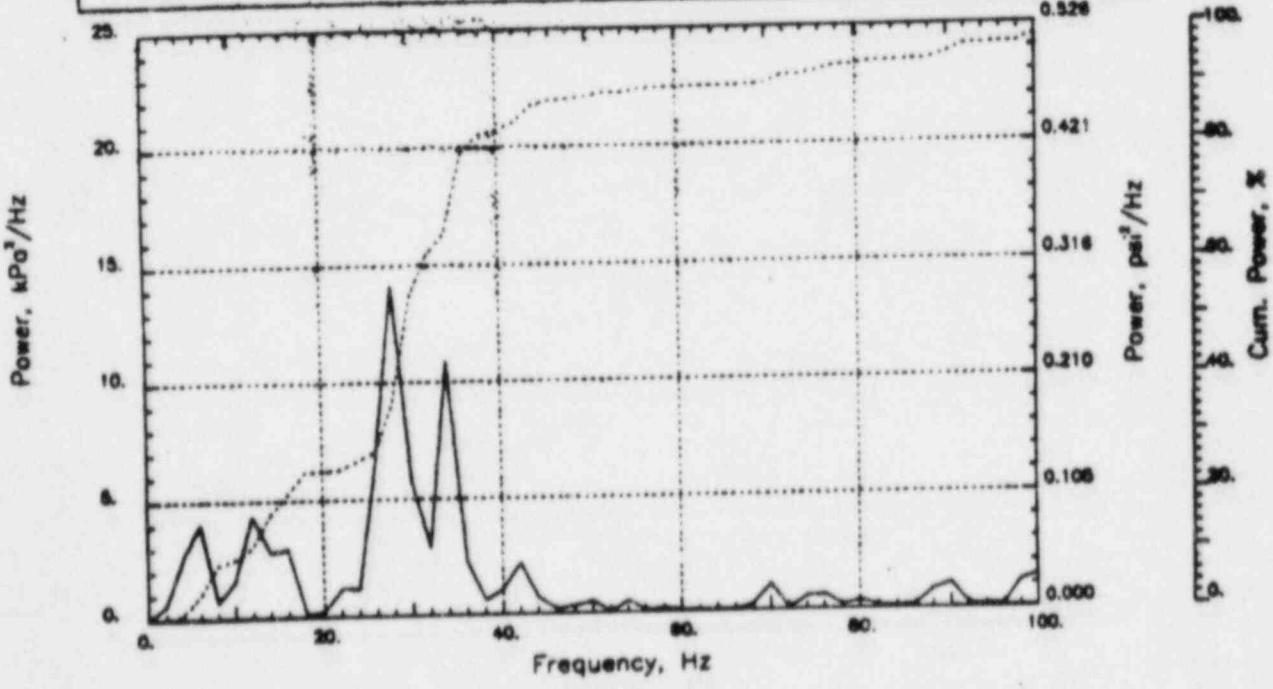

GGNS RHR CO (C=1067)

Output at point (12.65,28.00,2.18)

NAME - LEONG, TAI SENG
DATE - FEB 22, 1984
PROJECT NO. - 15026004

CHECKED _____
DATE _____
CALC NO. - AP-84-

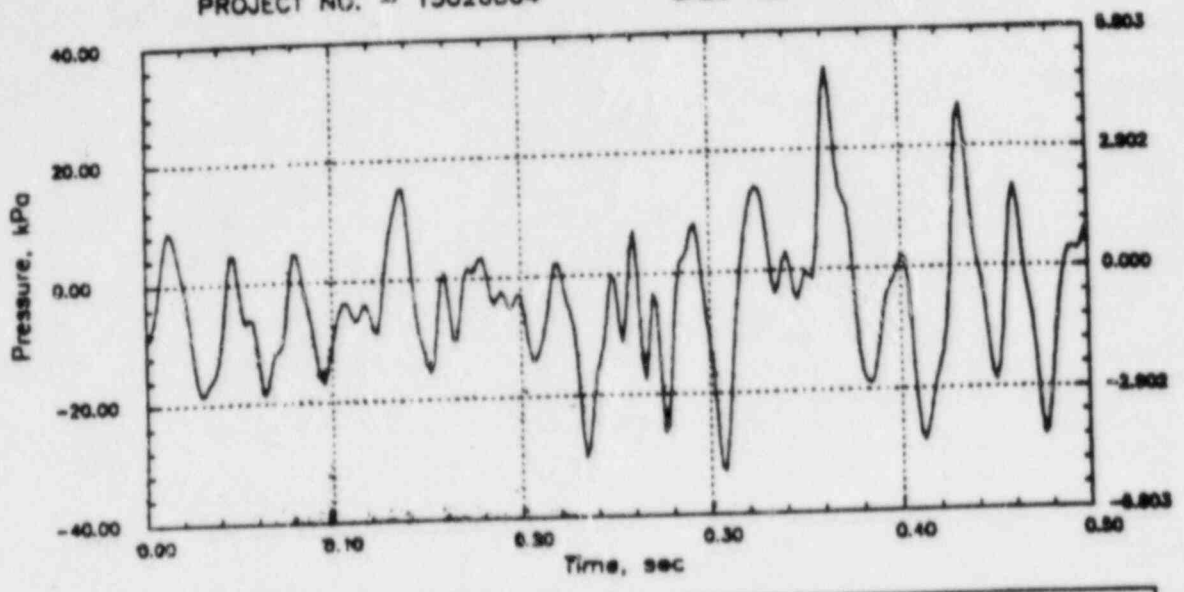

POP = 33.60 kPa PUP = -32.84 kPa MSP = 127.40 kPa²

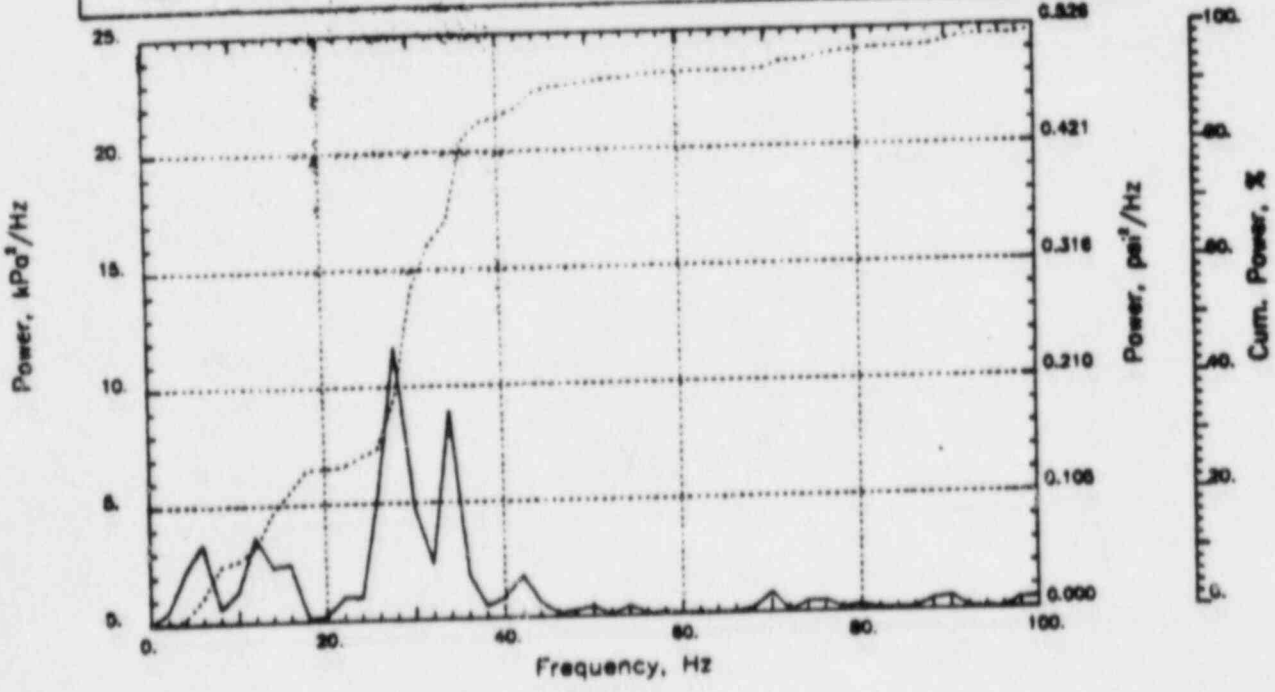

GGNS RHR CO (C=1067)

Output at point (12.65,28.00,2.82)

NAME - LEONG, TAI SENG
DATE - FEB 22, 1984
PROJECT NO. - 15026004

CHECKED _____
DATE _____
CALC NO. - AP-84-

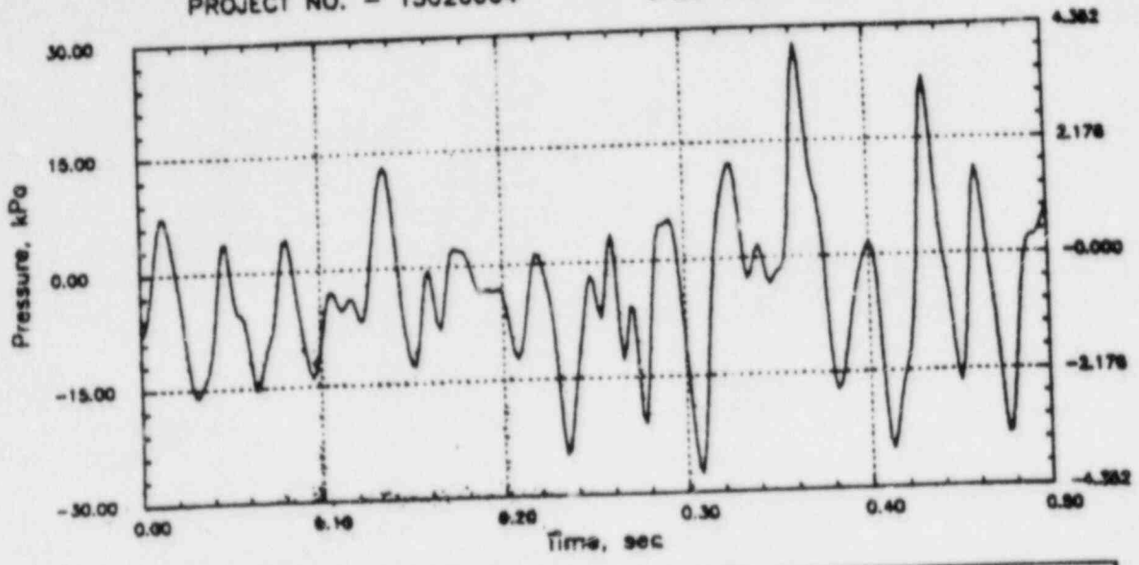

POP = 27.77 kPa PUP = -27.50 kPa MSP = 93.08 kPa²

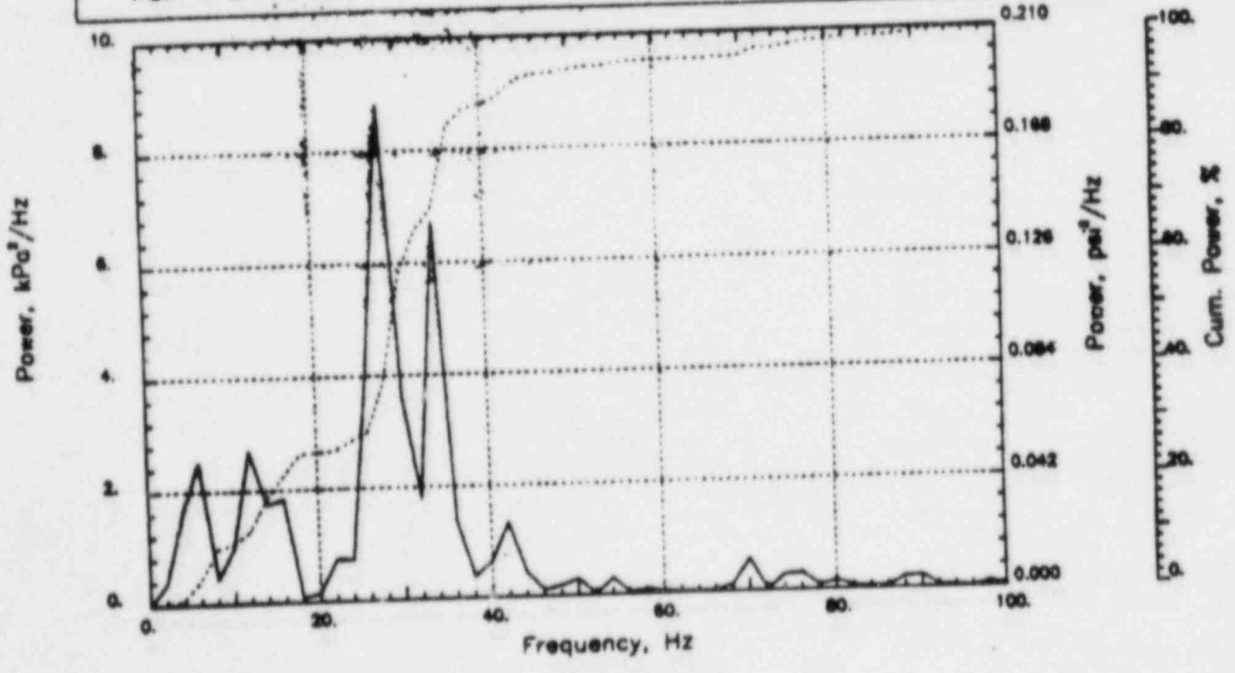

GGNS RHR CO (C=1067)

Output at point (12.65,28.00,3.45)

NAME - LEONG, TAI SENG
DATE - FEB 22, 1984
PROJECT NO. - 15026004

CHECKED _____
DATE _____
CALC NO. - AP-84-

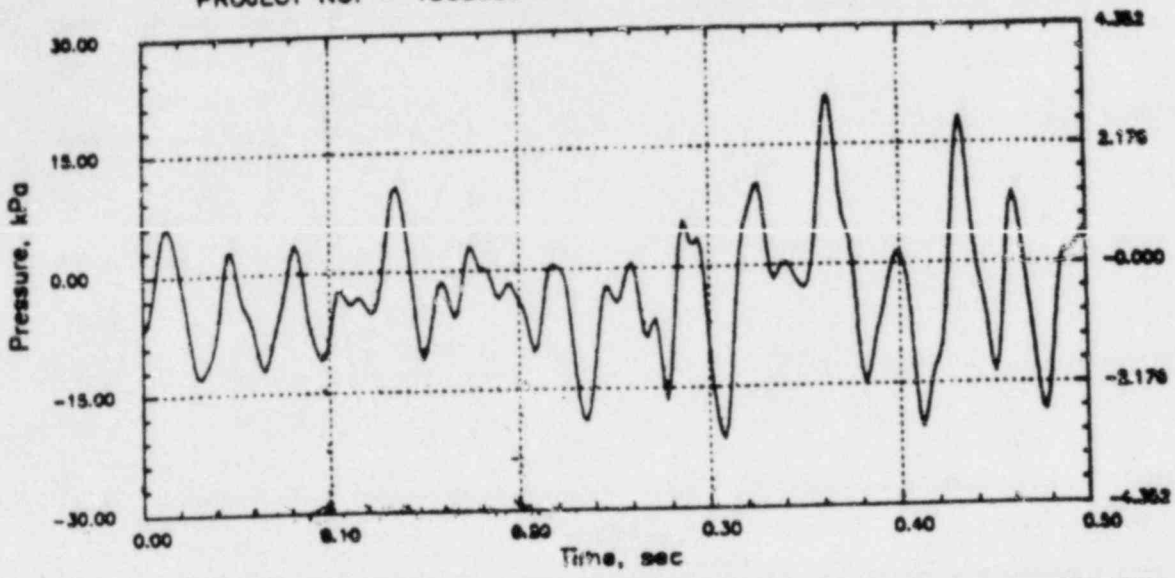

POP = 21.29 kPa PUP = -21.46 kPa MSP = 60.40 kPa²

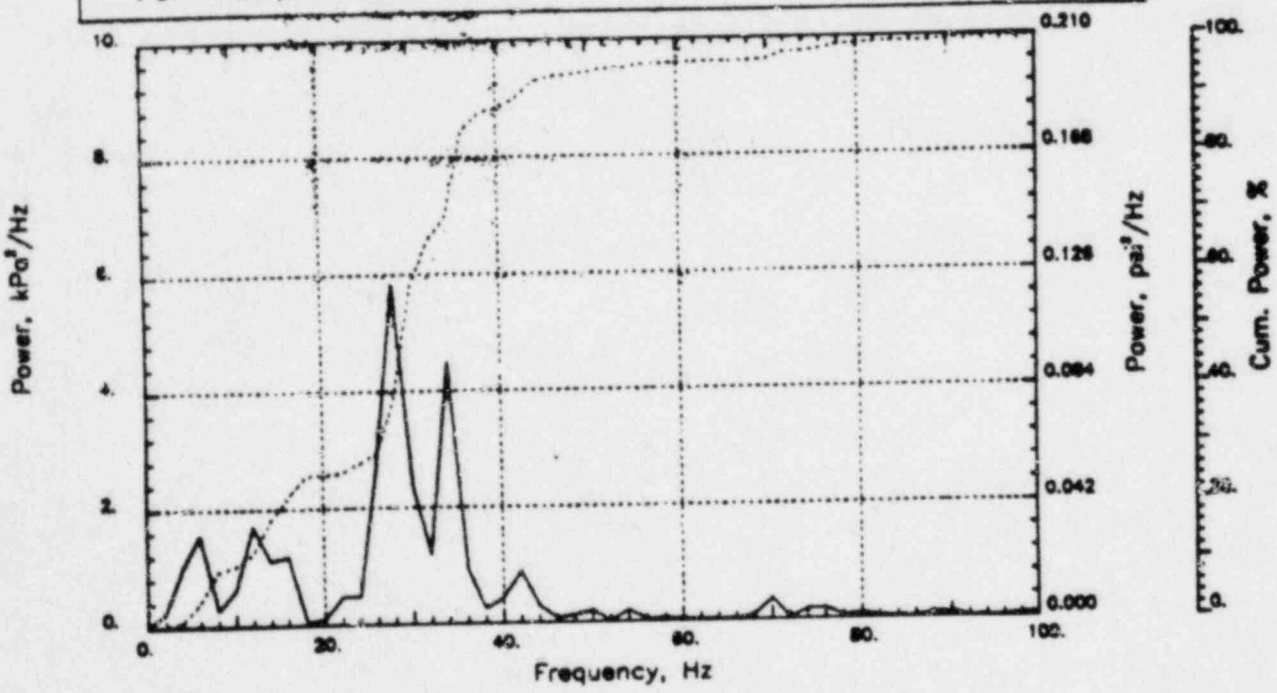

GGNS RHR CO (C=1067)

Output at point (12.65,28.00,4.09)

NAME - LEONG, TAI SENG
DATE - FEB 22, 1984
PROJECT NO. - 15026004

CHECKED _____
DATE _____
CALC NO. - AP-84-

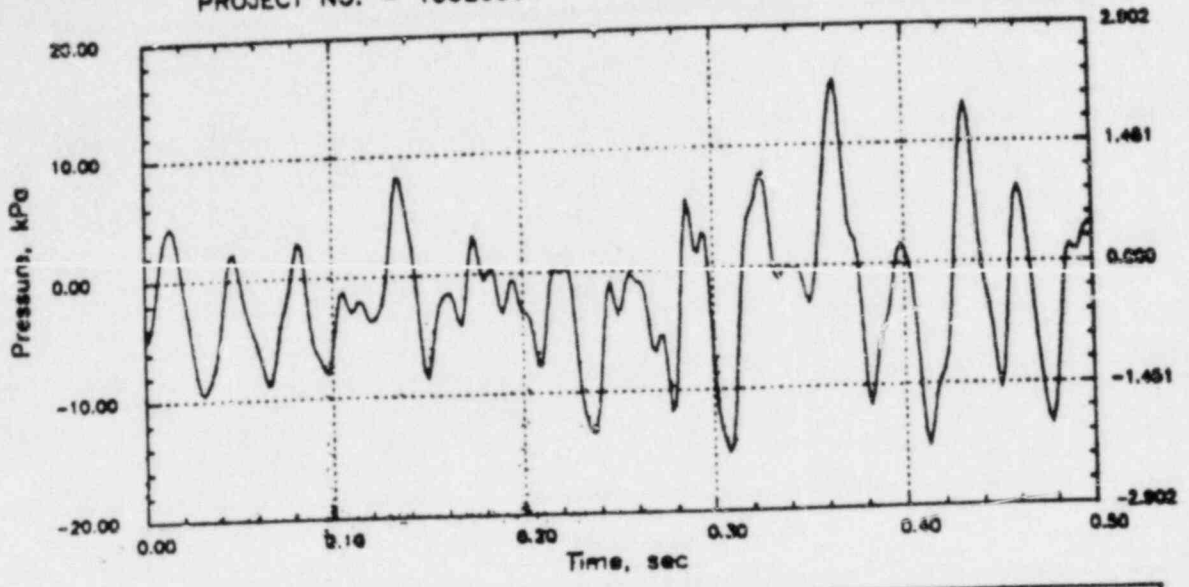

POP = 15.42 kPa PUP = -15.22 kPa MSP = 32.87 kPa²

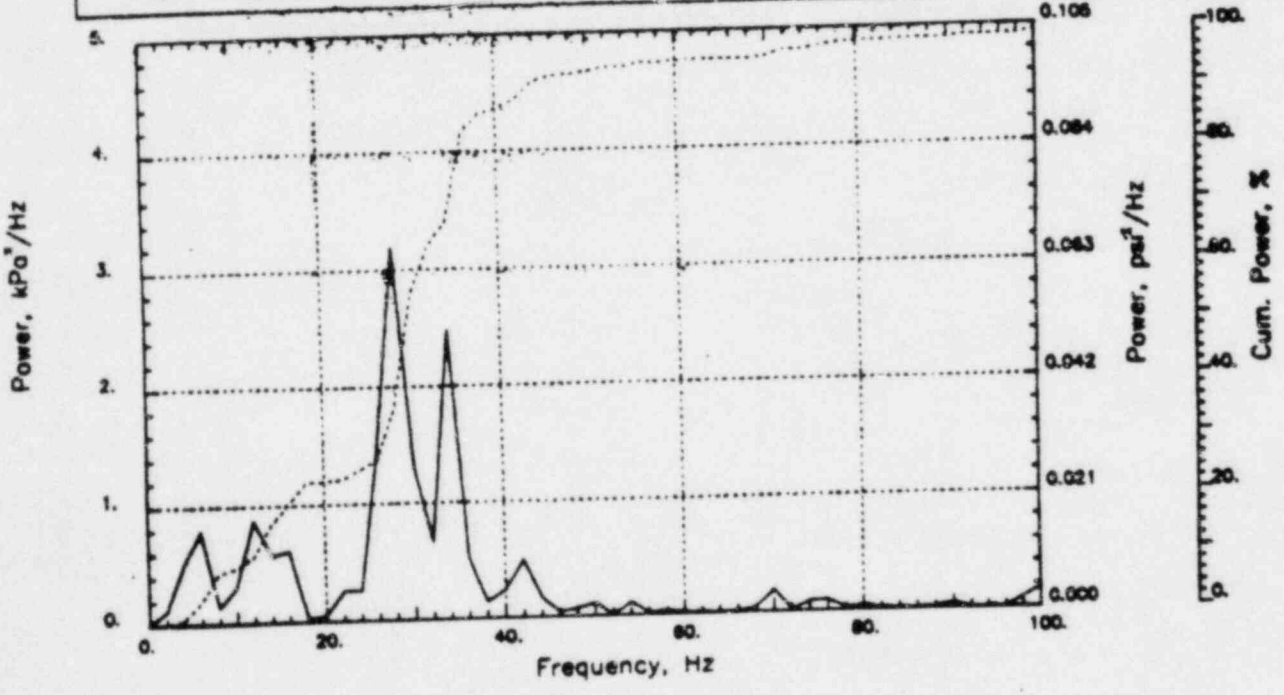

GGNS RHR CO (C=1067)

Output at point (12.65,28.00,4.91)

NAME - LEONG, TAI SENG
DATE - FEB 22, 1984
PROJECT NO. - 15026004

CHECKED _____
DATE _____
CALC NO. - AP-84-

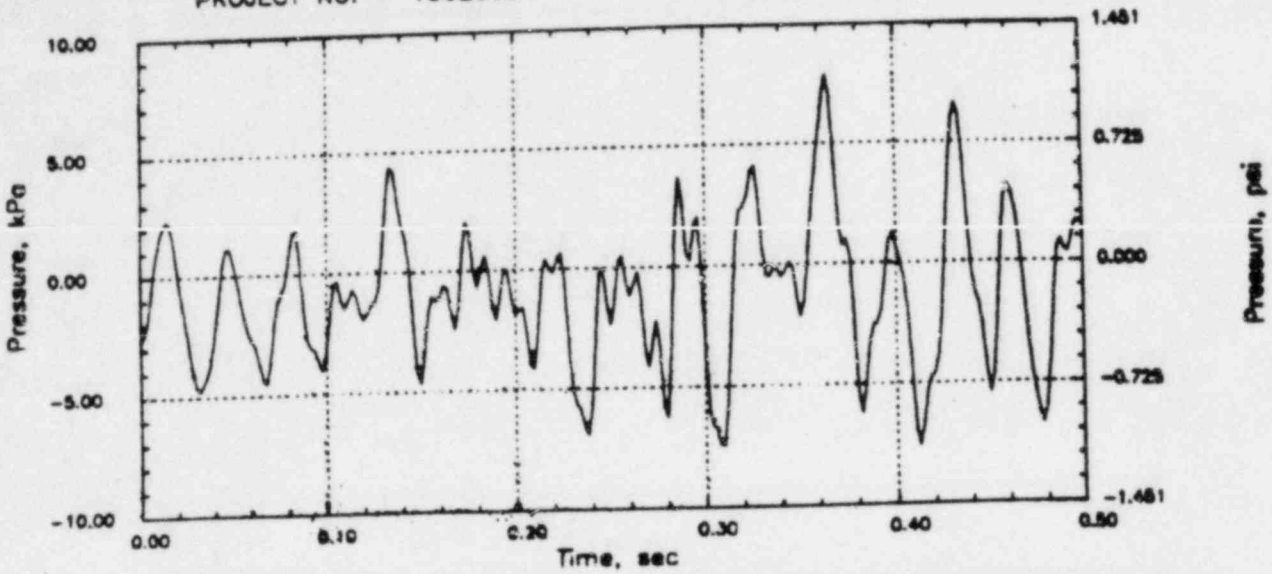

POP = 7.85 kPa PUP = -7.60 kPa MSP = 8.53 kPa²

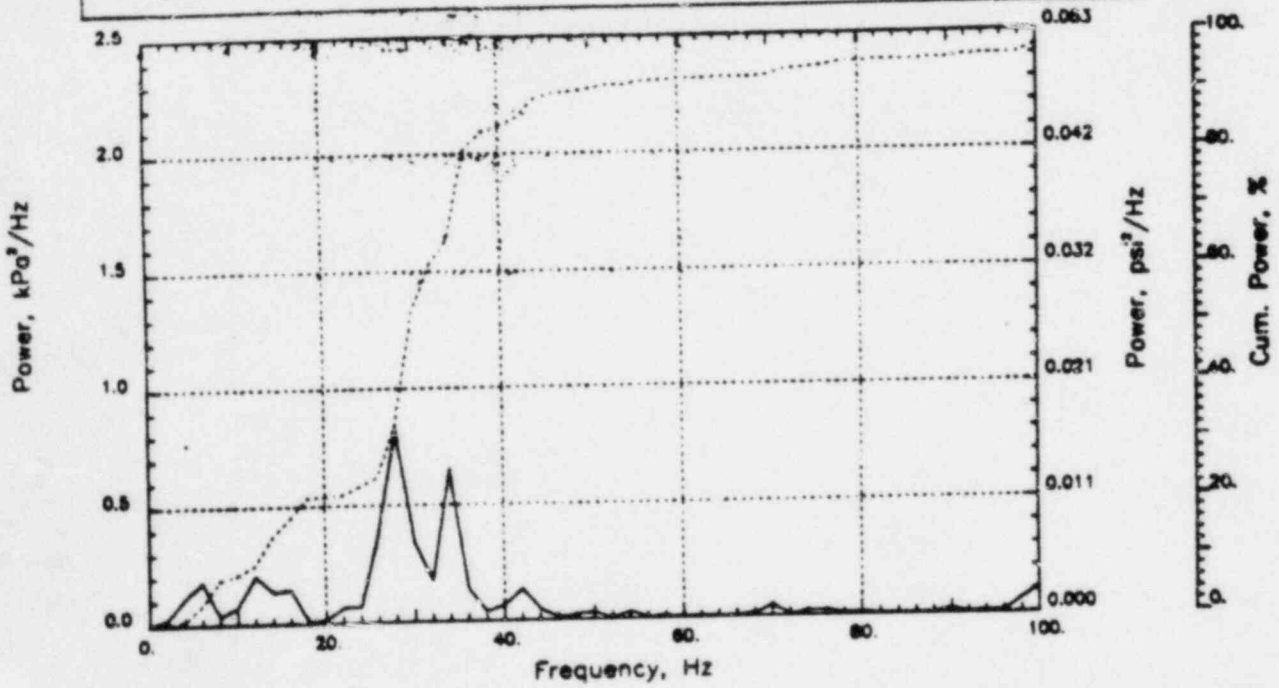

CLINTON RHR CO (C=1067)

Output at point (18.90,28.00,4.91)

NAME - LEONG, TAI SENG
DATE - FEB 22, 1984
PROJECT NO. - 15026004

CHECKED _____
DATE _____
CALC NO. - AP-84-

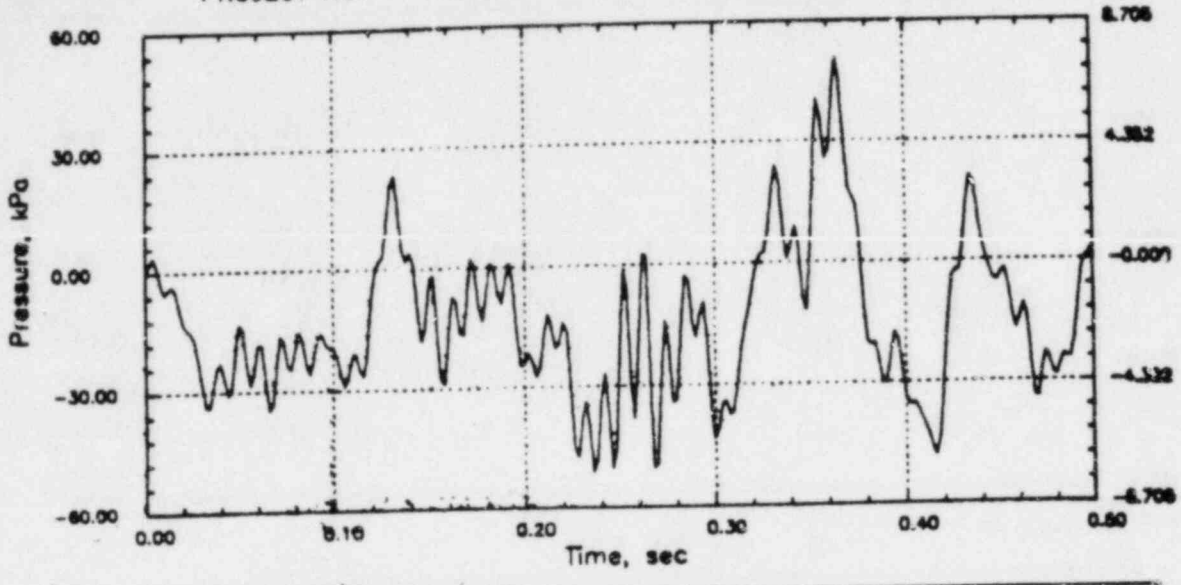

POP = 50.63 kPa PUP = -50.94 kPa MSP = 339.68 kPa²

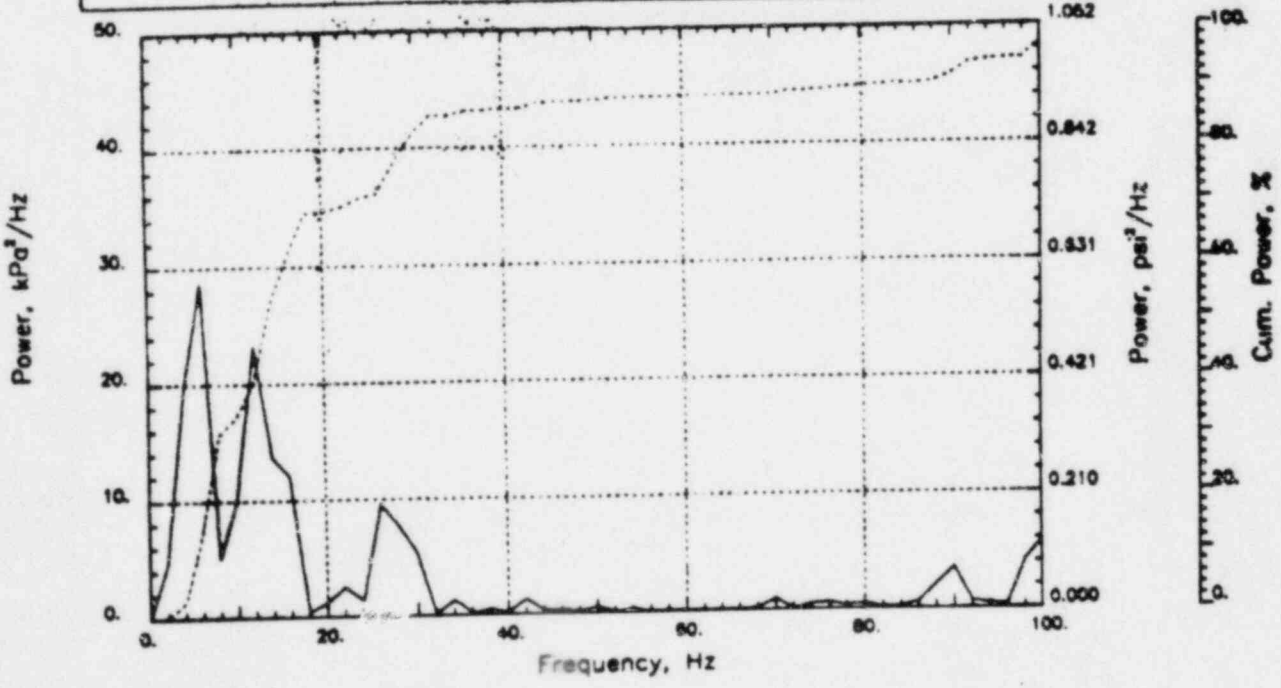

GGNS RHR CO (C=1067)

Output at point (18.90,28.00,4.91)

NAME - LEONG, TAI SENG
DATE - FEB 22, 1984
PROJECT NO. - 15026004

CHECKED _____
DATE _____
CALC NO. - AP-84-

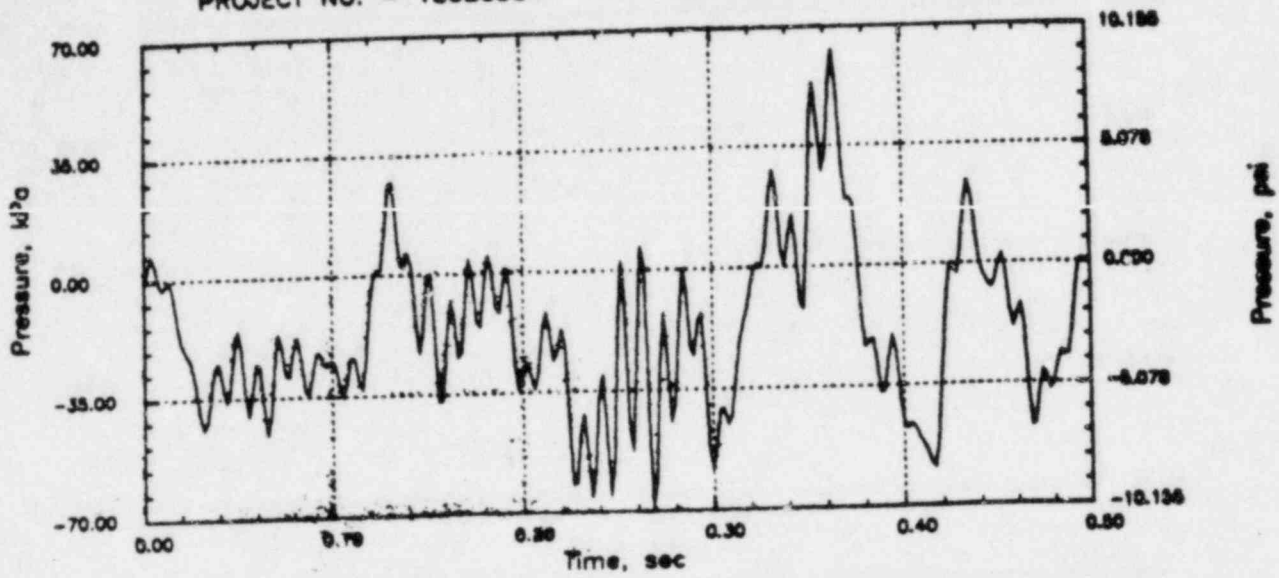

POP = 62.87 kPa PUP = -68.97 kPa MSP = 540.21 kPa²

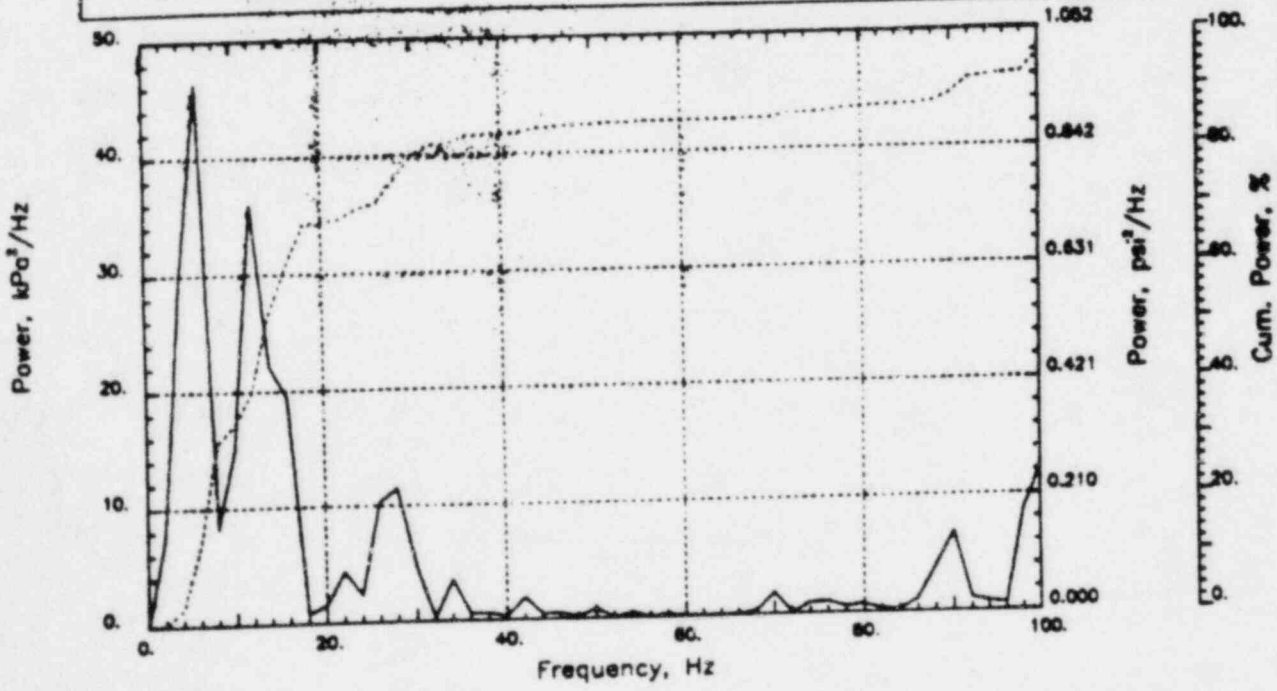

GGNS RHR CO (C=1067)

Output at point (18.90,28.00,4.09)

NAME - LEONG, TAI SENG
DATE - FEB 22, 1984
PROJECT NO. - 15026004

CHECKED _____
DATE _____
CALC NO. - AP-84-

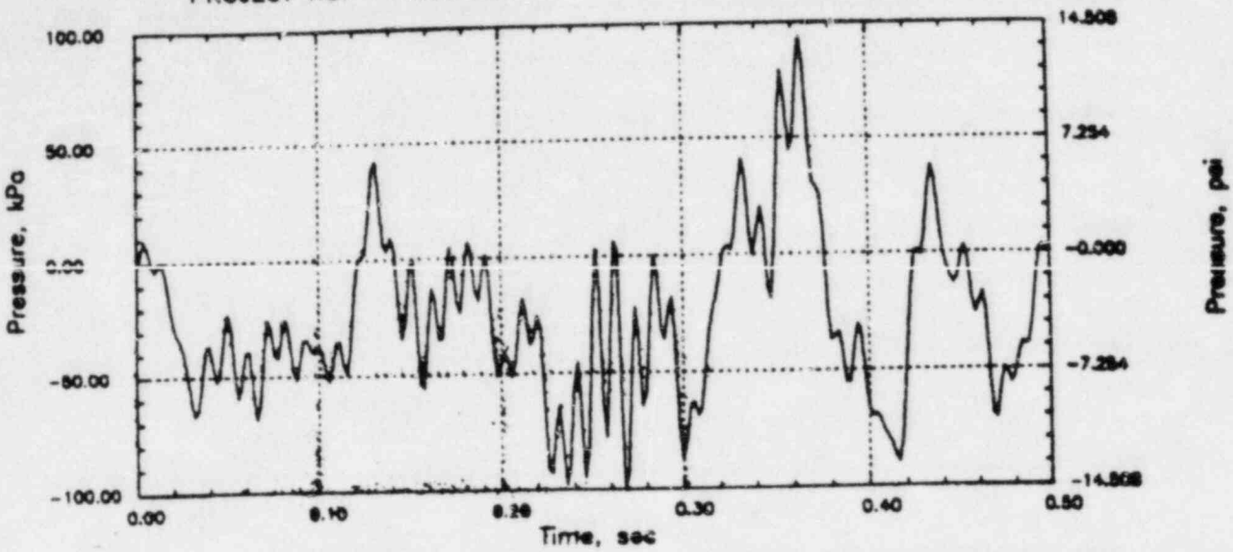

POP = 94.52 kPa PUP = -99.84 kPa MSP = 1220.43 kPa²

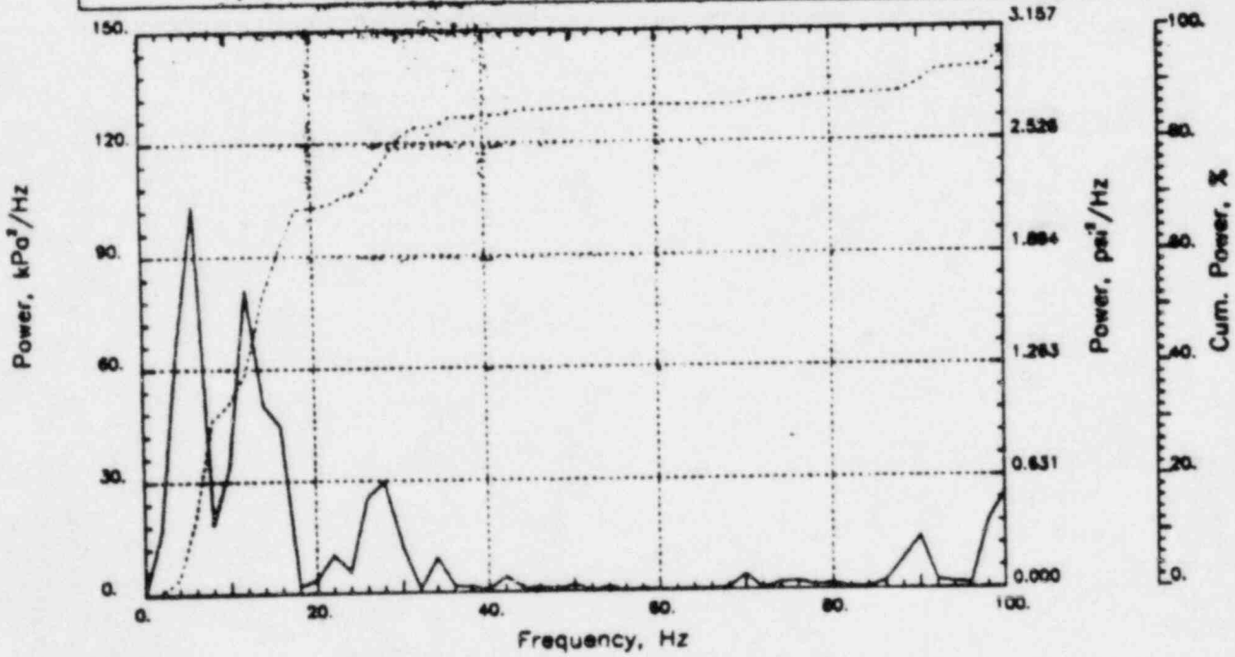

CLINTON RHR CO (C=1067)

Output at point (18.90,28.00,4.09)

NAME - LEONG, TAI SENG
DATE - FEB 22, 1984
PROJECT NO. - 15026004

CHECKED _____
DATE _____
CALC NO. - AP-84-

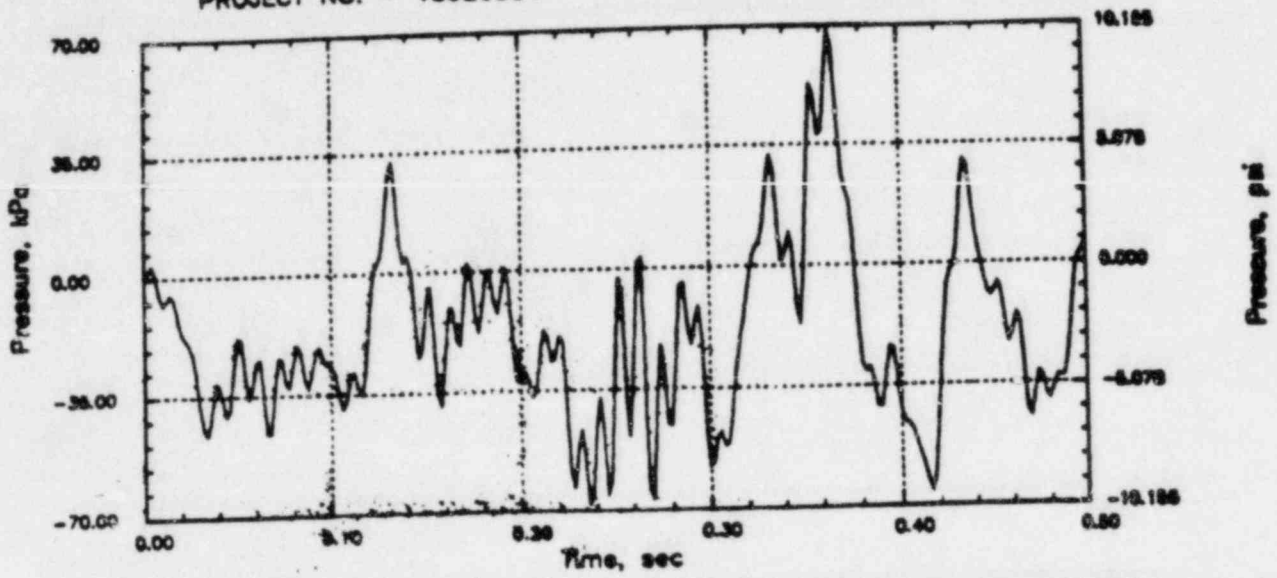

POP = 68.73 kPa PUP = -68.23 kPa MSP = 624.64 kPa²

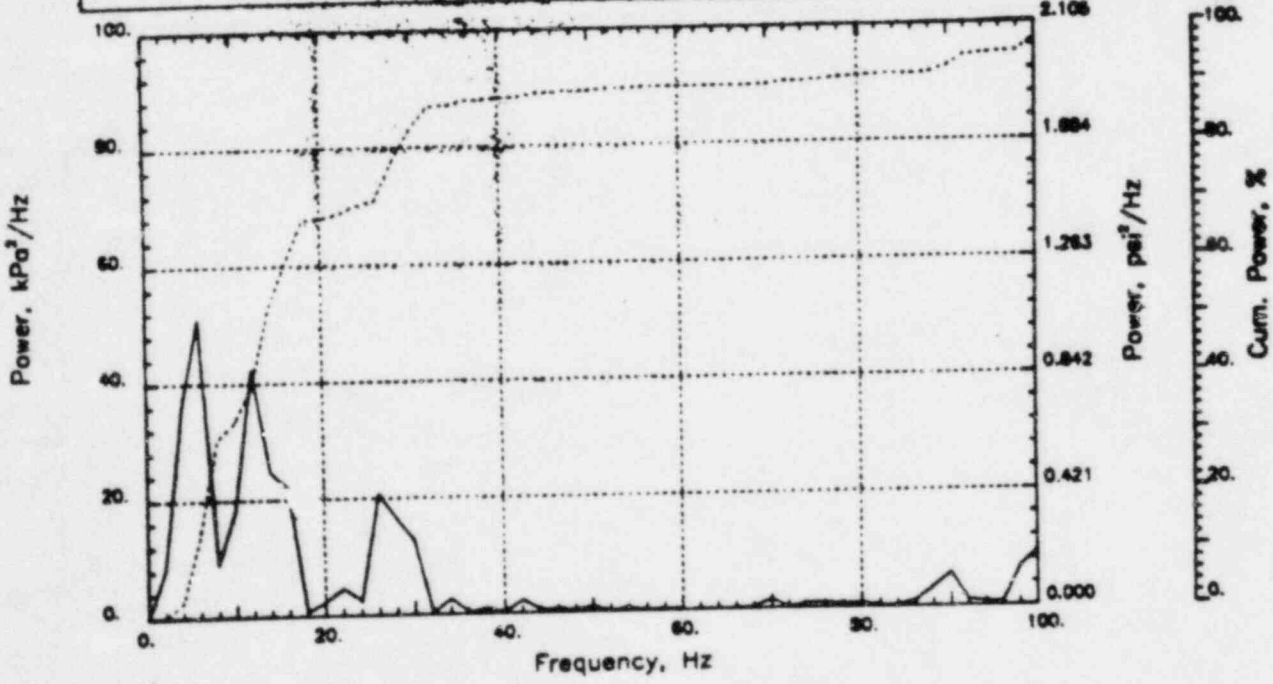

CLINTON RHR CO (C=1067)

Output at point (18.90,28.00,3.45)

NAME - LEONG, TAI SENG
DATE - FEB 22, 1984
PROJECT NO. - 15026004

CHECKED _____
DATE _____
CALC NO. - AP-84-

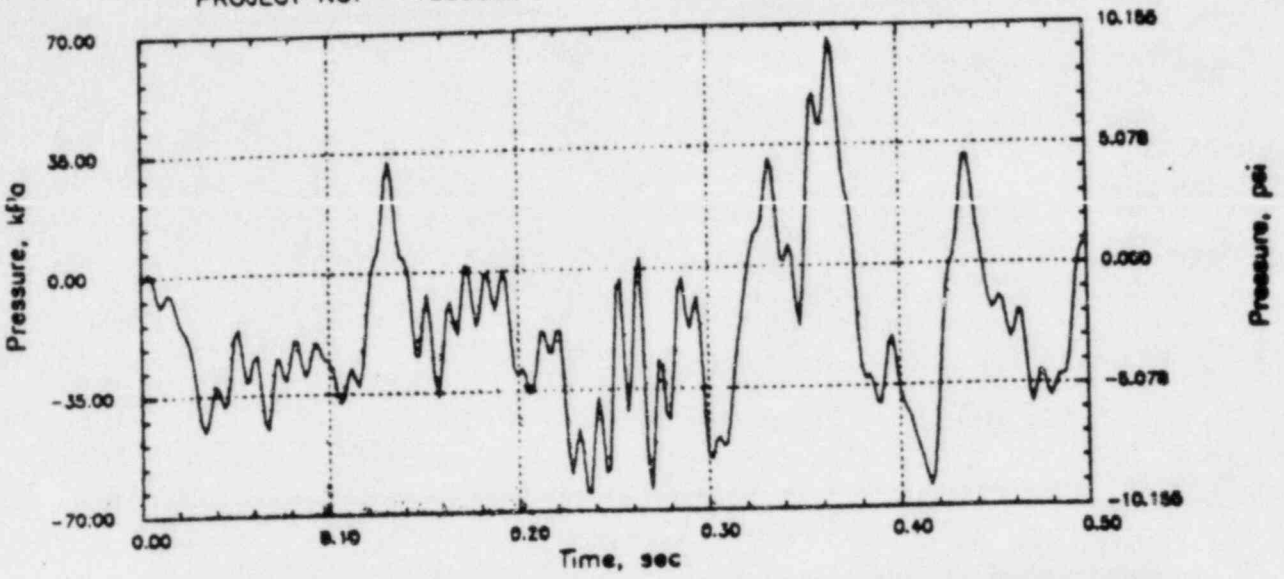

POP = 66.13 kPa PUP = -64.78 kPa MSP = 587.50 kPa²

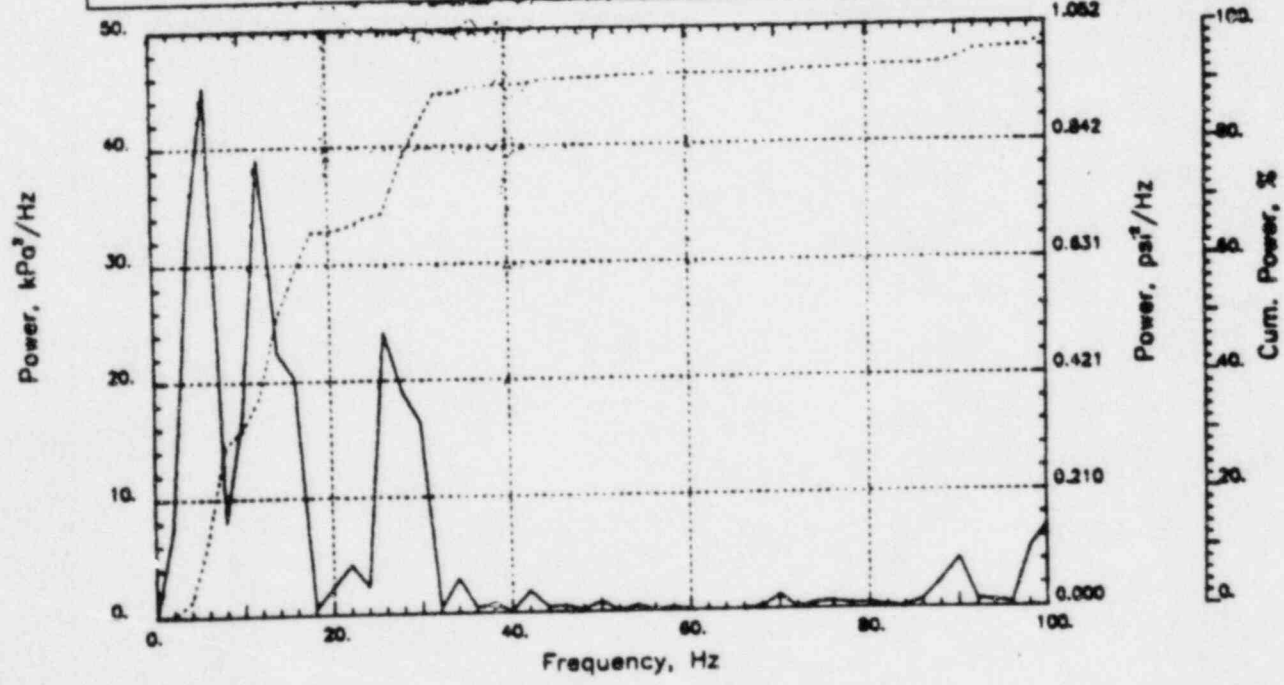

CLINTON RHR CO (C=1067)

Output at point (18.90,28.00,2.82)

NAME - LEONG, TAI SENG
DATE - FEB 22, 1984
PROJECT NO. - 15026004

CHECKED _____
DATE _____
CALC NO. - AP-84-

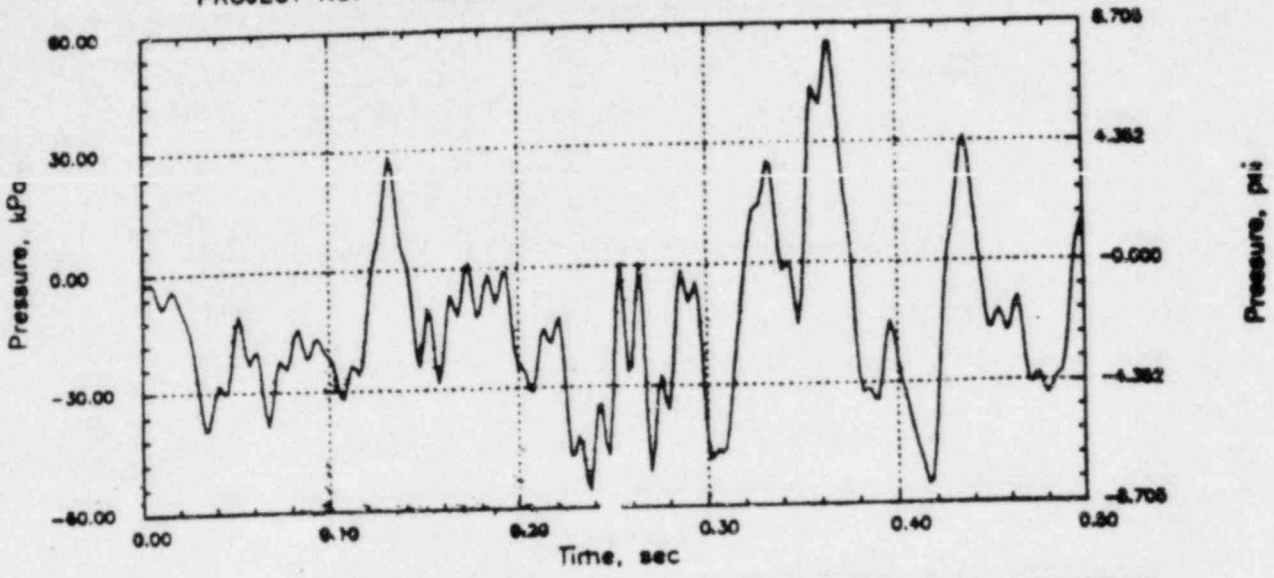

POP = 55.20 kPa PUP = -55.54 kPa MSP = 439.91 kPa²

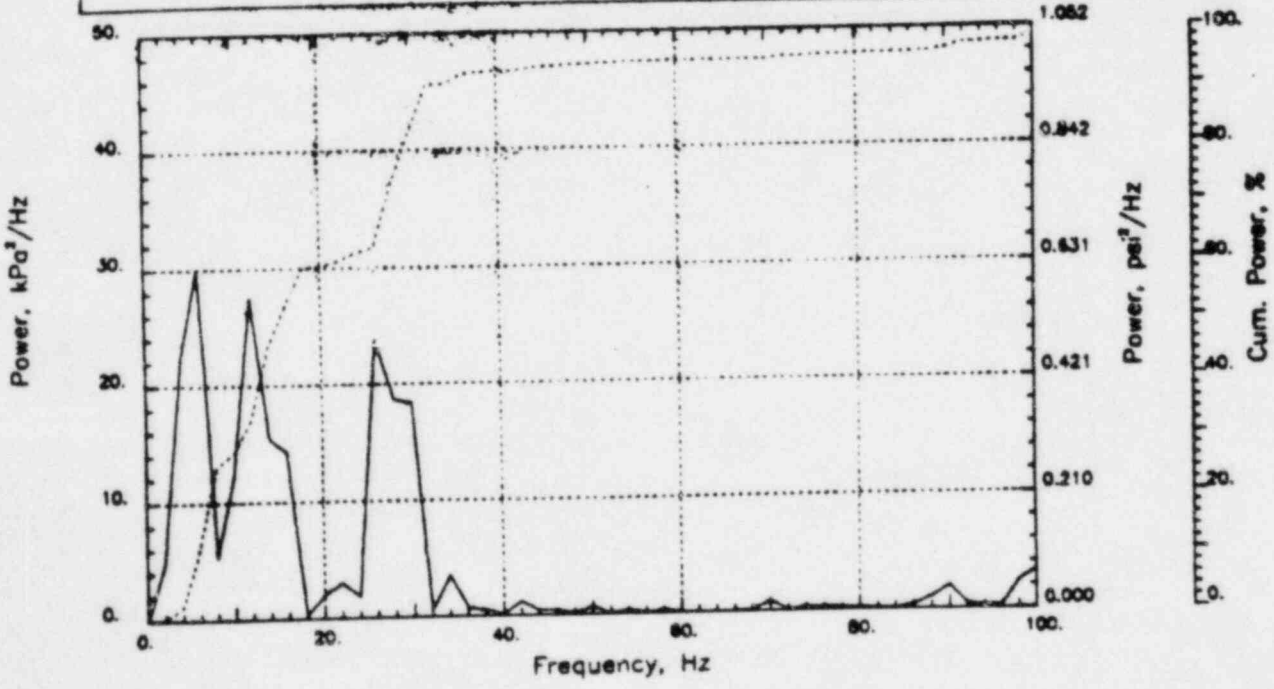

CLINTON RHR CO (C=1067)

Output at point (18.90,28.00,2.18)

NAME - LEONG, TAI SENG
DATE - FEB 22, 1984
PROJECT NO. - 15026004

CHECKED _____
DATE _____
CALC NO. - AP-84-

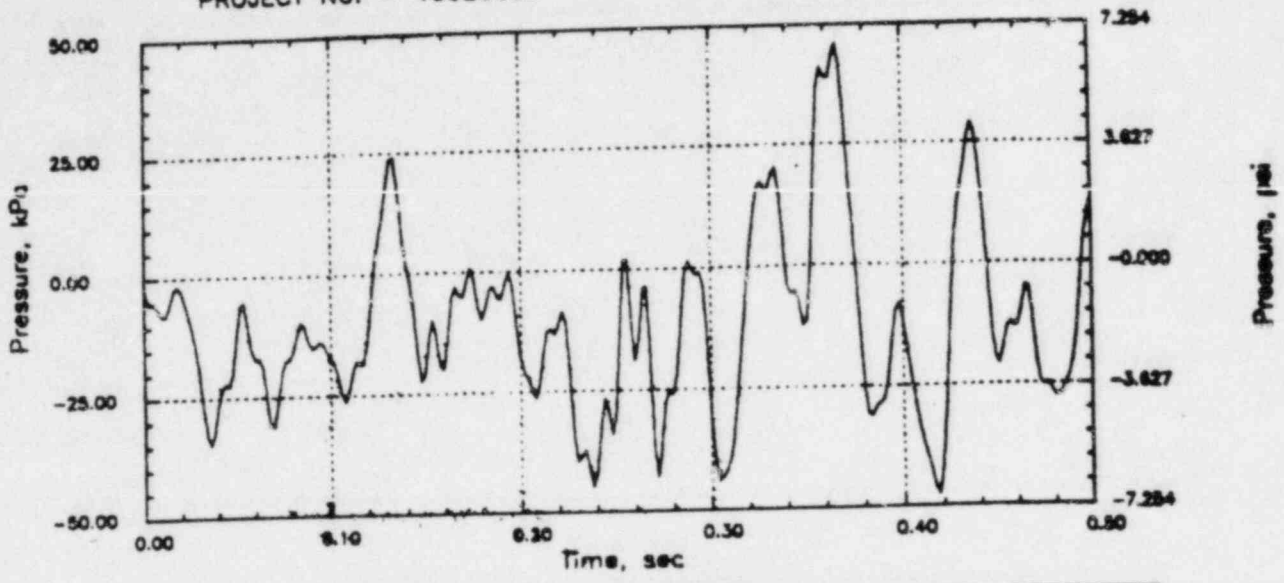

POP = 45.97 kPa PUP = -47.54 kPa MSP = 328.63 kPa²

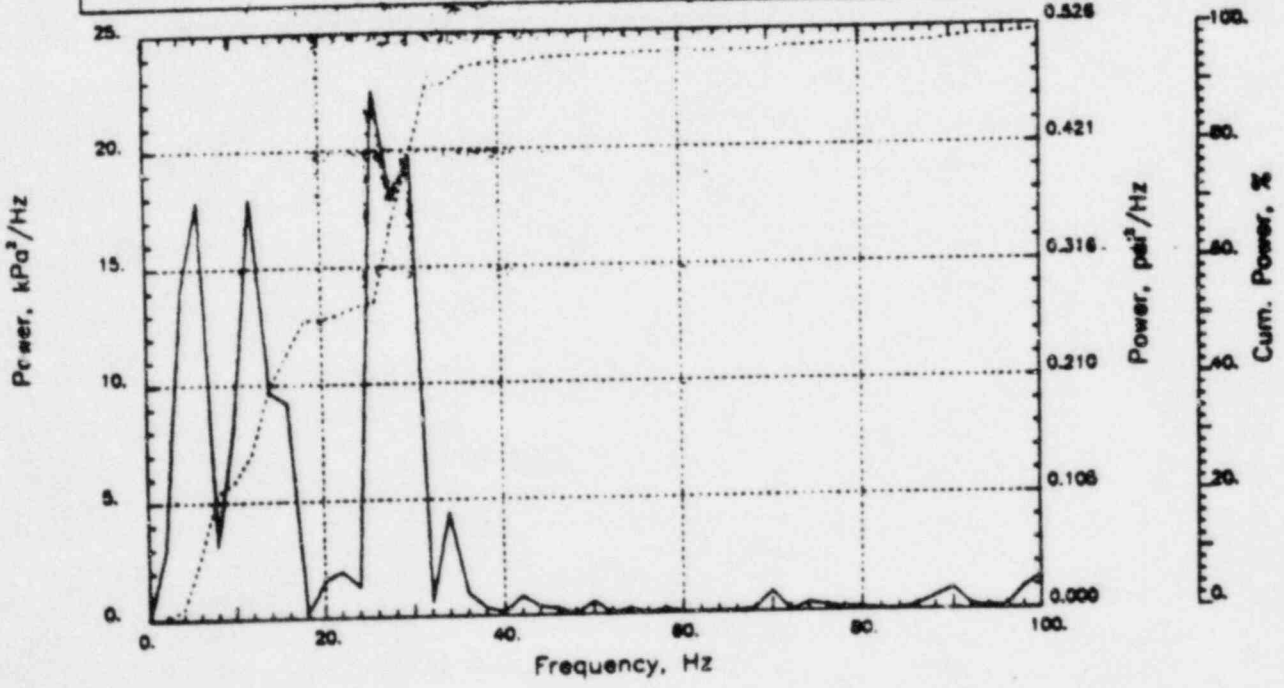

CLINTON RHR CO (C=1067)

Output at point (18.90,28.00,1.55)

NAME - LEONG, TAI SENG
DATE - FEB 22, 1984
PROJECT NO. - 15026004

CHECKED _____
DATE _____
CALC NO. - AP-84-

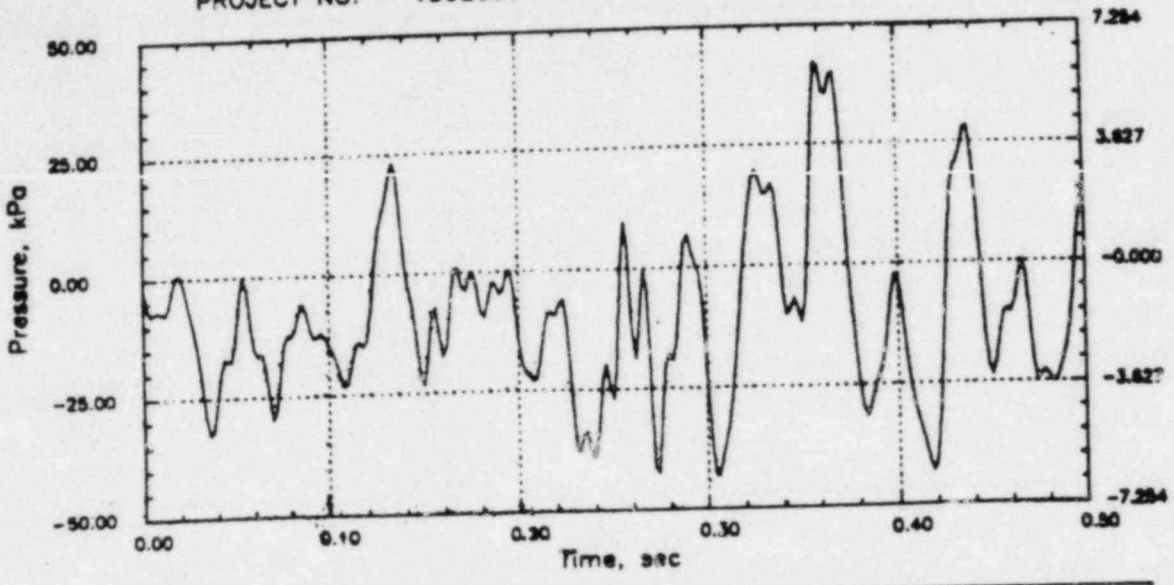

POP = 42.27 kPa PUP = -43.29 kPa MSP = 287.73 kPa²

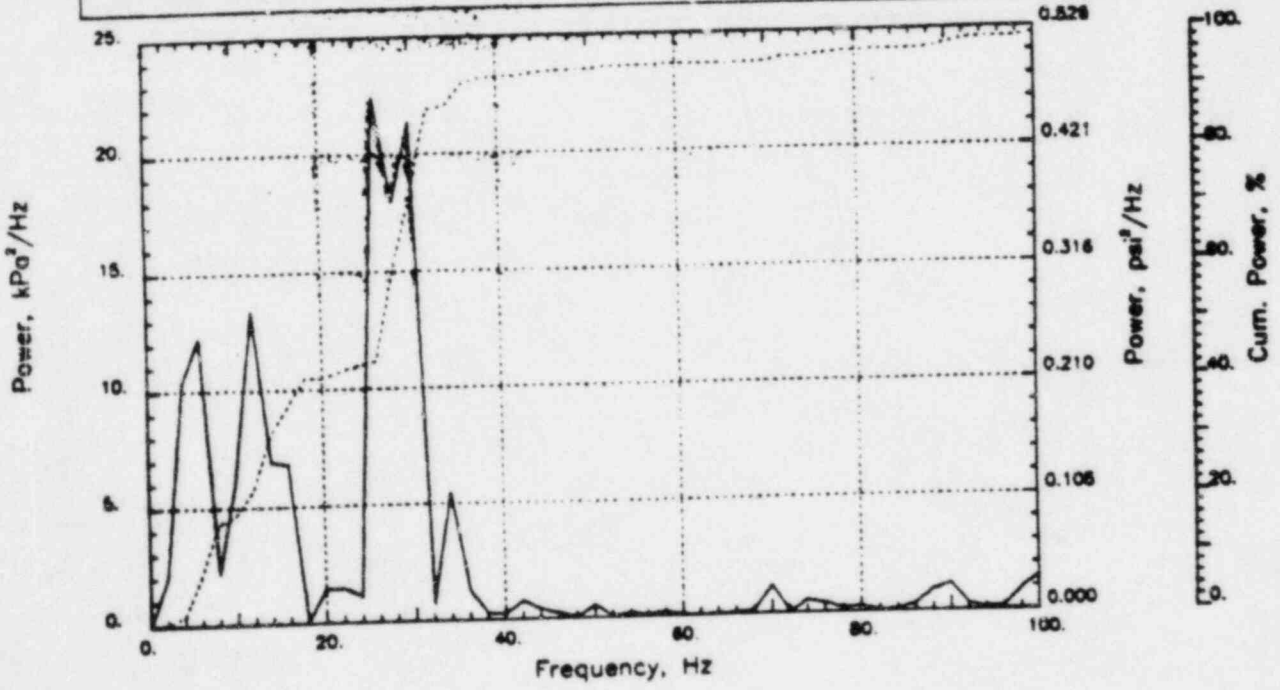

CLINTON RHR CO (C=1067)

Output at point (18.90,28.00,0.91)

NAME - LEONG, TAI SENG
DATE - FEB 22, 1984
PROJECT NO. - 15026004

CHECKED _____
DATE _____
CALC NO. - AP-84-

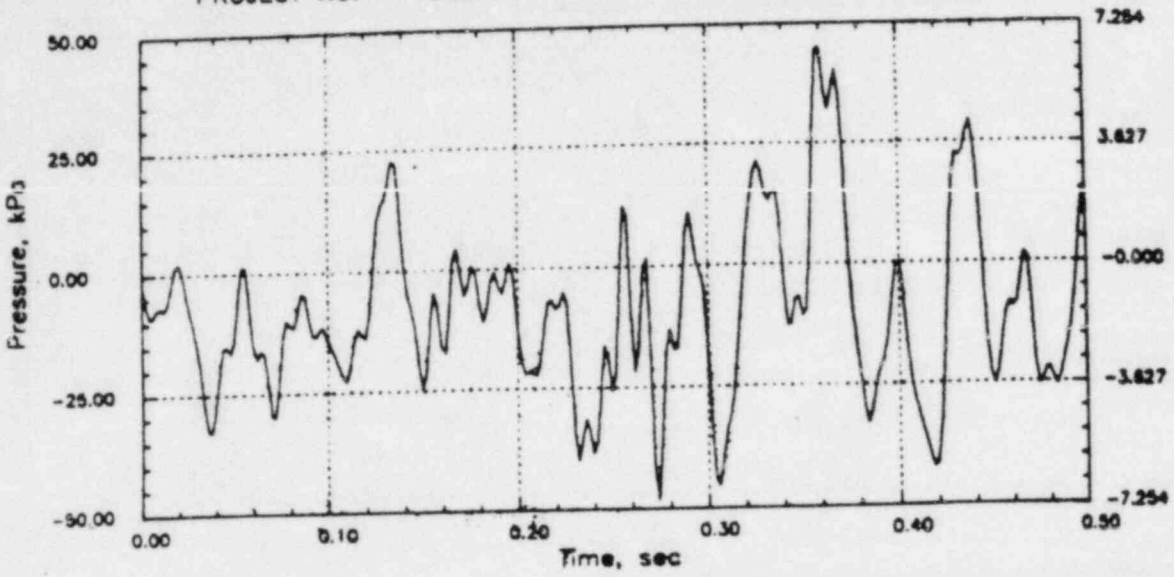

POP = 45.00 kPa PUP = -48.19 kPa MSP = 295.42 kPa²

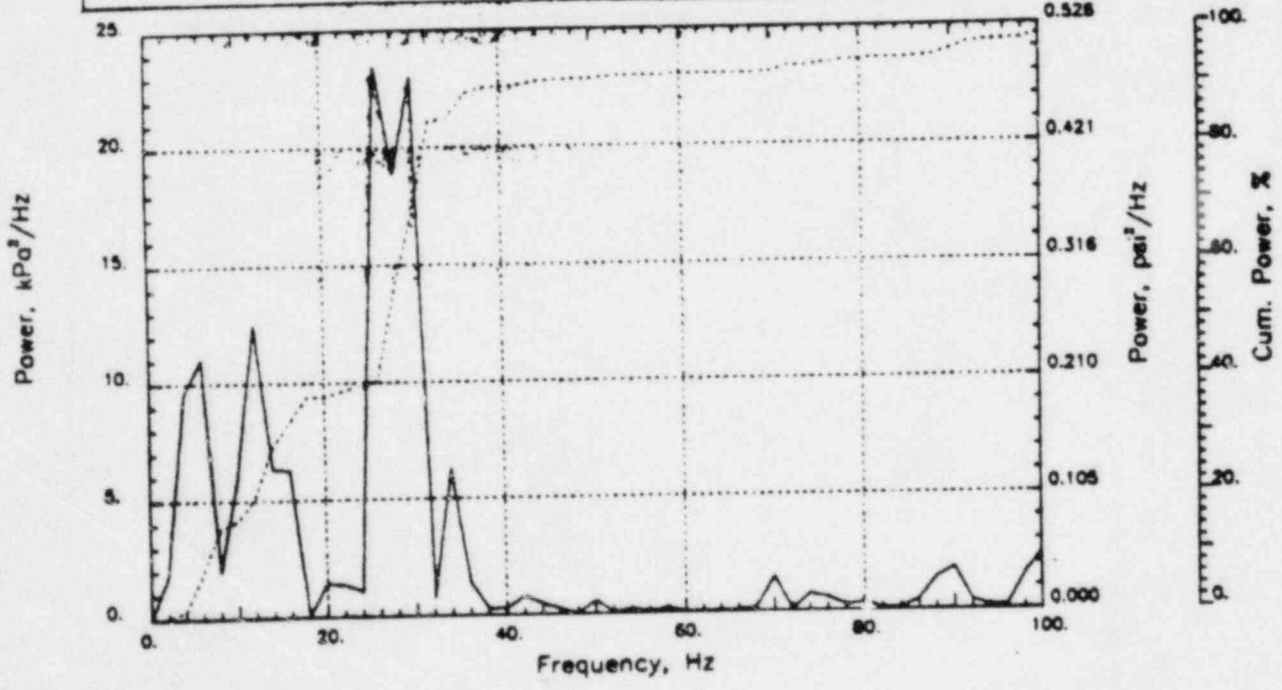

CLINTON RHR CO (C=1067)

Output at point (18.90,28.00,0.46)

NAME - LEONG, TAI SENG
DATE - FEB 22, 1984
PROJECT NO. - 15026004

CHECKED _____
DATE _____
CALC NO. - AP-84-

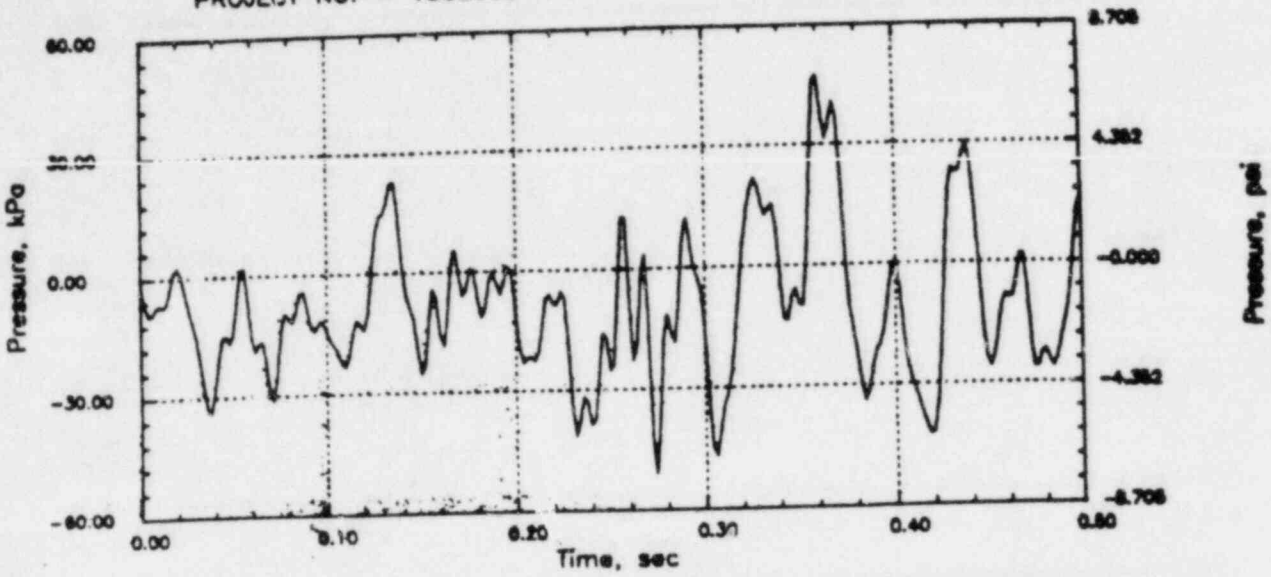

POP = 47.26 kPa PUP = -50.89 kPa MSP = 308.06 kPa²

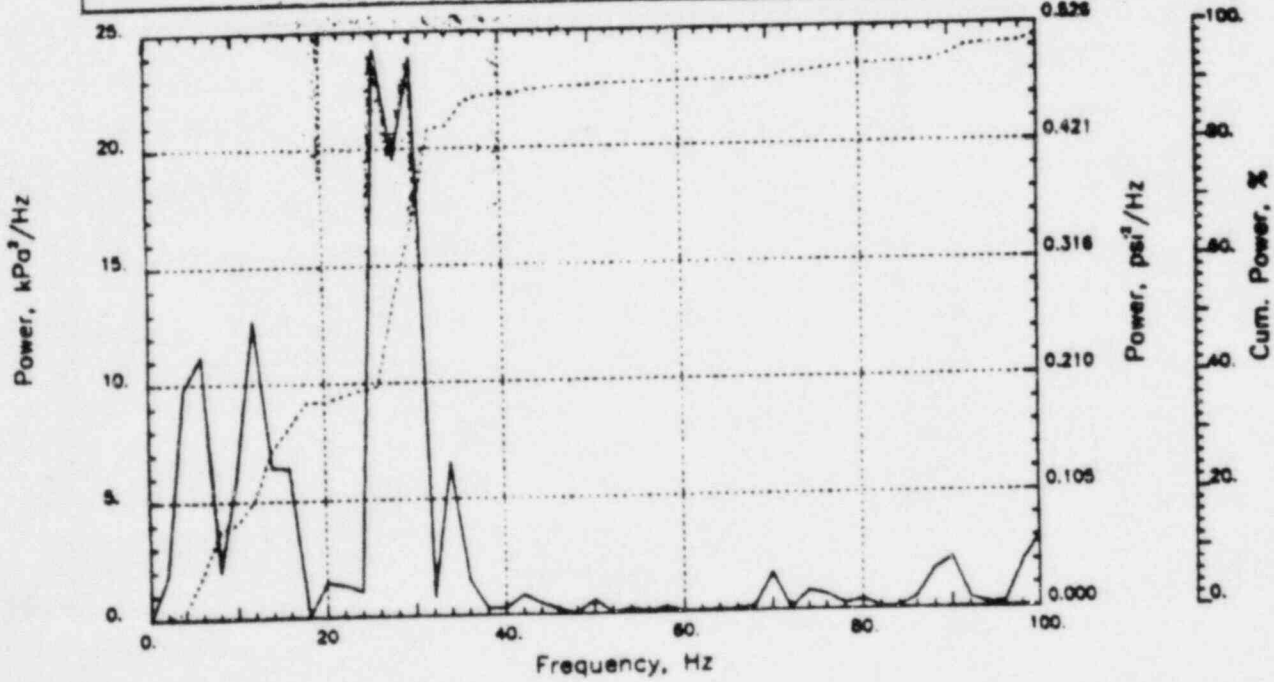

CLINTON RHR CO (C=1067)

Output at point (18.90,28.00,0.00)

NAME - LEONG, TAI SENG
DATE - FEB 22, 1984
PROJECT NO. - 15026004

CHECKED _____
DATE _____
CALC NO. - AP-84-

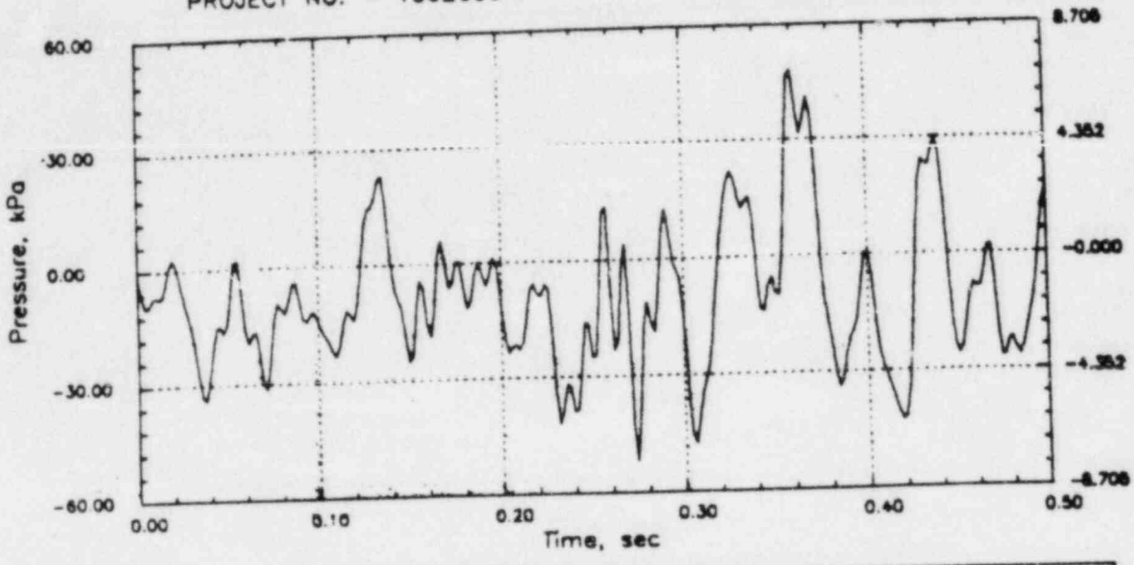

POP = 48.12 kPa PUP = -51.86 kPa MSP = 313.73 kPa²

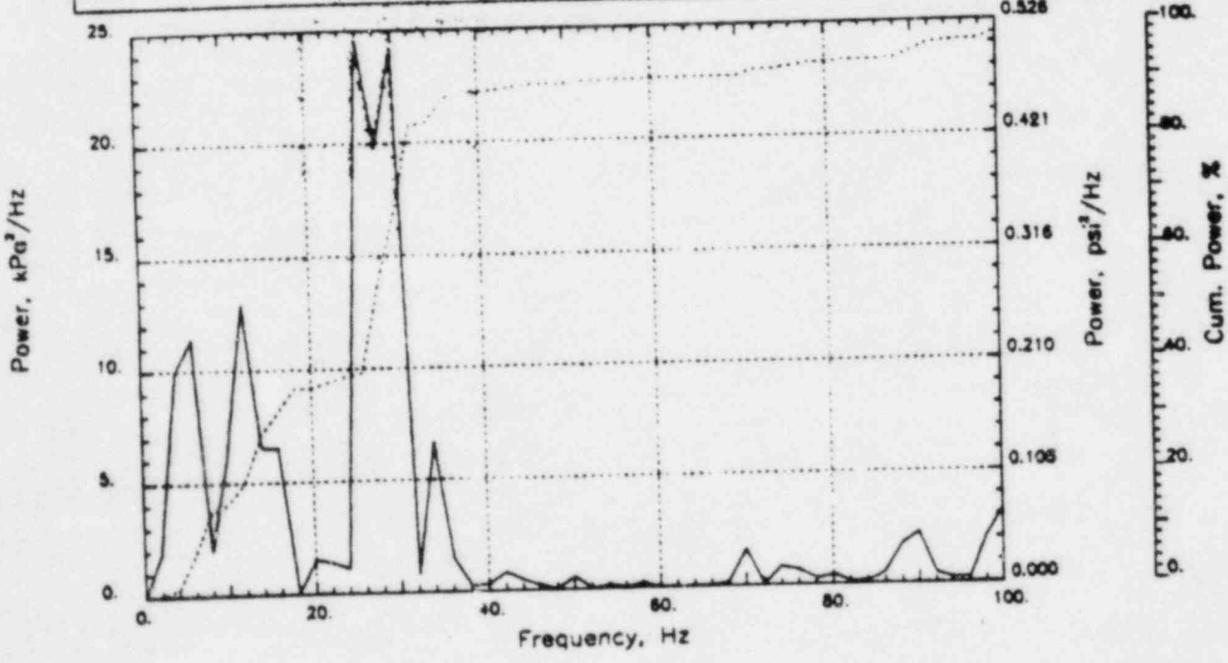

CLINTON RHR CO (C=1067)

Output at point (17.34,28.00,0.00)

NAME - LEONG, TAI SENG
DATE - FEB 22, 1984
PROJECT NO. - 15026004

CHECKED _____
DATE _____
CALC NO. - AP-84-

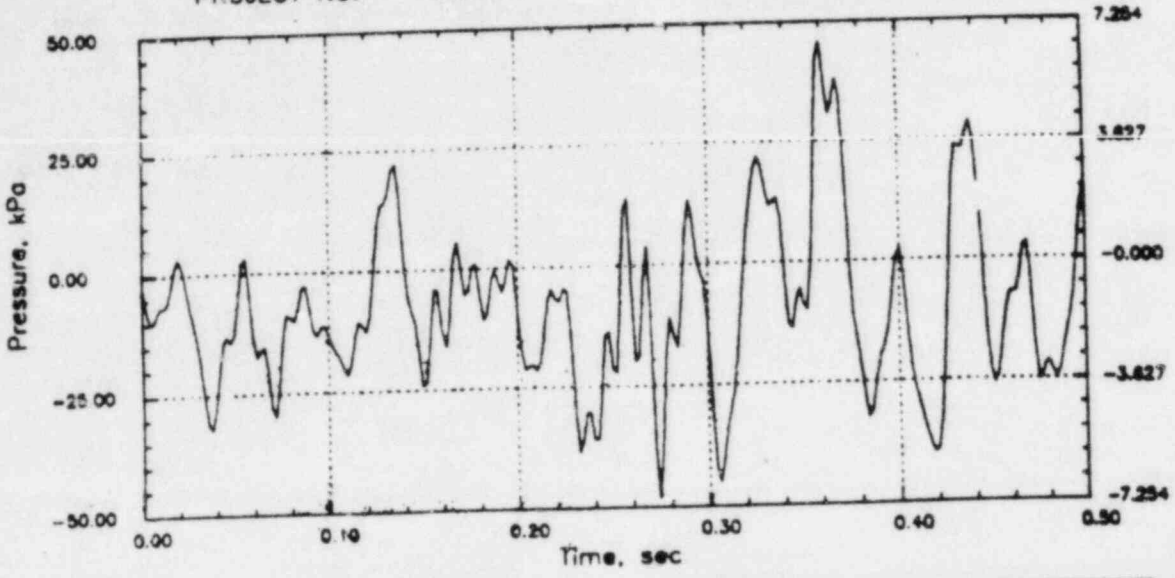

POP = 45.68 kPa PUP = -48.08 kPa MSP = 279.89 kPa²

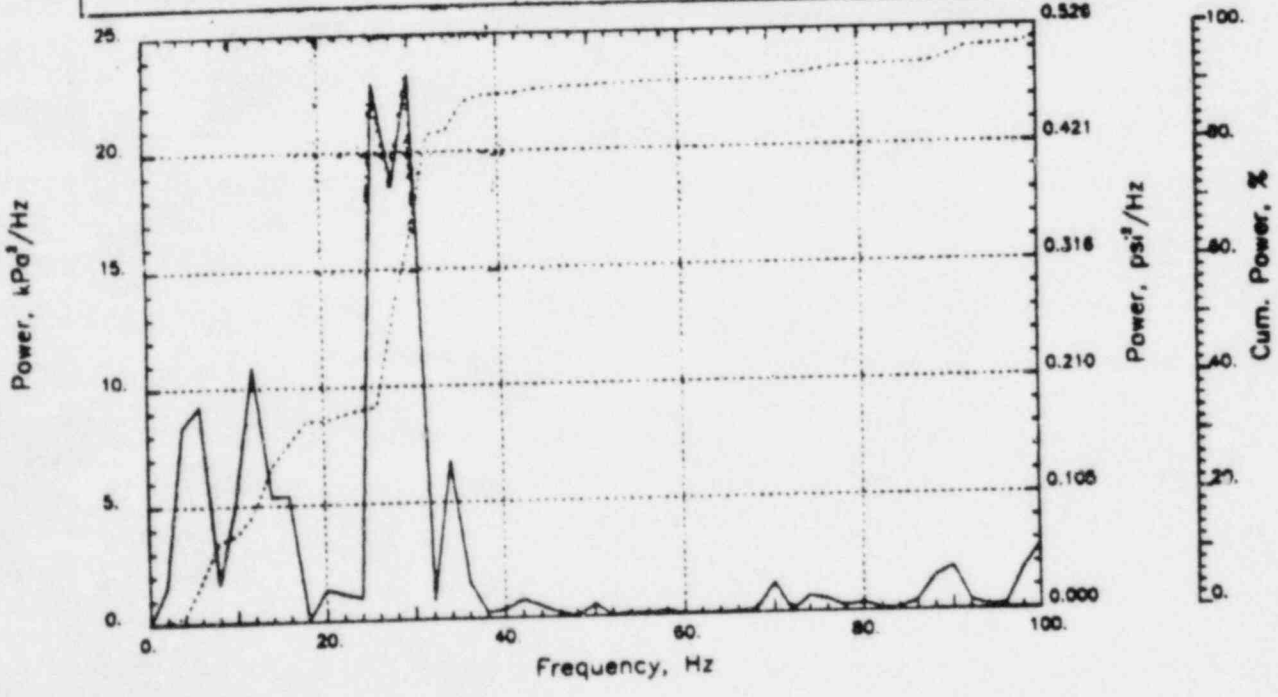

CLINTON RHR CO (C=1067)

Output at point (15.77,28.00,0.00)

NAME - LEONG, TAI SENG
DATE - FEB 22, 1984
PROJECT NO. - 15026004

CHECKED _____
DATE _____
CALC NO. - AP-84-

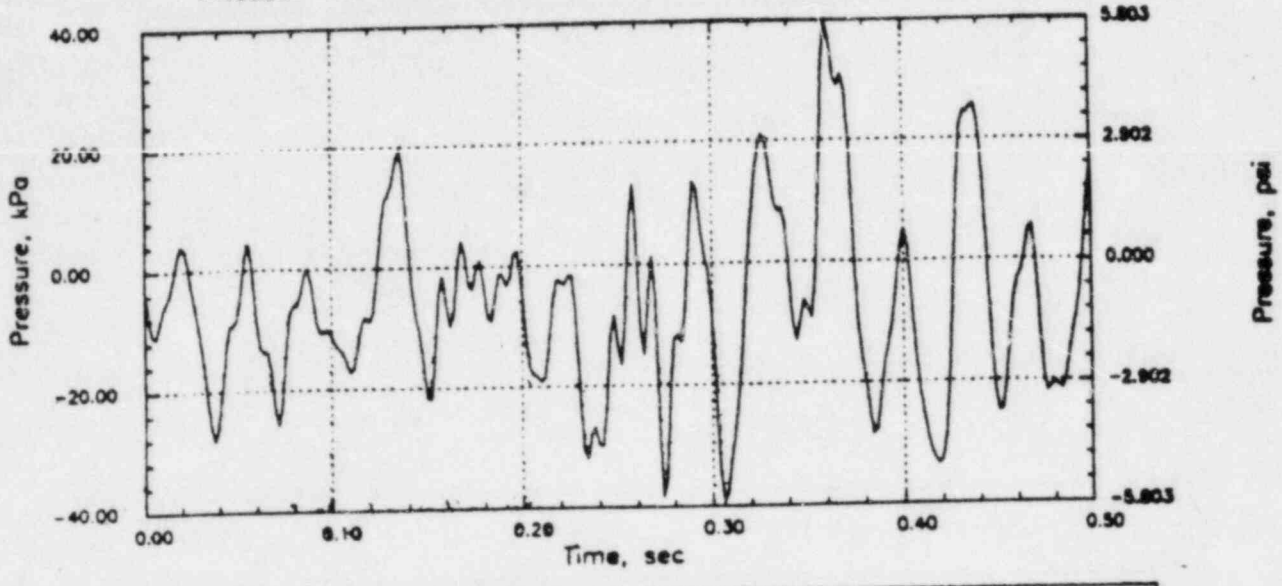

POP = 39.82 kPa PUP = -39.65 kPa MSP = 215.95 kPa²

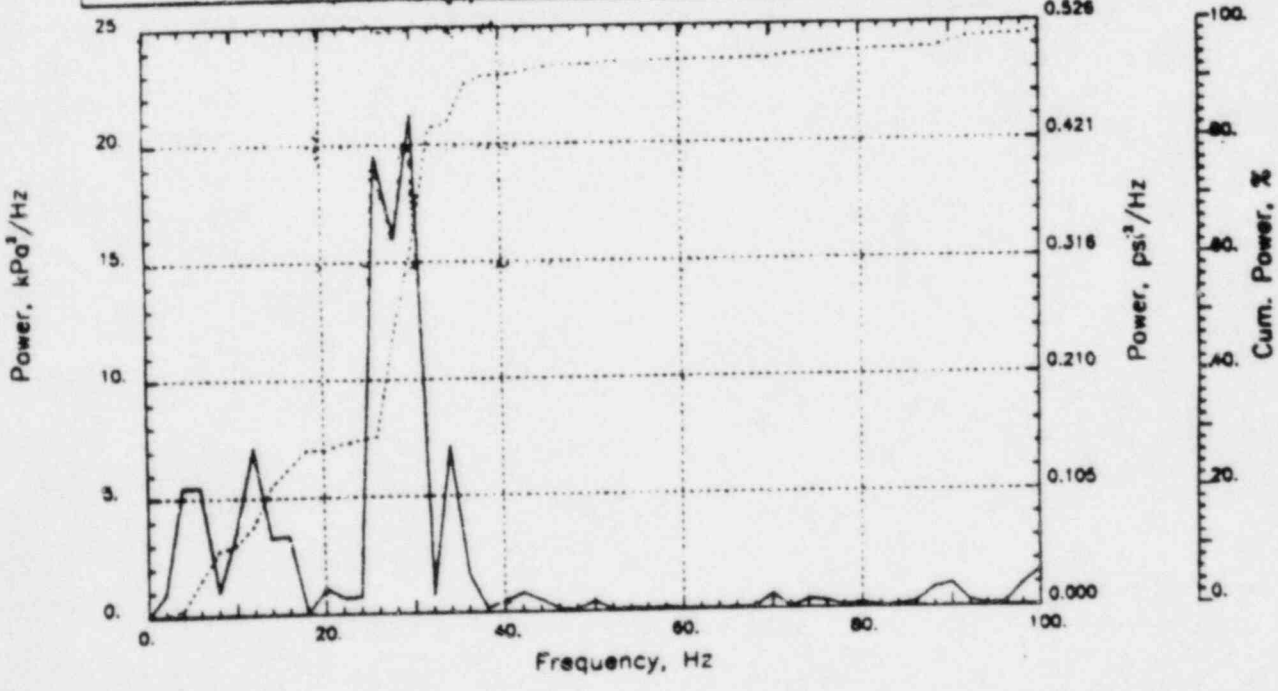

CLINTON RHR CO (C=1067)

Output at point (14.21,28.00,0.00)

NAME - LEONG, TAI SENG
DATE - FEB 22, 1984
PROJECT NO. - 15026004

CHECKED _____
DATE _____
CALC NO. - AP-84-

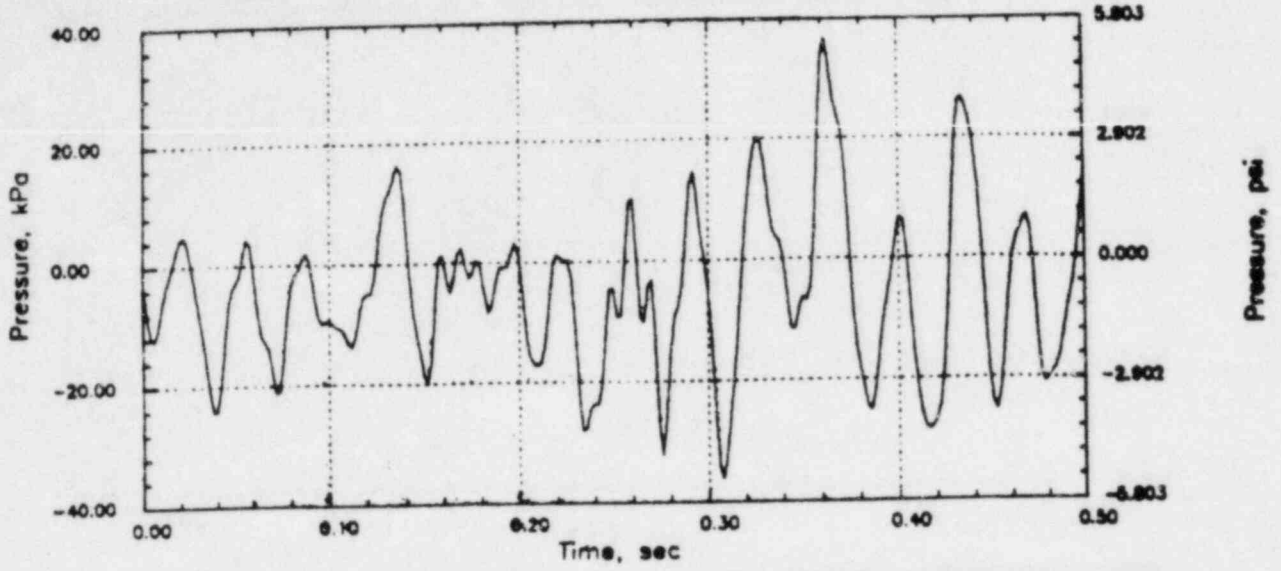

POP = 36.64 kPa PUP = -36.15 kPa MSP = 172.56 kPa²

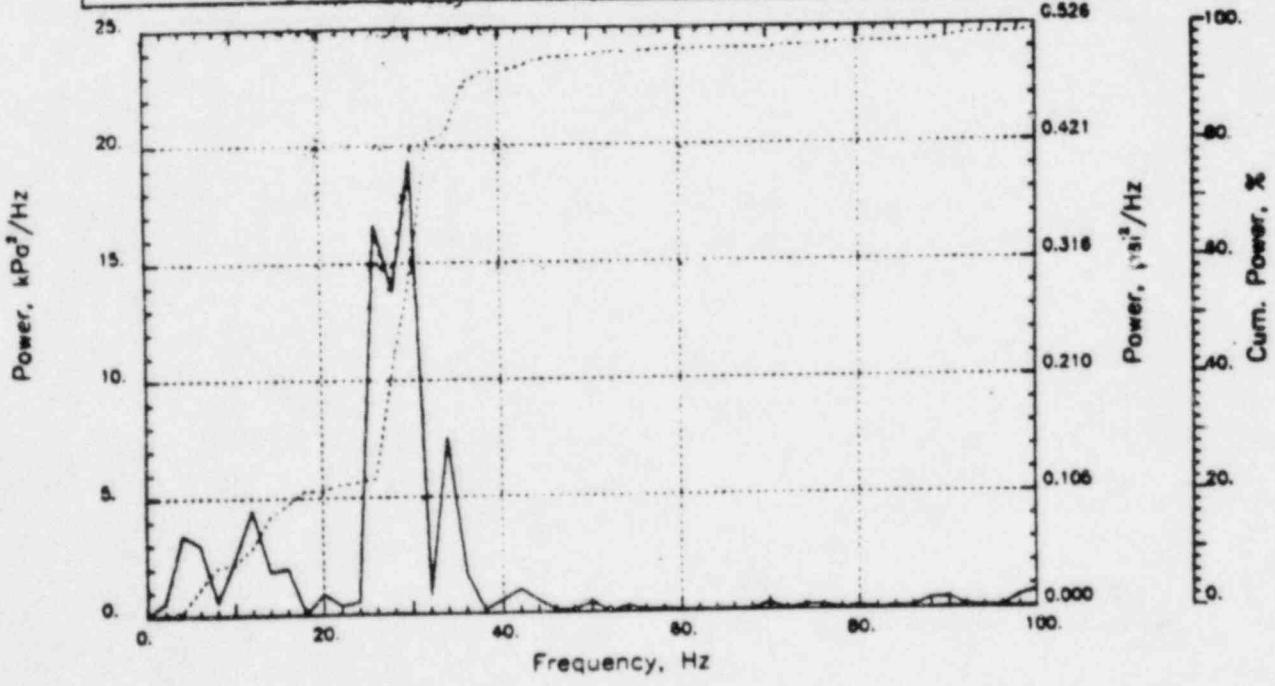

CLINTON RHR CO (C=1067)

Output at point (12.65,28.00,0.00)

NAME - LEONG, TAI SENG
DATE - FEB 22, 1984
PROJECT NO. - 15026004

CHECKED _____
DATE _____
CALC NO. - AP-84-

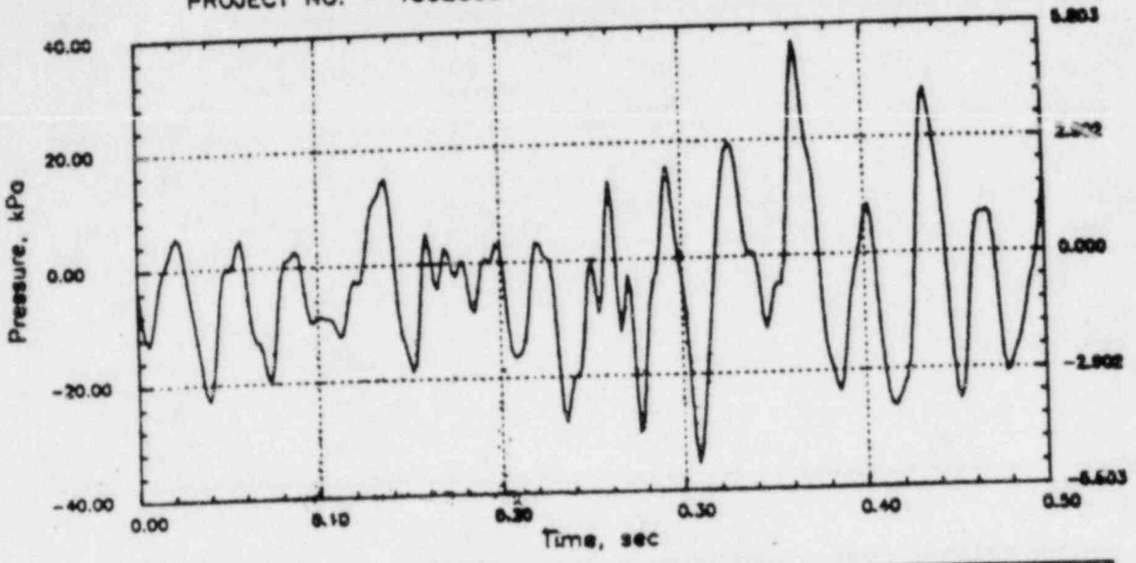

POP = 36.90 kPa PUP = -35.39 kPa MSP = 157.63 kPa²

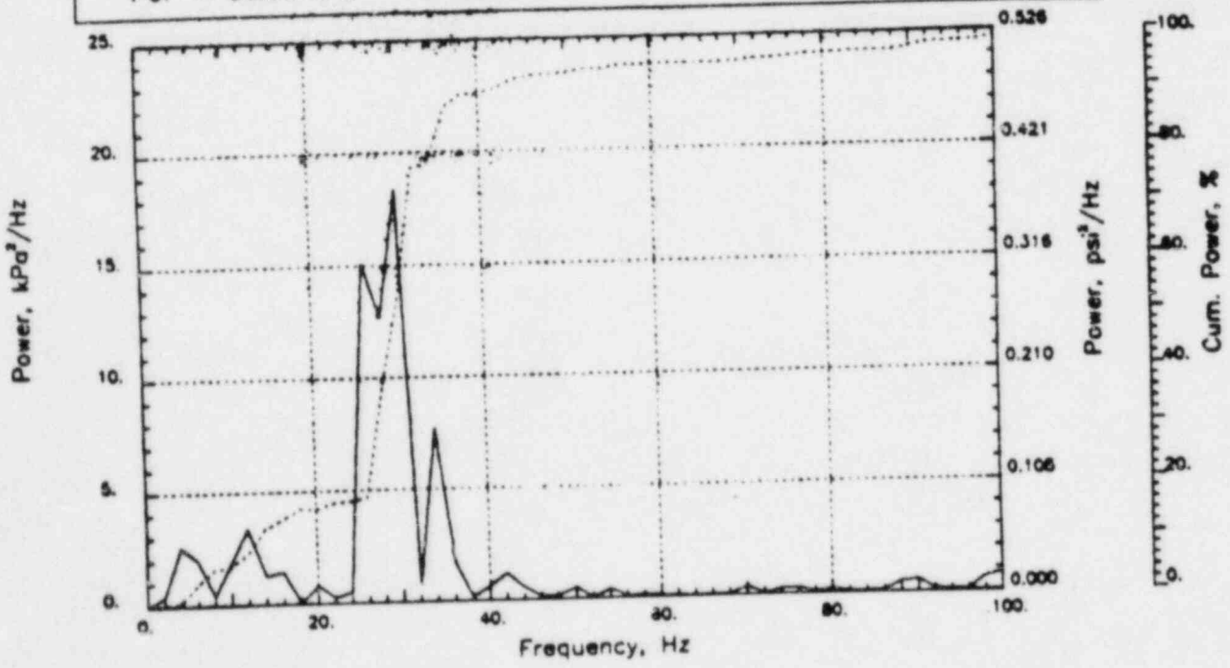

CLINTON RHR CO (C=1067)

Output at point (12.65,28.00,0.46)

NAME - LEONG, TAI SENG
DATE - FEB 22, 1984
PROJECT NO. - 15026004

CHECKED _____
DATE _____
CALC NO. - AP-84-

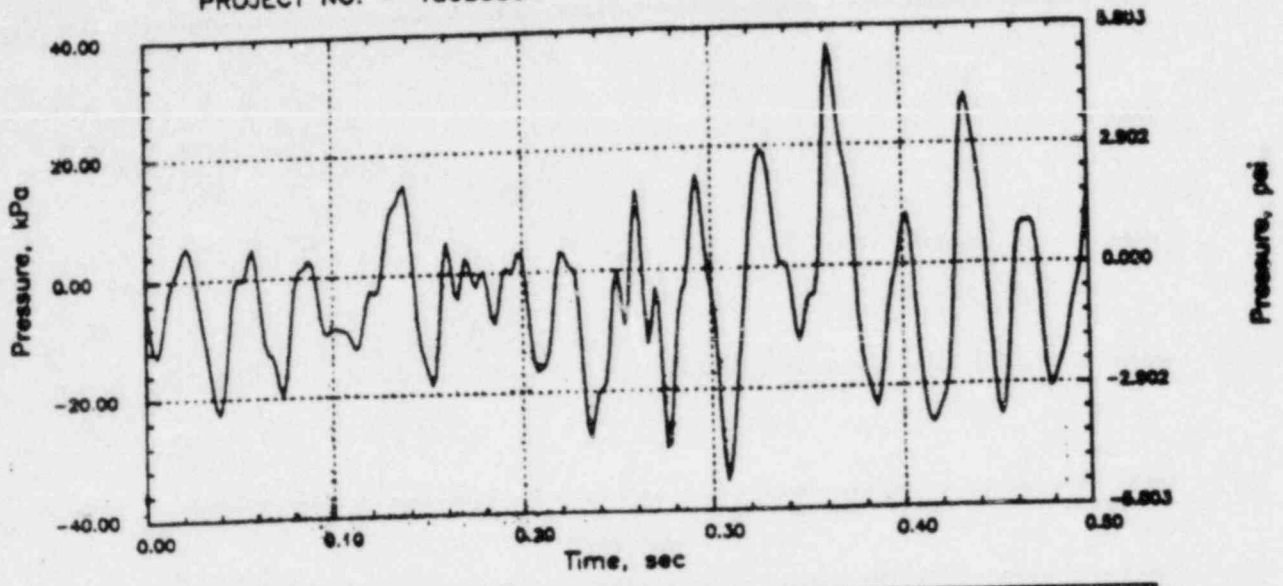

POP = 36.53 kPa PUP = -35.07 kPa MSP = 155.19 kPa²

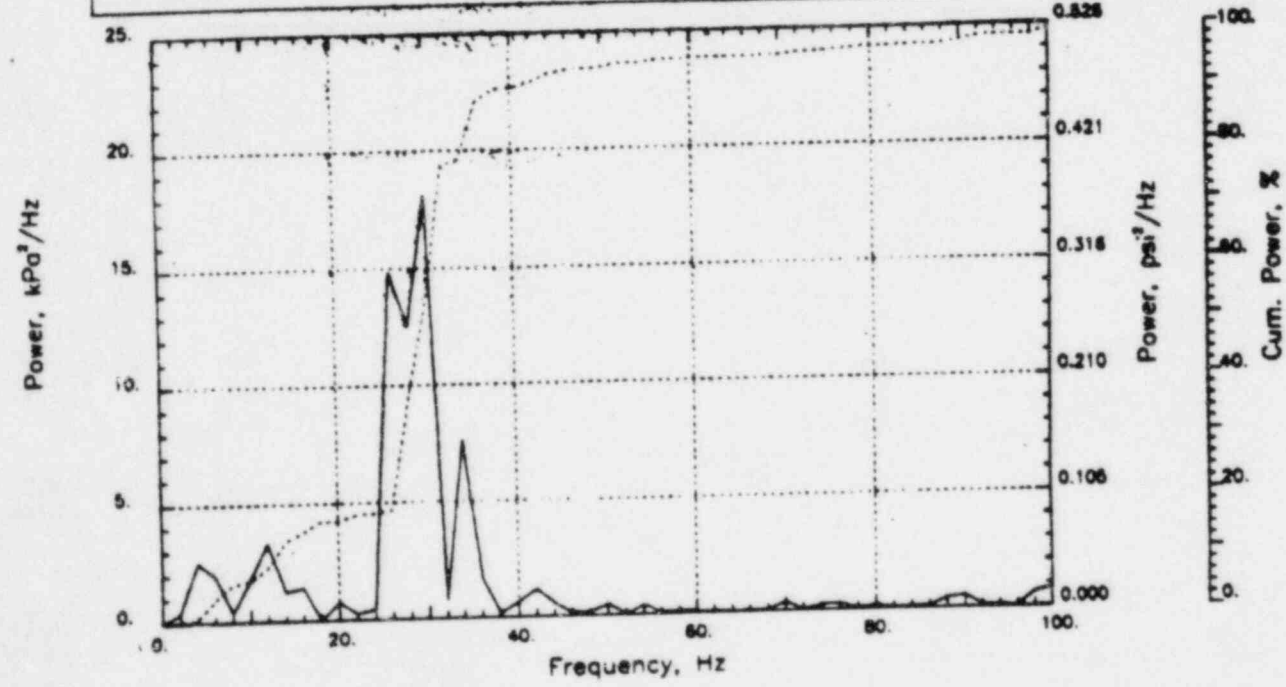

CLINTON RHR CO (C=1067)

Output at point (12.65,28.00,0.91)

NAME - LEONG, TAI SENG
DATE - FEB 22, 1984
PROJECT NO. - 15026004

CHECKED _____
DATE _____
CALC NO. - AP-84-

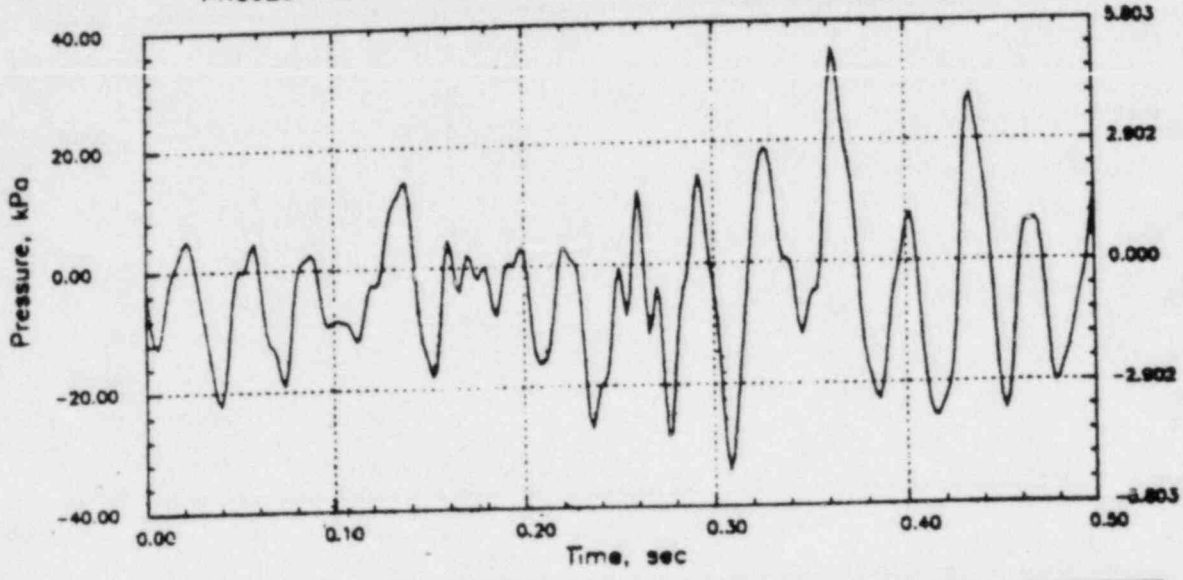

POP = 35.45 kPa PUP = -34.13 kPa MSP = 148.04 kPa²

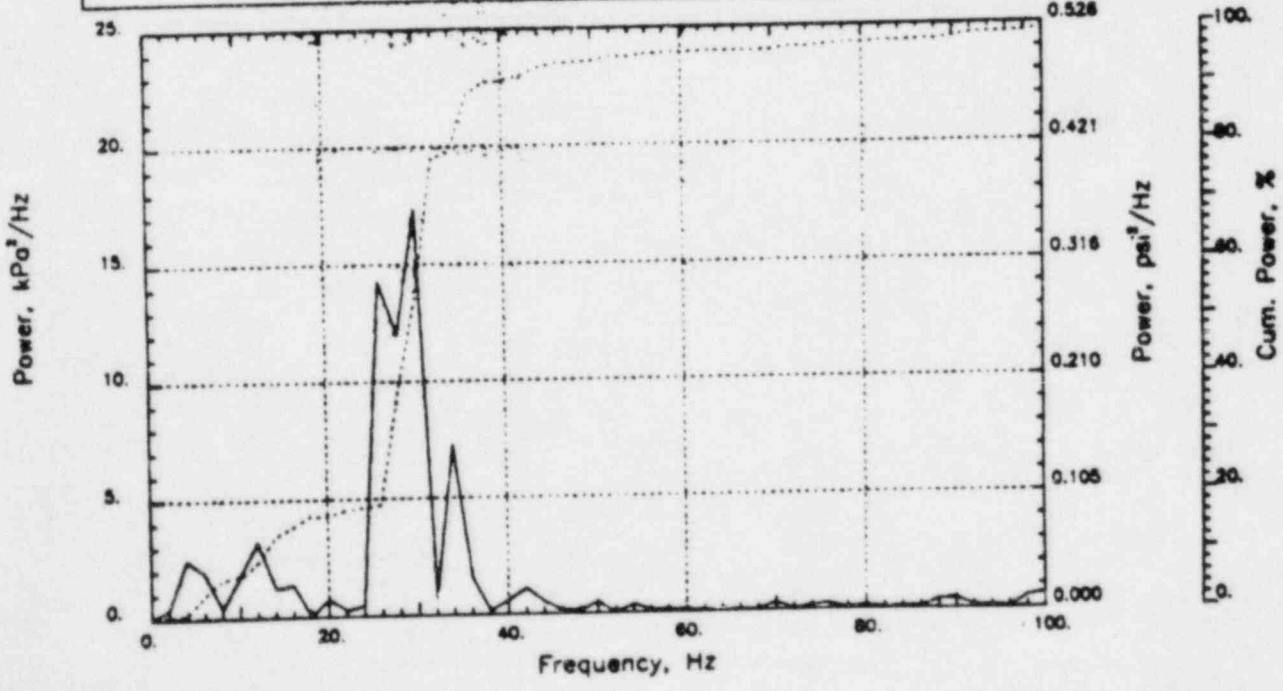

CLINTON RHR CO (C=1067)

Output at point (12.65,28.00,1.55)

NAME - LEONG, TAI SENG
DATE - FEB 22, 1984
PROJECT NO. - 15026004

CHECKED _____
DATE _____
CALC NO. - AP-84-

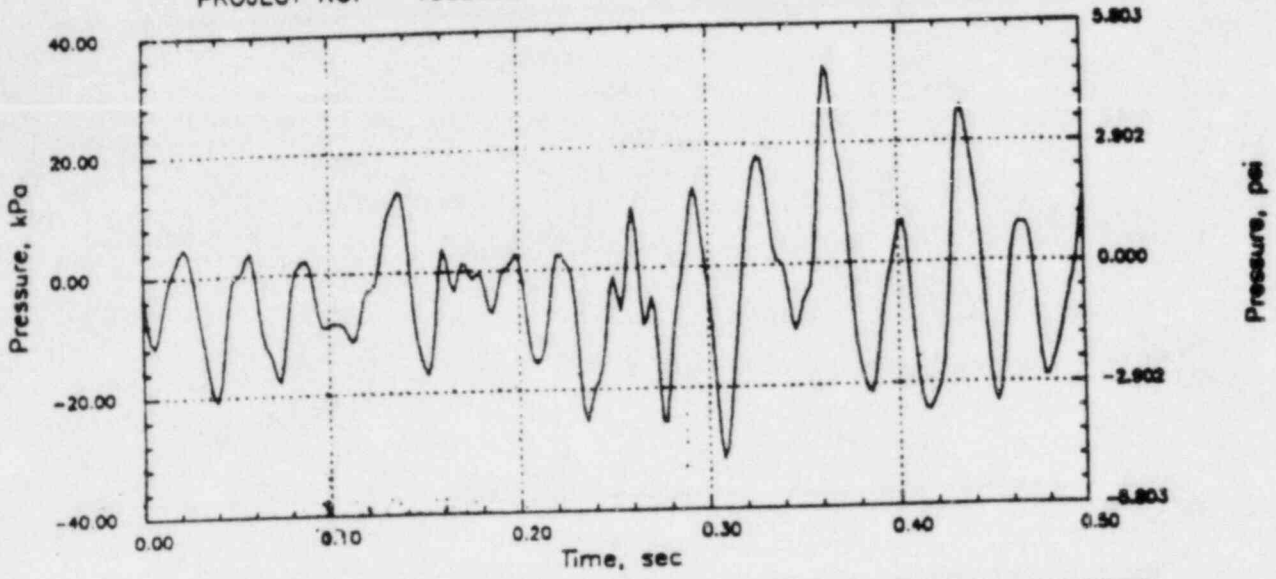

POP = 32.85 kPa PUP = -31.86 kPa MSP = 131.41 kPa²

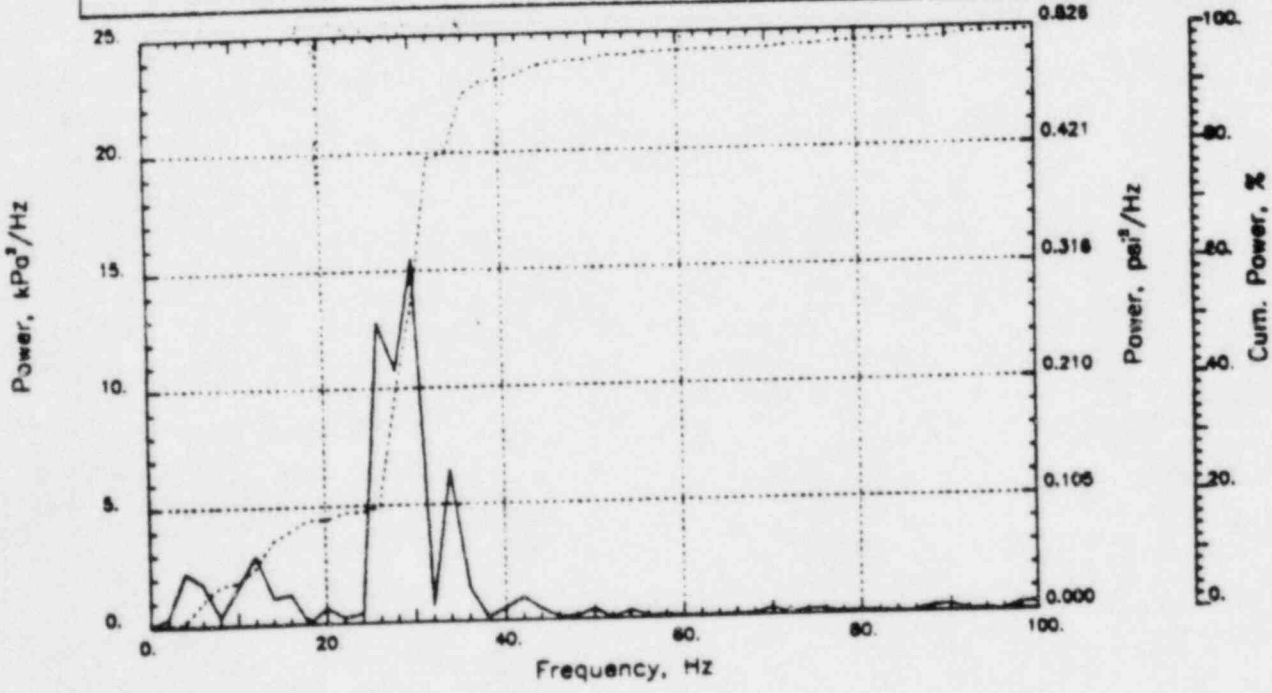

CLINTON RHR CO (C=1067)

Output at point (12.65,28.00,2.18)

NAME - LEONG, TAI SENG
DATE - FEB 22, 1984
PROJECT NO. - 15026004

CHECKED _____
DATE _____
CALC NO. - AP-84-

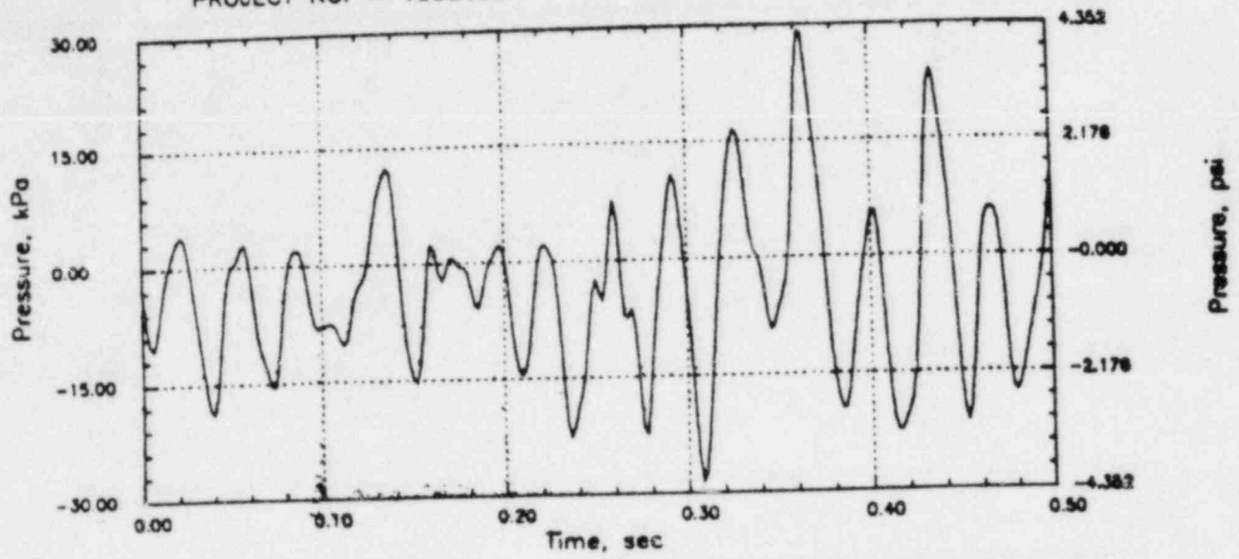

POP = 29.16 kPa PUP = -28.57 kPa MSP = 109.04 kPa²

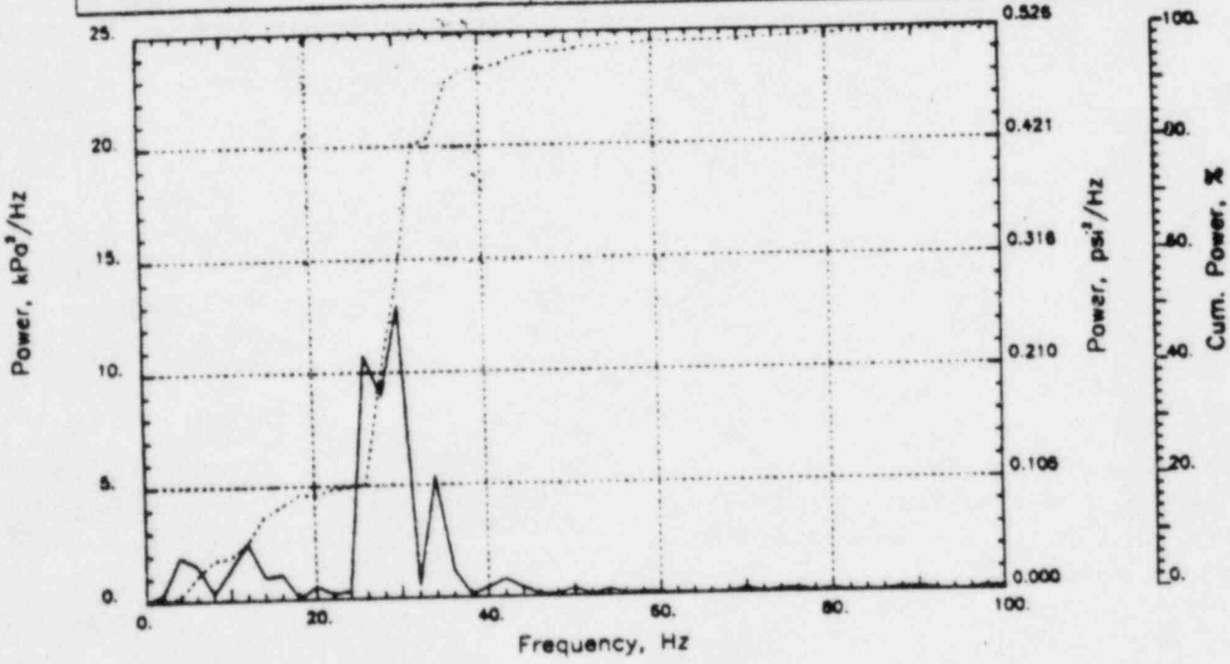

CLINTON RHR CO (C=1067)

Output at point (12.65,28.00,2.82)

NAME - LEONG, TAI SENG
DATE - FEB 22, 1984
PROJECT NO. - 15026004

CHECKED _____
DATE _____
CALC NO. - AP-84-

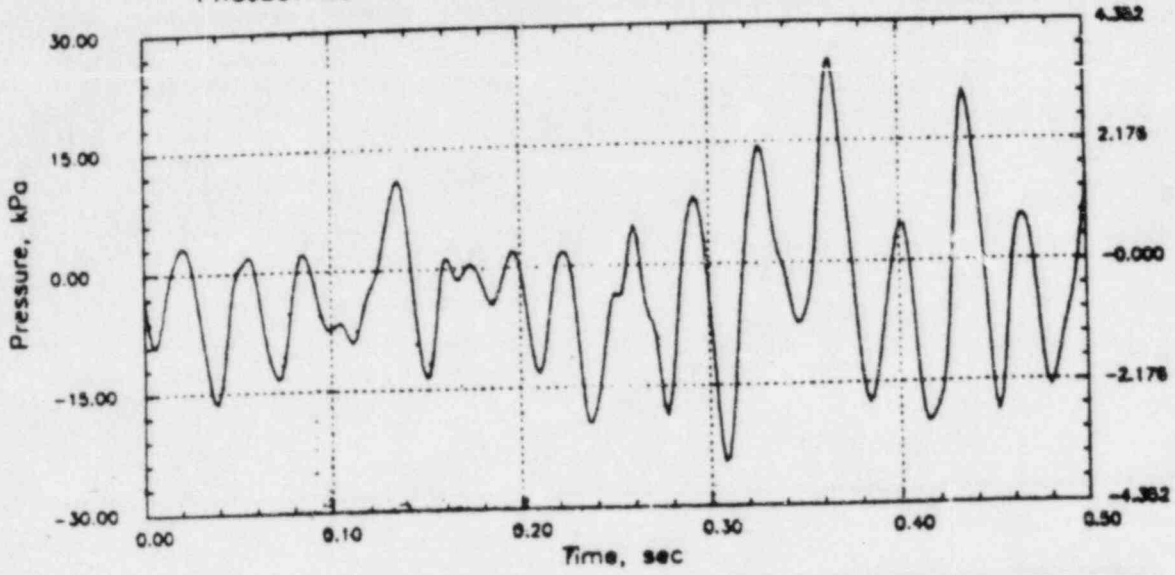

POP = 25.30 kPa PUP = -24.49 kPa MSP = 83.59 kPa²

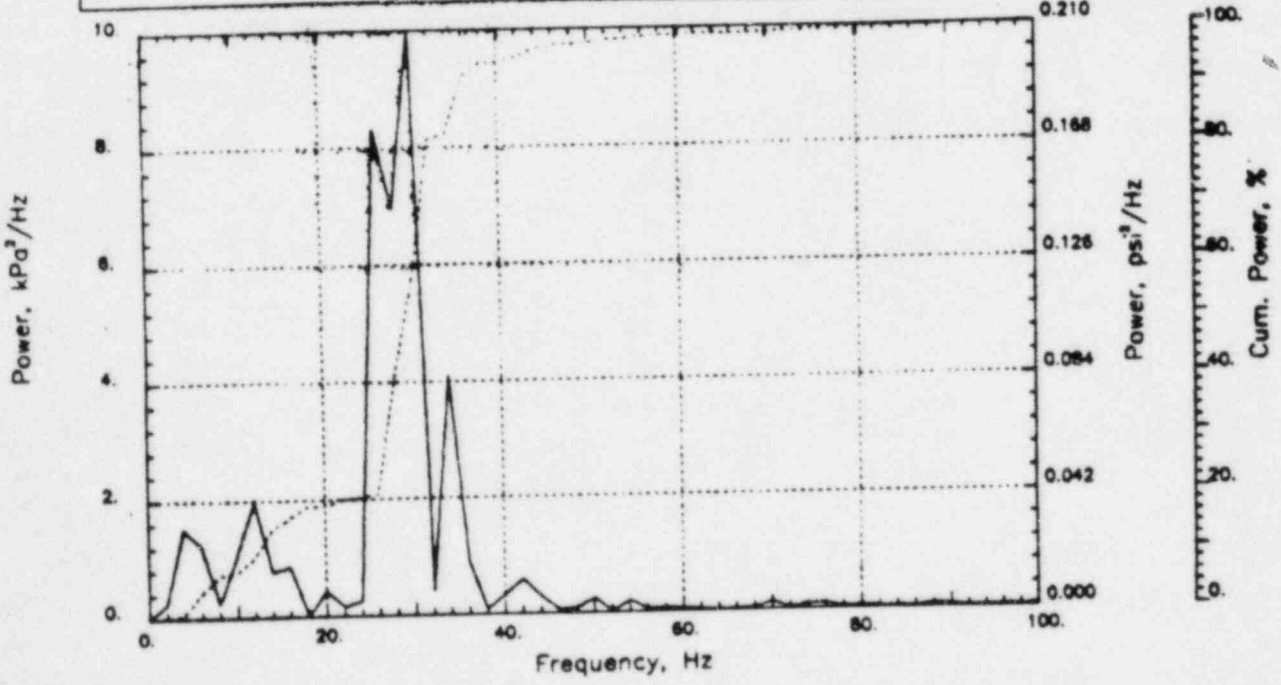

CLINTON RHR CO (C=1067)

Output at point (12.65,28.00,3.45)

NAME - LEONG, TAI SENG
DATE - FEB 22, 1984
PROJECT NO. - 15026004

CHECKED _____
DATE _____
CALC NO. - AP-84-

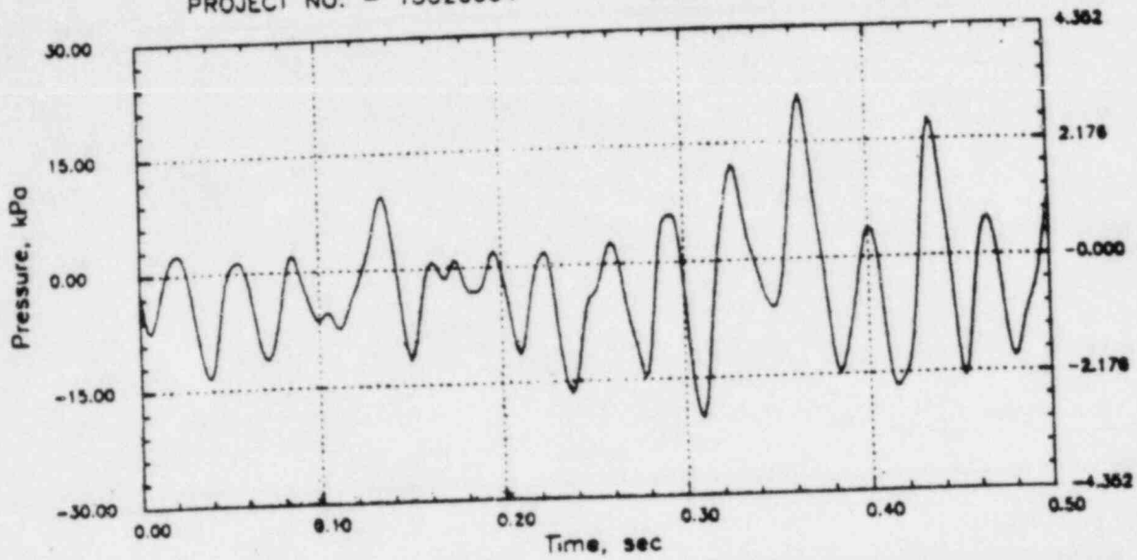

POP = 21.05 kPa PUP = -20.04 kPa MSP = 57.78 kPa²

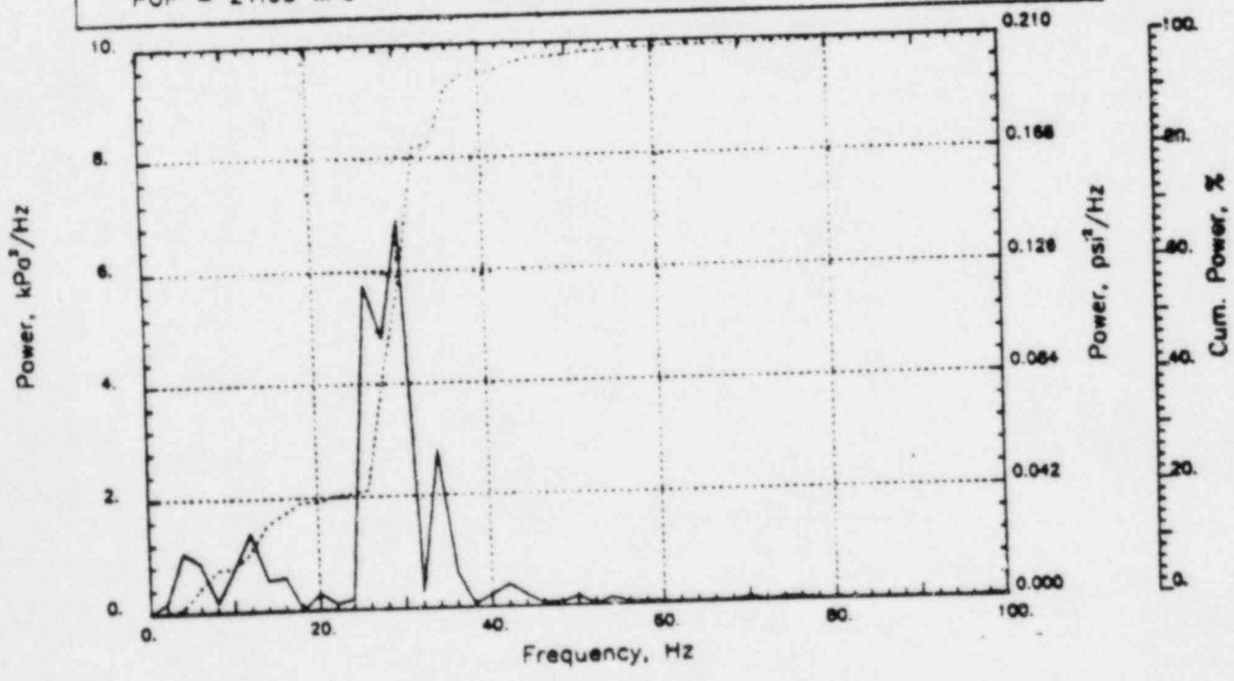

CLINTON RHR CO (C=1067)

Output at point (12.65.28.00,4.09)

NAME - LEONG, TAI SENG
DATE - FEB 22, 1984
PROJECT NO. - 15026004

CHECKED _____
DATE _____
CALC NO. - AP-84-

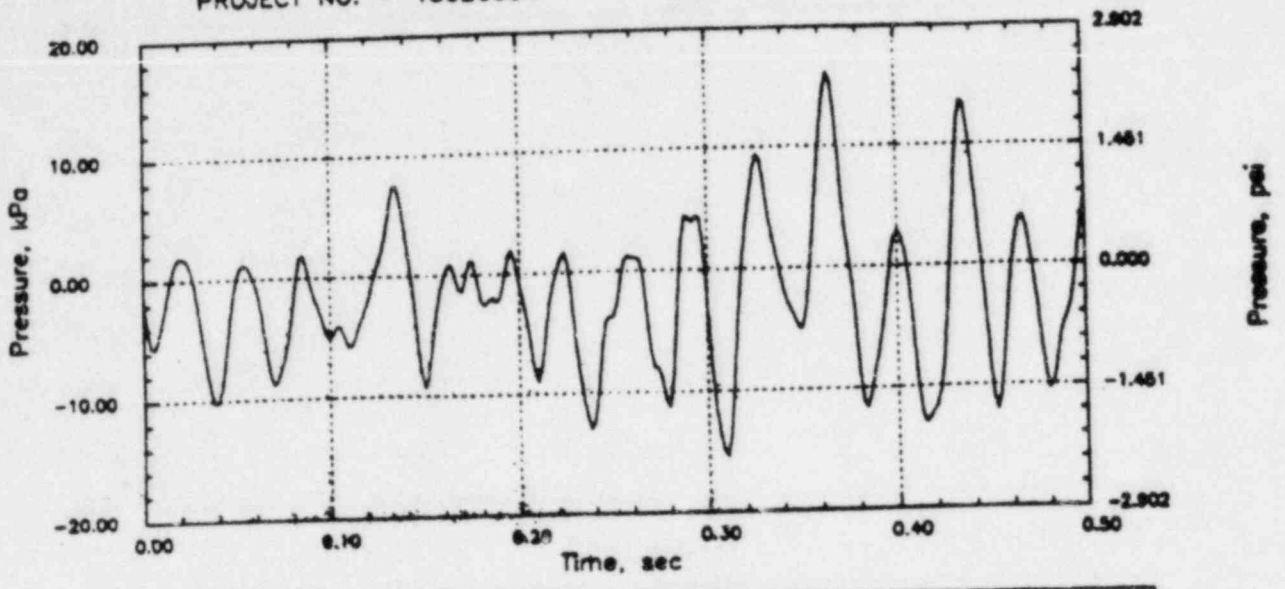

POP = 16.16 kPa PUP = -15.37 kPa MSP = 34.21 kPa²

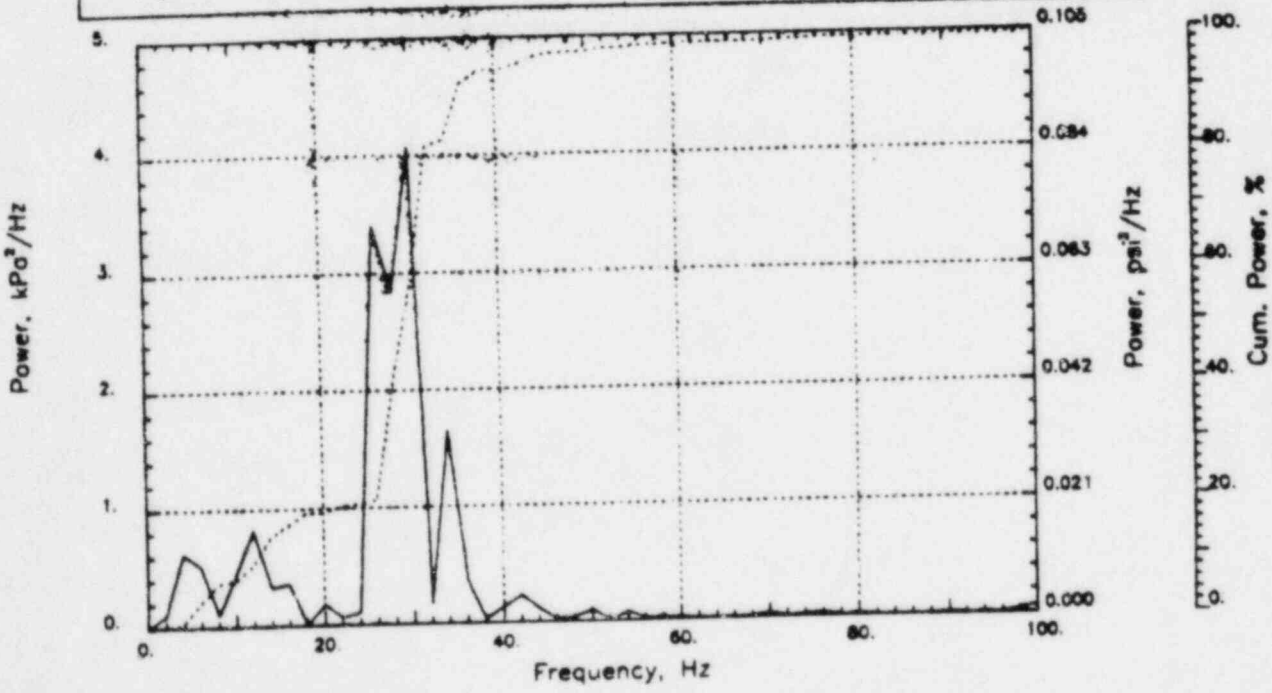

CLINTON RHR CO (C=1067)

Output at point (12.65,28.00,4.91)

NAME - LEONG, TAI SENG
DATE - FEB 22, 1984
PROJECT NO. - 15026004

CHECKED _____
DATE _____
CALC NO. - AP-84-

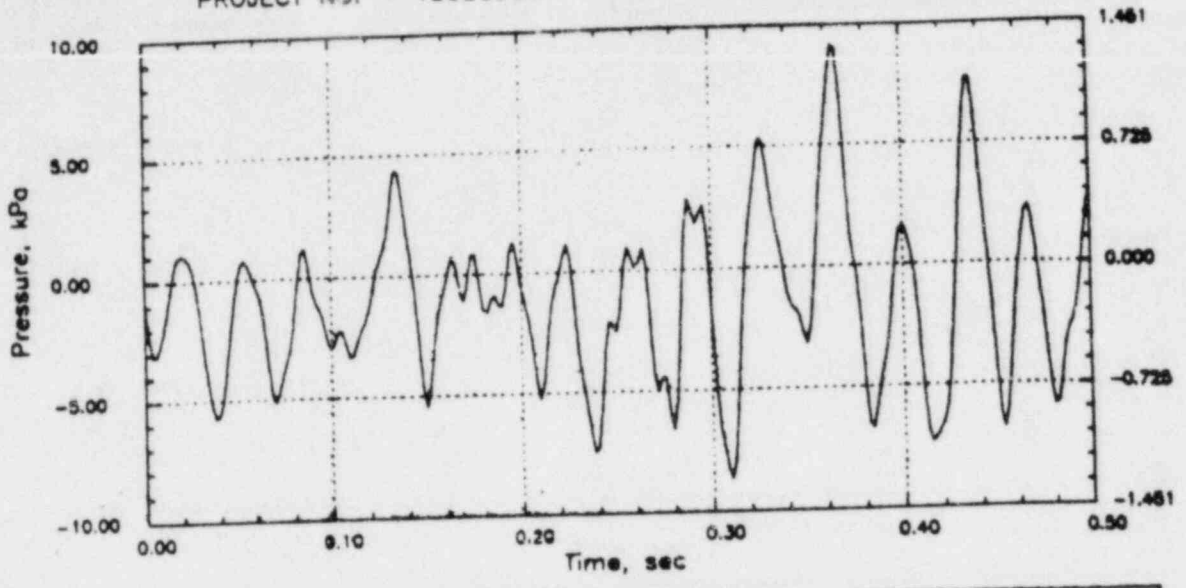

POP = 9.11 kPa PUP = -8.66 kPa MSP = 10.99 kPa²

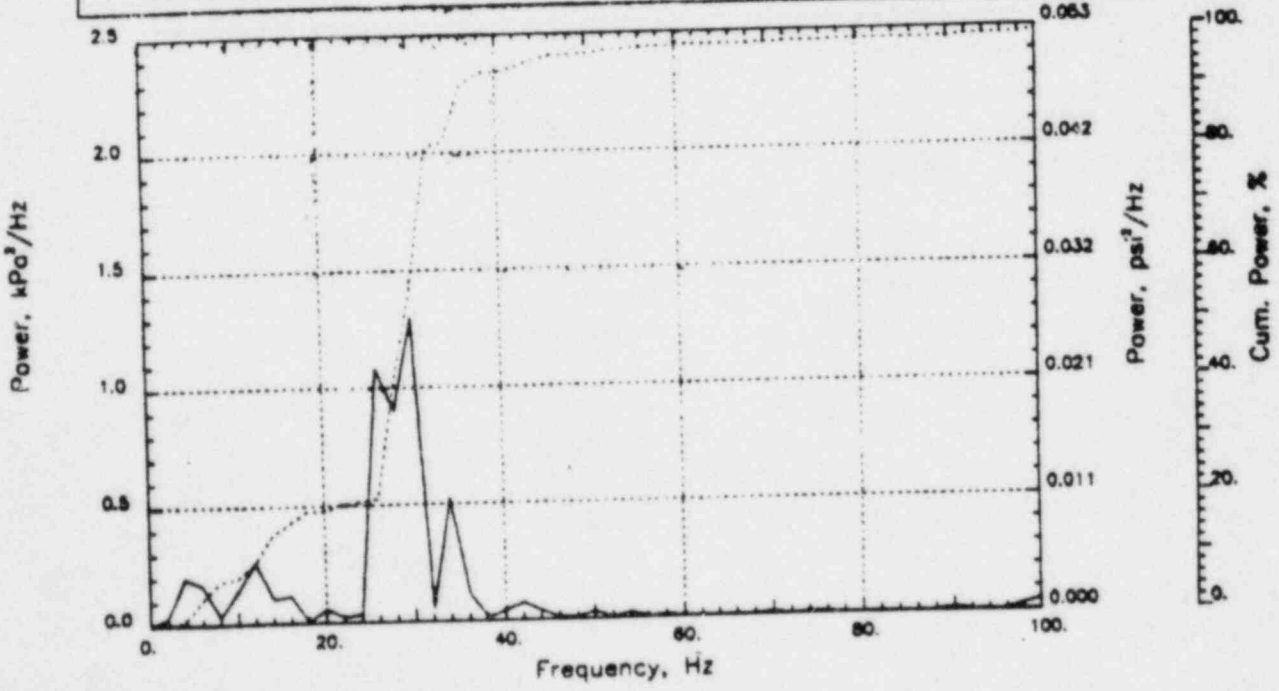

RIVER RHR CO (C=1067)

Output at point (18.90,28.00,4.91)

NAME - LEONG, TAI SENG
DATE - FEB 22, 1984
PROJECT NO. - 15026004

CHECKED _____
DATE _____
CALC NO. - AP-84-

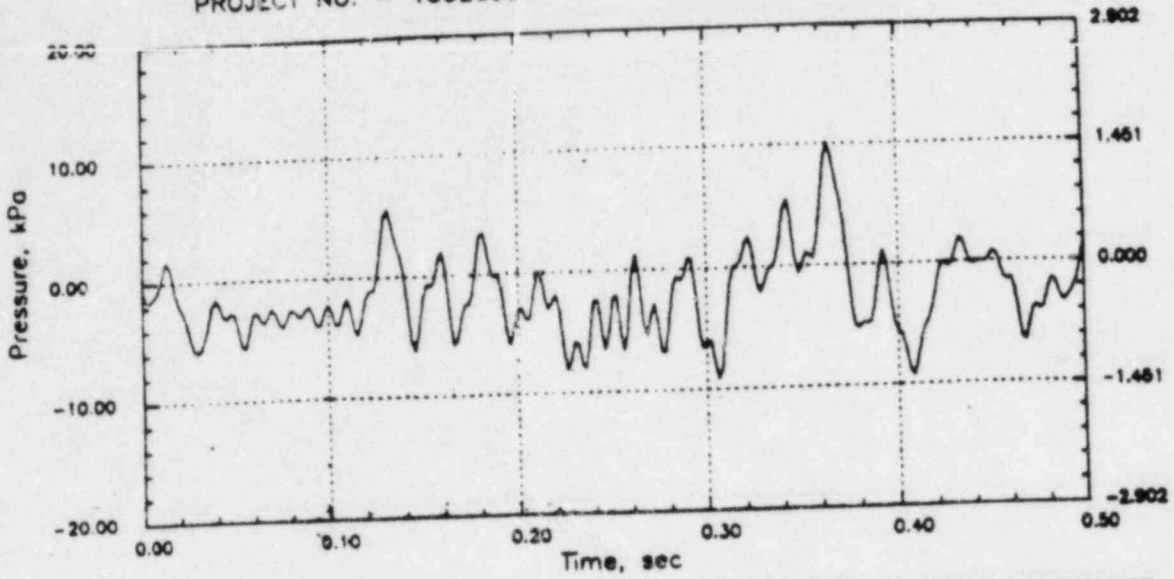

POP = 10.03 kPa PUP = -9.23 kPa MSP = 10.21 kPa²

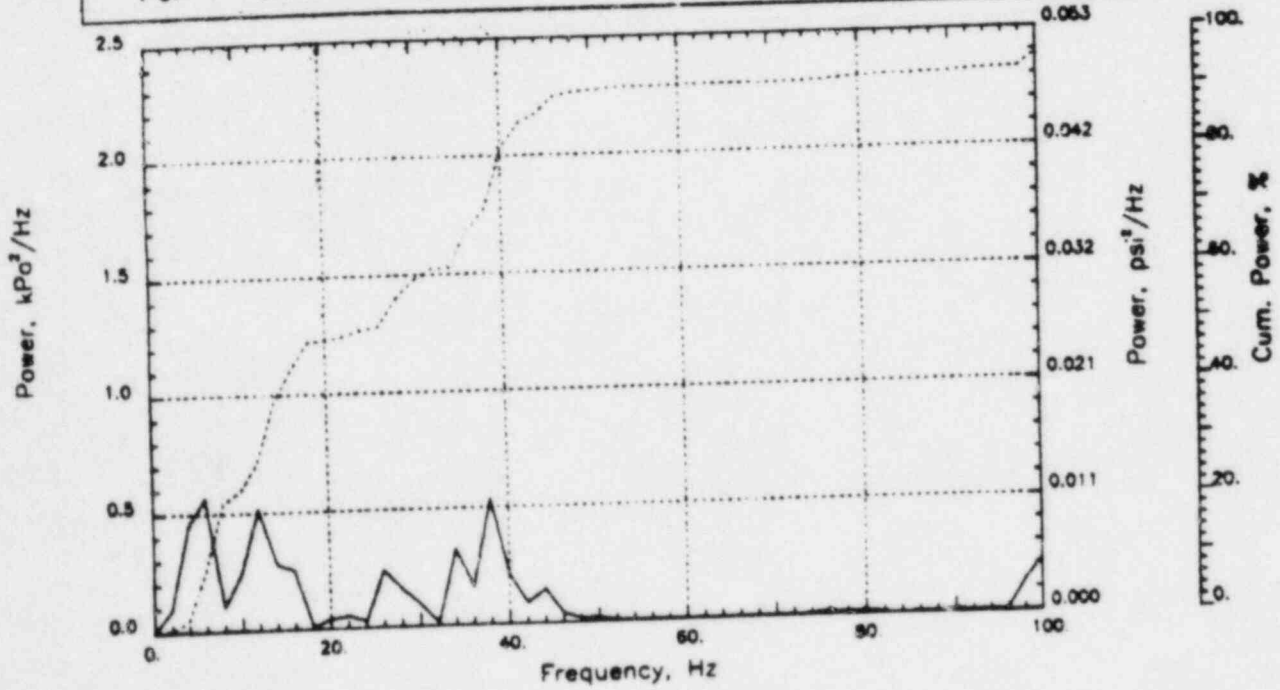

RIVER RHR CO (C=1067)

Output at point (18.90,28.00,4.09)

NAME - LEONG, TAI SENG
DATE - FEB 22, 1984
PROJECT NO. - 15026004

CHECKED _____
DATE _____
CALC NO. - AP-84-

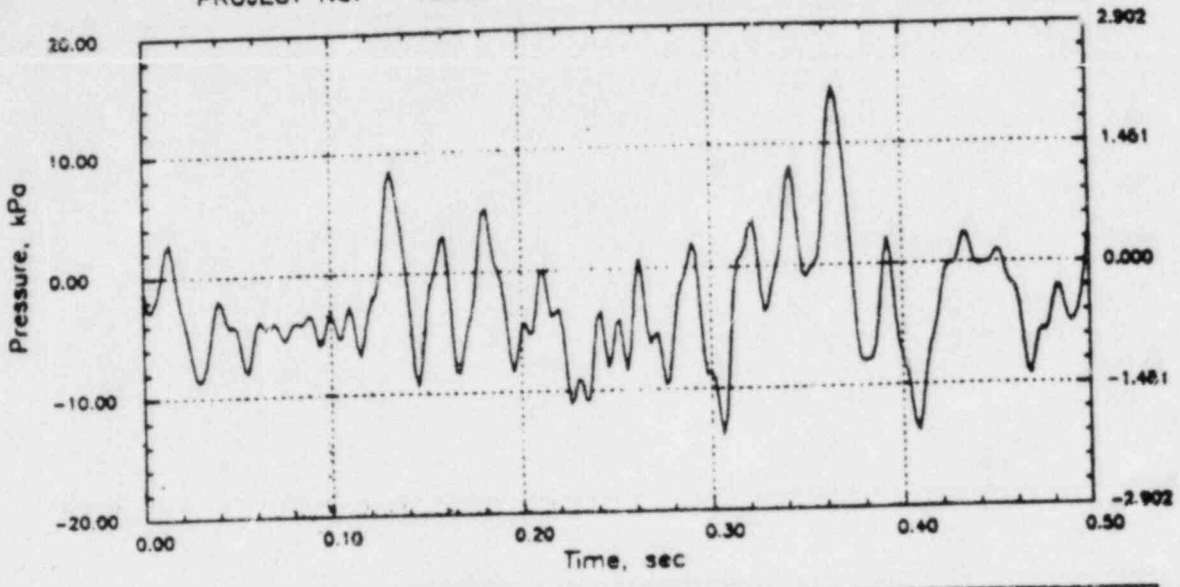

POP = 14.71 kPa PUP = -13.81 kPa MSP = 22.34 kPa²

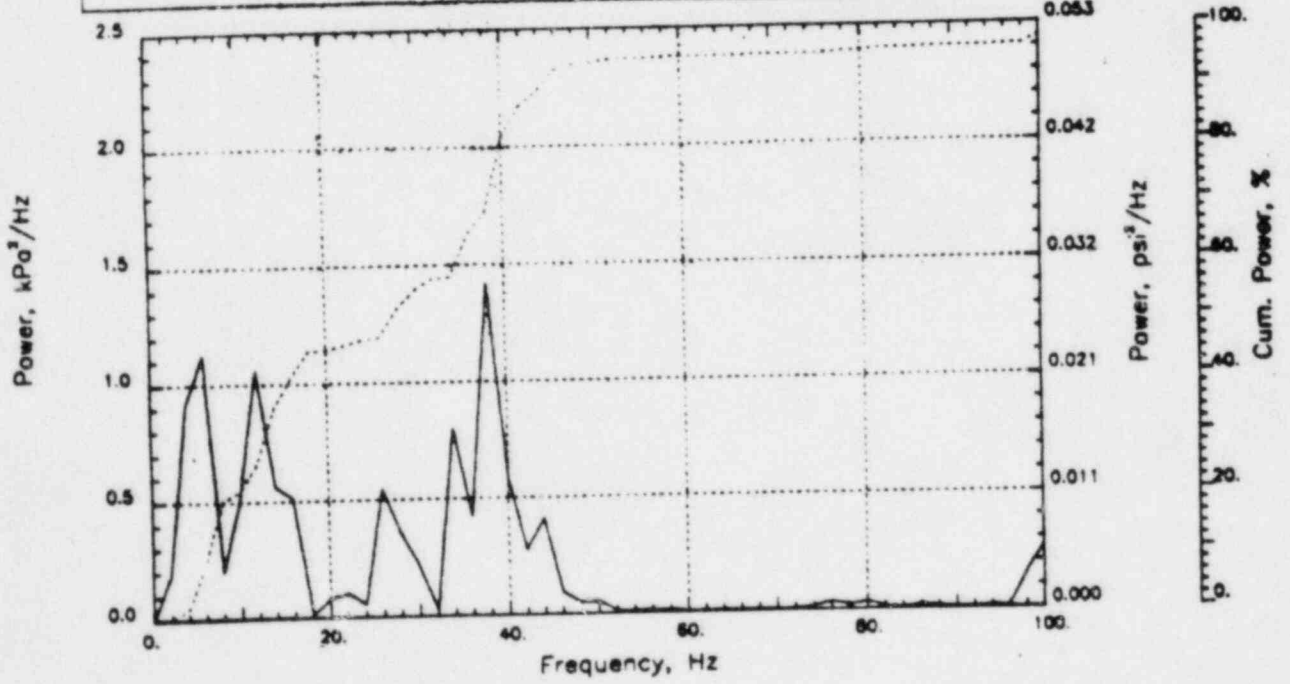

RIVER RHR CO (C=1067)

Output at point (18.90,28.00,3.45)

NAME - LEONG, TAI SENG
DATE - FEB 22, 1984
PROJECT NO. - 15026004

CHECKED _____
DATE _____
CALC NO. - AP-84-

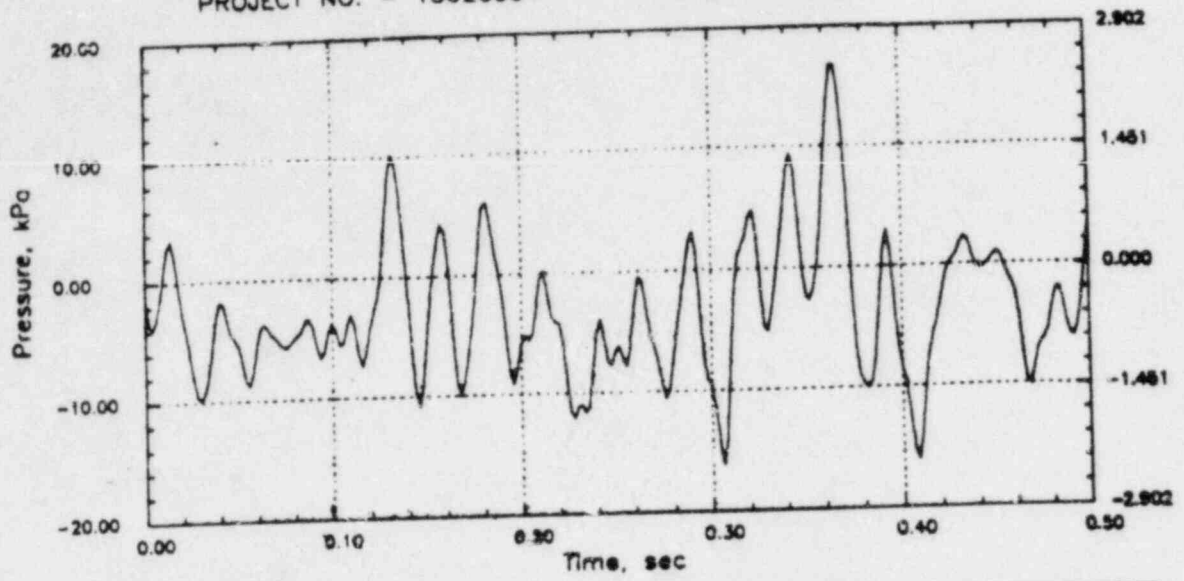

POP = 16.73 kPa PUP = -16.20 kPa MSP = 30.24 kPa²

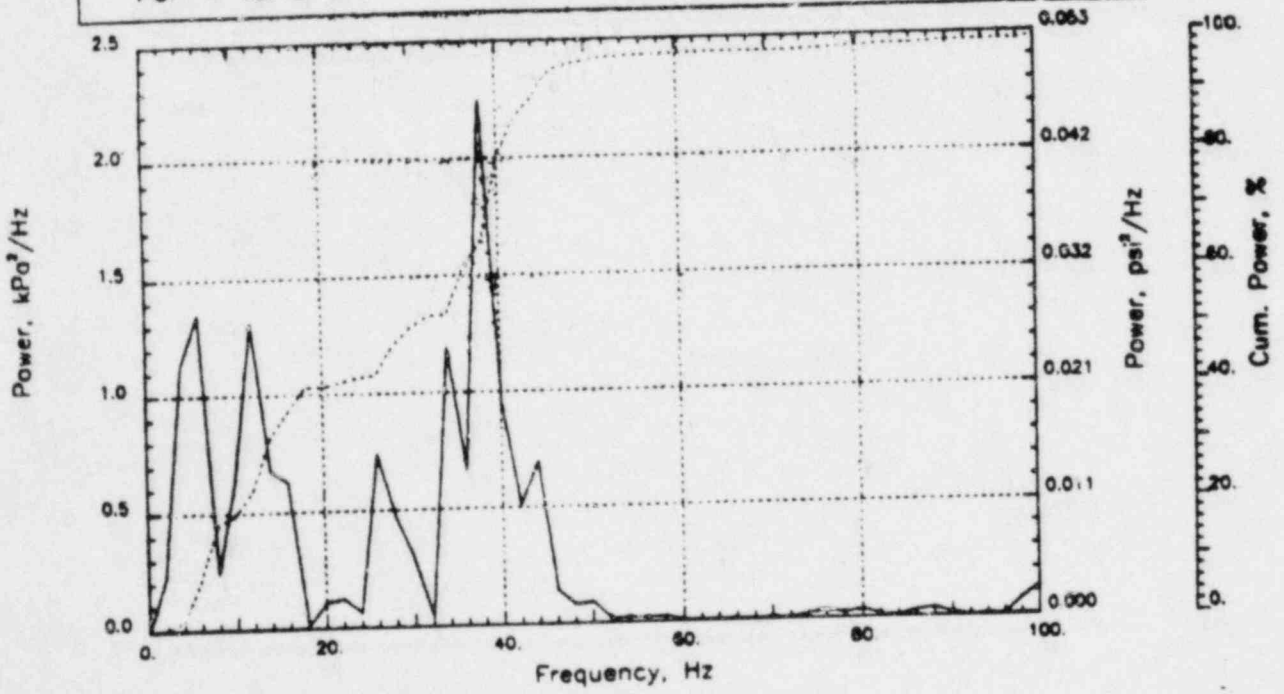

RIVER RHR CO (C=1067)

Output at point (18.90,28.00,2.82)

NAME - LEONG, TAI SENG
DATE - FEB 22, 1984
PROJECT NO. - 15026004

CHECKED _____
DATE _____
CALC NO. - AP-84-

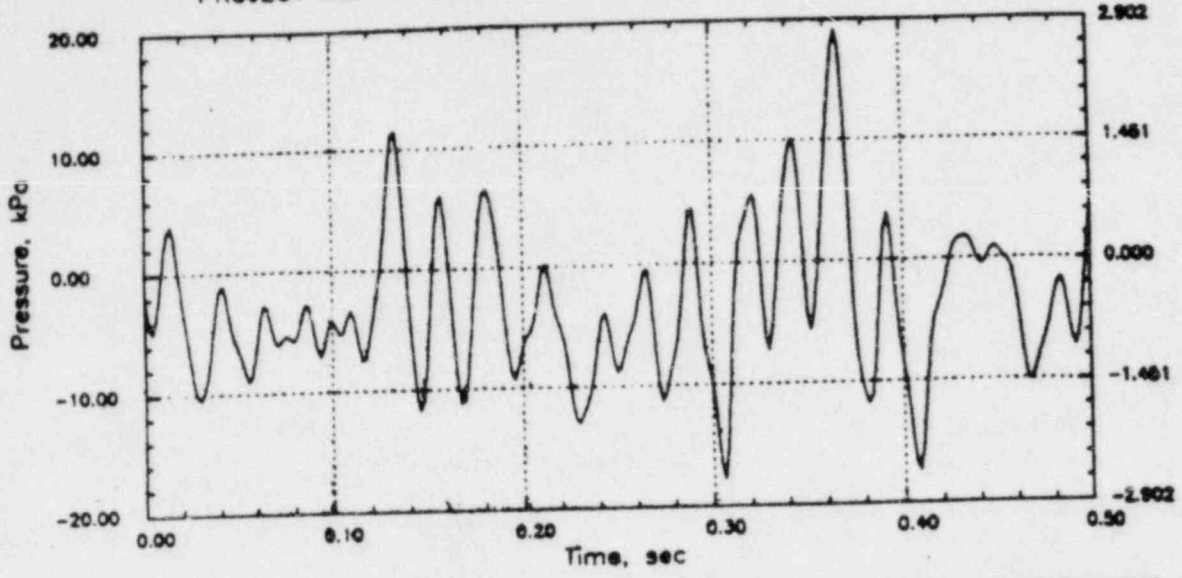

POP = 19.11 kPa PUP = -17.79 kPa MSP = 36.97 kPa²

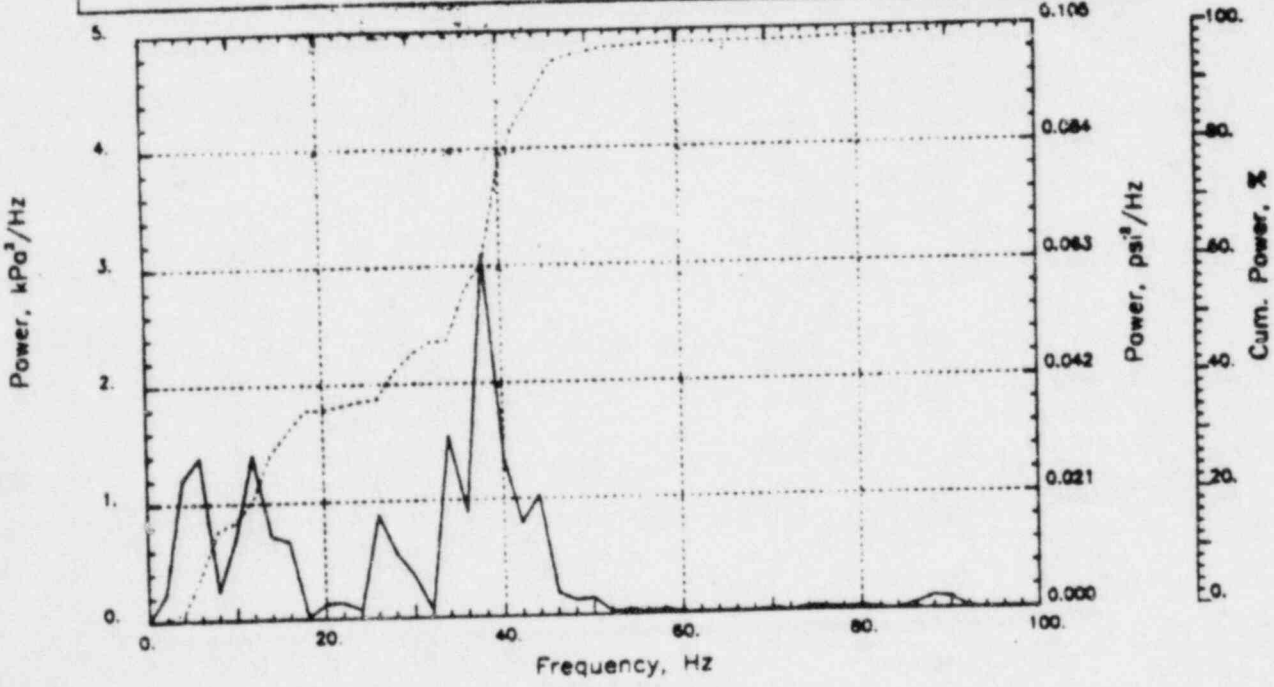

RIVER RHR CO (C=1067)

Output at point (18.90,28.00,2.18)

NAME - LEONG, TAI SENG
DATE - FEB 22, 1984
PROJECT NO. - 15026004

CHECKED _____
DATE _____
CALC NO. - AP-84-

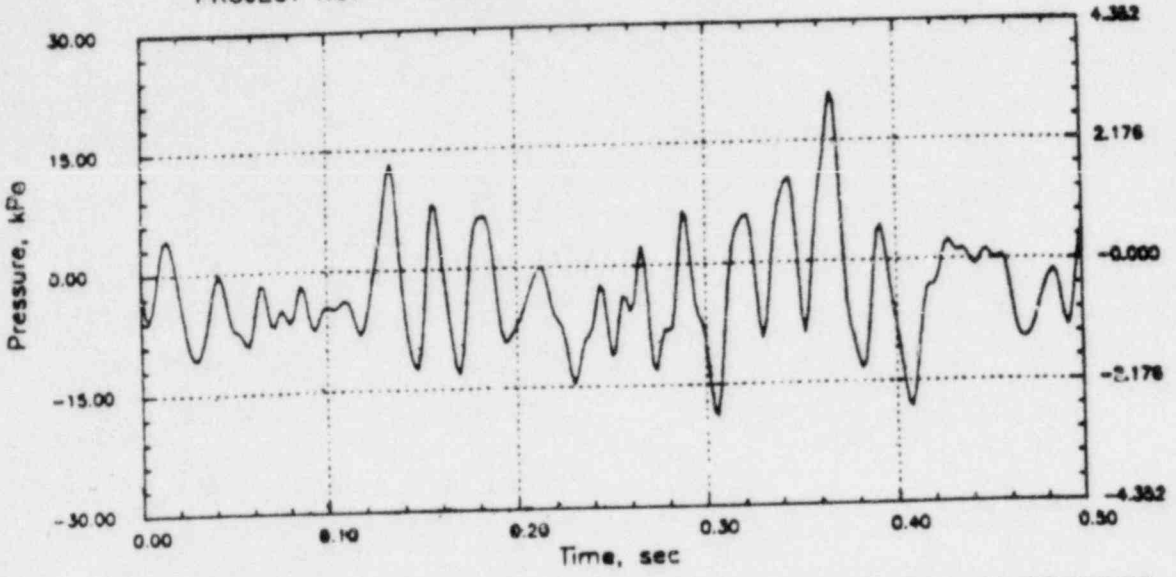

POP = 21.03 kPa PUP = -18.83 kPa MSP = 43.59 kPa²

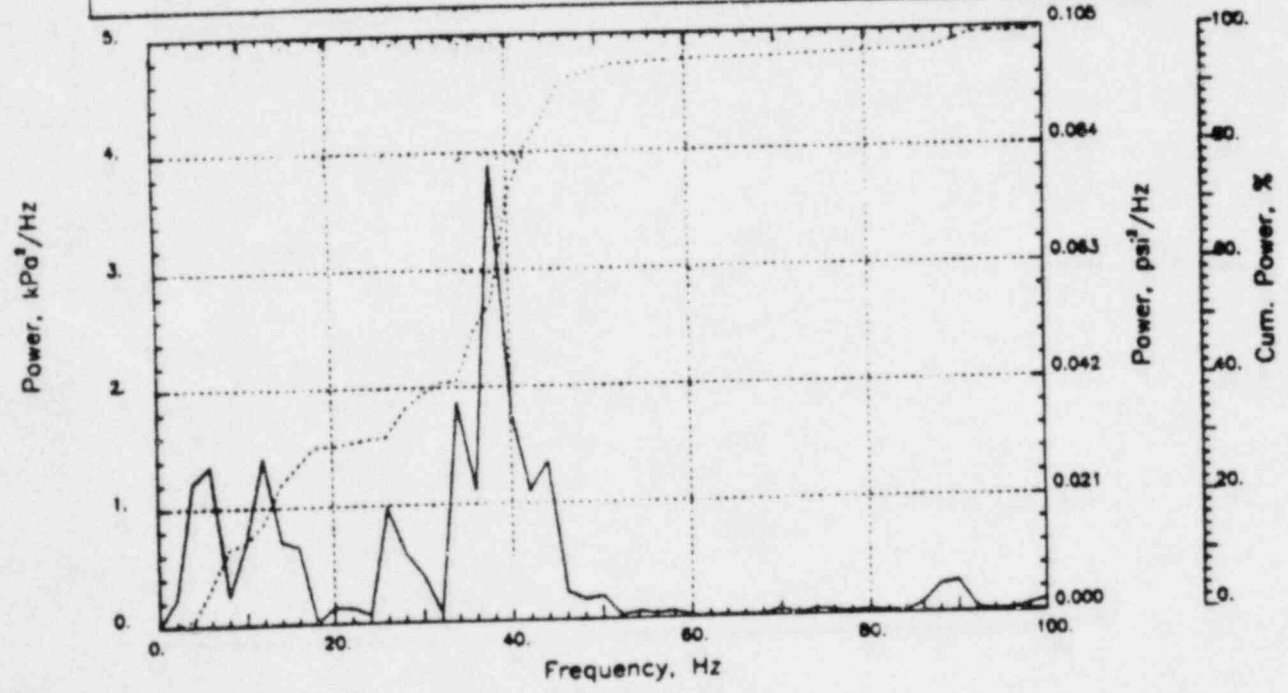

RIVER RHR CO (C=1067)

Output at point (18.90,28.00,1.55)

NAME - LEONG, TAI SENG
DATE - FEB 22, 1984
PROJECT NO. - 15026004

CHECKED _____
DATE _____
CALC NO. - AP-84-

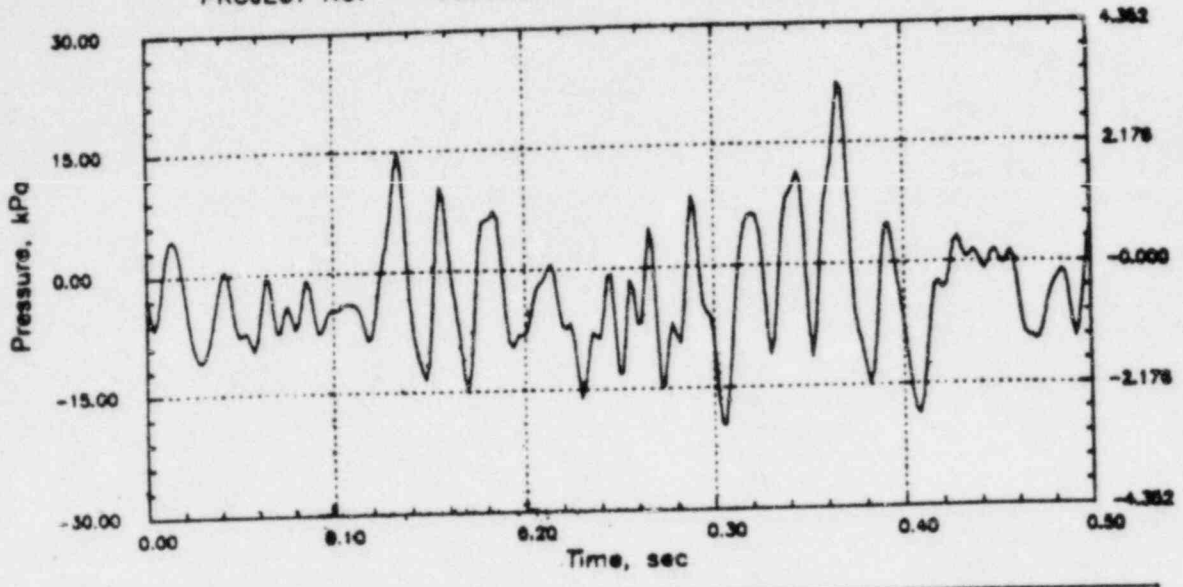

POP = 22.55 kPa PUP = -19.54 kPa MSP = 50.27 kPa²

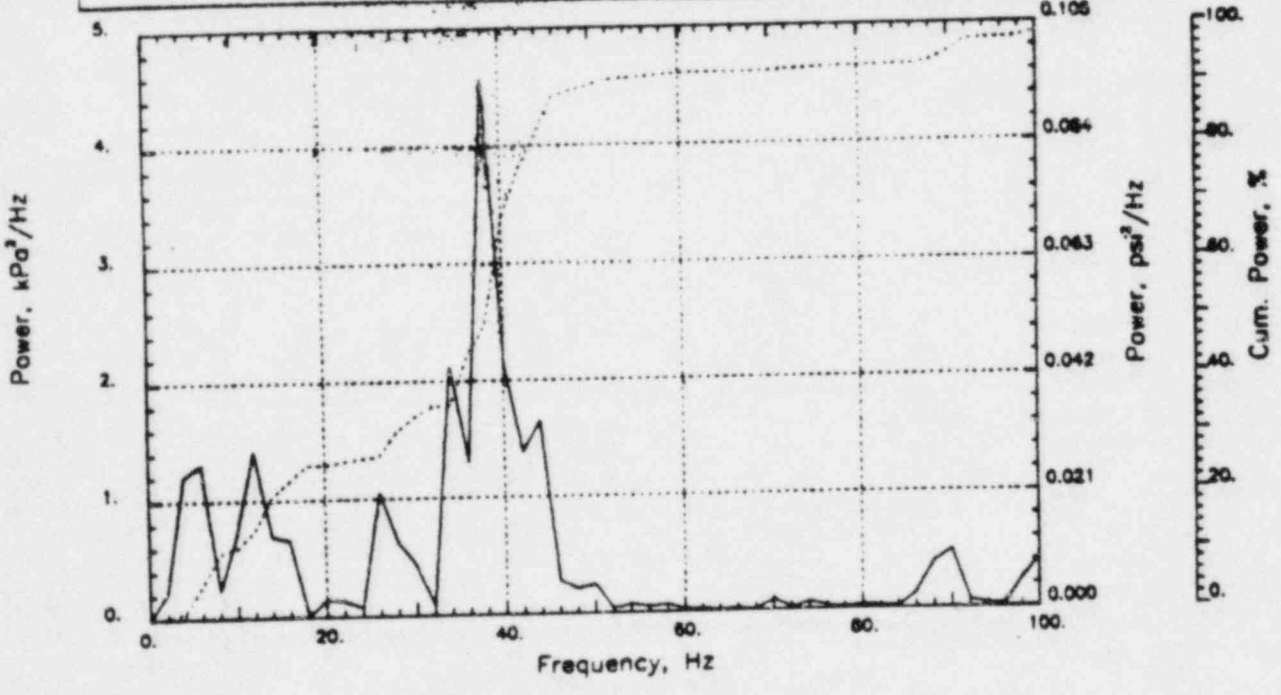

RIVER RHR CO (C=1067)

Output at point (18.90,28.00,0.91)

NAME - LEONG, TAI SENG
DATE - FEB 22, 1984
PROJECT NO - 15026004

CHECKED _____
DATE _____
CALC NO. - AP-84-

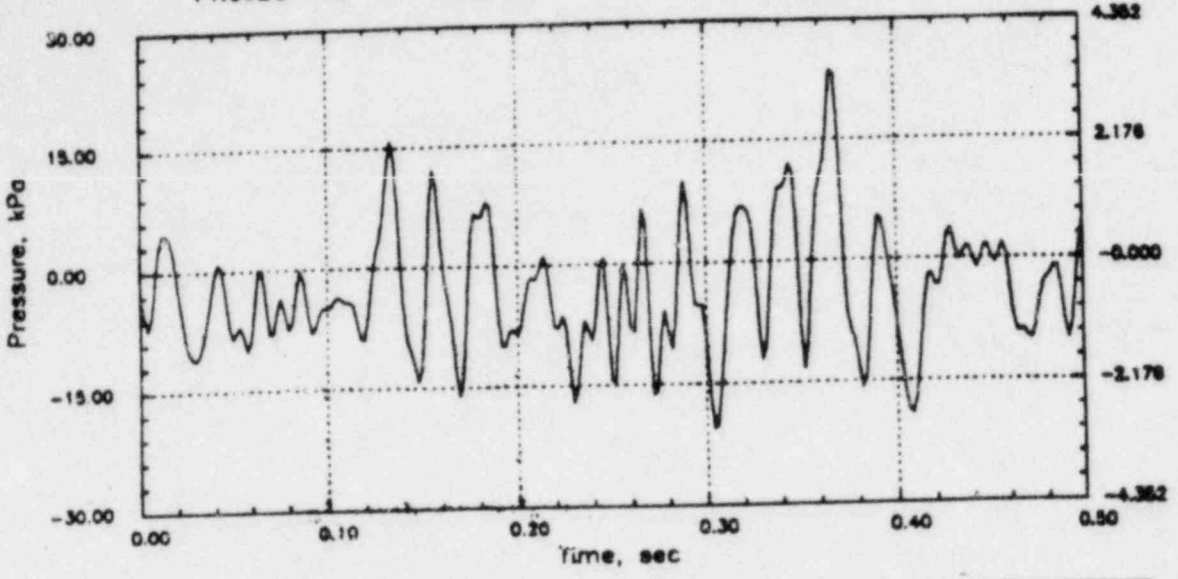

POP = 23.64 kPa PUP = -20.54 kPa MSP = 55.97 kPa²

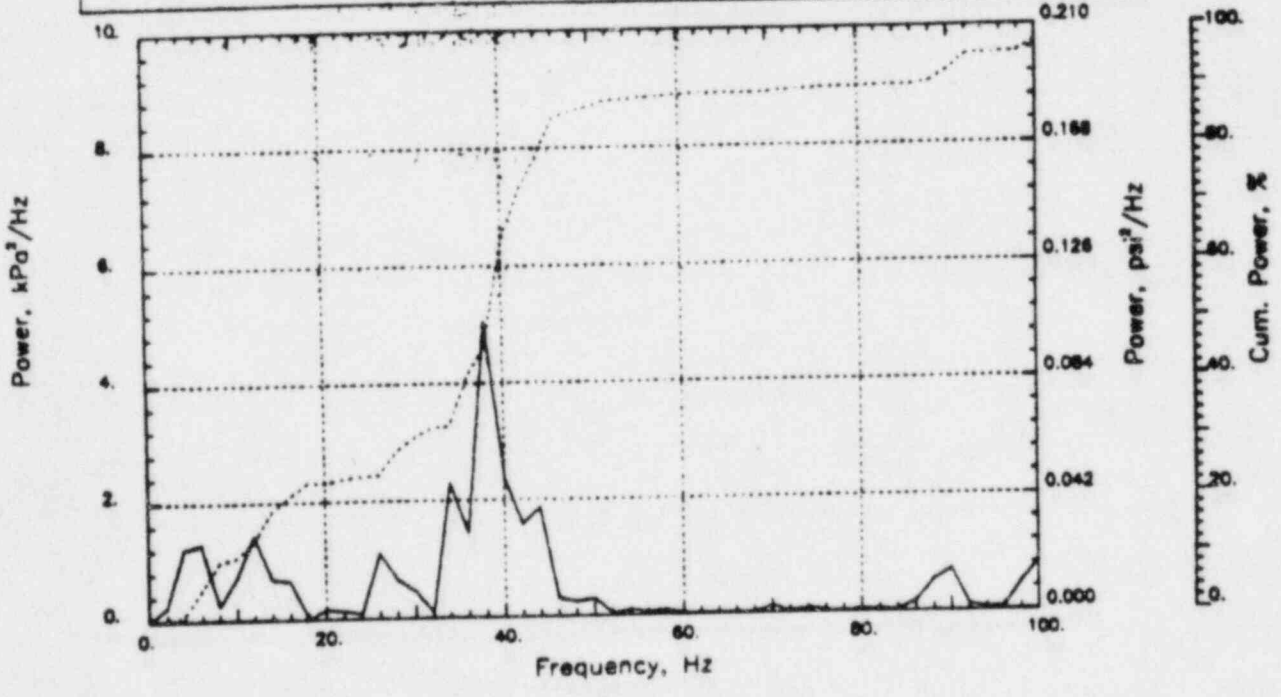

RIVER RHR CO (C=1067)

Output at point (18.90,28.00,0.46)

NAME - LEONG, TAI SENG
DATE - FEB 22, 1984
PROJECT NO. - 15026004

CHECKED _____
DATE _____
CALC NO. - AP-84-

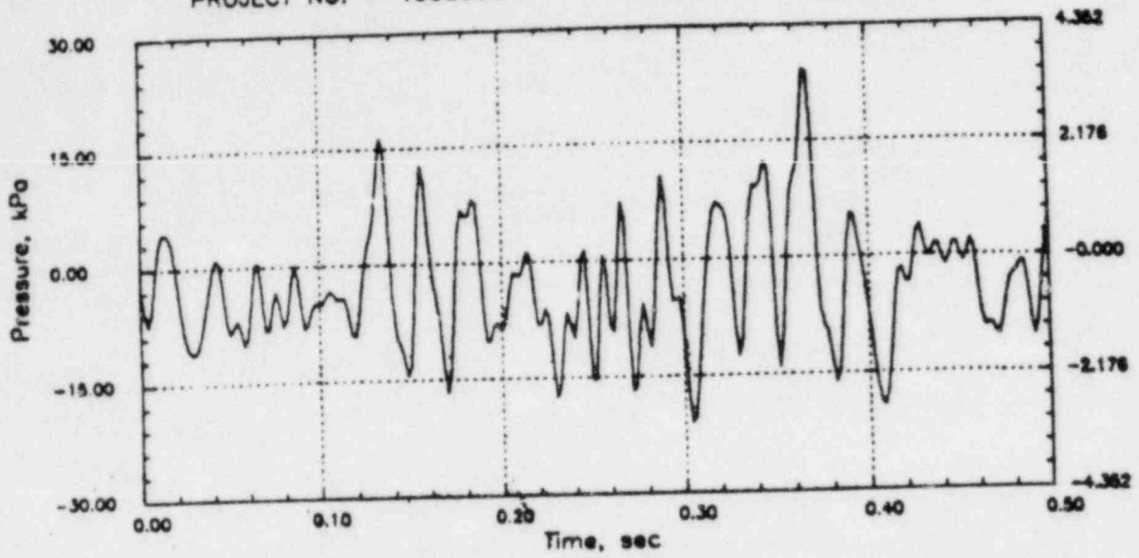

POP = 24.11 kPa PUP = -21.00 kPa MSP = 58.62 kPa²

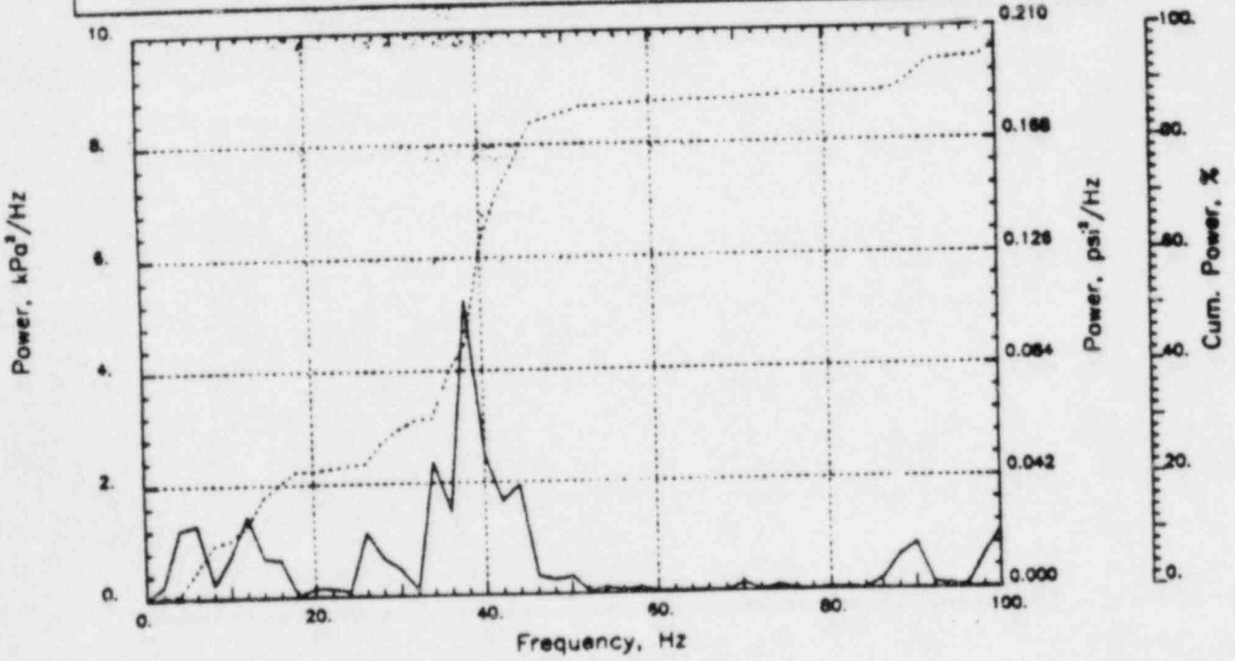

RIVER RHR CO (C=1067)

Output at point (18.90,28.00,0.00)

NAME - LEONG, TAI SENG
DATE - FEB 22, 1984
PROJECT NO. - 15026004

CHECKED _____
DATE _____
CALC NO. - AP-84-

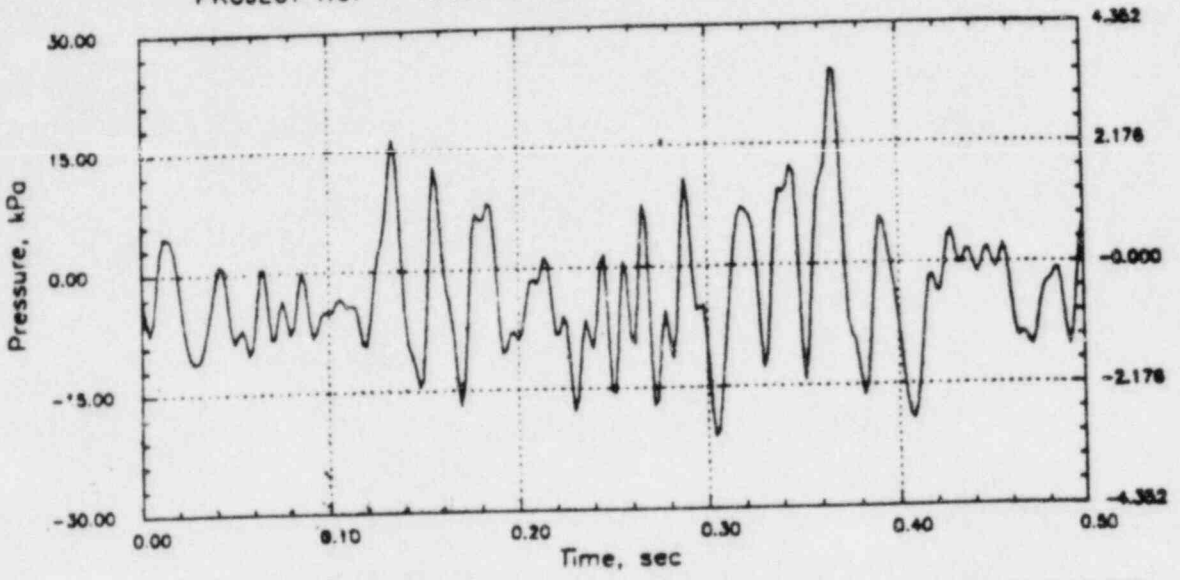

POP = 24.27 kPa PUP = -21.16 kPa MSP = 59.56 kPa²

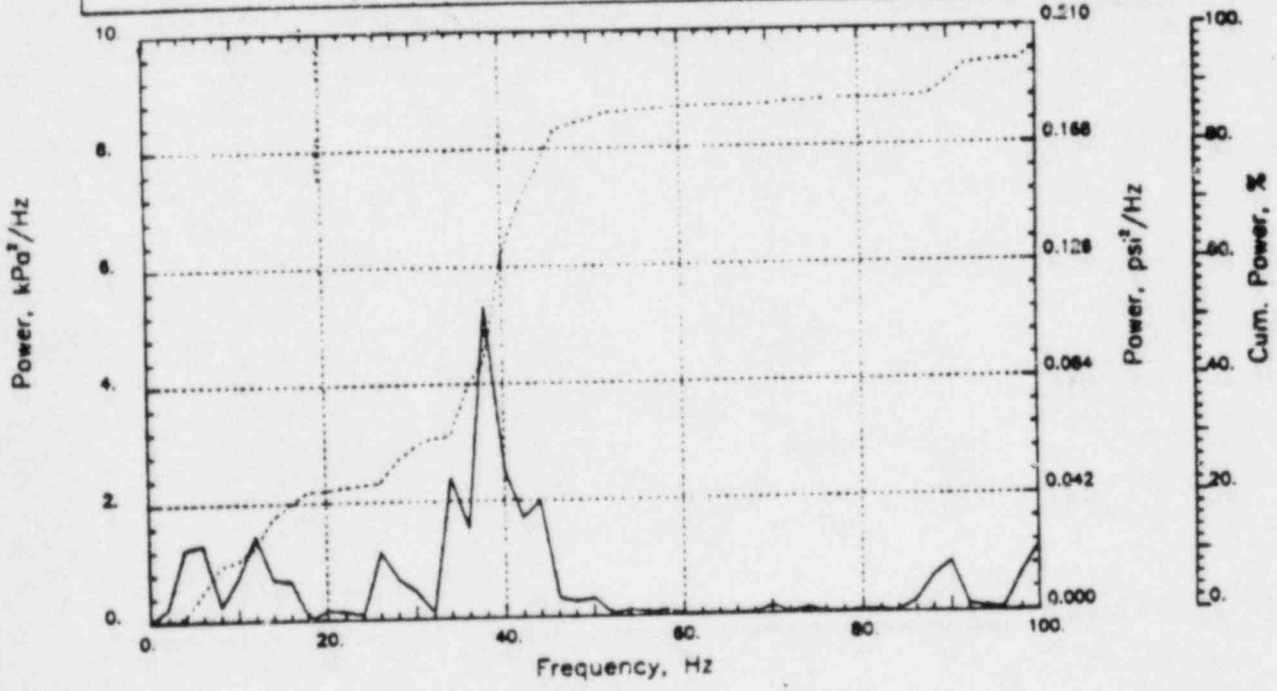

RIVER RHR CO (C=1067)

Output at point (17.34,28.00,0.00)

NAME - LEONG, TAI SENG
DATE - FEB 22, 1984
PROJECT NO. - 15026004

CHECKED _____
DATE _____
CALC NO. - AP-84-

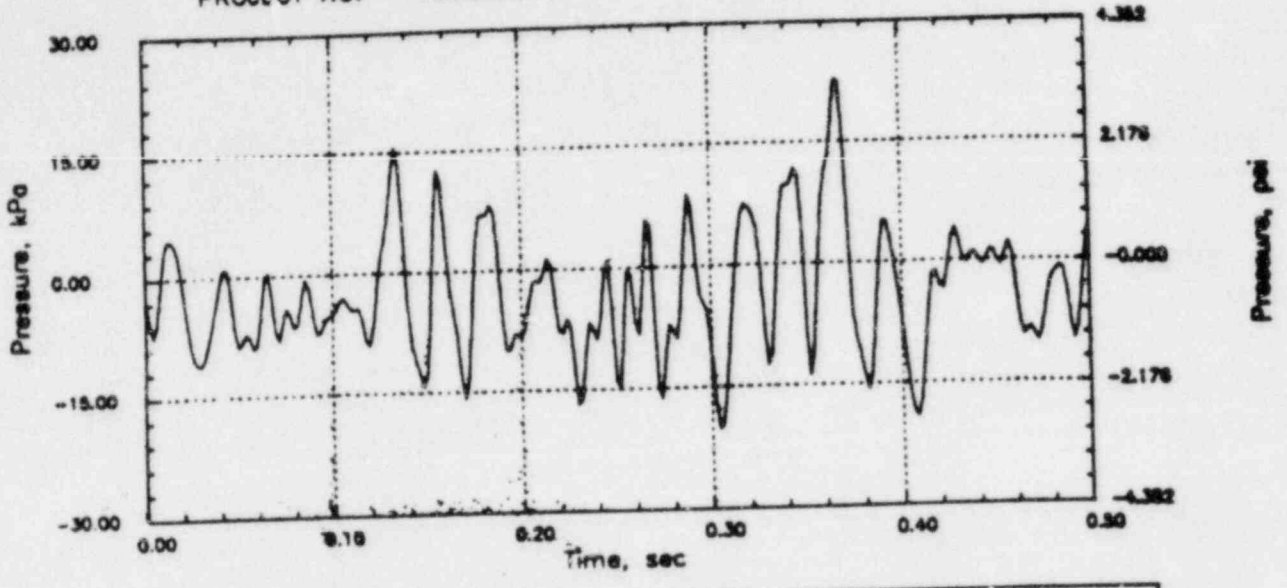

POP = 22.68 kPa PUP = -20.15 kPa MSP = 55.92 kPa²

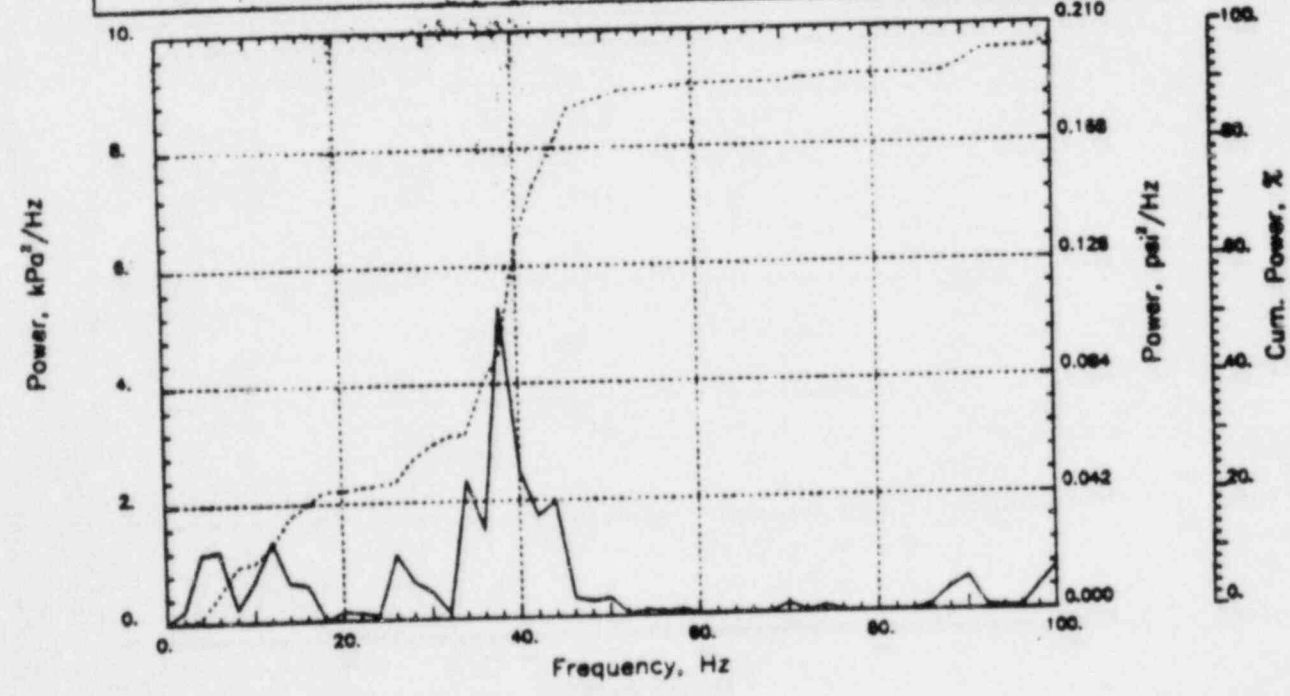

RIVER RHR CO (C=1067)

Output at point (14.21,28.00,0.00)

NAME - LEONG, TAI SENG
DATE - FEB 22, 1984
PROJECT NO. - 15026004

CHECKED _____
DATE _____
CALC NO. - AP-84-

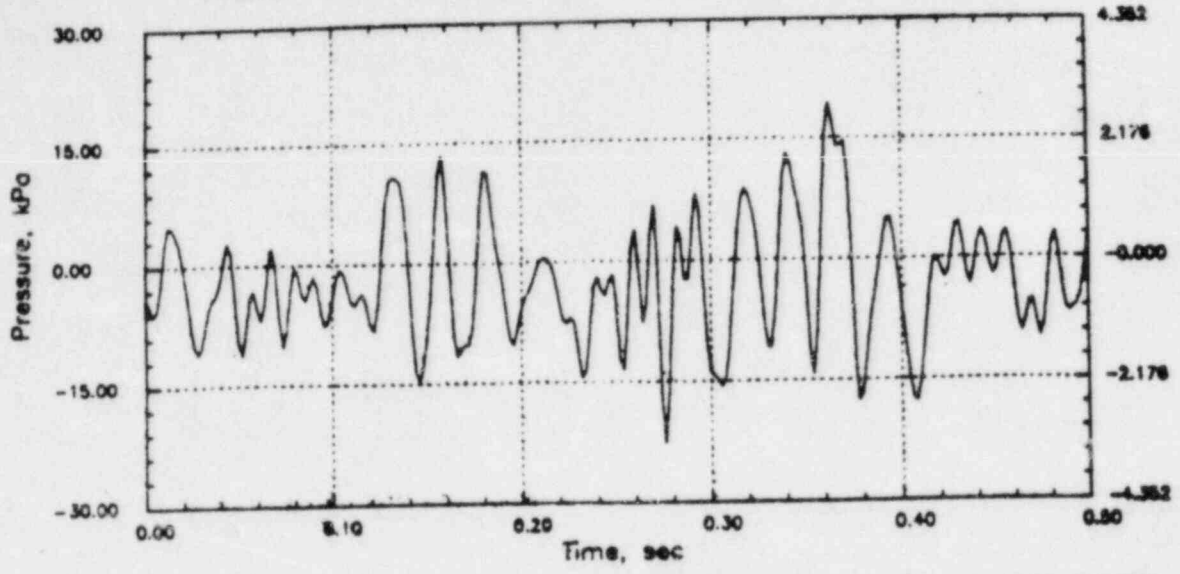

POP = 19.38 kPa PUP = -22.62 kPa MSP = 52.33 kPa²

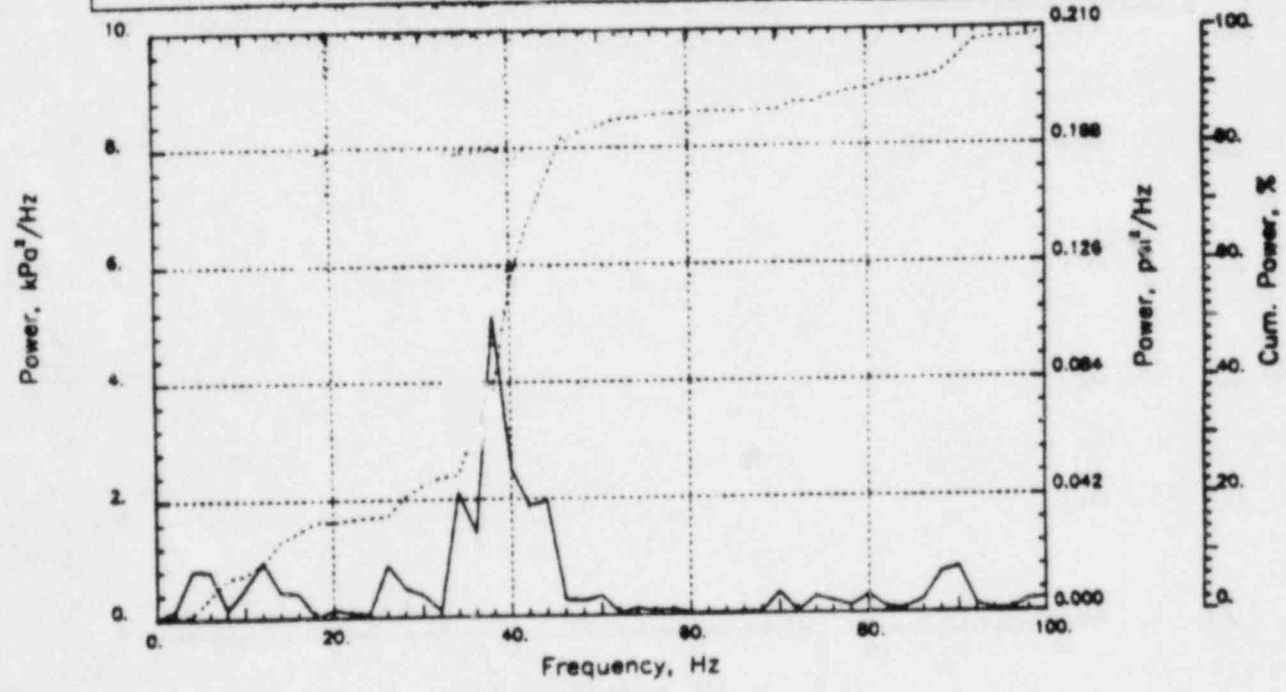

RIVER RHR CO (C=1067)

Output at point (12.65,28.00,0.00)

NAME - LEONG, TAI SENG
DATE - FEB 22, 1984
PROJECT NO - 15026004

CHECKED _____
DATE _____
CALC NO. - AP--84-

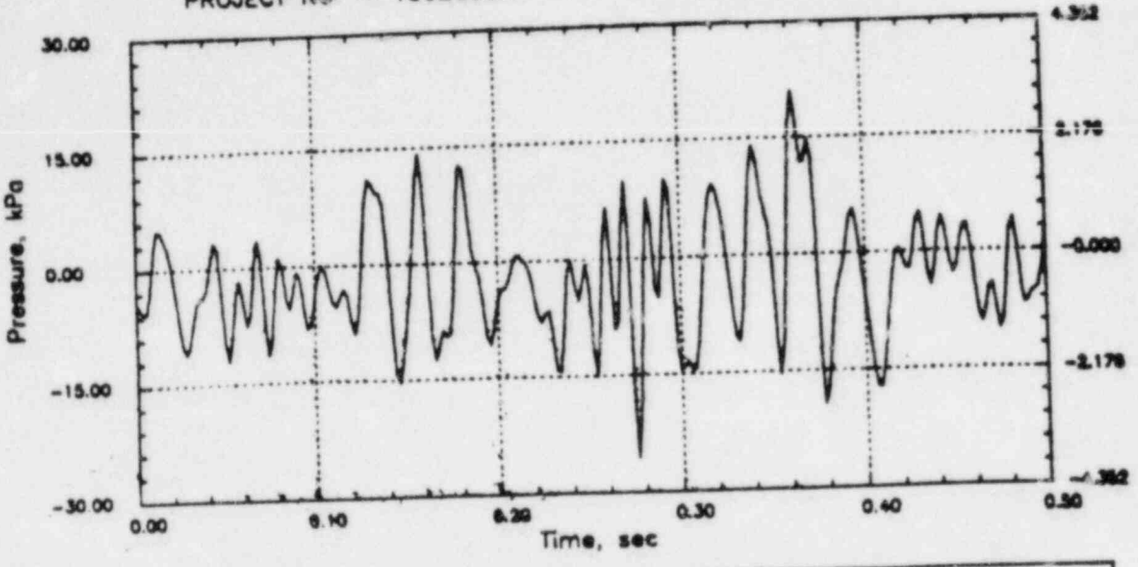

POP = 20.91 kPa PUP = -25.59 kPa MSP = 55.73 kPa²

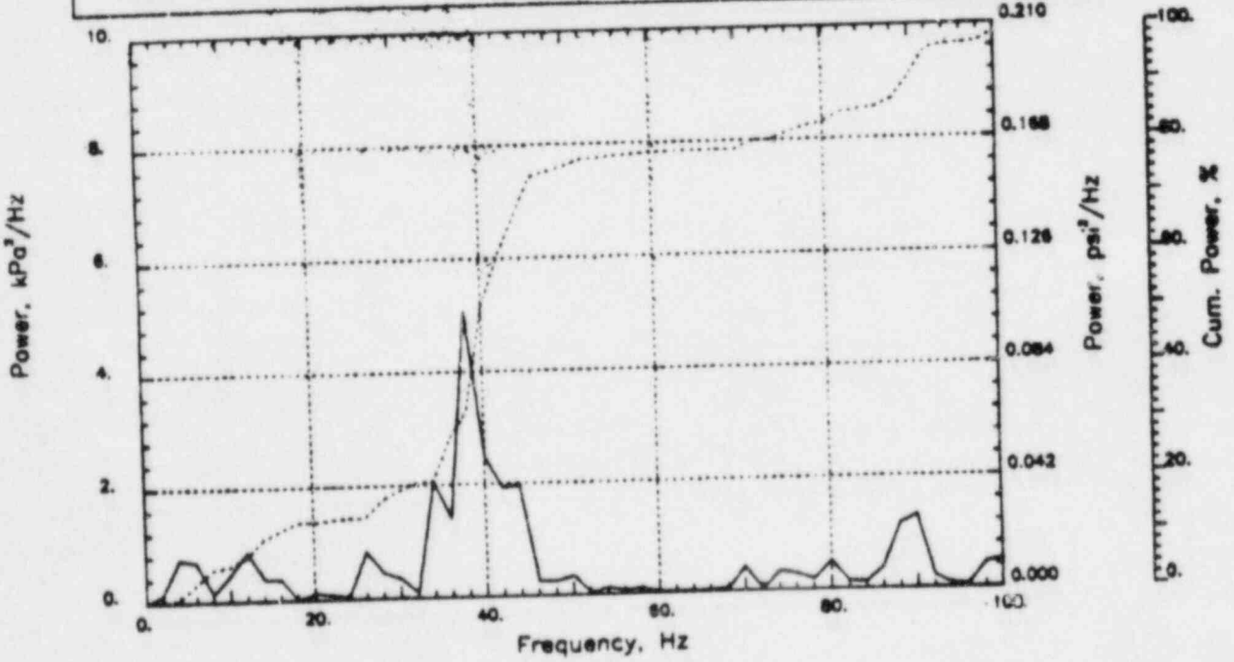

RIVER RHR CO (C=1067)

Output at point (12.65,28.00,0.46)

NAME - LEONG, TAI SENG
DATE - FEB 22, 1984
PROJECT NO. - 15026004

CHECKED _____
DATE _____
CALC NO. - AP-84-

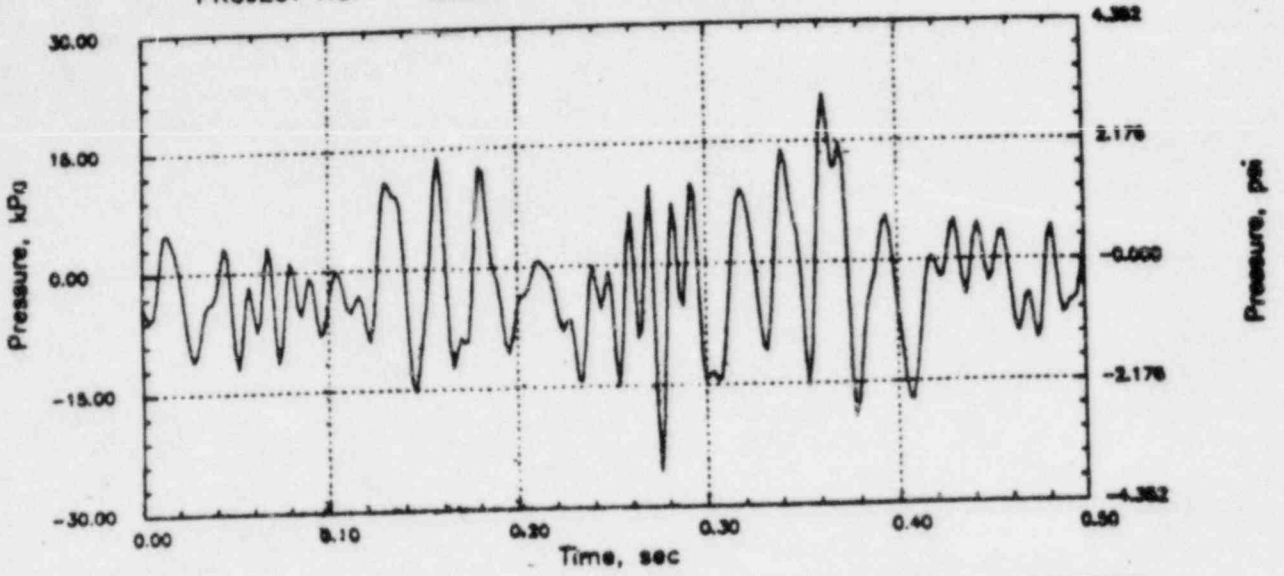

POP = 20.84 kPa PUP = -25.47 kPa MSP = 55.06 kPa²

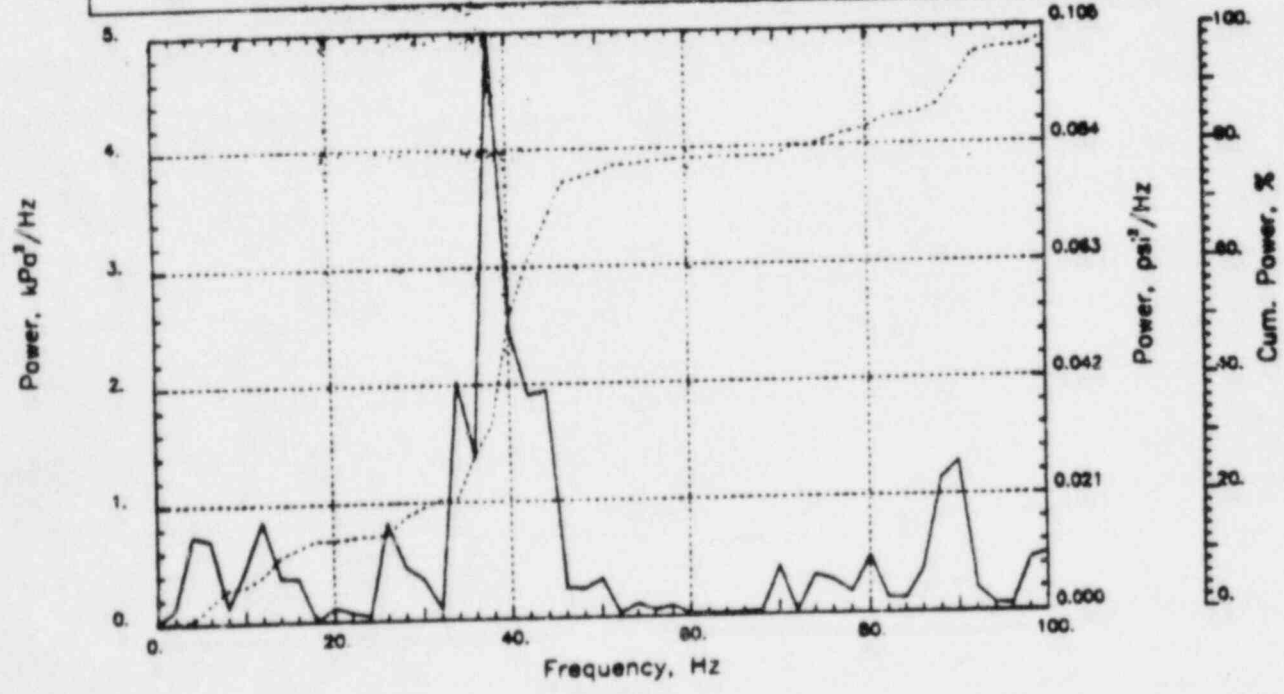

RIVER RHR CO (C=1067)

Output at point (12.65,28.00,0.91)

NAME - LEONG, TAI SENG
DATE - FEB 22, 1984
PROJECT NO. - 15026004

CHECKED _____
DATE _____
CALC NO. - AP-84-

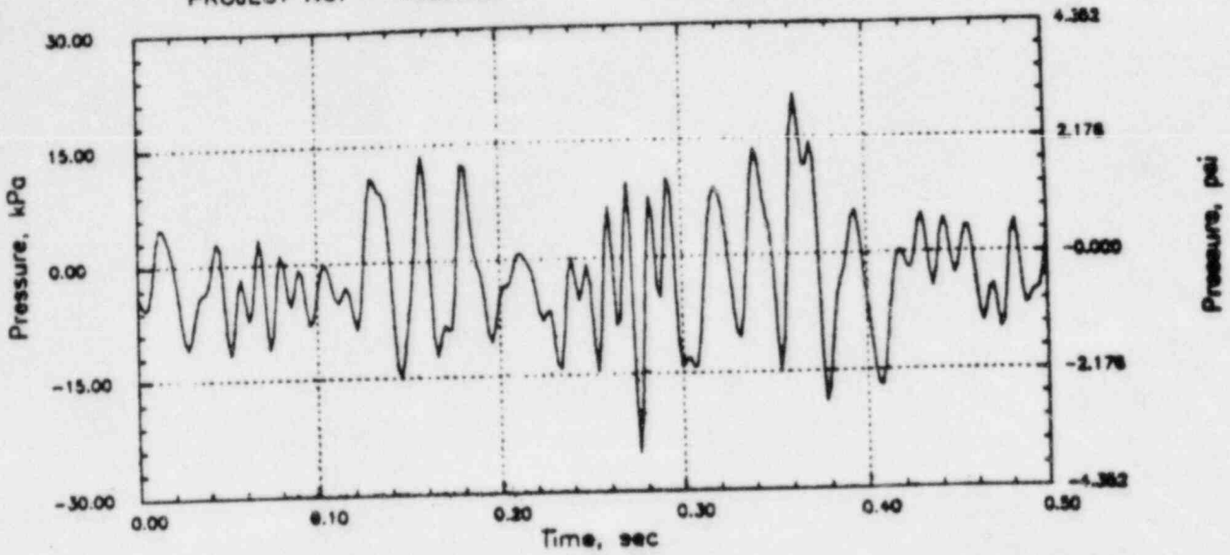

POP = 20.61 kPa PUP = -25.10 kPa MSP = 53.09 kPa²

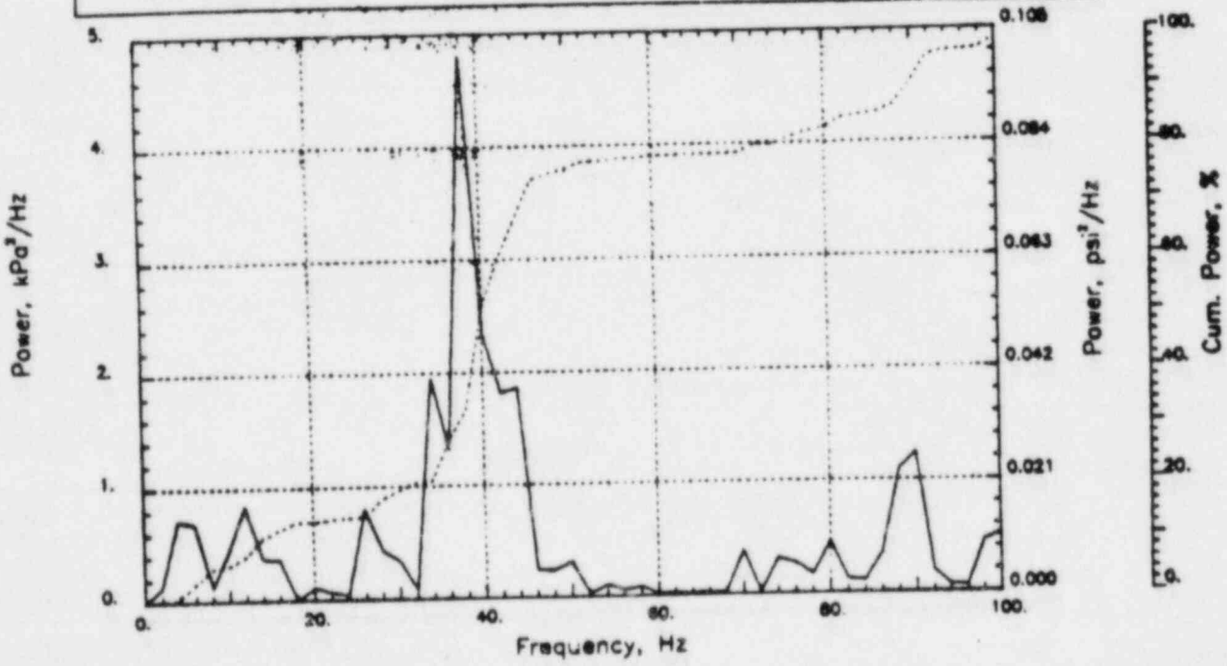

RIVER RHR CO (C=1067)

Output at point.(12.65,28.00,2.18)

NAME - LEONG, TAI SENG
DATE - FEB 22, 1984
PROJECT NO. - 15026004

CHECKED _____
DATE _____
CALC NO. - AP-84-

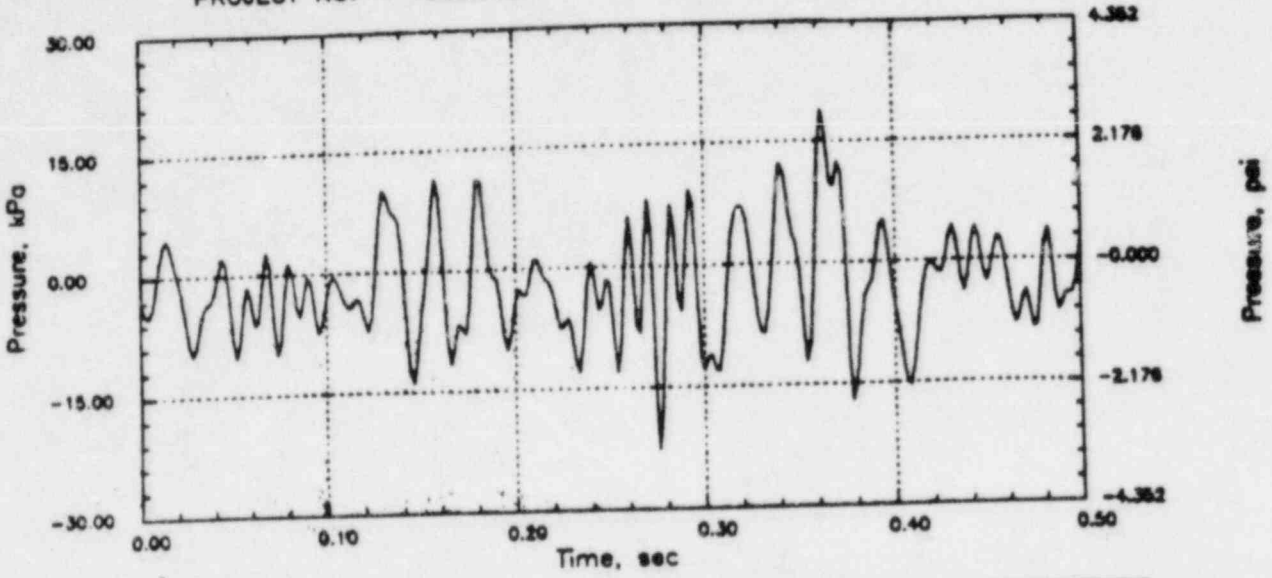

POP = 18.88 kPa PUP = -22.63 kPa MSP = 41.68 kPa²

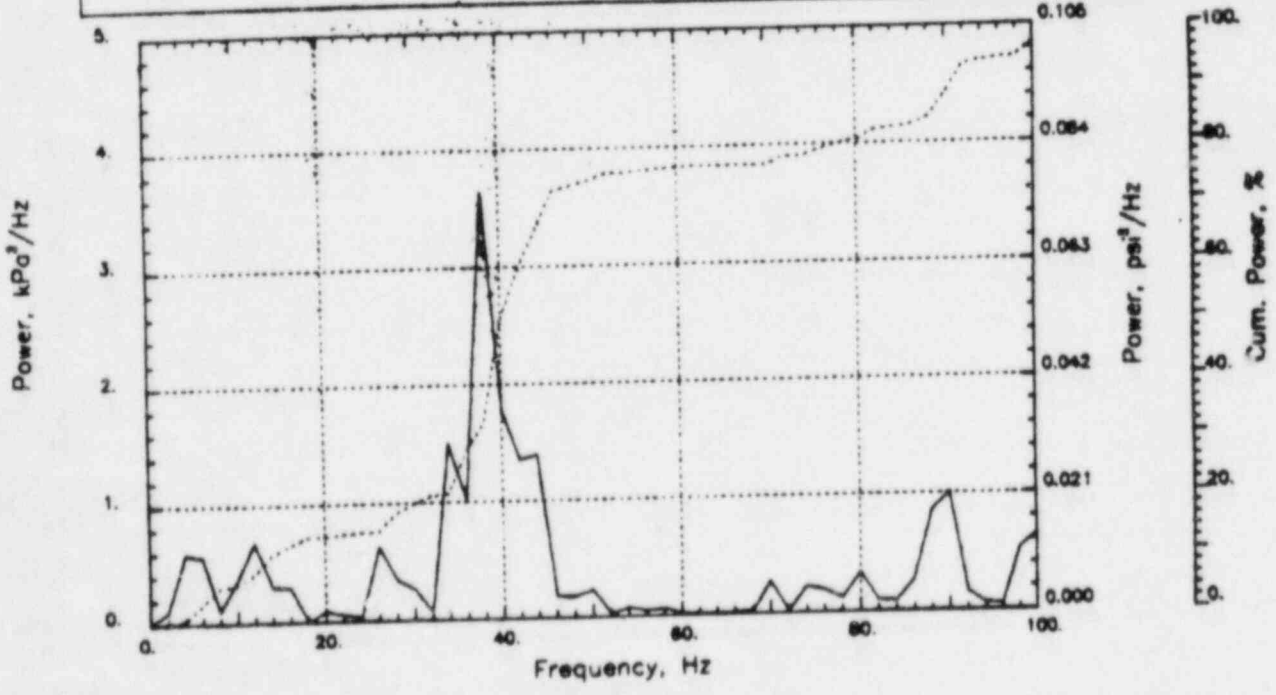

RIVER RHR CO (C=1067)

Output at point (12.65,28.00,3.45)

NAME - LEONG, TAI SENG
DATE - FEB 22, 1984
PROJECT NO. - 15026004

CHECKED _____
DATE _____
CALC NO. - AP-84-

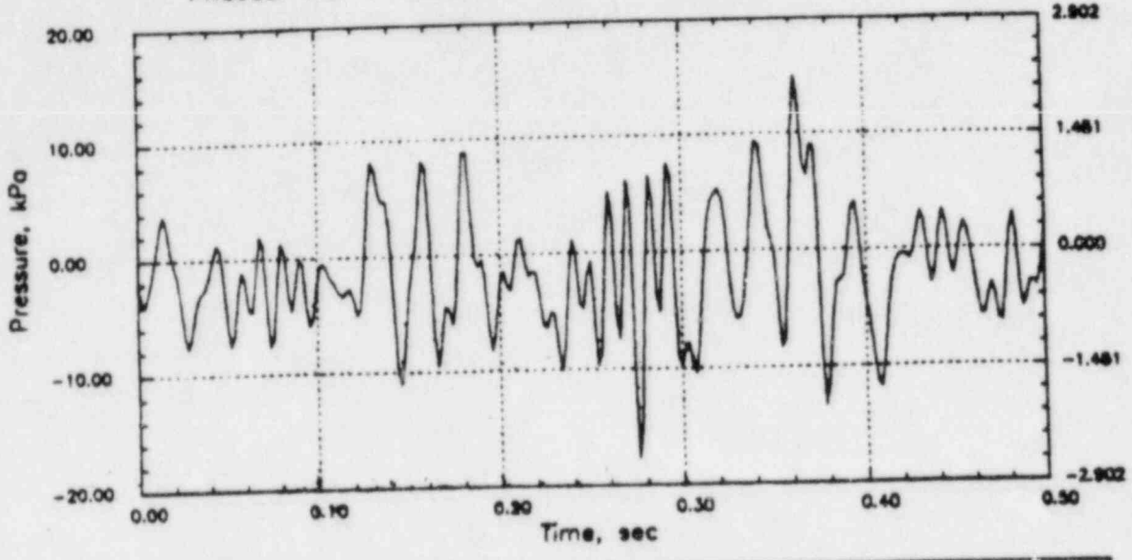

POP = 14.96 kPa PUP = -17.62 kPa MSP = 24.54 kPa²

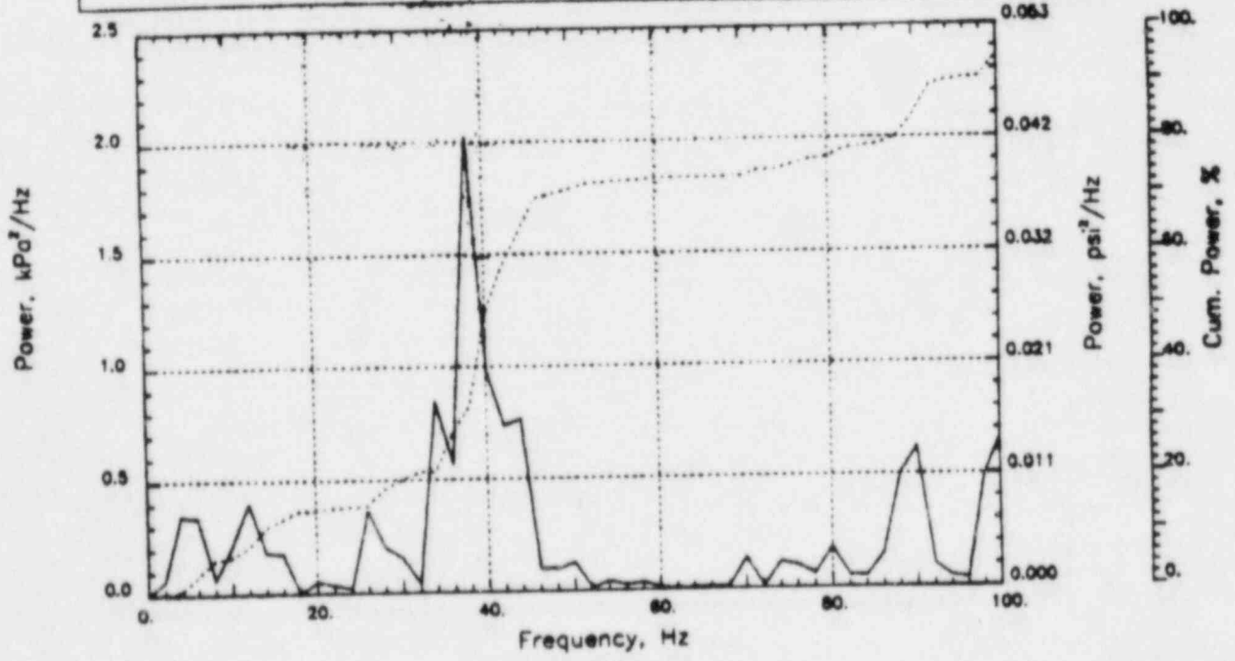

RIVER RHR CO (C=1067)

Output at point (12.65,28.00,4.09)

NAME - LEONG, TAI SENG
DATE - FEB 22, 1984
PROJECT NO. - 15020004

CHECKED _____
DATE _____
CALC NO. - AP-84-

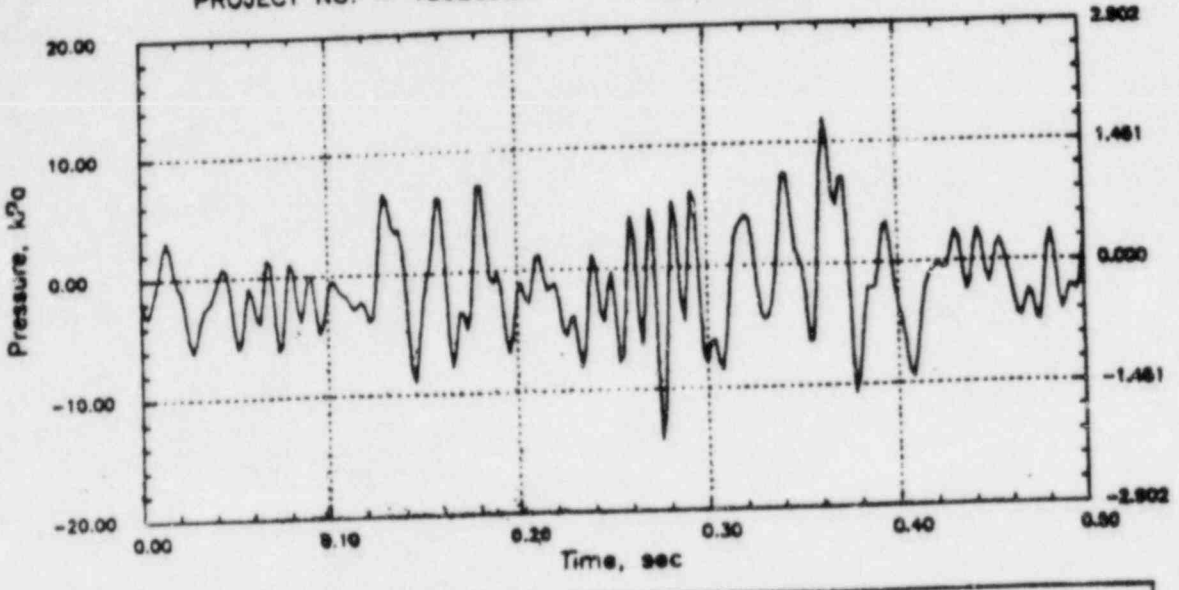

POP = 12.07 kPa PUP = -14.11 kPa MSP = 15.64 kPa²

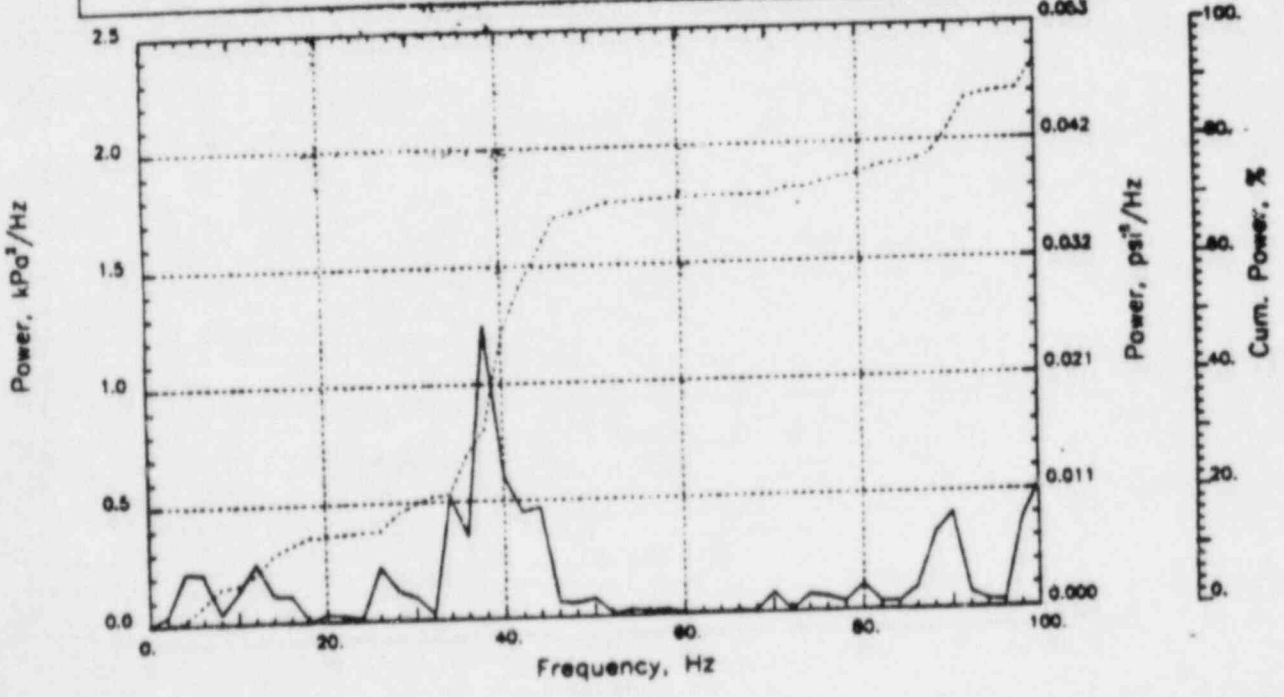

PERRY RHR CO (C=1067)

Output at point (18.90,28.00,4.91)

NAME - LEONG, TAI SENG
DATE - FEB 22, 1984
PROJECT NO. - 15026004

CHECKED _____
DATE _____
CALC NO. - AP-84-

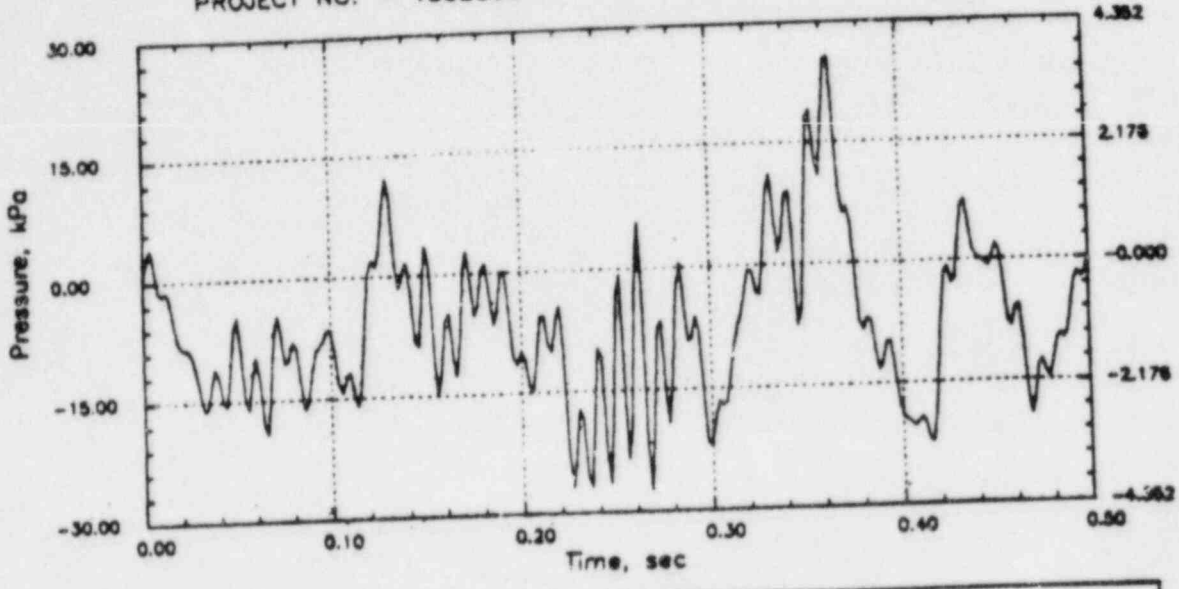

POP = 25.68 kPa PUP = -27.22 kPa MSP = 86.34 kPa²

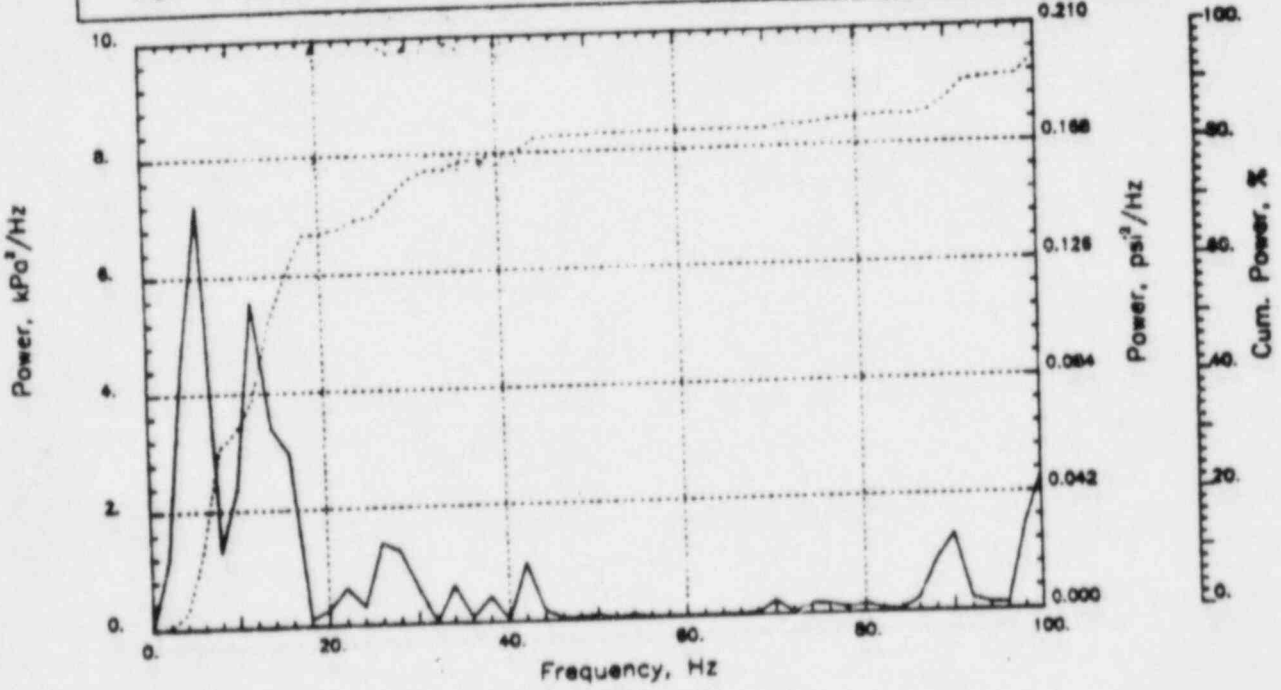

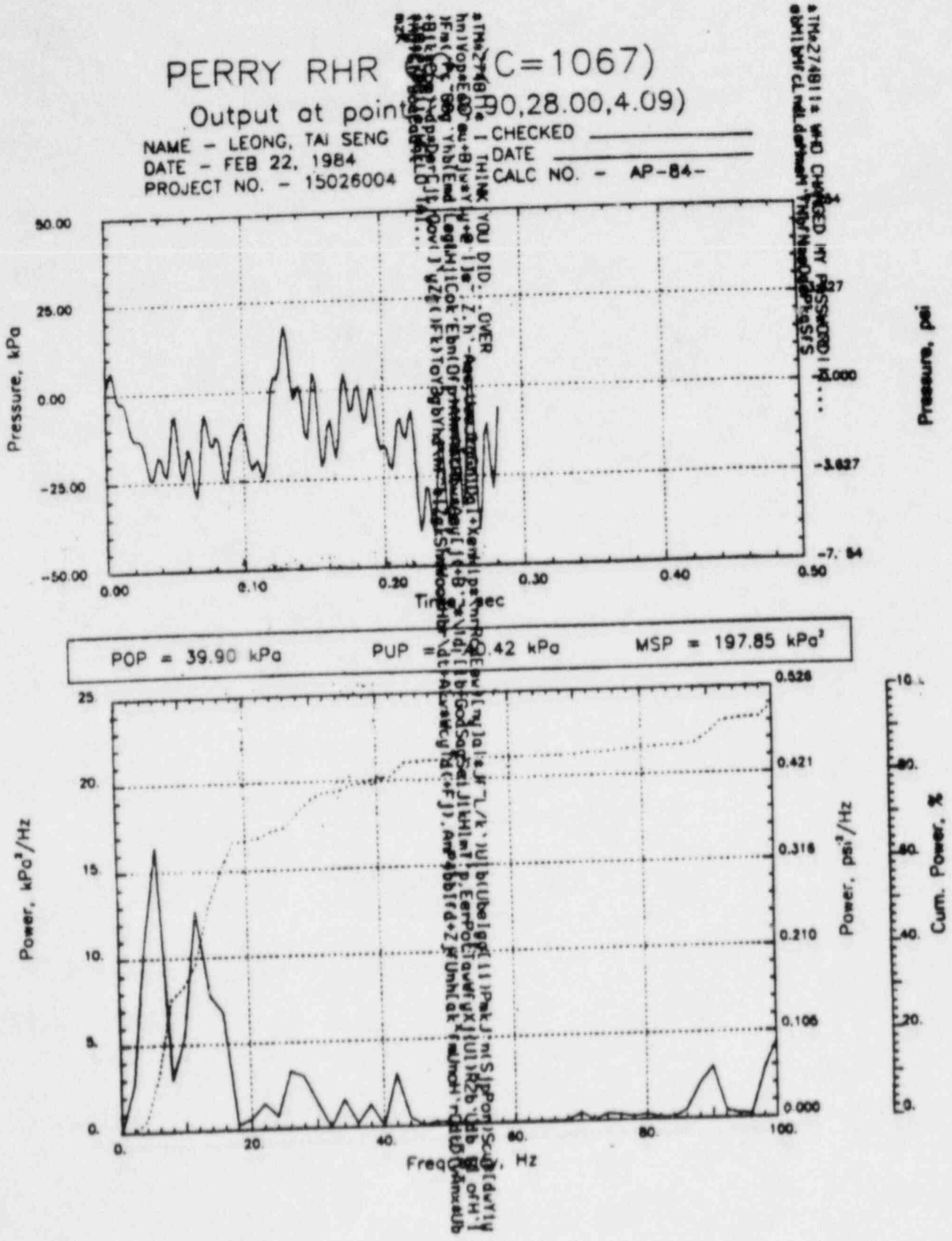
PERRY RHR (C=1067)
Output at point (30,28.00,4.09)
NAME - LEONG, TAI SENG
DATE - FEB 22, 1984
PROJECT NO. - 15026004
CHECKED
DATE
CALC NO. - AP-84-
Pressure, kPa
Time, sec
POP = 39.90 kPa
PUP = 20.42 kPa
MSP = 197.85 kPa²
Power, kPa²/Hz
Power, psi²/Hz
Cum. Power, %
Freq, Hz

PERRY RHR CO (C=1067)

Output at point (18.90,28.00,3.45)

NAME - LEONG, TAI SENG
DATE - FEB 22, 1984
PROJECT NO. - 15026004

CHECKED _____
DATE _____
CALC NO. - AP-84-

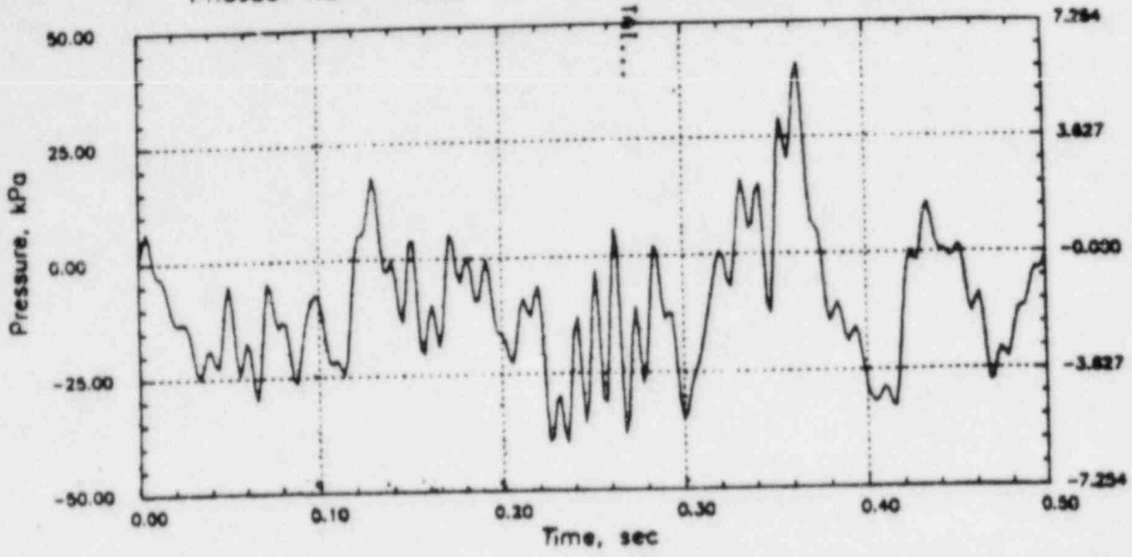

POP = 41.15 kPa PUP = -39.73 kPa MSP = 198.65 kPa²

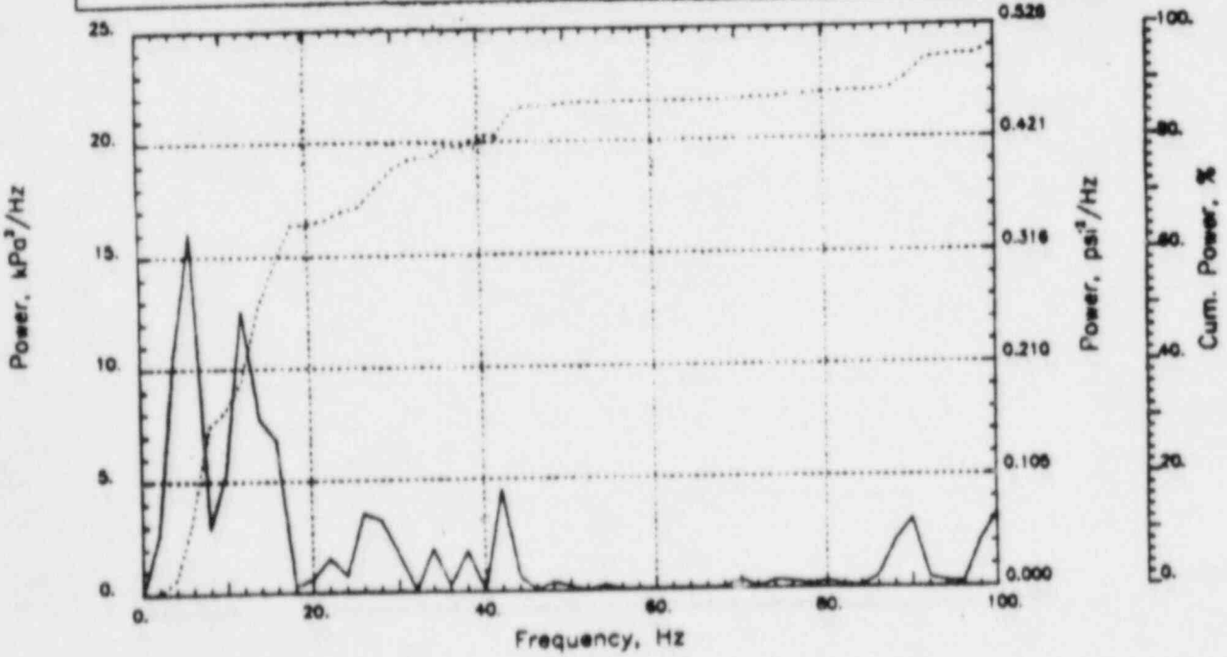

PERRY RHR CO (C=1067)

Output at point (18.90,28.00,2.82)

NAME - LEONG, TAI SENG
DATE - FEB 22, 1984
PROJECT NO. - 15026004

CHECKED _____
DATE _____
CALC NO. - AP-84-

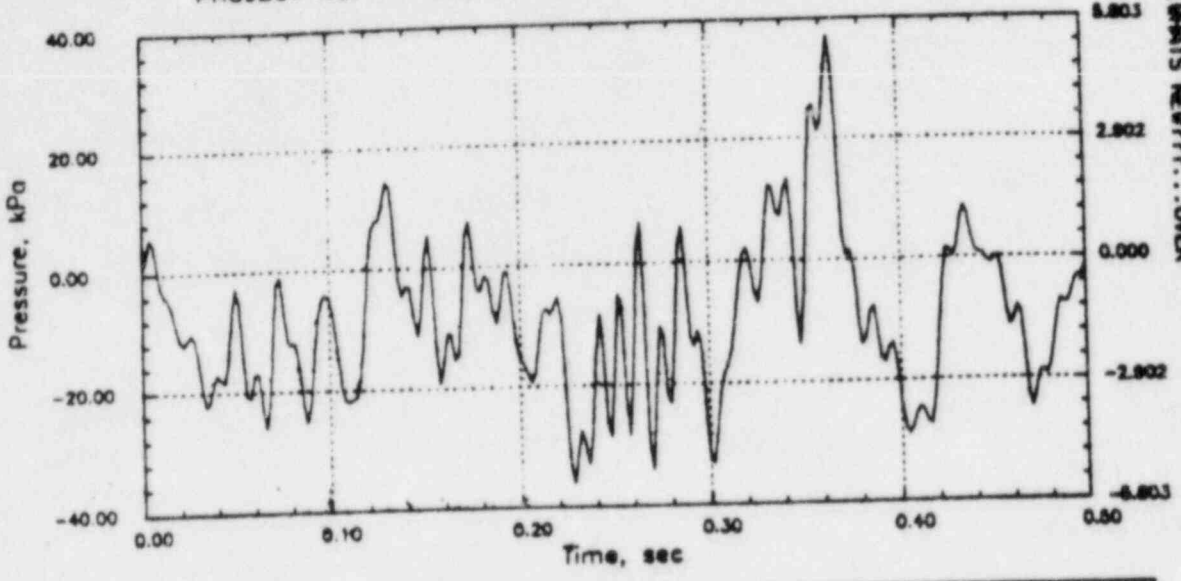

POP = 37.02 kPa PUP = -36.09 kPa MSP = 156.12 kPa²

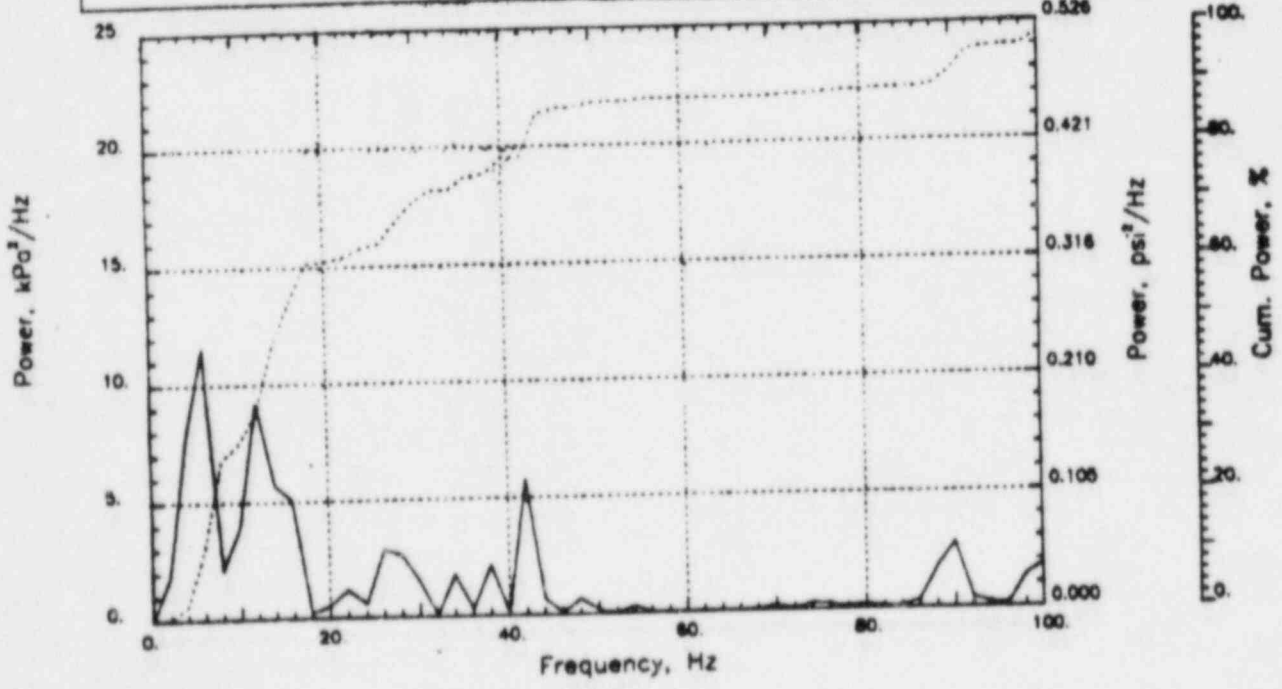

PERRY RHR CO (C=1067)

Output at point (18.90,28.00,2.18)

NAME - LEONG, TAI SENG
DATE - FEB 22, 1984
PROJECT NO. - 15026004

CHECKED _____
DATE _____
CALC NO. - AP-84-

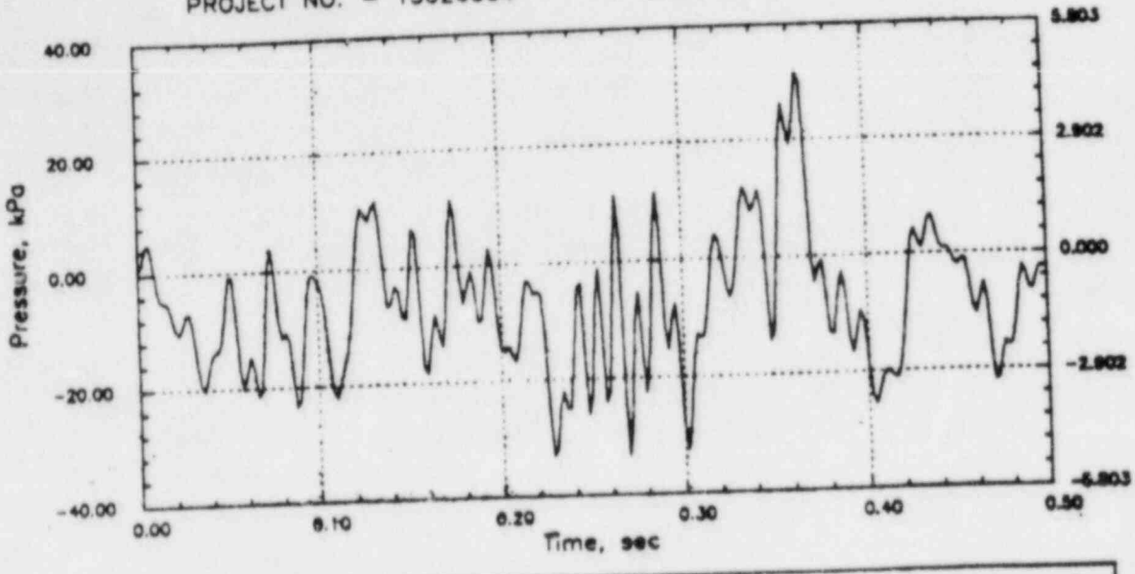

POP = 31.83 kPa PUP = -33.30 kPa MSP = 126.27 kPa²

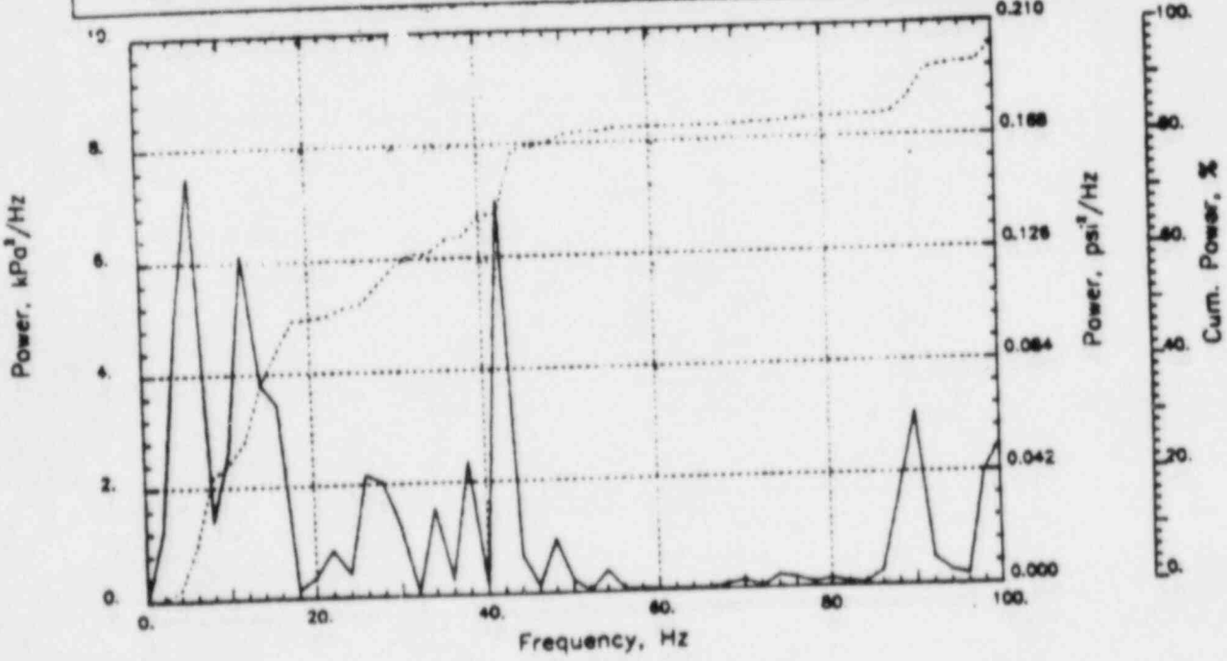

PERRY RHR CO (C=1067)

Output at point (18.90,28.00,1.55)

NAME - LEONG, TAI SENG
DATE - FEB 22, 1984
PROJECT NO. - 15026004

CHECKED _____
DATE _____
CALC NO. - AP-84-

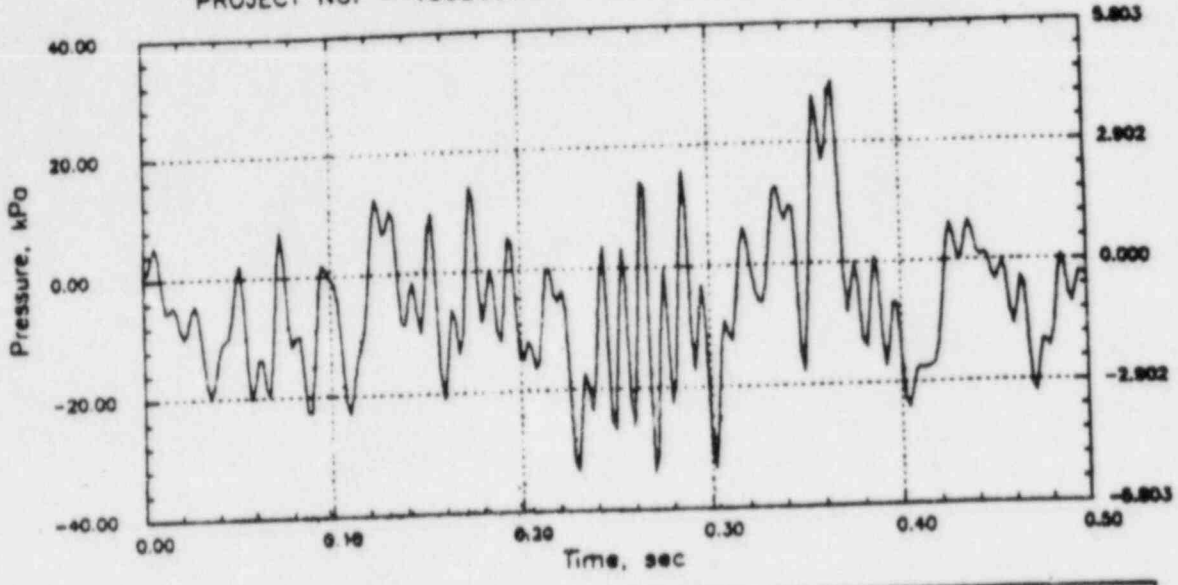

POP = 30.02 kPa PUP = -33.77 kPa MSP = 124.73 kPa²

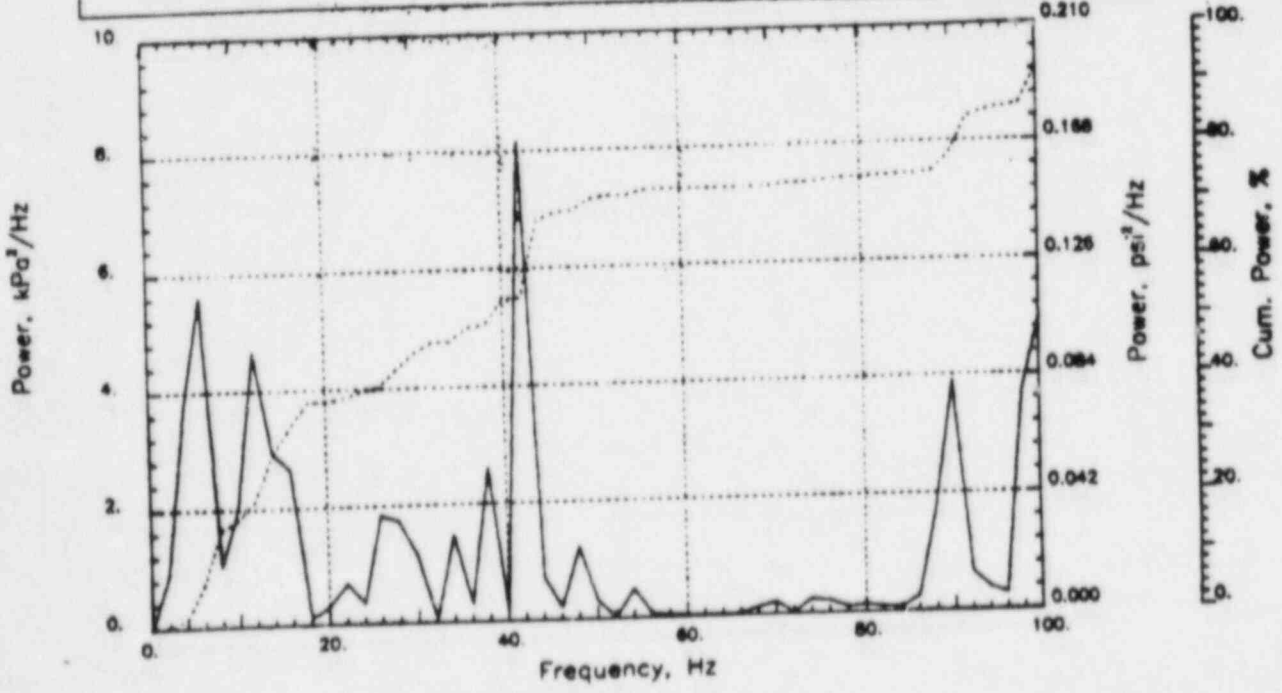

PERRY RHR CO (C=1067)

Output at point (18.90,28.00,0.46)

NAME - LEONG, TAI SENG
DATE - FEB 22, 1984
PROJECT NO. - 15026004

CHECKED _____
DATE _____
CALC NO. - AP-84-

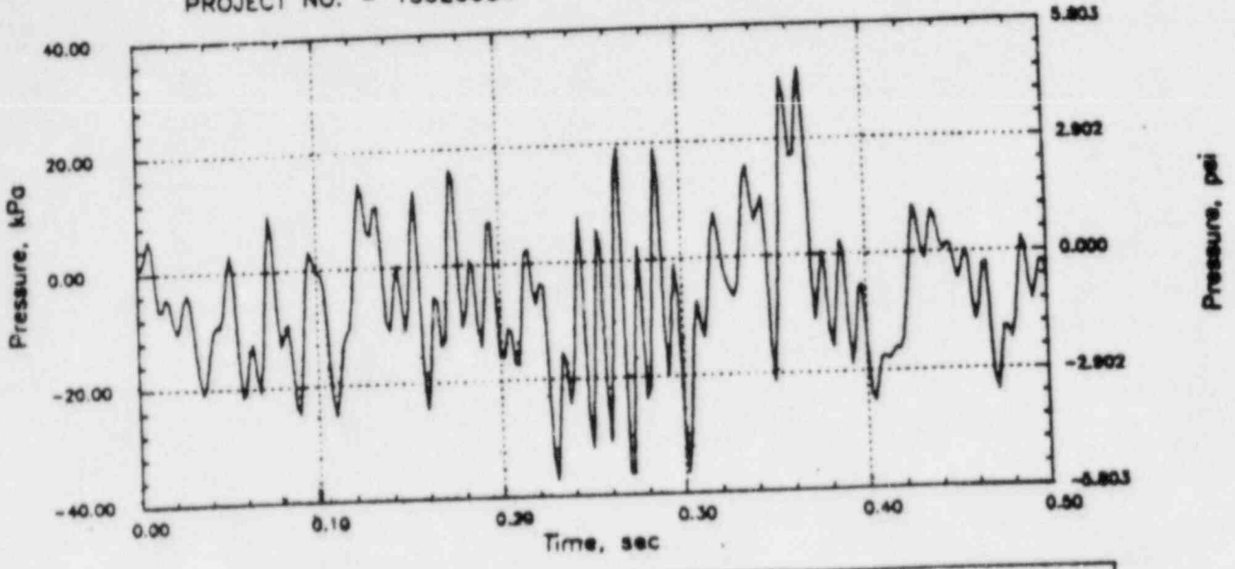

POP = 32.27 kPa PUP = -37.07 kPa MSP = 147.03 kPa²

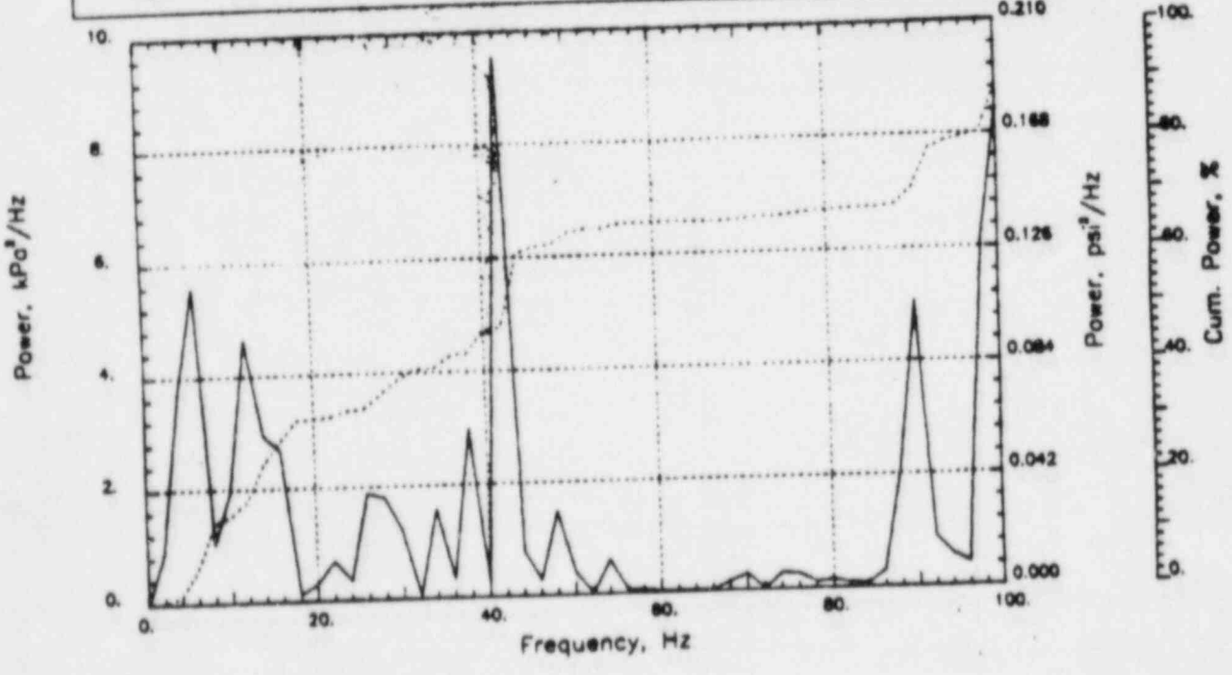

PERRY RHR CO (C=1067)

Output at point (18.90,28.00,0.00)

NAME - LEONG, TAI SENG
DATE - FEB 22, 1984
PROJECT NO. - 15026004

CHECKED _____
DATE _____
CALC NO. - AP-84-

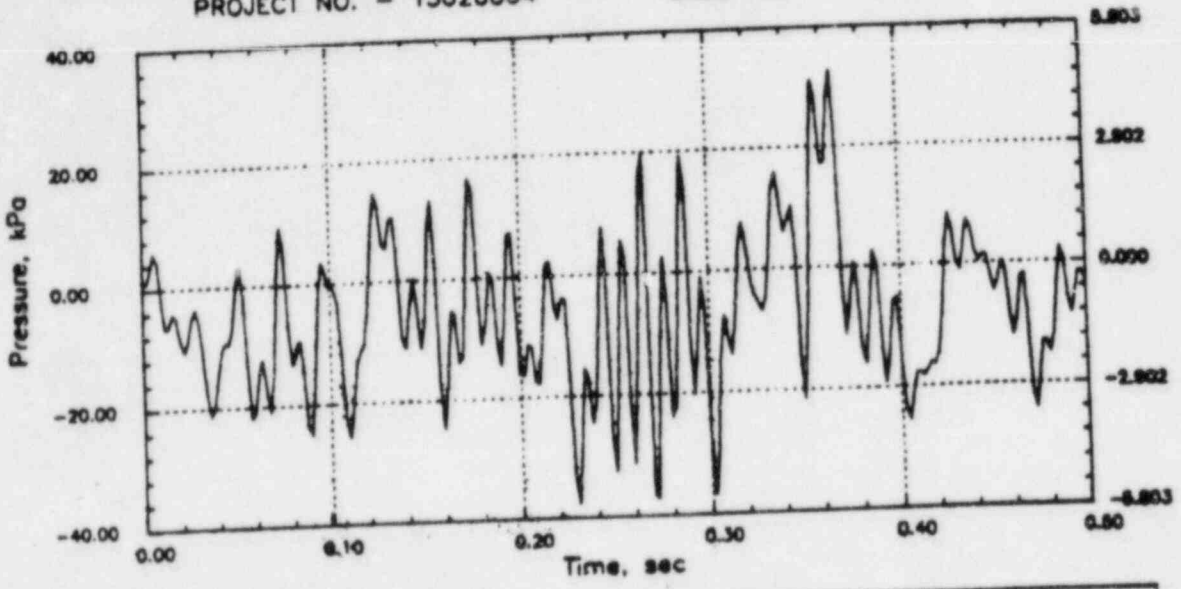

POP = 32.64 kPa PUP = -37.61 kPa MSP = 150.62 kPa²

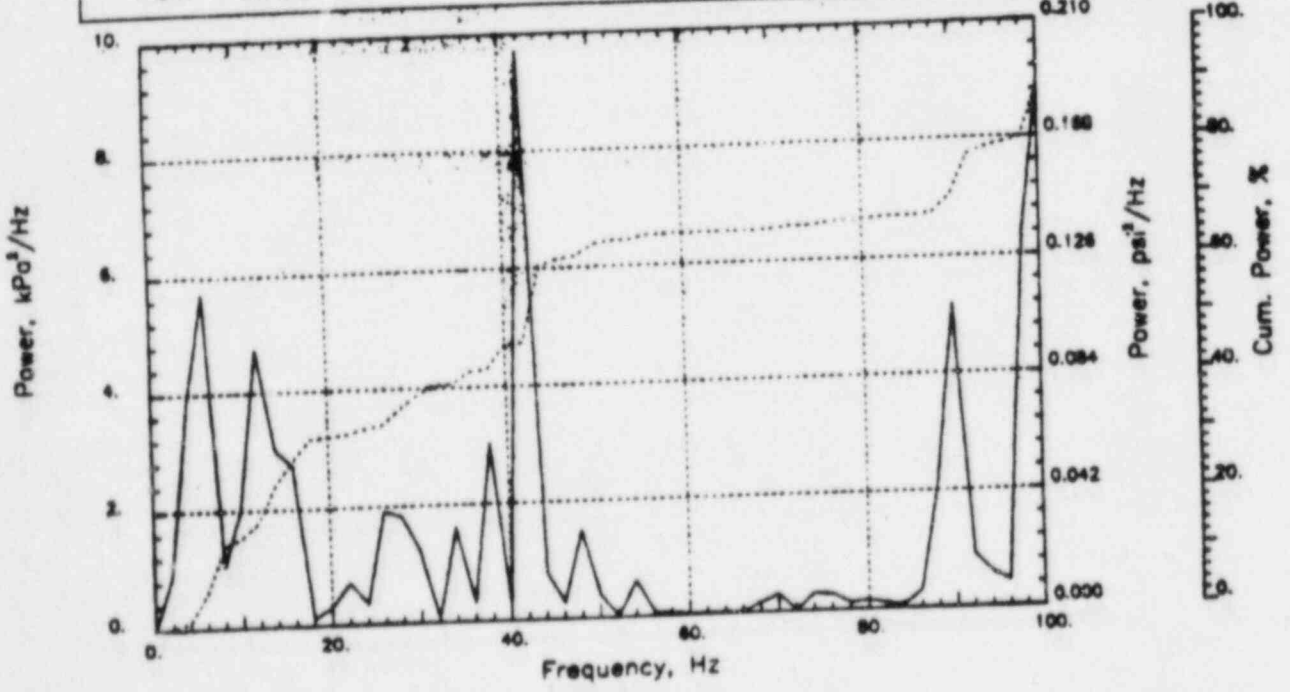

PERRY RHR CO (C=1067)

Output at point (17.34,28.00,0.00)

NAME - LEONG, TAI SENG
DATE - FEB 22, 1984
PROJECT NO. - 15026004

CHECKED _____
DATE _____
CALC NO. - AP-84-

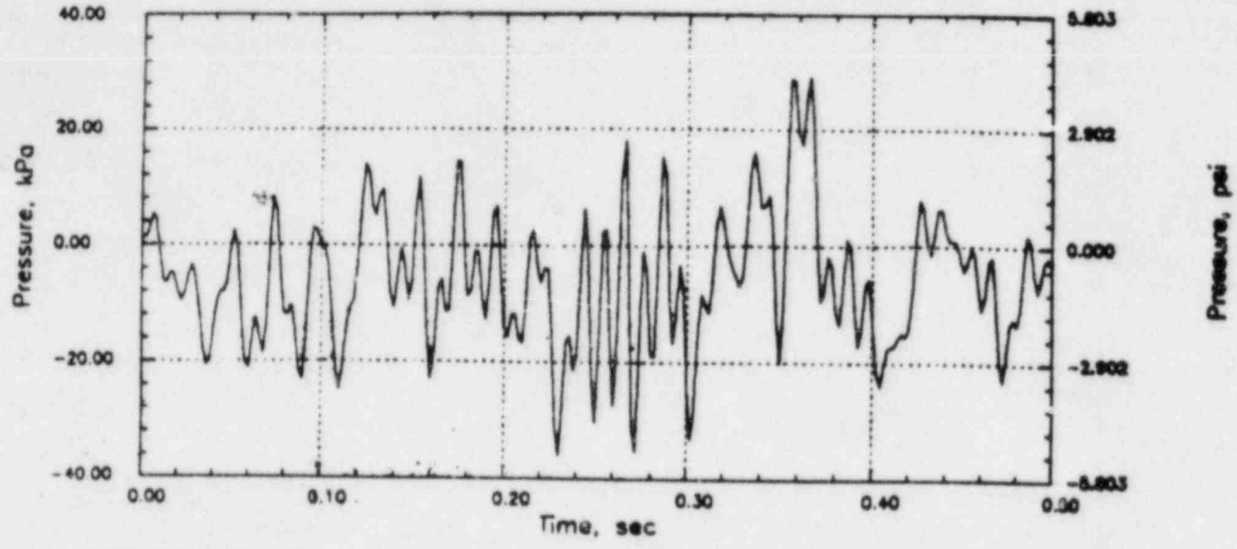

POP = 29.15 kPa PUP = -36.10 kPa MSP = 129.70 kPa²

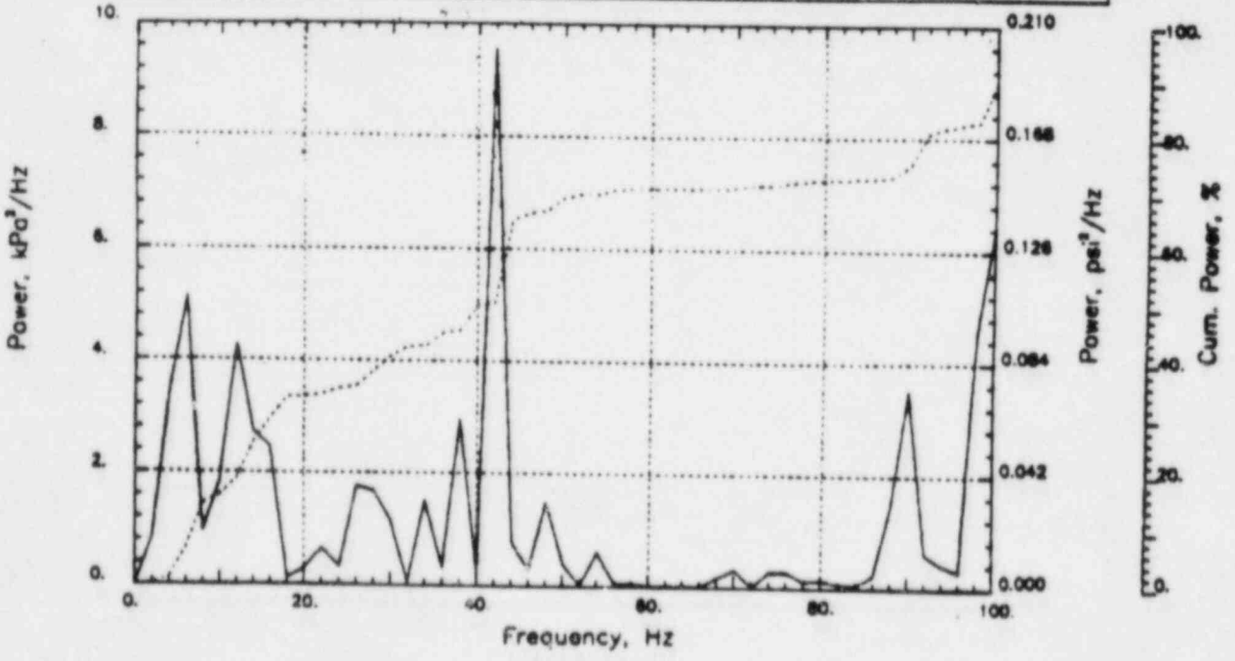

PERRY RHR CO (C=1067)

Output at point (15.77,28.00,0.00)

NAME - LEONG, TAI SENG
DATE - FEB 22, 1984
PROJECT NO. - 15026004

CHECKED _____
DATE _____
CALC NO. - AP-84-

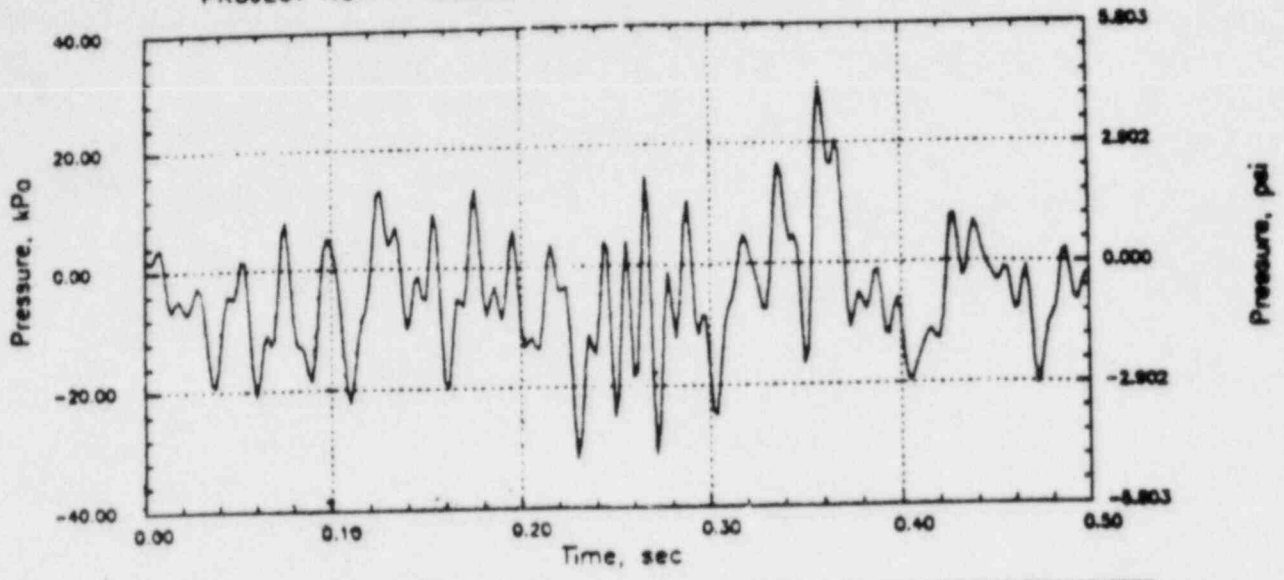

POP = 30.03 kPa PUP = -31.89 kPa MSP = 95.49 kPa²

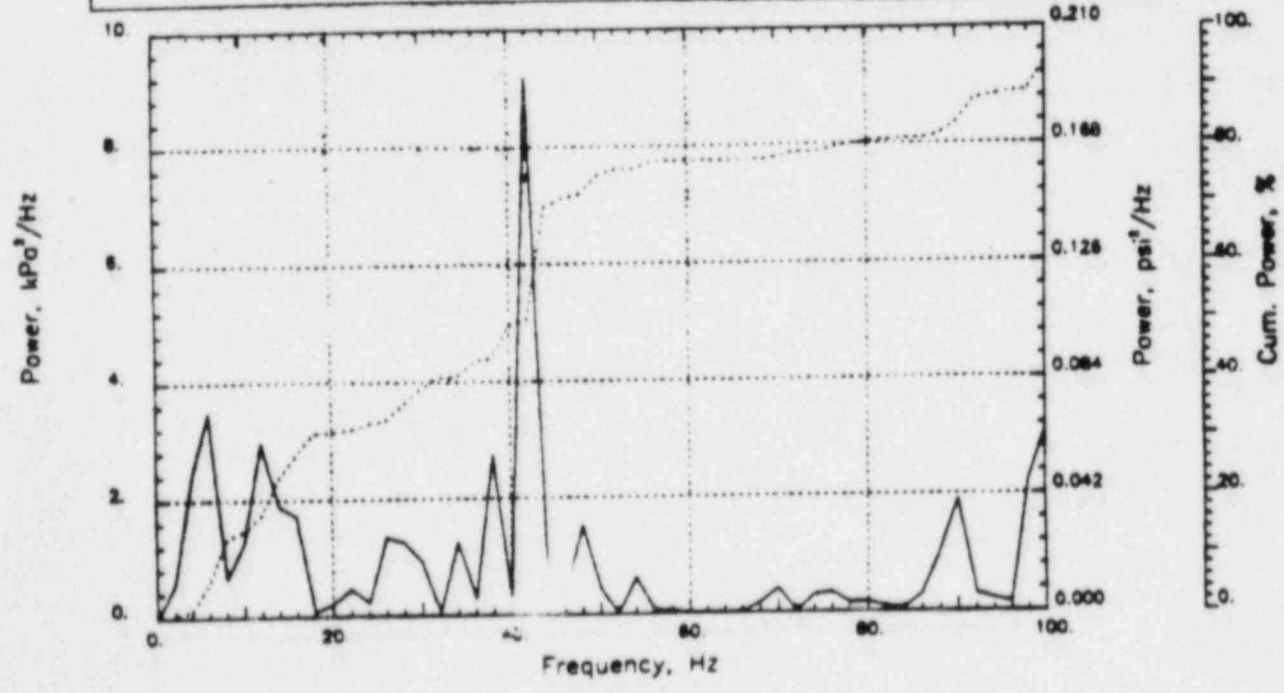

PERRY RHR CO (C=1067)

Output at point (12.65,28.00,0.00)

NAME - LEONG, TAI SENG
DATE - FEB 22, 1984
PROJECT NO. - 15026004

CHECKED _____
DATE _____
CALC NO. - AP-84-

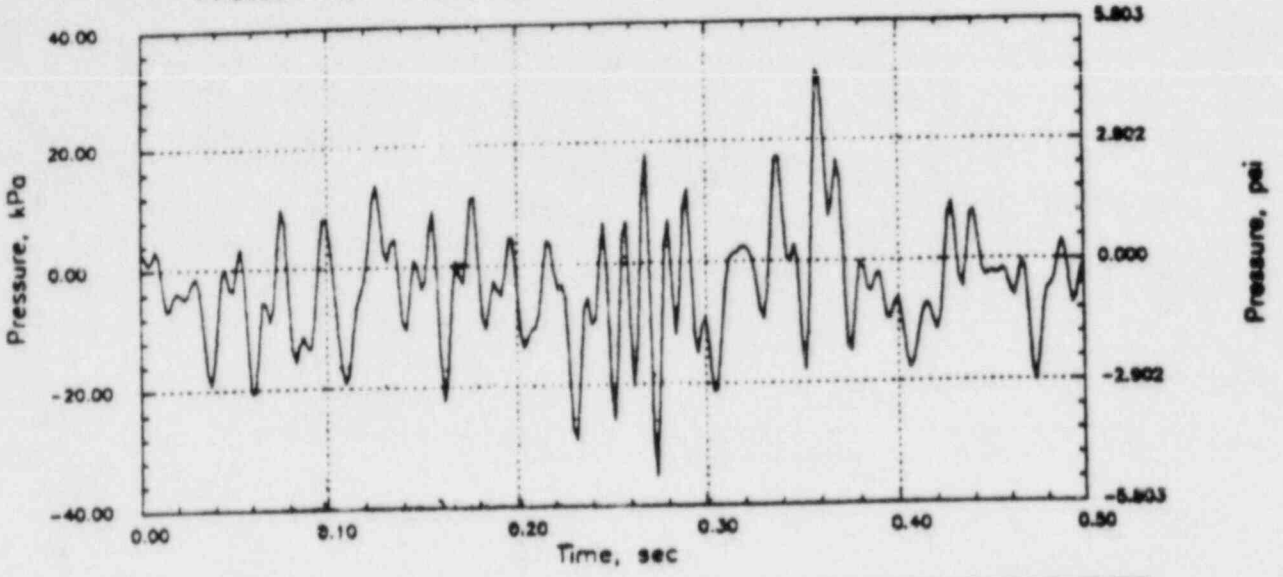

POP = 31.85 kPa PUP = -35.13 kPa MSP = 90.11 kPa²

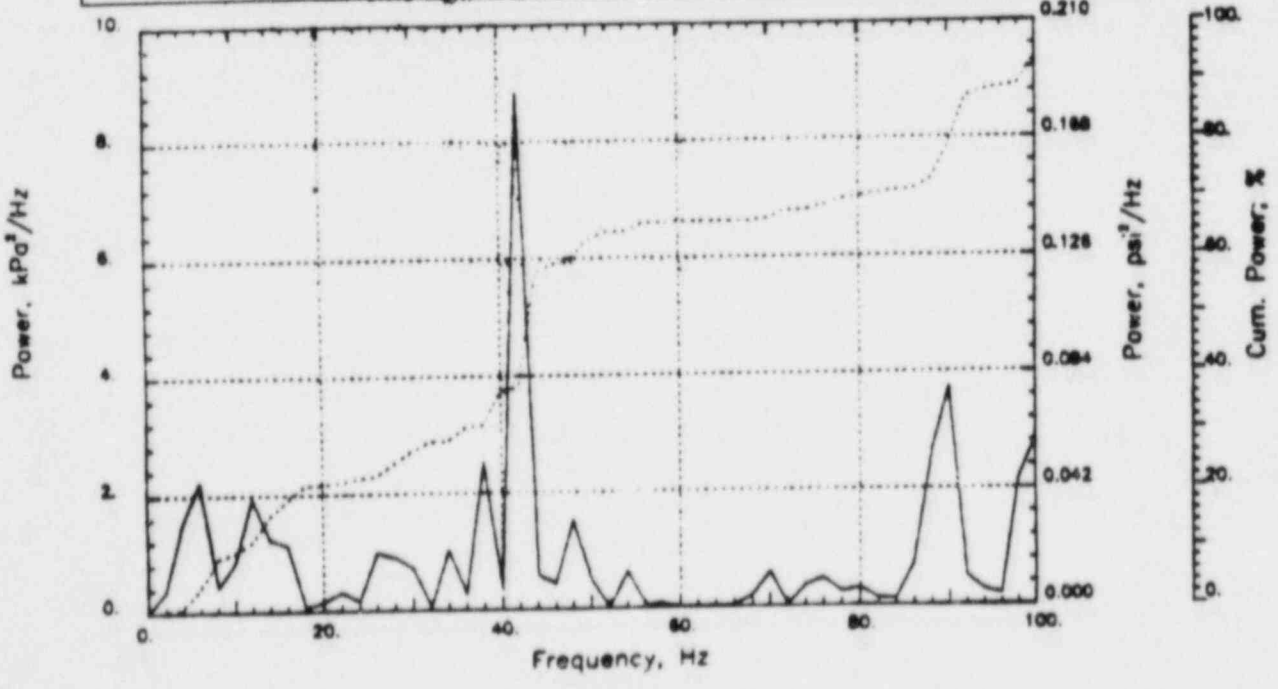

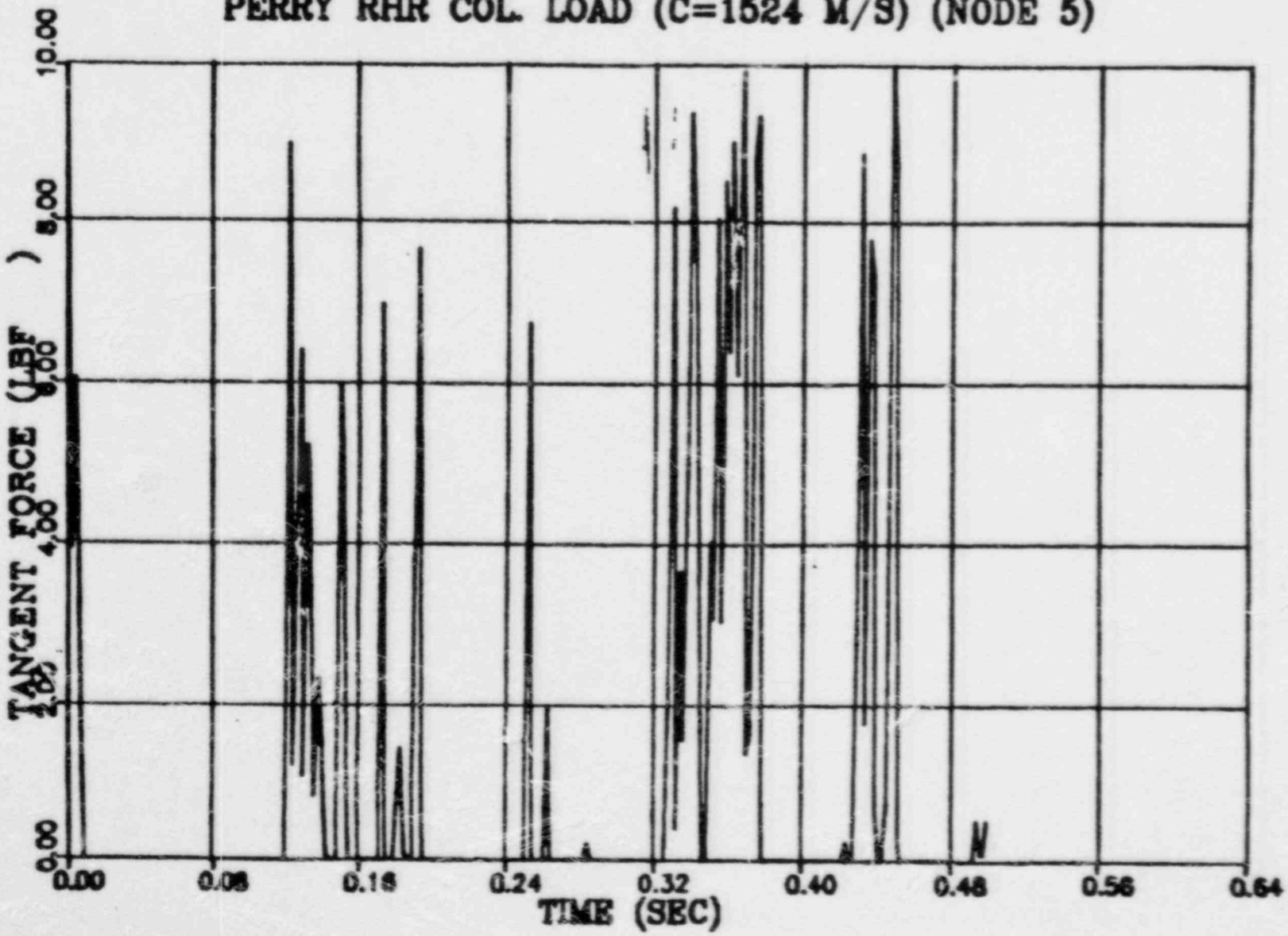
PERRY RHR COL. LOAD (C=1524 M/S) (NODE 5)
TANGENT FORCE (LBF)
10.00
8.00
6.00
4.00
2.00
0.00
0.00
0.08
0.16
0.24
0.32
0.40
0.48
0.56
0.64
TIME (SEC)

PERRY RHR CO (C=1067)

Output at point (12.65,28.00,0.91)

NAME - LEONG, TAI SENG
DATE - FEB 22, 1984
PROJECT NO. - 15026004

CHECKED _____
DATE _____
CALC NO. - AP-84-

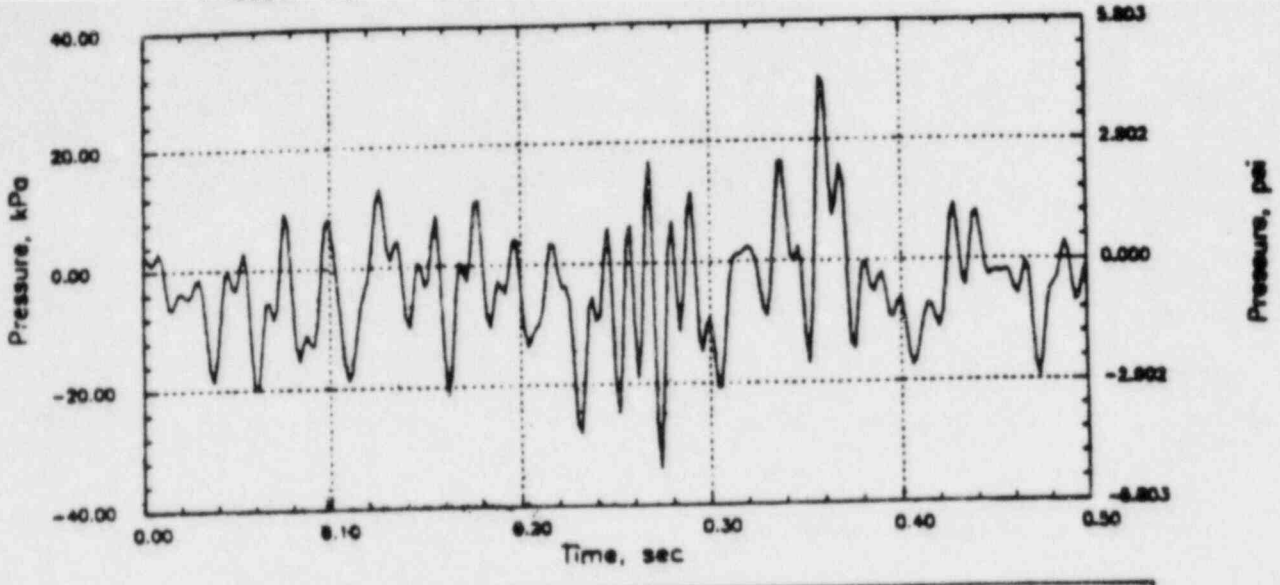

POP = 30.58 kPa PUP = -33.79 kPa MSP = 83.50 kPa²

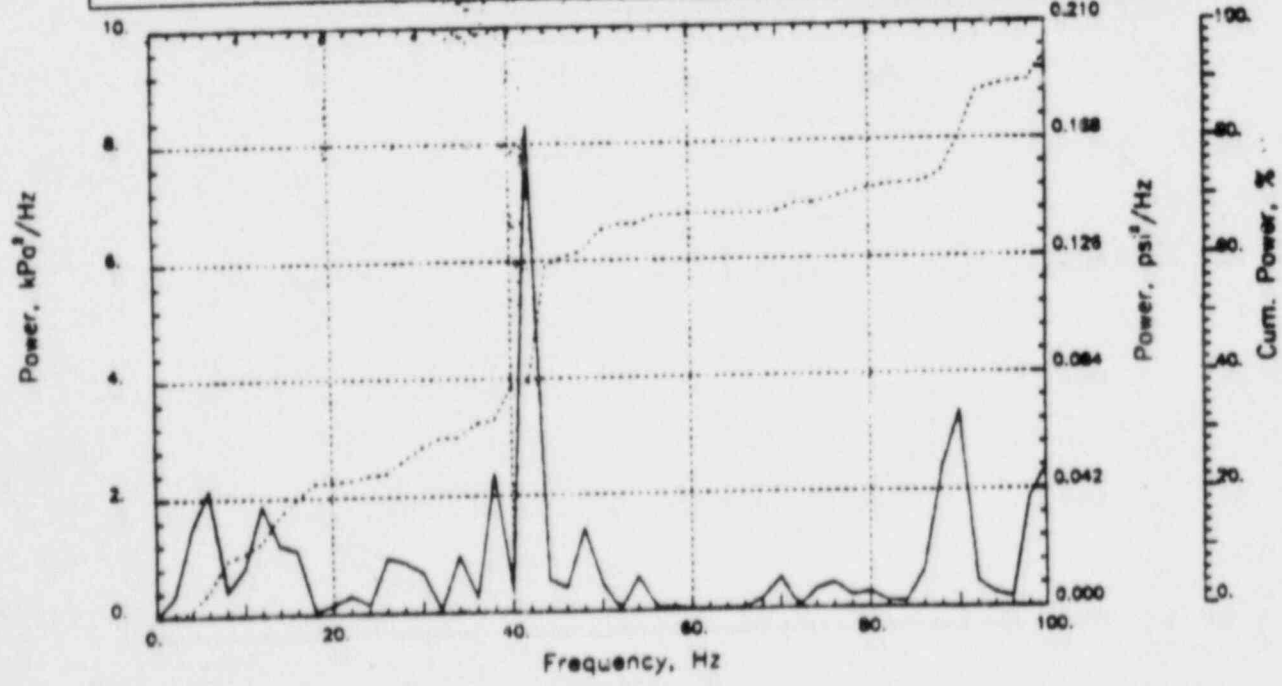

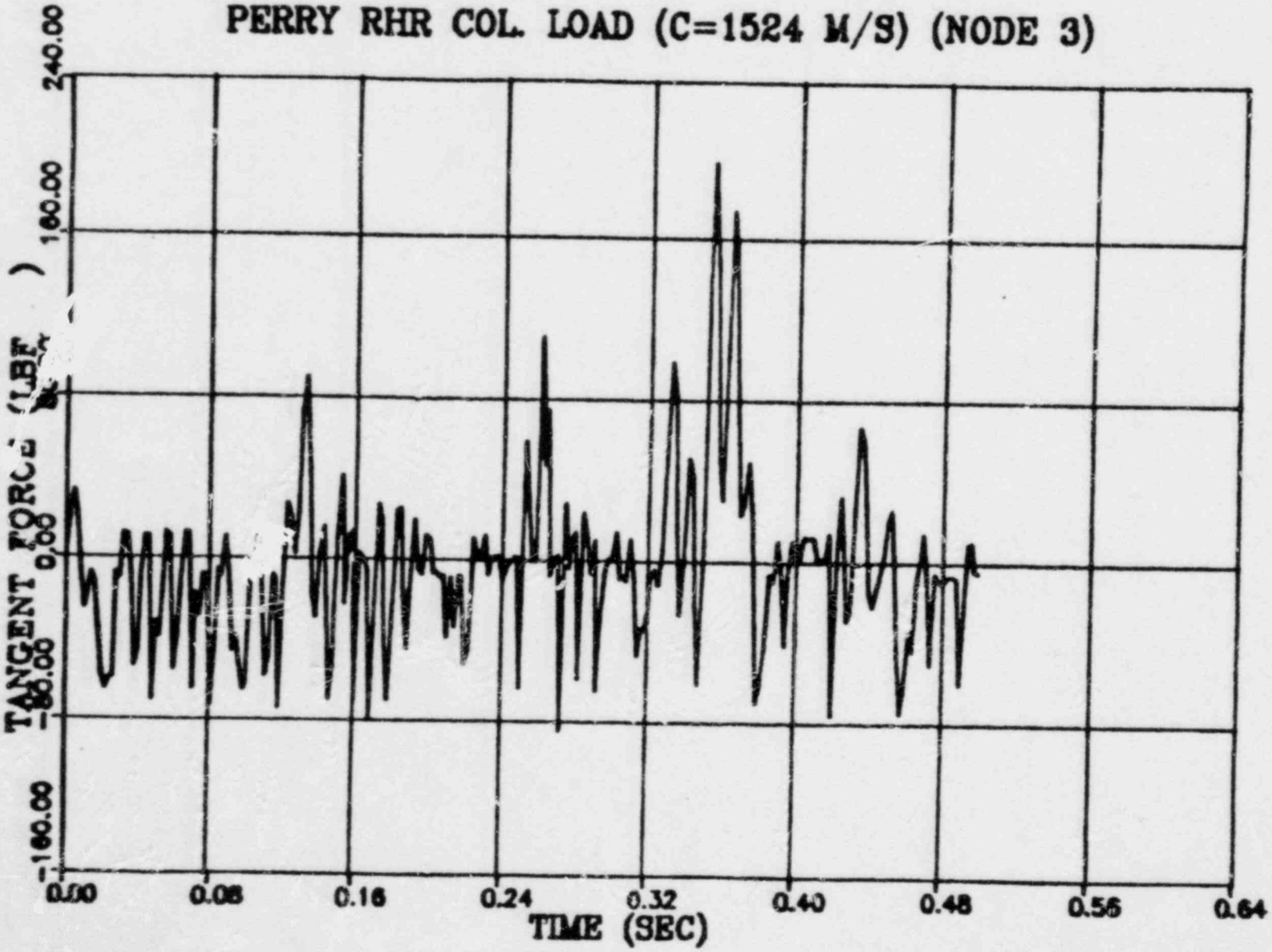
PERRY RHR COL. LOAD (C=1524 M/S) (NODE 3)
TANGENT FORCE (LBF)
240.00
160.00
80.00
0.00
-80.00
-160.00
0.00
0.08
0.16
0.24
0.32
0.40
0.48
0.56
0.64
TIME (SEC)

PERRY RHR CO (C=1067)

Output at point (12.65,28.00,2.18)

NAME - LEONG, TAI SENG
DATE - FEB 22, 1984
PROJECT NO. - 15026004

CHECKED _____
DATE _____
CALC NO. - AP-84-

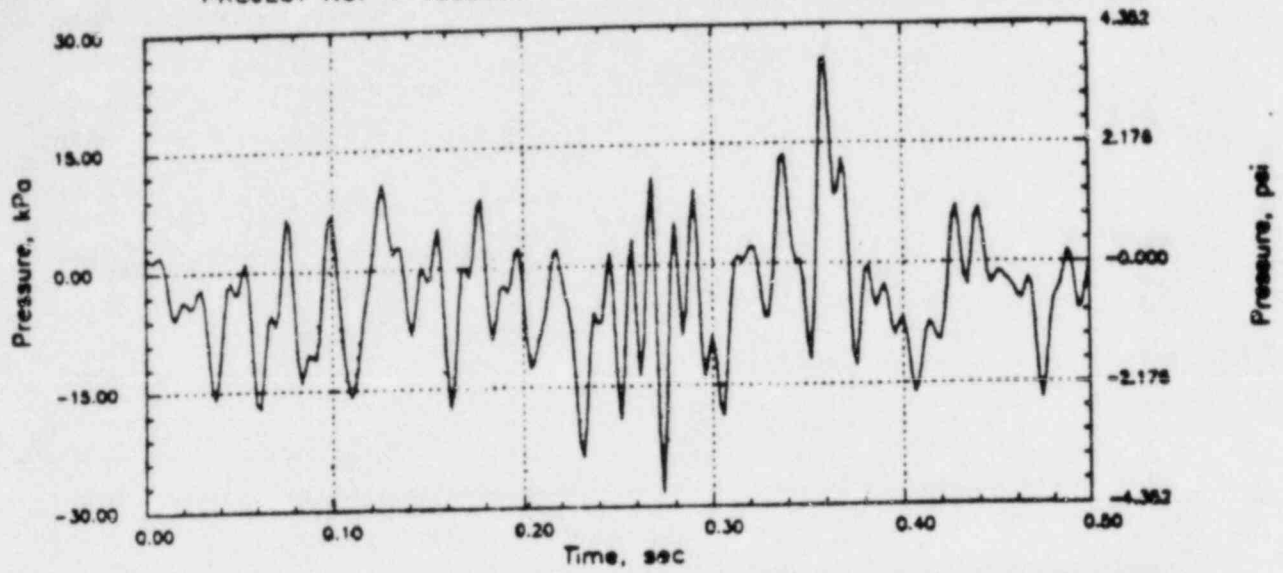

POP = 25.75 kPa PUP = -28.15 kPa MSP = 59.91 kPa²

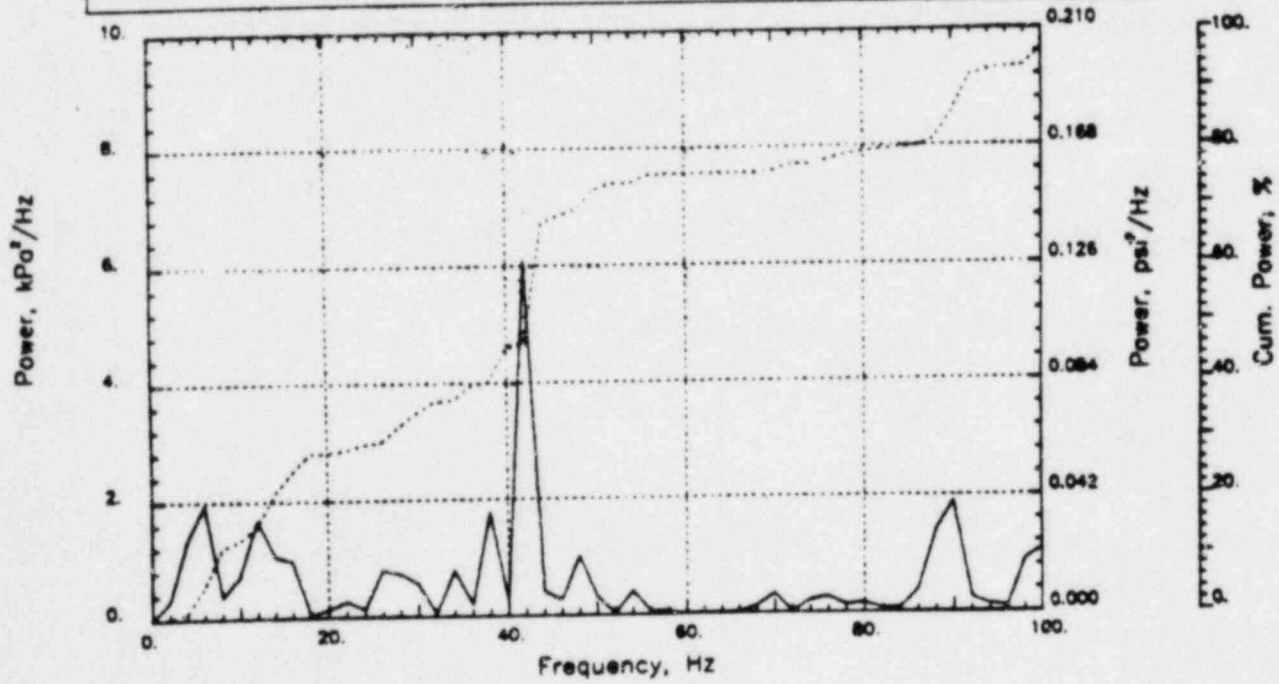

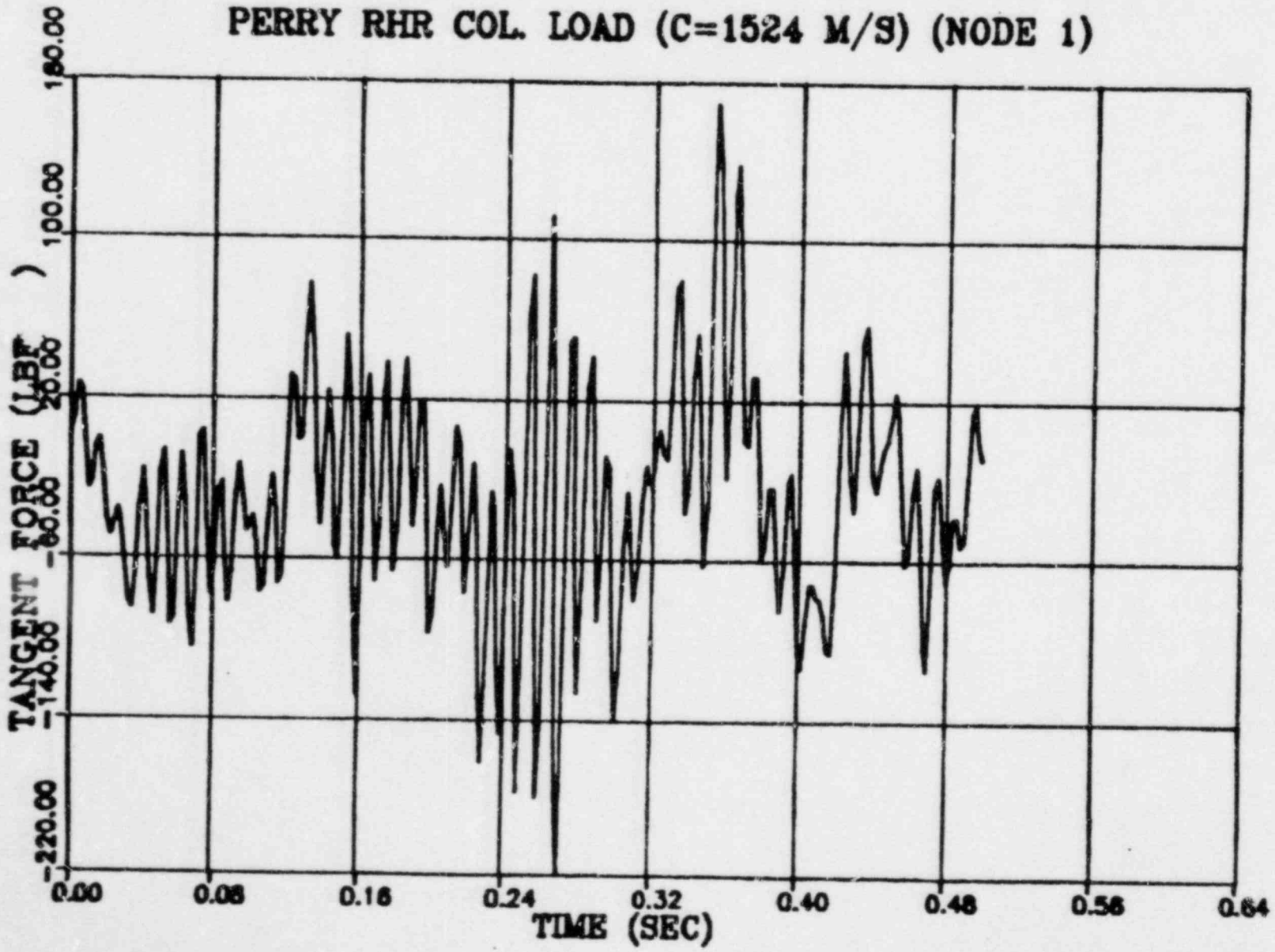
PERRY RHR COL. LOAD (C=1524 M/S) (NODE 1)
TANGENT FORCE (LBF)
180.00
100.00
20.00
-60.00
-140.00
-220.00
0.00
0.08
0.16
0.24
0.32
0.40
0.48
0.56
0.64
TIME (SEC)

PERRY RHR CO (C=1067)

Output at point (12.65,28.00,3.45)

NAME - LEONG, TAI SENG
DATE - FEB 22, 1984
PROJECT NO. - 15026004

CHECKED _____
DATE _____
CALC NO. - AP-84-

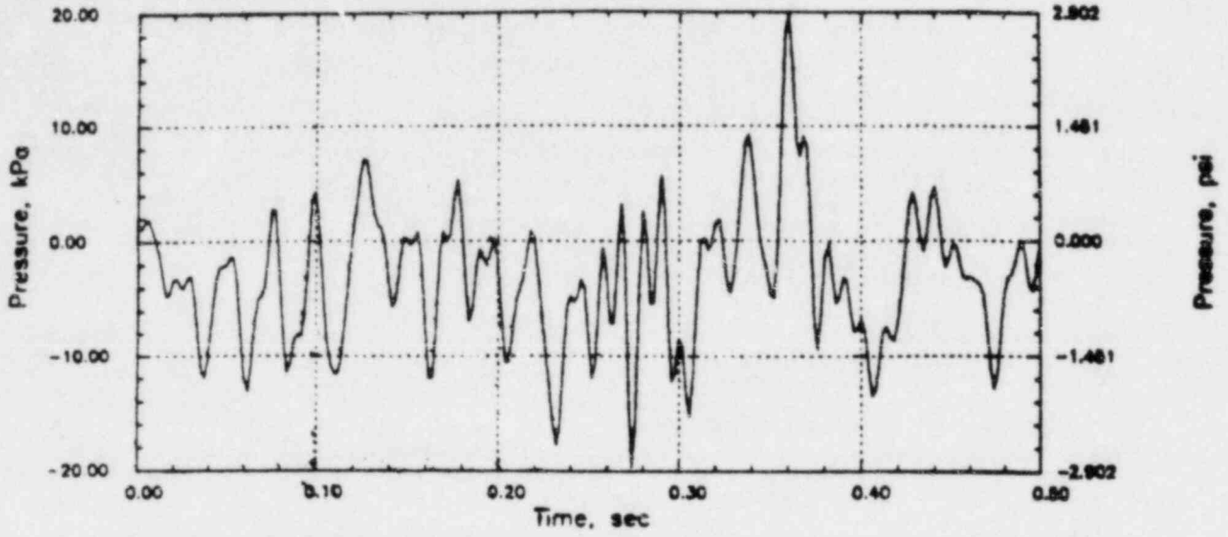

POP = 19.85 kPa PUP = -19.64 kPa MSP = 33.99 kPa²

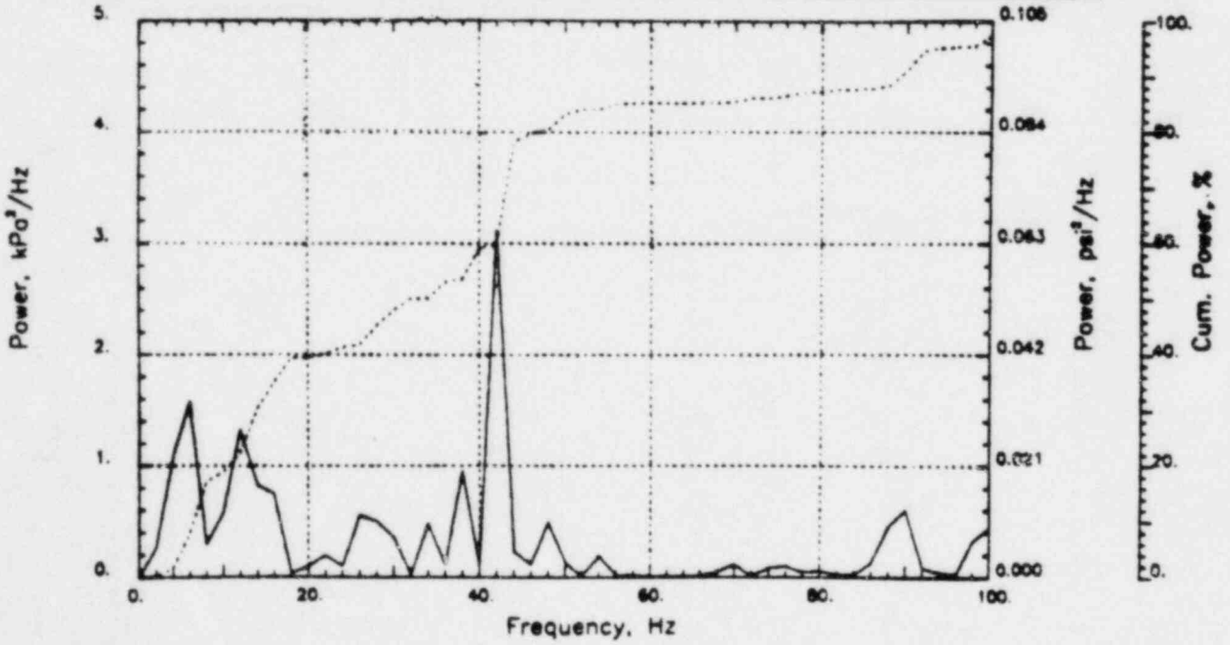

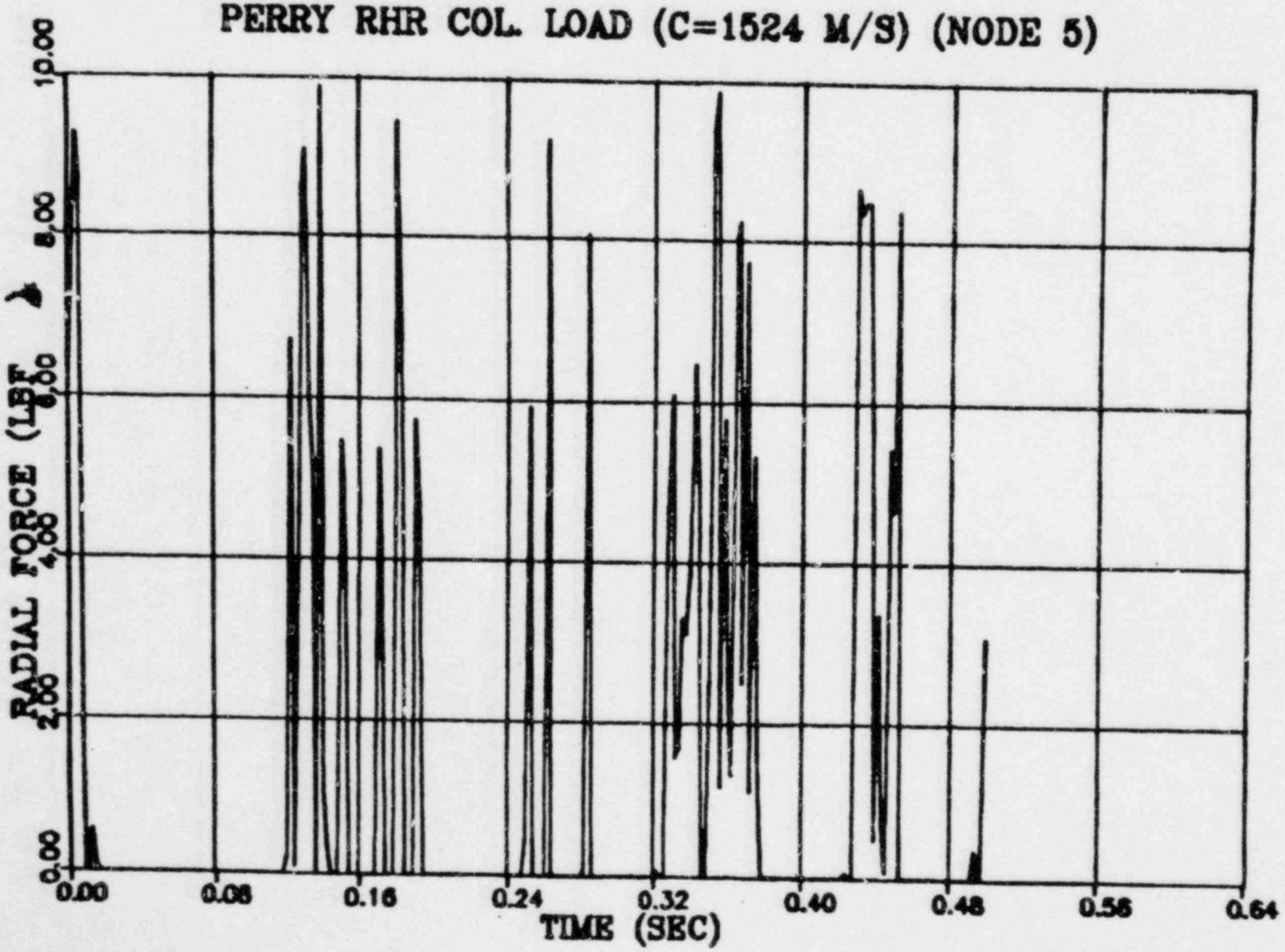
PERRY RHR COL. LOAD (C=1524 M/S) (NODE 5)
RADIAL FORCE (LBF)
10.00
8.00
6.00
4.00
2.00
0.00
0.00
0.08
0.16
0.24
0.32
0.40
0.48
0.56
0.64
TIME (SEC)

PERRY RHR CO (C=1067)

Output at point (12.65,28.00,4.91)

NAME - LEONG, TAI SENG
DATE - FEB 22, 1984
PROJECT NO. - 15026004

CHECKED _____
DATE _____
CALC NO. - AP-84-

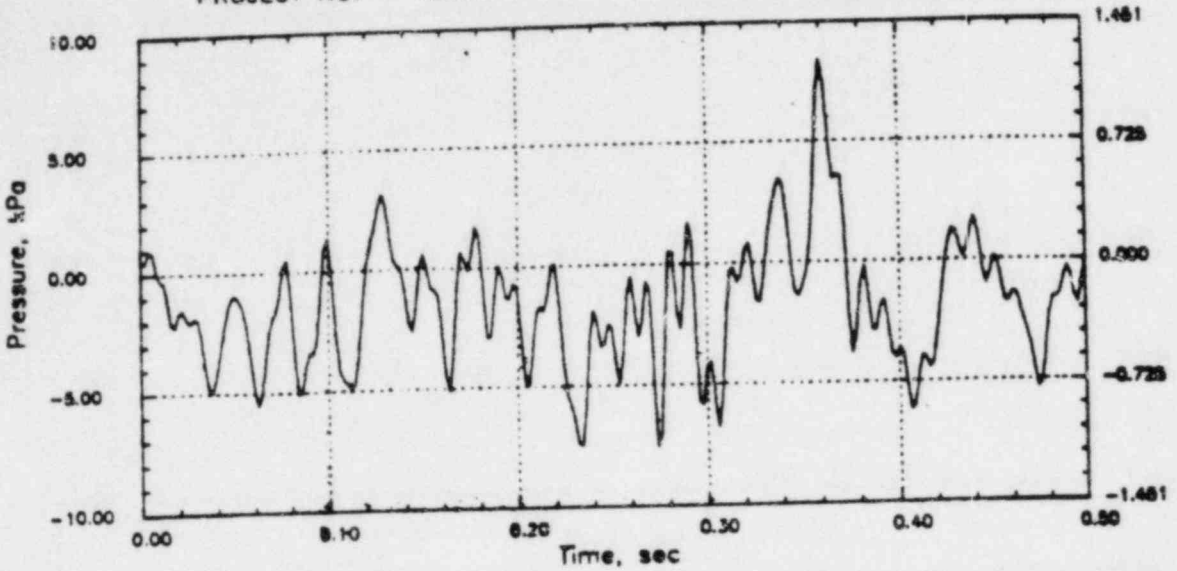

POP = 8.41 kPa PUP = -7.53 kPa MSP = 6.45 kPa²

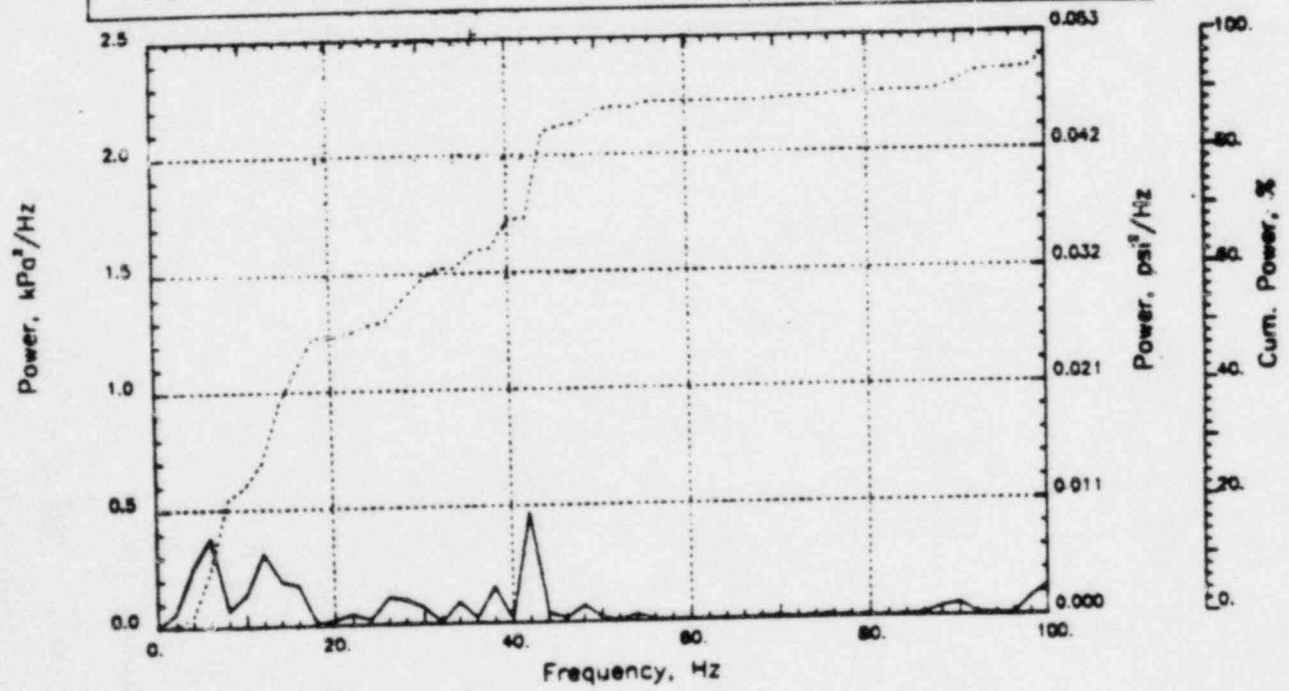

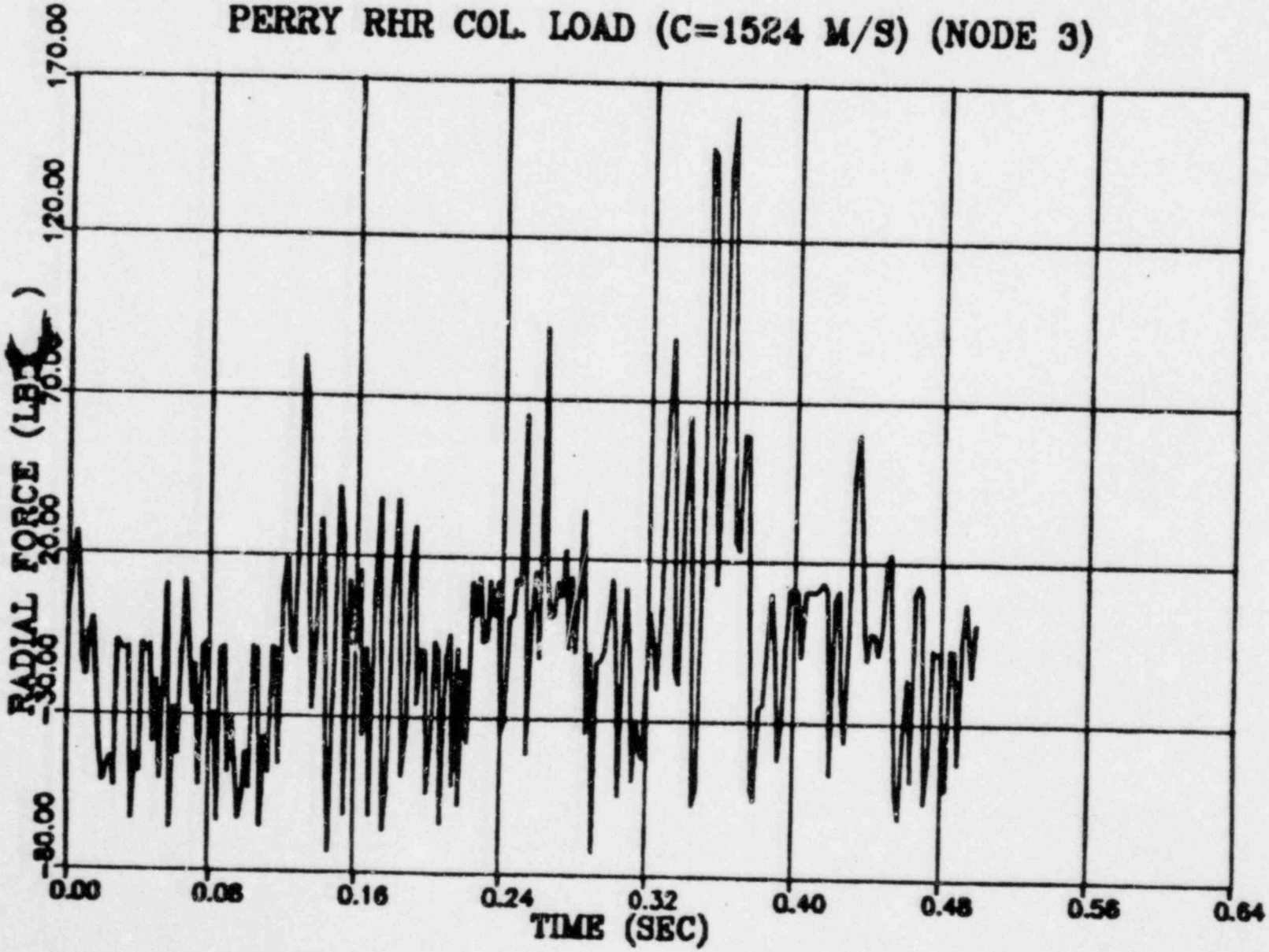
PERRY RHR COL. LOAD (C=1524 M/S) (NODE 3)
RADIAL FORCE (LBF)
170.00
120.00
70.00
20.00
-30.00
-80.00
0.00
0.08
0.16
0.24
0.32
0.40
0.48
0.56
0.64
TIME (SEC)

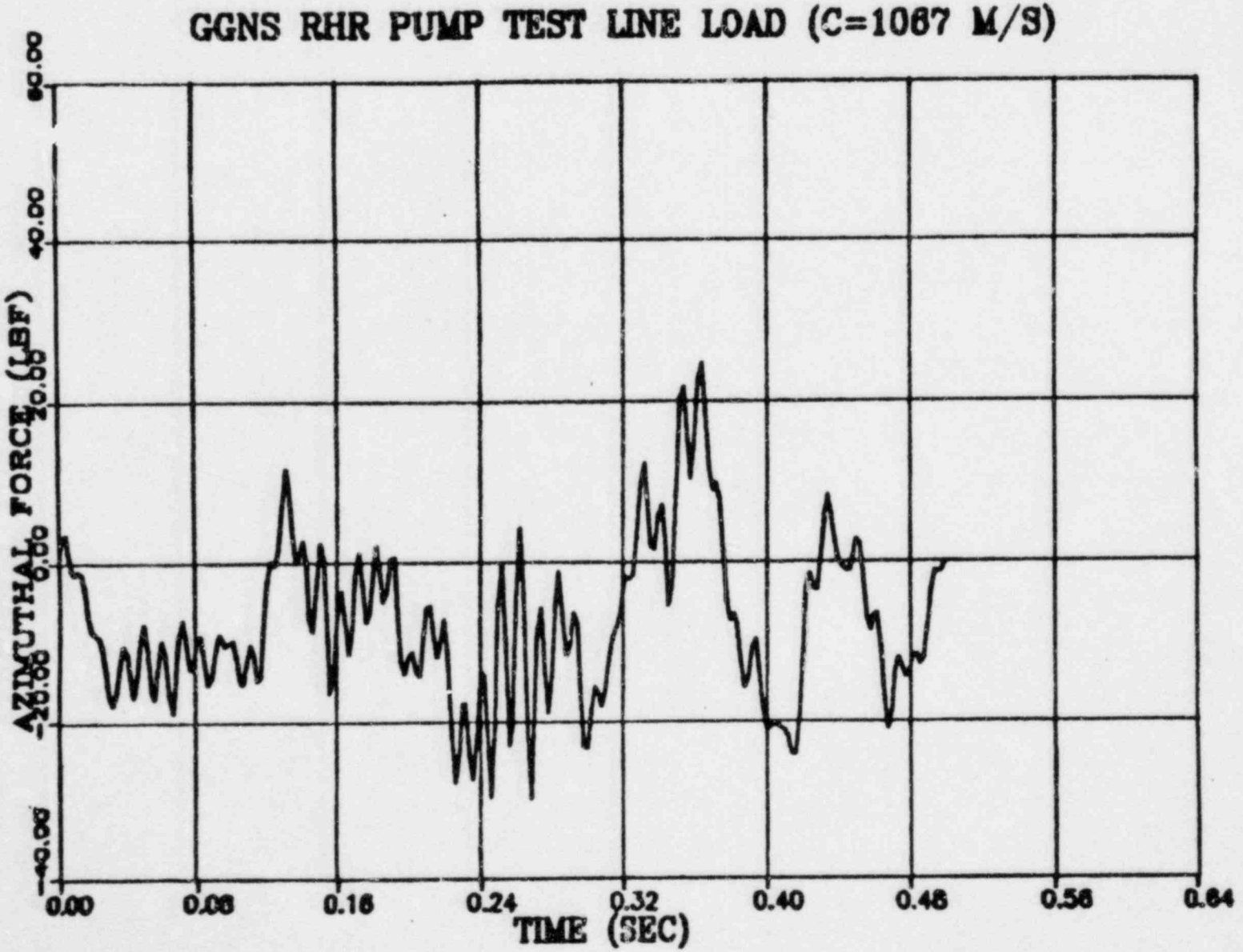
GGNS RHR PUMP TEST LINE LOAD (C=1067 M/S)
AZIMUTHAL FORCE (LBF)
40.00
20.00
0.00
-20.00
-40.00
0.00
0.08
0.16
0.24
0.32
0.40
0.48
0.56
0.64
TIME (SEC)

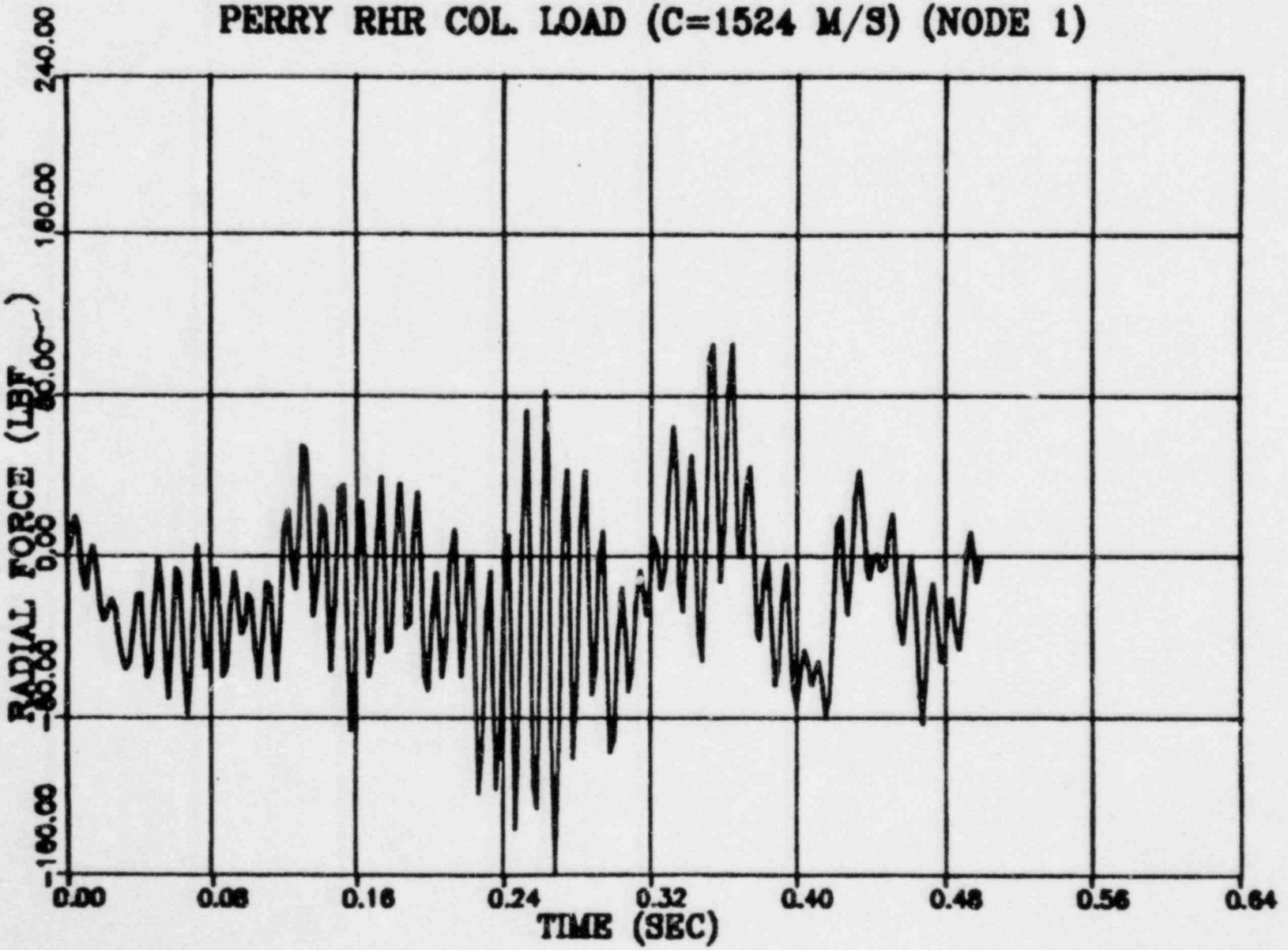
PERRY RHR COL. LOAD (C=1524 M/S) (NODE 1)
RADIAL FORCE (LBF)
240.00
160.00
80.00
0.00
-80.00
-160.00
0.00
0.08
0.16
0.24
0.32
0.40
0.48
0.56
0.64
TIME (SEC)

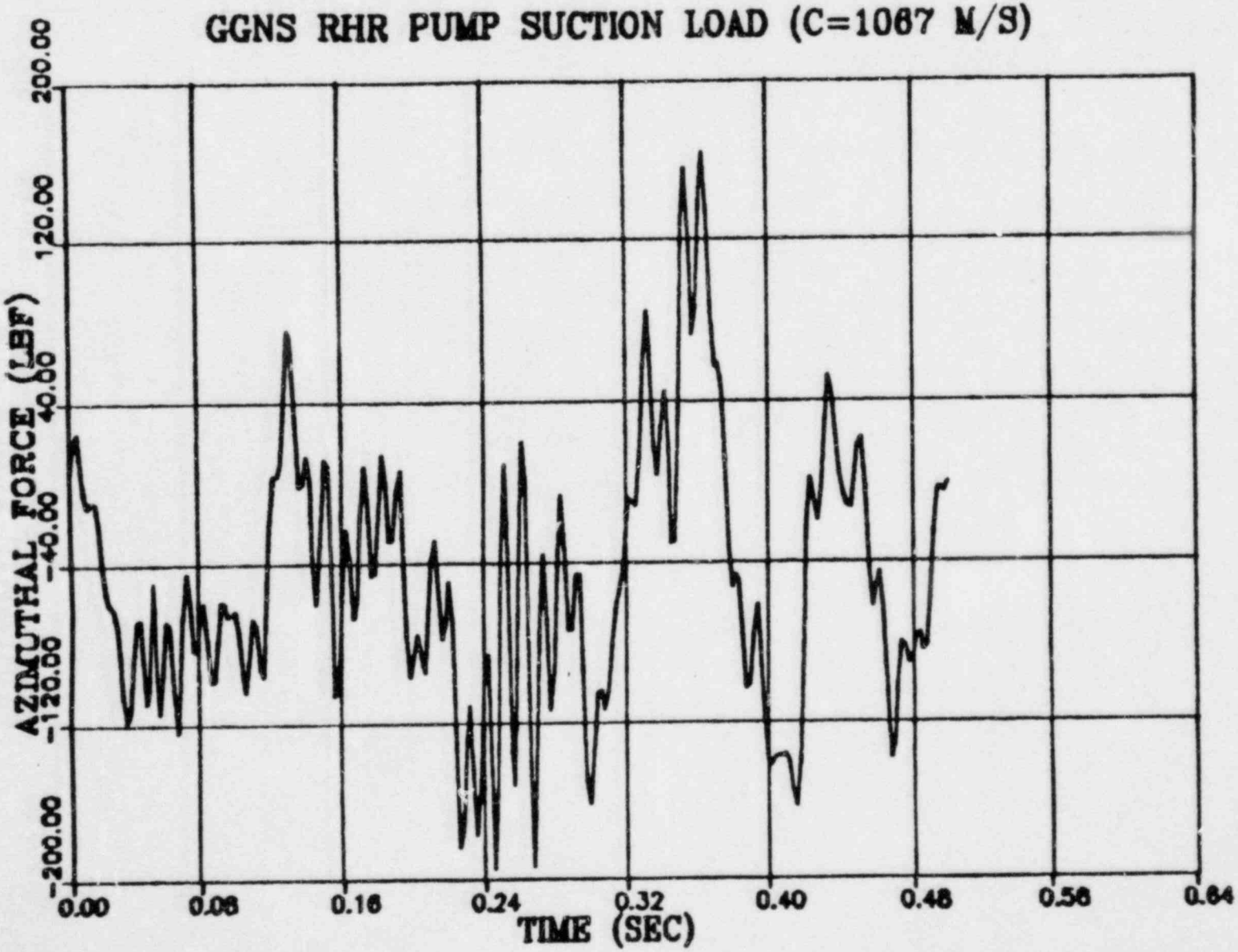
GGNS RHR PUMP SUCTION LOAD (C=1067 M/S)
AZIMUTHAL FORCE (LBF)
200.00
120.00
40.00
-40.00
-120.00
-200.00
0.00
0.08
0.16
0.24
0.32
0.40
0.48
0.56
0.64
TIME (SEC)

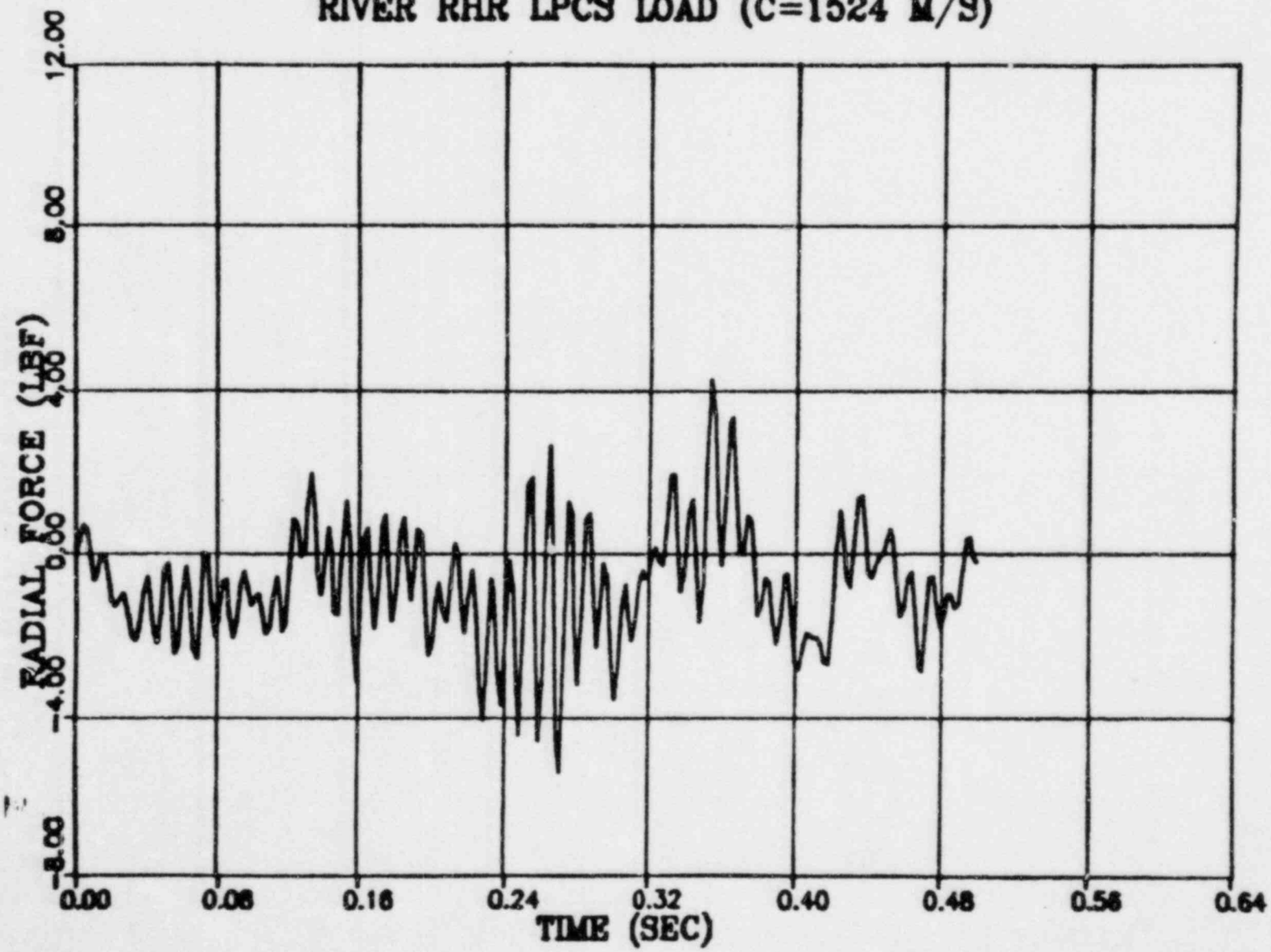
RIVER RHR LPCS LOAD (C=1524 M/S)
RADIAL FORCE (LBF)
12.00
8.00
4.00
0.00
-4.00
-8.00
0.00
0.08
0.16
0.24
0.32
0.40
0.48
0.56
0.64
TIME (SEC)

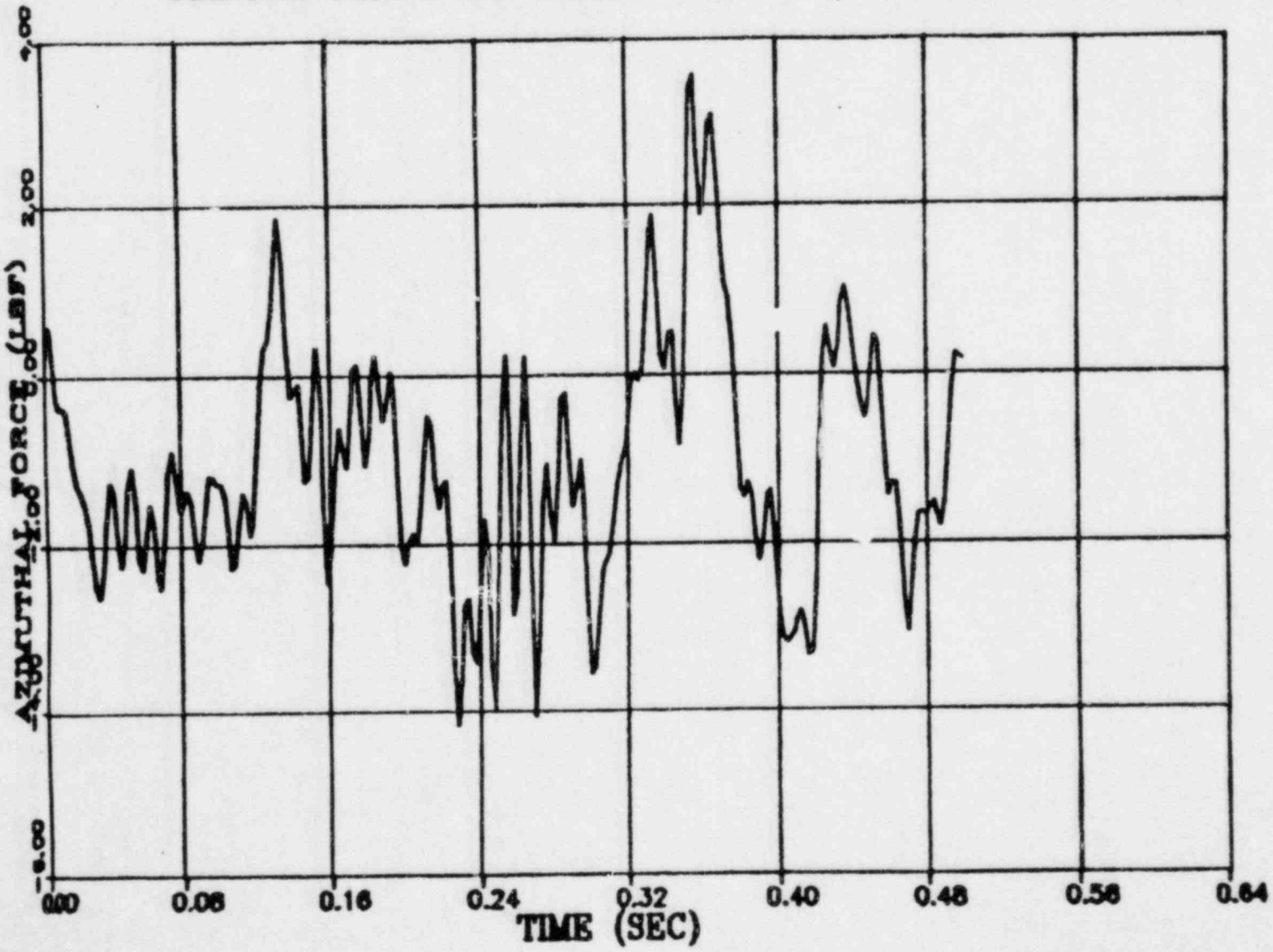
CLINTON RHR PUMP SUCTION LOAD (C=1067 M/S)
AZIMUTHAL FORCE (LBF)
4.00
2.00
0.00
-2.00
0.00
0.08
0.16
0.24
0.32
0.40
0.48
0.56
0.64
TIME (SEC)

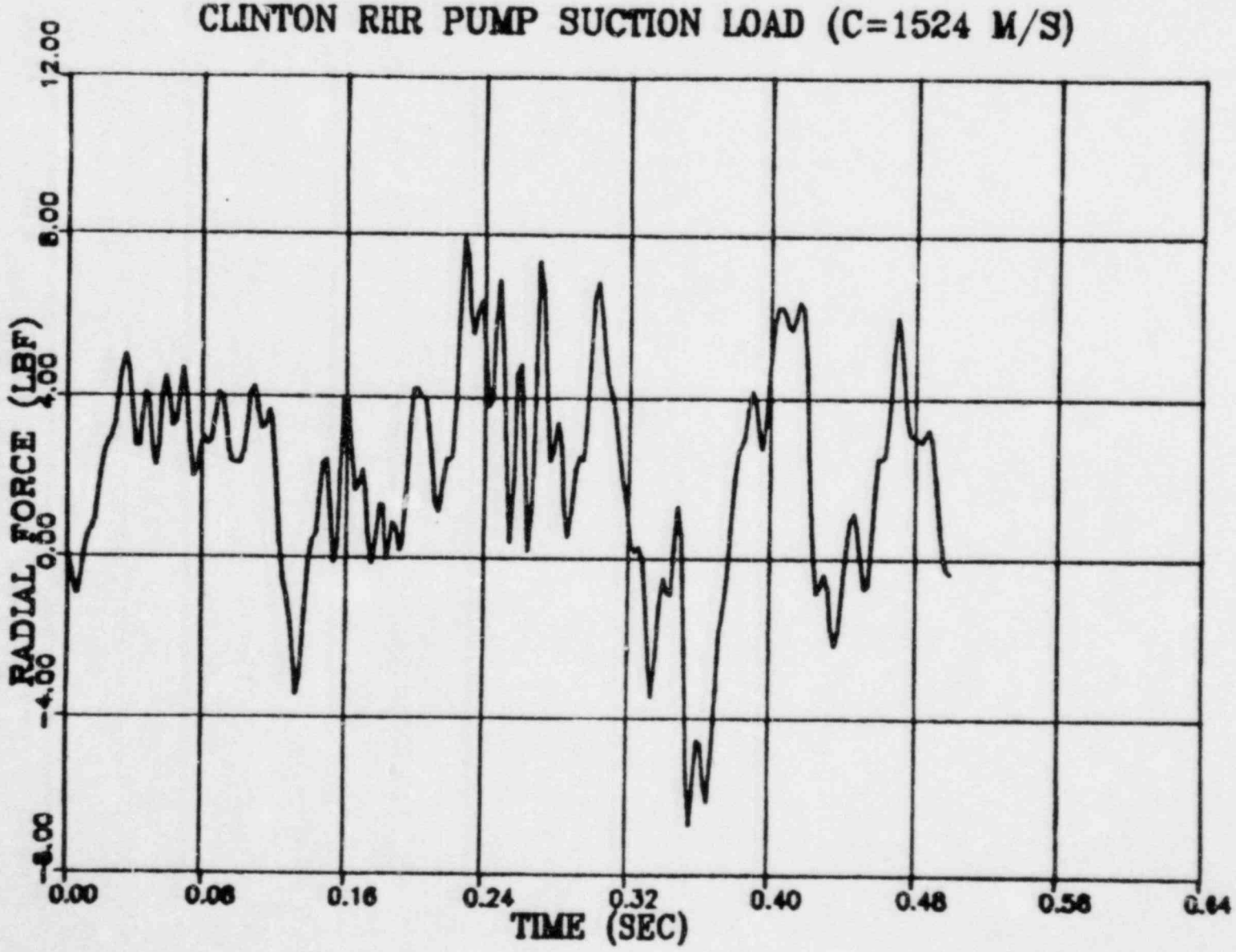
CLINTON RHR PUMP SUCTION LOAD (C=1524 M/S)
RADIAL FORCE (LBF)
12.00
8.00
4.00
0.00
-4.00
-8.00
0.00
0.08
0.16
0.24
0.32
0.40
0.48
0.56
0.64
TIME (SEC)

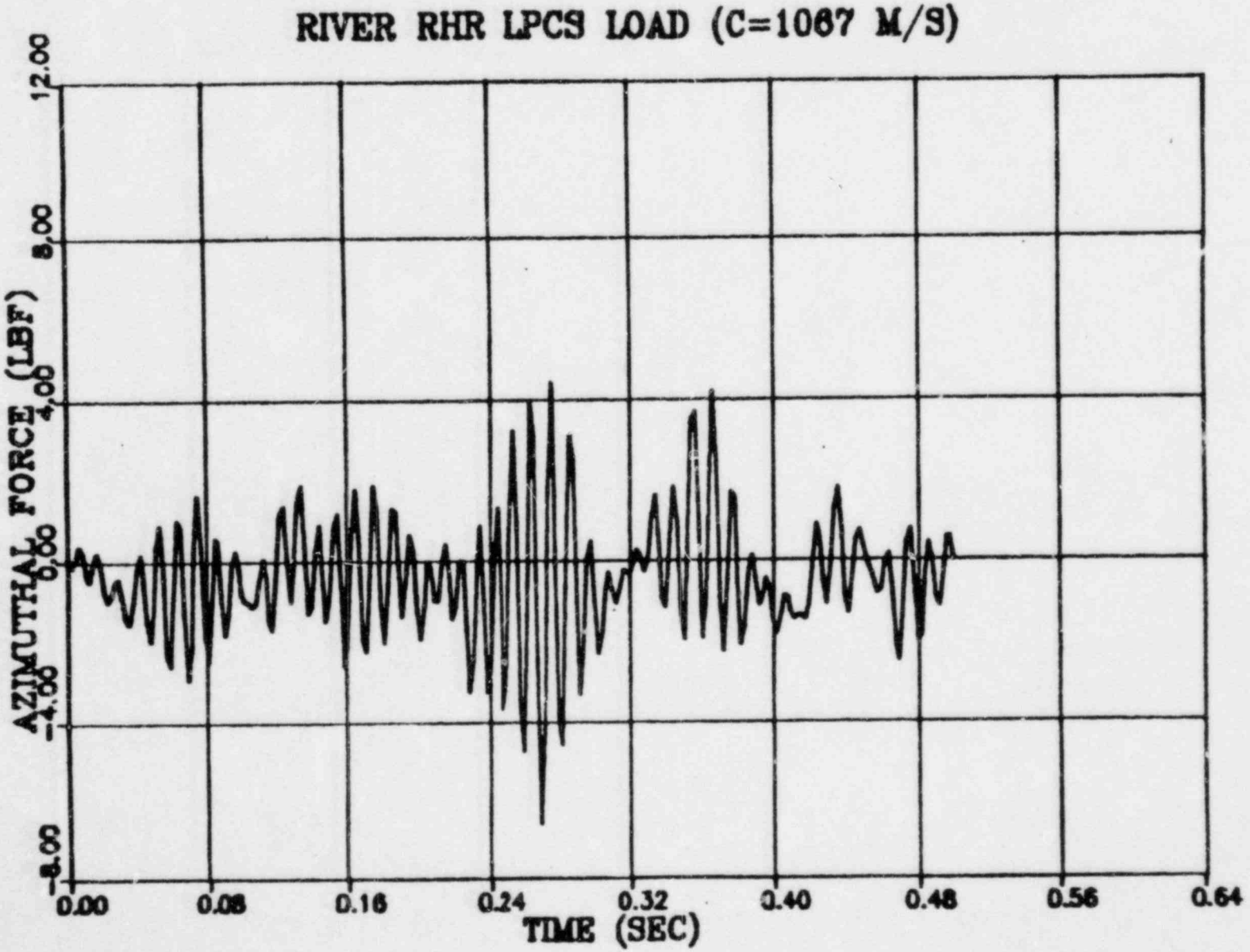
RIVER RHR LPCS LOAD (C=1067 M/S)
AZIMUTHAL FORCE (LBF)
12.00
8.00
4.00
0.00
-4.00
-8.00
0.00
0.08
0.16
0.24
0.32
0.40
0.48
0.56
0.64
TIME (SEC)

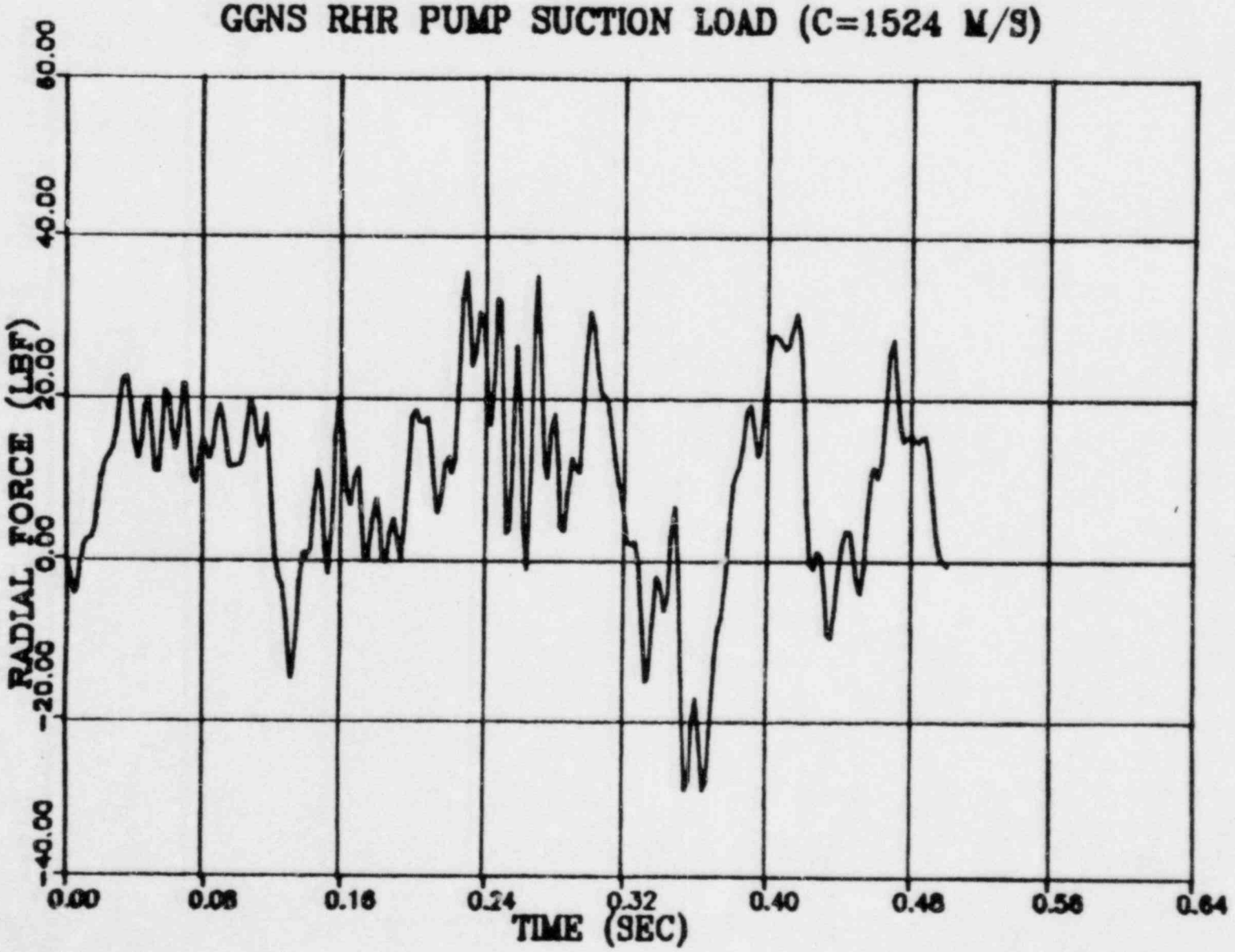
GGNS RHR PUMP SUCTION LOAD (C=1524 M/S)
RADIAL FORCE (LBF)
60.00
40.00
20.00
0.00
-20.00
-40.00
0.00
0.08
0.16
0.24
0.32
0.40
0.48
0.56
0.64
TIME (SEC)

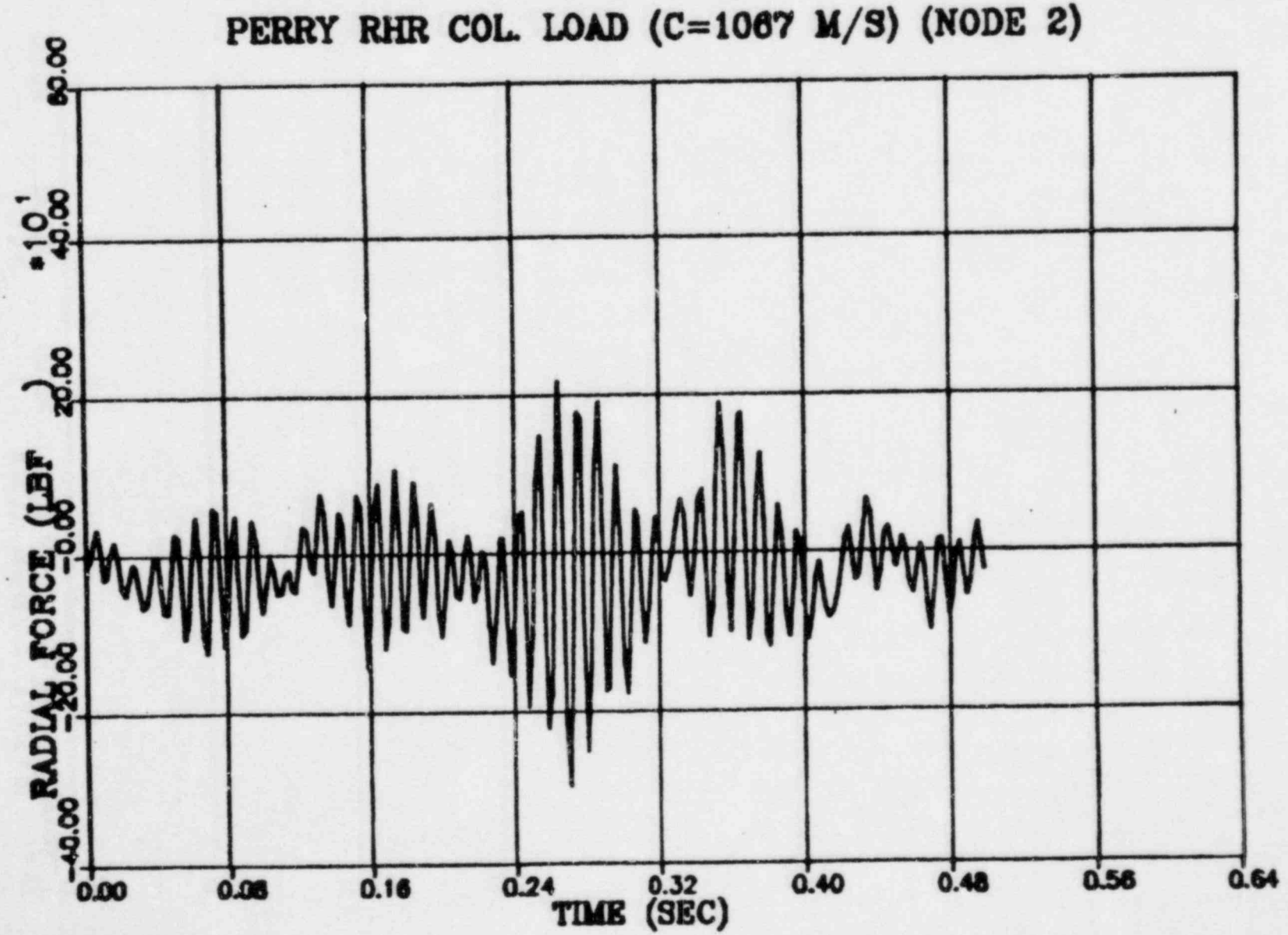
PERRY RHR COL. LOAD (C=1067 M/S) (NODE 2)
RADIAL FORCE (LBF *10^1)
60.00
40.00
20.00
-0.00
-20.00
-40.00
0.00
0.08
0.16
0.24
0.32
0.40
0.48
0.56
0.64
TIME (SEC)

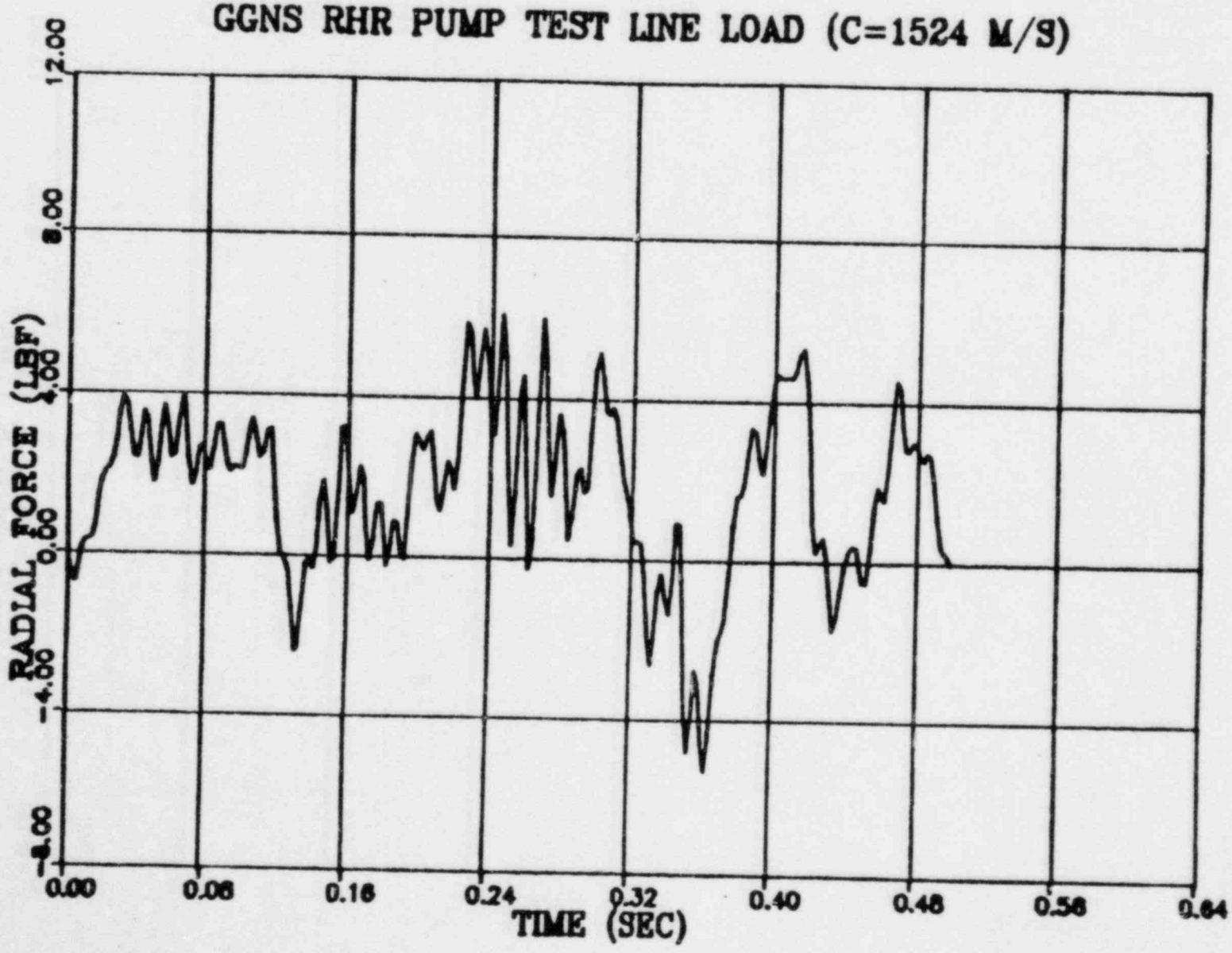
GGNS RHR PUMP TEST LINE LOAD (C=1524 M/S)
RADIAL FORCE (LBF)
12.00
8.00
4.00
0.00
-4.00
-8.00
0.00
0.08
0.16
0.24
0.32
0.40
0.48
0.56
0.64
TIME (SEC)

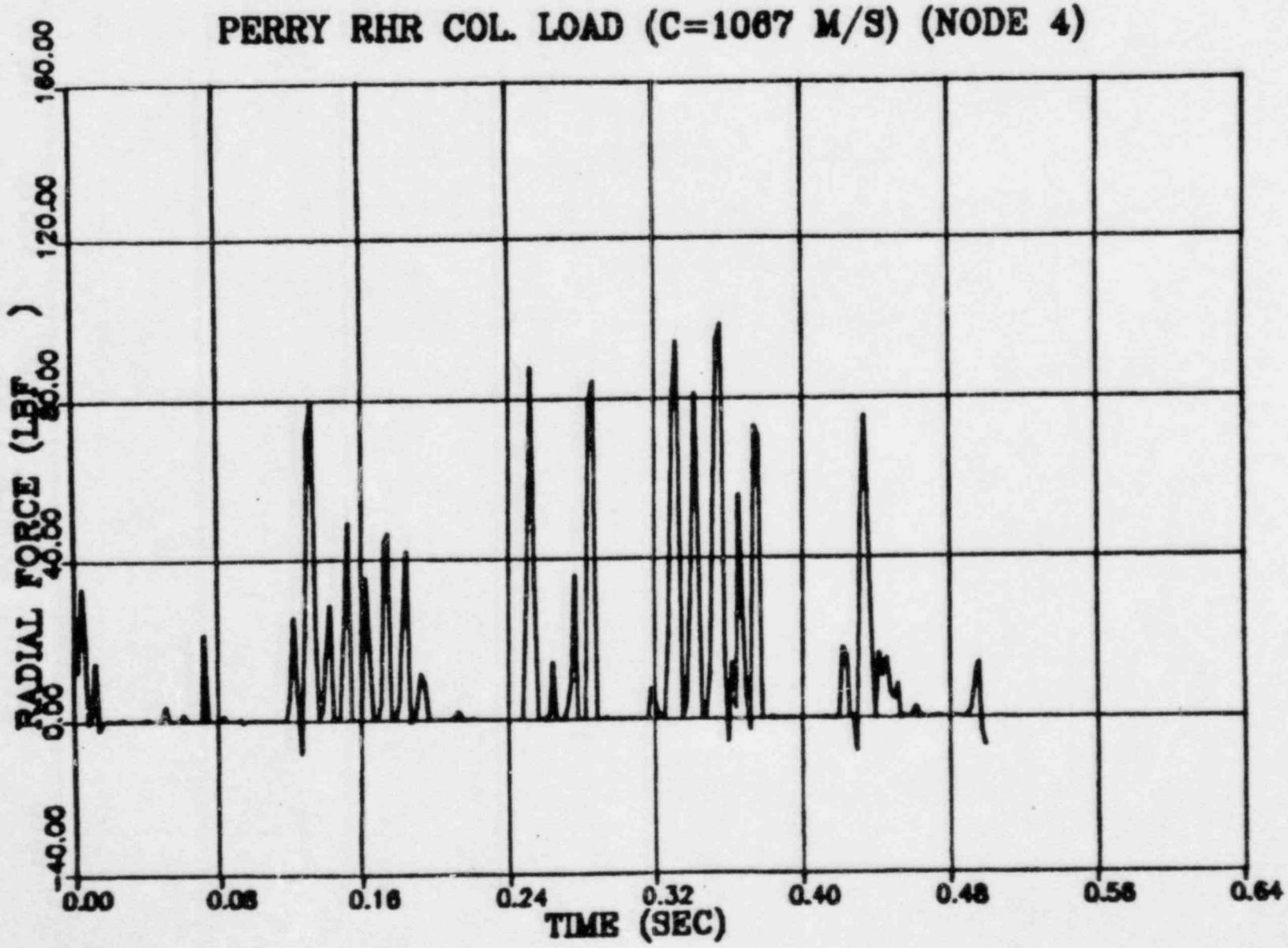
PERRY RHR COL. LOAD (C=1067 M/S) (NODE 4)
RADIAL FORCE (LBF)
160.00
120.00
80.00
40.00
0.00
-40.00
0.00
0.08
0.16
0.24
0.32
0.40
0.48
0.56
0.64
TIME (SEC)

PERRY RHR CO

Output at point (12.65,28.00,4.09)

NAME - LEONG, TAI SENG
DATE - FEB 21, 1984
PROJECT NO. - 15026004

CHECKED _____
DATE _____
CALC NO. - AP-84-

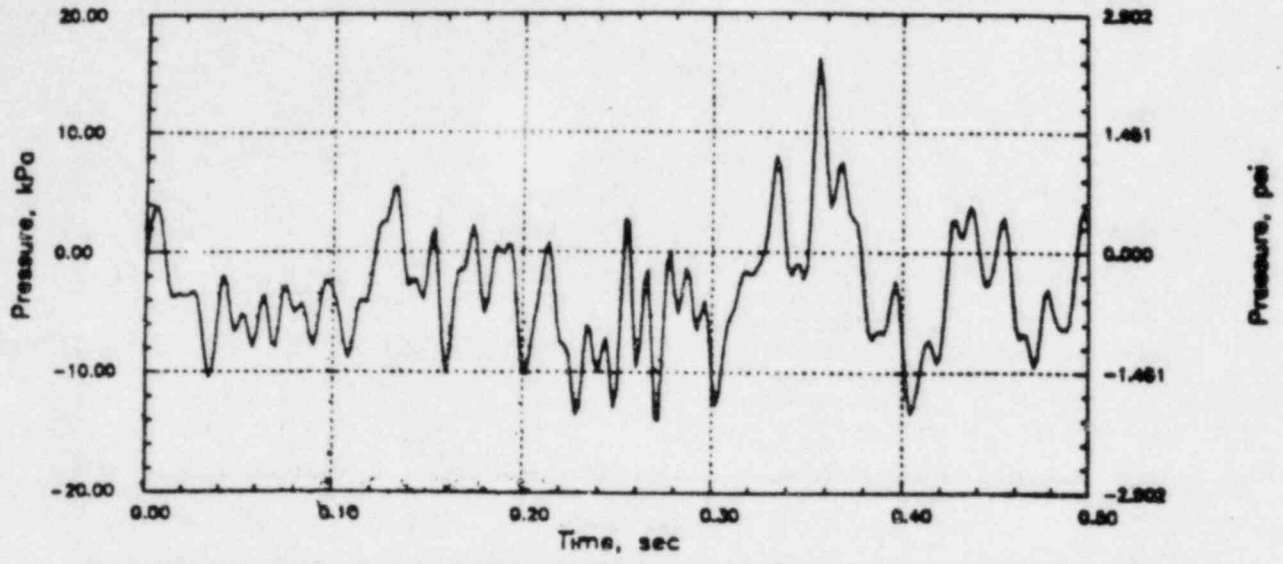

POP = 16.28 kPa PUP = -13.97 kPa MSP = 24.06 kPa²

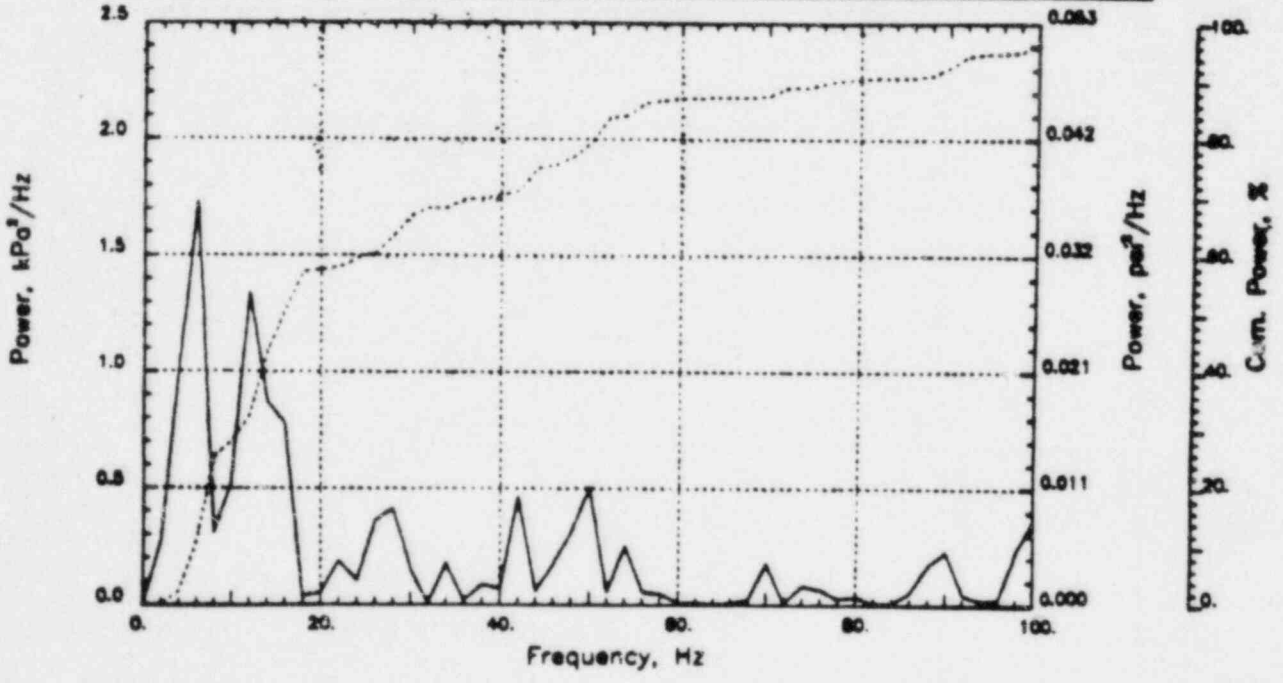

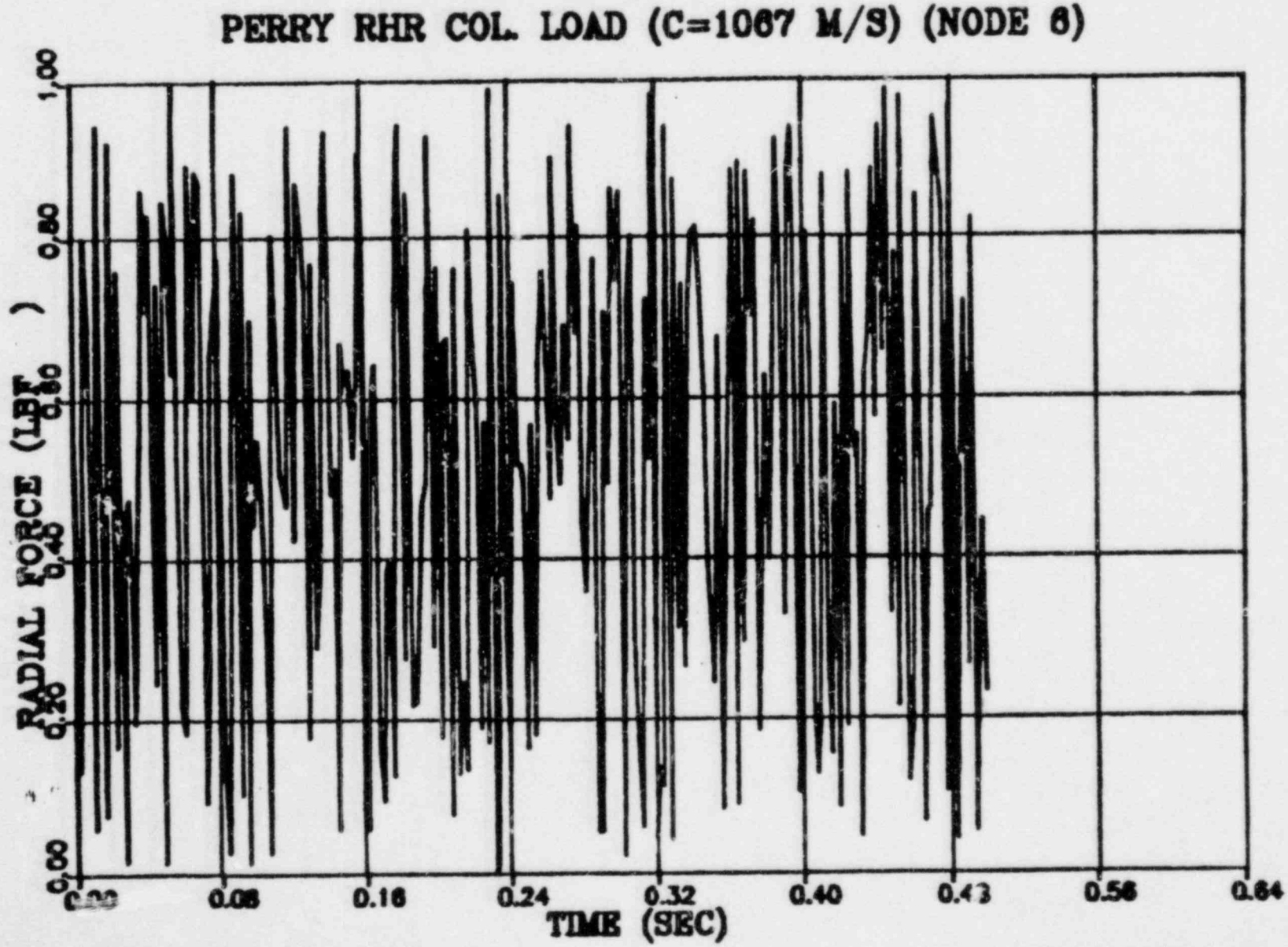
PERRY RHR COL. LOAD (C=1067 M/S) (NODE 6)
RADIAL FORCE (LBF)
1.00
0.80
0.60
0.40
0.20
0.00
0.08
0.16
0.24
0.32
0.40
0.48
0.56
0.64
TIME (SEC)

PERRY RHR CO

Output at point (12.65,28.00,2.82)

NAME - LEONG, TAI SENG
DATE - FEB 21, 1984
PROJECT NO. - 15026004

CHECKED _____
DATE _____
CALC NO. - AP-84-

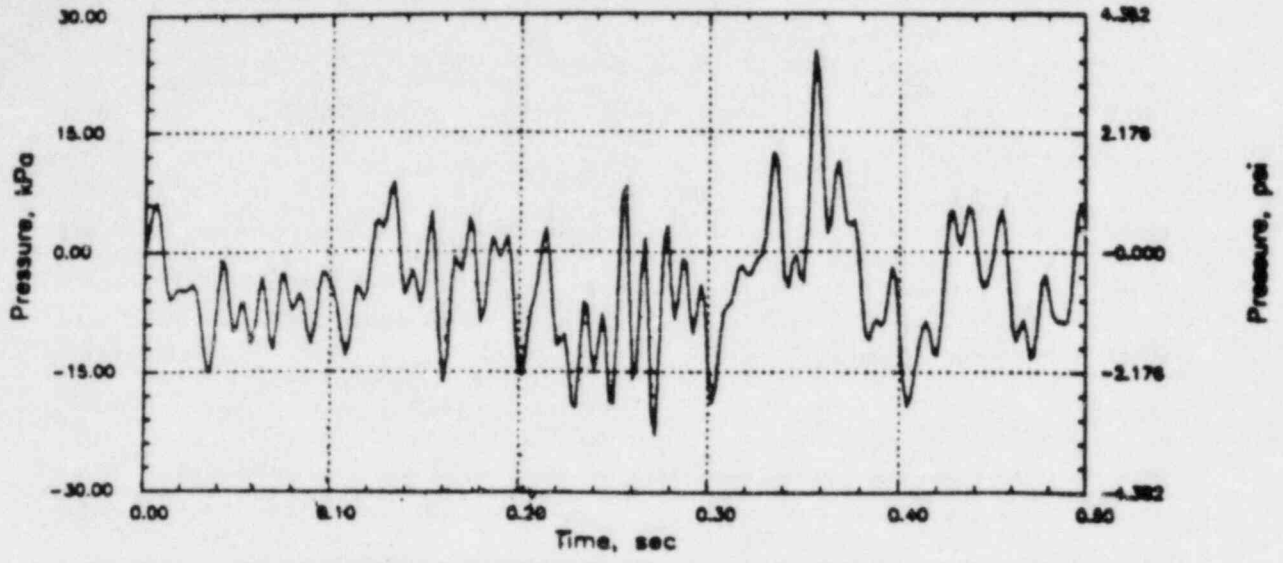

POP = 25.33 kPa PUP = -22.83 kPa MSP = 52.42 kPa²

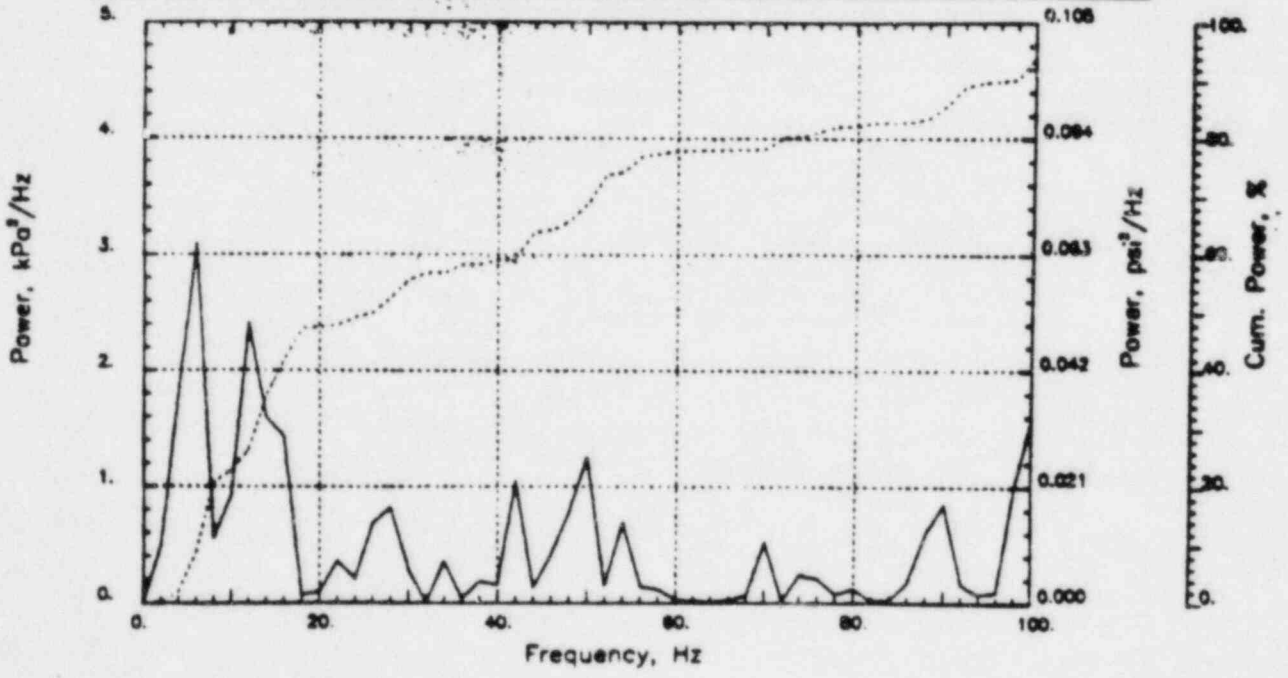

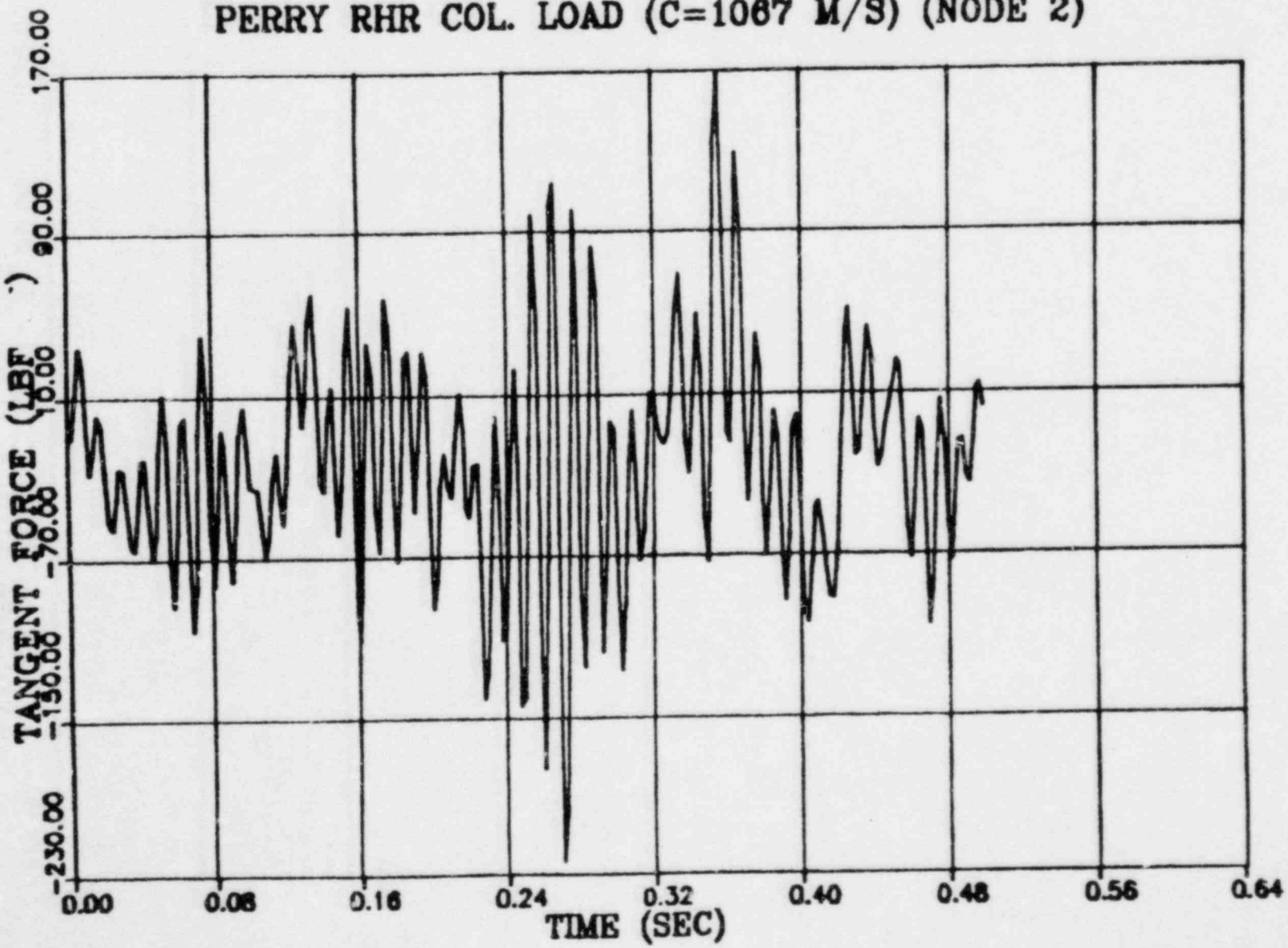
PERRY RHR COL. LOAD (C=1067 M/S) (NODE 2)
TANGENT FORCE (LBF)
170.00
90.00
10.00
-70.00
-150.00
-230.00
0.00
0.08
0.16
0.24
0.32
0.40
0.48
0.56
0.64
TIME (SEC)

PERRY RHR CO

Output at point (12.65,28.00,1.55)

NAME - LEONG, TAI SENG
DATE - FEB 21, 1984
PROJECT NO. - 15026004

CHECKED _____
DATE _____
CALC NO. - AP-84-

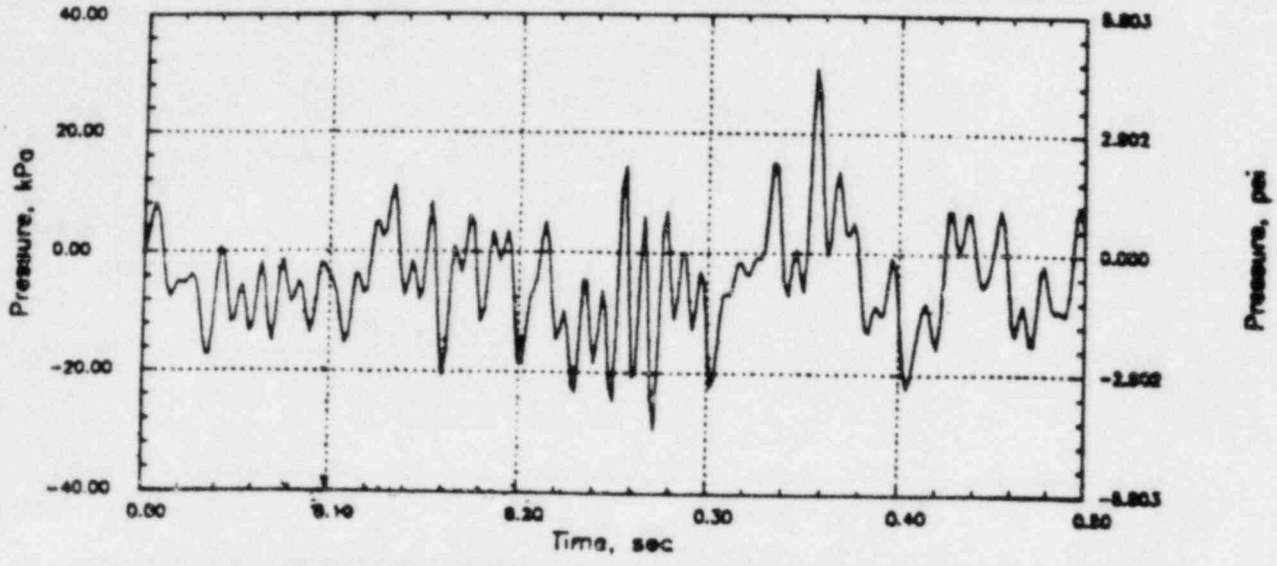

POP = 31.14 kPa PUP = -29.22 kPa MSP = 75.89 kPa²

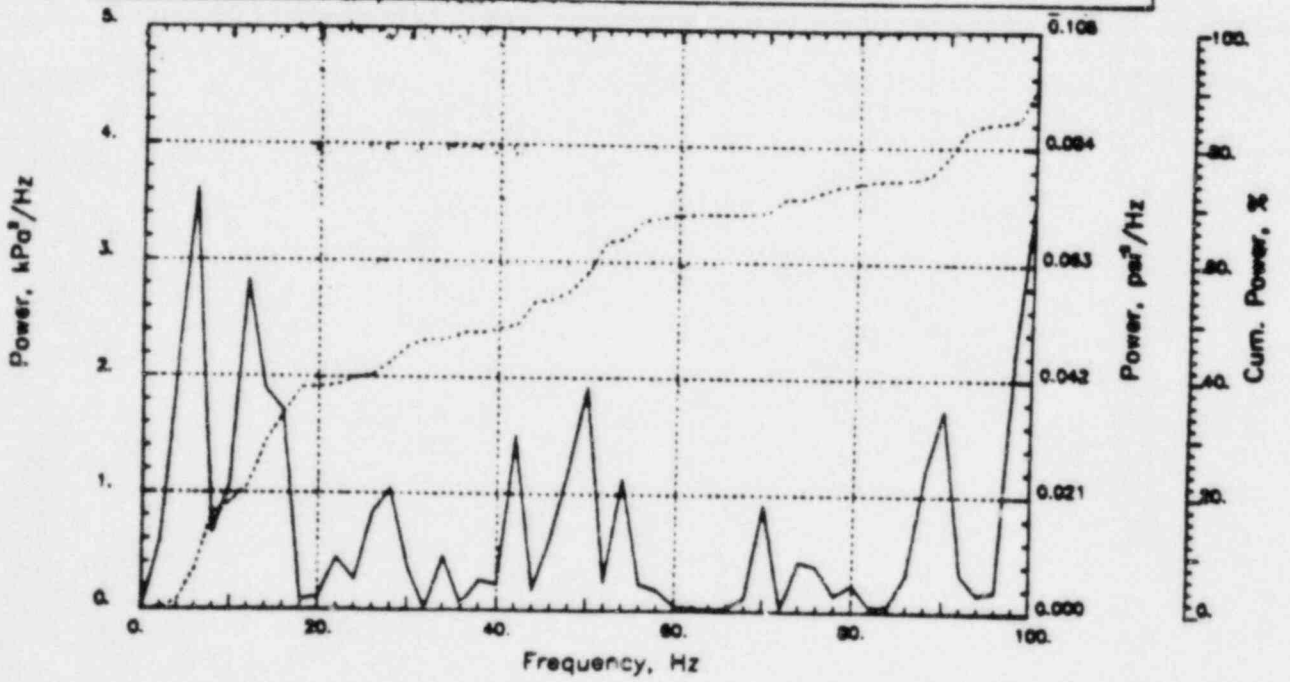

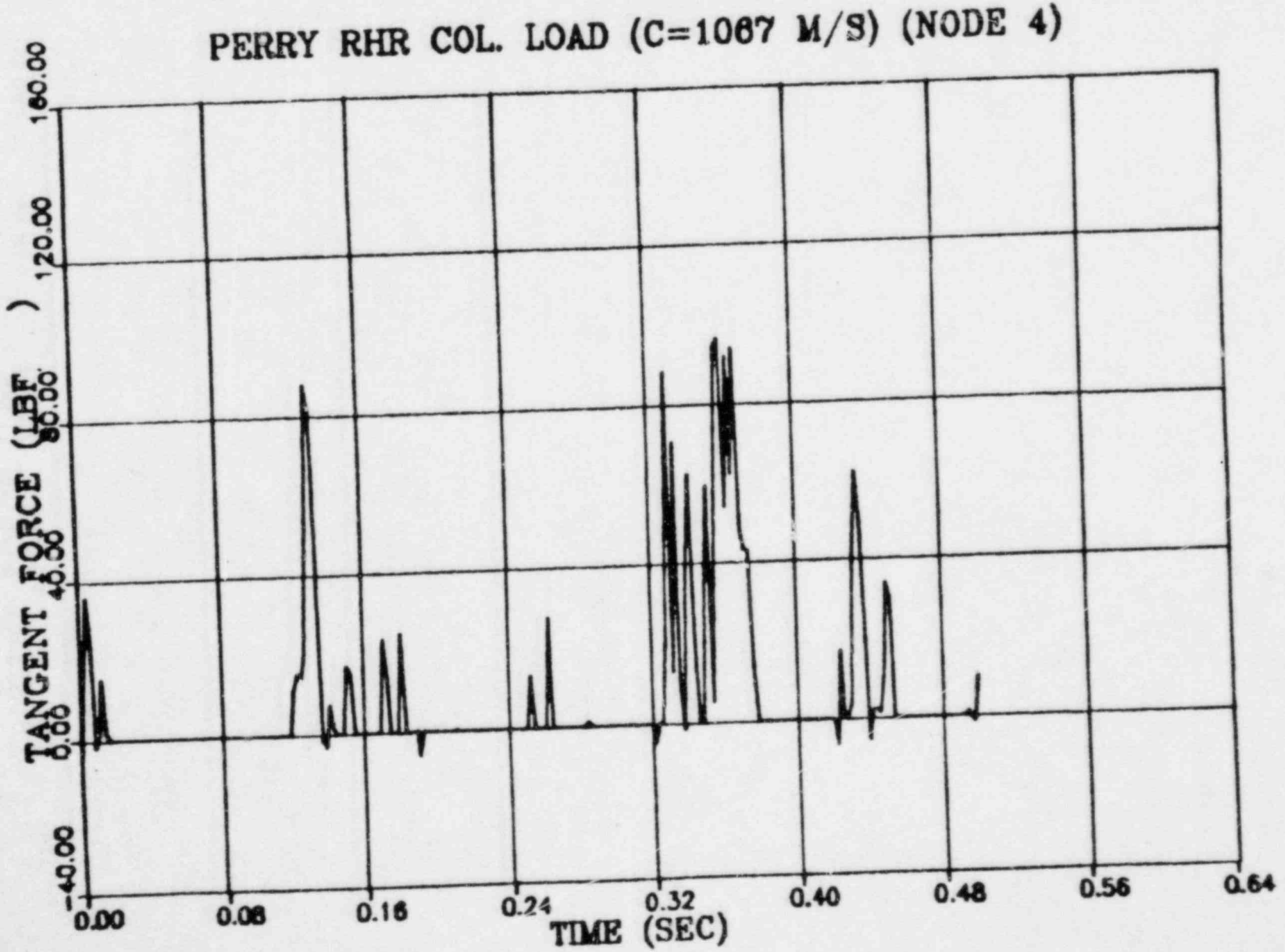
PERRY RHR COL. LOAD (C=1067 M/S) (NODE 4)
TANGENT FORCE (LBF)
160.00
120.00
80.00
40.00
0.00
-40.00
0.00
0.08
0.16
0.24
0.32
0.40
0.48
0.56
0.64
TIME (SEC)

PERRY RHR CO

Output at point (12.65,28.00,0.46)

NAME - LEONG, TAI SENG
DATE - FEB 21, 1984
PROJECT NO. - 15026004

CHECKED _____
DATE _____
CALC NO. - AP-84-

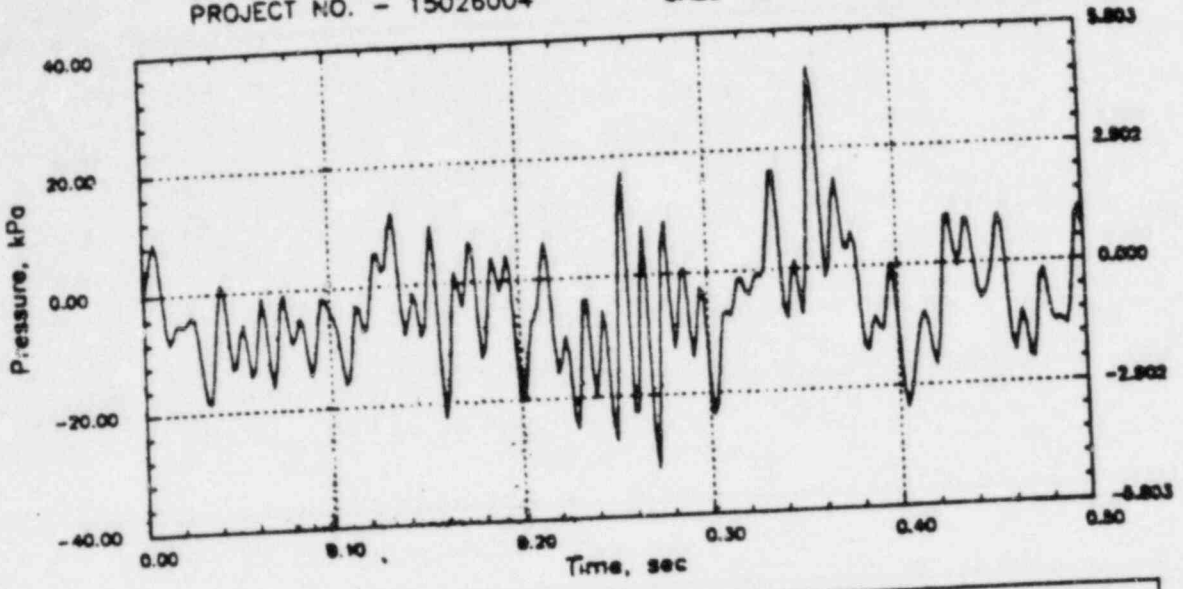

POP = 33.60 kPa PUP = -32.05 kPa MSP = 87.95 kPa²

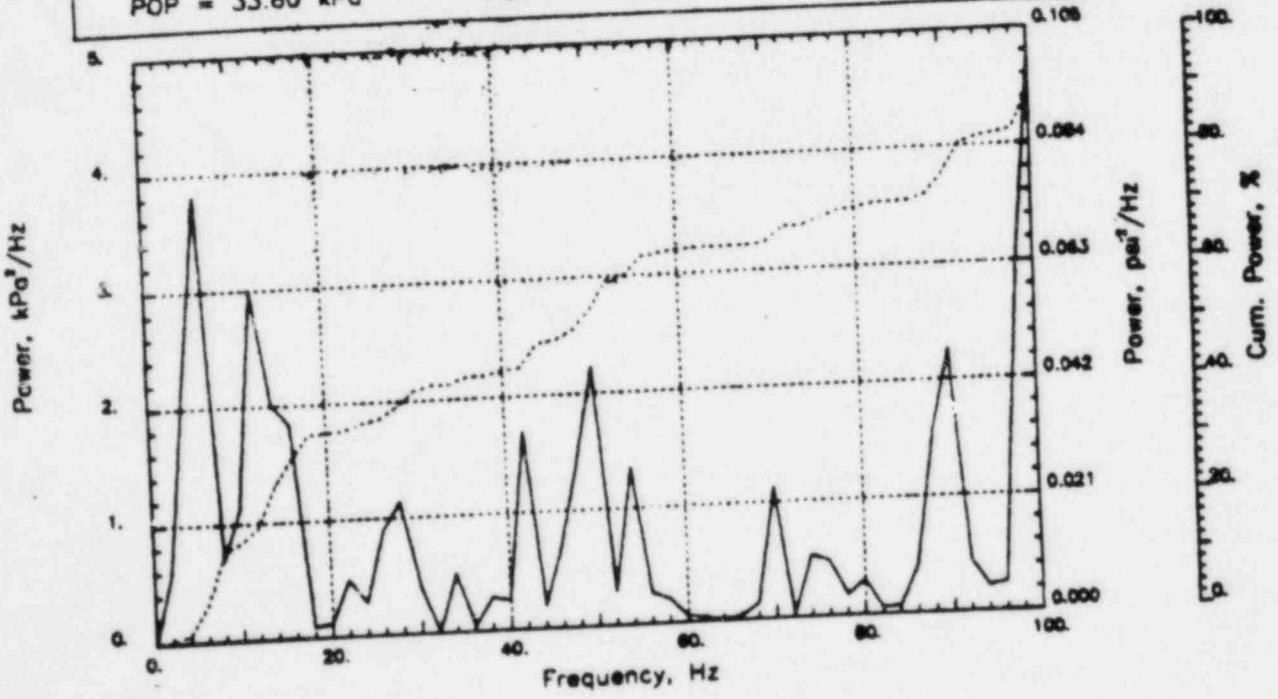

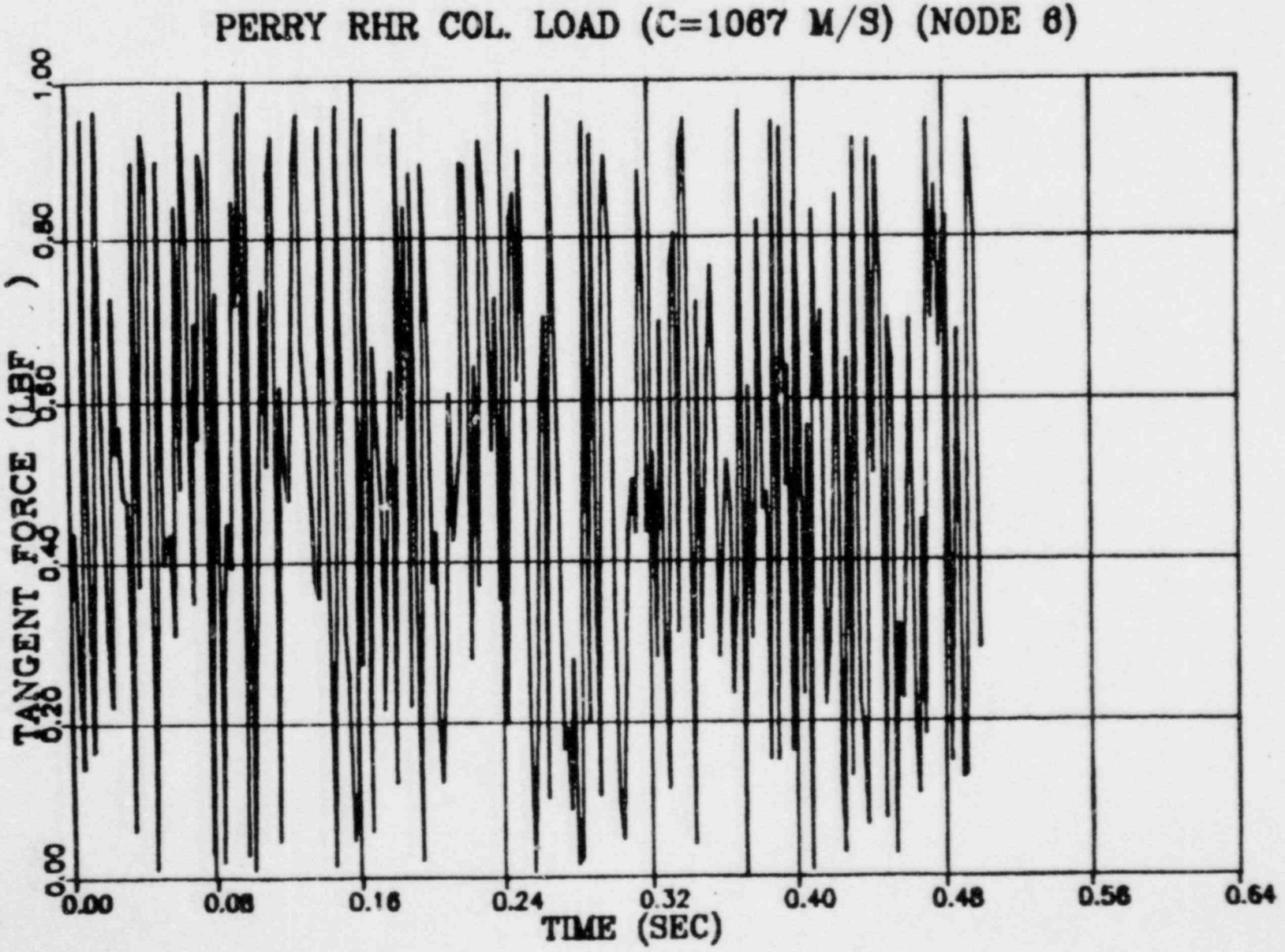
PERRY RHR COL. LOAD (C=1067 M/S) (NODE 6)
TANGENT FORCE (LBF)
1.00
0.80
0.60
0.40
0.20
0.00
0.00
0.08
0.16
0.24
0.32
0.40
0.48
0.56
0.64
TIME (SEC)

PERRY RHR CO

Output at point (14.21,28.00,0.00)

NAME - LEONG, TAI SENG
DATE - FEB 21, 1984
PROJECT NO. - 15026004

CHECKED _____
DATE _____
CALC NO. - AP-84-

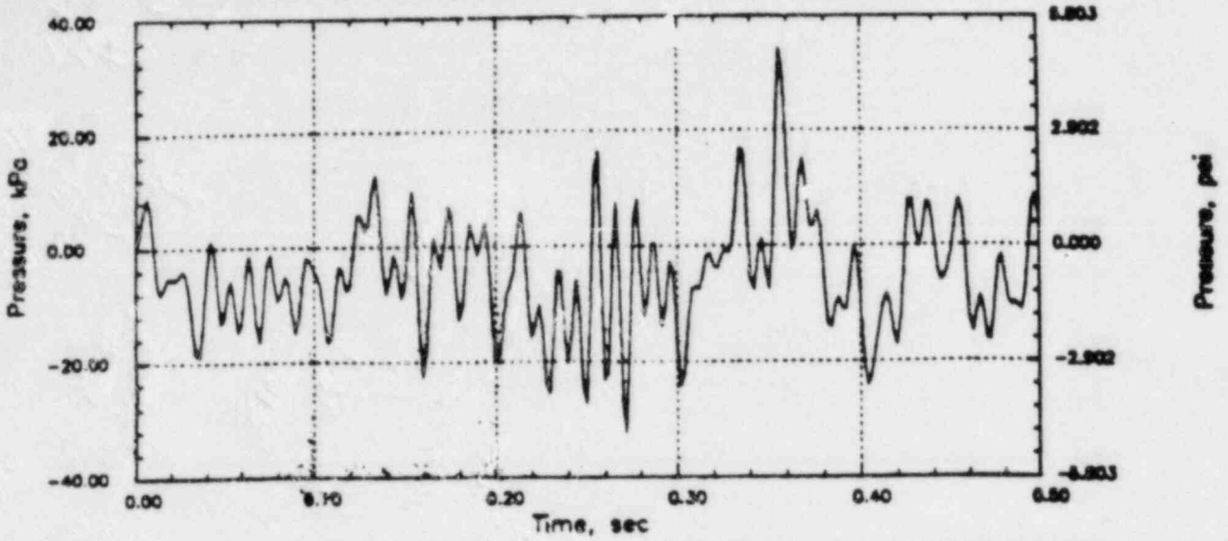

POP = 34.26 kPa PUP = -32.18 kPa MSP = 91.07 kPa²

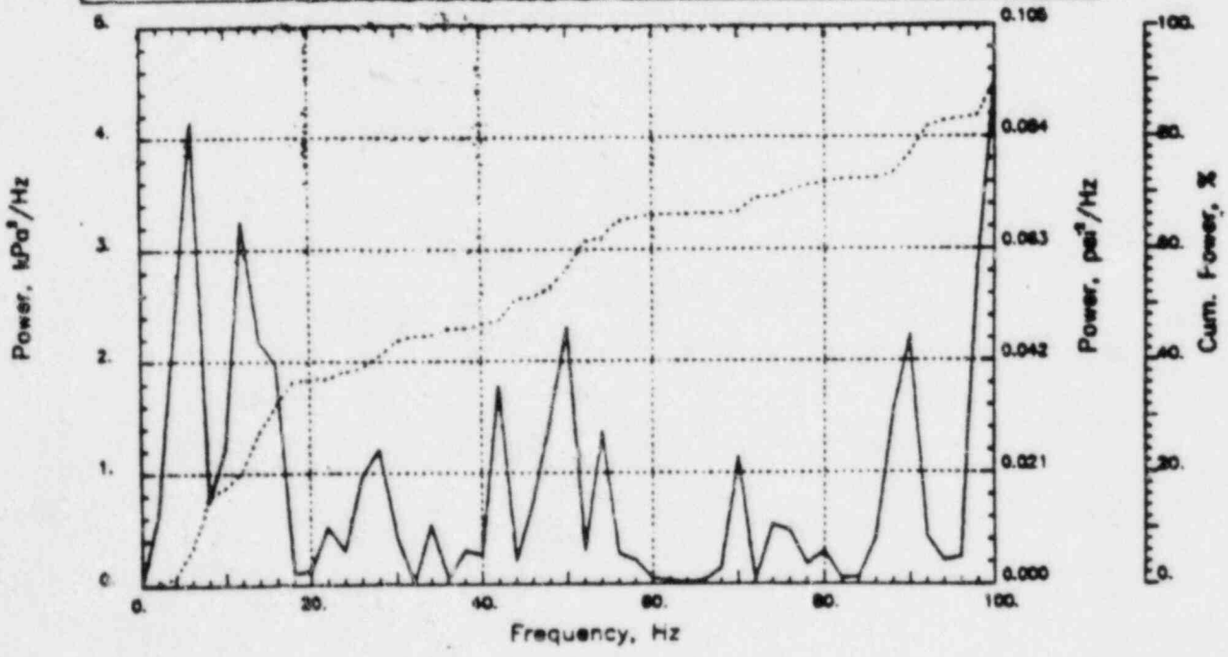

APPENDIX C

PLANT PRESSURE TIME-HISTORIES AND PLANT SUBMERGED STRUCTURES FORCE TIME-HISTORIES WITH C = 1524 m/s

PERRY RHR CO

Output at point (18.90,28.00,0.00)

NAME - LEONG, TAI SENG
DATE - FEB 21, 1984
PROJECT NO. - 15026004

CHECKED _____
DATE _____
CALC NO. - AP-84-

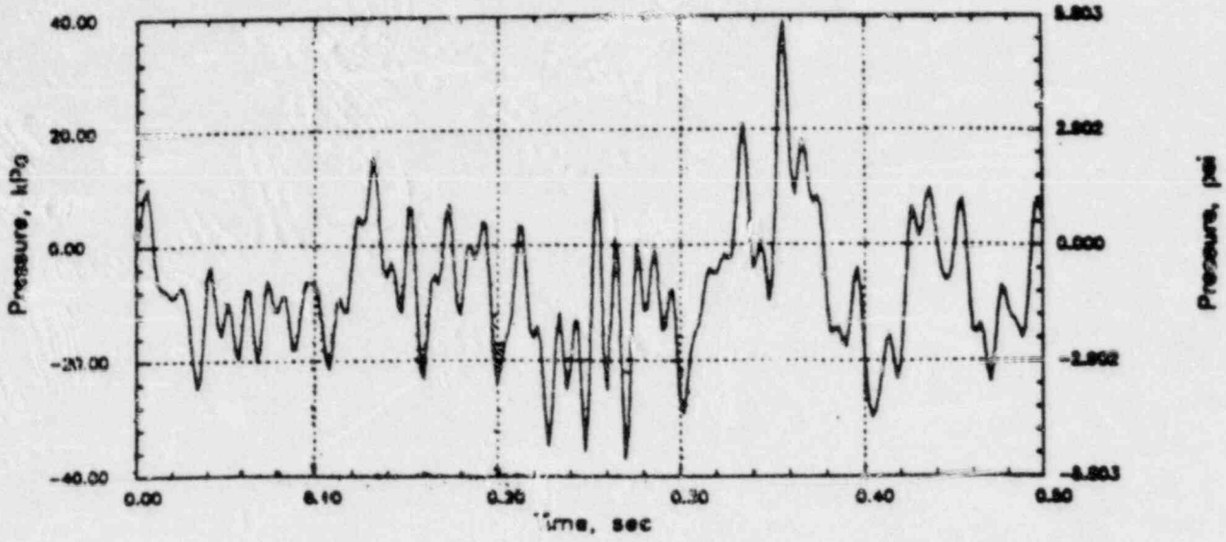

POP = 39.01 kPa PU.' = -37.05 kPa MSP = 137.43 kPc²

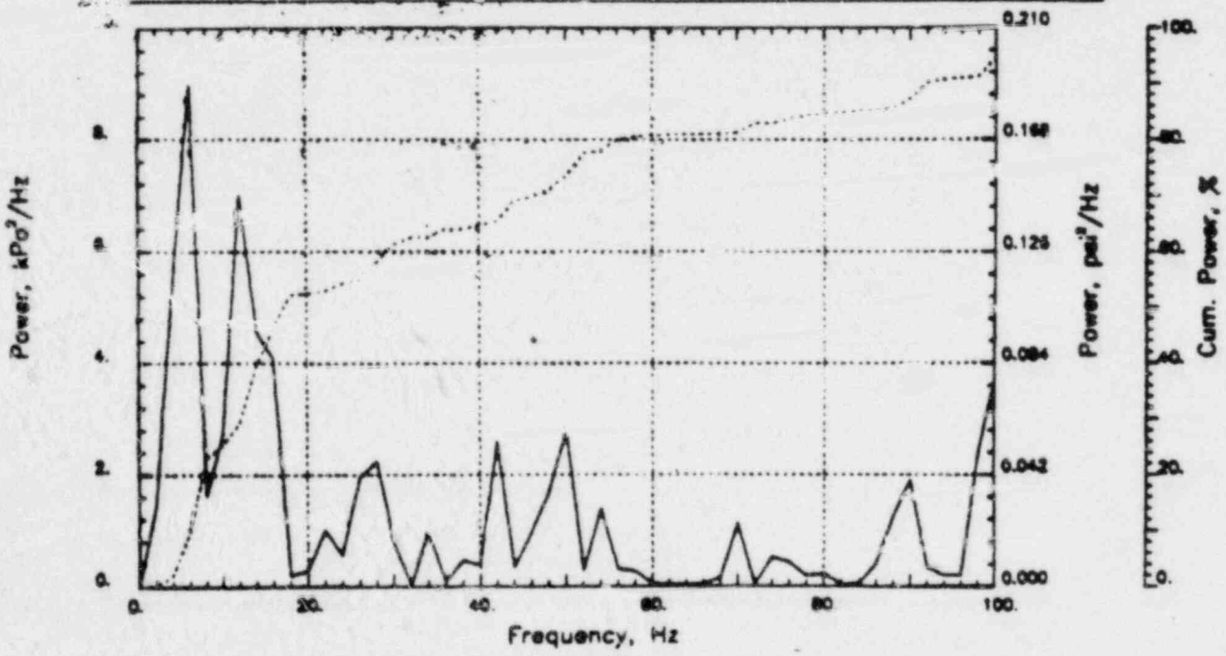

GGNS RHR CO

Output at point (18.90,28.00,4.91)

NAME - LEONG, TAI SENG
DATE - FEB 21, 1984
PROJECT NO. - 15026004

CHECKED _____
DATE _____
CALC NO. - AP-84-

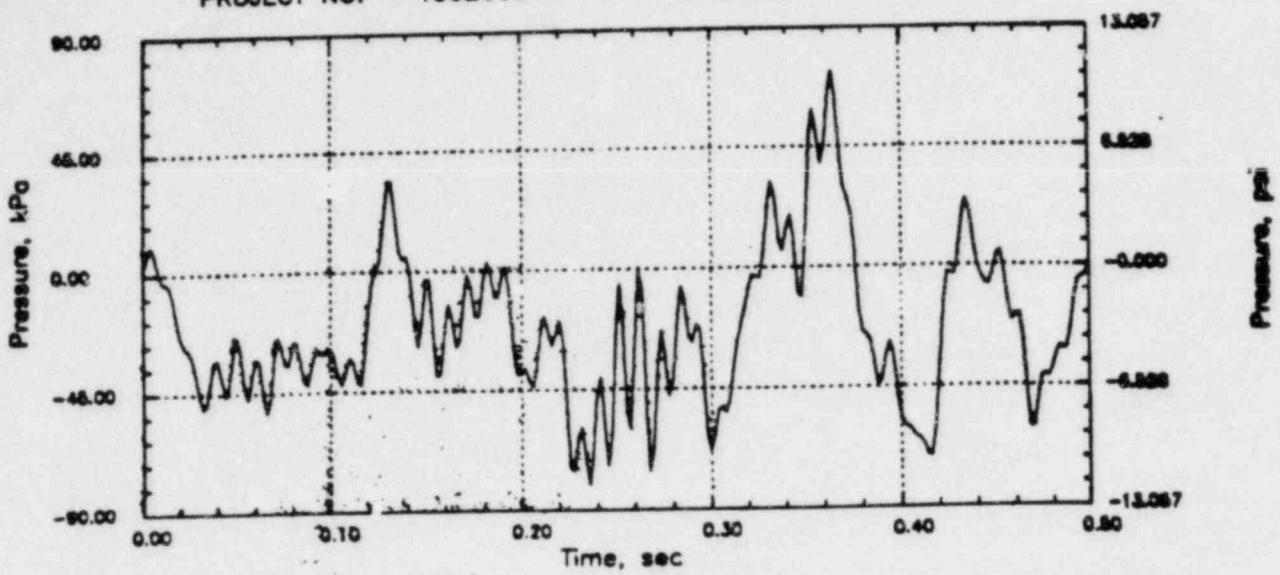

POP = 78.44 kPa PUP = -80.12 kPa MSP = 785.13 kPa²

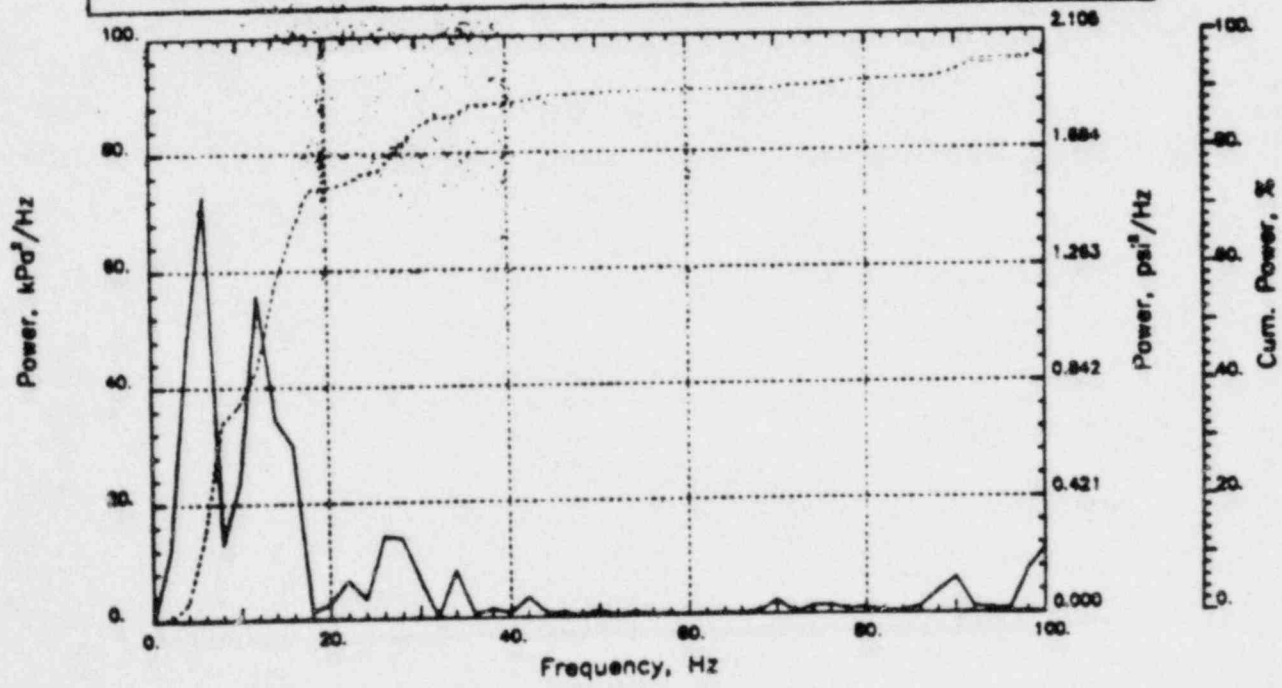

PERRY RHR CO

Output at point (18.90,28.00,0.91)

NAME - LEONG, TAI SENG
DATE - FEB 21, 1984
PROJECT NO. - 15026004

CHECKED _____
DATE _____
CALC NO. - AP-84-

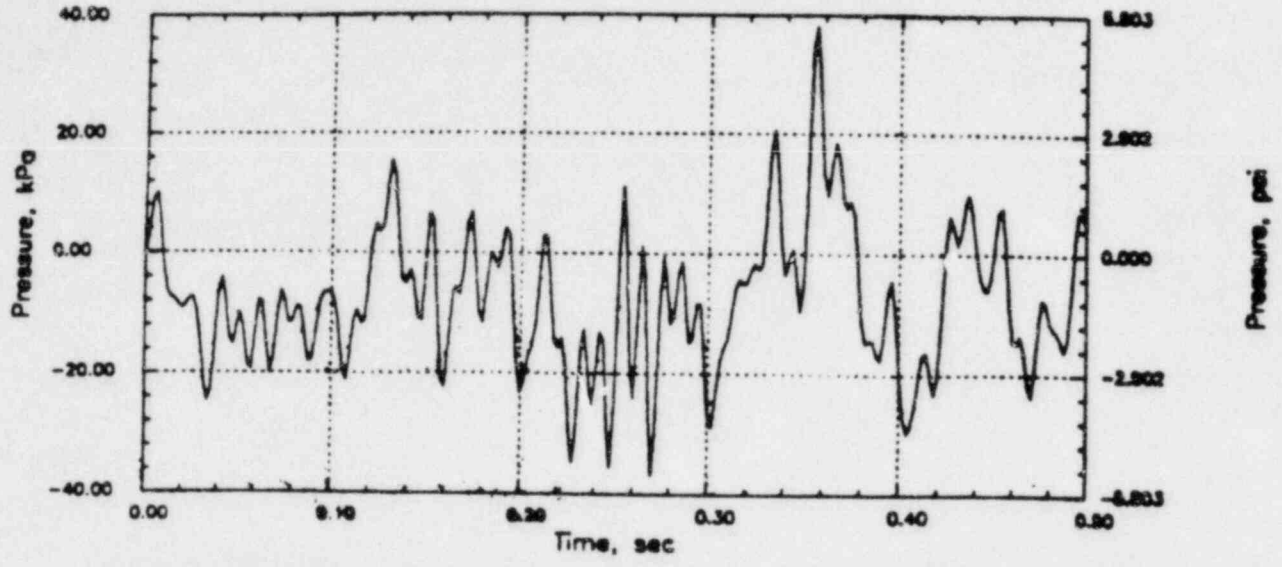

POP = 38.20 kPa PUP = -36.74 kPa MSP = 136.49 kPa²

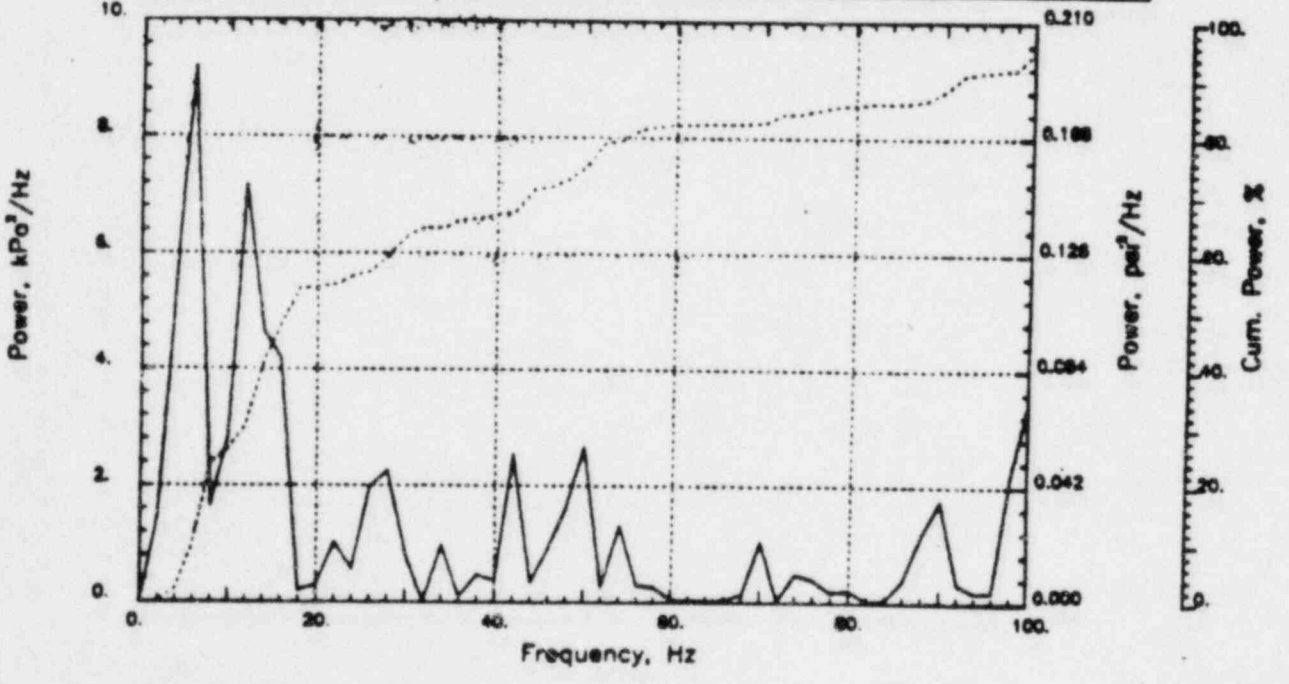

GGNS RHR CO

Output at point (18.90,28.00,3.45)

NAME - LEONG, TAI SENG
DATE - FEB 21, 1984
PROJECT NO. - 15026004

CHECKED _____
DATE _____
CALC NO. - AP-84-

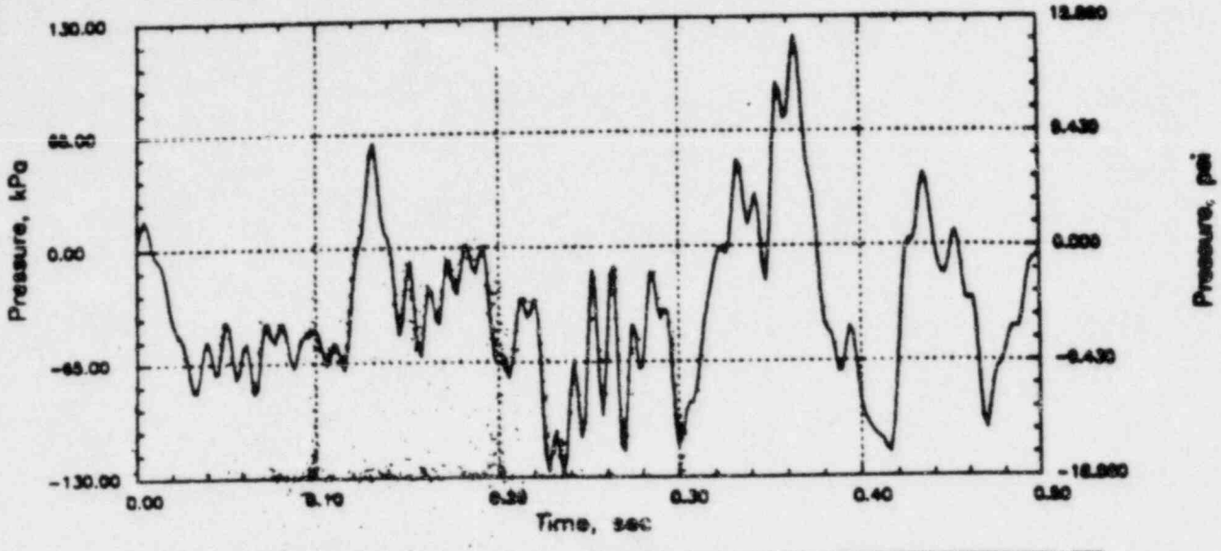

POP = 119.16 kPa PUP = -129.92 kPa MSP = 2098.24 kPa²

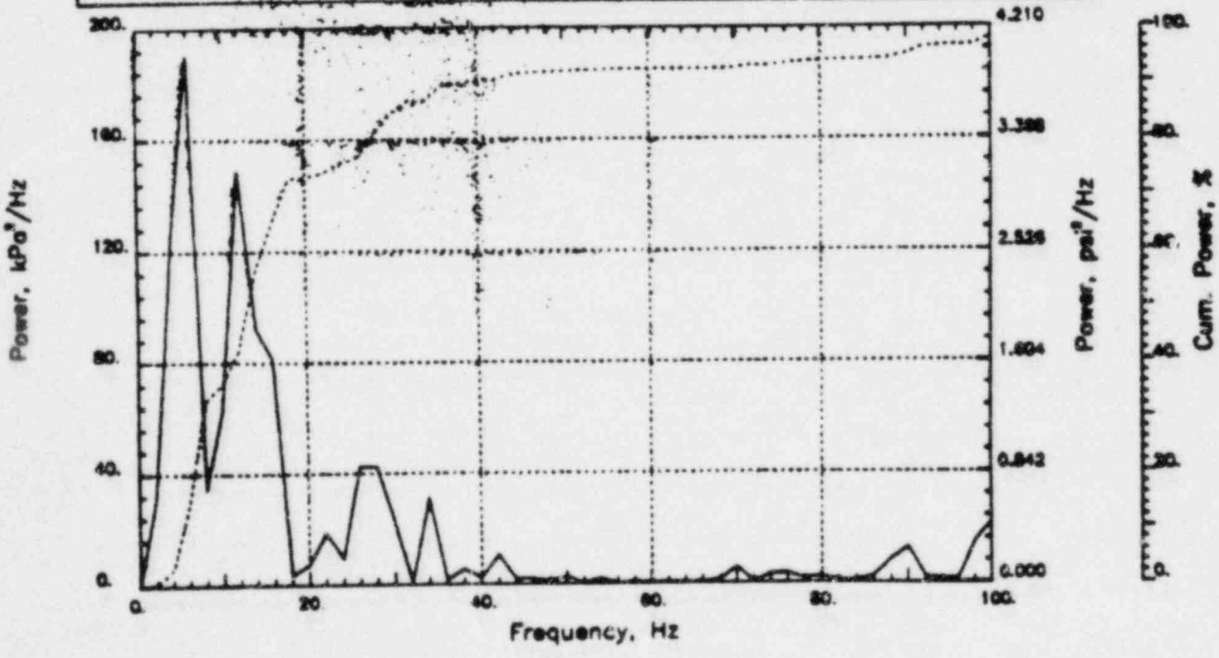

PERRY RHR CO

Output at point (18.90,28.00,2.18)

NAME - LEONG, TAI SENG
DATE - FEB 21, 1984
PROJECT NO. - 15026004

CHECKED _____
DATE _____
CALC NO. - AP-84-

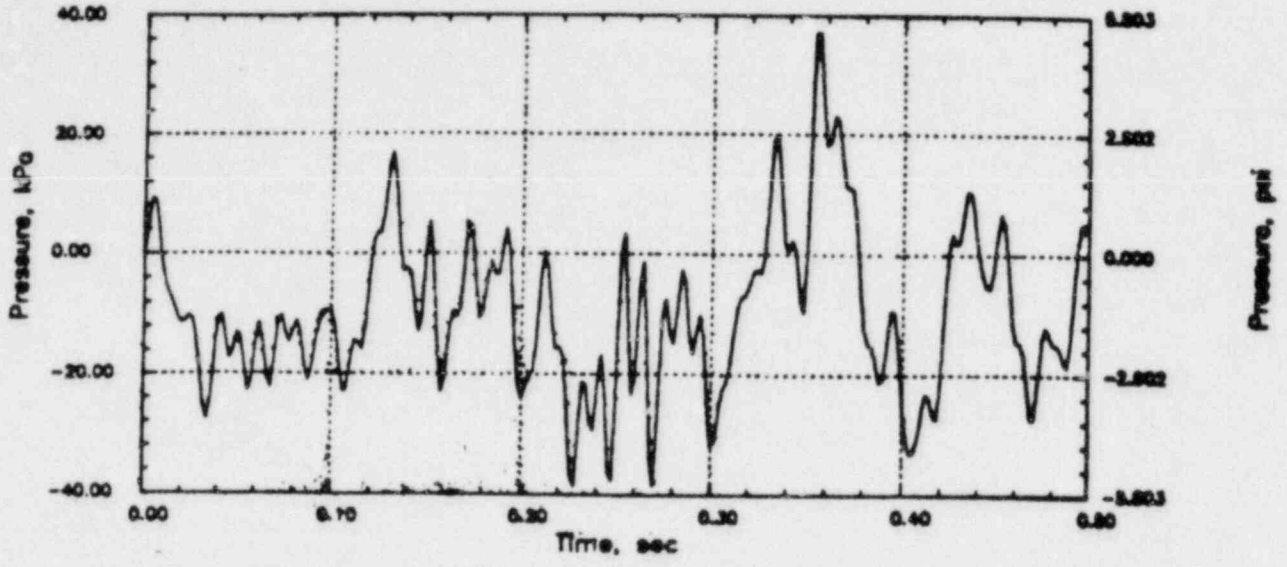

POP = 37.11 kPa PUP = -38.61 kPa MSP = 175.32 kPa²

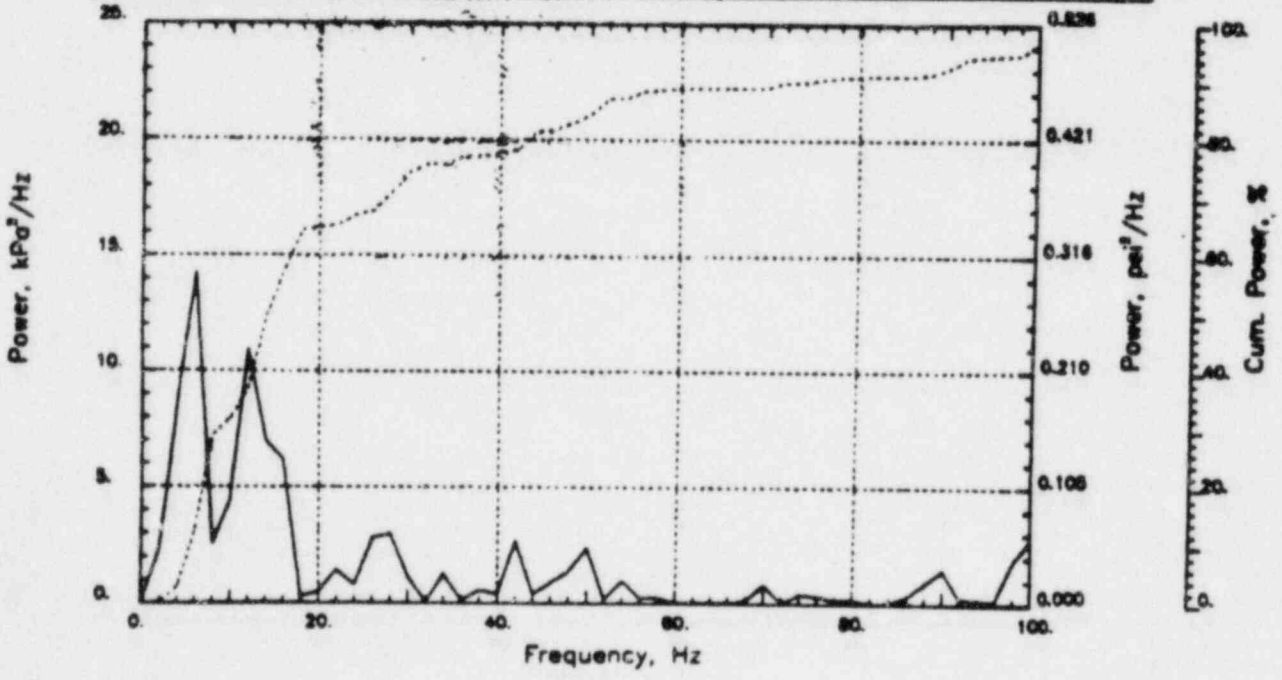

APPENDIX C

PLANT PRESSURE TIME-HISTORIES AND PLANT SUBMERGED STRUCTURES FORCE TIME-HISTORIES WITH C = 1524 m/s

GGNS RHR CO

Output at point (18.90,28.00,4.91)

NAME - LEONG, TAI SENG
DATE - FEB 21, 1984
PROJECT NO. - 15026004

CHECKED _____
DATE _____
CALC NO. - AP-84-

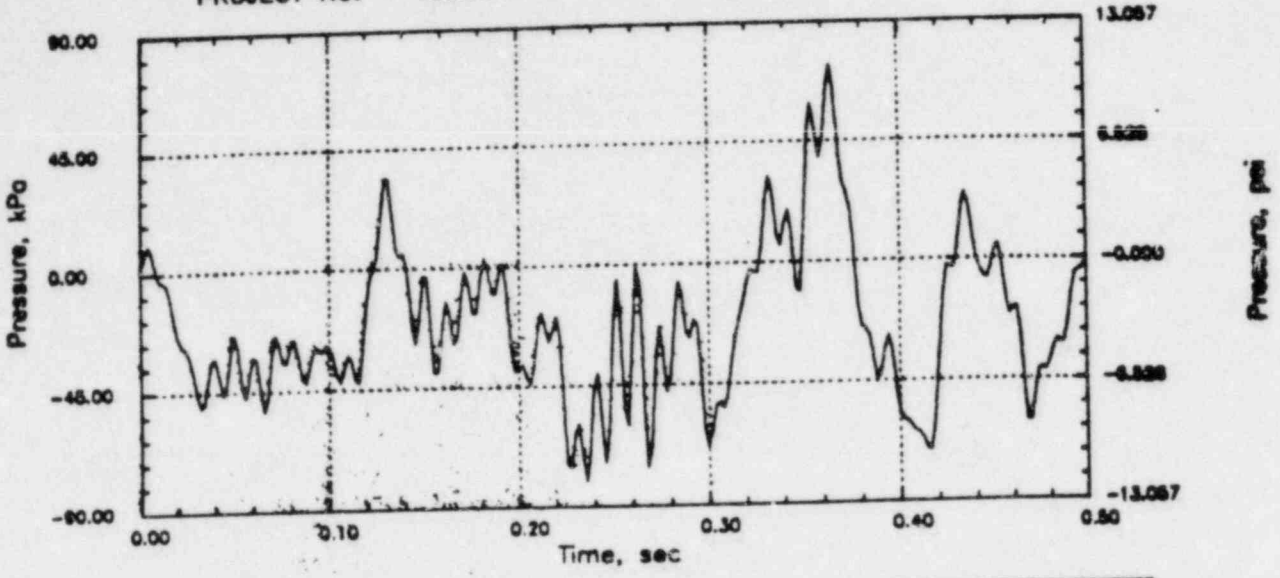

POP = 73.44 kPa PUP = -80.12 kPa MSP = 785.13 kPa²

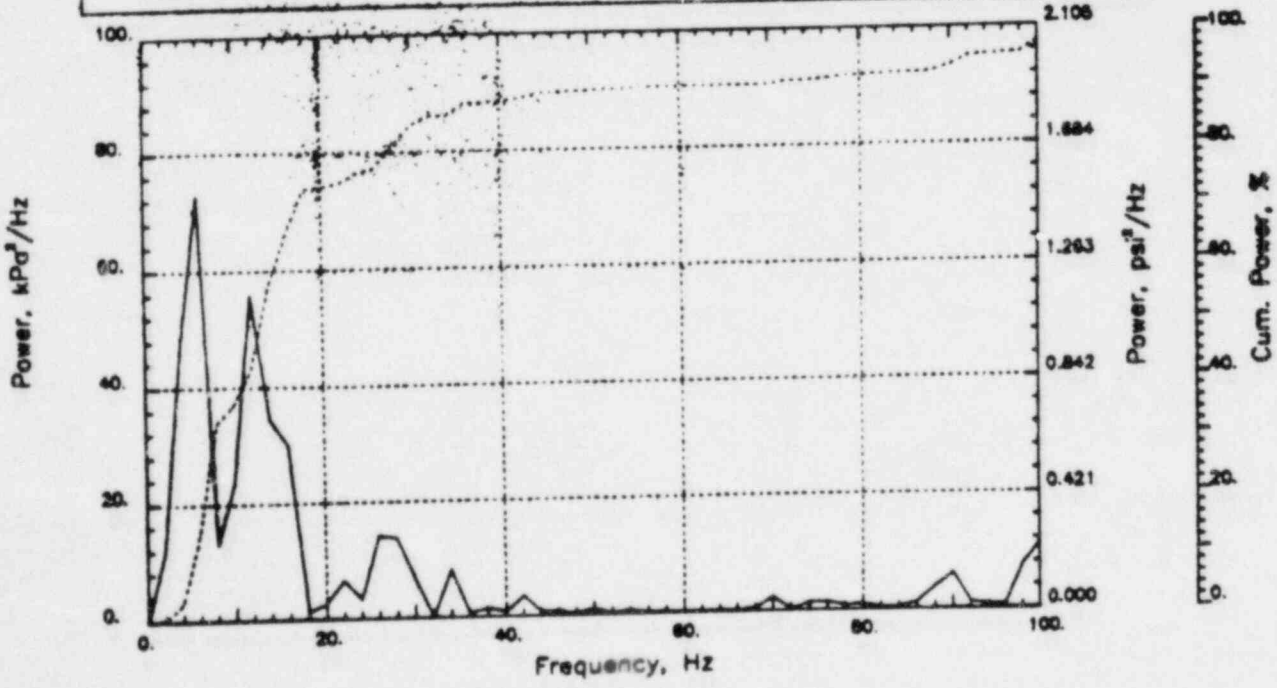

GGNS RHR CO

Output at point (18.90,28.00,4.09)

NAME - LEONG, TAI SENG
DATE - FEB 21, 1984
PROJECT NO. - 15026004

CHECKED _____
DATE _____
CALC NO. - AP-84-

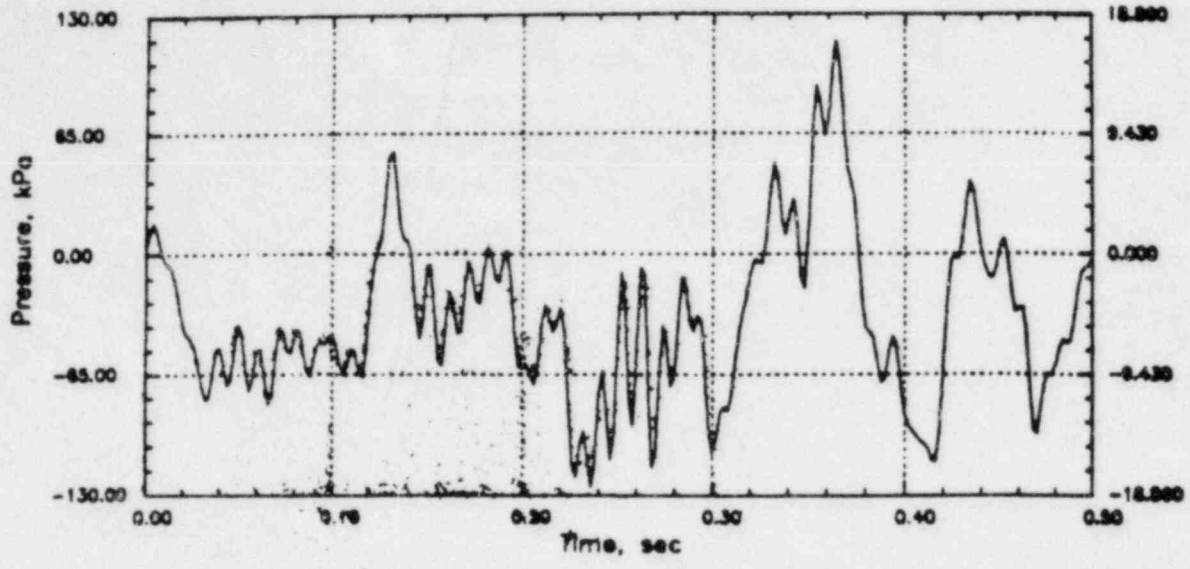

POP = 115.14 kPa PUP = -125.54 kPa MSP = 1934.52 kPa²

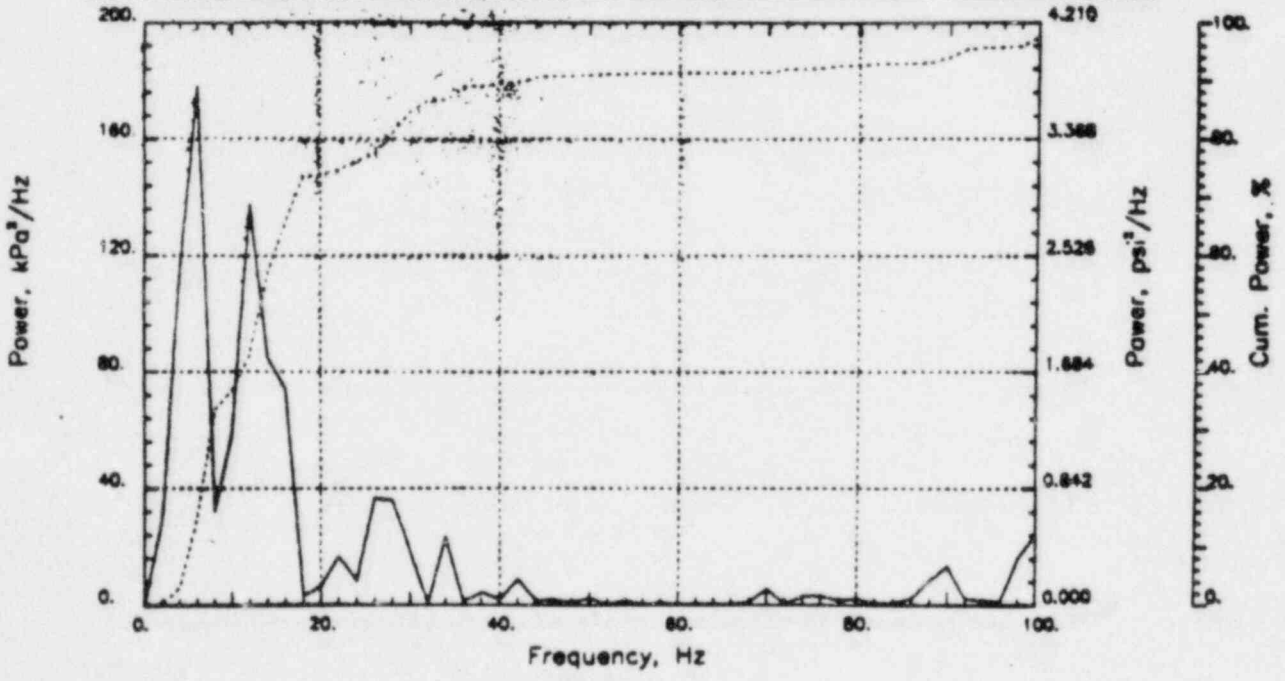

GGNS RHR CO

Output at point (18.90,28.00,3.45)

NAME - LEONG, TAI SENG
DATE - FEB 21, 1984
PROJECT NO. - 15026004

CHECKED _____
DATE _____
CALC NO. - AP-84-

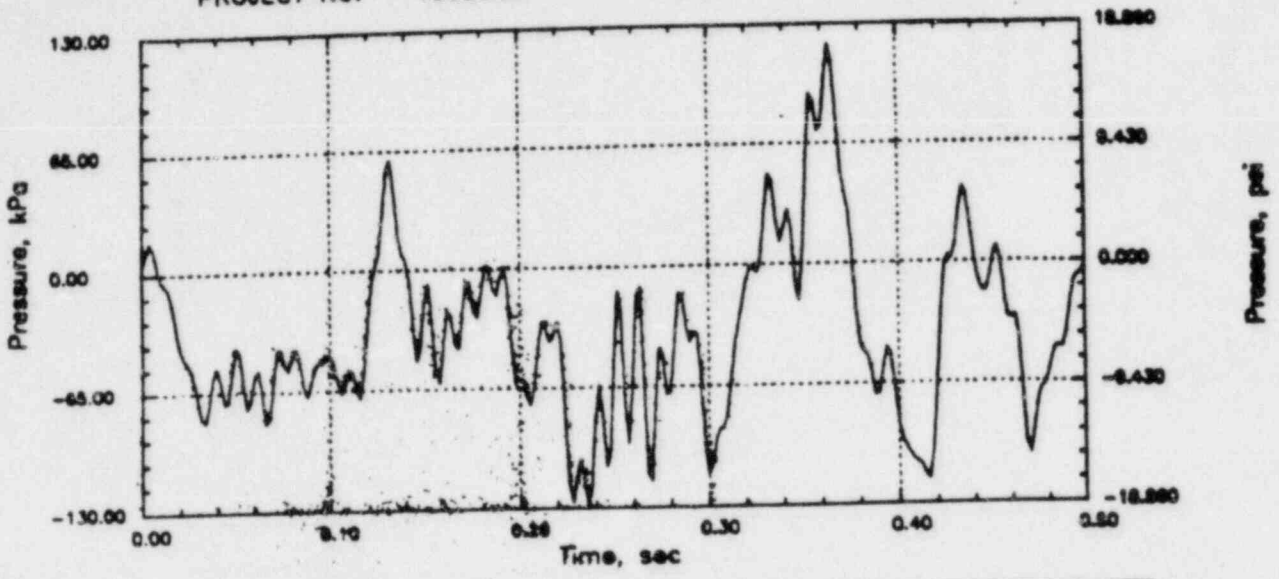

POP = 119.16 kPa PUP = -129.92 kPa MSP = 2098.24 kPa²

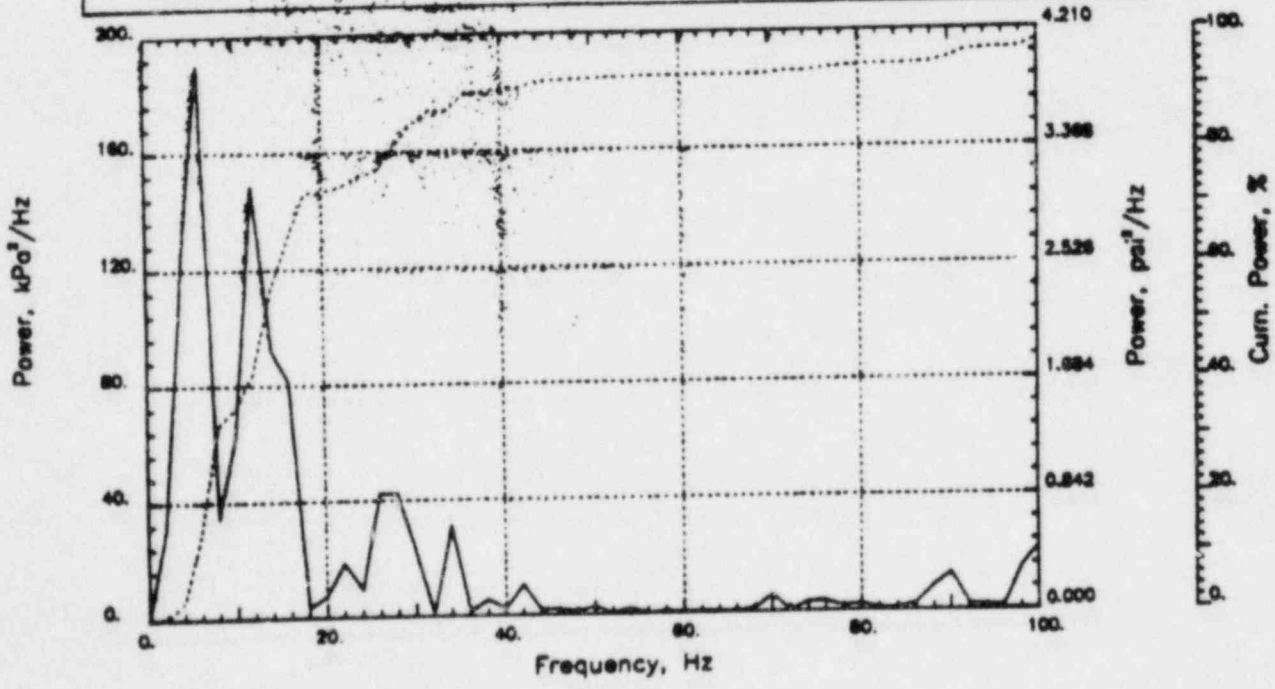

GGNS RHR CO

Output at point (18.90,28.00,2.82)

NAME - LEONG, TAI SENG
DATE - FEB 21, 1984
PROJECT NO. - 15028004

CHECKED _____
DATE _____
CALC NO. - AP-84-

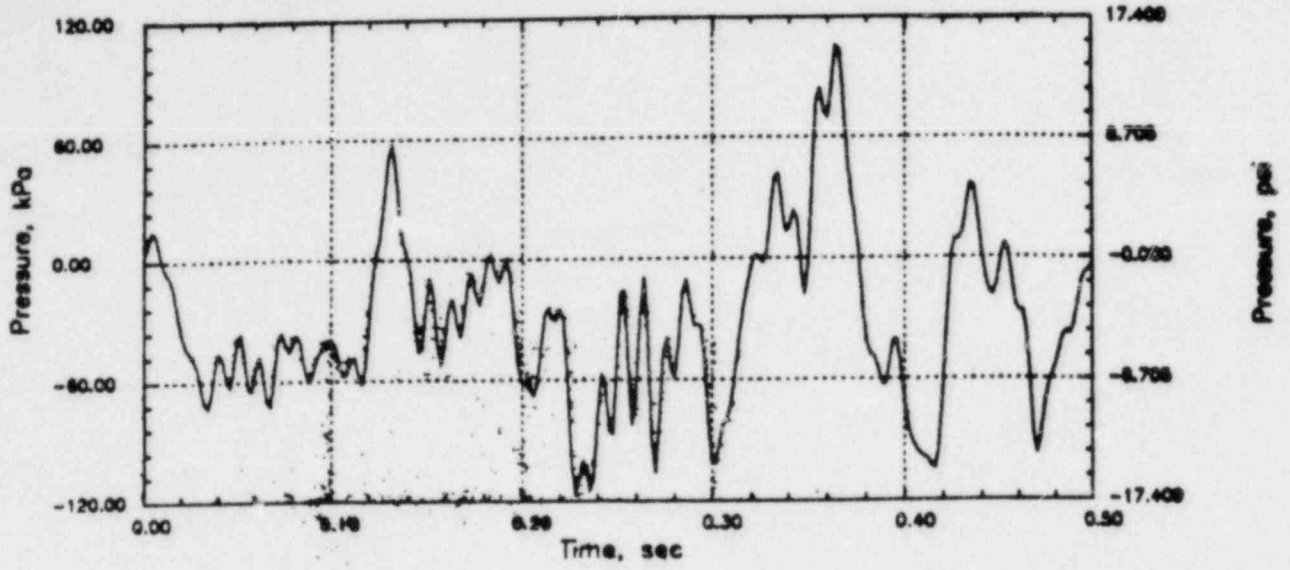

POP = 105.64 kPa PUP = -117.15 kPa MSP = 1720.45 kPa²

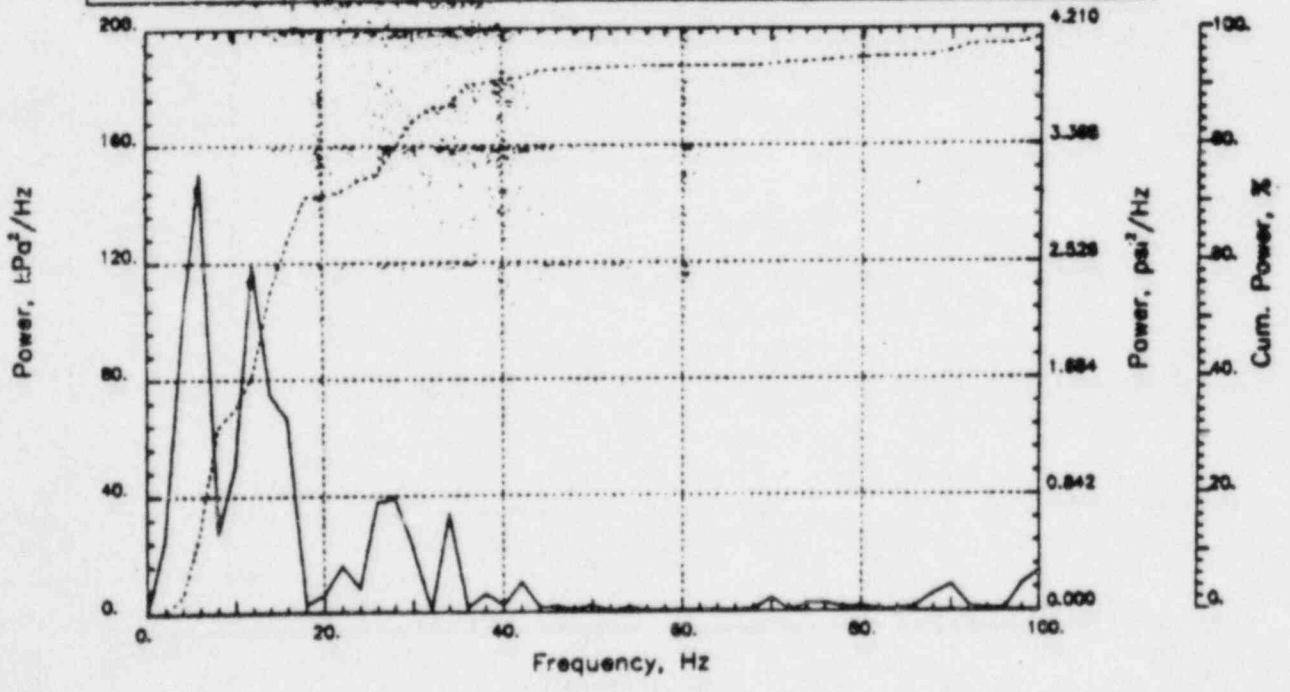

GGNS RHR CO

Output at point (18.90,28.00,2.18)

NAME - LEONG, TAI SENG
DATE - FEB 21, 1984
PROJECT NO. - 15028004

CHECKED _____
DATE _____
CALC NO. - AP-84-

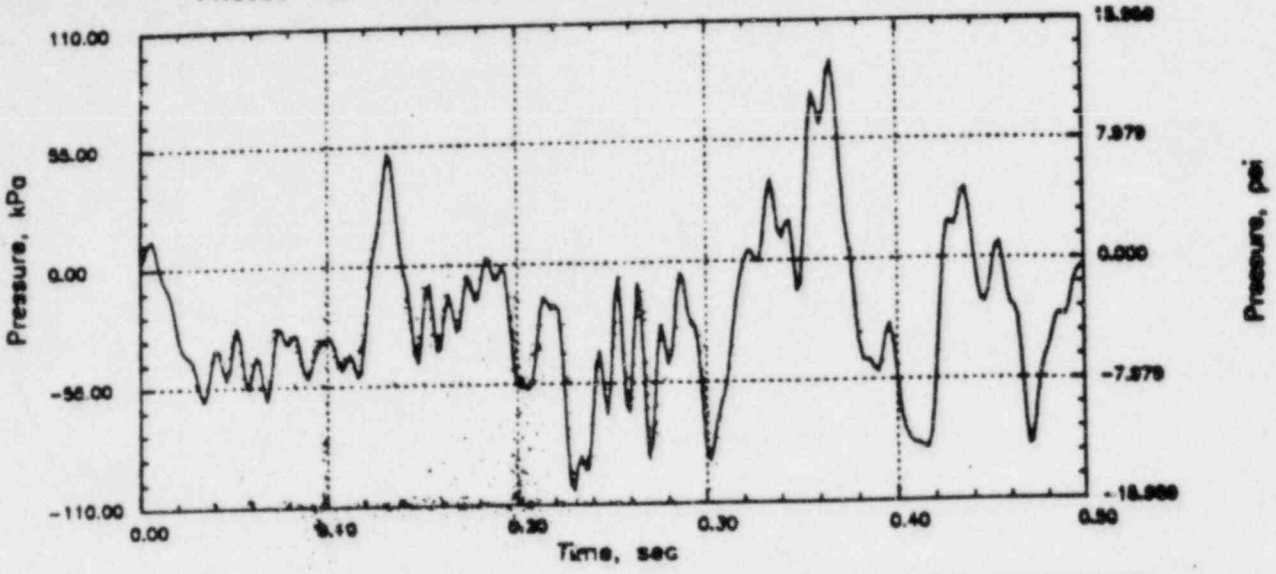

POP = 81.42 kPa PUP = -103.72 kPa MSP = 1260.08 kPa²

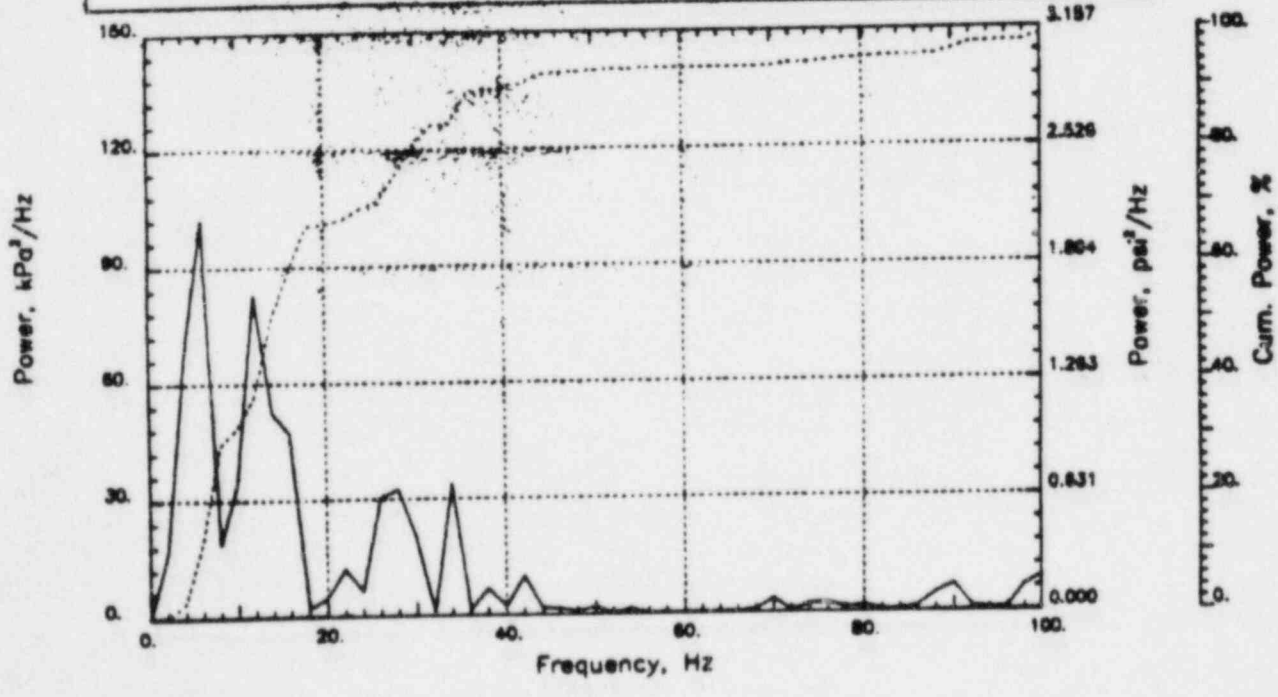

GGNS RHR CO

Output at point (18.90,28.00,1.55)

NAME - LEONG, TAI SENG
DATE - FEB 21, 1984
PROJECT NO. - 15026004

CHECKED _____
DATE _____
CALC NO. - AP-84-

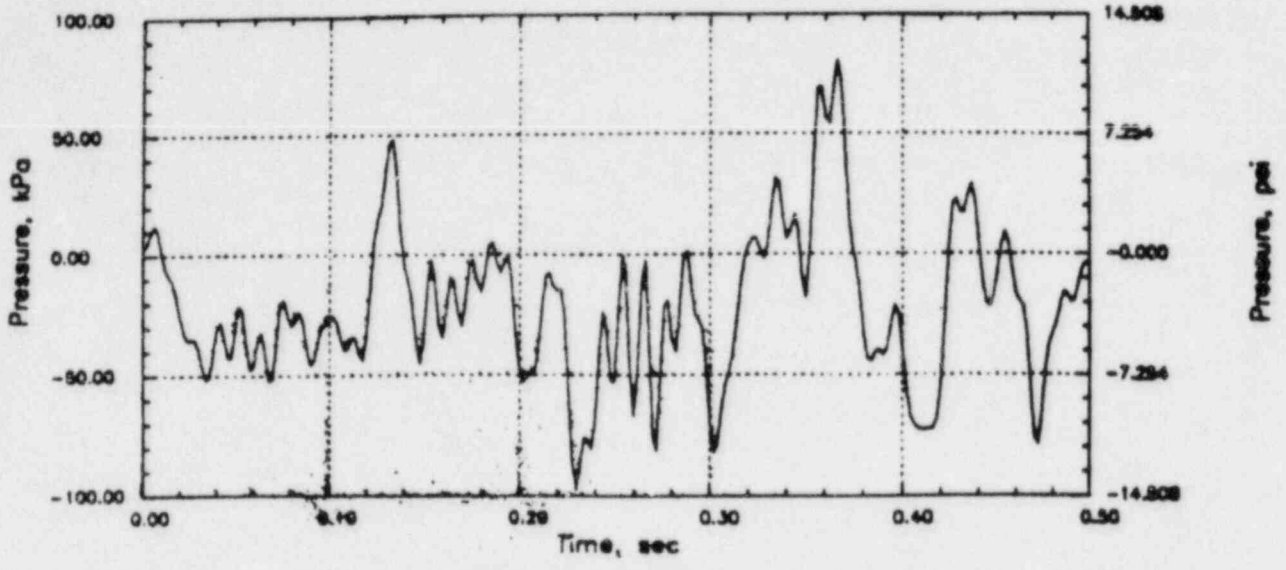

POP = 80.97 kPa PUP = -97.39 kPa MSP = 972.77 kPa²

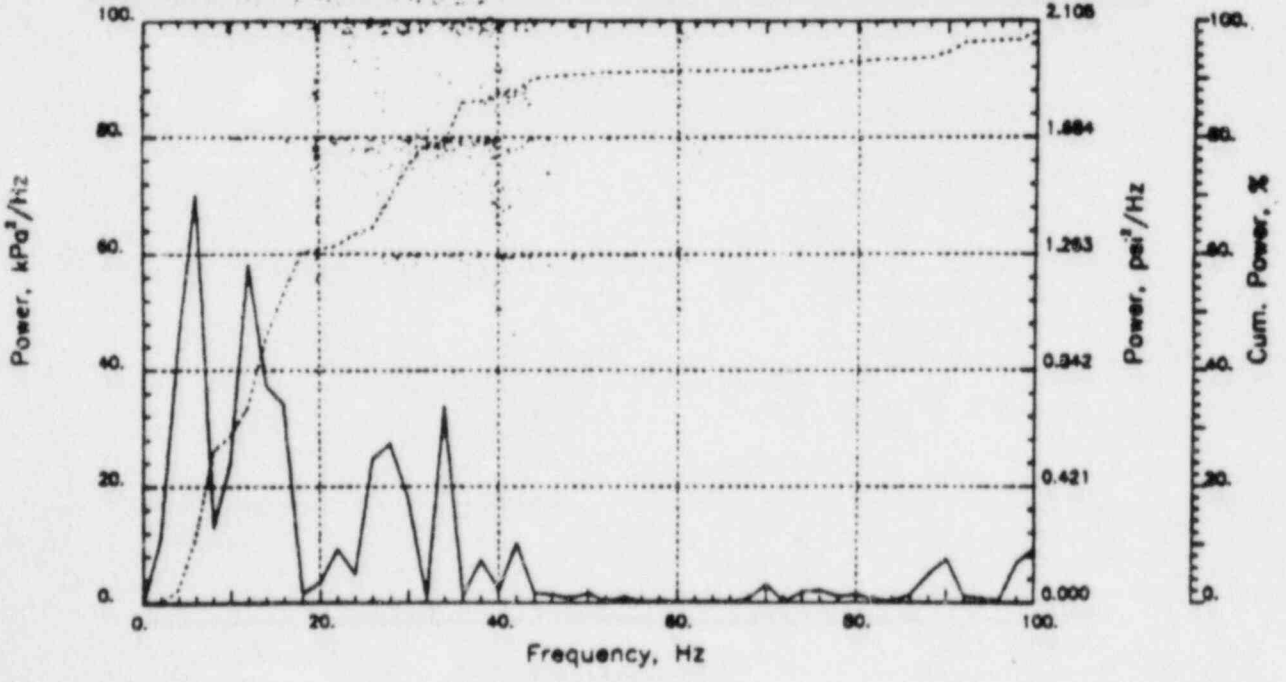

GGNS RHR CO

Output at point (18.90,28.00,0.91)

NAME - LEONG, TAI SENG
DATE - FEB 21, 1984
PROJECT NO. - 15026004

CHECKED _____
DATE _____
CALC NO. - AP-84-

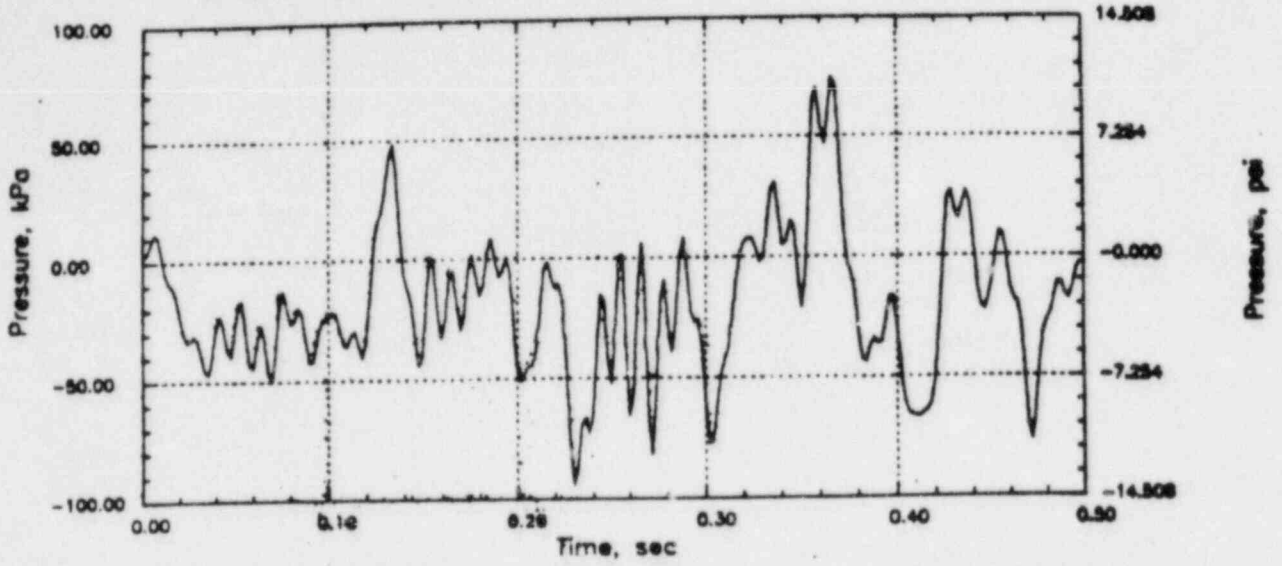

POP = 74.71 kPa PUP = -94.43 kPa MSP = 856.28 kPa²

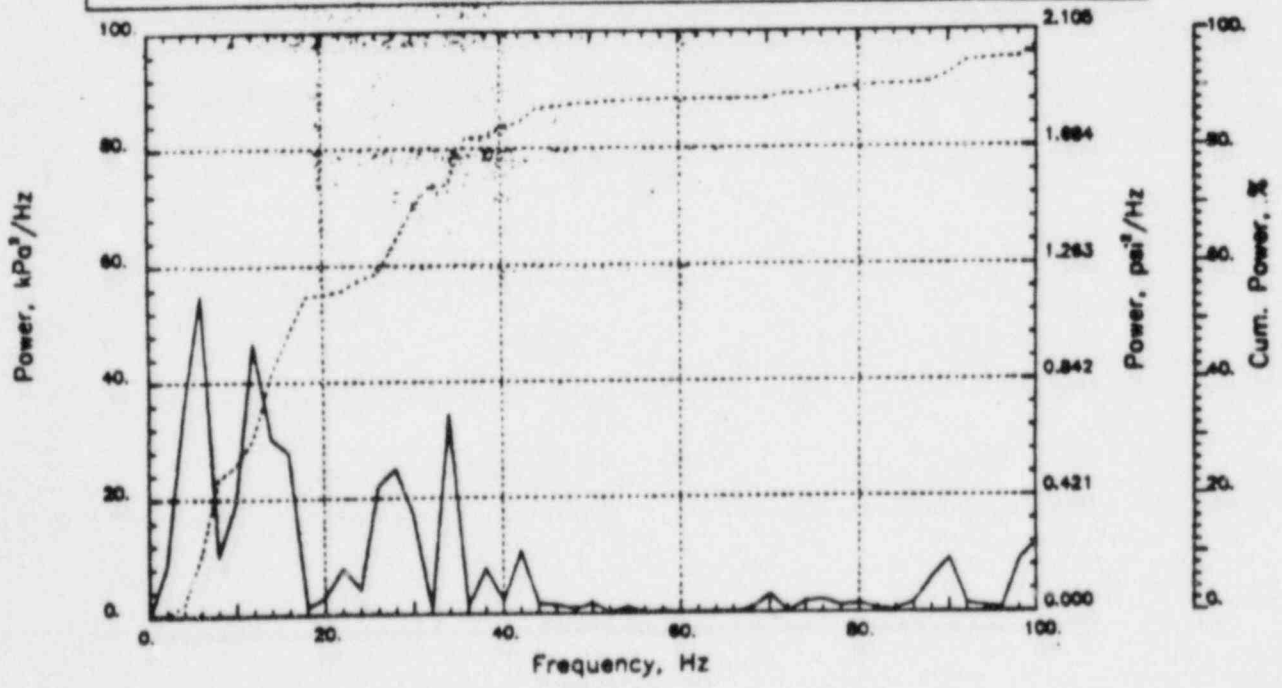

GGNS RHR CO

Output at point (18.90,28.00,0.46)

NAME - LEONG, TAI SENG
DATE - FEB 21, 1984
PROJECT NO. - 15026004

CHECKED _____
DATE _____
CALC NO. - AP-84-

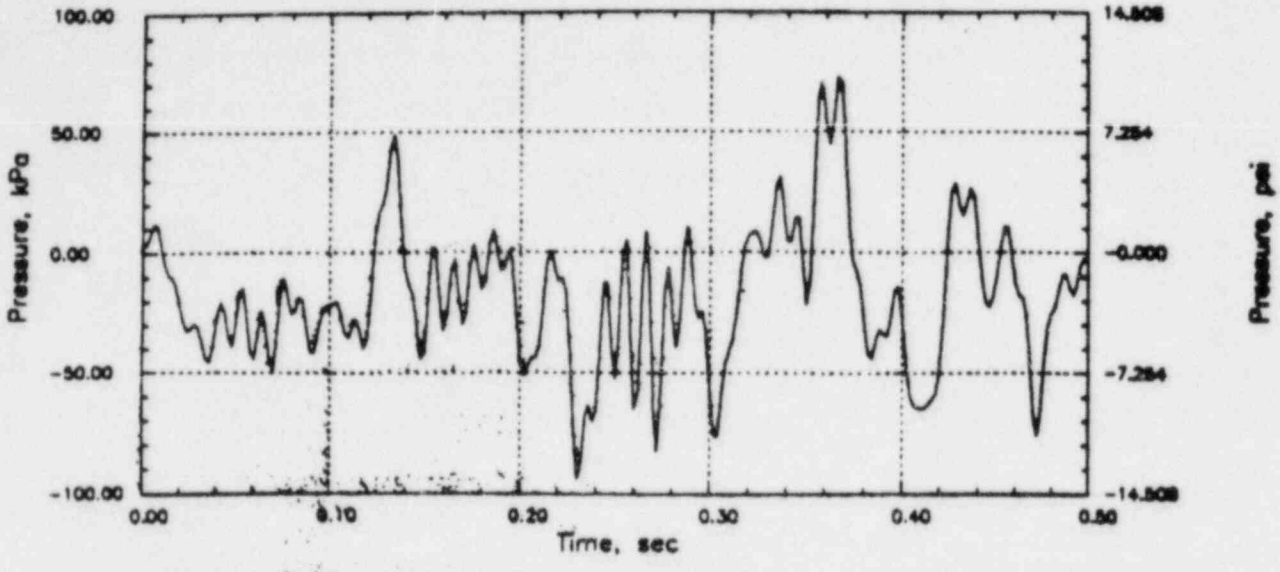

POP = 72.65 kPa PUP = -93.82 kPa MSP = 830.54 kPa²

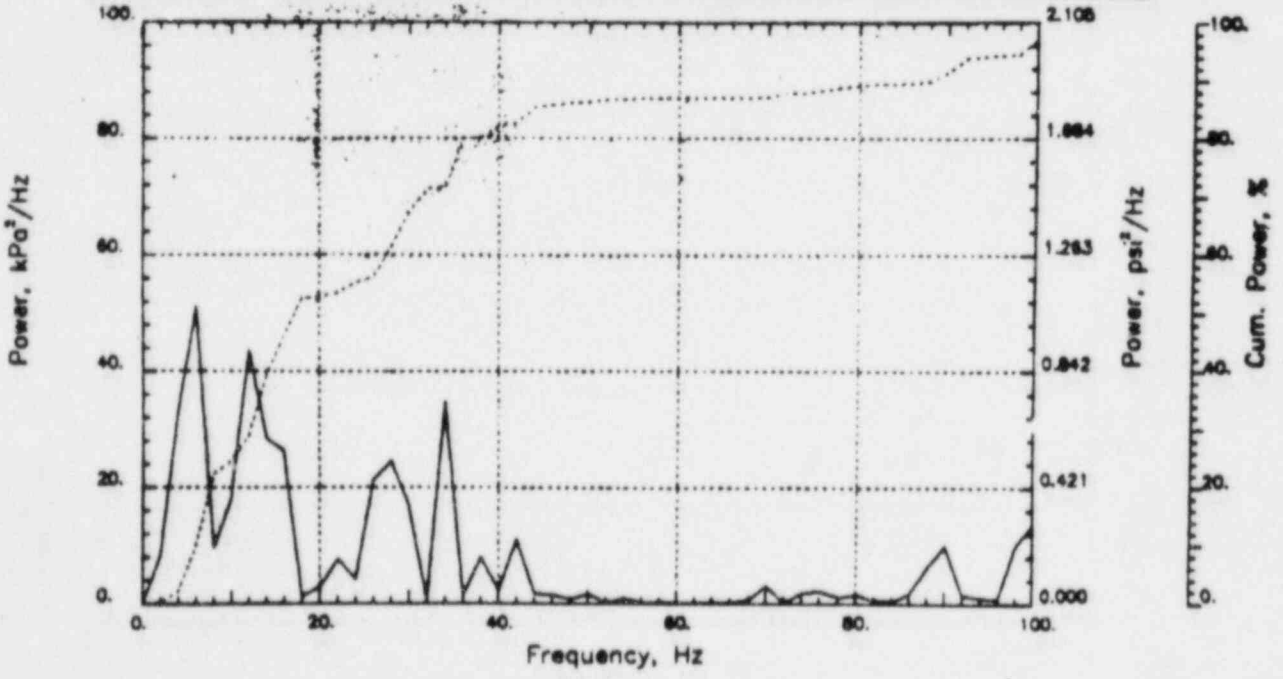

GGNS RHR CO

Output at point (18.90,28.00,0.00)

NAME - LEONG, TAI SENG
DATE - FEB 21, 1984
PROJECT NO. - 15026004

CHECKED _____
DATE _____
CALC NO. - AP-84-

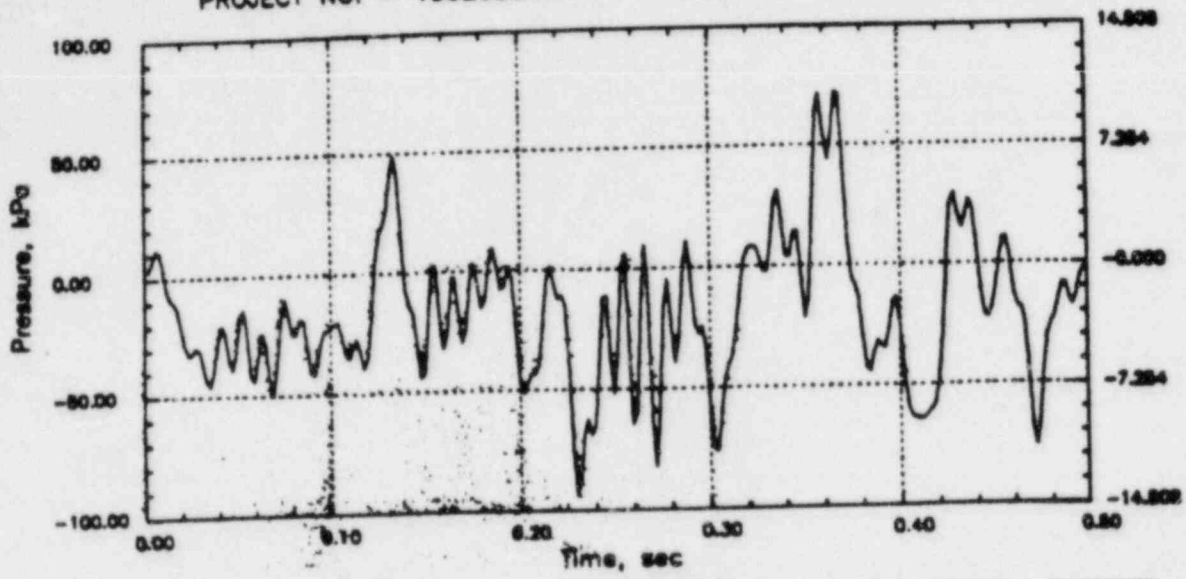

POP = 72.04 kPa PUP = -93.72 kPa MSP = 824.88 kPa²

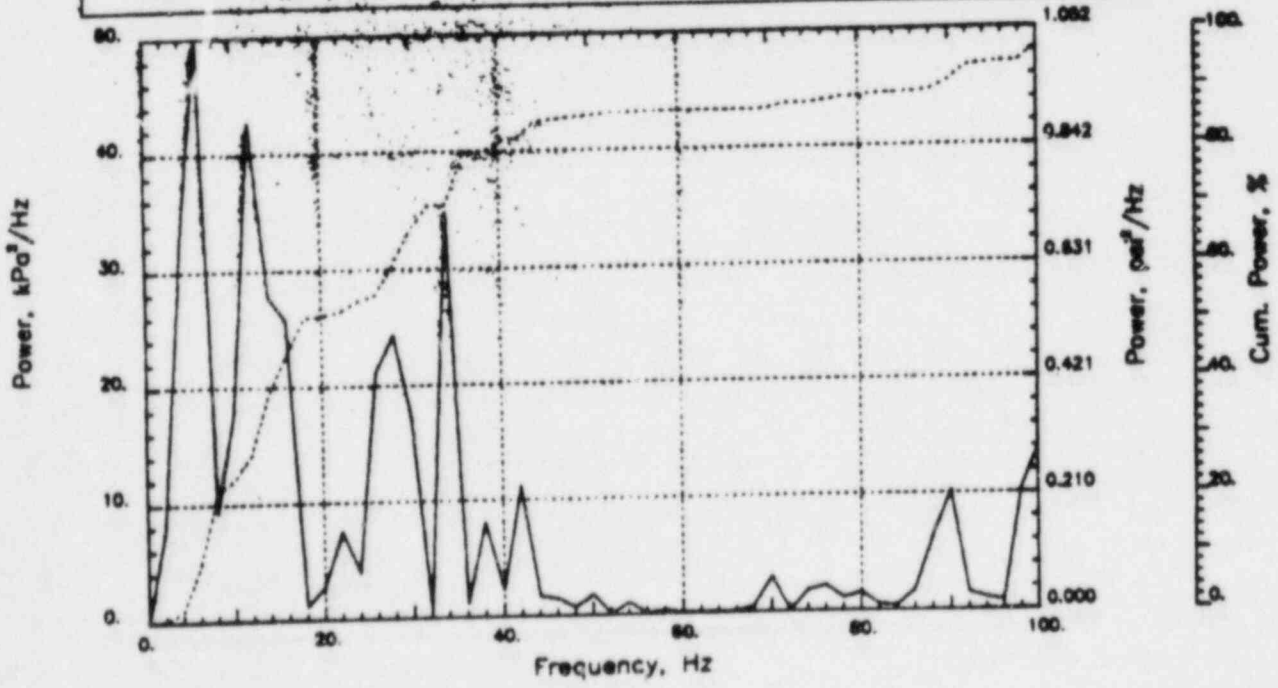

GGNS RHR CO

Output at point (17.34,28.00,0.00)

NAME - LEONG, TAI SENG
DATE - FEB 21, 1984
PROJECT NO. - 15026004

CHECKED _____
DATE _____
CALC NO. - AP-84-

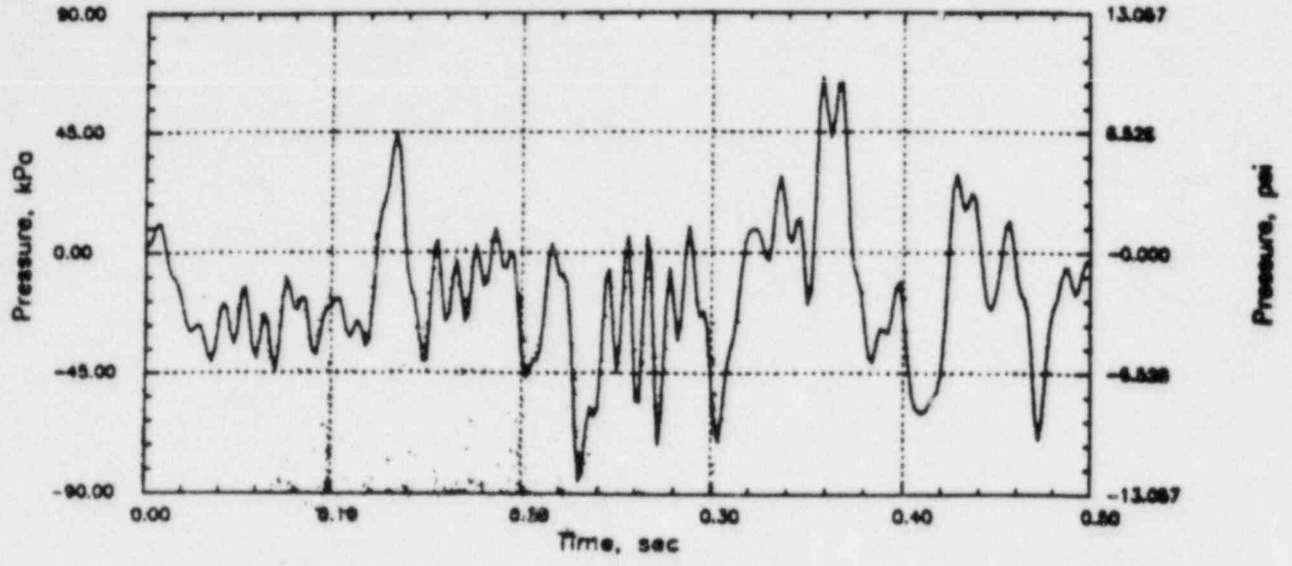

POP = 65.58 kPa PUP = -85.35 kPa MSP = 684.31 kPa²

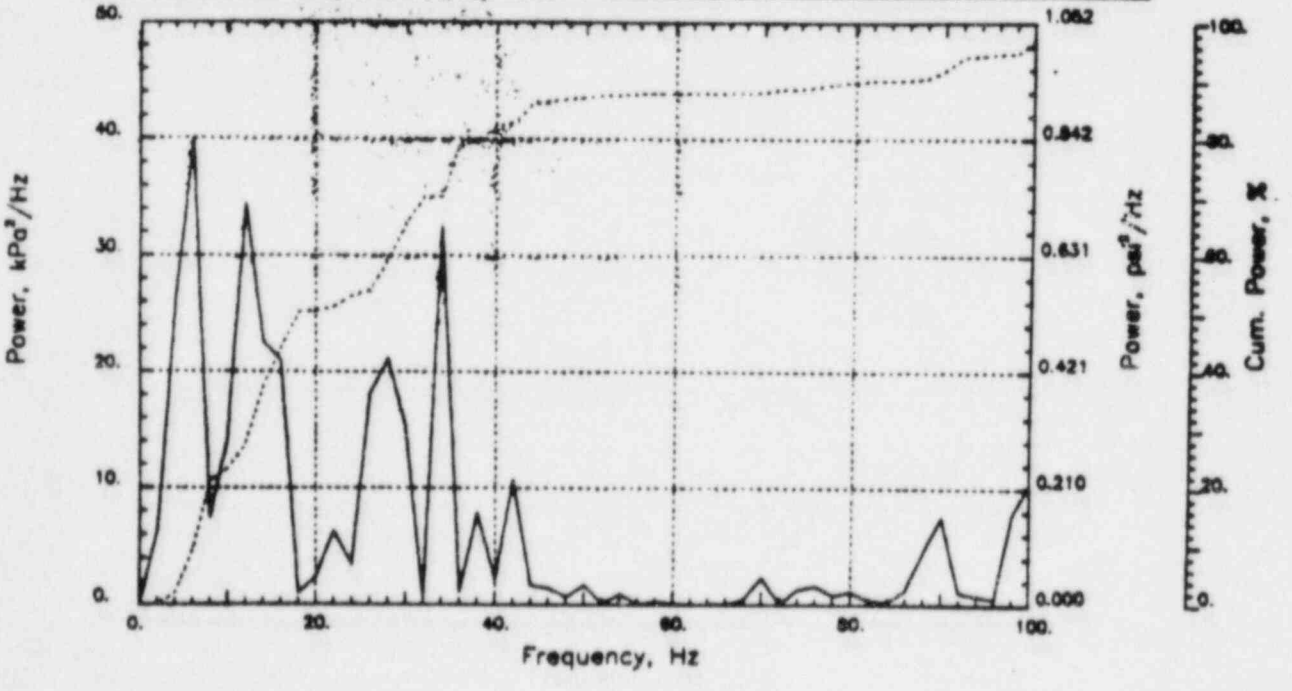

GGNS RHR CO

Output at point (15.77,28.00,0.00)

NAME - LEONG, TAI SENG
DATE - FEB 21, 1984
PROJECT NO. - 15026004

CHECKED _____
DATE _____
CALC NO. - AP-84-

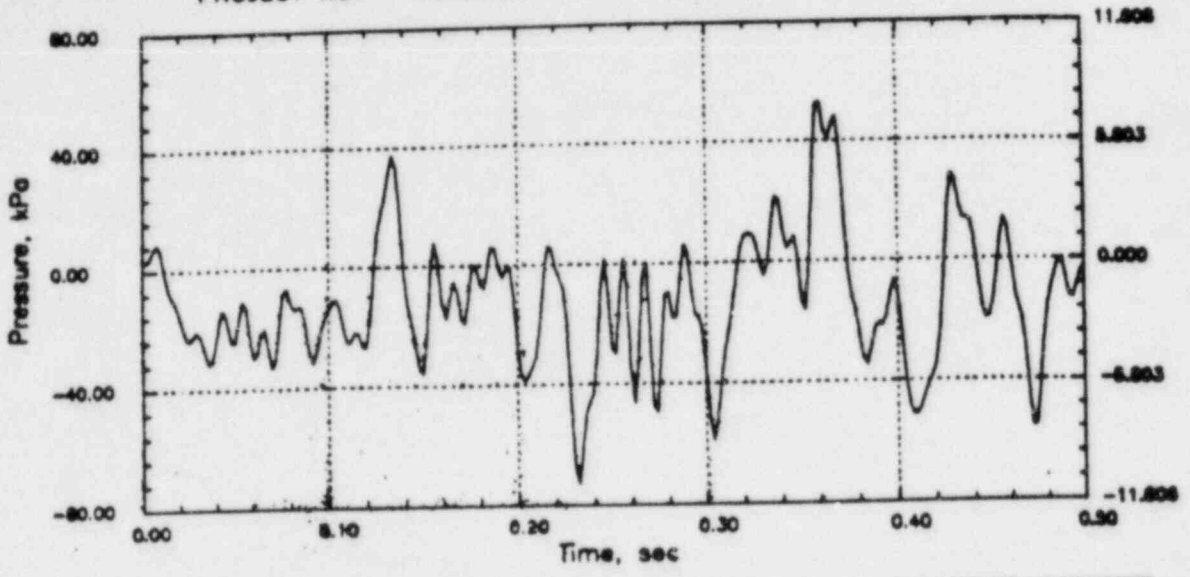

POP = 52.79 kPa PUP = -73.06 kPa MSP = 456.53 kPa²

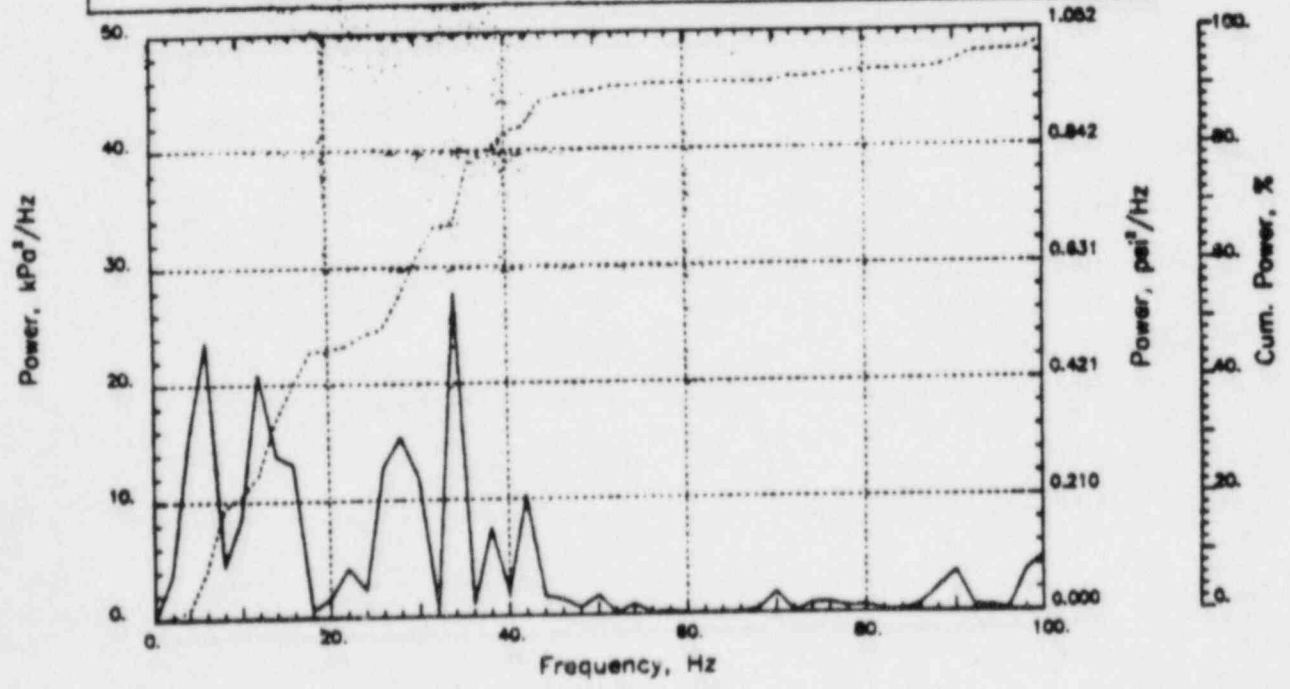

GGNS RHR CO

Output at point (14.21,28.00,0.00)

NAME - LEONG, TAI SENG
DATE - FEB 21, 1984
PROJECT NO. - 15026004

CHECKED _____
DATE _____
CALC NO. - AP-84-

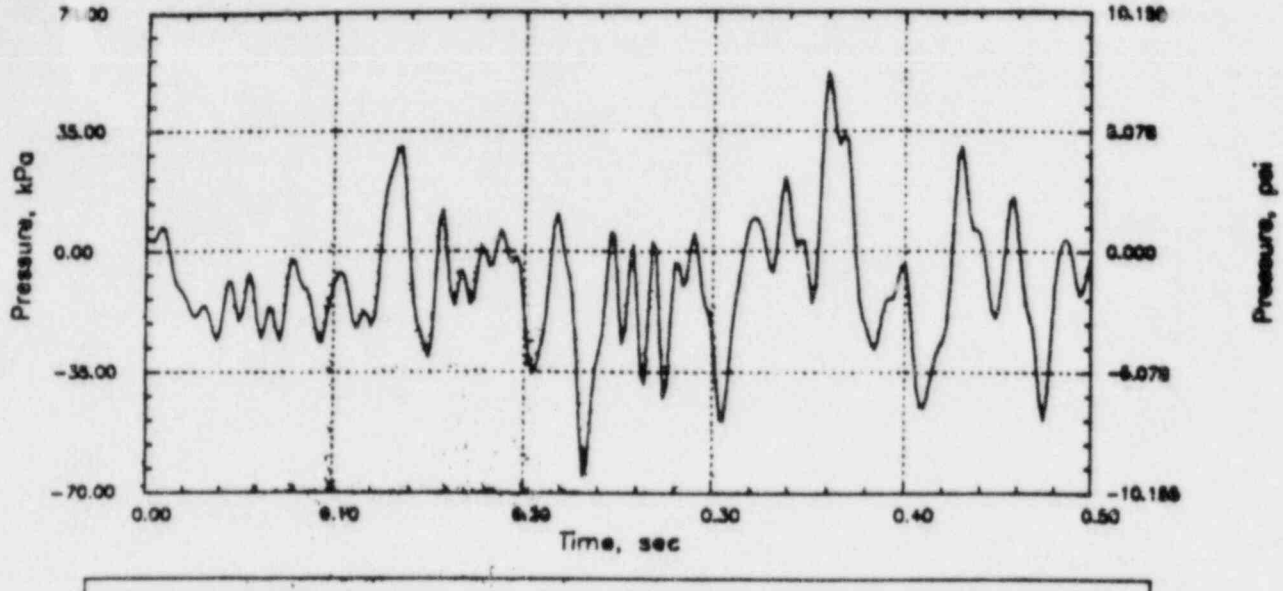

POP = 52.46 kPa PUP = -65.30 kPa MSP = 337.96 kPa²

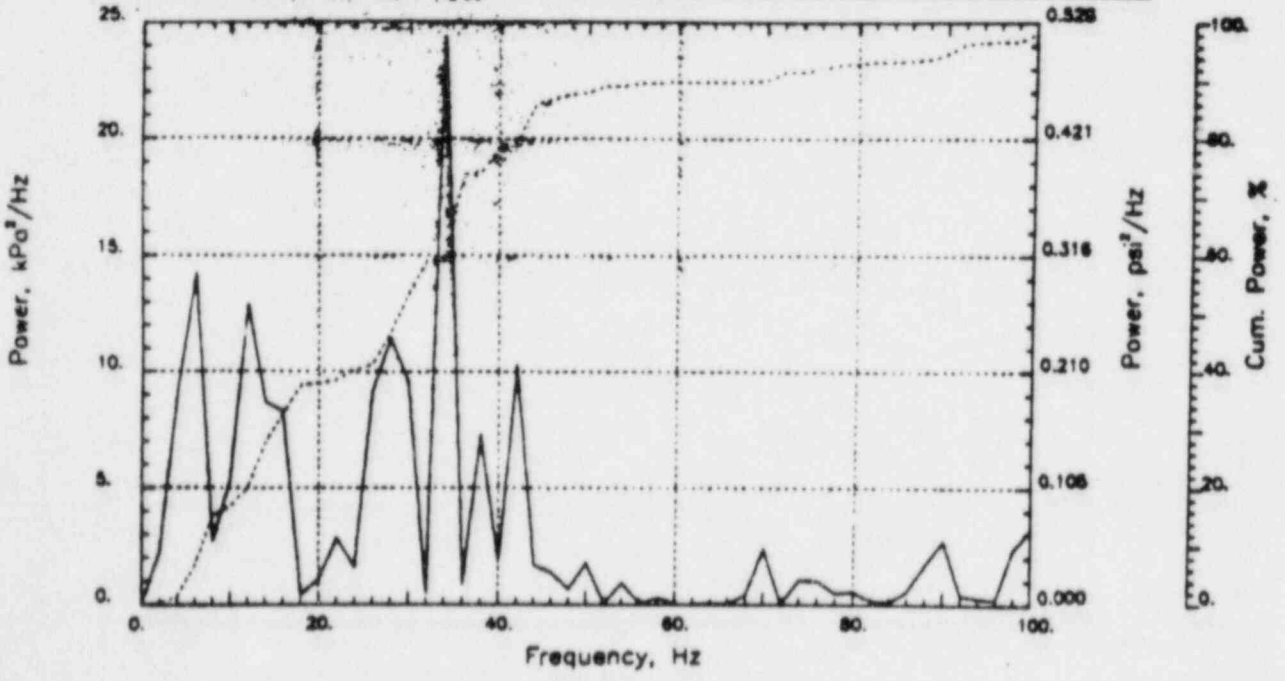

GGNS RHR CO

Output at point (12.65,28.00,0.00)

NAME - LEONG, TAI SENG
DATE - FEB 21, 1984
PROJECT NO. - 15026004

CHECKED _____
DATE _____
CALC NO. - AP-84-

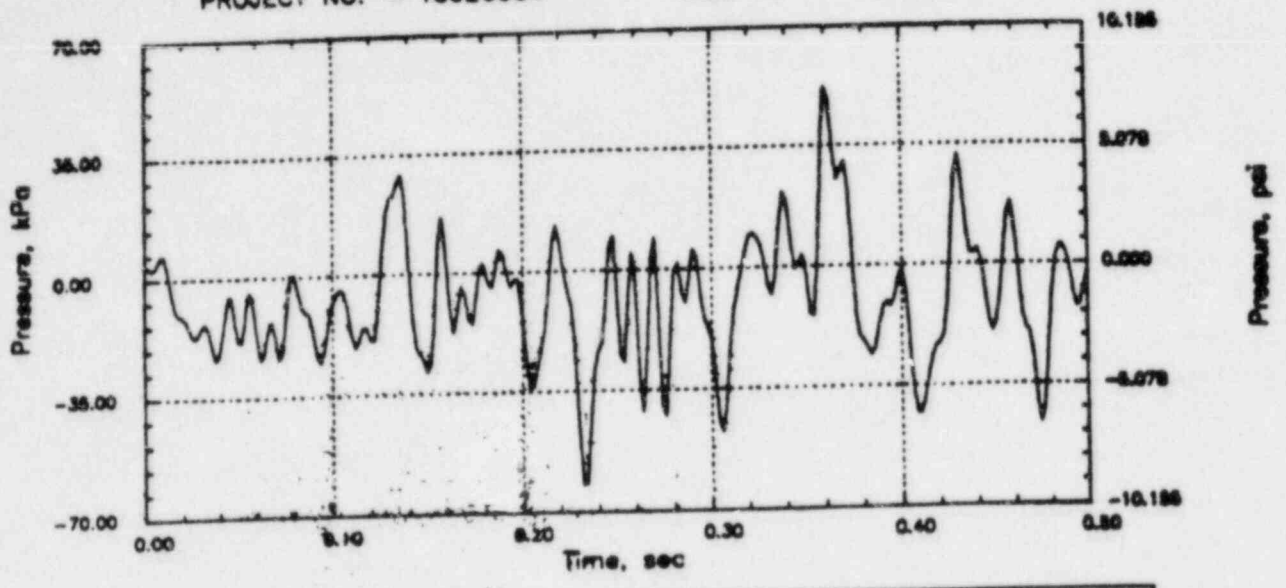

P_{UP} = 52.17 kPa PUP = -61.92 kPa MSP = 310.14 kPa^2

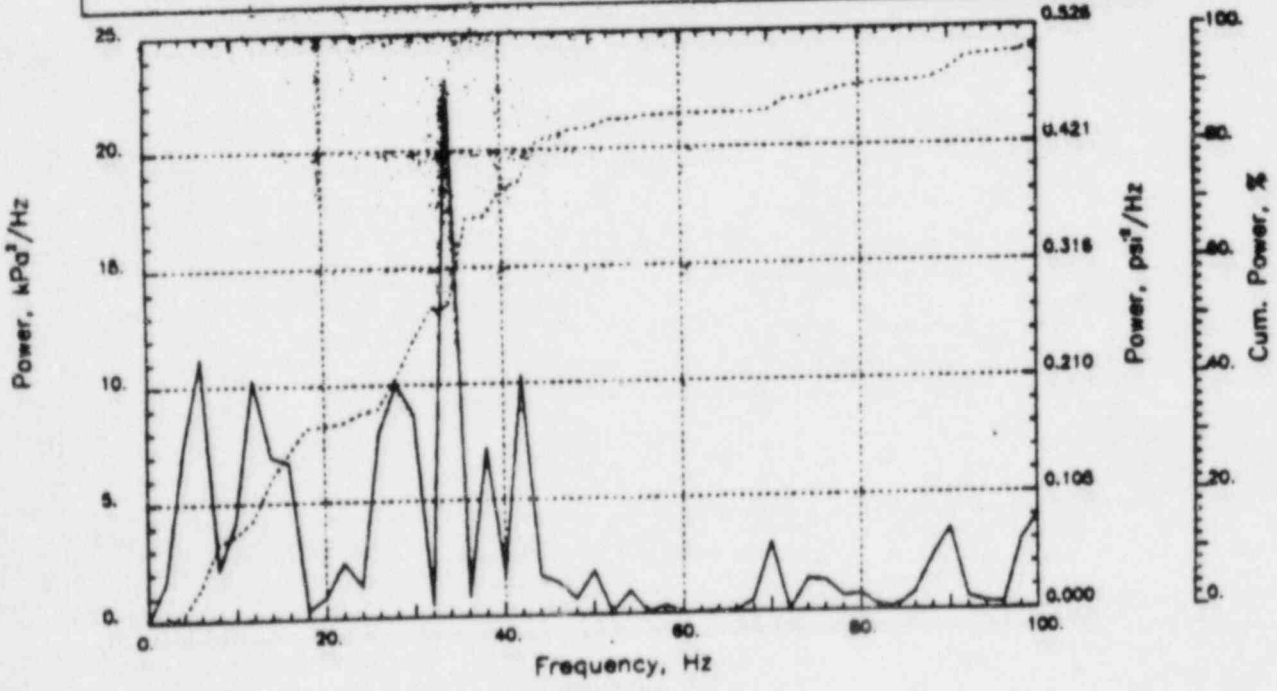

GGNS RHR CO

Output at point (12.65,28.00,0.46)

NAME - LEONG, TAI SENG
DATE - FEB 21, 1984
PROJECT NO. - 15026004

CHECKED _____
DATE _____
CALC NO. - AP-84-

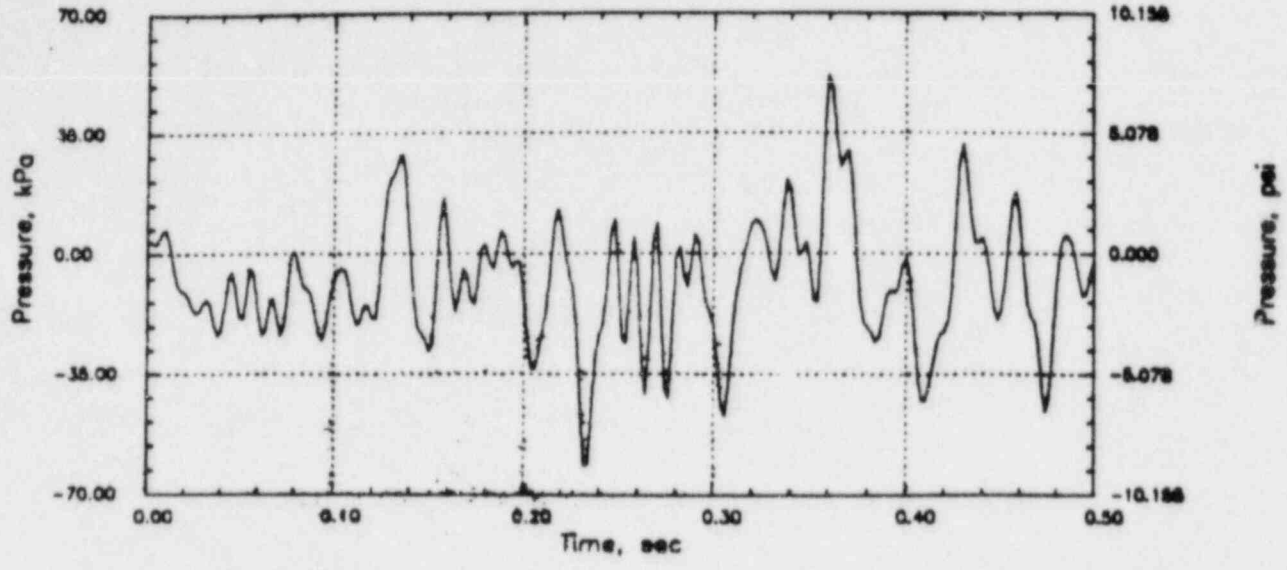

POP = 51.72 kPa PUP = -61.42 kPa MSP = 305.42 kPa²

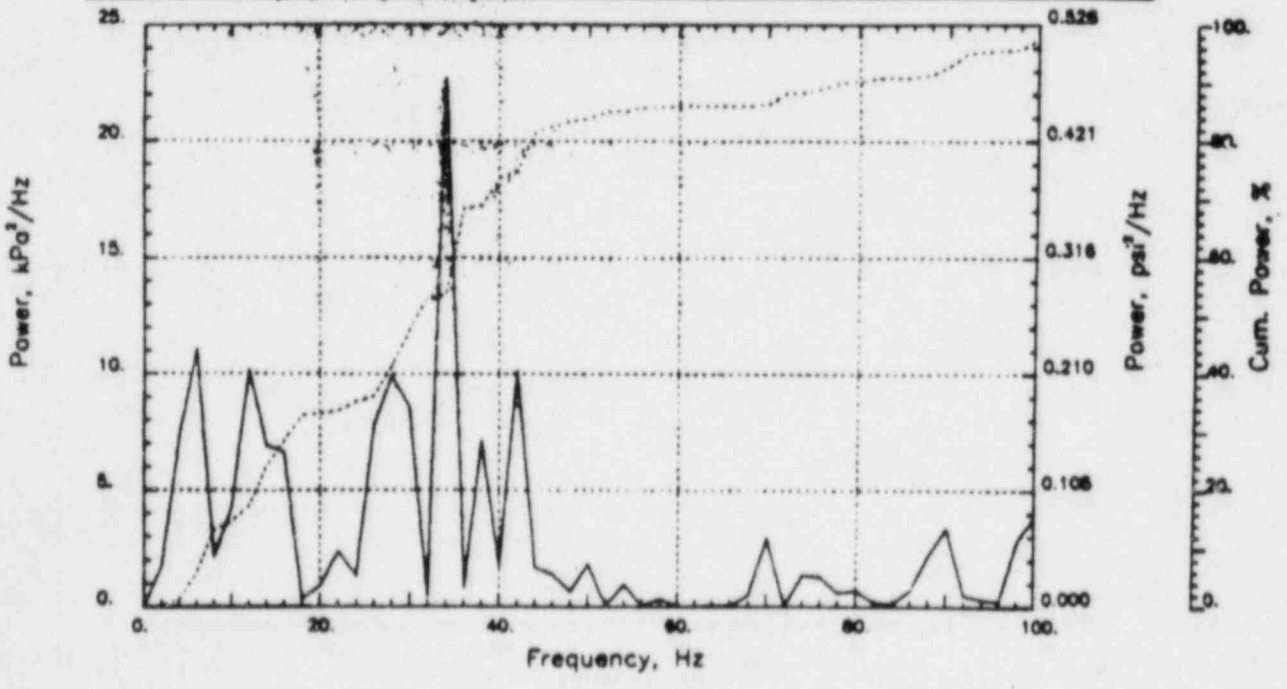

GGNS RHR CO

Output at point (12.65,28.00,0.91)

NAME - LEONG, TAI SENG
DATE - FEB 21, 1984
PROJECT NO. - 15026004

CHECKED _____
DATE _____
CALC NO. - AP-84-

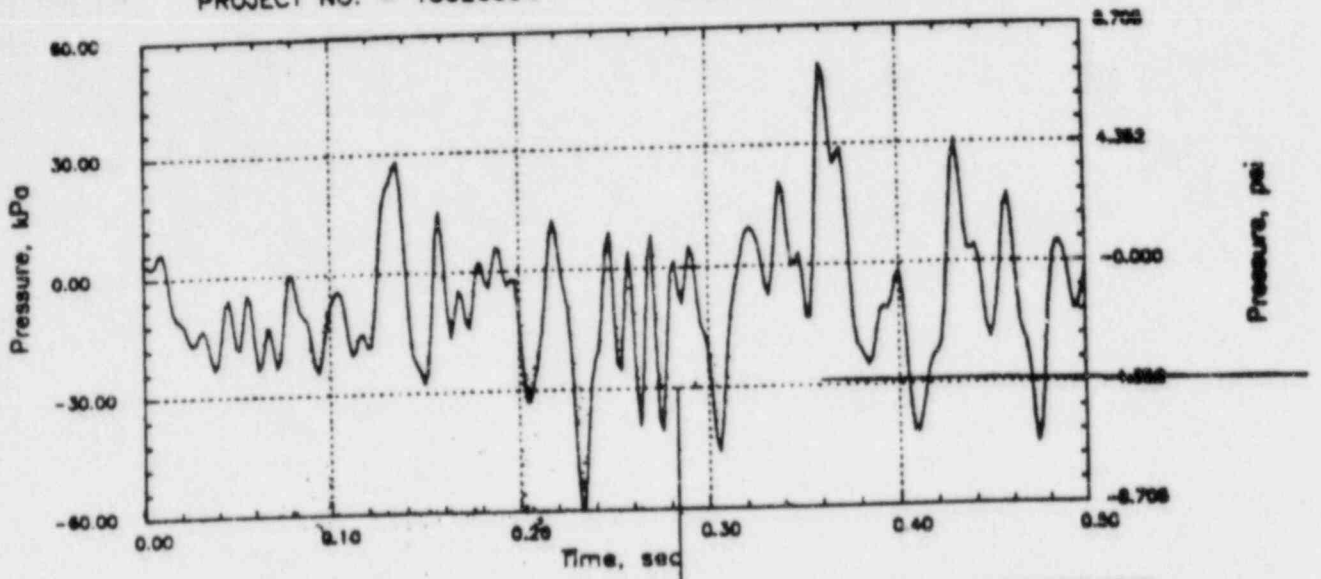

POP = 50.36 kPa PUP = -59.94 kPa MSP = 291.48 kPa²

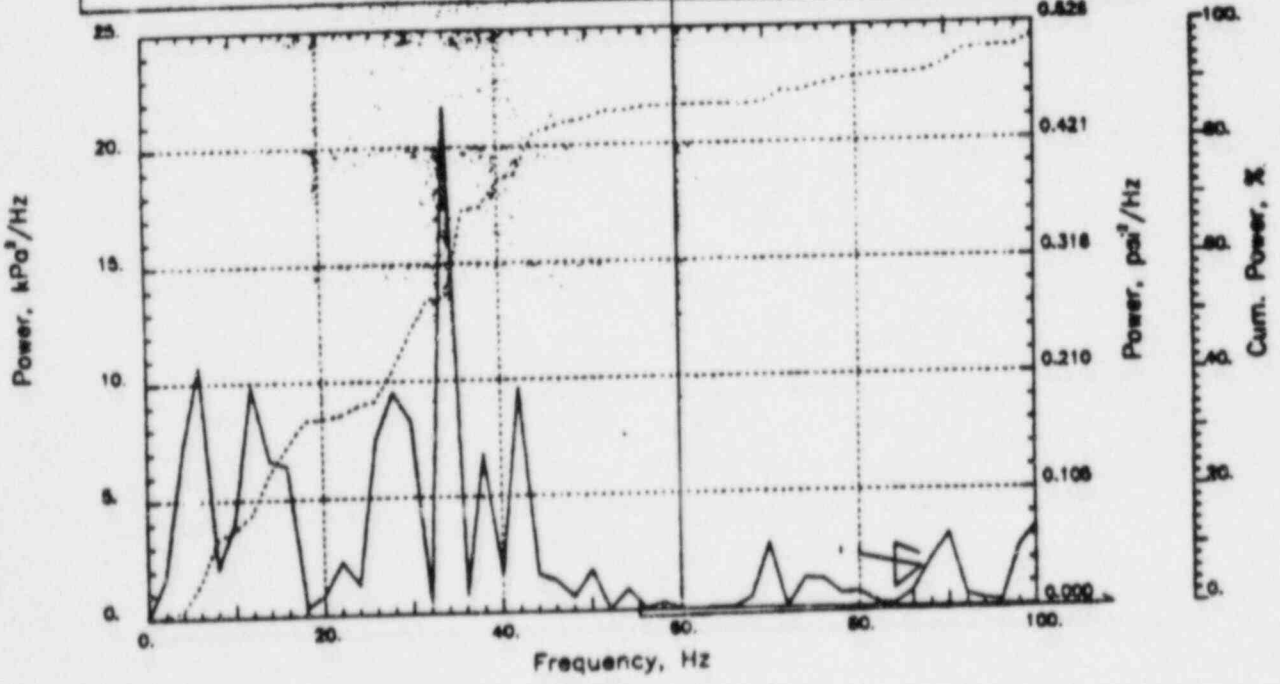

GGNS RHR CO

Output at point (12.65,28.00,1.55)

NAME - LEONG, TAI SENG
DATE - FEB 21, 1984
PROJECT NO. - 15026004

CHECKED _____
DATE _____
CALC NO. - AP-84-

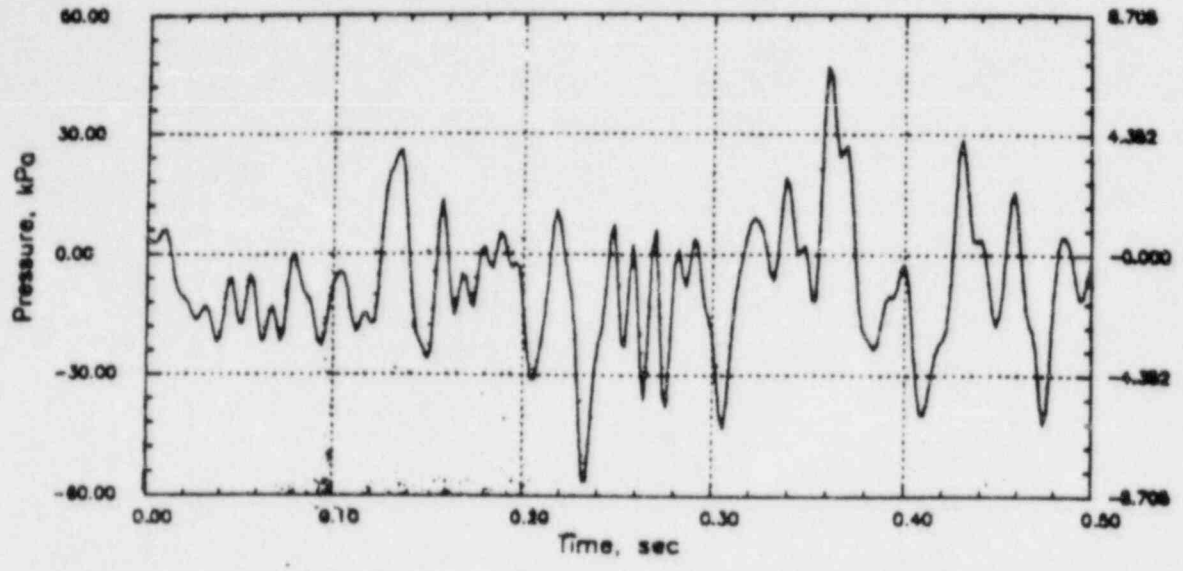

POP = 47.03 kPa PUP = -56.26 kPa MSP = 258.23 kPa²

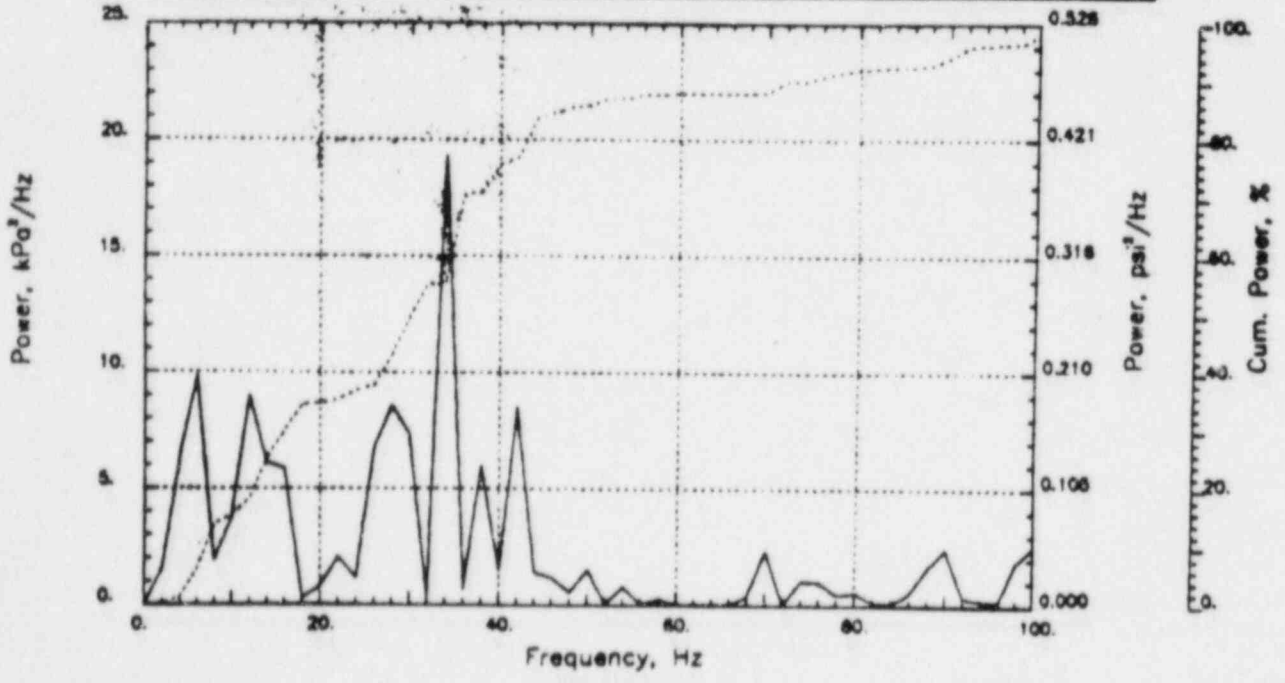

GGNS RHR CO

Output at point (12.65,28.00,2.18)

NAME - LEONG, TAI SENG
DATE - FEB 21, 1984
PROJECT NO. - 15026004

CHECKED _____
DATE _____
CALC NO. - AP-84-

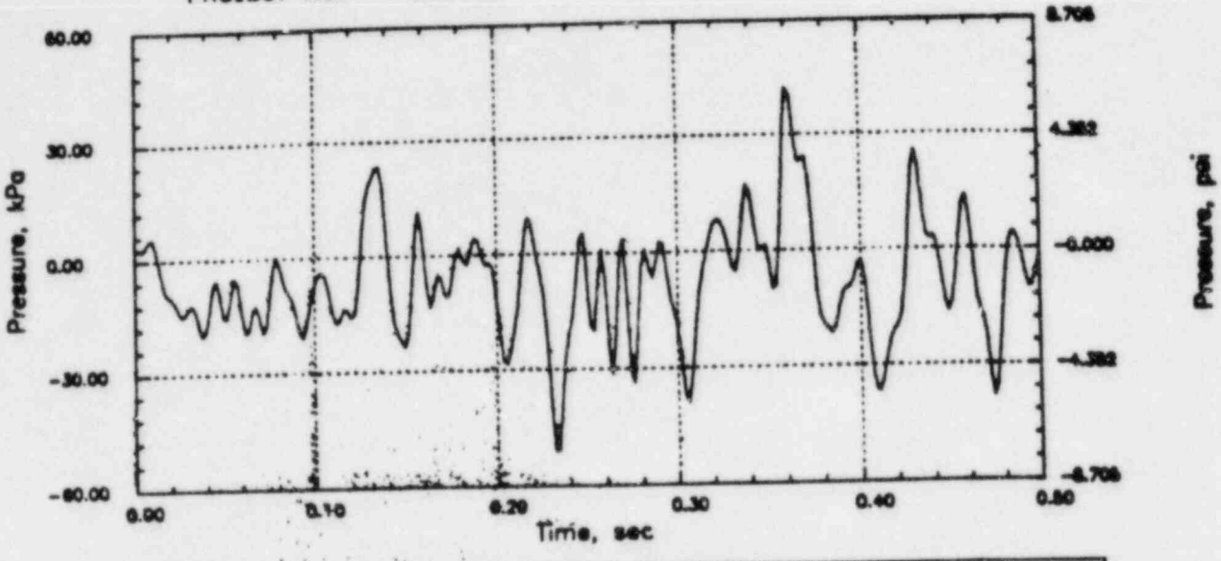

POP = 42.12 kPa PUP = -50.85 kPa MSP = 212.18 kPa²

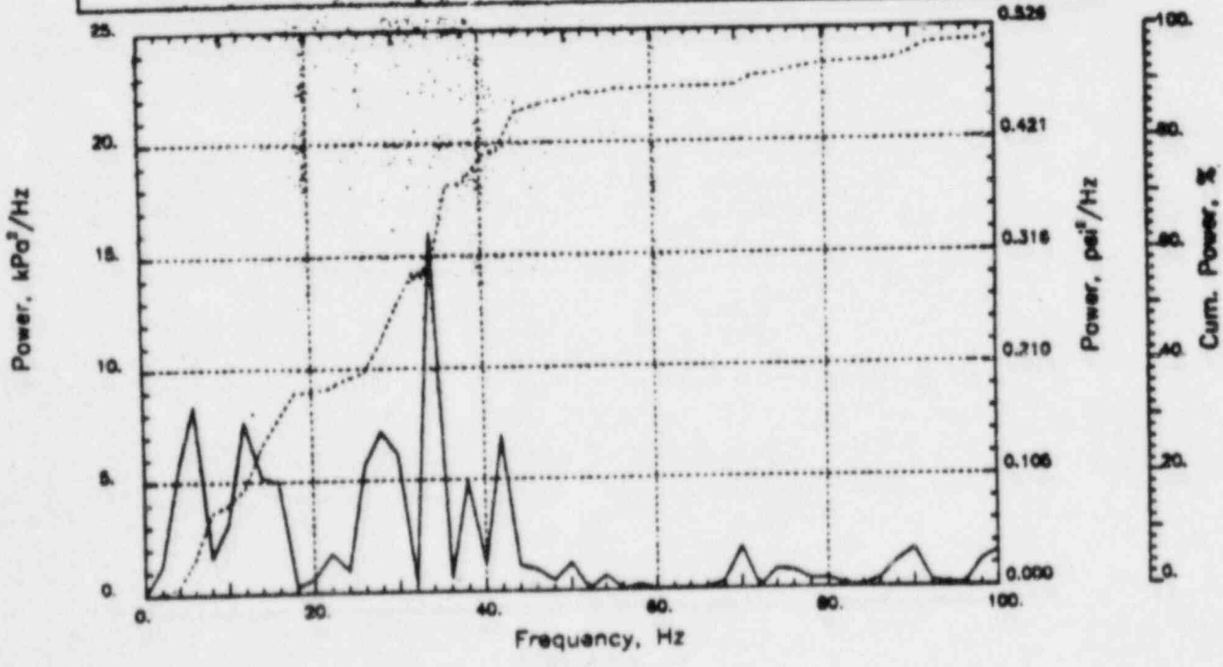

GGNS RHR CO

Output at point (12.65,28.00,2.82)

NAME - LEONG, TAI SENG
DATE - FEB 21, 1984
PROJECT NO. - 15026004

CHECKED _____
DATE _____
CALC NO. - AP-84-

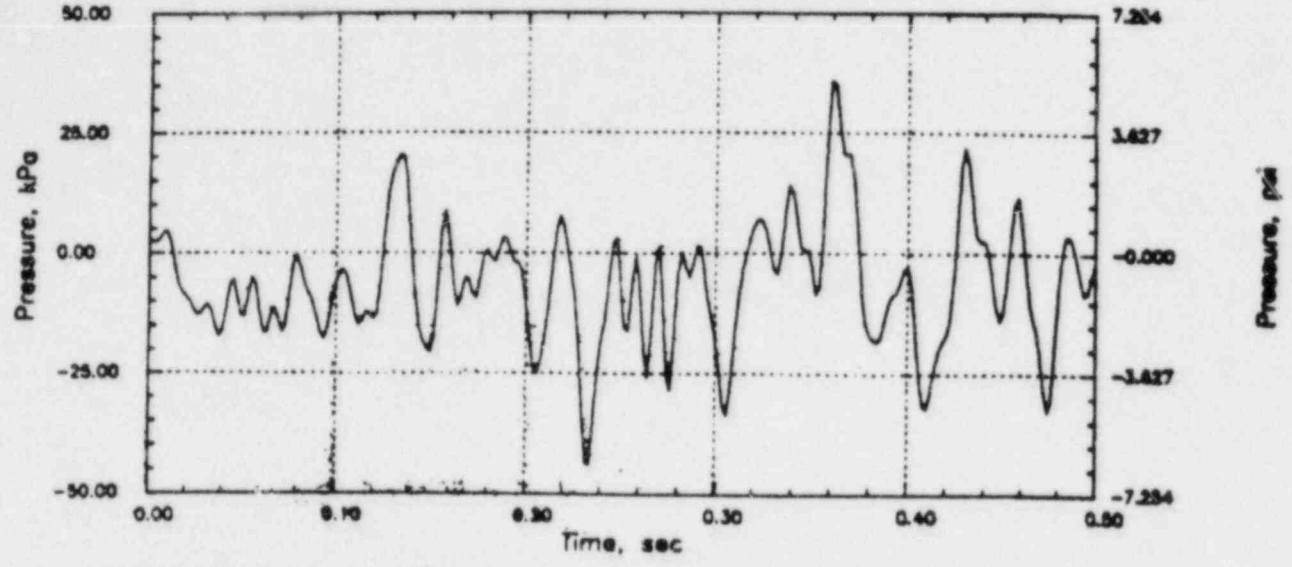

POP = 35.87 kPa PUP = -43.78 kPa MSP = 158.82 kPa²

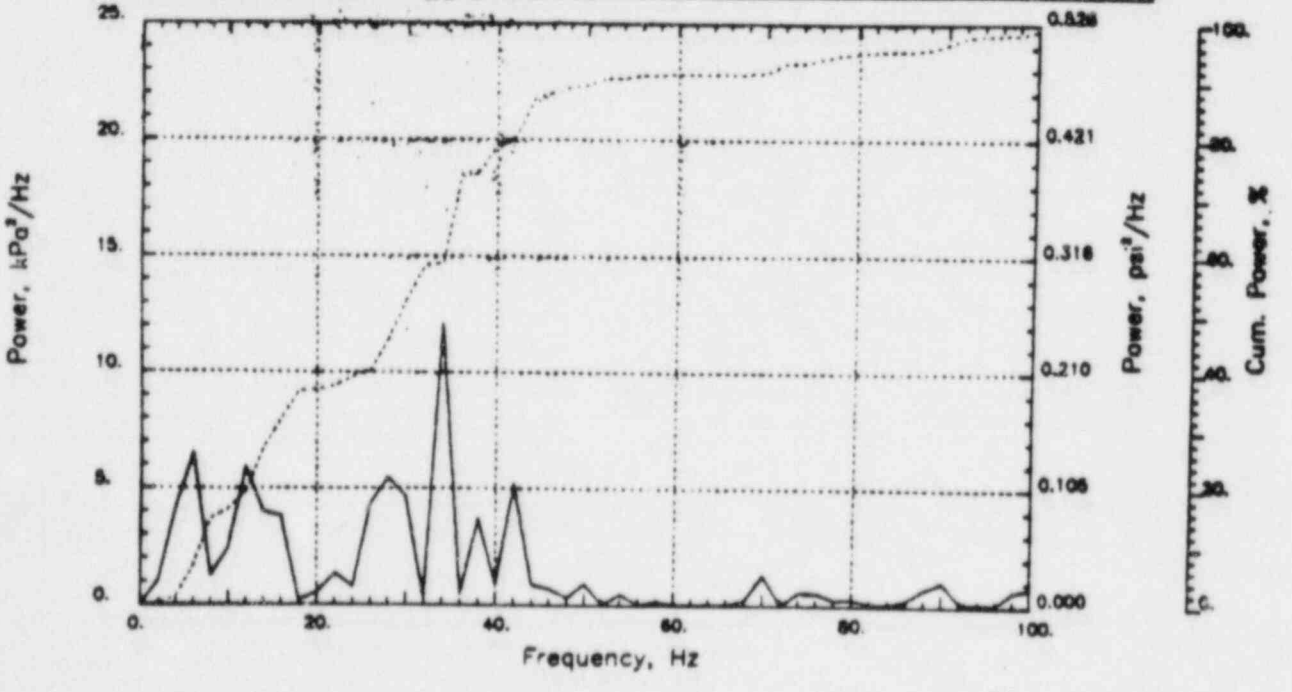

GGNS RHR CO

Output at point (12.65,28.00,3.45)

NAME - LEONG, TAI SENG
DATE - FEB 21, 1984
PROJECT NO. - 15026004

CHECKED _____
DATE _____
CALC NO. - AP-84-

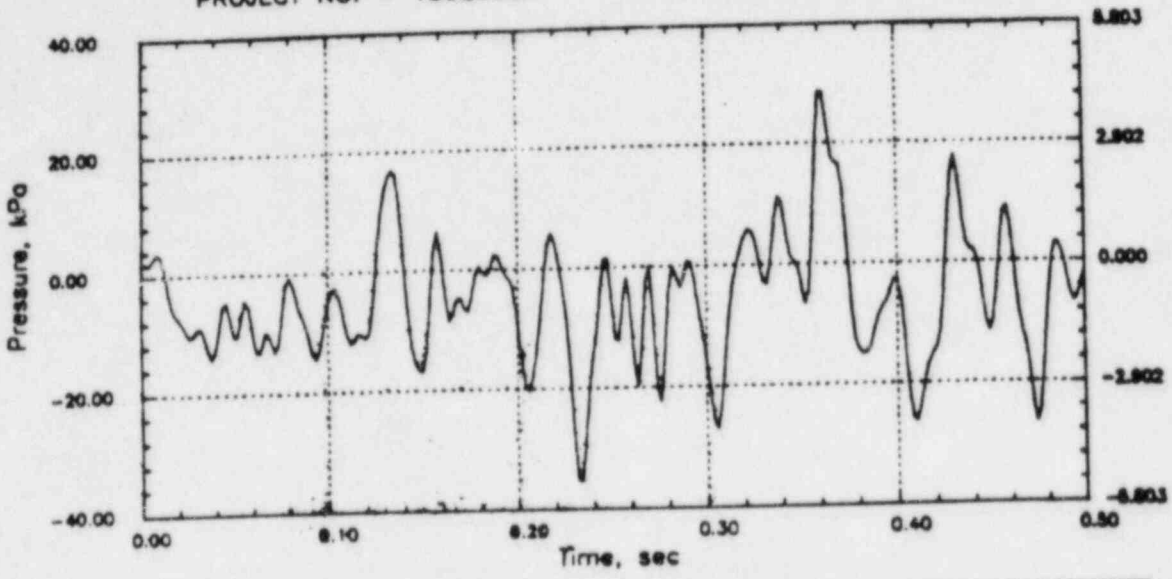

POP = 28.65 kPa PUP = -35.34 kPa MSP = 104.99 kPa²

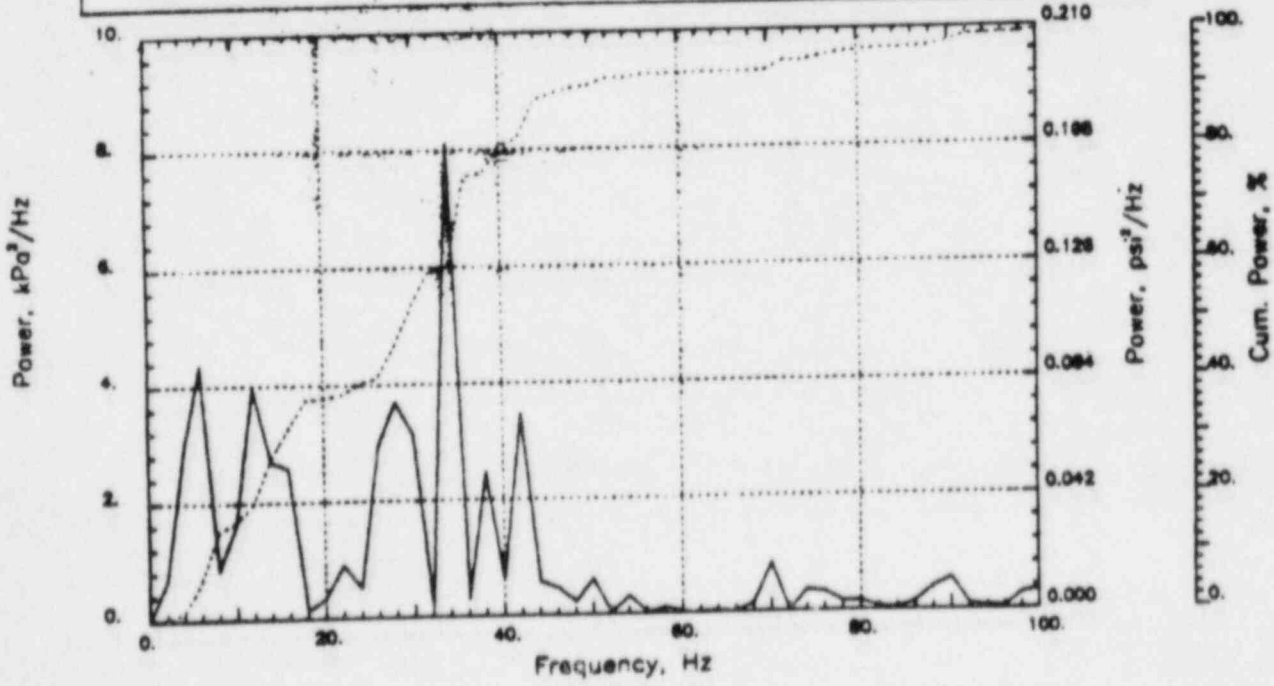

GGNS RHR CO

Output at point (12.65,28.00,4.09)

NAME - LEONG, TAI SENG
DATE - FEB 21, 1984
PROJECT NO. - 15026004

CHECKED _____
DATE _____
CALC NO. - AP-84-

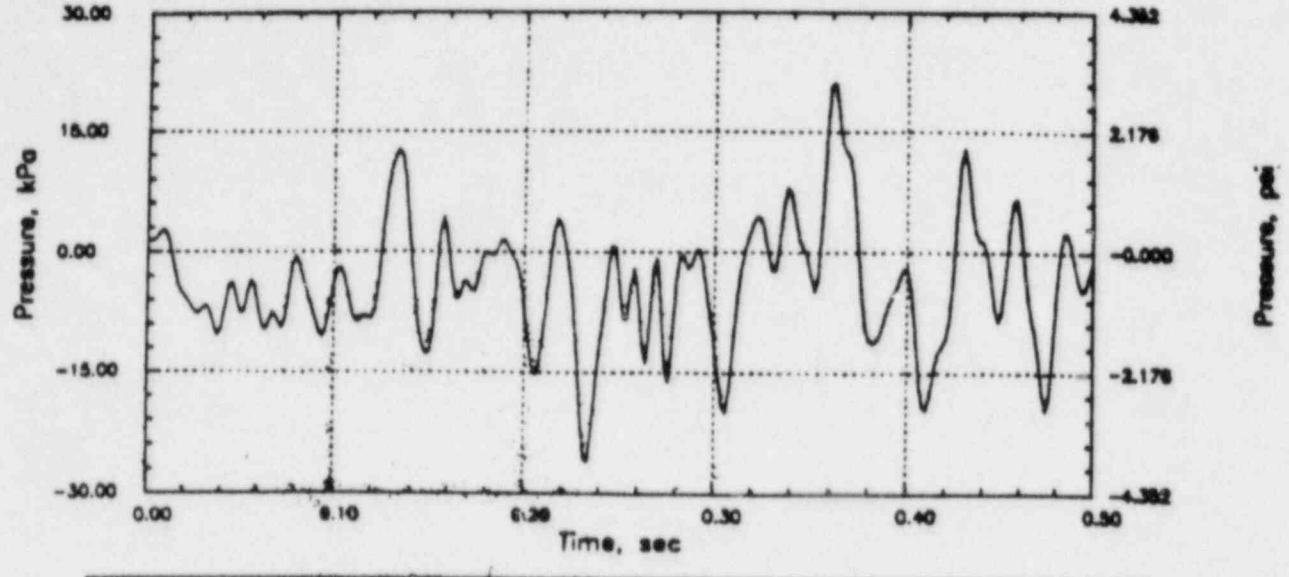

POP = 21.01 kPa PUP = -25.98 kPa MSP = 57.68 kPa²

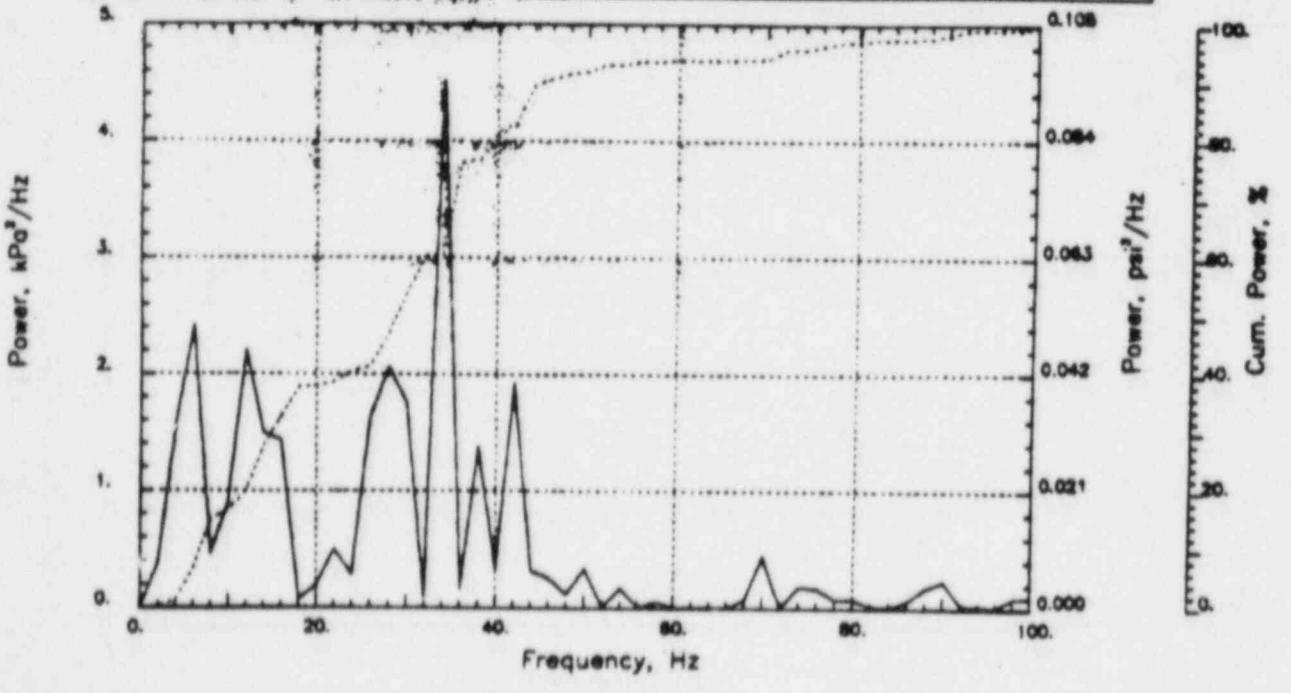

GGNS RHR CO

Output at point (12.65,28.00,4.91)

NAME - LEONG, TAI SENG
DATE - FEB 21, 1984
PROJECT NO. - 15026004

CHECKED _____
DATE _____
CALC NO. - AP-84-

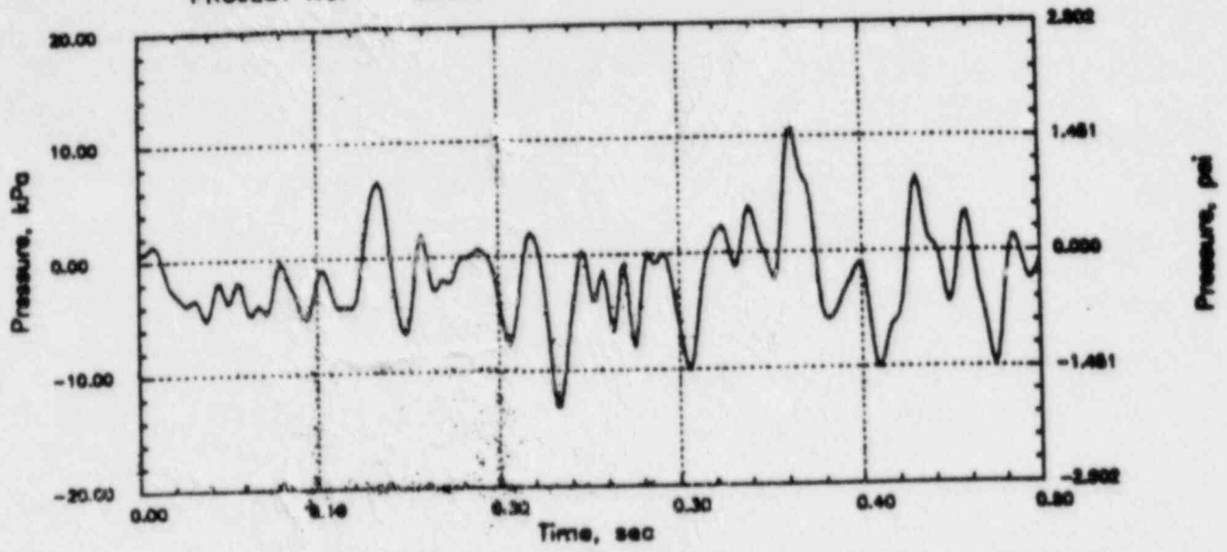

POP = 10.86 kPa PUP = -13.11 kPa MSP = 14.97 kPa²

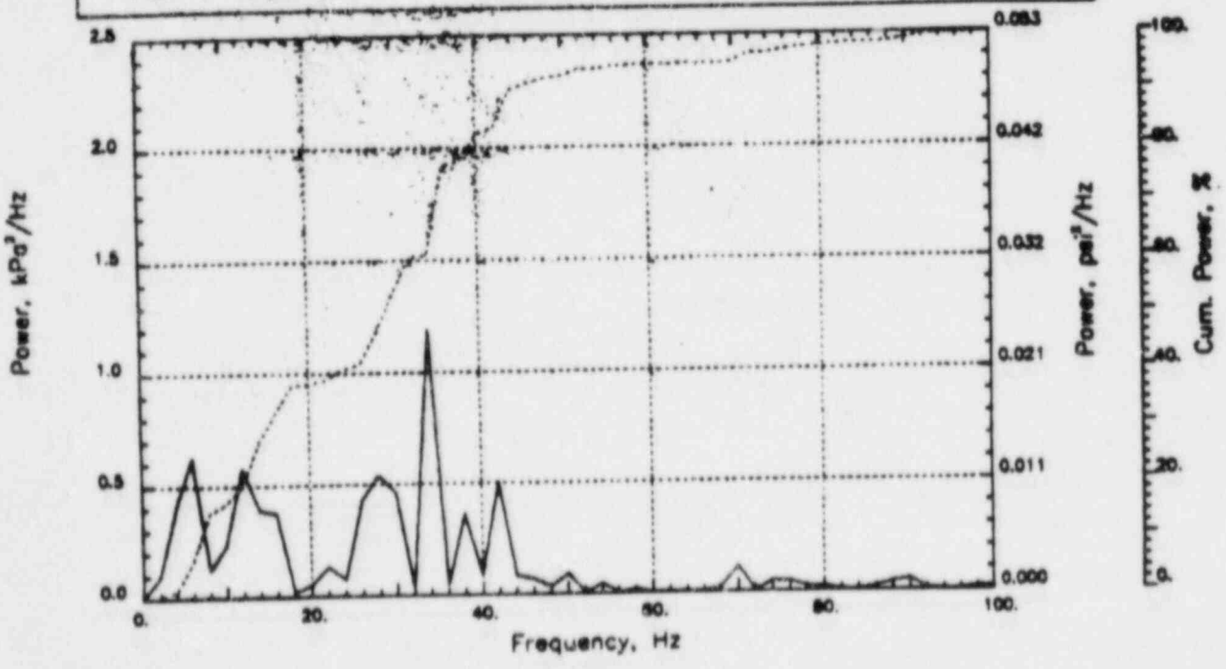

CLINTON RHR CO

Output at point (18.90,28.00,4.91)

NAME - LEONG, TAI SENG
DATE - FEB 21, 1984
PROJECT NO. - 15026004

CHECKED _____
DATE _____
CALC NO. - AP-84-

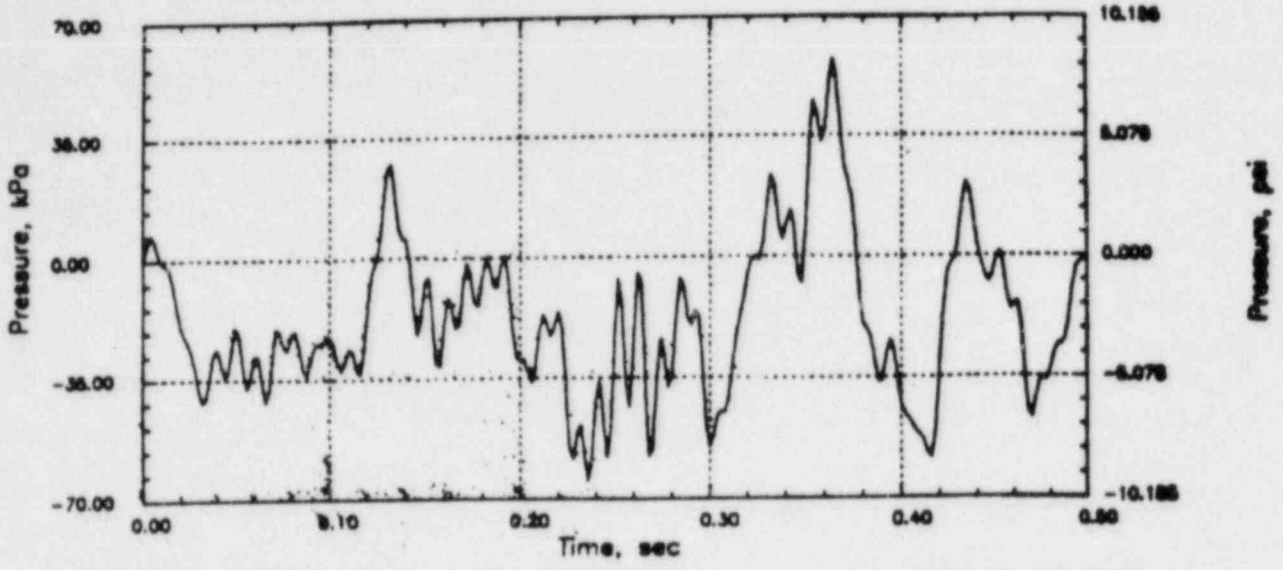

POP = 57.46 kPa PUP = -64.55 kPa MSP = 508.07 kPa²

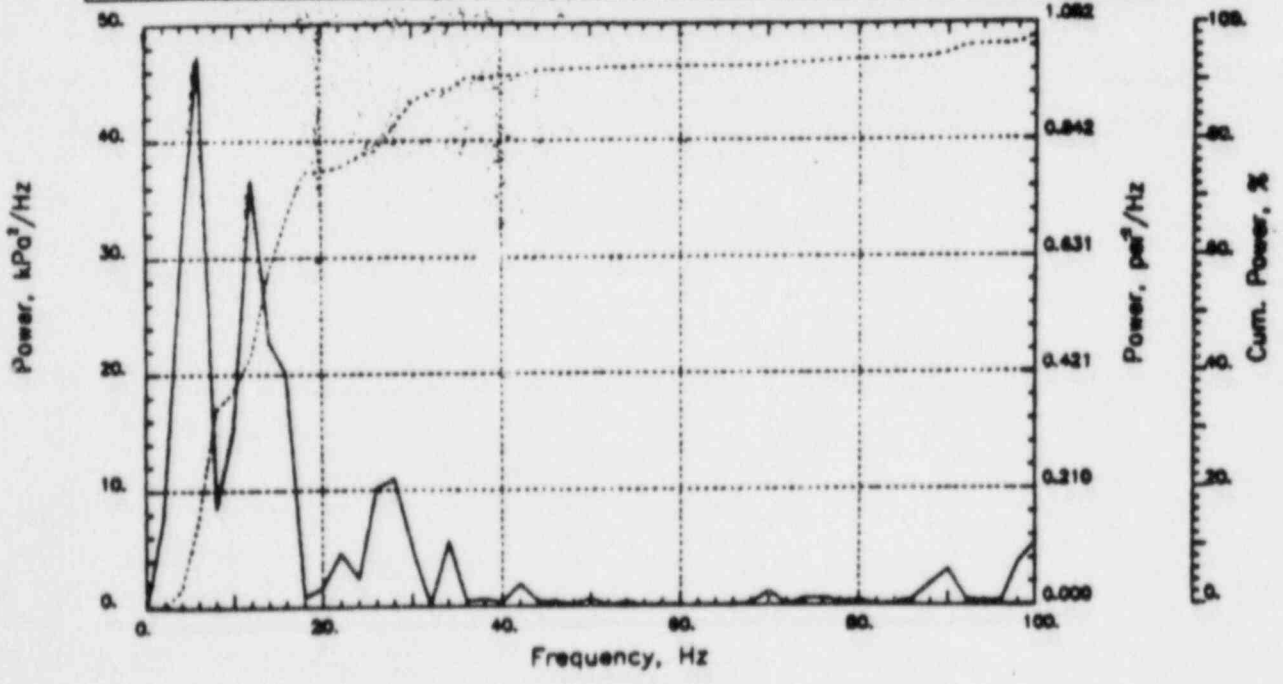

CLINTON RHR CO

Output at point (18.90,28.00,4.09)

NAME - LEONG, TAI SENG
DATE - FEB 21, 1984
PROJECT NO. - 15026004

CHECKED _____
DATE _____
CALC NO. - AP-84-

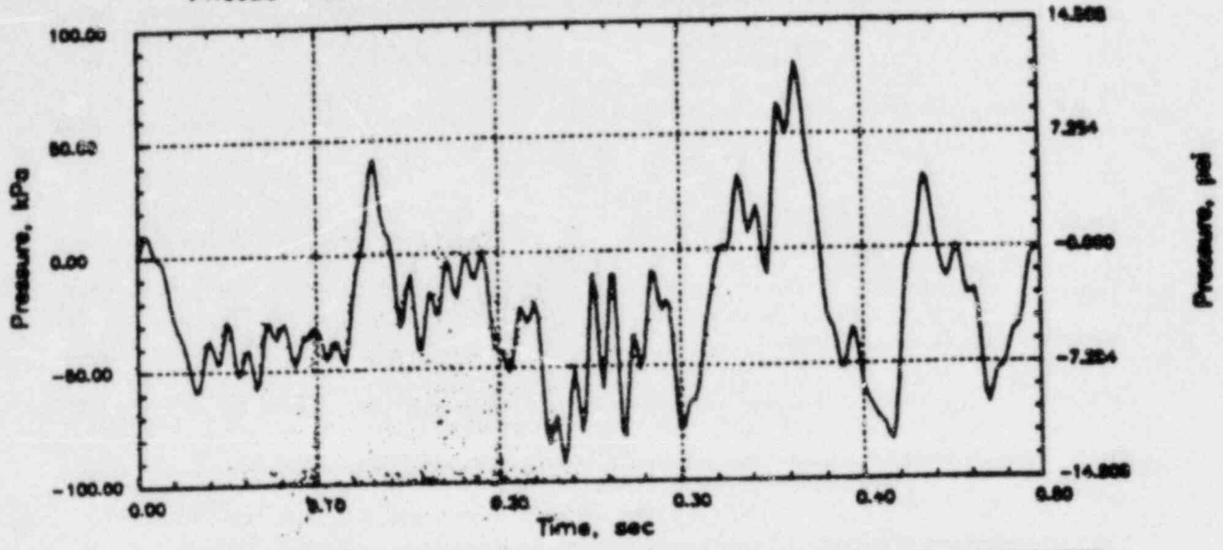

POP = 81.08 kPa PUP = -91.82 kPa MSP = 1032.37 kPa²

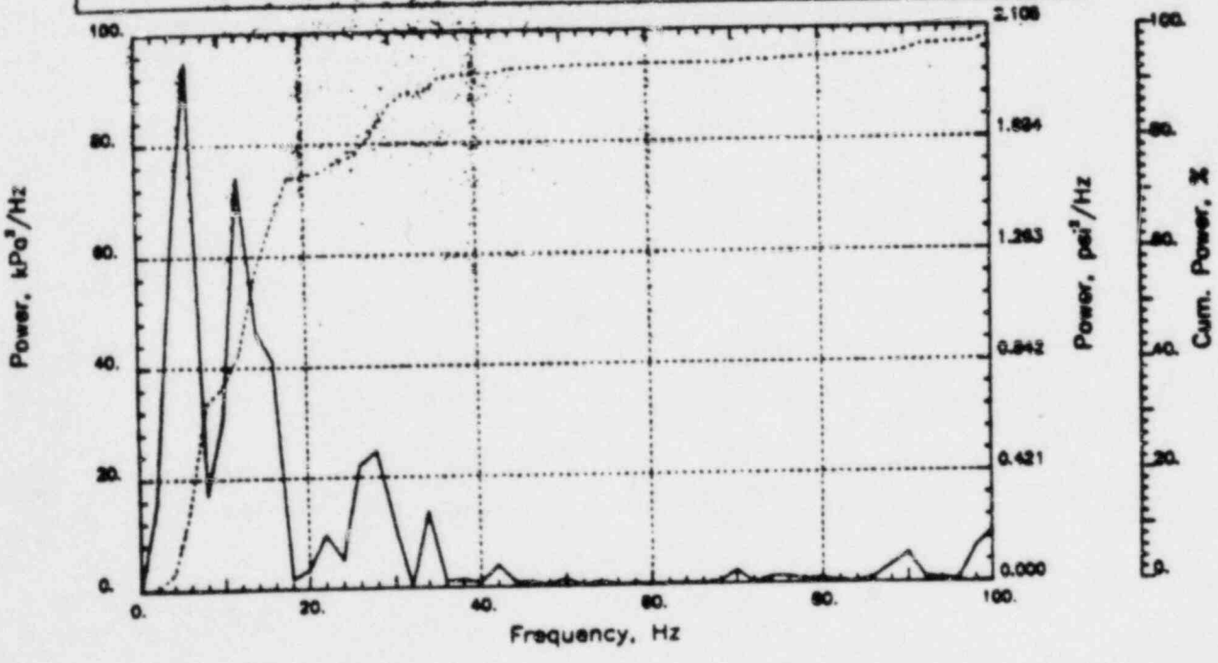

CLINTON RHR CO

Output at point (18.90,28.00,3.45)

NAME - LEONG, TAI SENG
DATE - FEB 21, 1984
PROJECT NO. - 15026004

CHECKED _____
DATE _____
CALC NO. - AP-84-

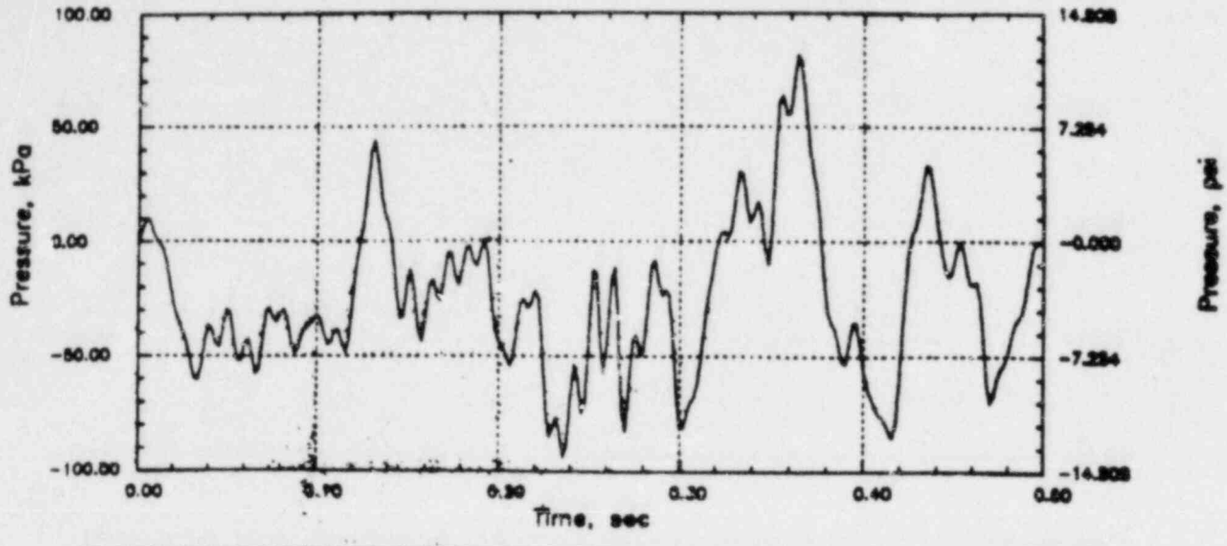

POP = 81.80 kPa PUP = -93.80 kPa MSP = 1092.60 kPa²

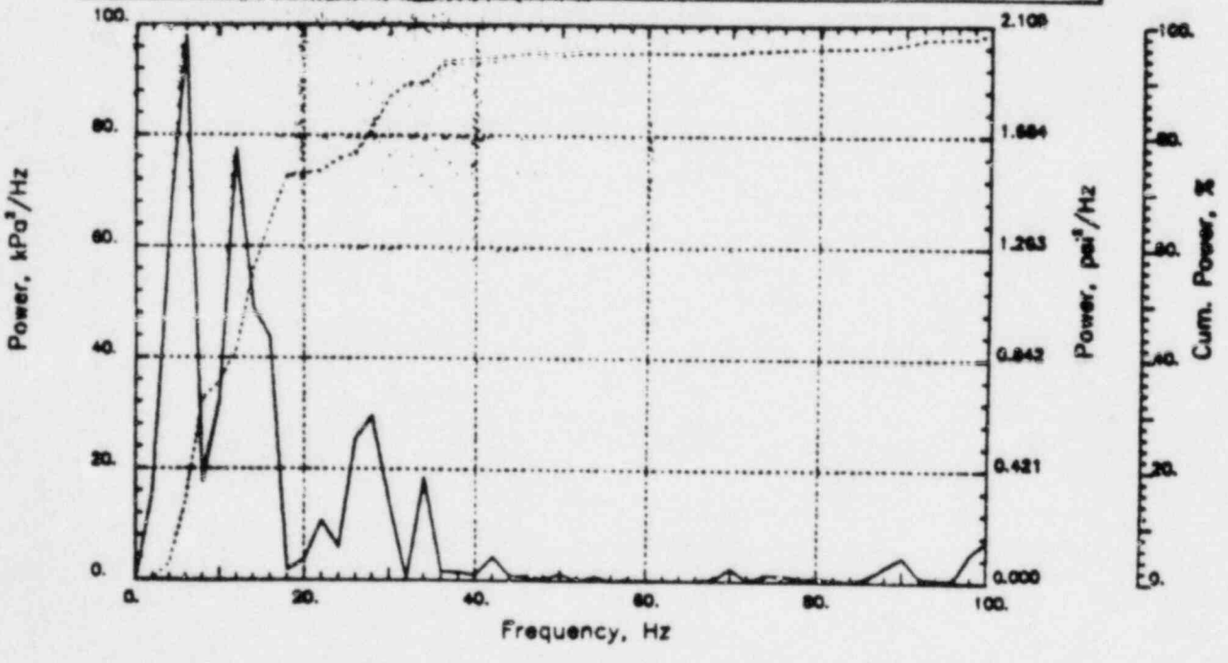

CLINTON RHR CO

Output at point (18.90,28.00,2.82)

NAME - LEONG, TAI SENG
DATE - FEB 21, 1984
PROJECT NO. - 15026004

CHECKED _____
DATE _____
CALC NO. - AP-84-

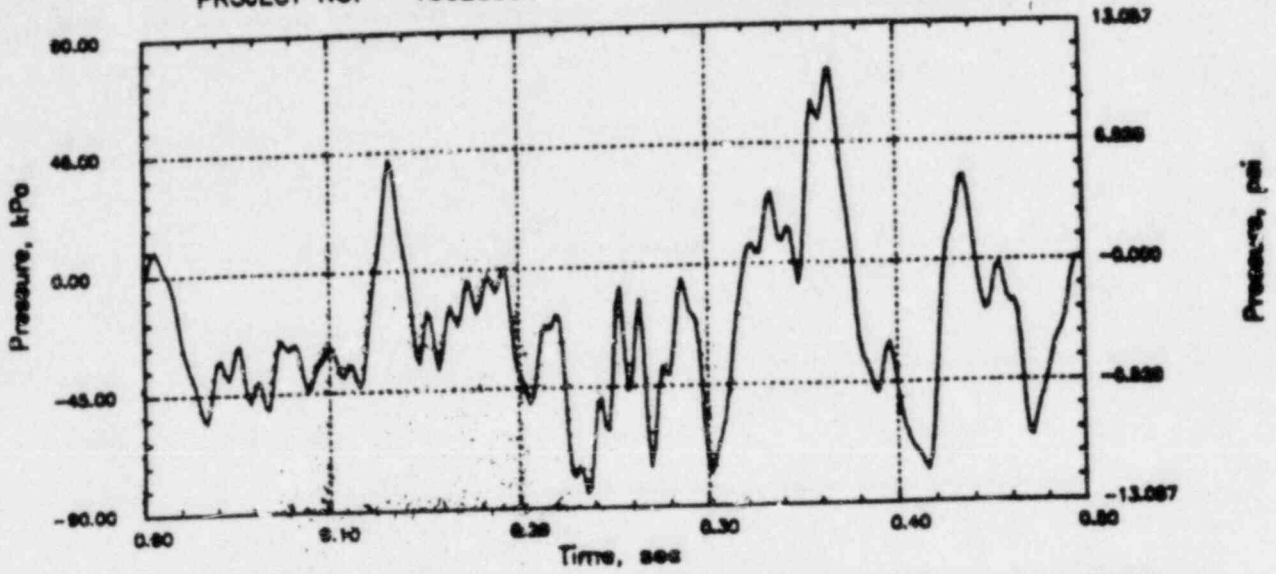

POP = 72.90 kPa PUP = -84.89 kPa MSP = 929.67 kPa²

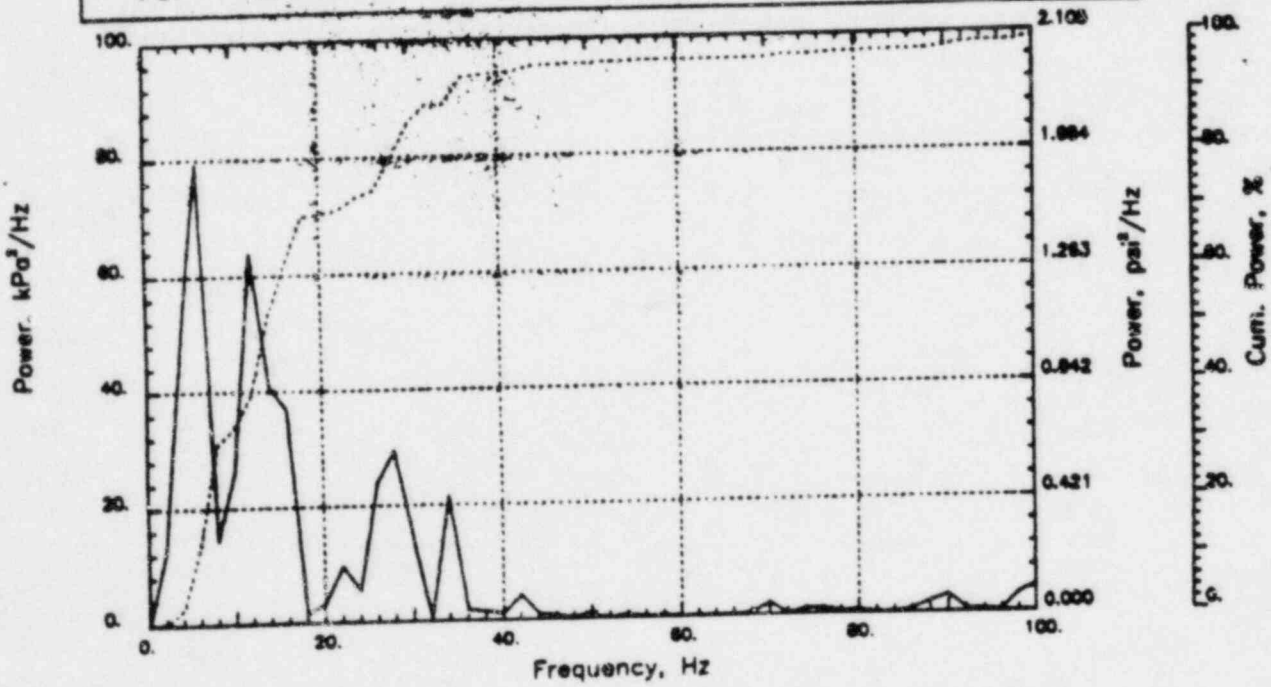

CLINTON RHR CO

Output at point (18.90,28.00,2.18)

NAME - LEONG, TAI SENG
DATE - FEB 21, 1984
PROJECT NO. - 15026004

CHECKED _____
DATE _____
CALC NO. - AP-84-

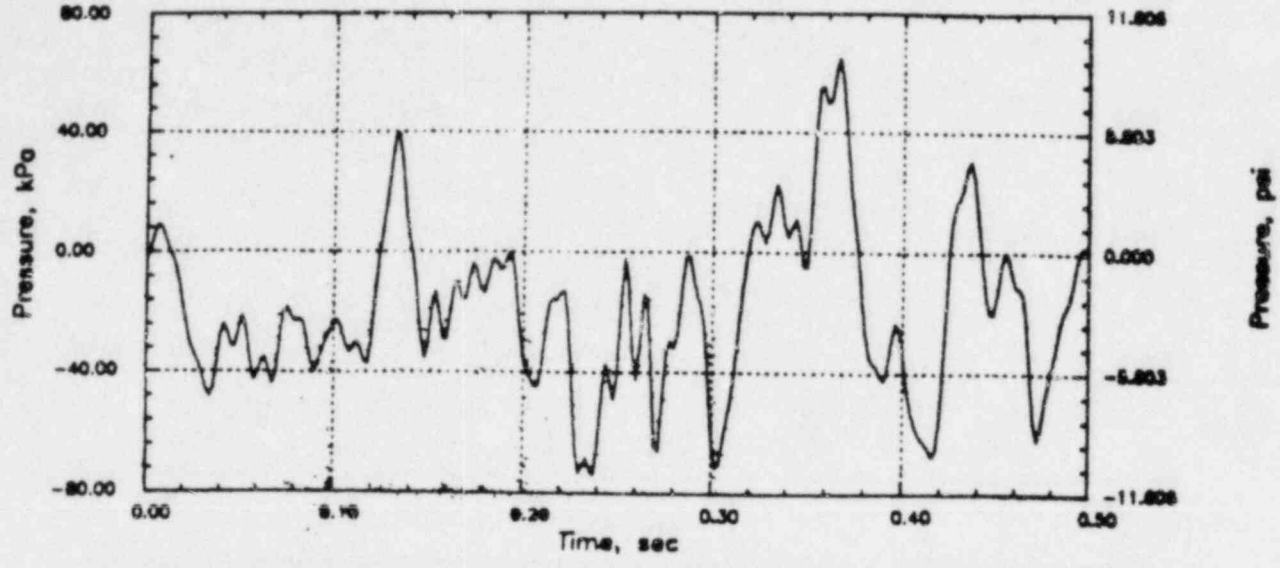

POP = 64.80 kPa PUP = -74.12 kPa MSP = 736.36 kPa²

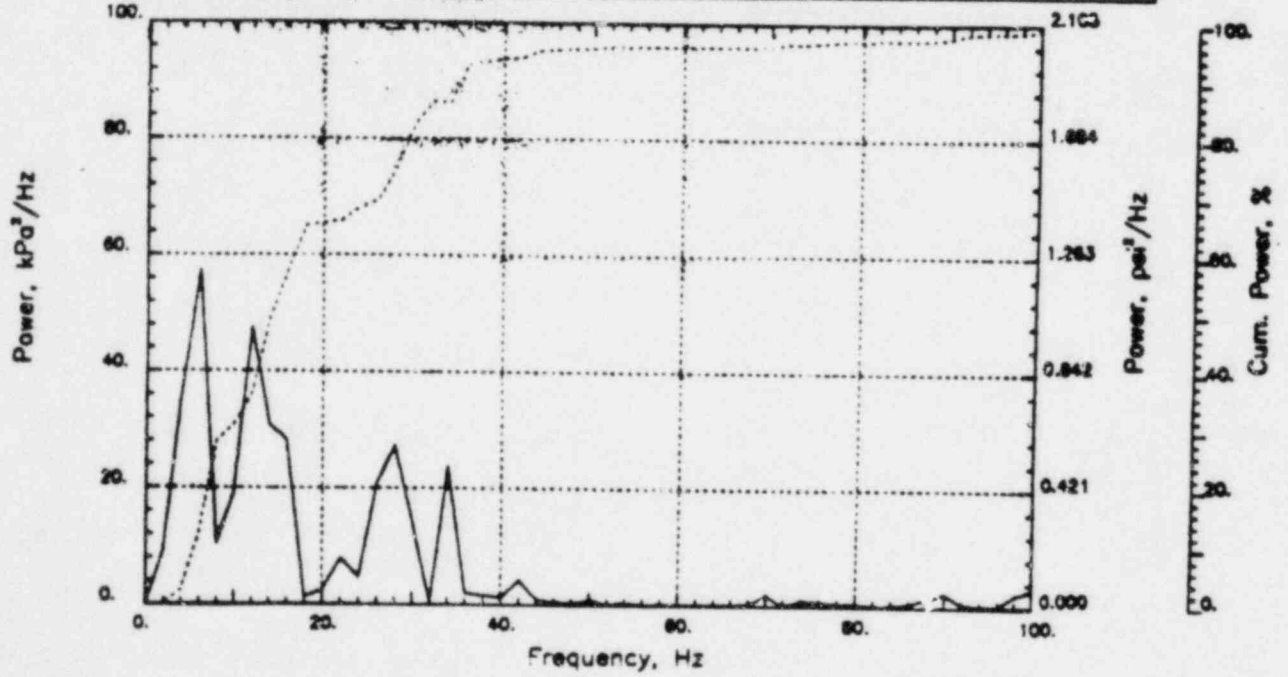

CLINTON RHR CO

Output at point (18.90,28.00,1.55)

NAME - LEONG, TAI SENG
DATE - FEB 21, 1984
PROJECT NO. - 15026004

CHECKED _____
DATE _____
CALC NO. - AP-84-

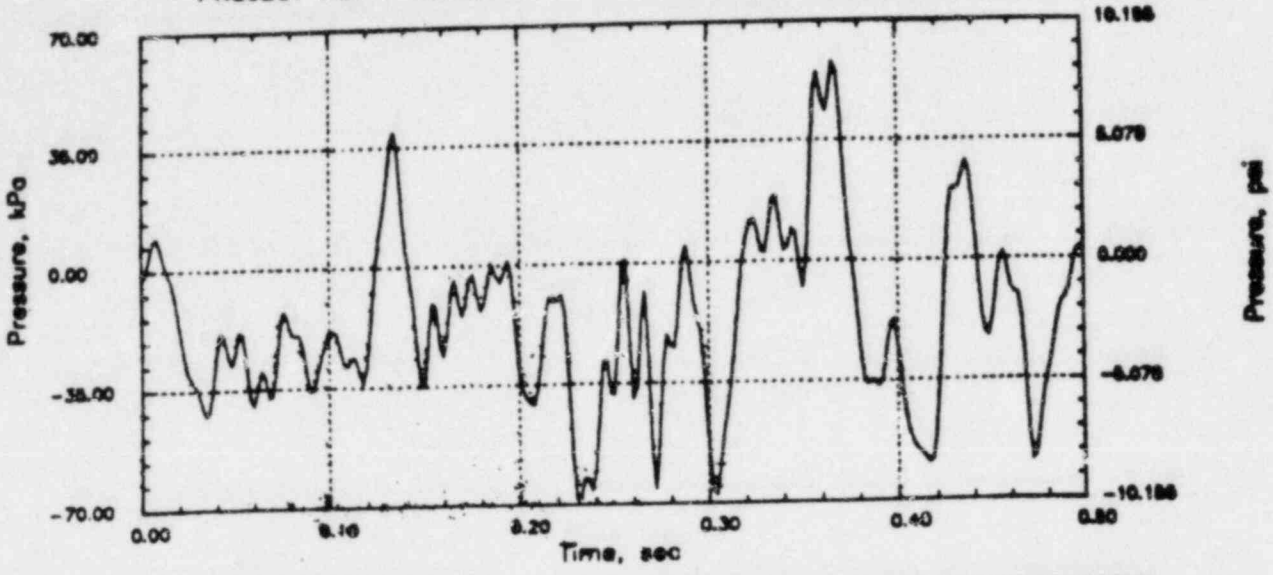

POP = 57.84 kPa PUP = -68.57 kPa MSP = 614.62 kPa²

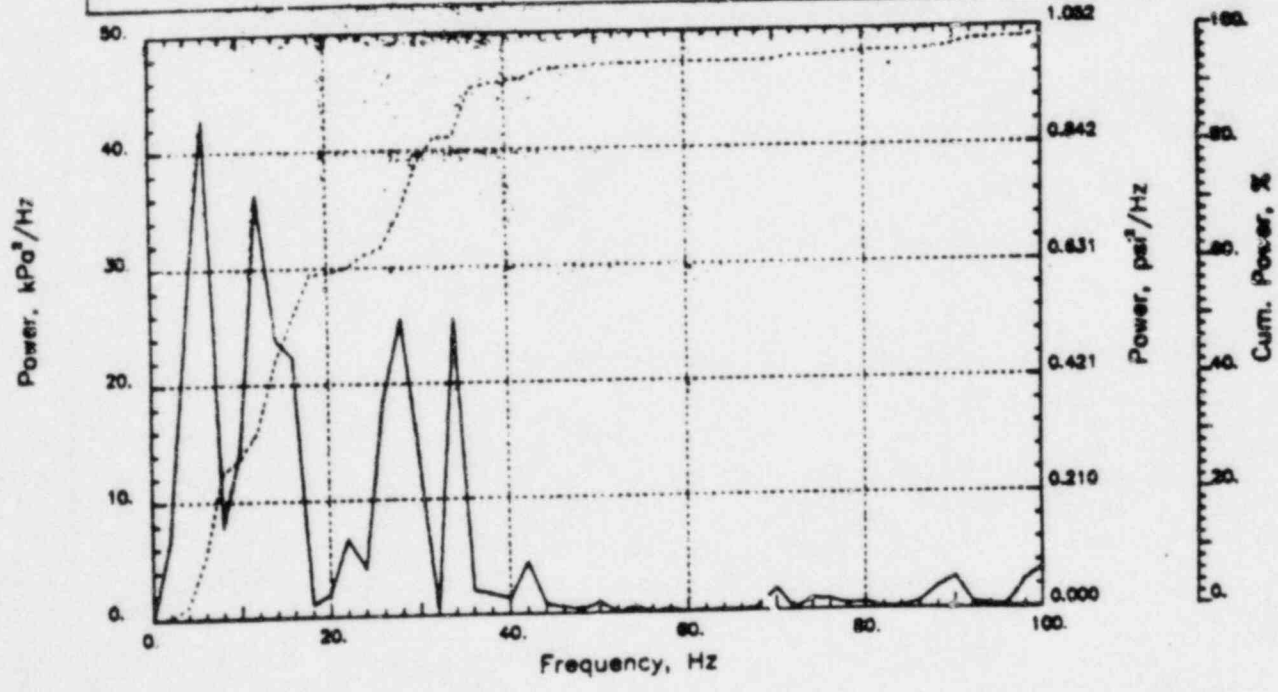

CLINTON RHR CO

Output at point (18.90,28.00,0.91)

NAME - LEONG, TAI SENG
DATE - FEB 21, 1984
PROJECT NO. - 15026004

CHECKED _____
DATE _____
CALC NO. - AP-(3)4-

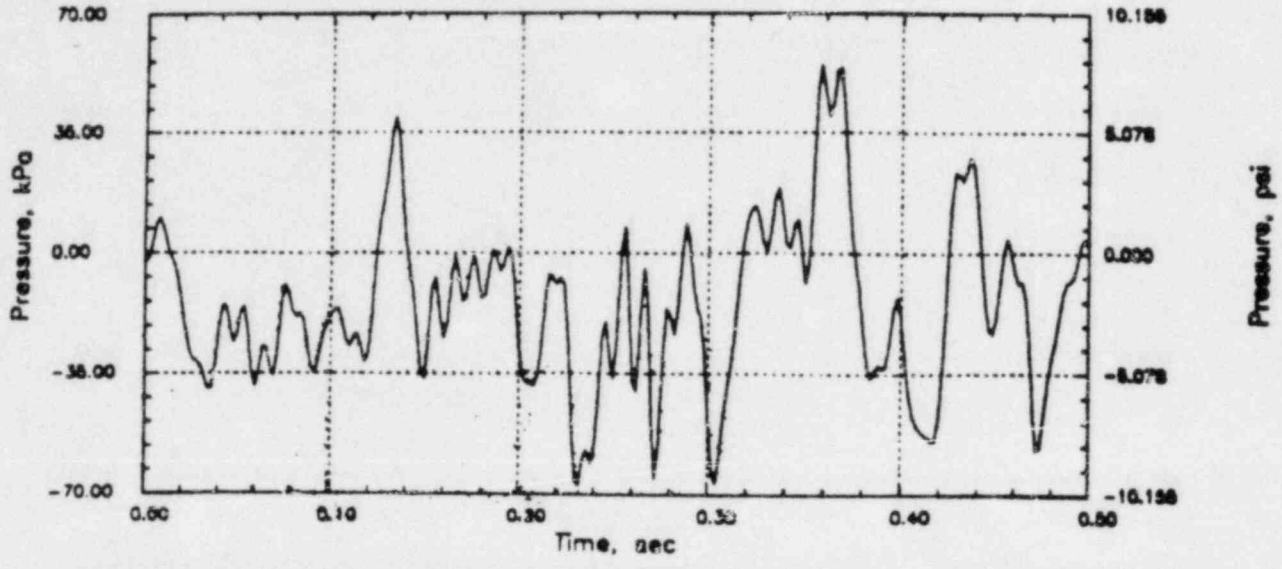

POP = 55.05 kPa PUP = -67.47 kPa MSP = 564.89 kPa²

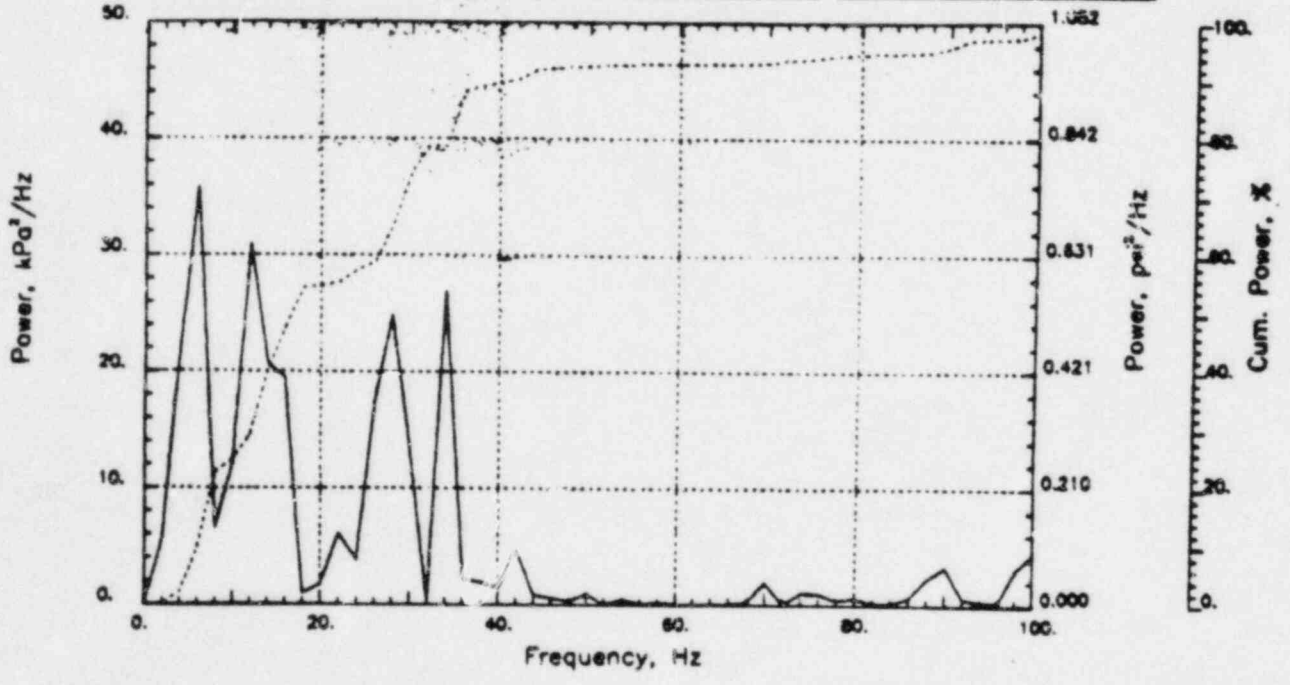

CLINTON RHR CO

Output at point (18.90,28.00,0.46)

NAME - LEONG, TAI SENG
DATE - FEB 21, 1984
PROJECT NO. - 150260C4

CHECKED _____
DATE _____
CALC NO. - AP-84-

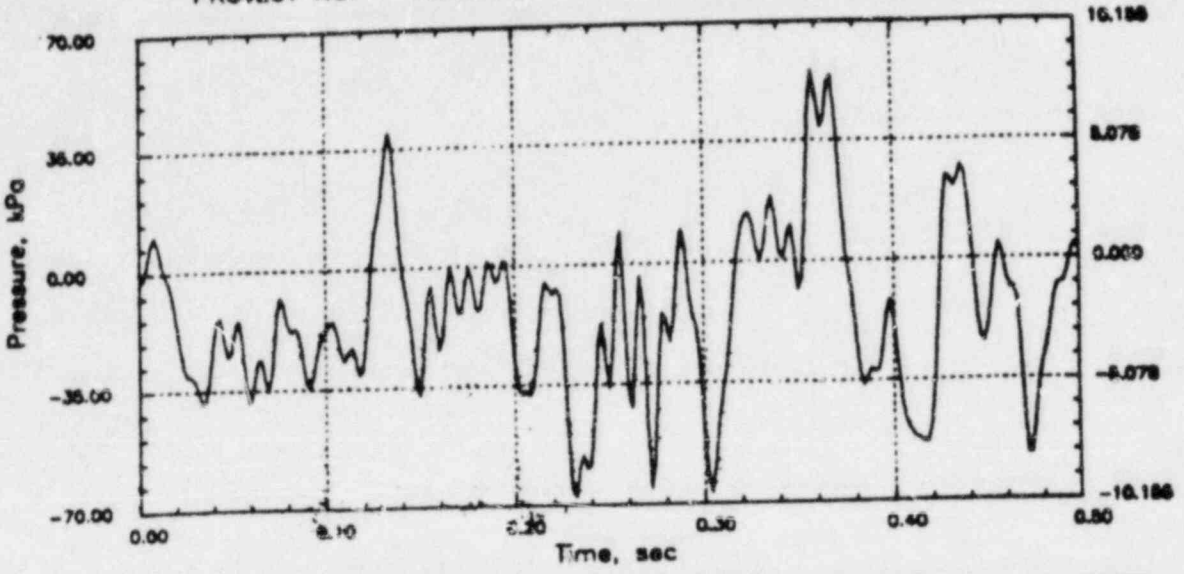

POP = 55.43 kPa PUP = -67.74 kPa MSP = 554.25 kPa²

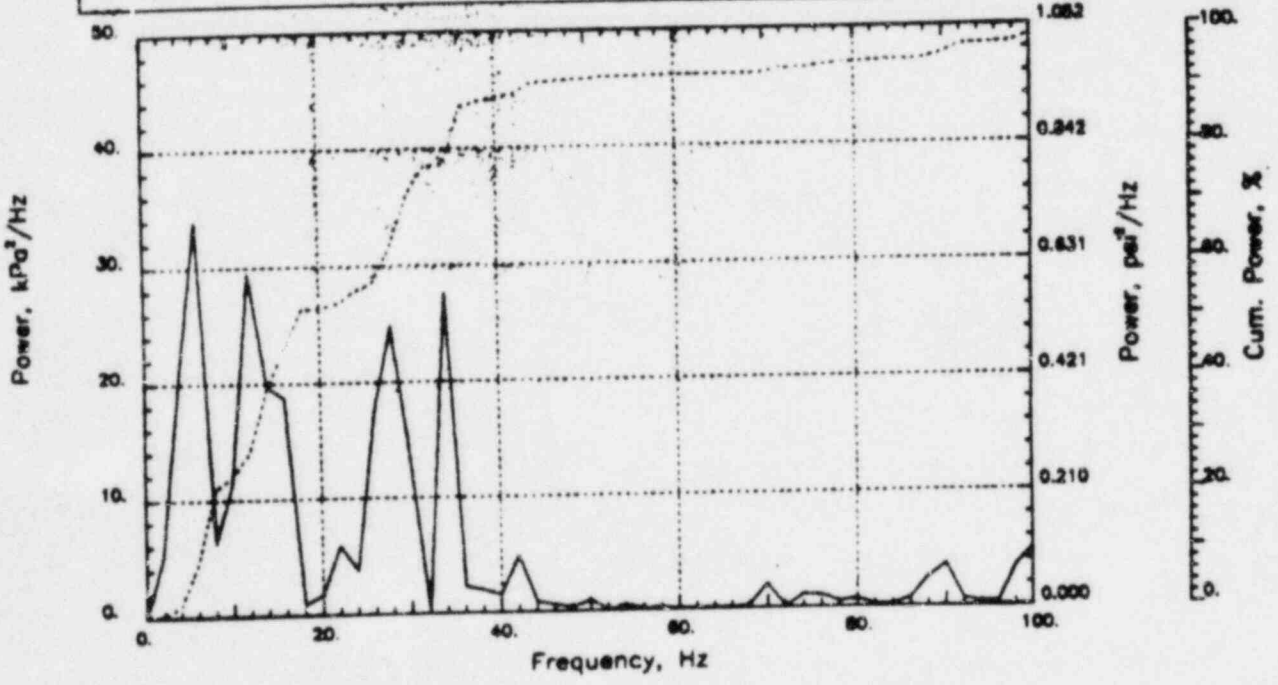

CLINTON RHR CO

Output at point (18.90,28.00,0.00)

NAME - LEONG, TAI SENG
DATE - FEB 21, 1984
PROJECT NO. - 15026004

CHECKED _____
DATE _____
CALC NO. - AP-84-

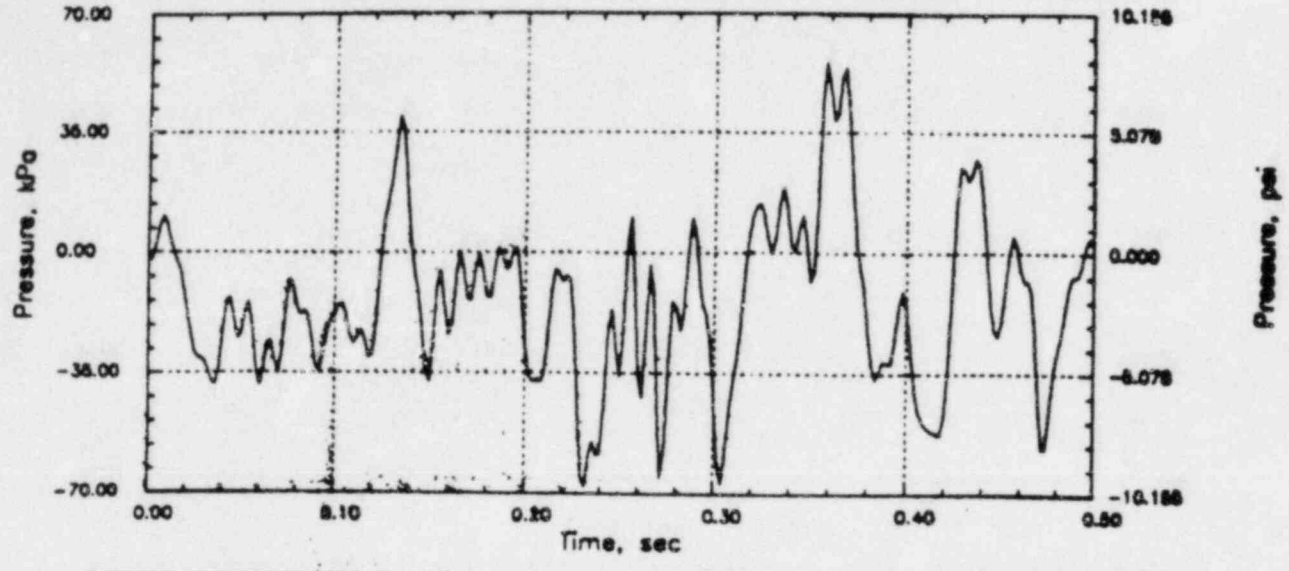

POP = 55.60 kPa PUP = -67.91 kPa MSP = 552.05 kPa²

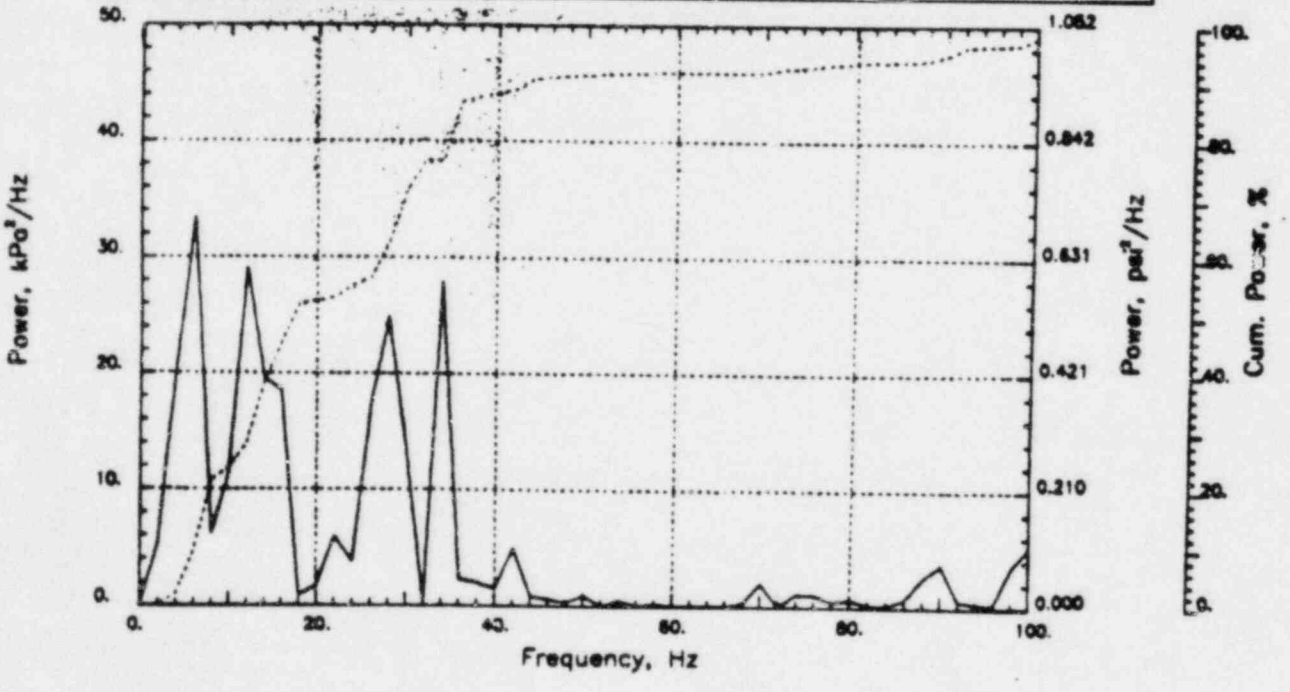

CLINTON RHR CO

Output at point (17.34,28.00,0.00)

NAME - LEONG, TAI SENG
DATE - FEB 21, 1984
PROJECT NO. - 15026004

CHECKED _____
DATE _____
CALC NO. - AP-84-

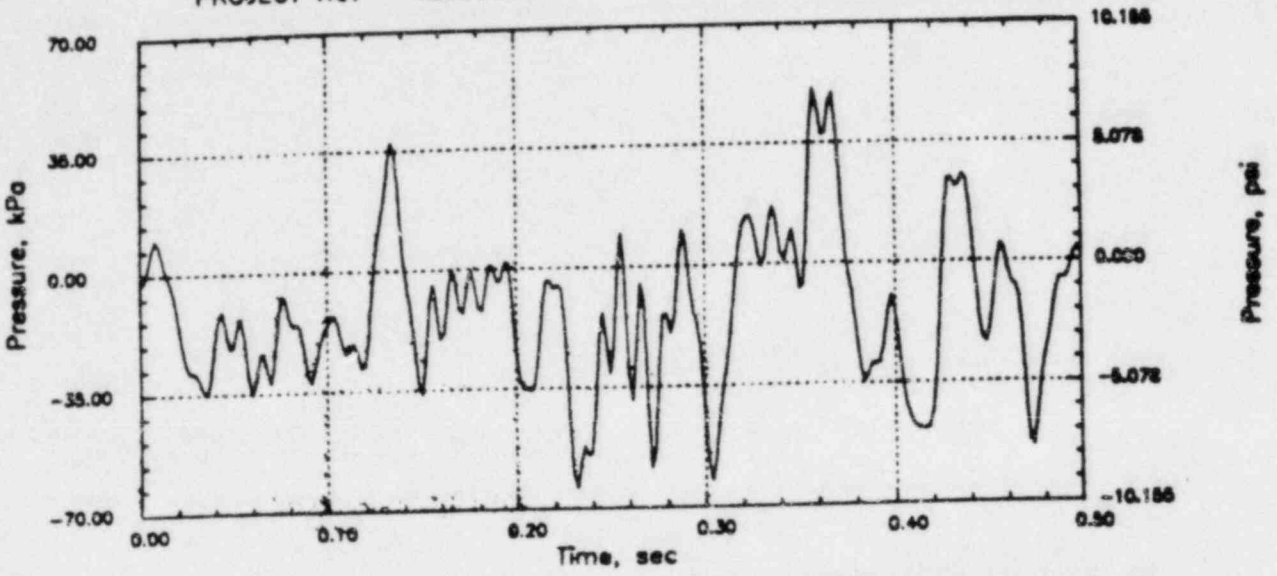

POP = 50.96 kPa PUP = -63.93 kPa MSP = 479.08 kPa²

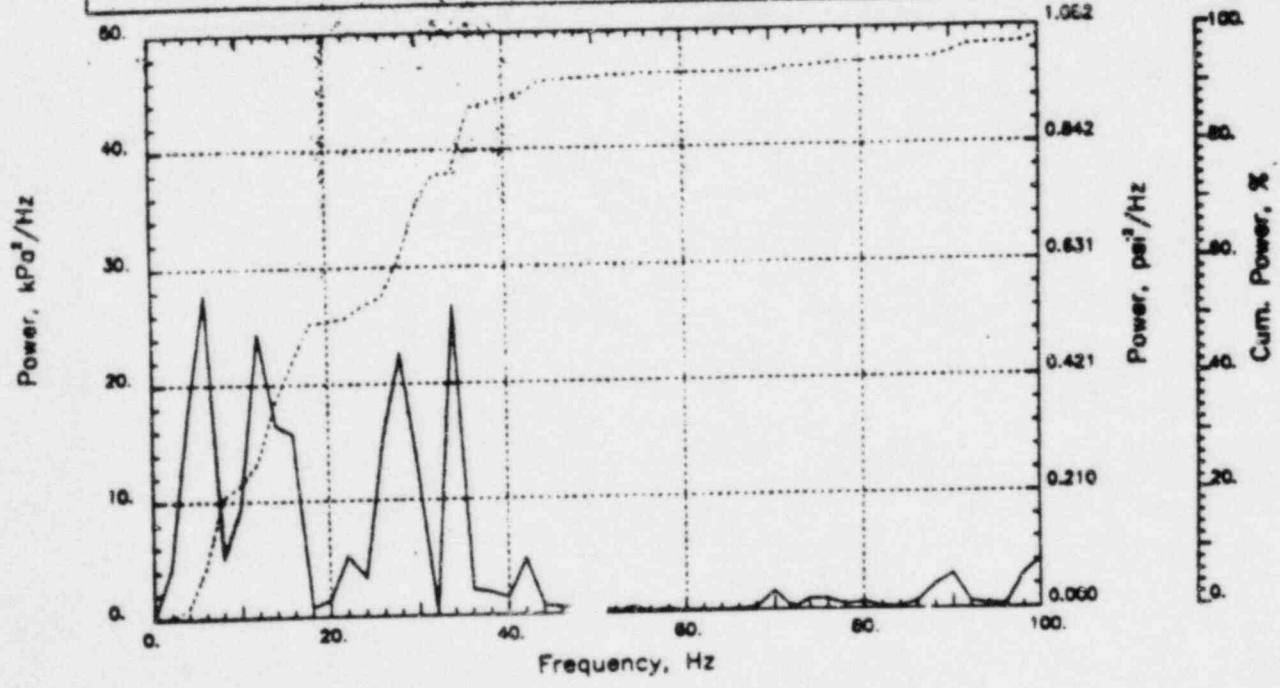

CLINTON RHR CO

Output at point (14.21,28.00,0.00)

NAME - LEONG, TAI SENG
DATE - FEB 21, 1984
PROJECT NO. - 15026004

CHECKED _____
DATE _____
CALC NO. - AP-84-

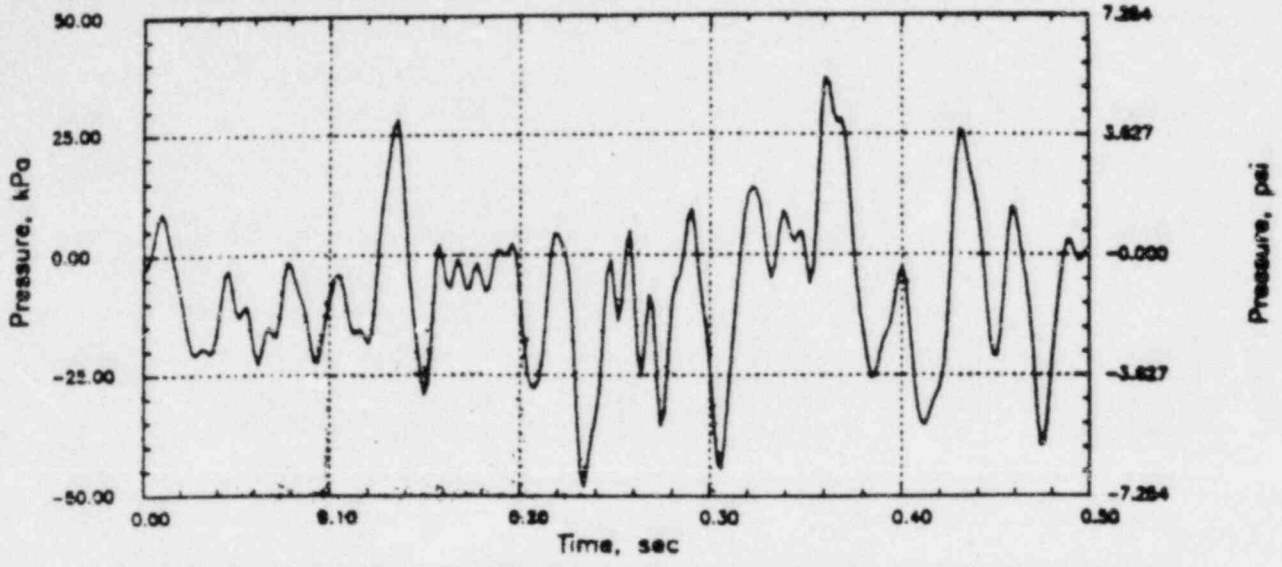

POP = 36.90 kPa PUP = -48.18 kPa MSP = 245.71 kPa²

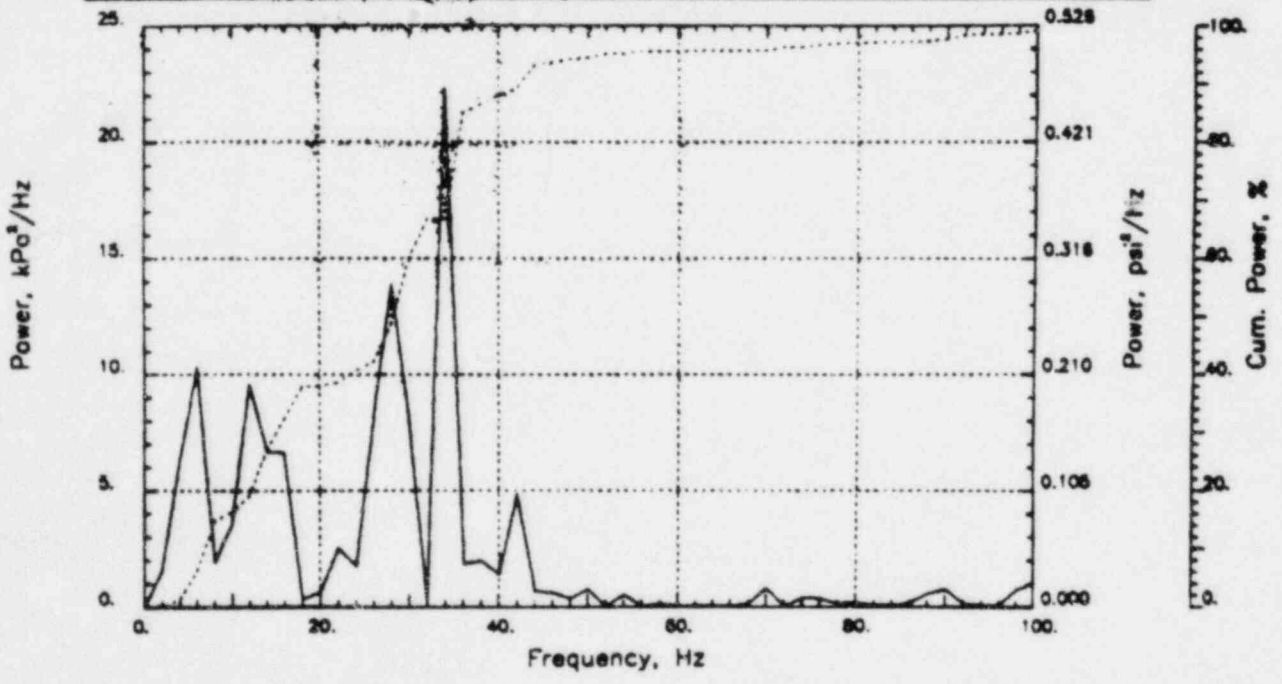

CLINTON RHR CO

Output at point (12.65,28.00,0.00)

NAME - LEONG, TAI SENG
DATE - FEB 21, 1984
PROJECT NO. - 15026004

CHECKED _____
DATE _____
CALC NO. - AP-84-

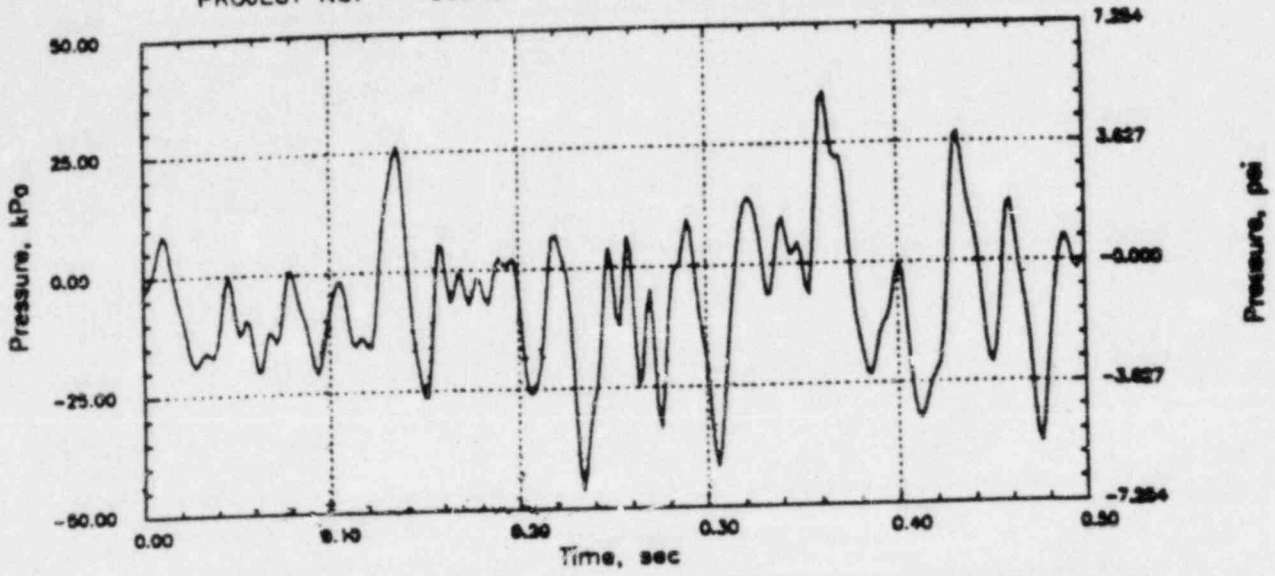

POP = 35.74 kPa PUP = -46.34 kPa MSP = 209.71 kPa²

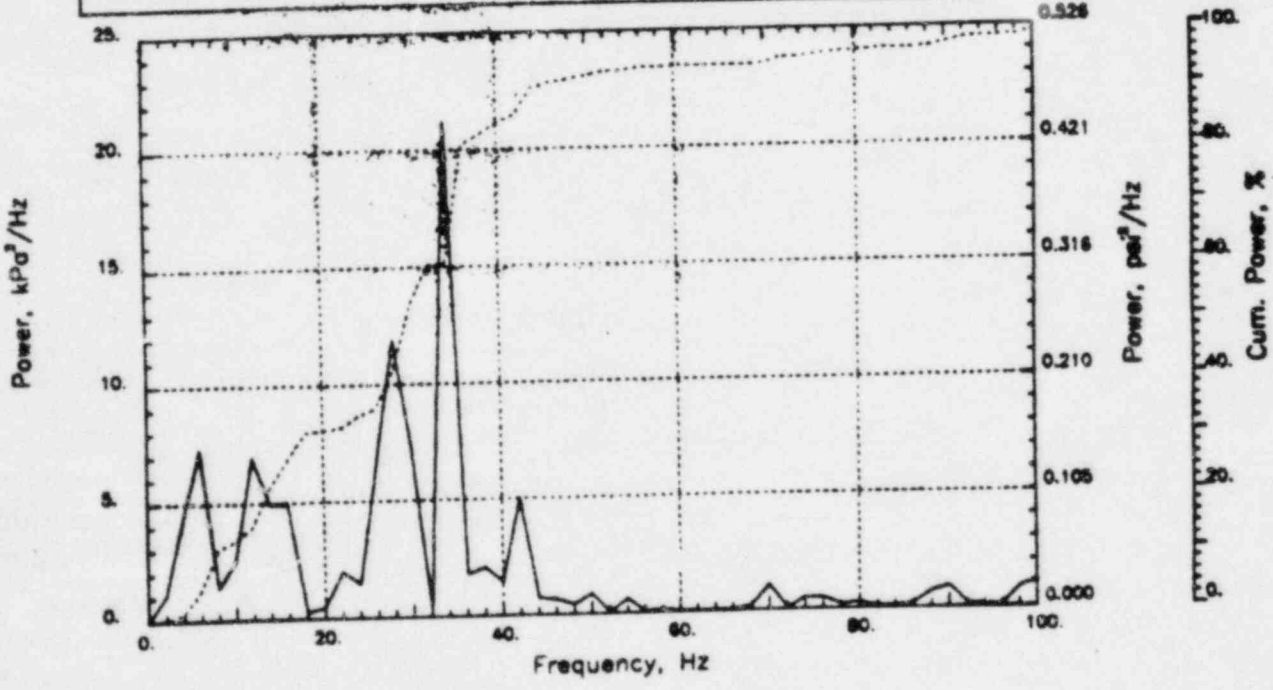

CLINTON RHR CO

Output at point (12.65,28.00,0.46)

NAME - LEONG, TAI SENG
DATE - FEB 21, 1984
PROJECT NO. - 15026004

CHECKED _____
DATE _____
CALC NO. - AP-84-

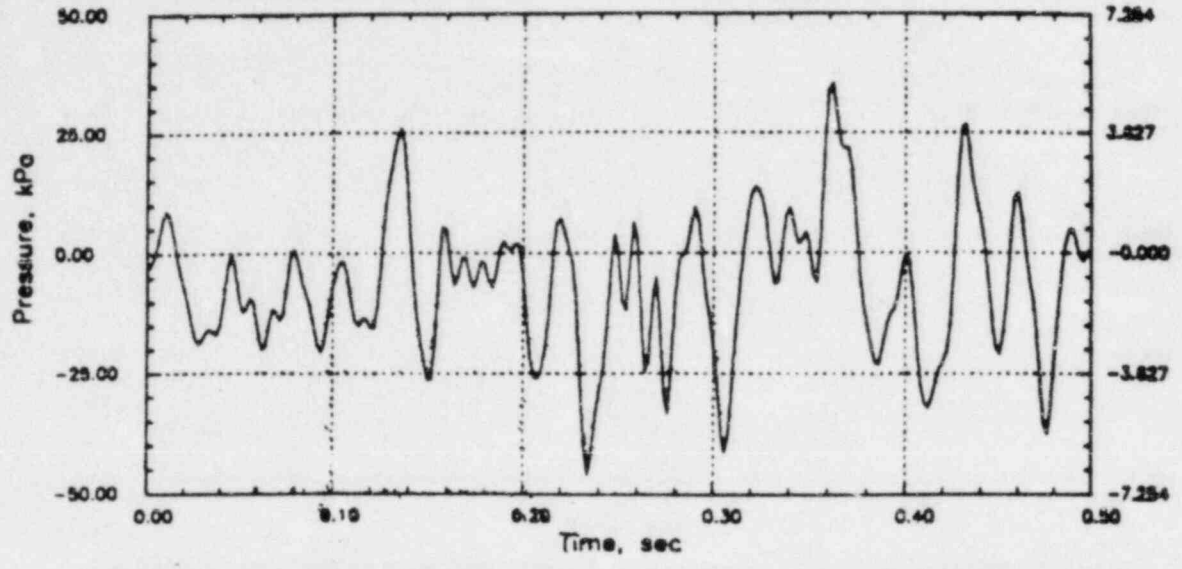

POP = 35.48 kPa PUP = -46.00 kPa MSP = 206.78 kPa²

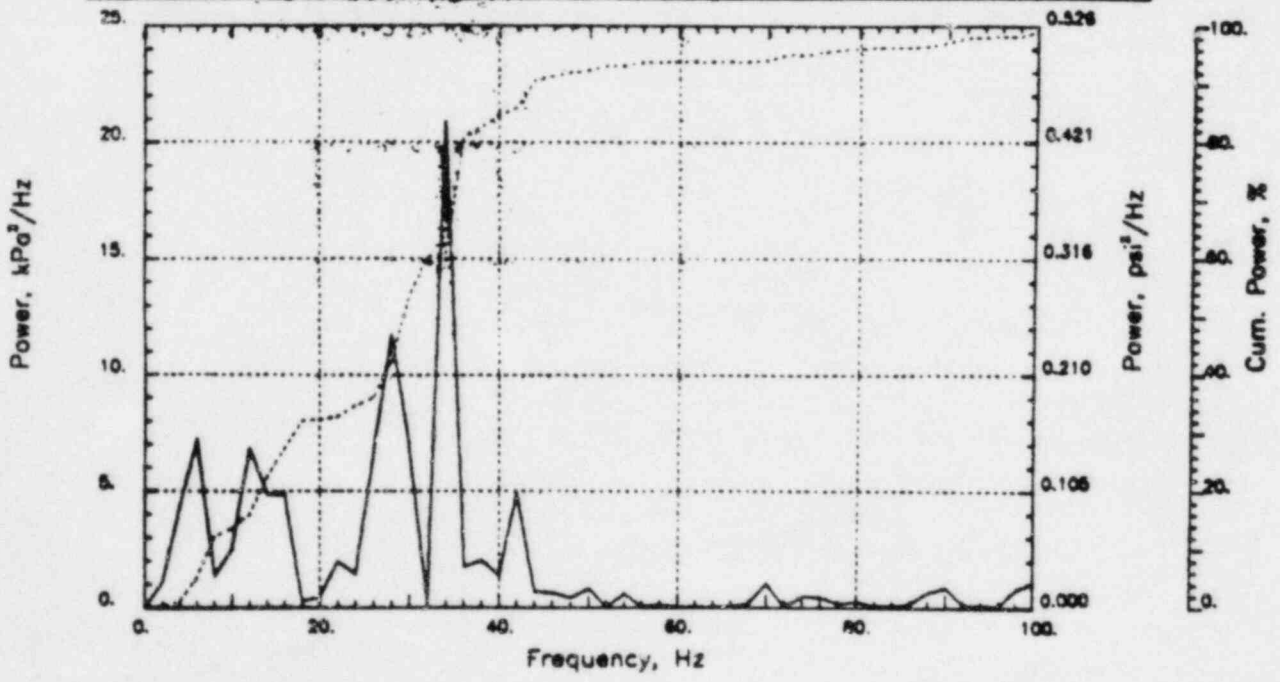

CLINTON RHR CO

Output at point (12.65,28.00,0.91)

NAME - LEONG, TAI SENG
DATE - FEB 21, 1984
PROJECT NO. - 15026004

CHECKED _____
DATE _____
CALC NO. - AP-84-

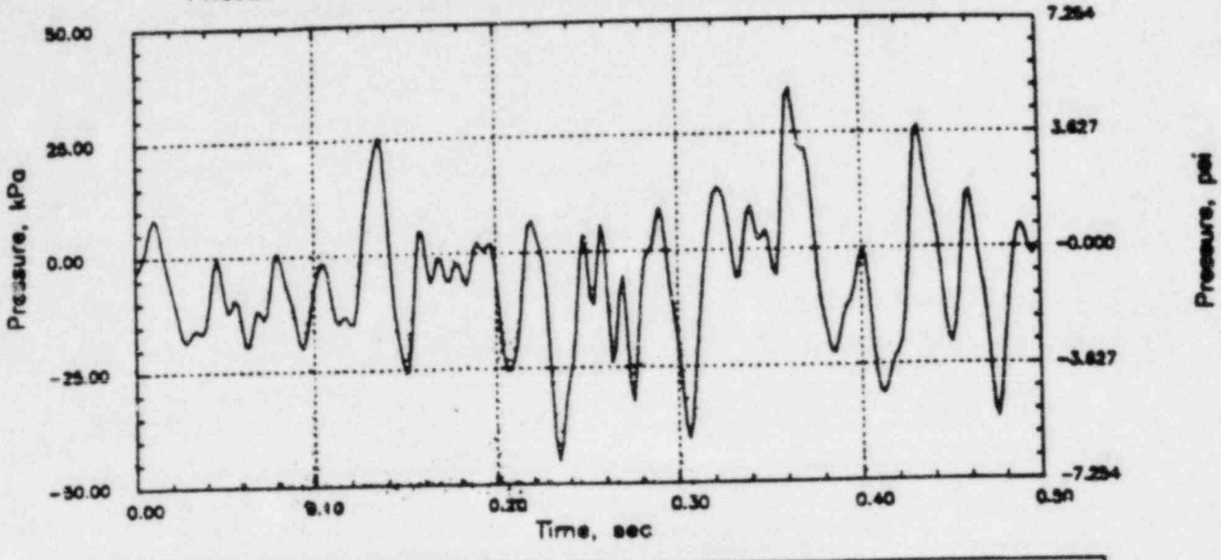

POP = 34.71 kPa PUP = -44.96 kPa MSP = 198.13 kPa²

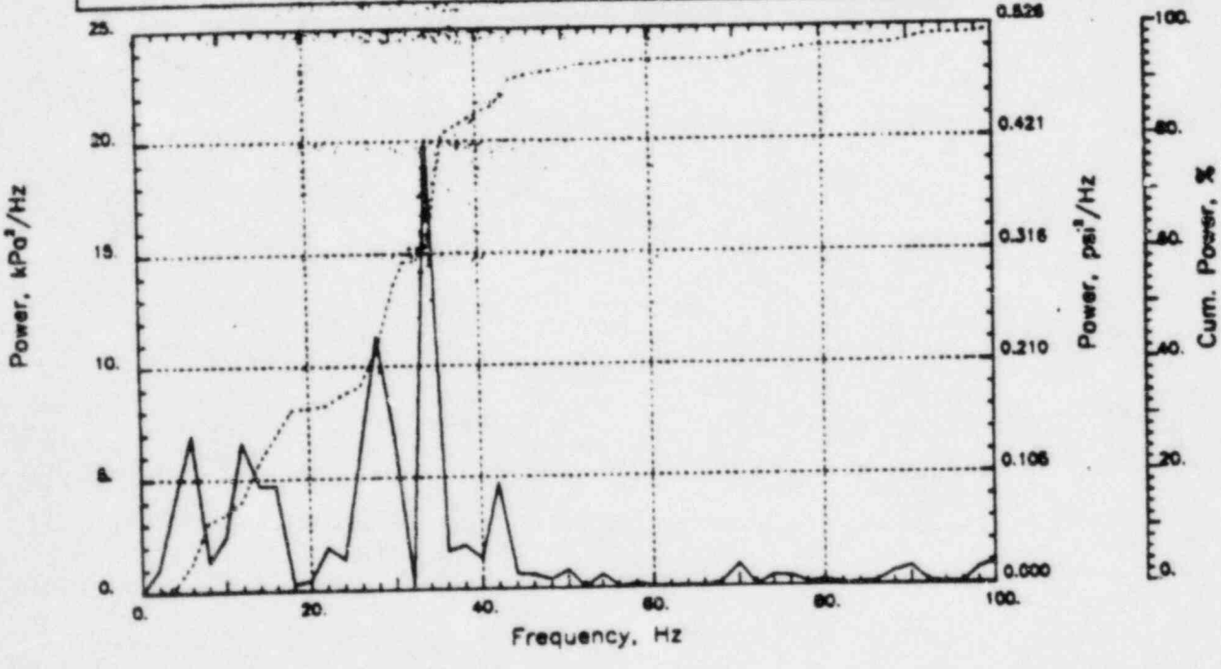

CLINTON RHR CO

Output at point (12.65,28.00,1.55)

NAME - LEONG, TAI SENG
DATE - FEB 21, 1984
PROJECT NO. - 15026004

CHECKED _____
DATE _____
CALC NO. - AP-84-

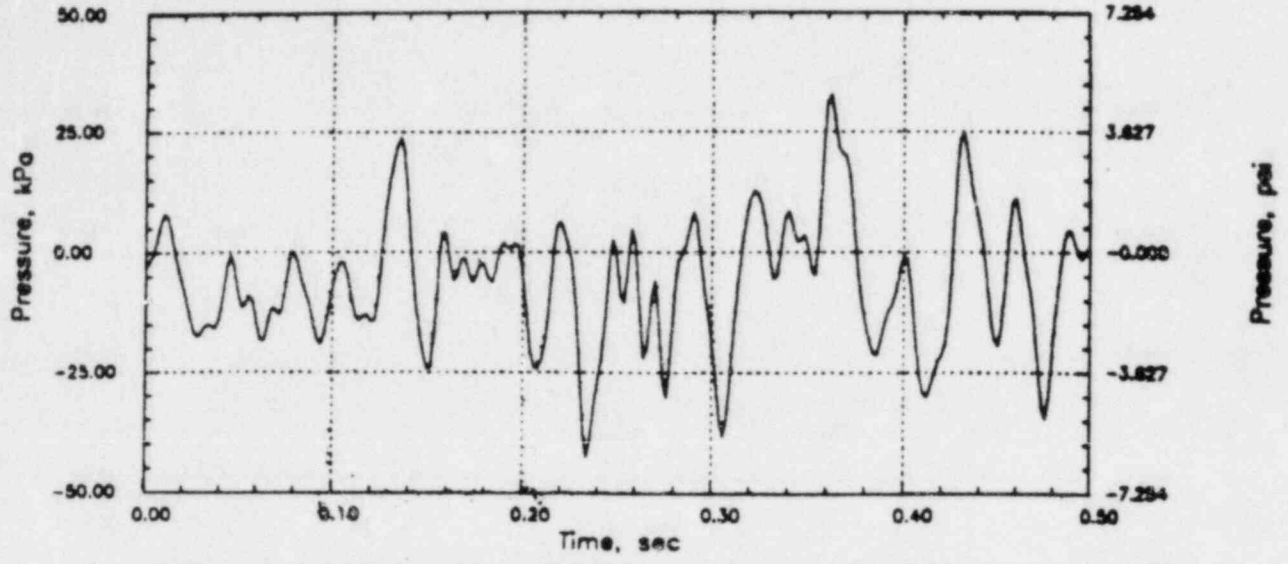

POP = 32.81 kPa PUP = -42.39 kPa MSP = 177.52 kPa²

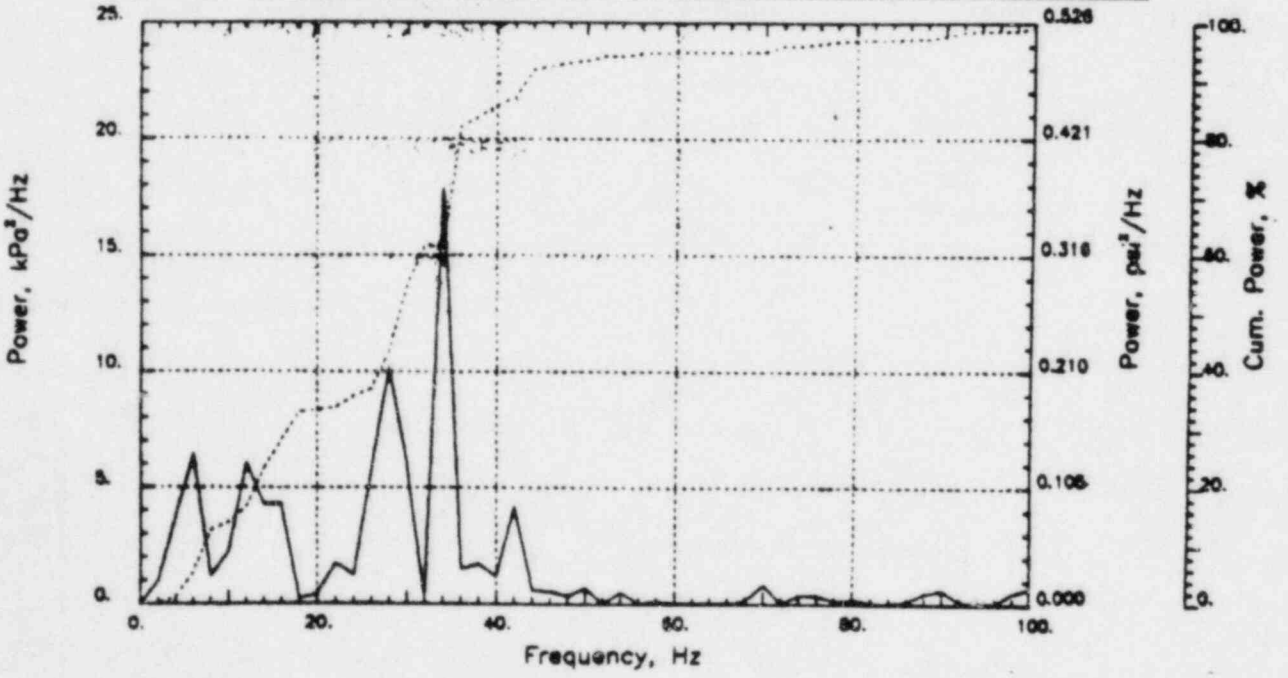

CLINTON RHR CO

Output at point (12.65,28.00,2.18)

NAME - LEONG, TAI SENG
DATE - FEB 21, 1984
PROJECT NO. - 15026004

CHECKED _____
DATE _____
CALC NO. - AP-84-

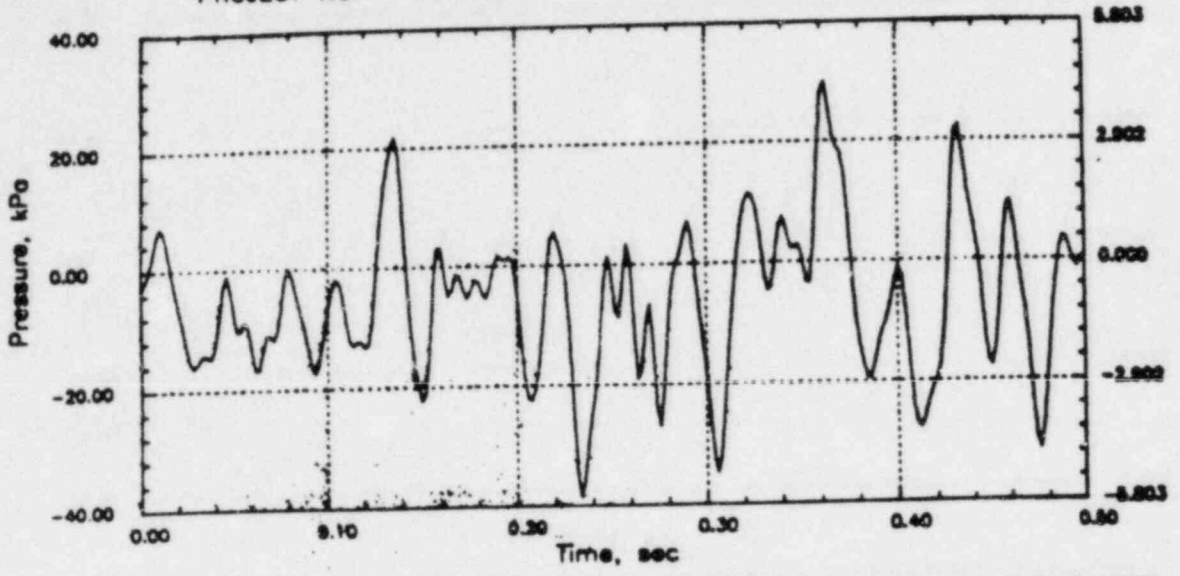

POP = 29.96 kPa PUP = -38.59 kPa MSP = 148.87 kPa²

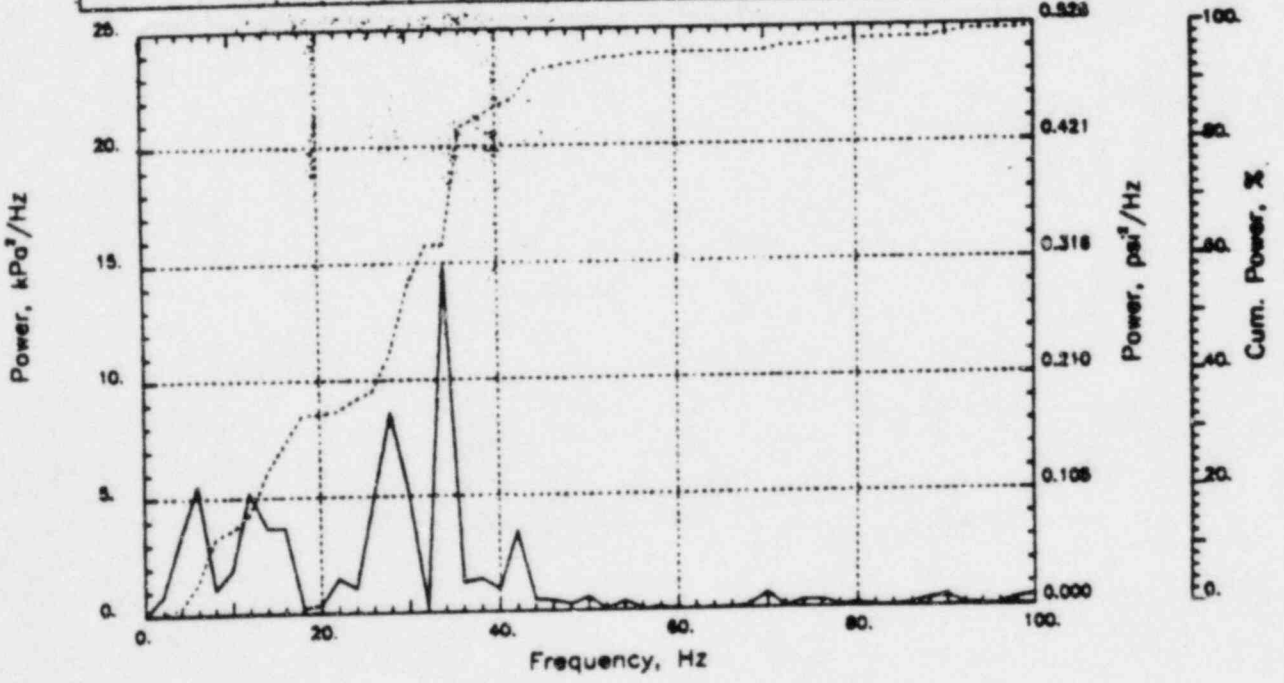

CLINTON RHR CO

Output at point (12.65,28.00,2.82)

NAME - LEONG, TAI SENG
DATE - FEB 21, 1984
PROJECT NO. - 15026004

CHECKED _____
DATE _____
CALC NO. - AP-84-

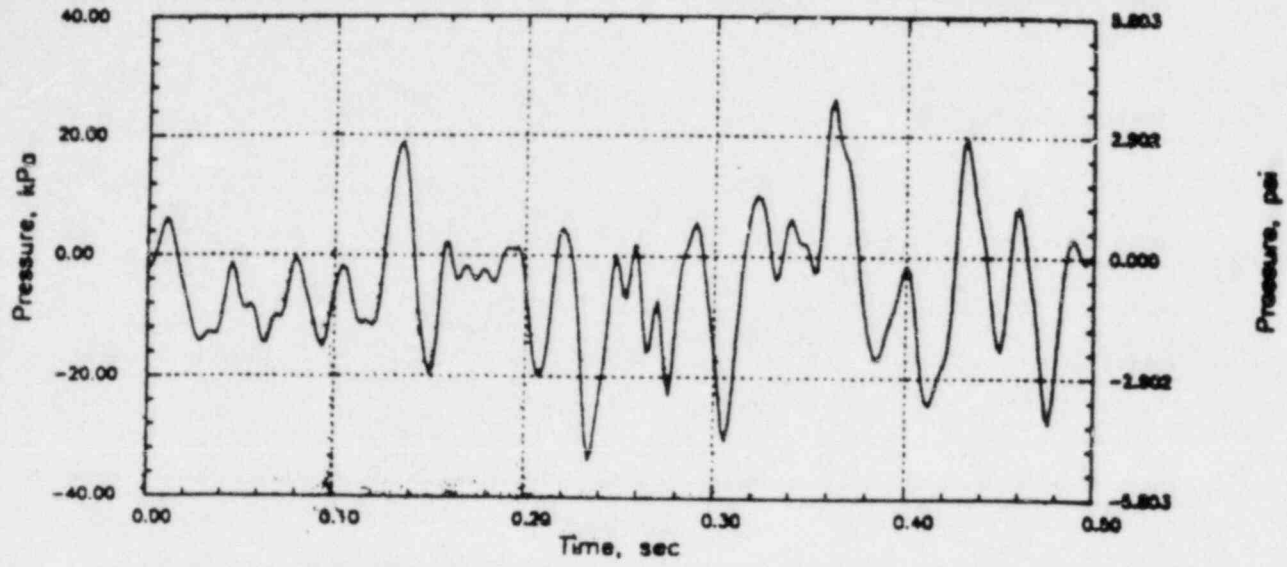

POP = 26.22 kPa PUP = -33.67 kPa MSP = 115.16 kPa²

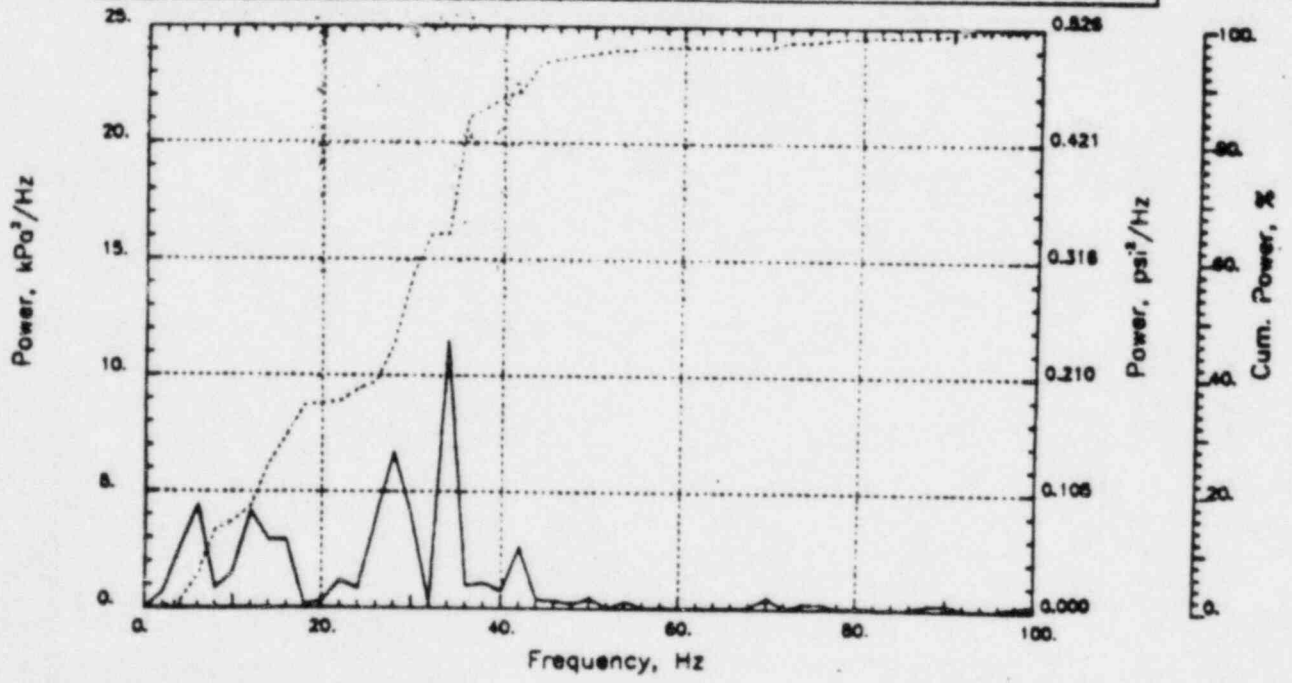

CLINTON RHR CO

Output at point (12.65,28.00,3.45)

NAME - LEONG, TAI SENG
DATE - FEB 21, 1984
PROJECT NO. - 15026004

CHECKED _____
DATE _____
CALC NO. - AP-84-

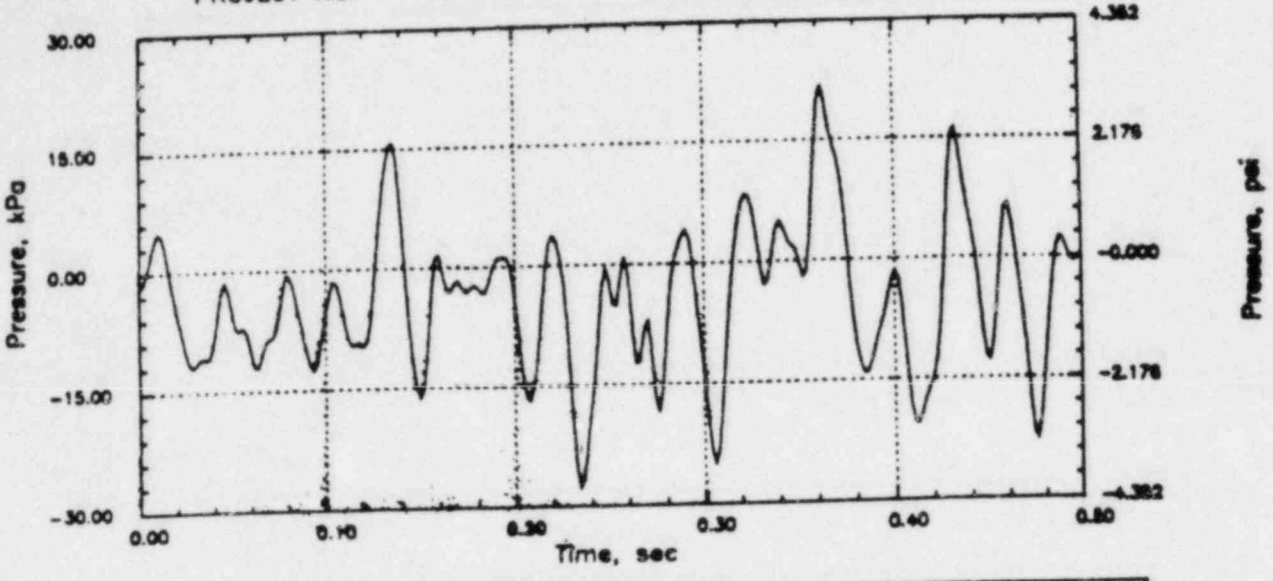

POP = 21.72 kPa PUP = -27.80 kPa MSP = 80.02 kPa²

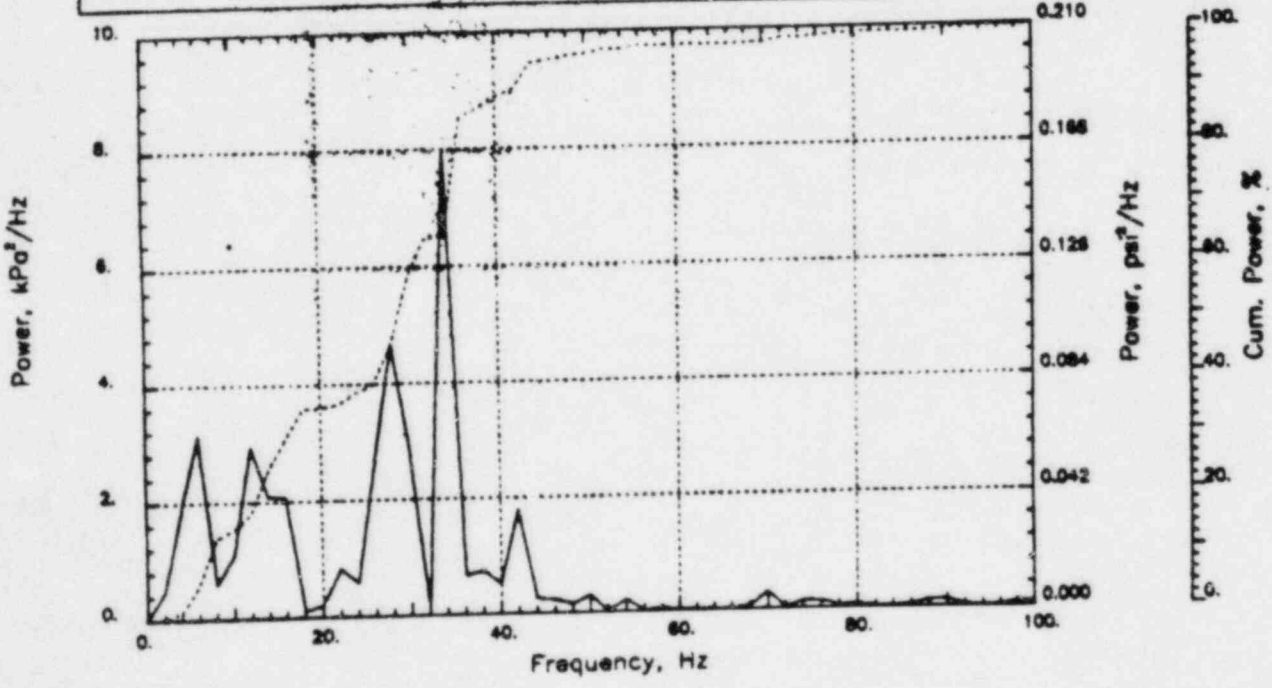

CLINTON RHR CO

Output at point (12.65,28.00,4.09)

NAME - LEONG, TAI SENG
DATE - FEB 21, 1984
PROJECT NO. - 15026004

CHECKED _____
DATE _____
CALC NO. - AP-84-

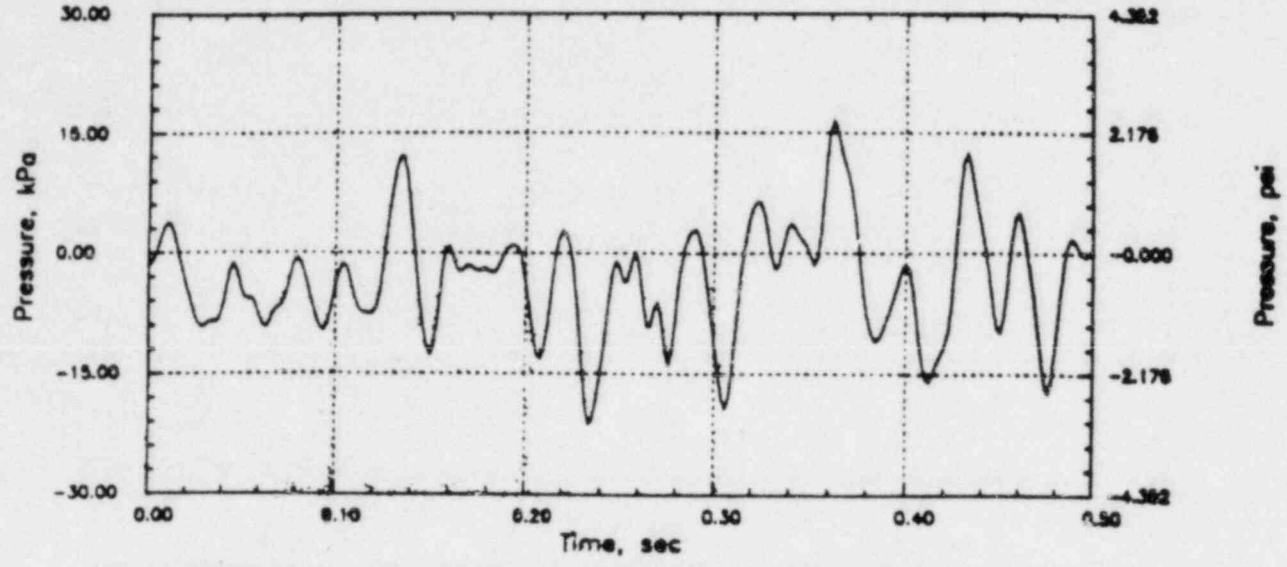

POP = 16.61 kPa PUP = -21.20 kPa MSP = 47.44 kPa²

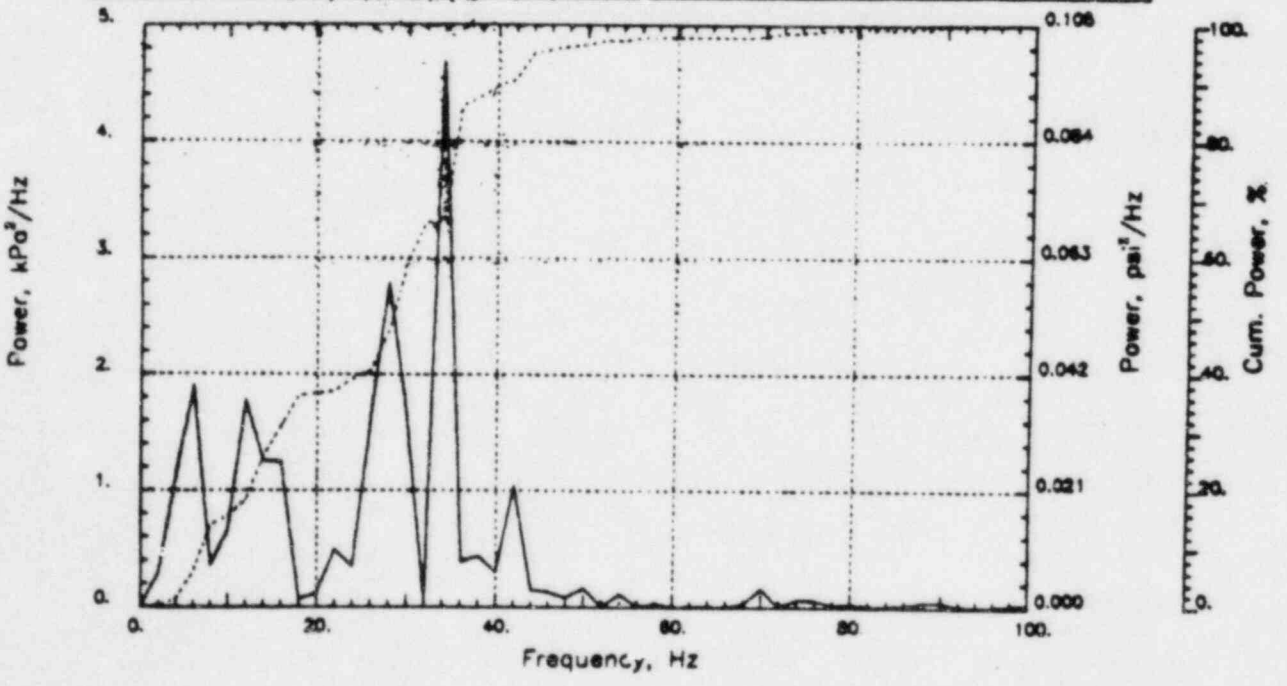

RIVER RHR CO

Output at point (18.90,28.00,2.82)

NAME - LEONG, TAI SENG
DATE - FEB 21, 1984
PROJECT NO. - 15026004

CHECKED _____
DATE _____
CALC NO. - AP-84-

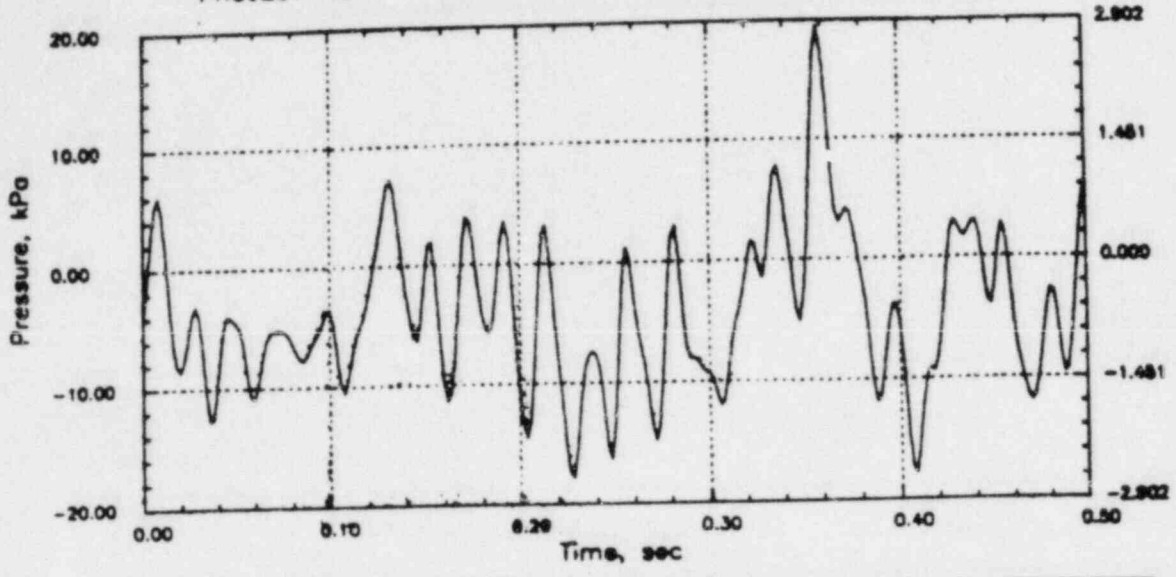

POP = 19.52 kPa PUP = -17.84 kPa MSP = 39.38 kPa²

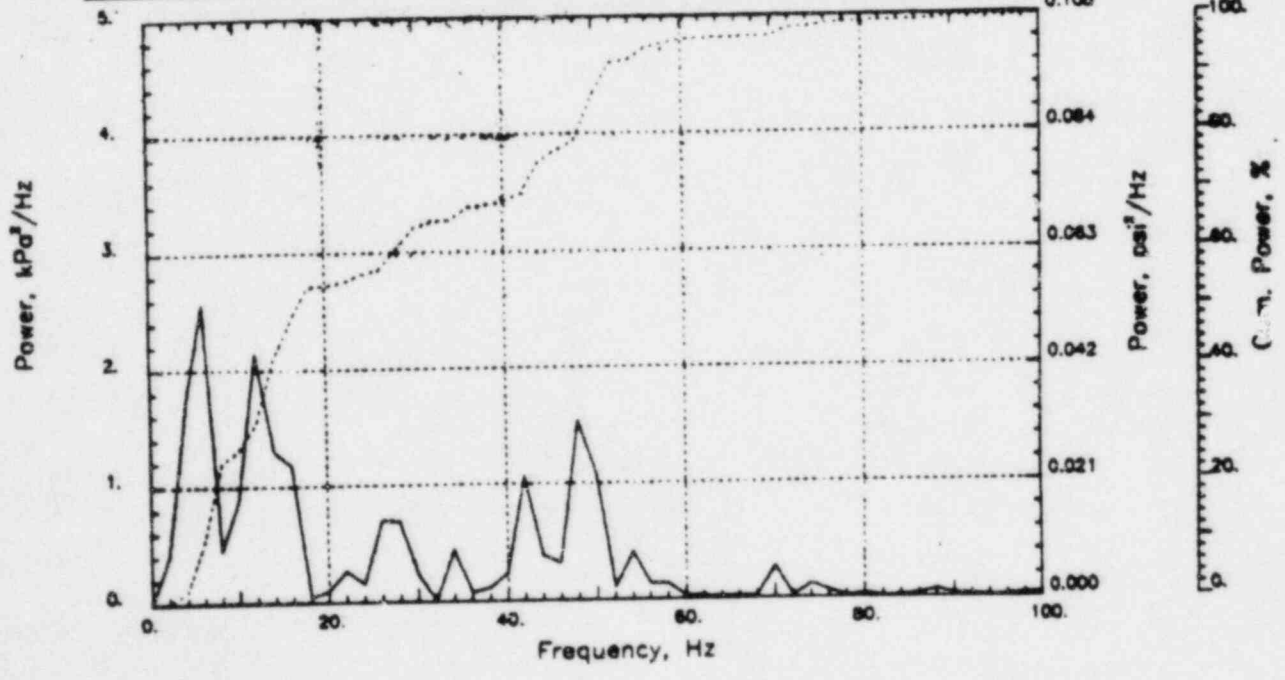

RIVER RHR CO

Output at point (18.90,28.00,2.18)

NAME - LEONG, TAI SENG
DATE - FEB 21, 1984
PROJECT NO. - 15026004

CHECKED _____
DATE _____
CALC NO. - AP-84-

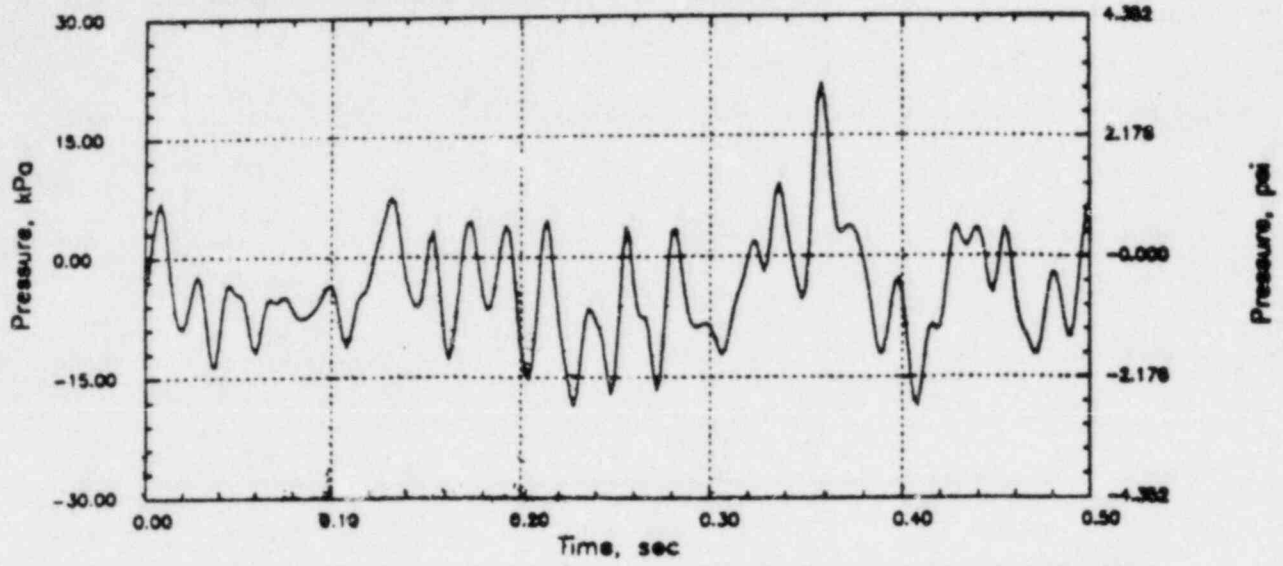

POP = 21.56 kPa PUP = -18.51 kPa MSP = 43.10 kPa²

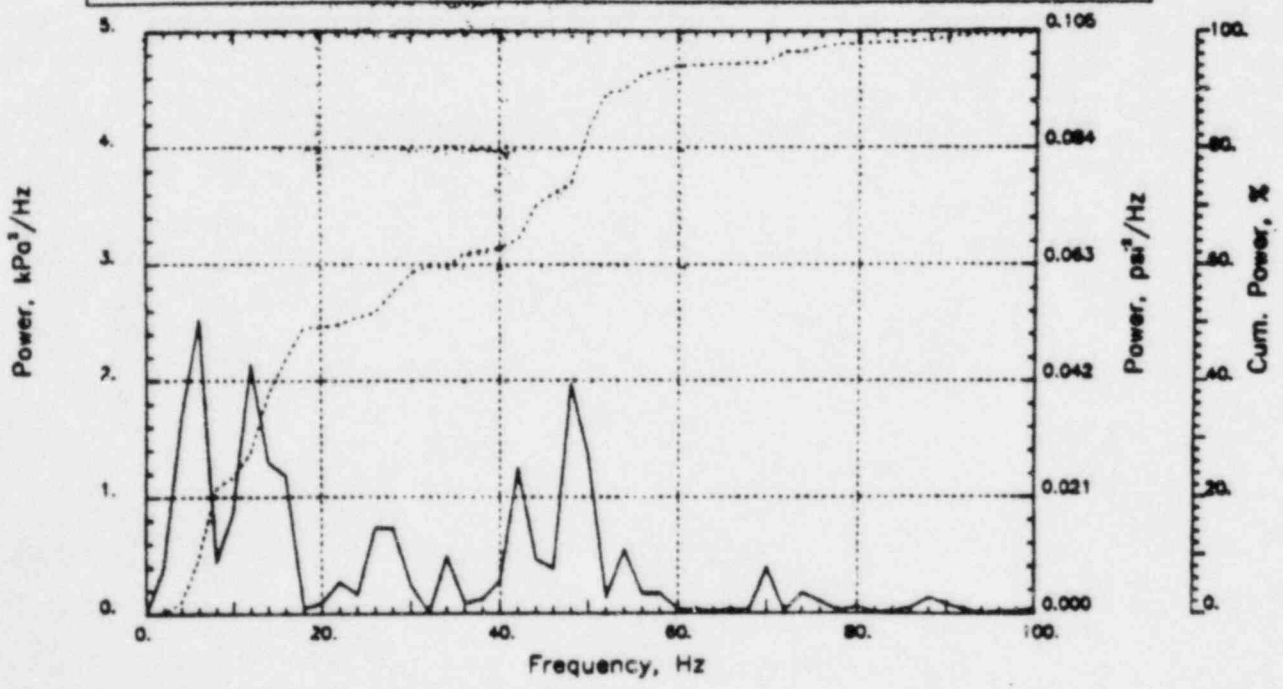

RIVER RHR CO

Output at point (18.90,28.00,1.55)

NAME - LEONG, TAI SENG
DATE - FEB 21, 1984
PROJECT NO. - 15026004

CHECKED _____
DATE _____
CALC NO. - AP-84-

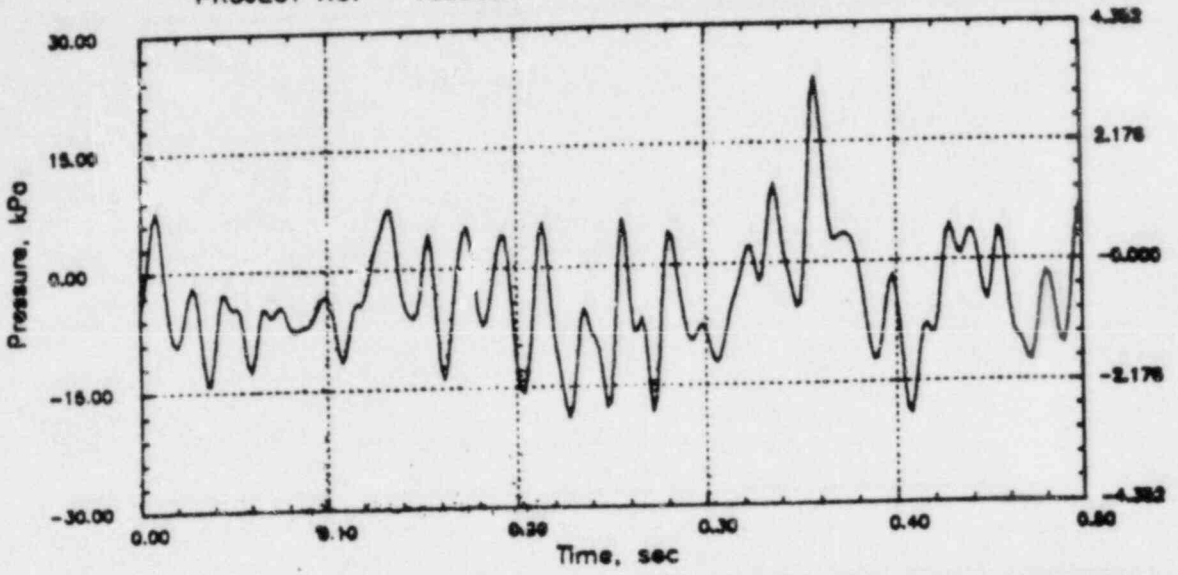

POP = 23.16 kPa PUP = -18.96 kPa MSP = 46.29 kPa²

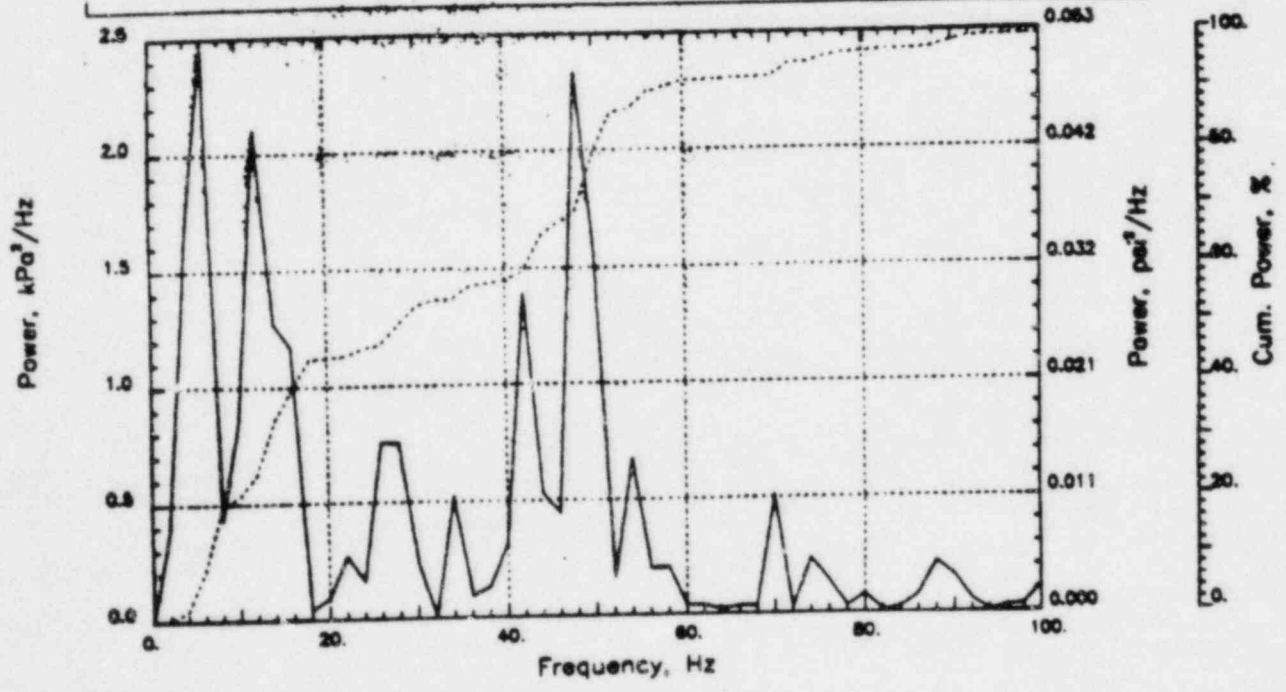

RIVER RHR CO

Output at point (18.90,28.00,0.91)

NAME - LEONG, TAI SENG
DATE - FEB 21, 1984
PROJECT NO. - 15026004

CHECKED _____
DATE _____
CALC NO. - AP-84-

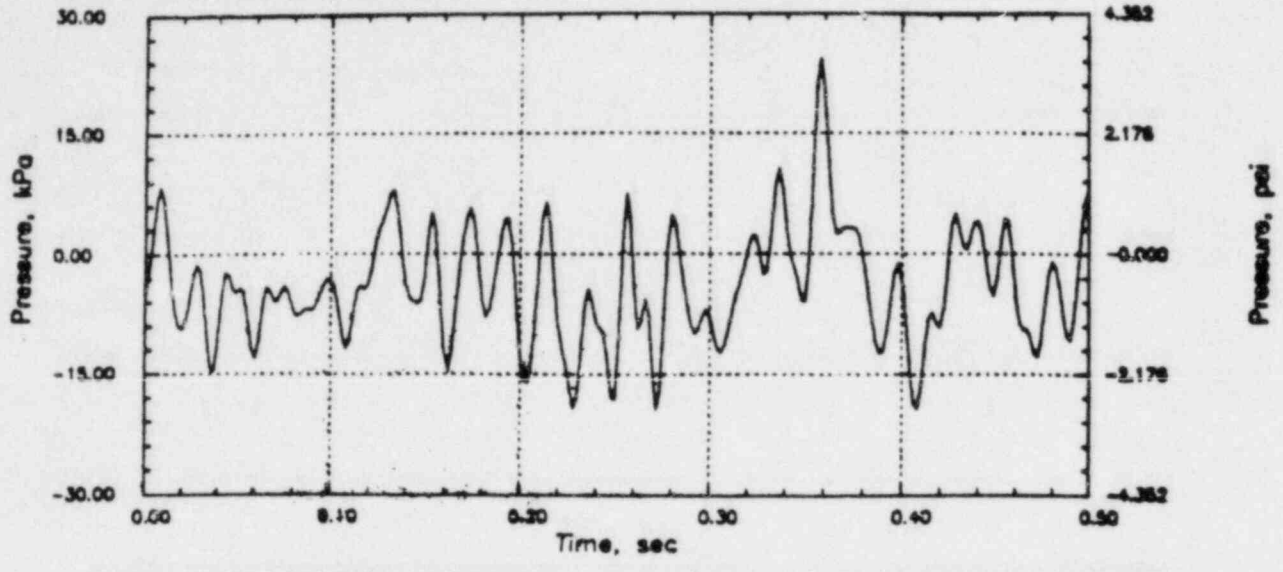

POP = 24.29 kPa PUP = -19.32 kPa MSP = 48.92 kPa²

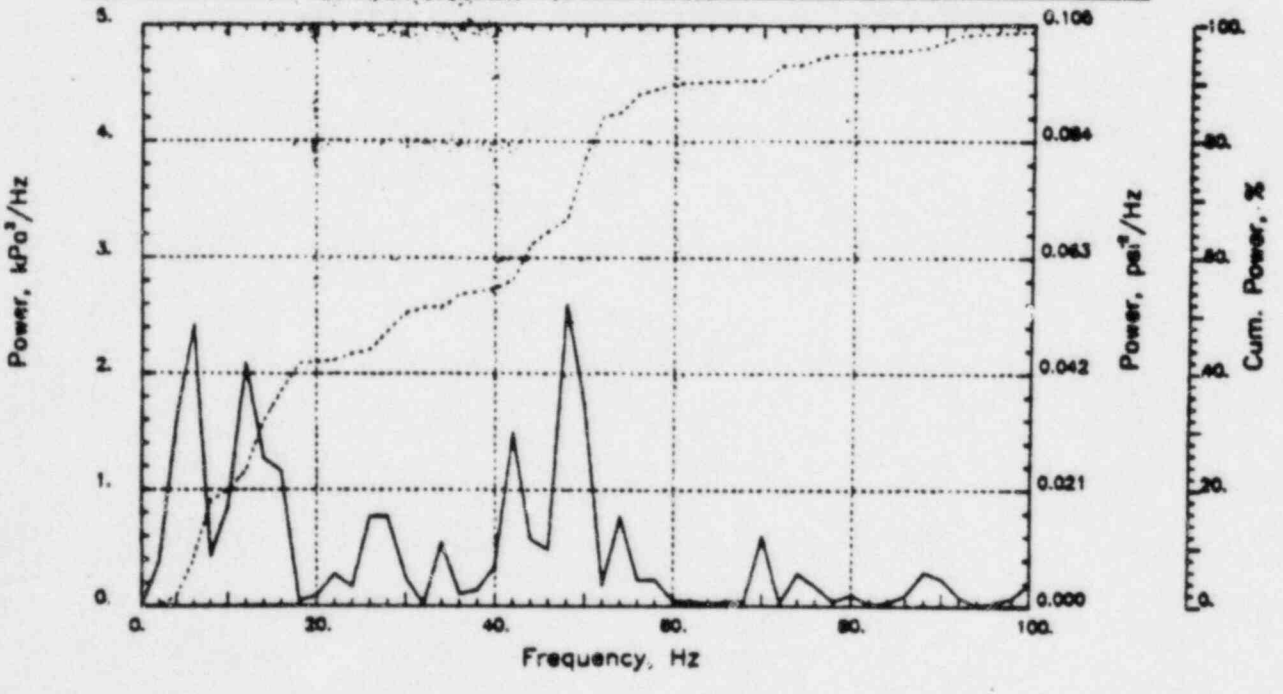

CLINTON RHR CO

Output at point (12.65,28.00,4.91)

NAME - LEONG, TAI SENG
DATE - FEB 21, 1984
PROJECT NO. - 15026004

CHECKED _____
DATE _____
CALC NO. - AP-84--

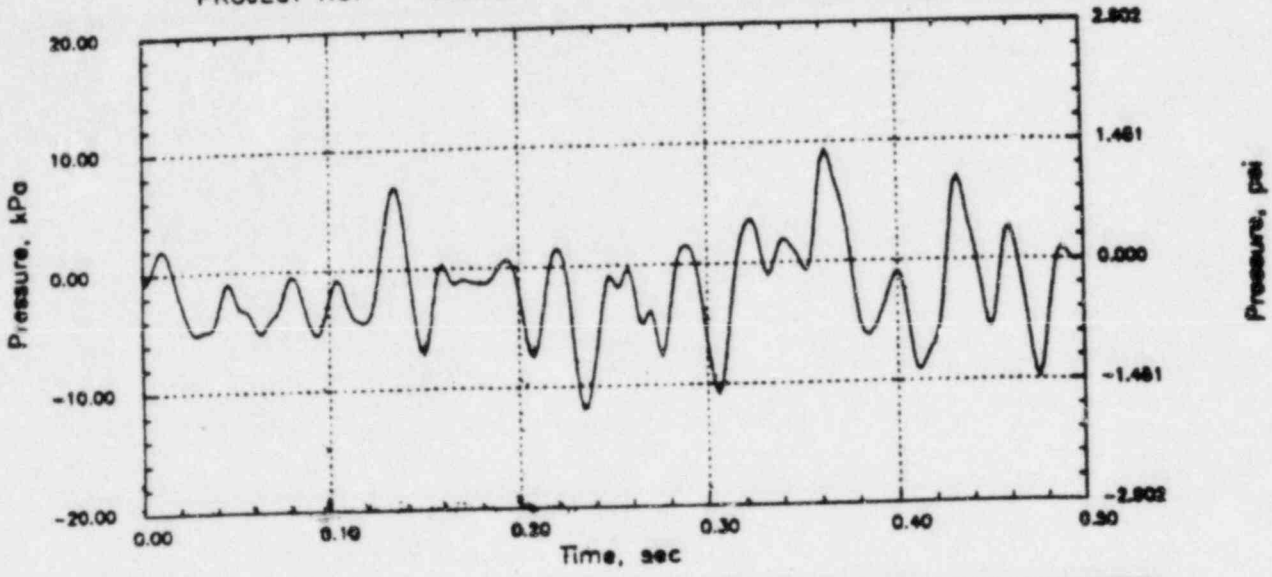

POP = 9.33 kPa PUP = -11.88 kPa MSP = 15.21 kPa²

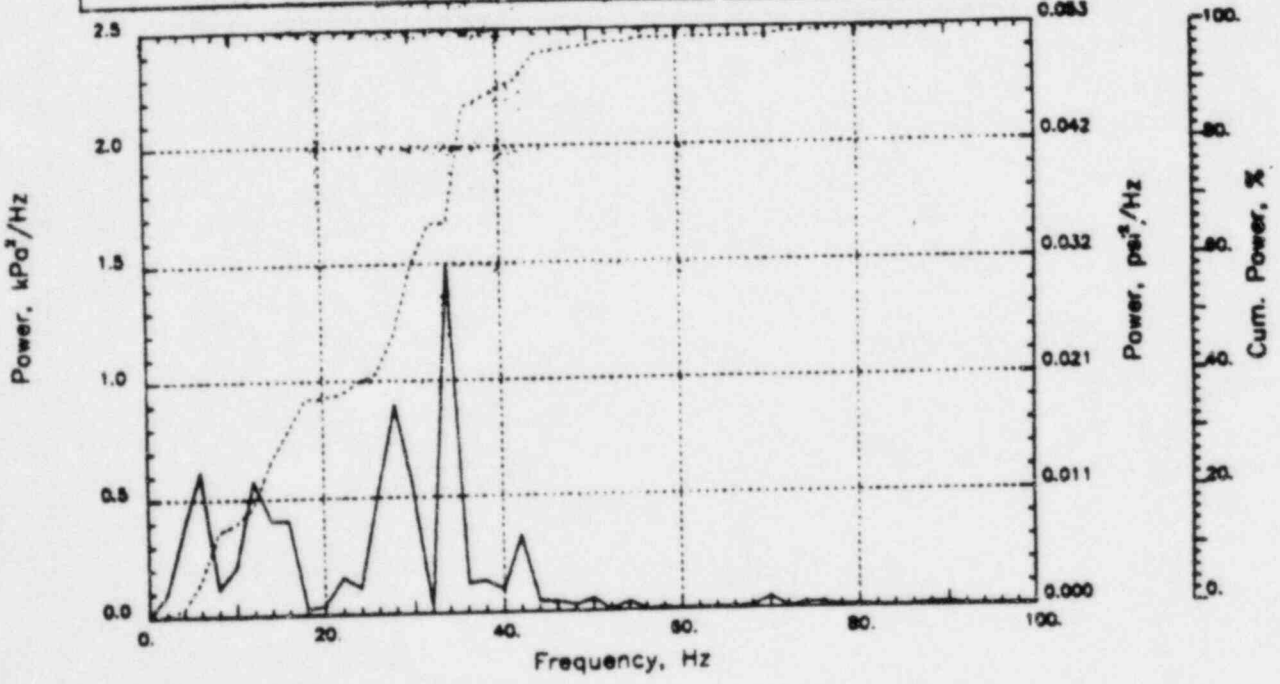

RIVER RHR CO

Output at point (18.90,28.00,4.91)

NAME - LEONG, TAI SENG
DATE - FEB 21, 1984
PROJECT NO. - 15026004

CHECKED _____
DATE _____
CALC NO. - AP-84-

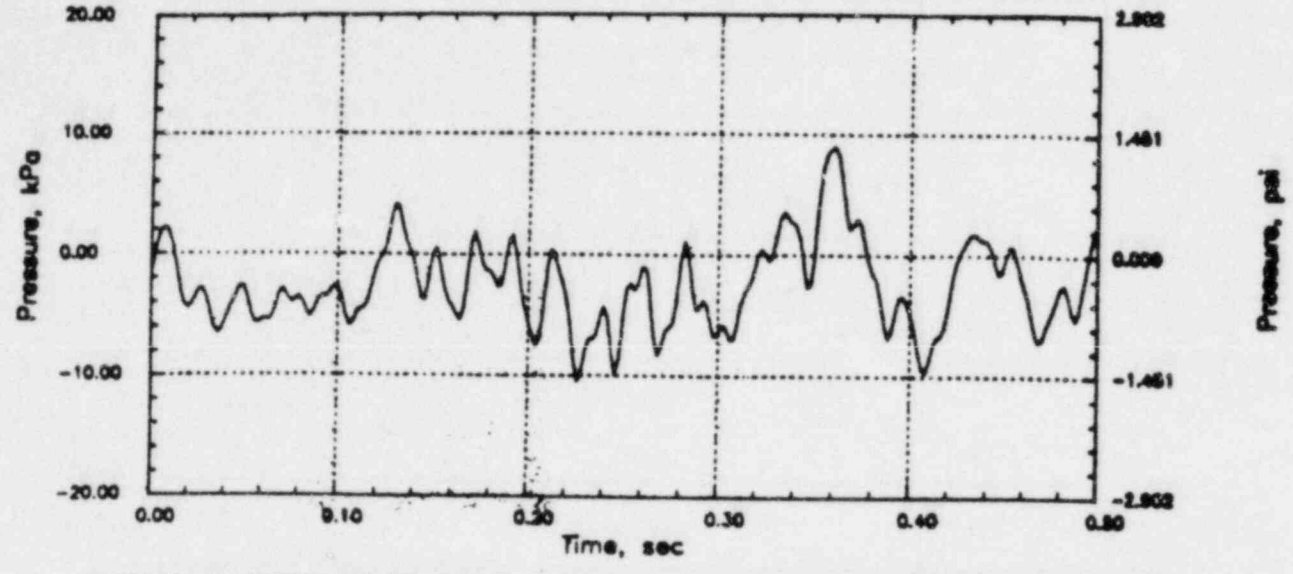

POP = 9.01 kPa PUP = -10.43 kPa MSP = 12.24 kPa²

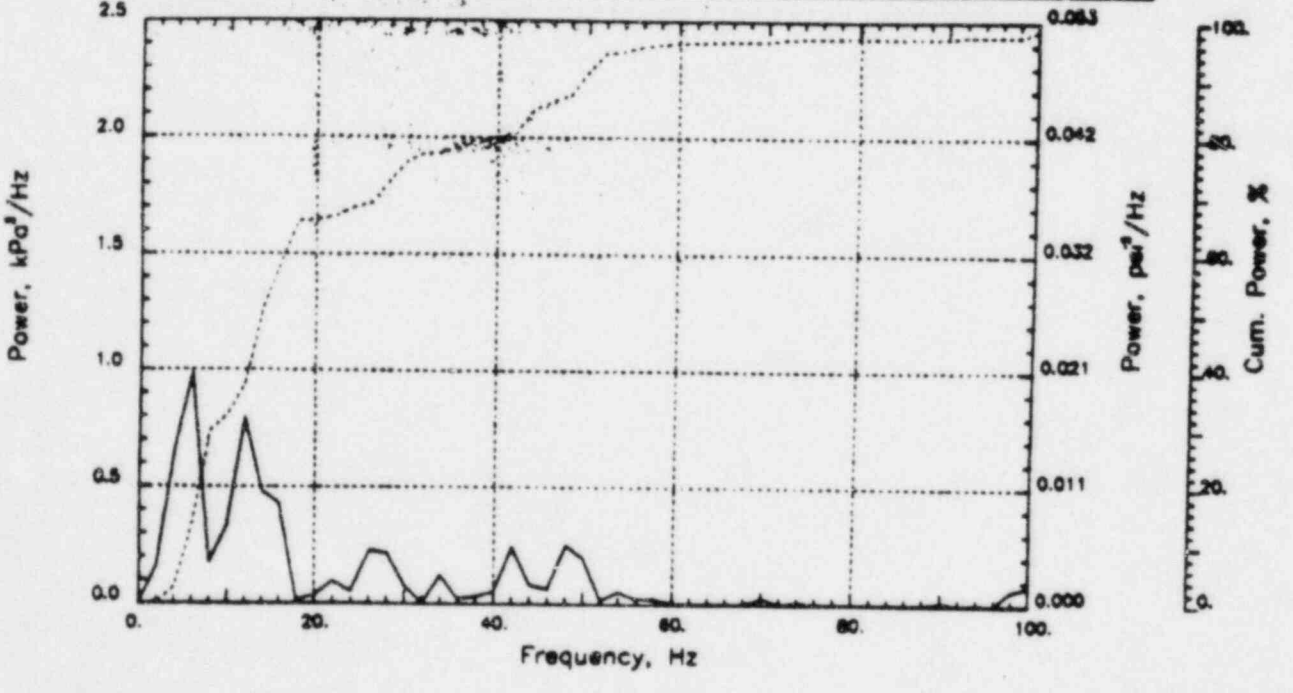

RIVER RHR CO

Output at point (18.90,28.00,4.09)

NAME - LEONG, TAI SENG
DATE - FEB 21, 1984
PROJECT NO. - 15026004

CHECKED _____
DATE _____
CALC NO. - AP-84-

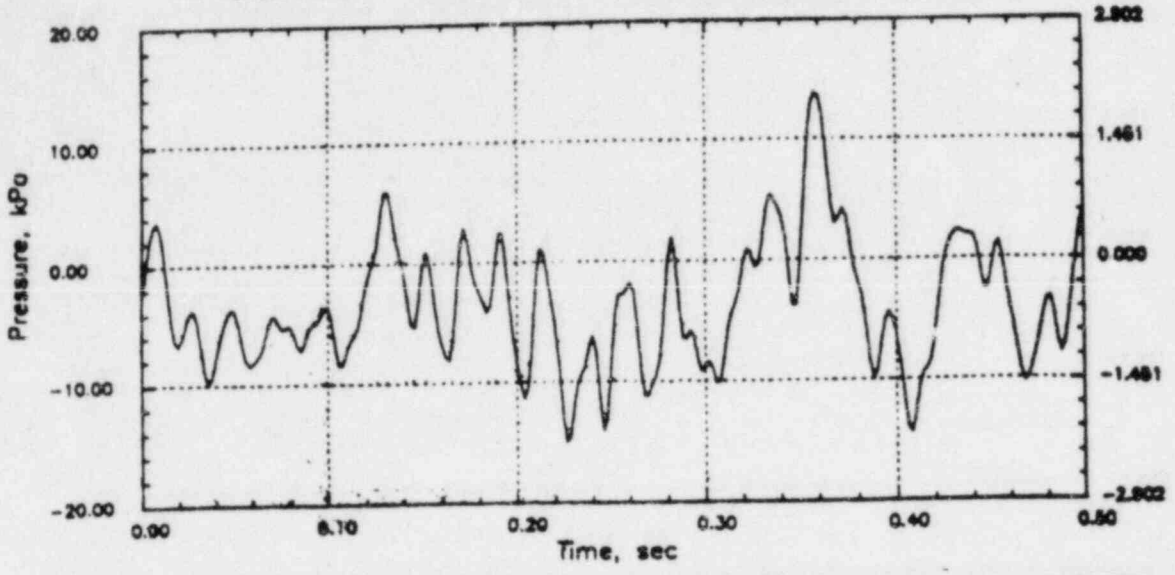

POP = 13.87 kPa PUP = -15.00 kPa MSP = 26.20 kPa²

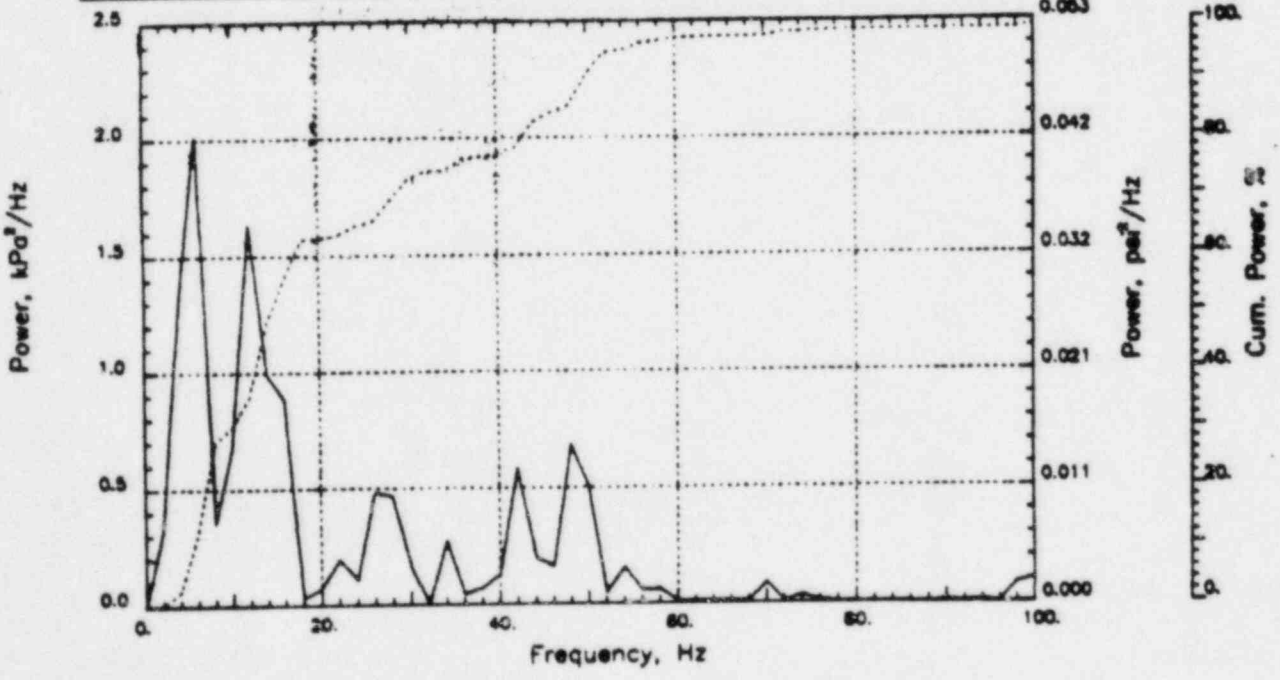

RIVER RHR CO

Output at point (18.90,28.00,3.45)

NAME - LEONG, TAI SENG
DATE - FEB 21, 1984
PROJECT NO. - 15026004

CHECKED _____
DATE _____
CALC NO. - AP-84-

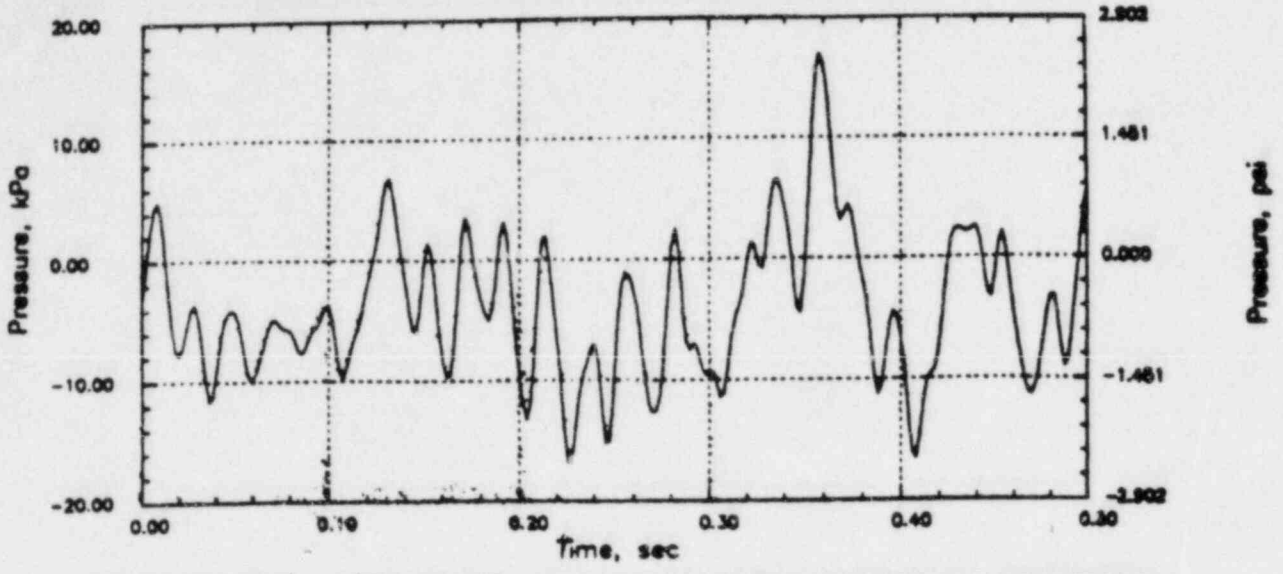

POP = 17.00 kPa PUP = -16.68 kPa MSP = 34.18 kPa²

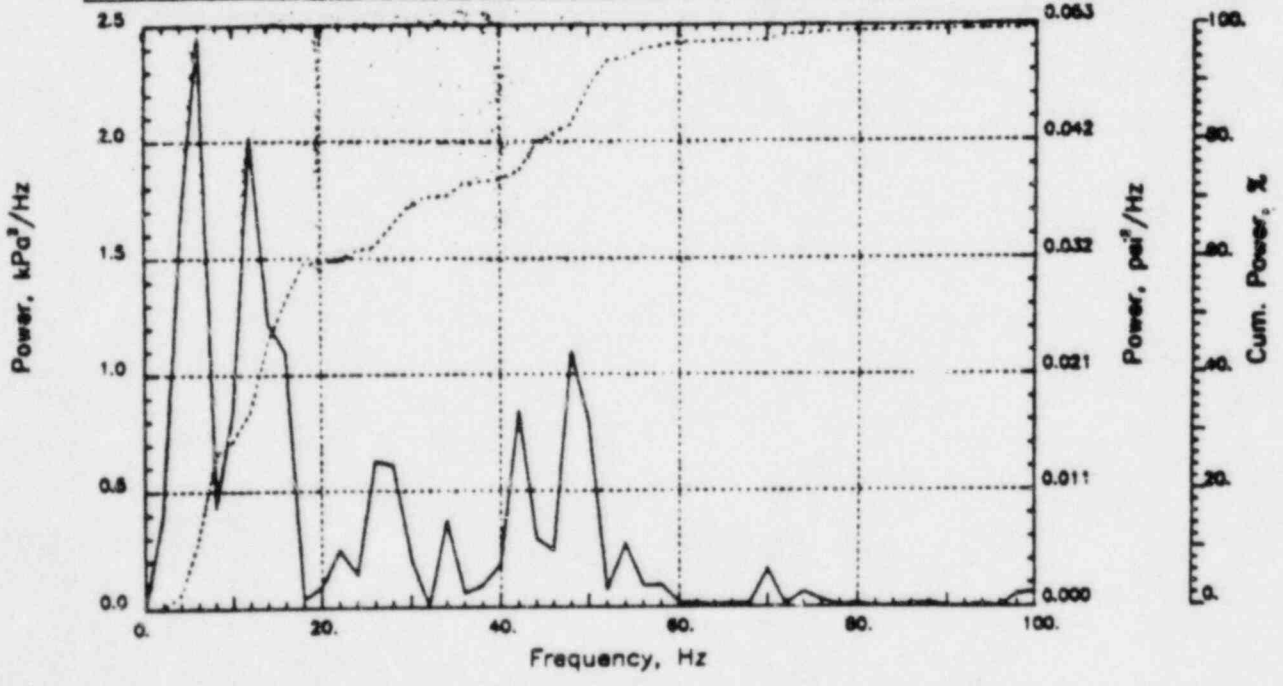

RIVER RHR CO

Output at point (18.90,28.00,0.46)

NAME - LEONG, TAI SENG
DATE - FEB 21, 1984
PROJECT NO. - 15026004

CHECKED _____
DATE _____
CALC NO. - AP-84-

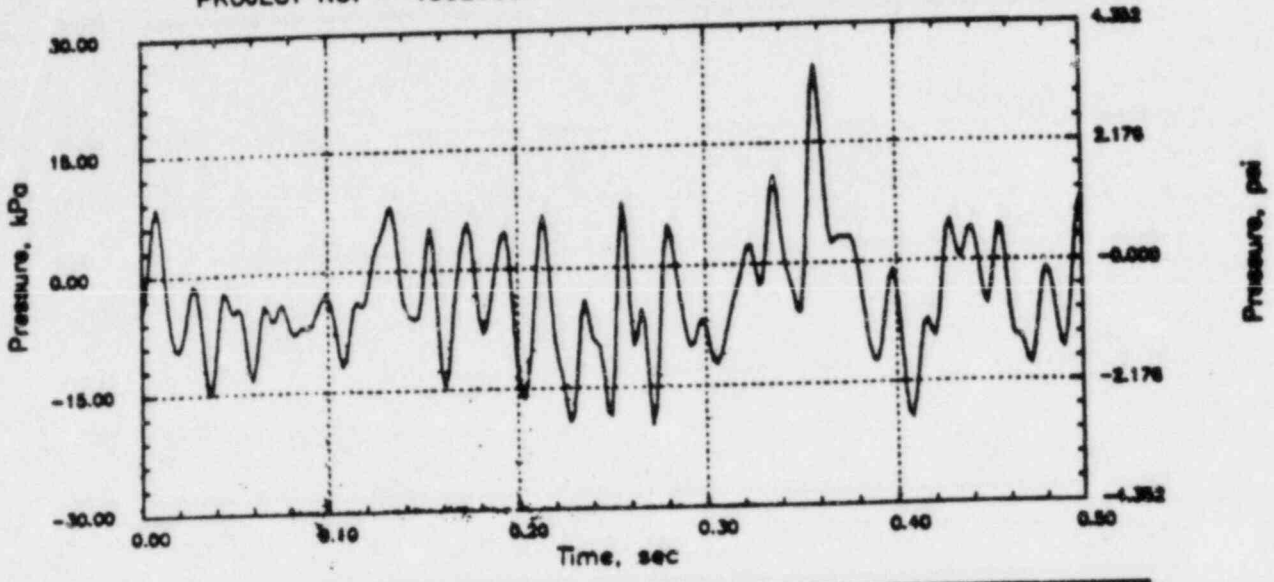

POP = 24.77 kPa PUP = -19.79 kPa MSP = 50.15 kPa²

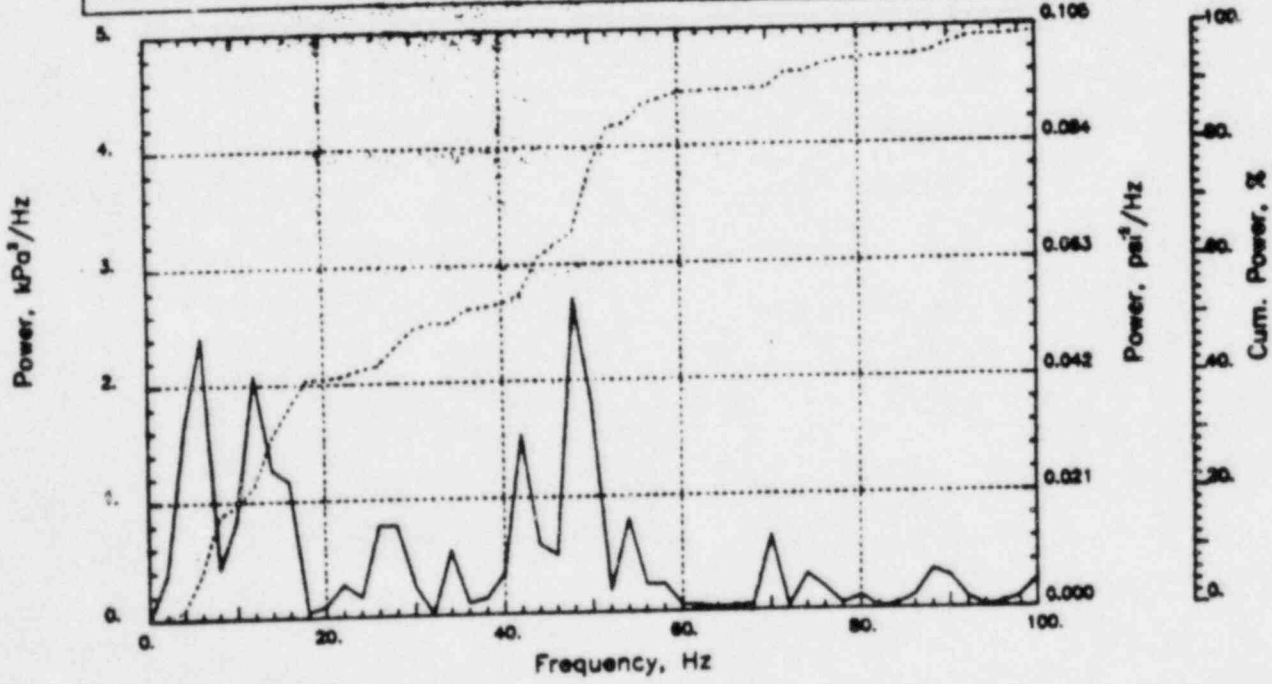

RIVER RHR CO

Output at point (18.90,28.00,0.00)

NAME - LEONG, TAI SENG
DATE - FEB 21, 1984
PROJECT NO. - 15026004

CHECKED _____
DATE _____
CALC NO. - AP-84-

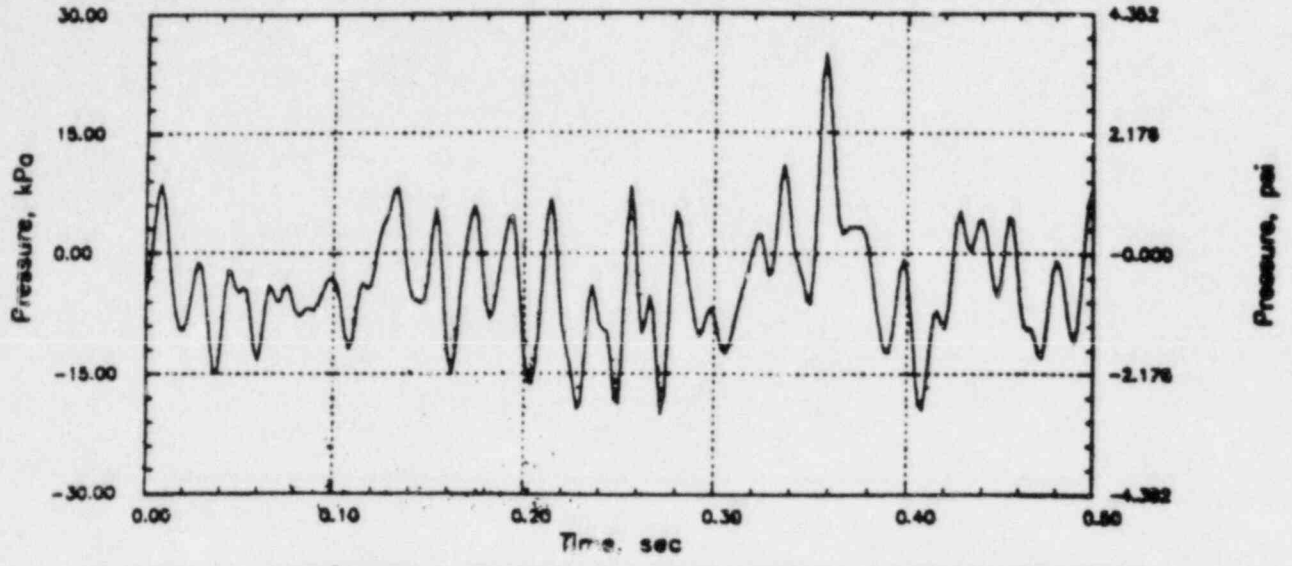

POP = 24.93 kPa PUP = -19.95 kPa MSP = 50.59 kPa²

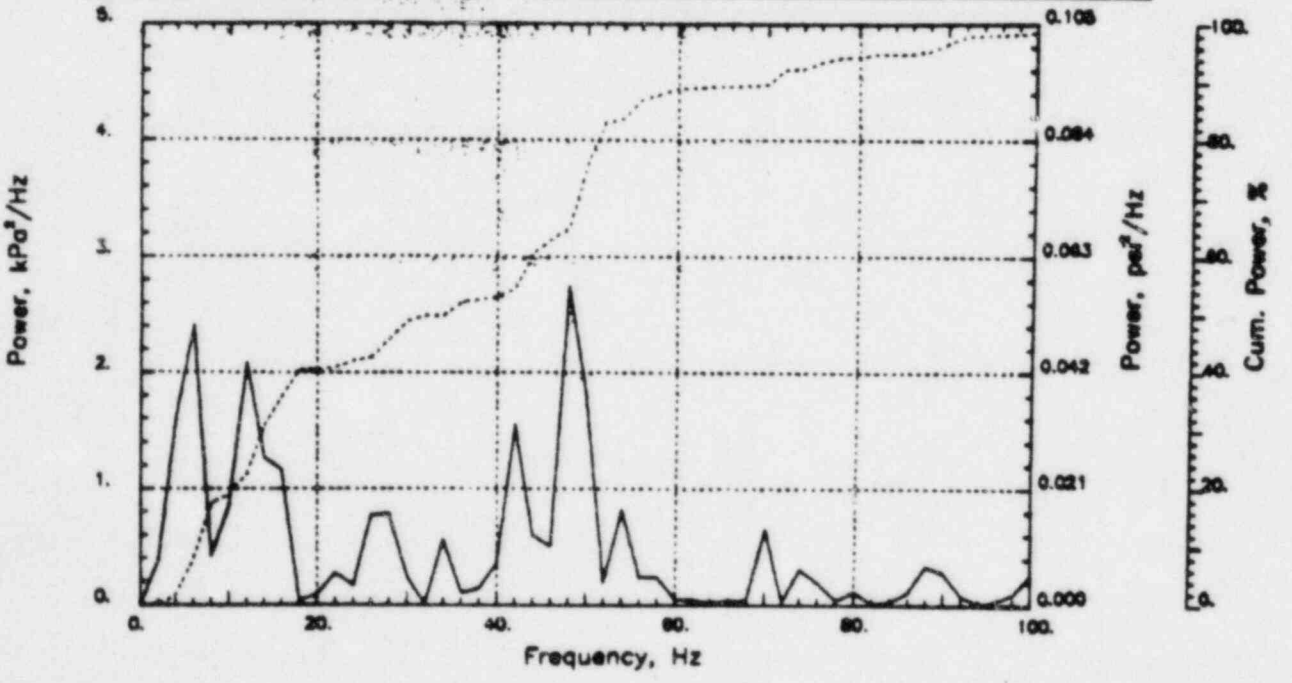

RIVER RHR CO

Output at point (17.34,28.00,0.00)

NAME - LEONG, TAI SENG
DATE - FEB 21, 1984
PROJECT NO. - 15026004

CHECKED _____
DATE _____
CALC NO. - AP-84-

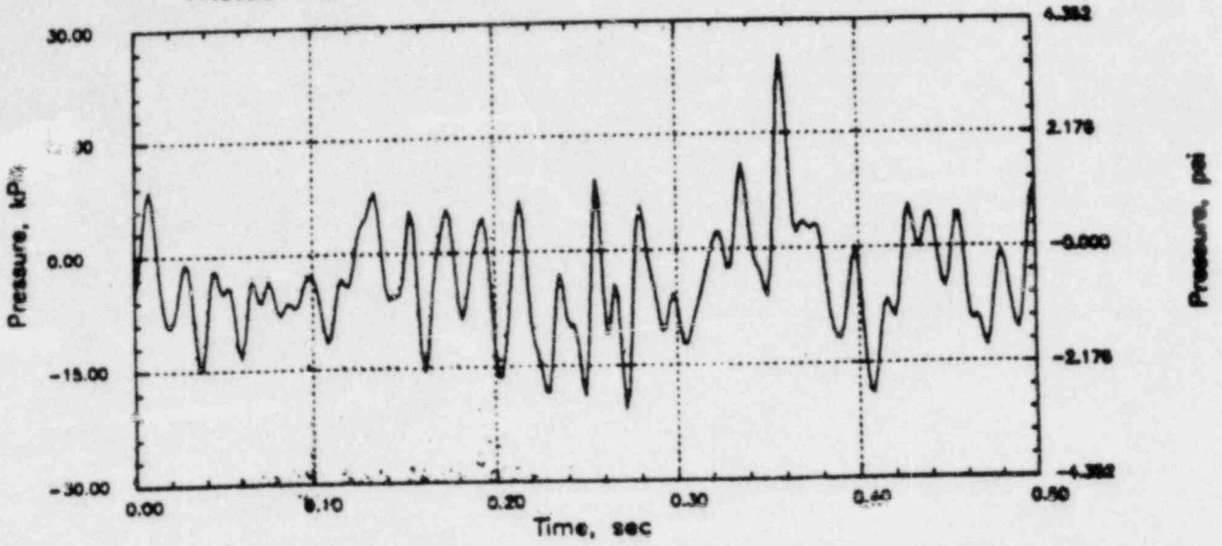

POP = 25.31 kPa PUP = -20.55 kPa MSP = 49.82 kPa²

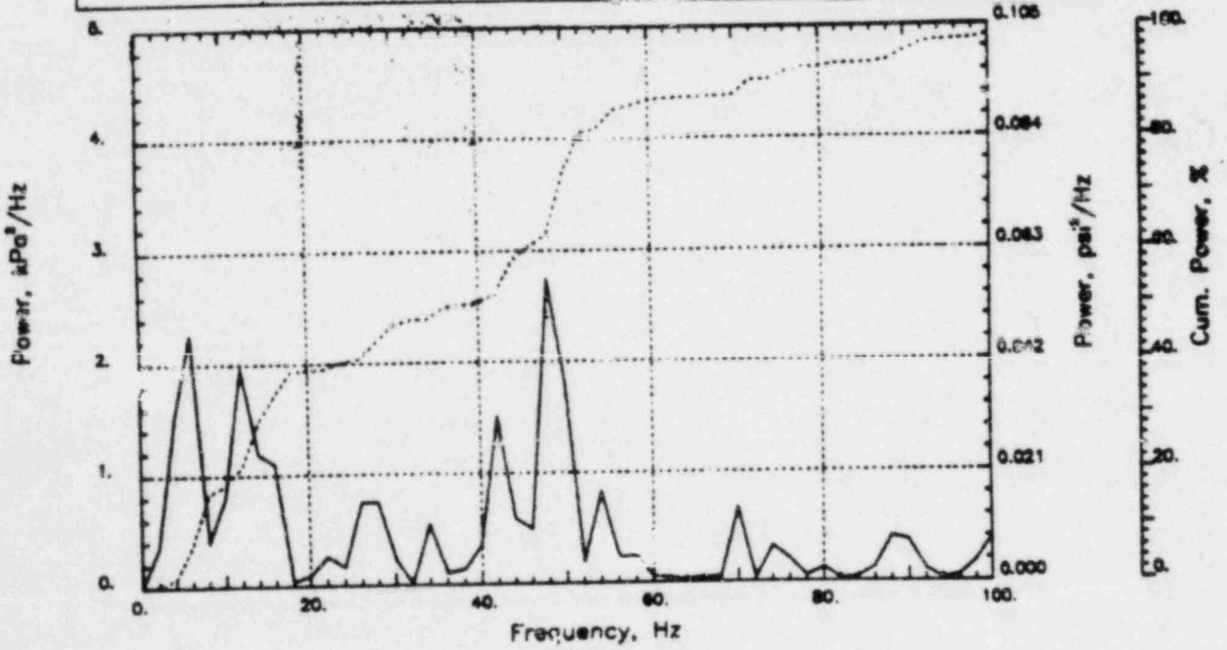

RIVER RHR CO

Output at point (15.77,28.00,0.00)

NAME - LEONG, TAI SENG
DATE - FEB 21, 1984
PROJECT NO. - 15026004

CHECKED _____
DATE _____
CALC NO. - AP-84-

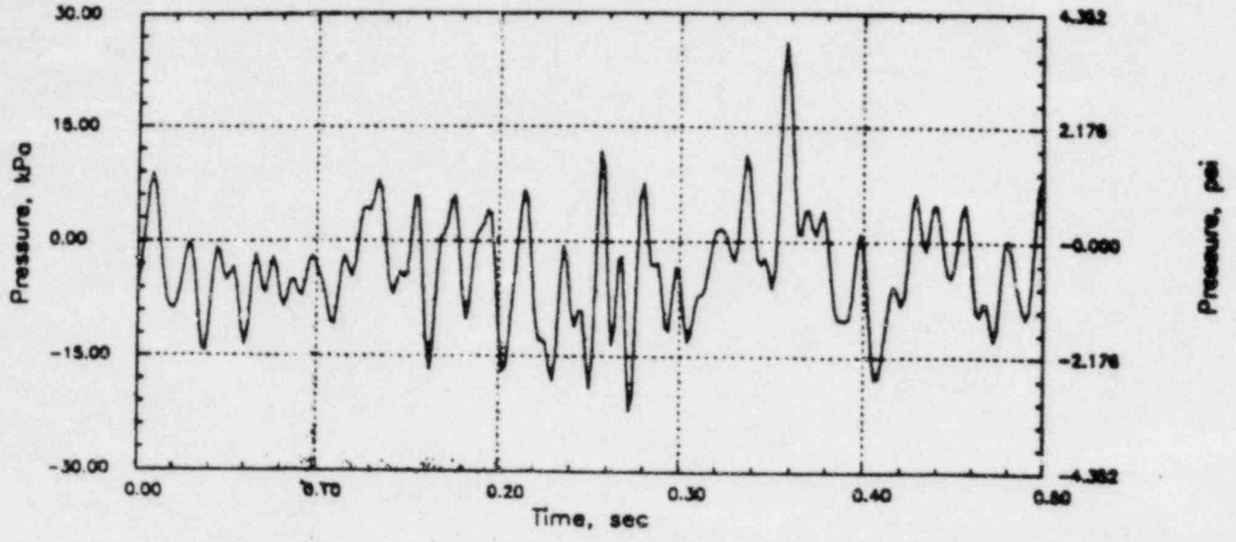

POP = 26.32 kPa PUP = -22.12 kPa MSP = 49.51 kPa²

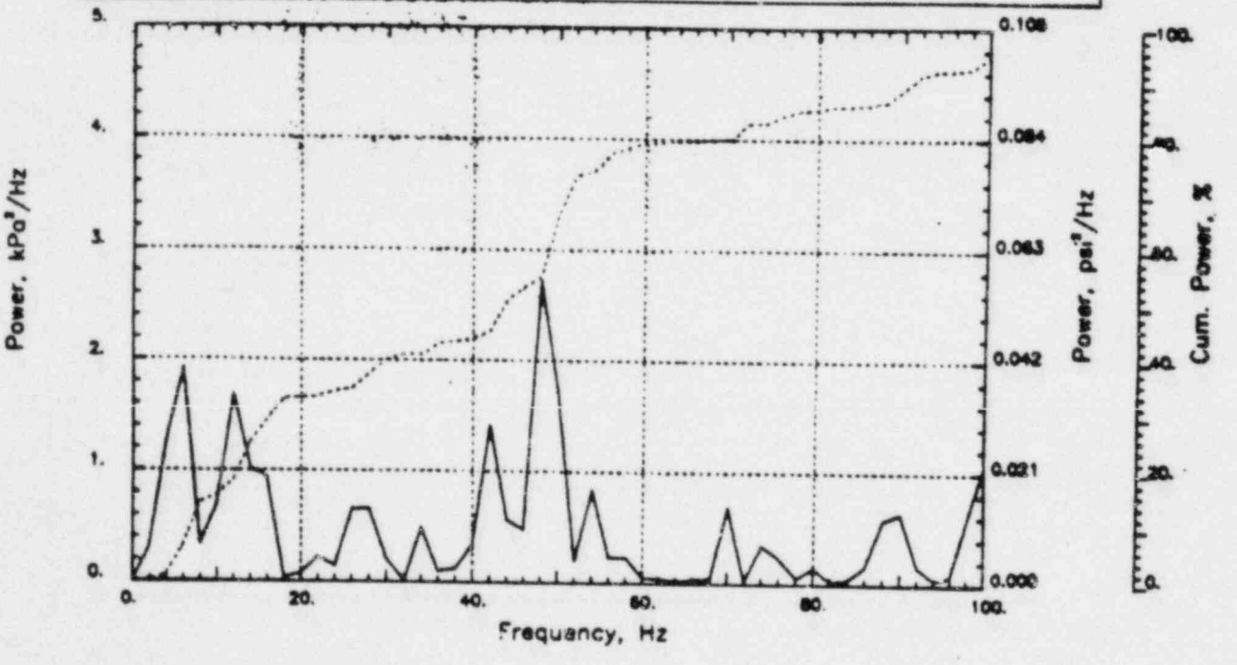

RIVER RHR CO

Output at point (14.21,28.00,0.00)

NAME - LEONG, TAI SENG
DATE - FEB 21, 1984
PROJECT NO. - 15026004

CHECKED _____
DATE _____
CALC NO. - AP-84-

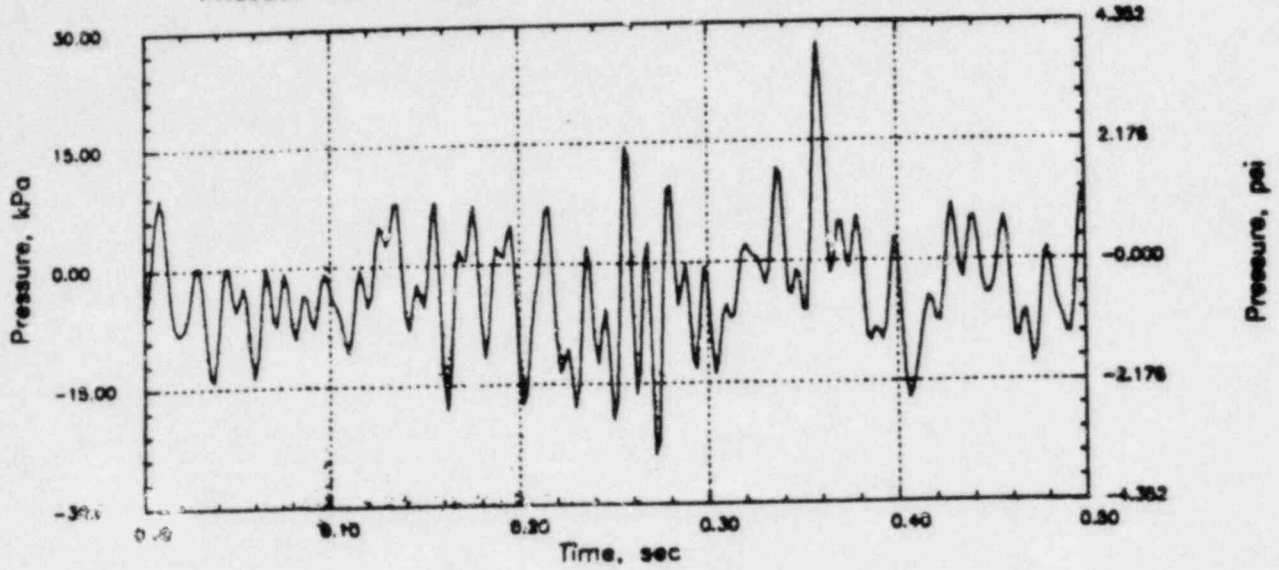

POP = 27.39 kPa PUP = -23.81 kPa MSP = 51.63 kPa²

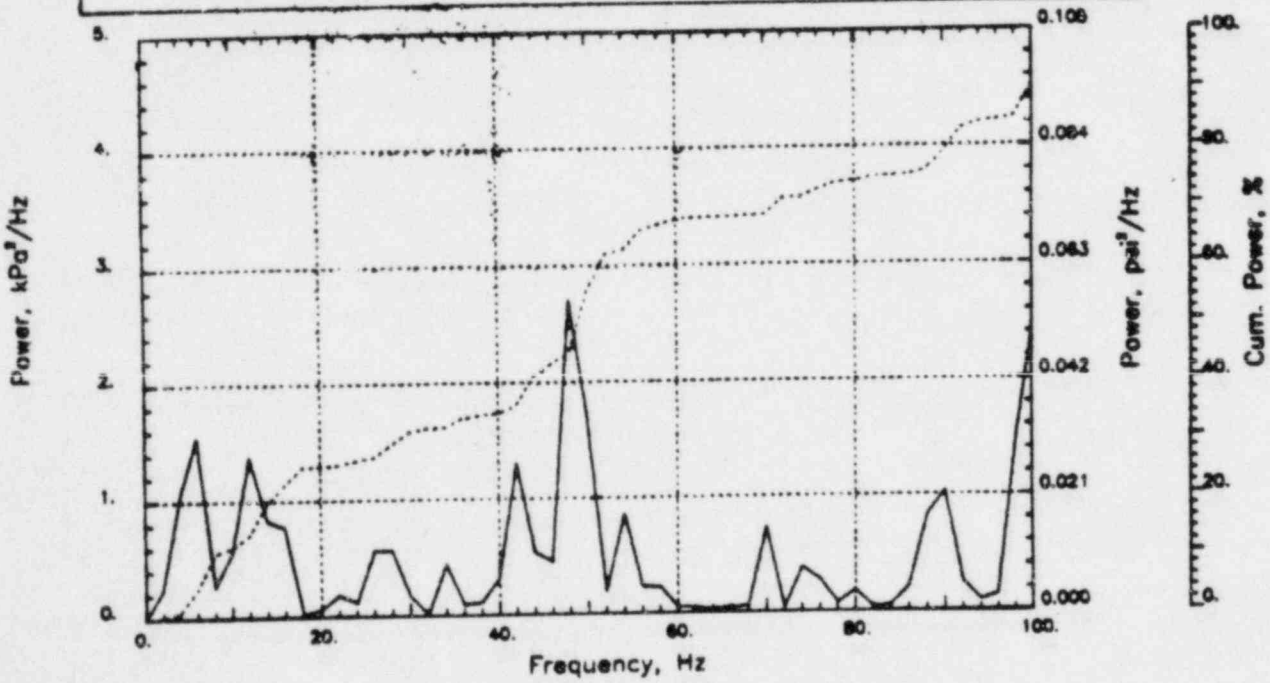

RIVER RHR CO

Output at point (12.65,28.00,0.00)

NAME - LEONG, TAI SENG
DATE - FEB 21, 1984
PROJECT NO. - 15026004

CHECKED _____
DATE _____
CALC NO. - AP-84-

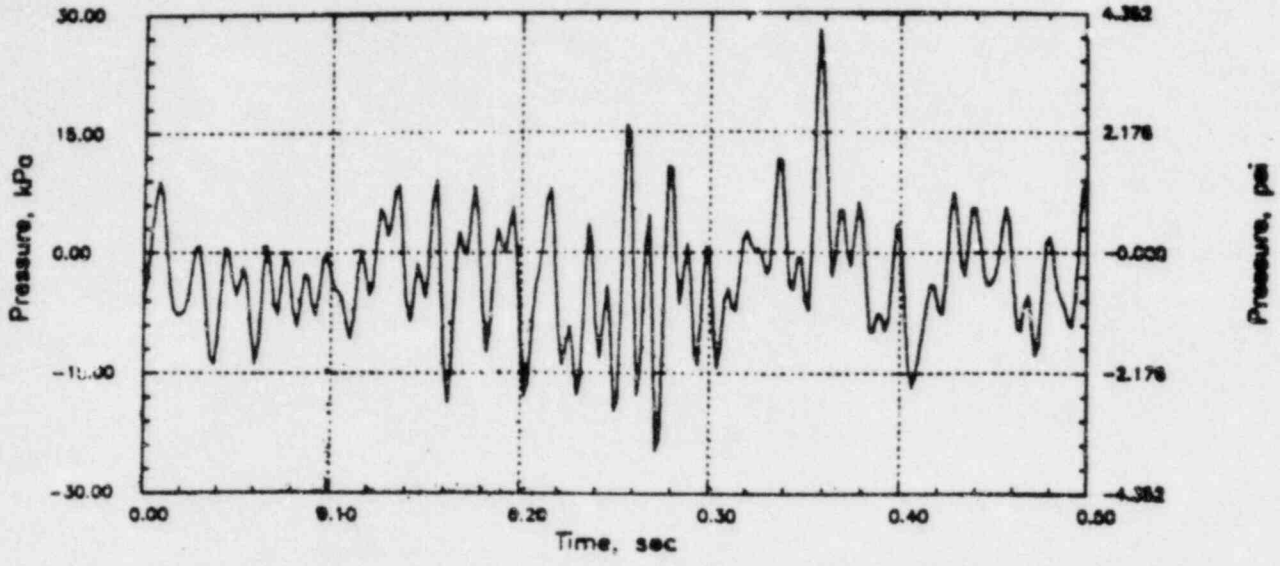

POP = 27.91 kPa PUP = -24.65 kPa MSP = 53.71 kPa²

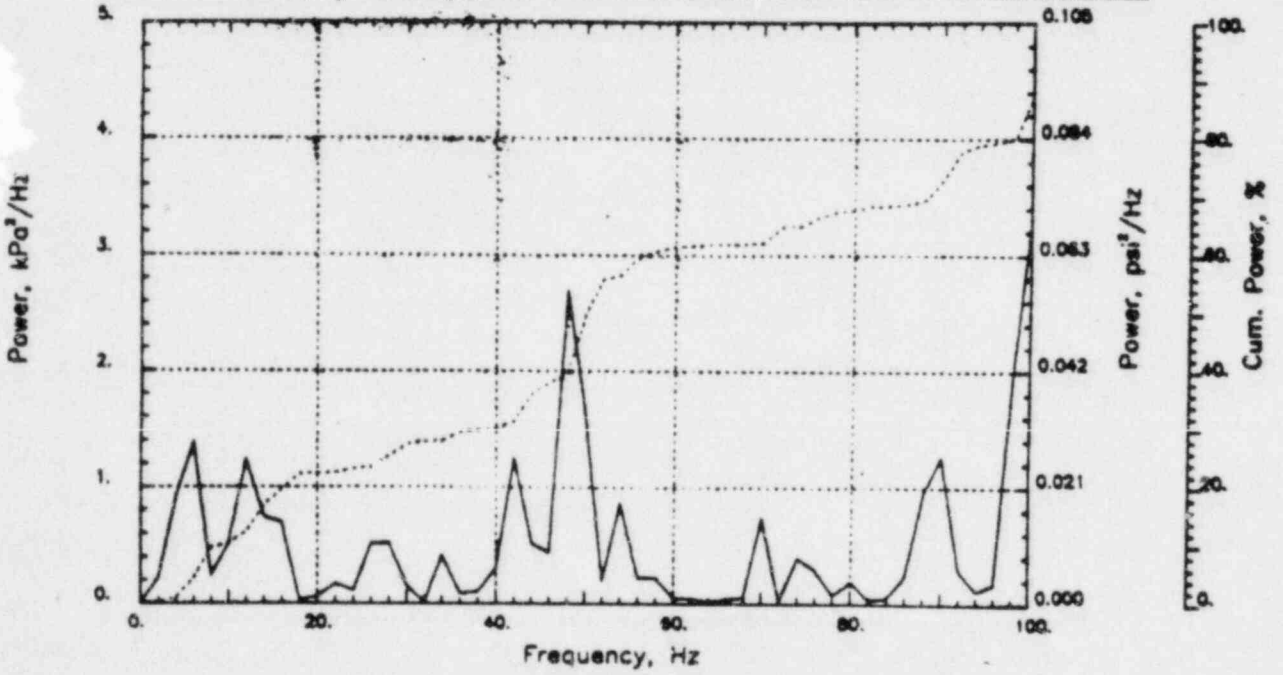

RIVER RHR CO

Output at point (12.65,28.00,0.46)

NAME - LEONG, TAI SENG
DATE - FEB 21, 1984
PROJECT NO. - 15026004

CHECKED _____
DATE _____
CALC NO. - AP-84-

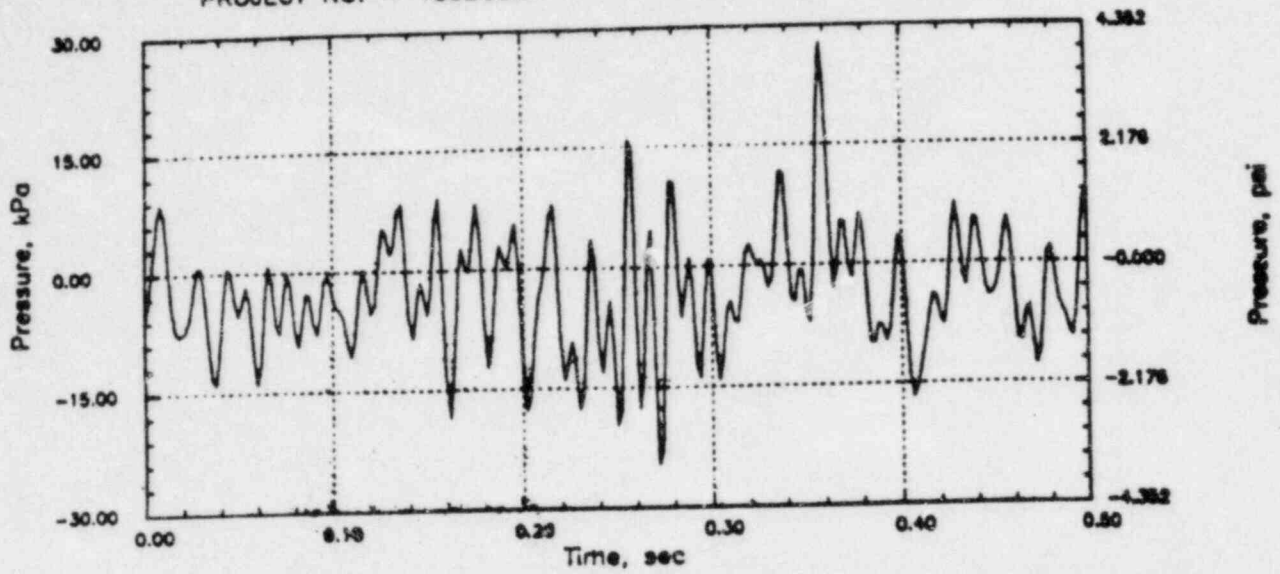

POP = 27.72 kPa PUP = -24.46 kPa MSP = 52.95 kPa²

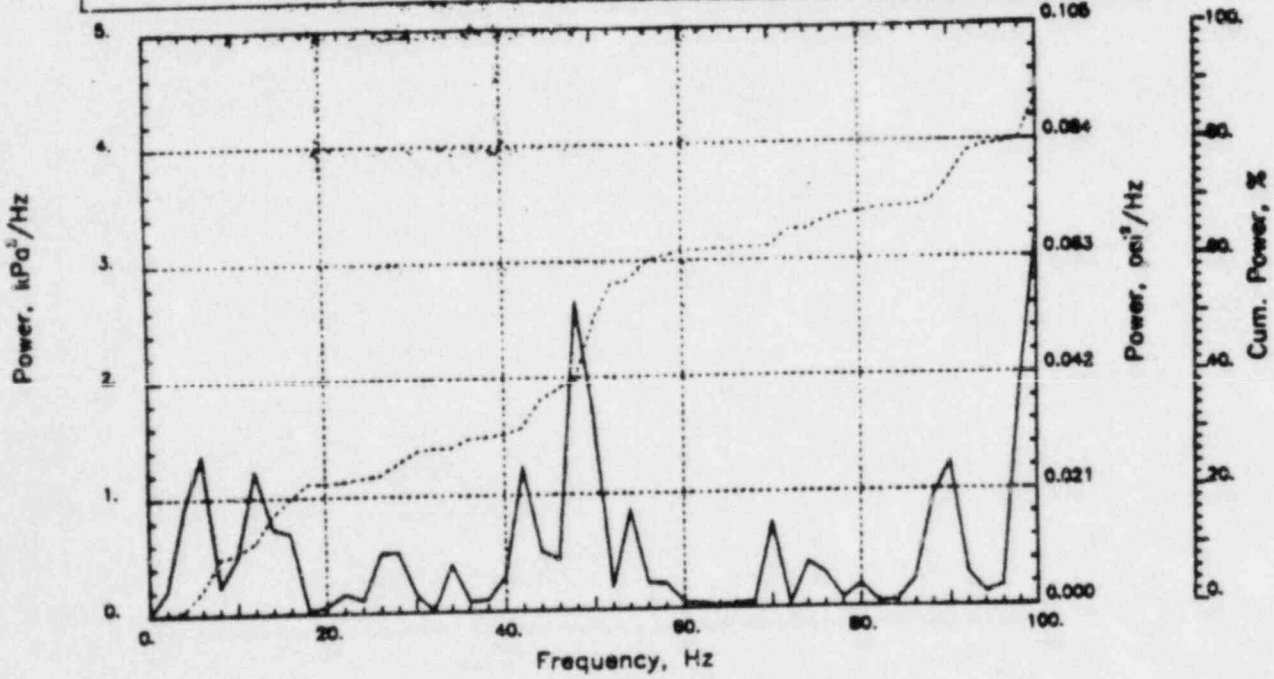

RIVER RHR CO

Output at point (12.65,28.00,0.91)

NAME - LEONG, TAI SENG
DATE - FEB 21, 1984
PROJECT NO. - 15026004

CHECKED _____
DATE _____
CALC NO. - AP-84-

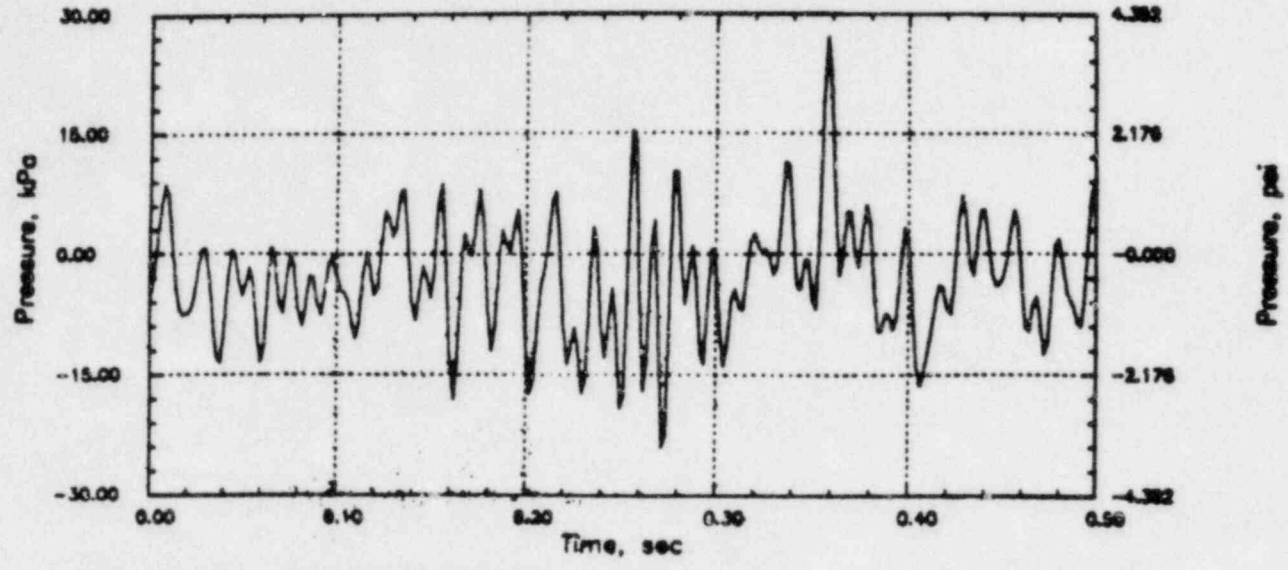

POP = 27.13 kPa PUP = -23.91 kPa MSP = 50.72 kPa²

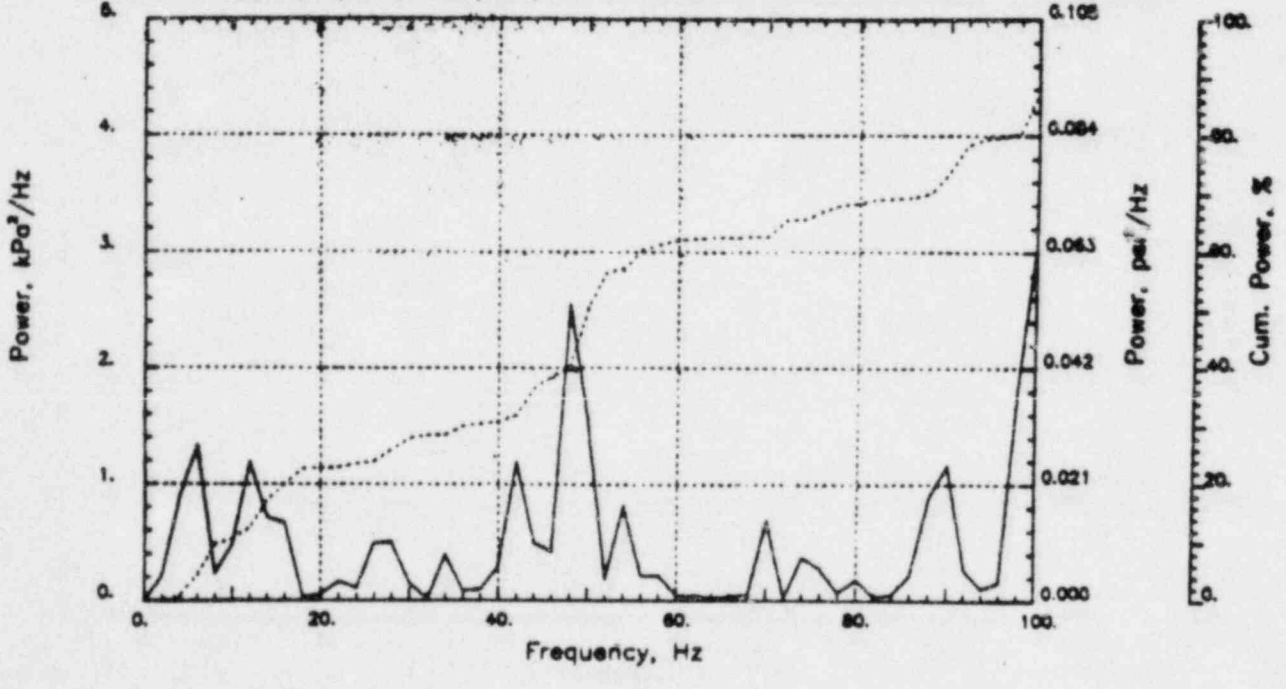

RIVER RHR CO

Output at point (12.65,28.00,1.55)

NAME - LEONG, TAI SENG
DATE - FEB 21, 1984
PROJECT NO. - 15026004

CHECKED _____
DATE _____
CALC NO. - AP-84-

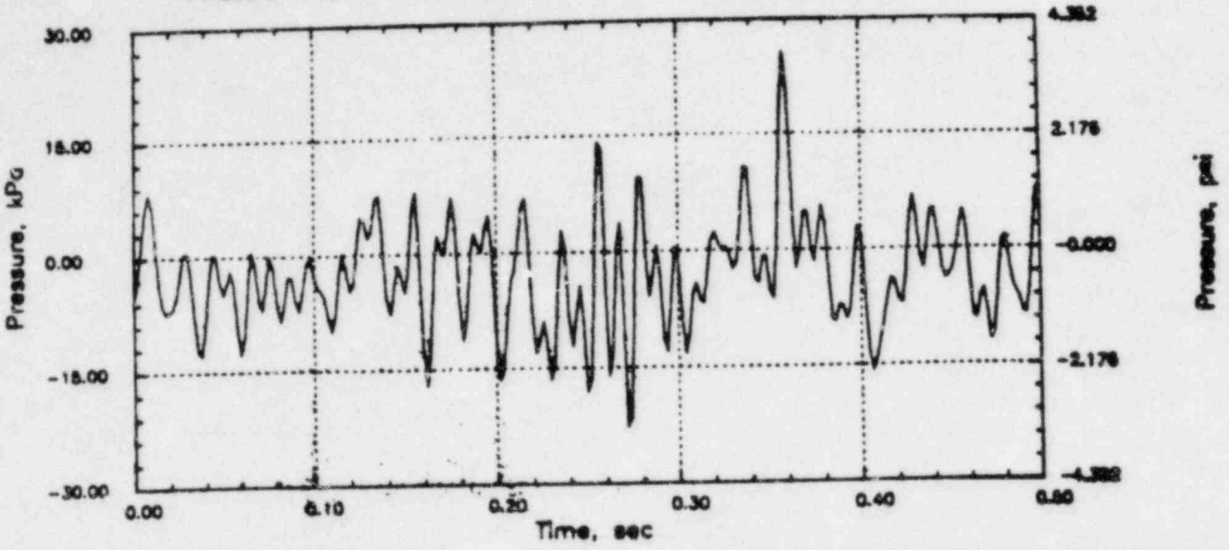

POP = 25.68 kPa PUP = -22.57 kPa MSP = 45.46 kPa

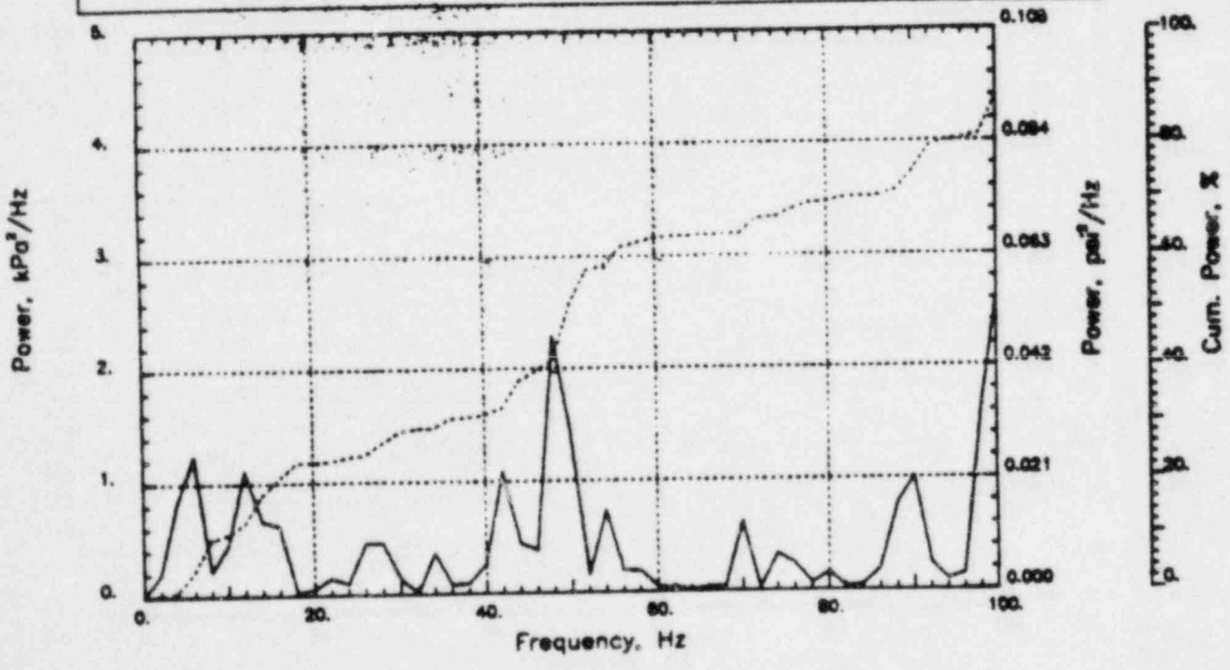

RIVER RHR CO

Output at point (12.65,28.00,2.18)

NAME - LEONG, TAI SENG
DATE - FEB 21, 1984
PROJECT NO. - 15026004

CHECKED _____
DATE _____
CALC NO. - AP-84-

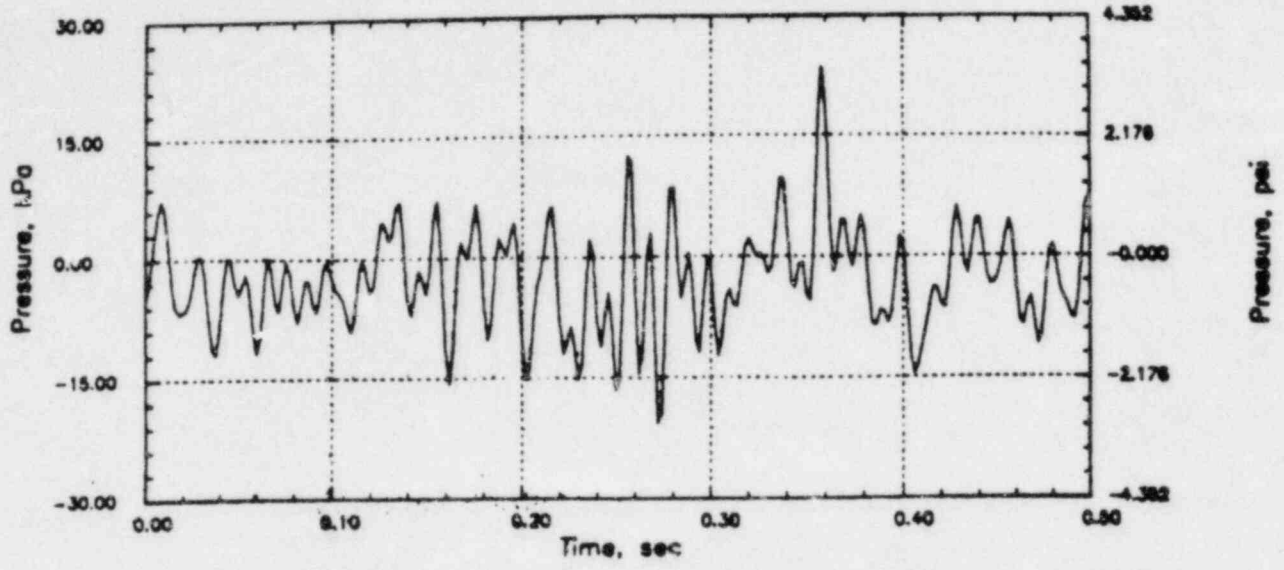

POP = 23.54 kPa PUP = -2[illegible].60 kPa MSP = 38.22 kPa²

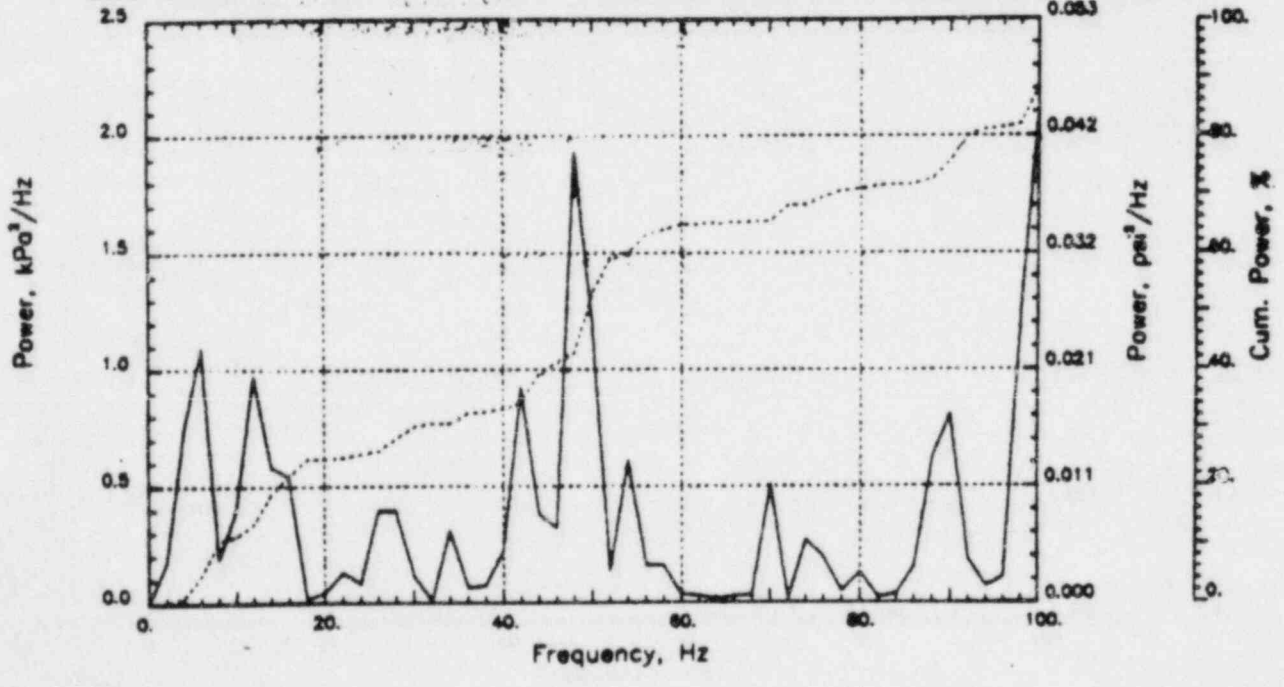

RIVER RHR CO

Output at point (12.65,28.00,2.82)

NAME - LEONG, TAI SENG
DATE - FEB 21, 1984
PROJECT NO. - 15026004

CHECKED _____
DATE _____
CALC NO. - AP-84-

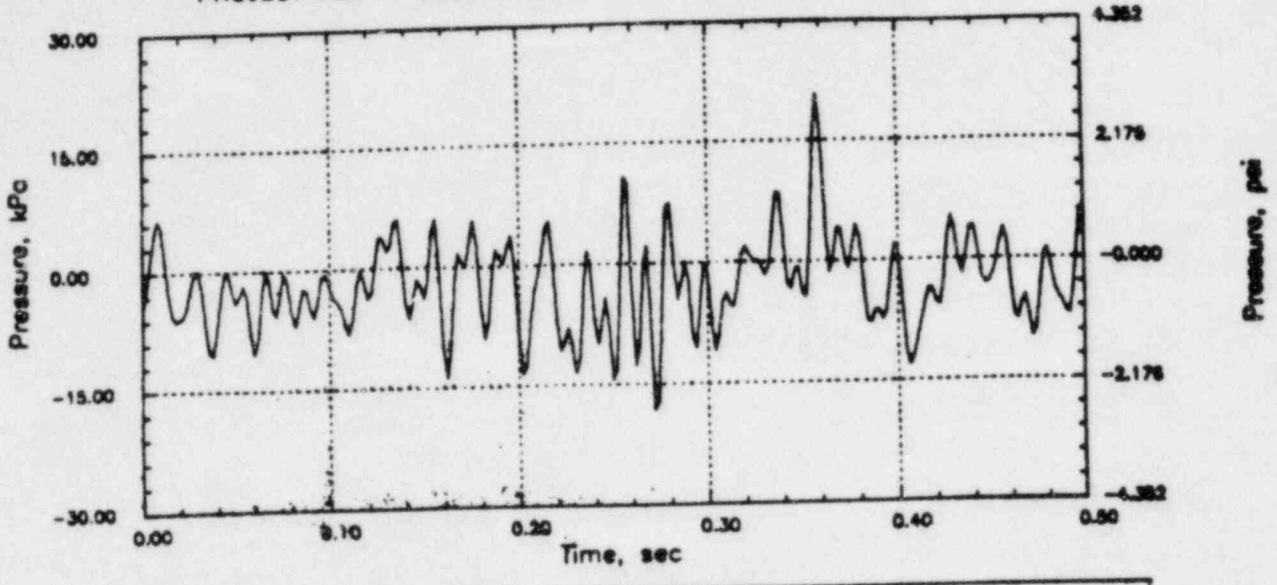

POP = 20.77 kPa PUP = -18.08 kPa MSP = 29.80 kPa²

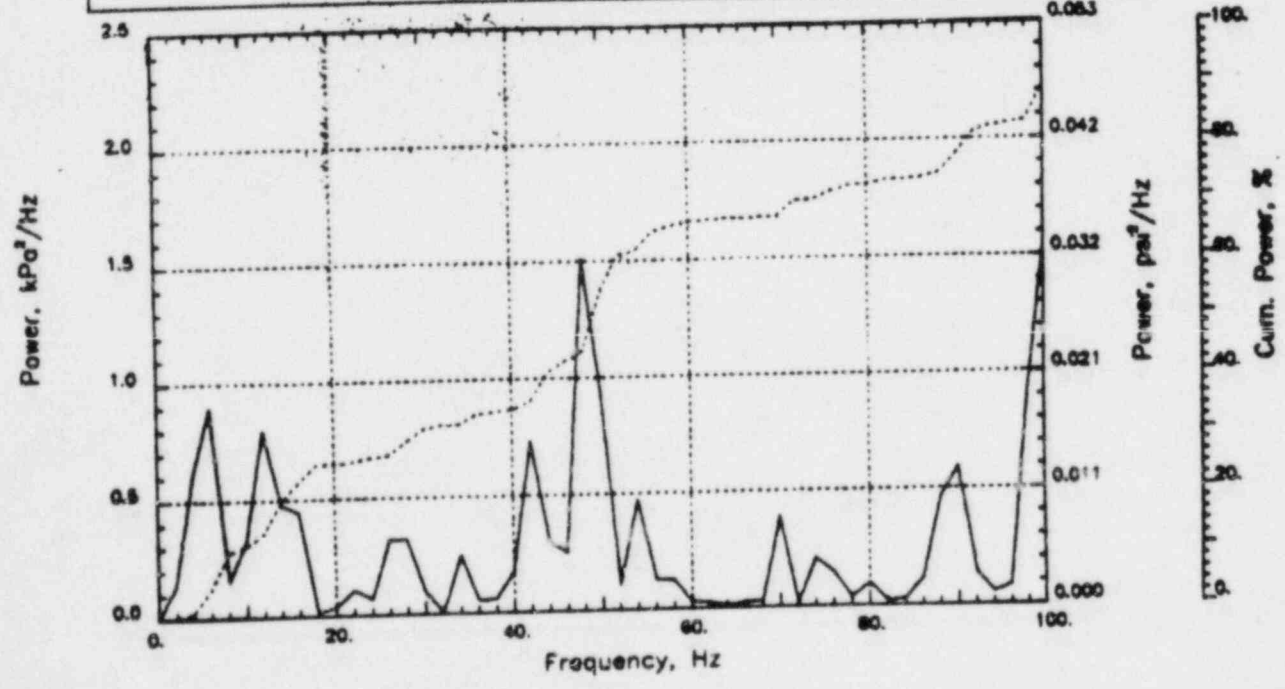

RIVER RHR CO

Output at point (12.65,28.00,3.45)

NAME - LEONG, TAI SENG
DATE - FEB 21, 1984
PROJECT NO. - 15026004

CHECKED _____
DATE _____
CALC NO. - AP-84-

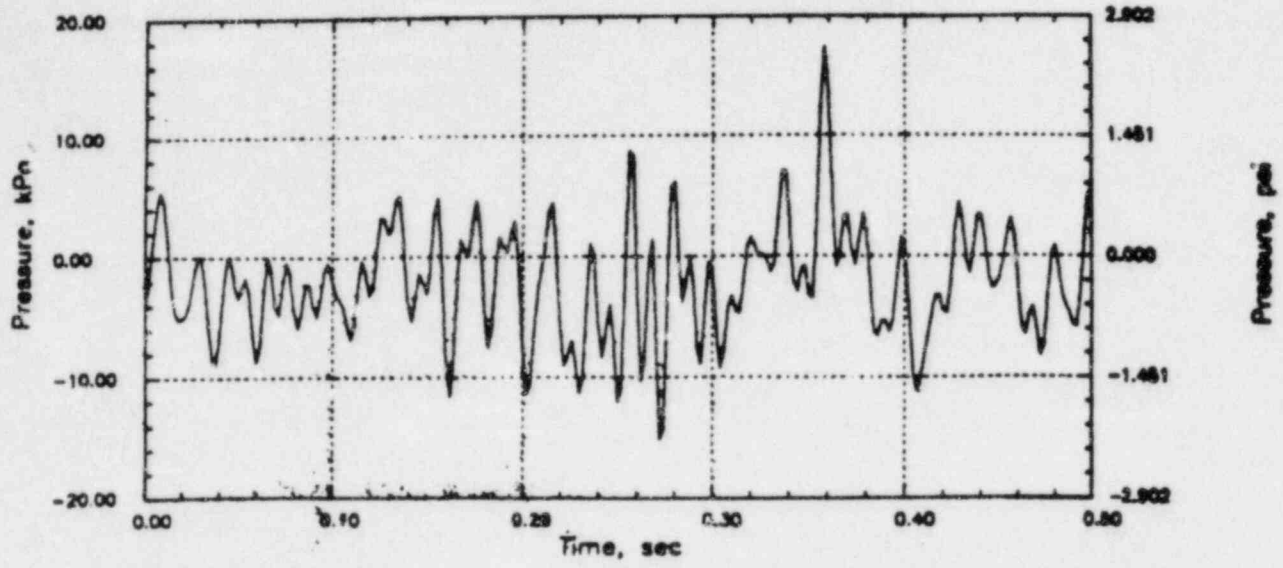

POP = 17.45 kPa PUP = -15.11 kPa MSP = 21.09 kPa²

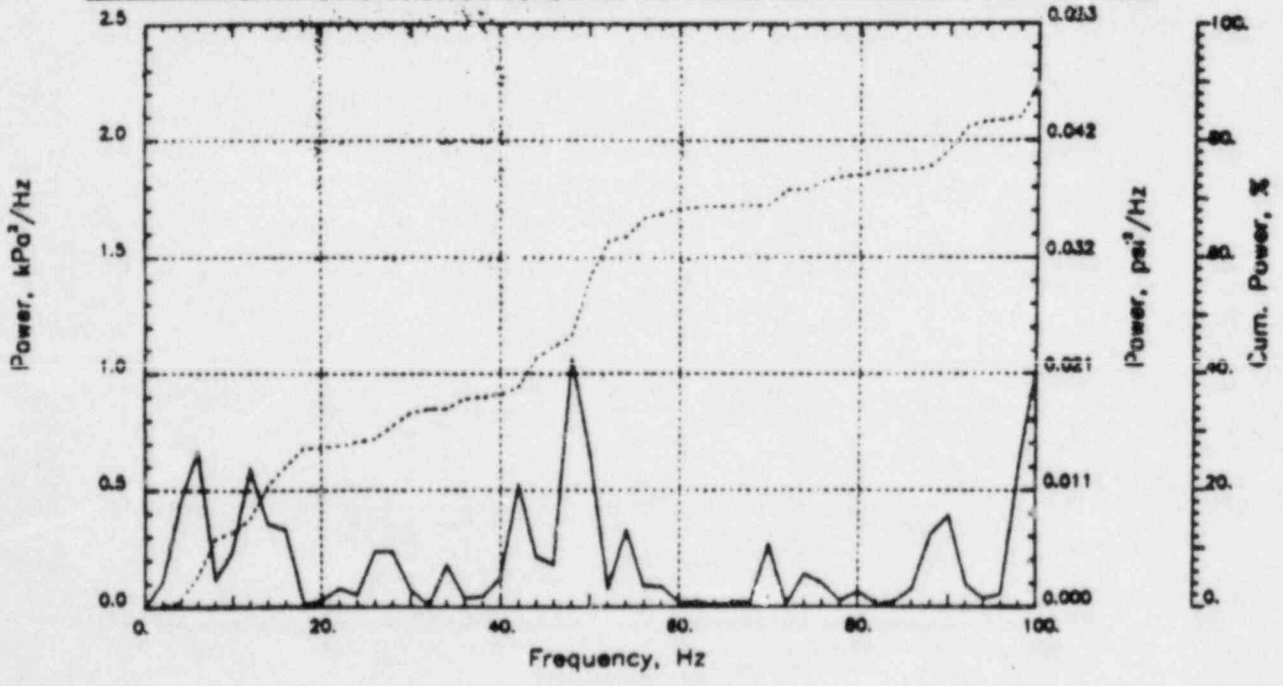

RIVER RHR CO

Output at point (12.65,28.00,4.09)

NAME - LEONG, TAI SENG
DATE - FEB 21, 1984
PROJECT NO. - 15026004

CHECKED _____
DATE _____
CALC NO. - AP-84-

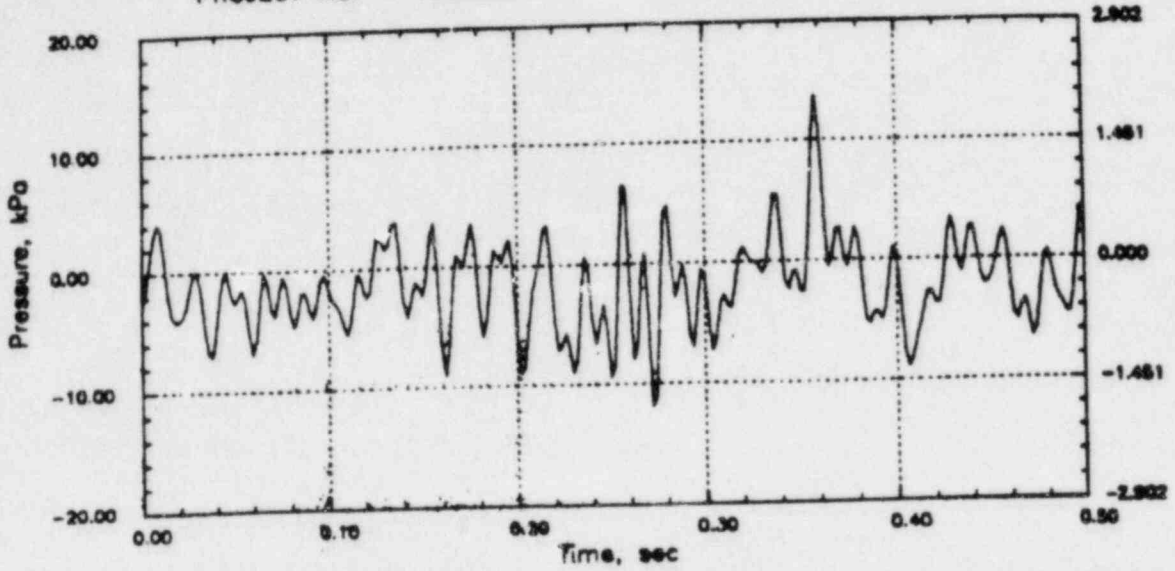

POP = 13.68 kPa PUP = -11.78 kPa MSP = 13.00 kPa²

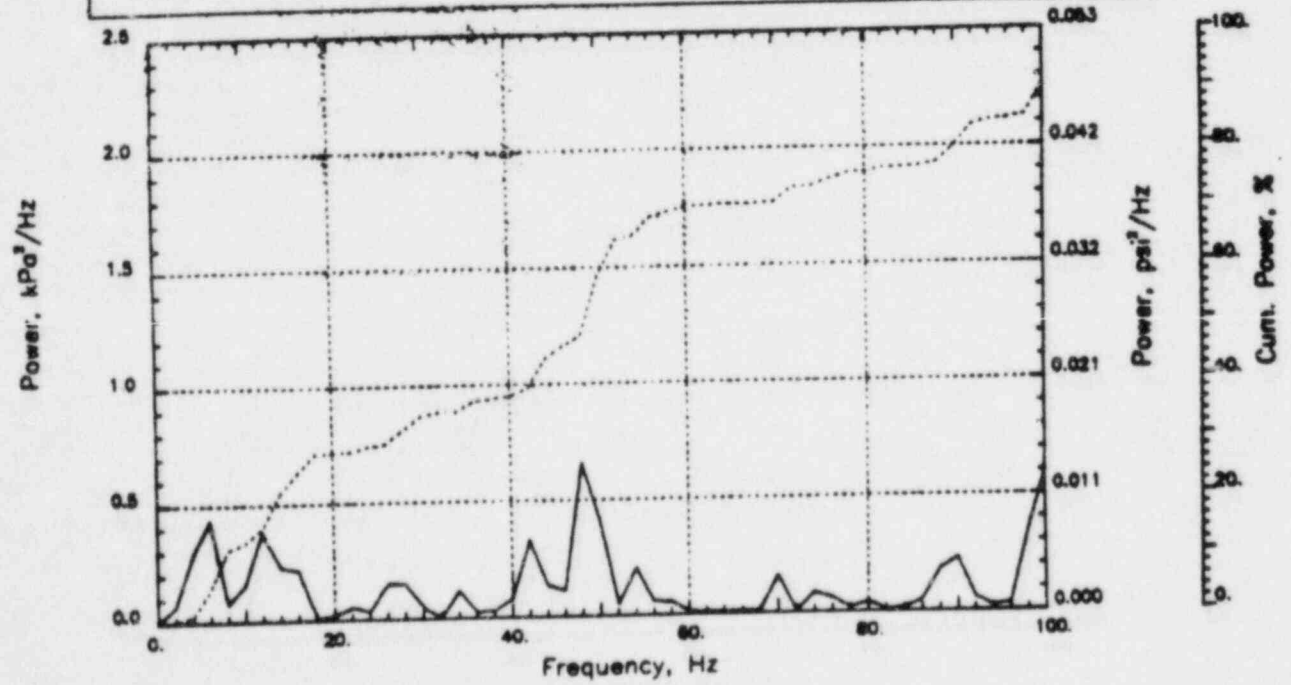

RIVER RHR CO

Output at point (12.65,28.00,4.91)

NAME - LEONG, TAI SENG
DATE - FEB 21, 1984
PROJECT NO. - 15026004

CHECKED _____
DATE _____
CALC NO. - AP-84-

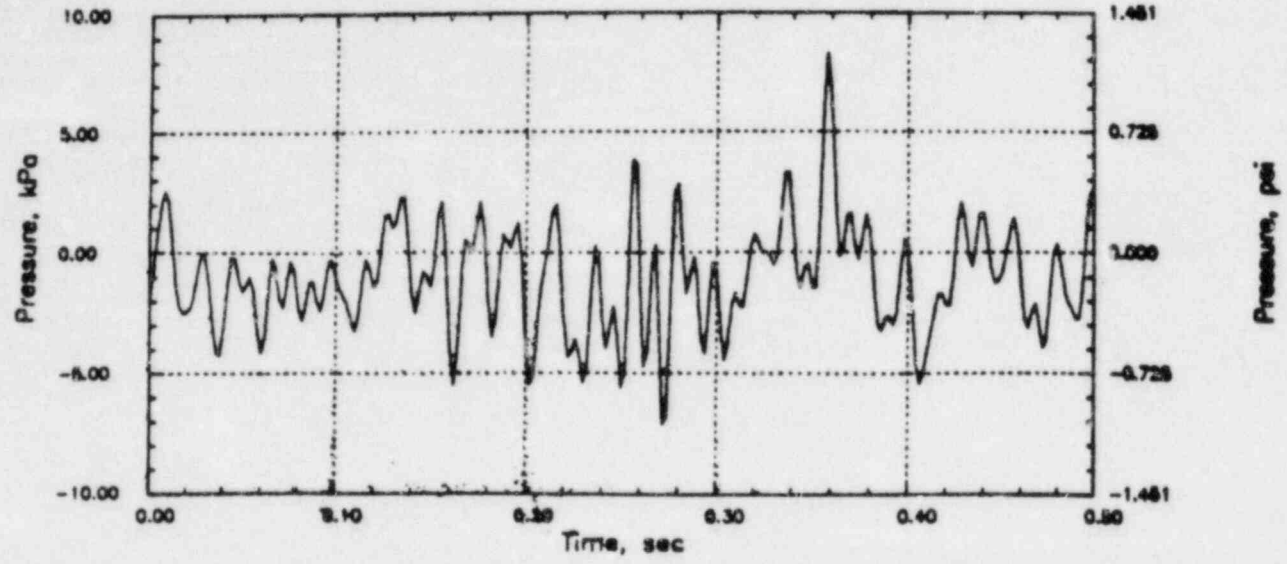

POP = 8.27 kPa PUP = -7.09 kPa MSP = 4.78 kPa²

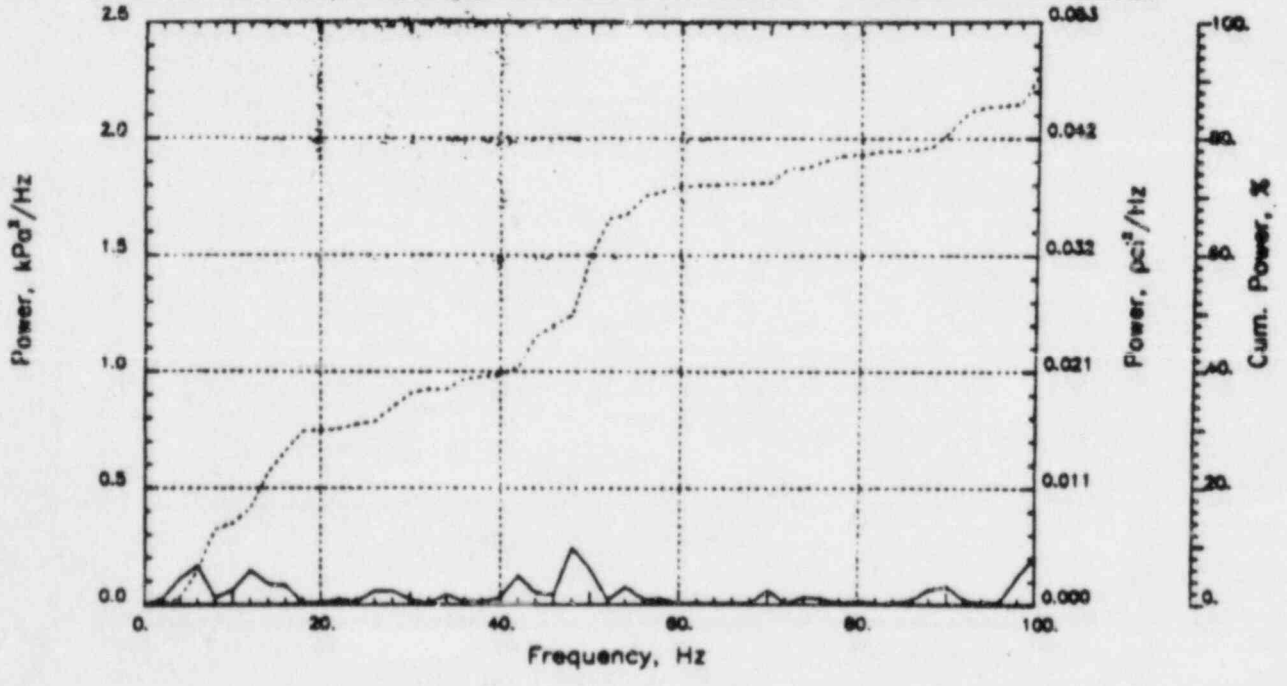

PERRY RHR CO

Output at point (18.90,28.00,4.91)

NAME - LEONG, TAI SENG
DATE - FEB 21, 1984
PROJECT NO. - 15026004

CHECKED _____
DATE _____
CALC NO. - AP-84-

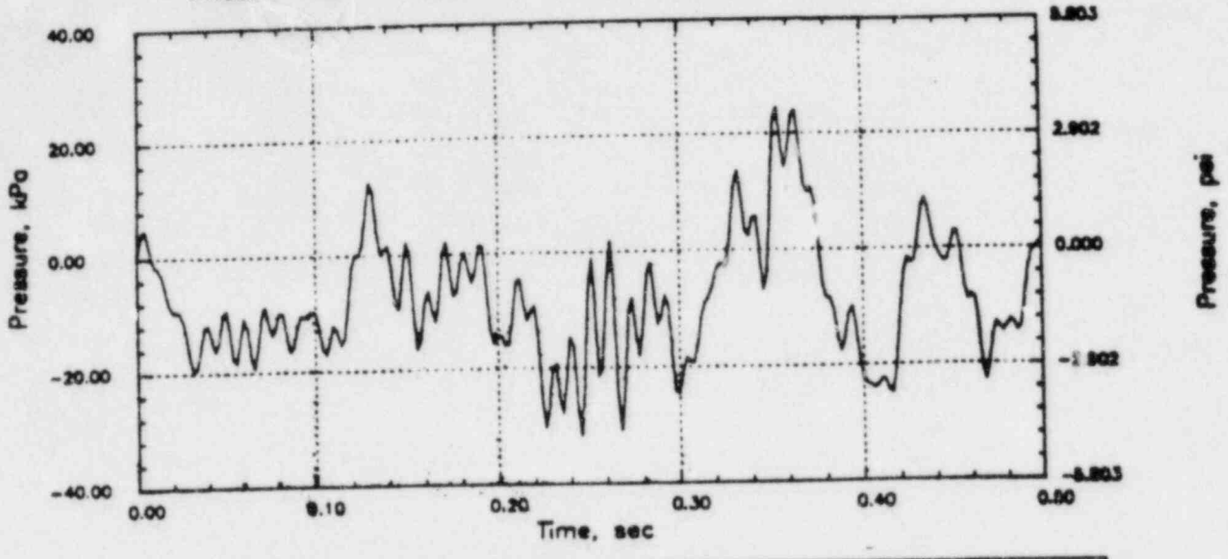

POP = 24.63 kPa PUP = -31.53 kPa MSP = 109.00 kPa²

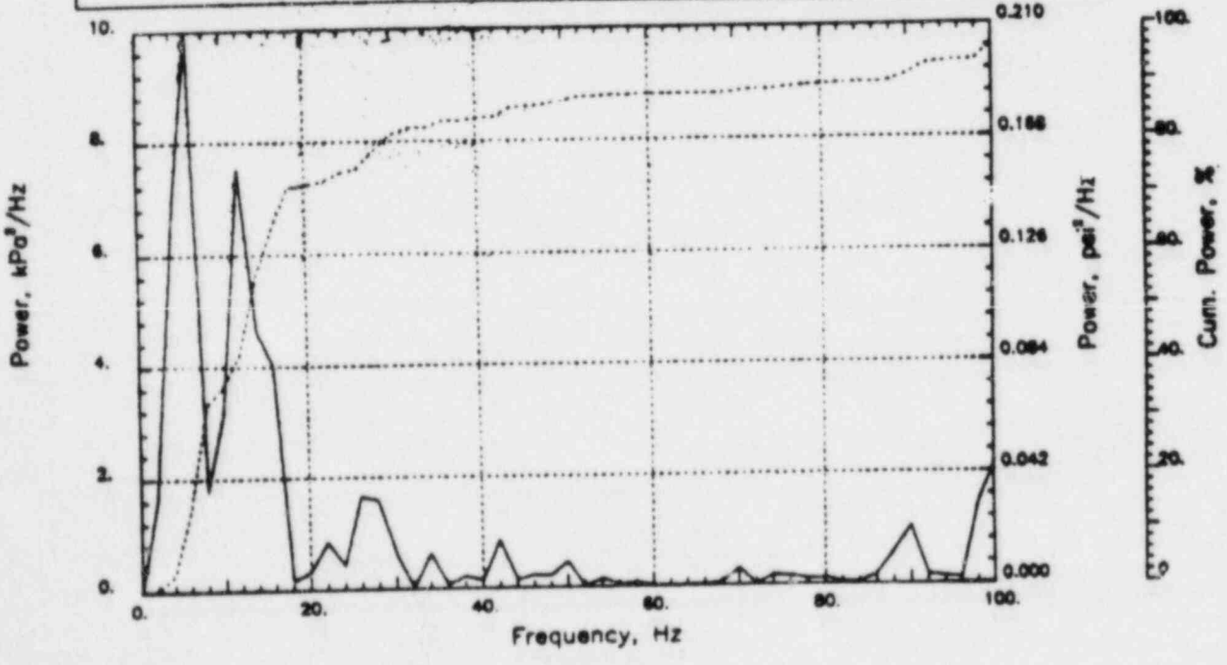

PERRY RHR CO

Output at point (18.90,28.00,4.09)

NAME - LEONG, TAI SENG
DATE - FEB 21, 1984
PROJECT NO. - 15026004

CHECKED _____
DATE _____
CA.C NO. - AP-84-

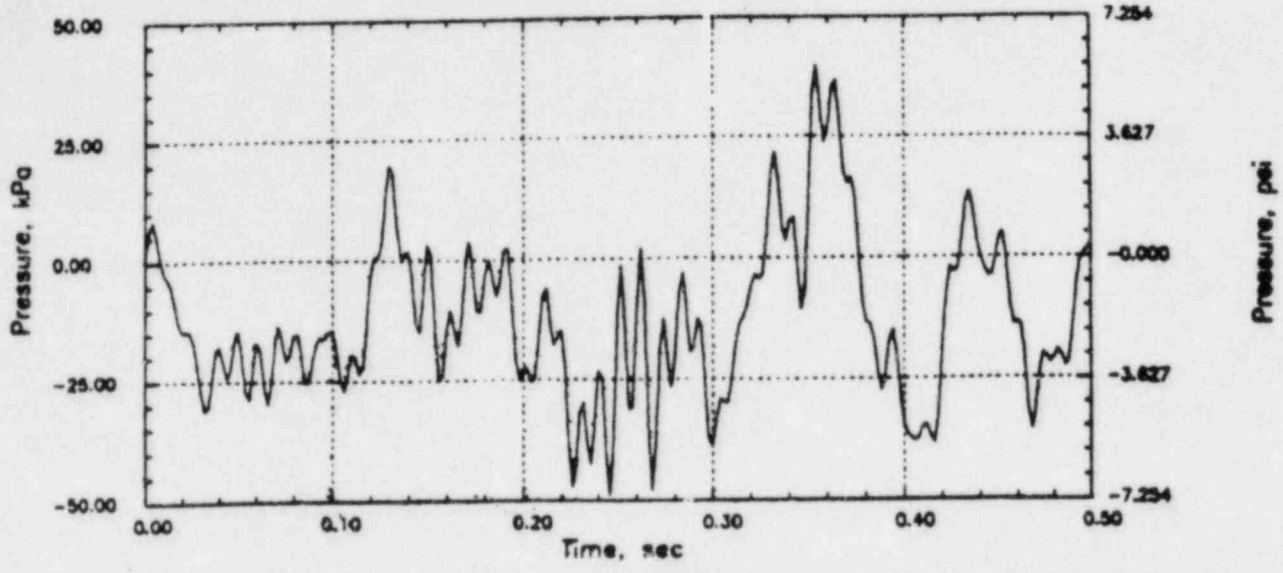

POP = 39.61 kPa PUP = -49.00 kPa MSP = 264.68 kPa²

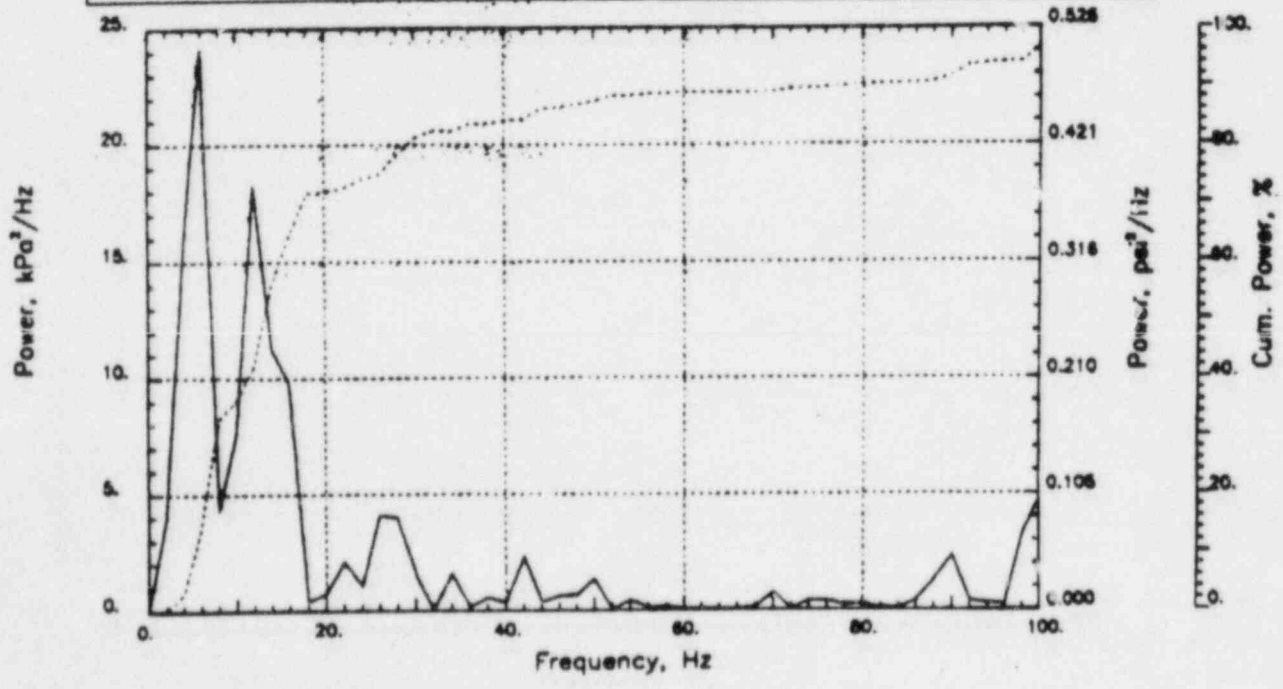

PERRY RHR CO

Output at point (18.90,28.00,3.45)

NAME - LEONG, TAI SENG
DATE - FEB 21, 1984
PROJECT NO. - 15026004

CHECKED _____
DATE _____
CALC NO. - AP-84-

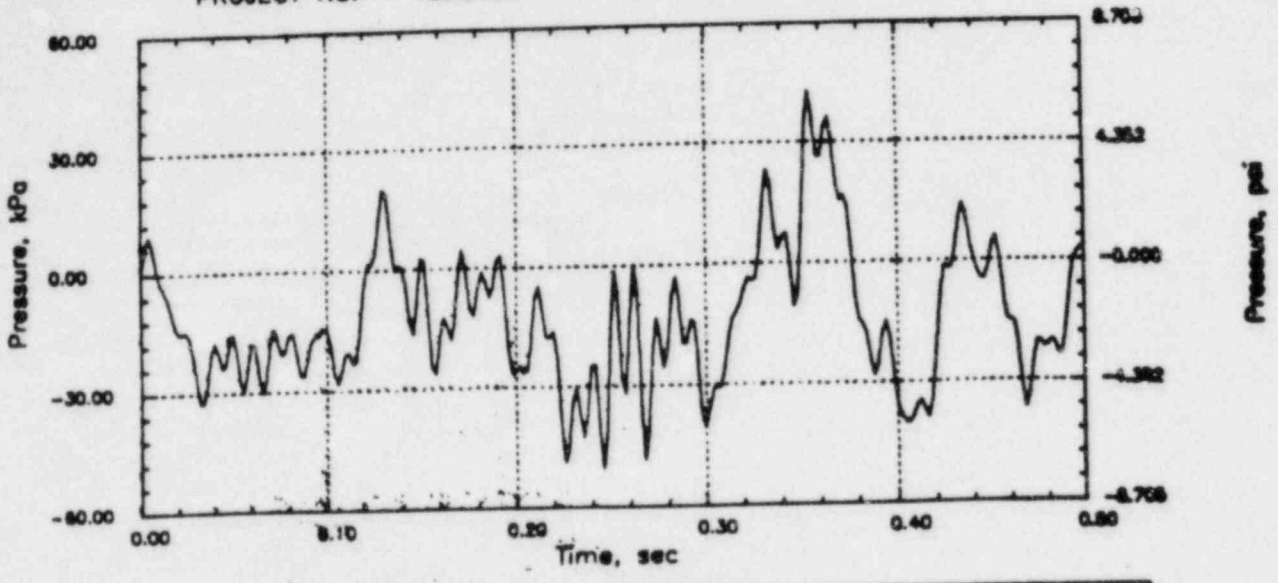

POP = 42.72 kPa PUP = -50.24 kPa MSP = 283.51 kPa²

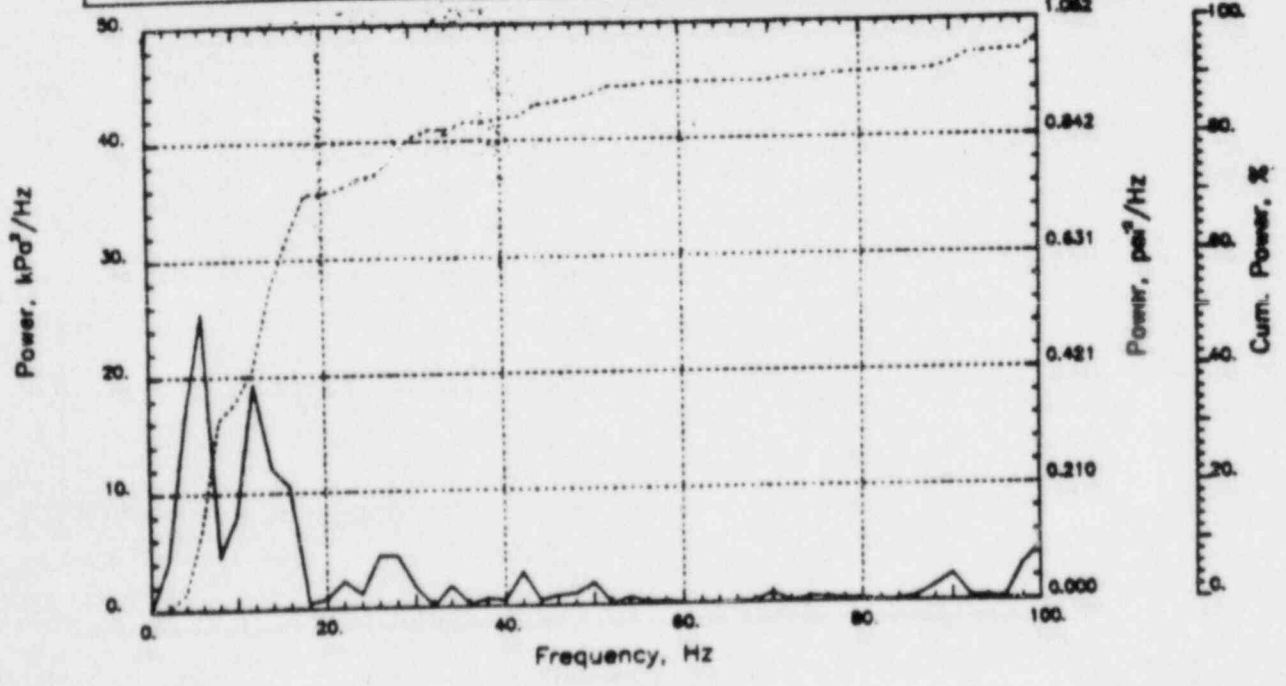

PERRY RHR CO

Output at point (18.90,28.00,2.82)

NAME - LEONG, TAI SENG
DATE - FEB 21, 1984
PROJECT NO. - 15026004

CHECKED _____
DATE _____
CALC NO. - AP-84-

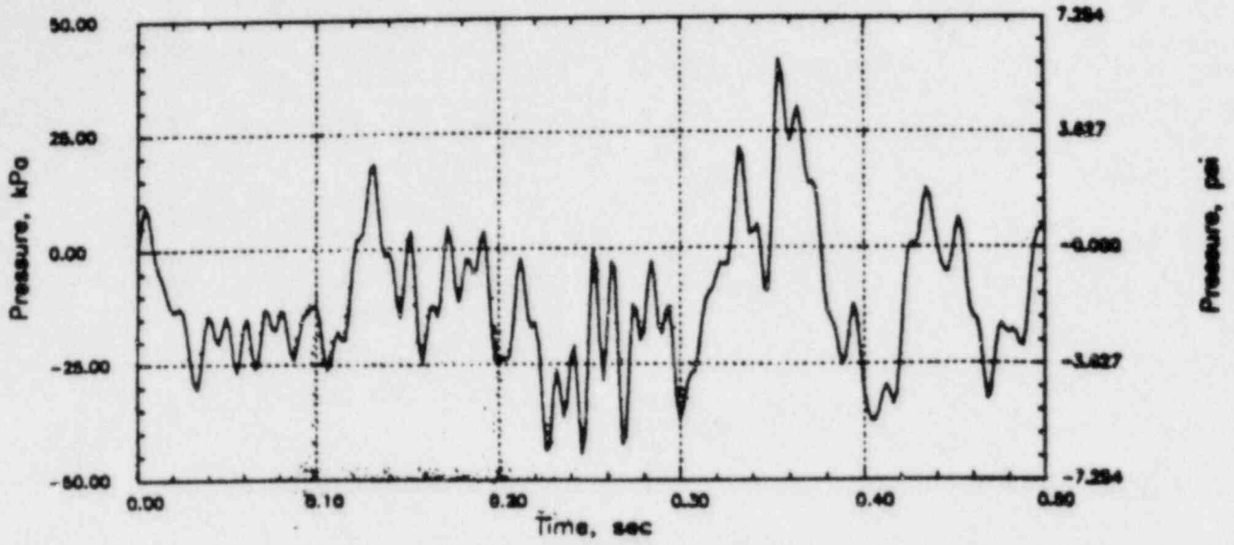

POP = 40.75 kPa PUP = -44.28 kPa MSP = 232.21 kPa²

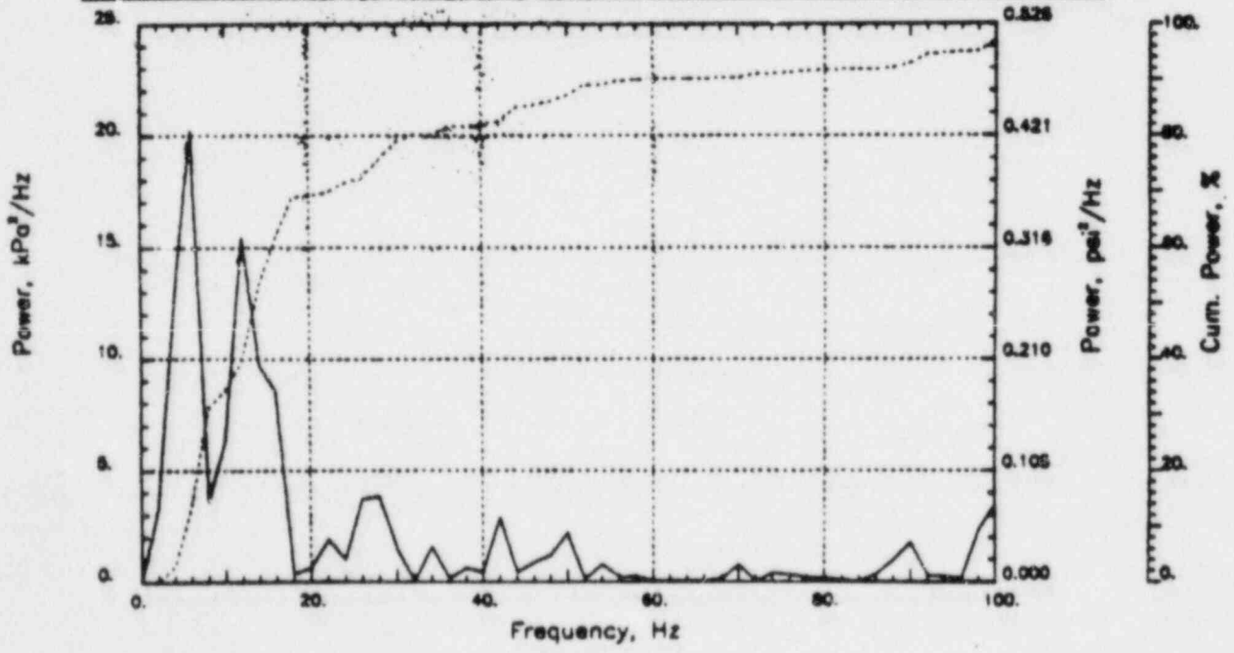

PERRY RHR CO

Output at point (18.90,28.00,2.18)

NAME - LEONG, TAI SENG
DATE - FEB 21, 1984
PROJECT NO. - 15026004

CHECKED _____
DATE _____
CALC NO. - AP-84-

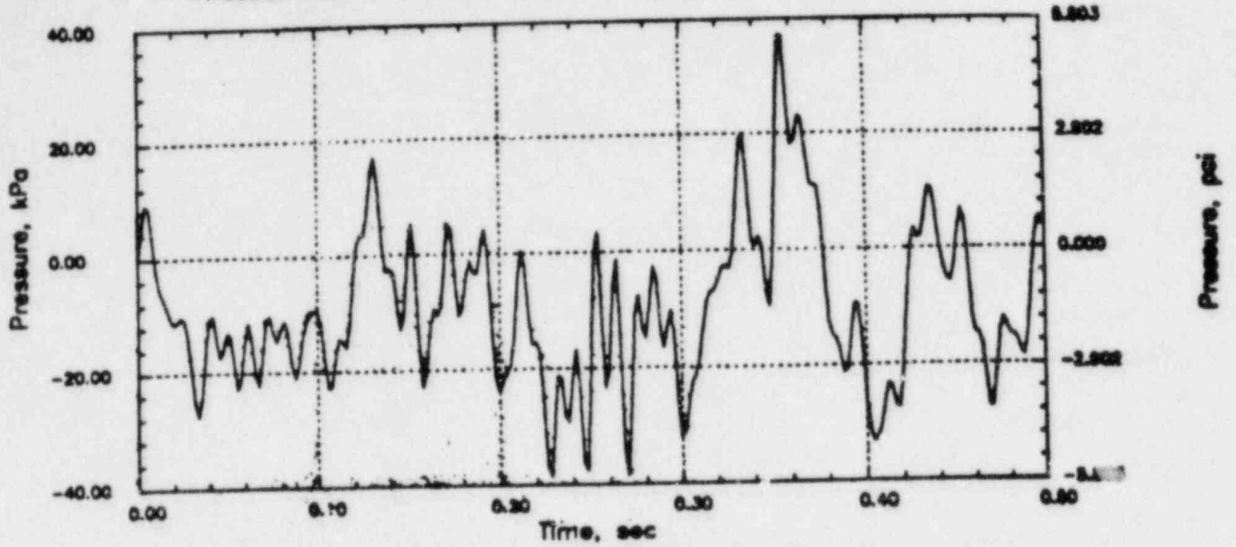

POP = 37.11 kPa PUP = -38.61 kPa MSP = 175.32 kPa²

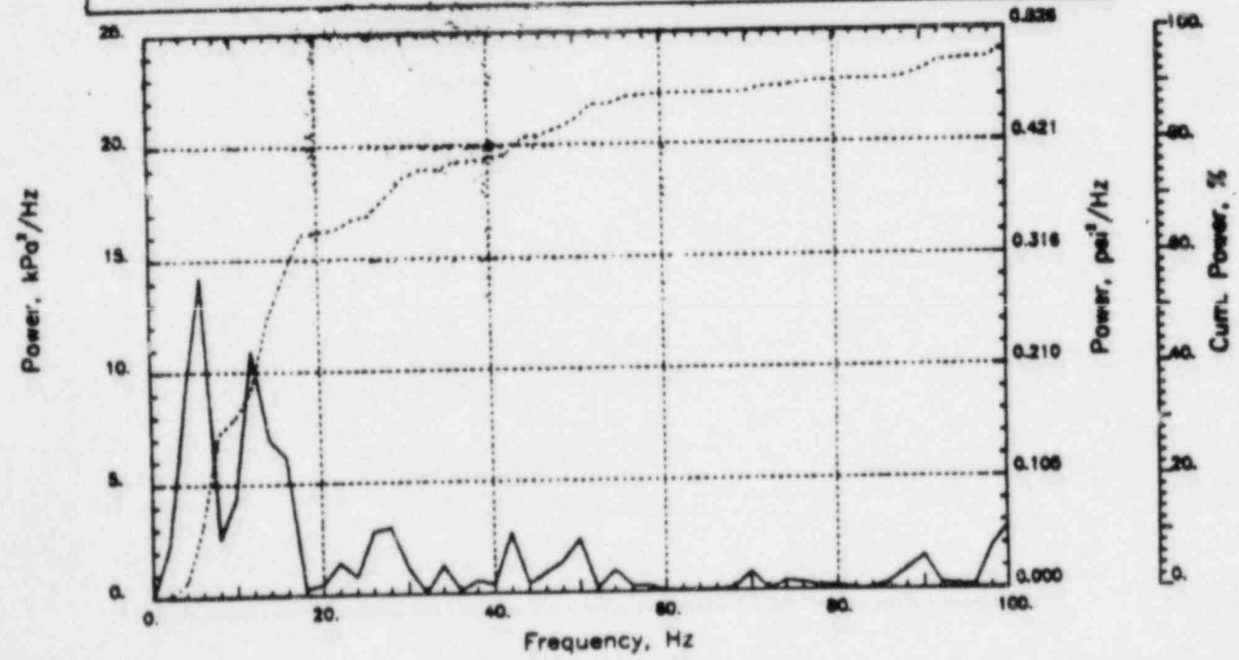

PERRY RHR CO

Output at point (18.90,28.00,1.55)

NAME - LEONG, TAI SENG
DATE - FEB 21, 1984
PROJECT NO. - 15026004

CHECKED _____
DATE _____
CALC NO. - AP-84-

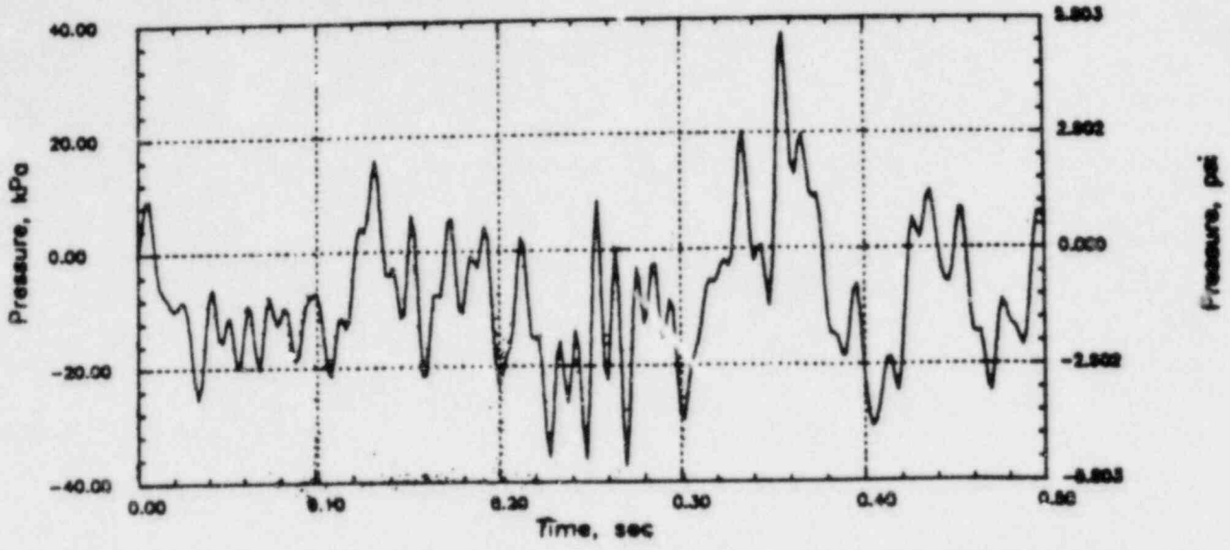

POP = 37.35 kPa PUP = -37.00 kPa MSP = 144.61 kPa²

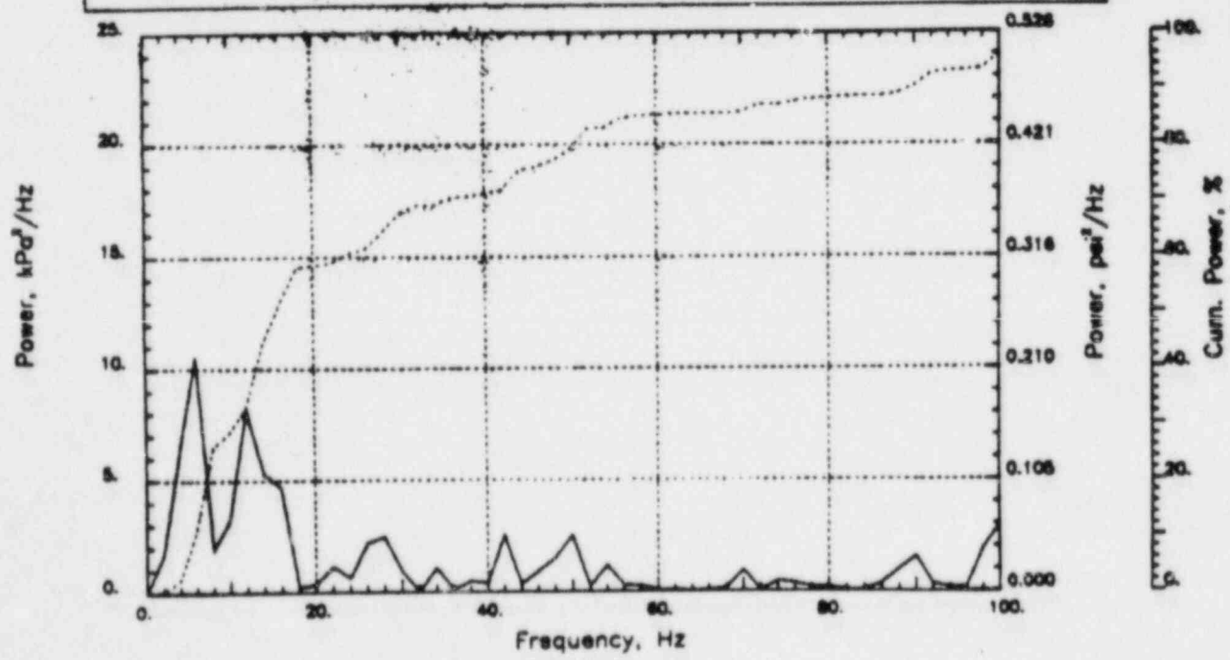

PERRY RHR CO

Output at point (18.90,28.00,0.91)

NAME - LEONG, TAI SENG
DATE - FEB 21, 1984
PROJECT NO. - 15026004

CHECKED _____
DATE _____
CALC NO. - AP-84-

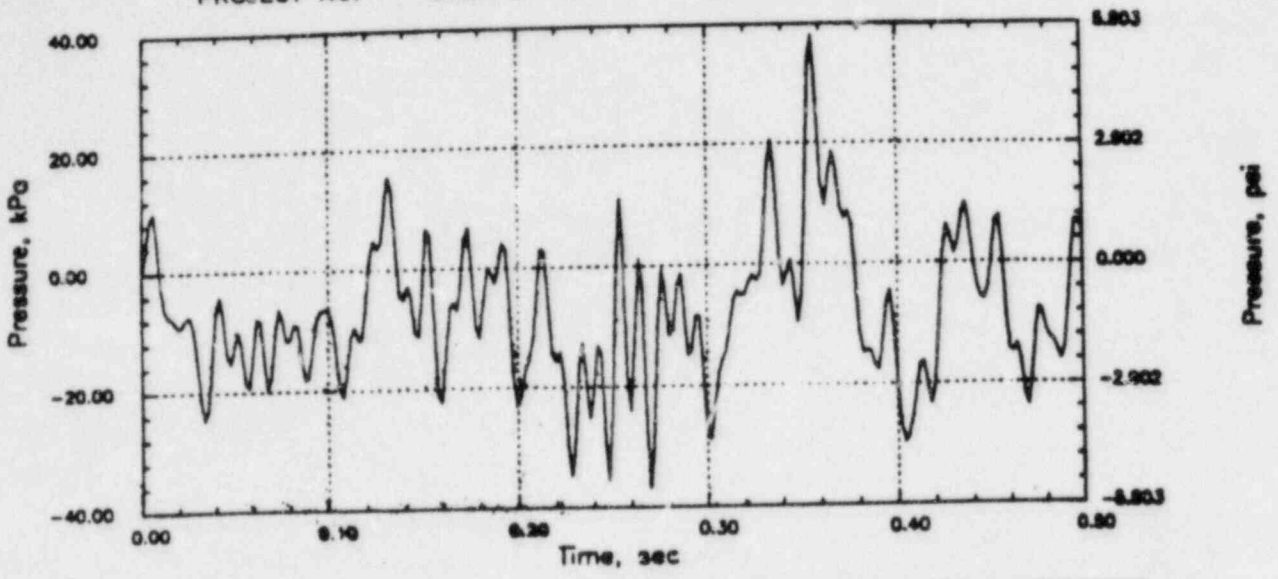

POP = 38.20 kPa PUP = -36.74 kPa MSP = 136.49 kPa²

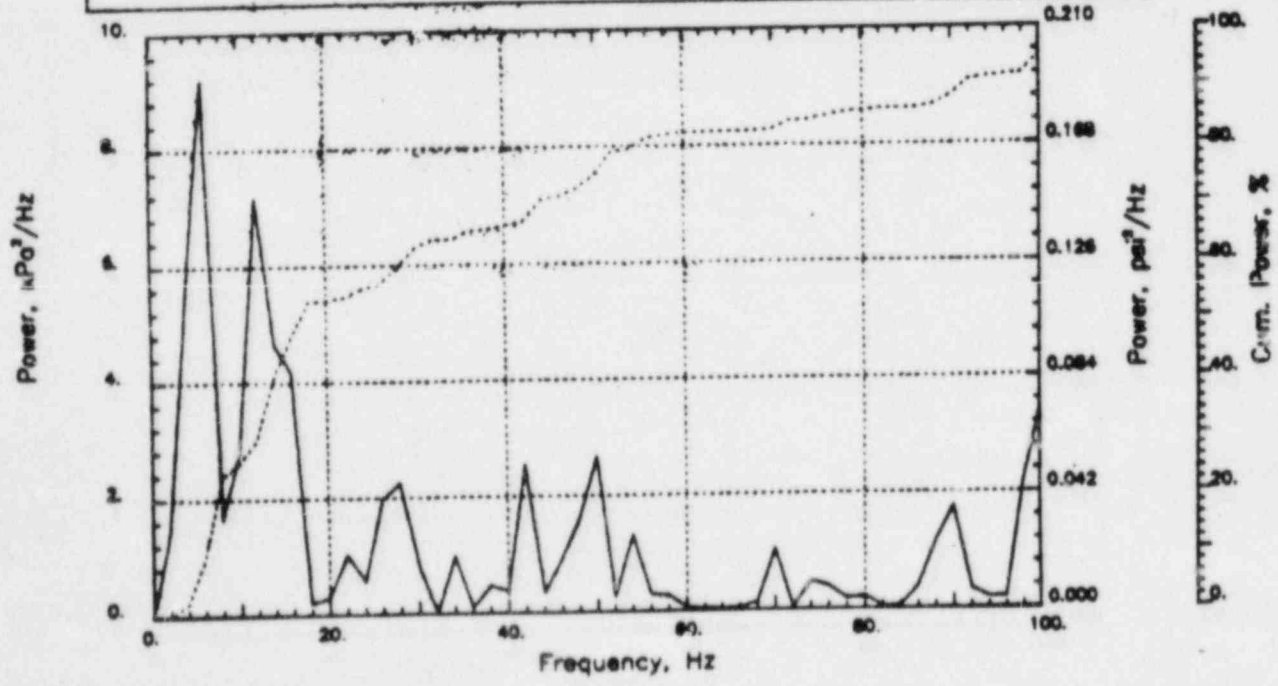

PERRY RHR CO

Output at point (18.90,28.00,0.46)

NAME - LEONG, TAI SENG
DATE - FEB 21, 1984
PROJECT NO. - 15026004

CHECKED _____
DATE _____
CALC NO. - AP-84-

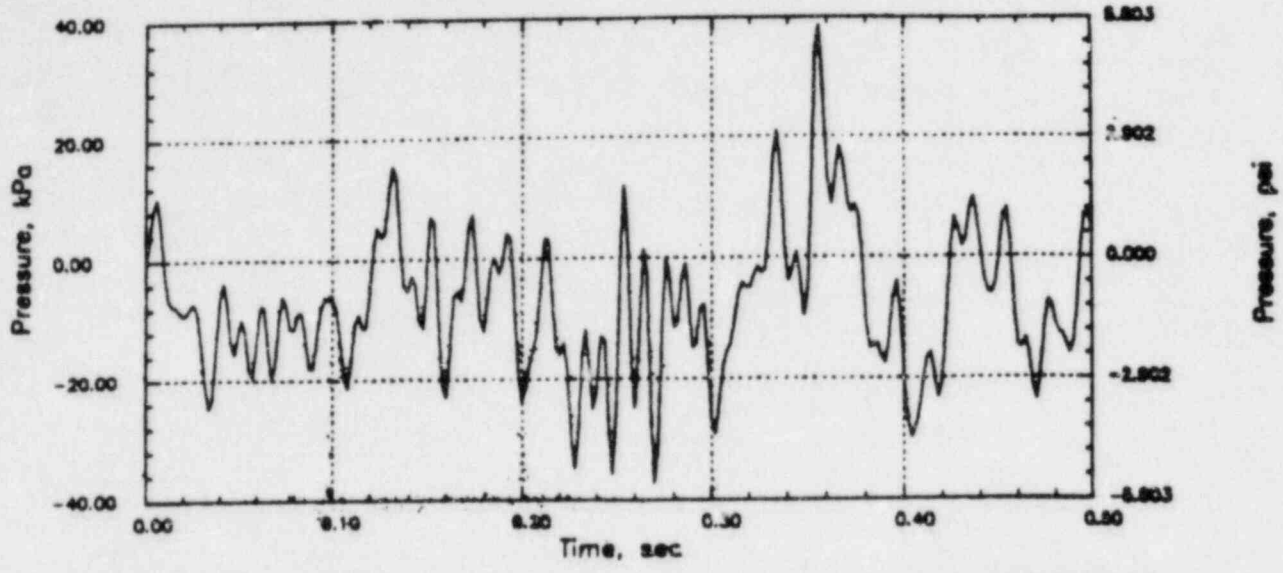

POP = 38.78 kPa PUP = -36.94 kPa MSP = 136.80 kPa²

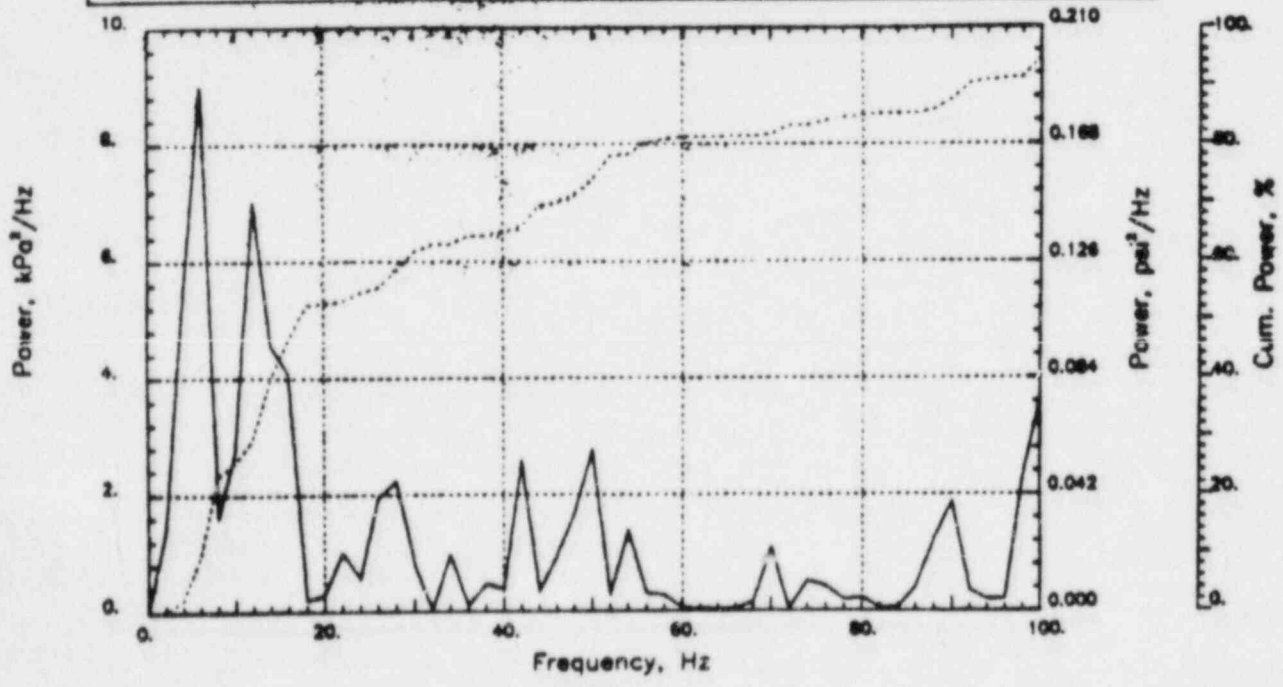

PERRY RHR CO

Output at point (18.90,28.00,0.00)

NAME - LEONG, TAI SENG
DATE - FEB 21, 1984
PROJECT NO. - 15026004

CHECKED _____
DATE _____
CALC NO. - AP-84-

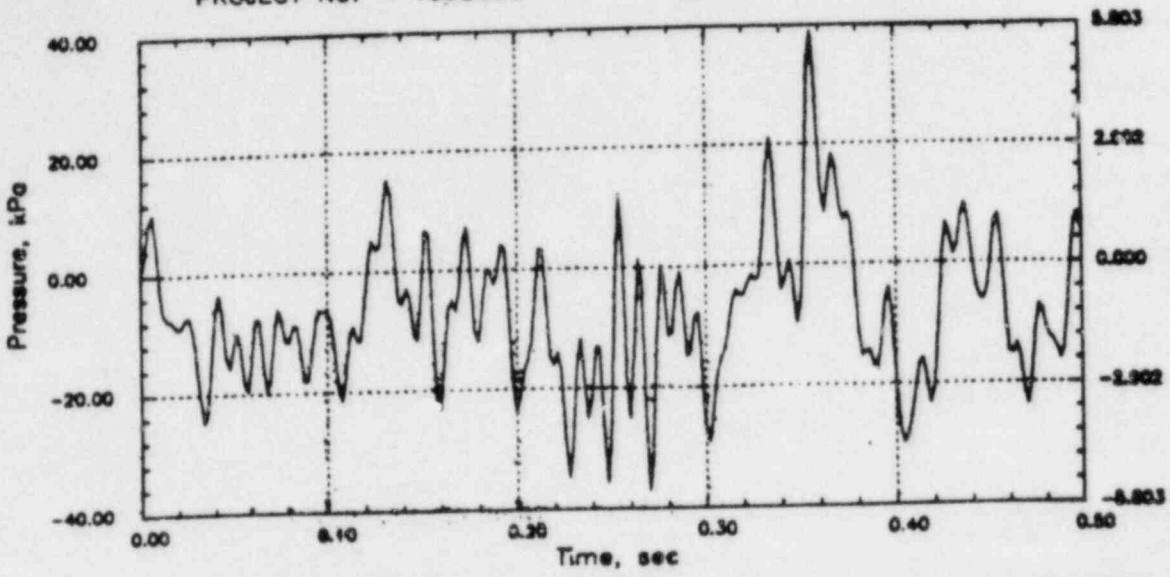

POP = 39.01 kPa PUP = -37.05 kPa MSP = 137.43 kPa²

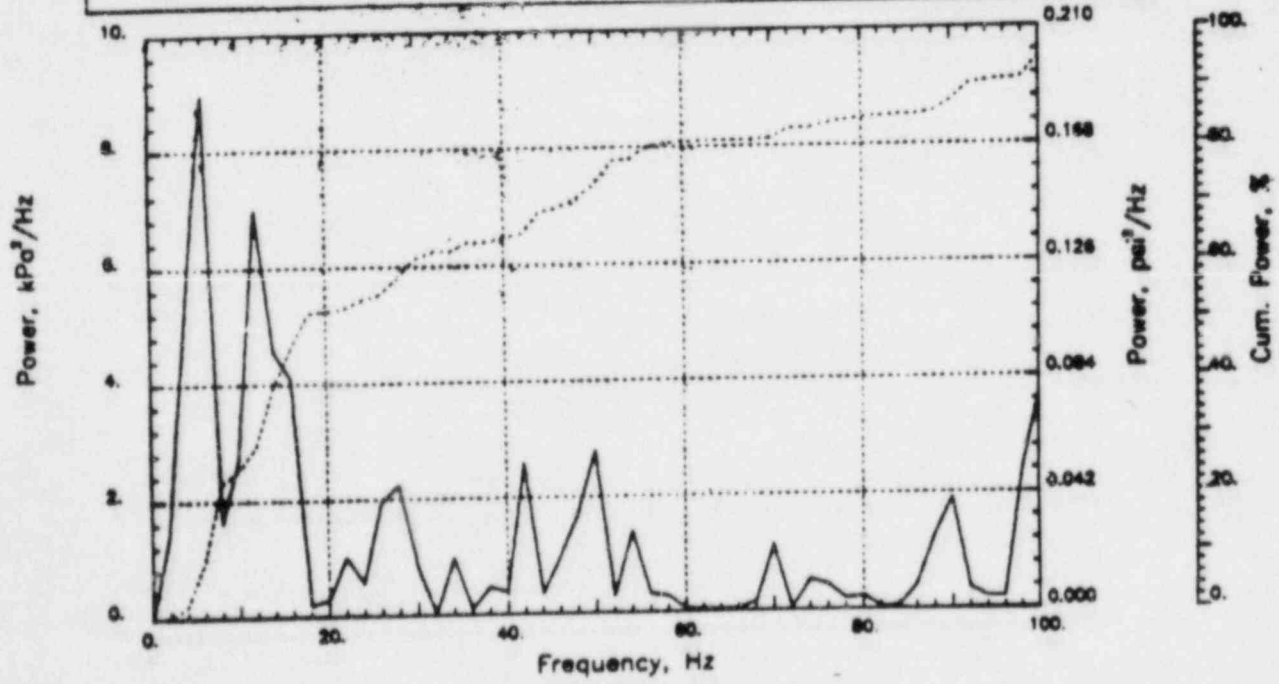

PERRY RHR CO

Output at point (17.34,28.00,0.00)

NAME - LEONG, TAI SENG
DATE - FEB 21, 1984
PROJECT NO. - 15026004

CHECKED _____
DATE _____
CALC. NO. - AP-84-

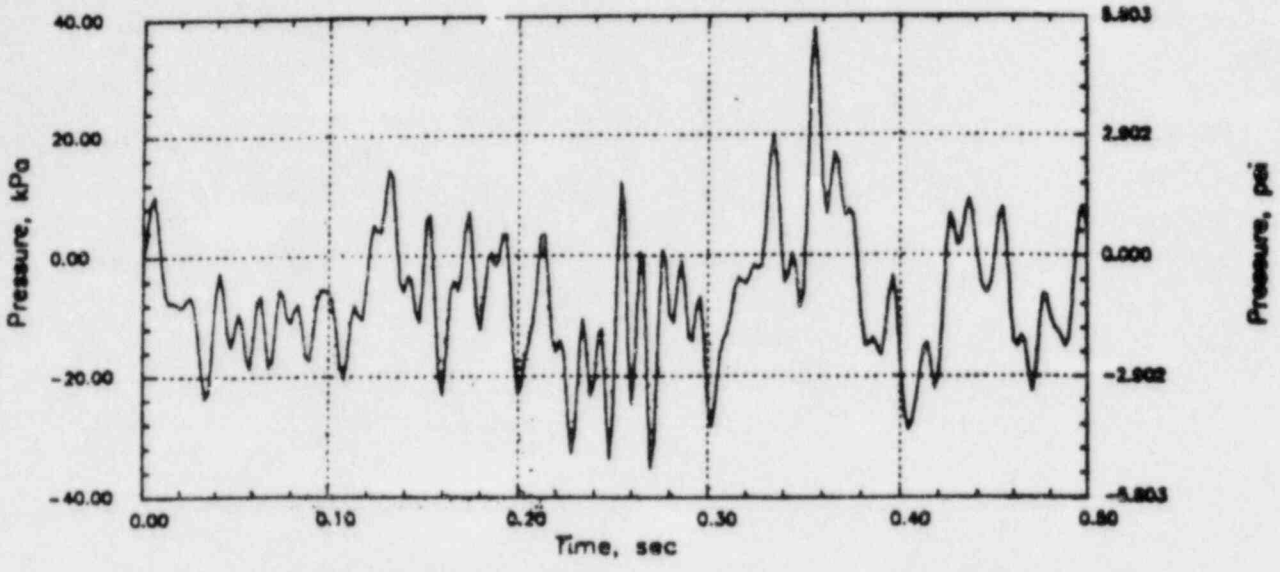

POP = 38.20 kPa PUP = -35.14 kPa MSP = 126.22 kPa²

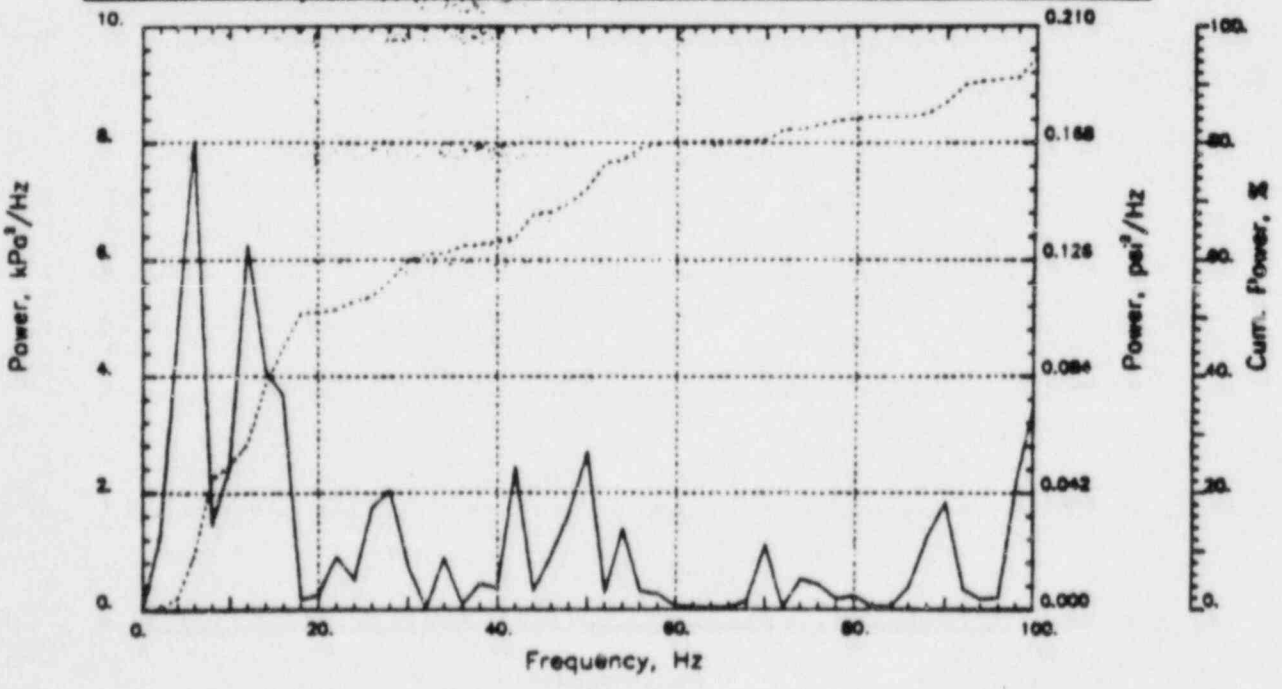

PERRY RHR CO

Output at point (14.21,28.00,0.00)

NAME - LEONG, TAI SENG
DATE - FEB 21, 1984
PROJECT NO. - 15026004

CHECKED _____
DATE _____
CALC NO. - AP-84-

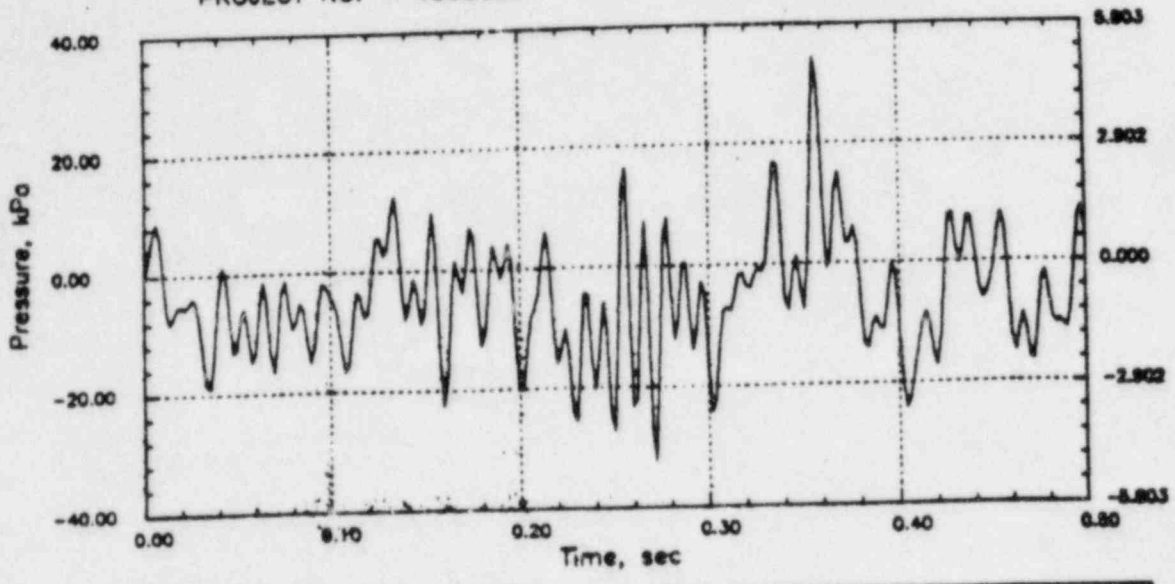

POP = 34.26 kPa PUP = -32.18 kPa MSP = 91.07 kPa²

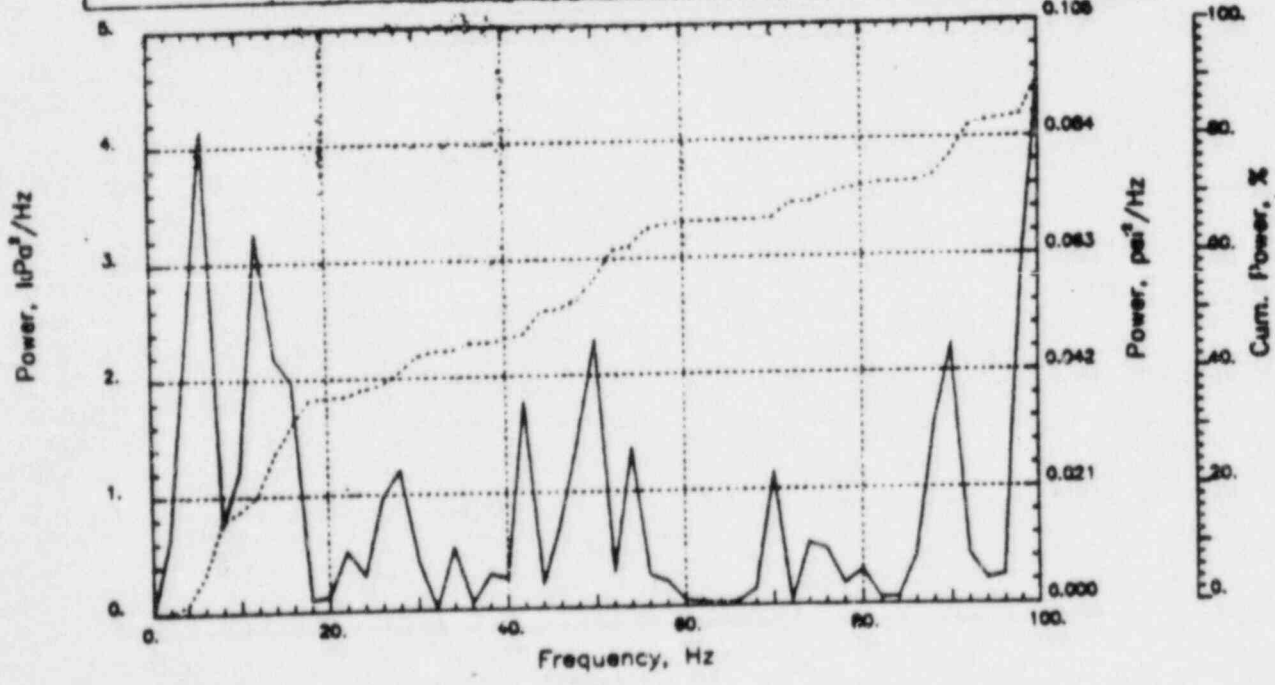

PERRY RHR CO

Output at point (15.77,28.00,0.00)

NAME - LEONG, TAI SENG
DATE - FEB 21, 1984
PROJECT NO. - 15026004

CHECKED _____
DATE _____
CALC NO. - AP-84-

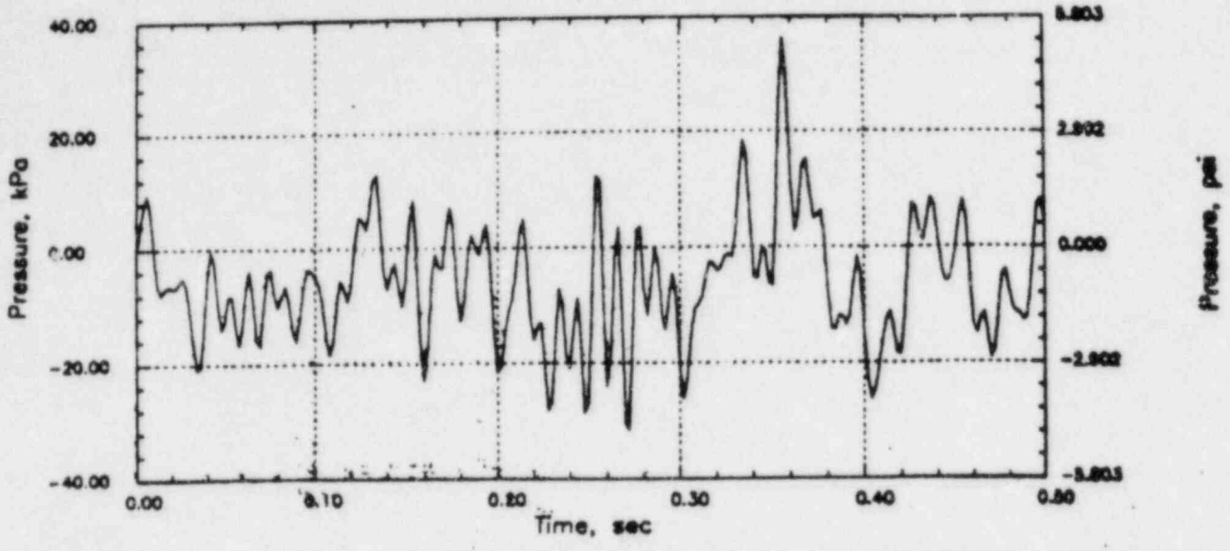

POP = 36.16 kPa PUP = -31.44 kPa MSP = 103.95 kPa²

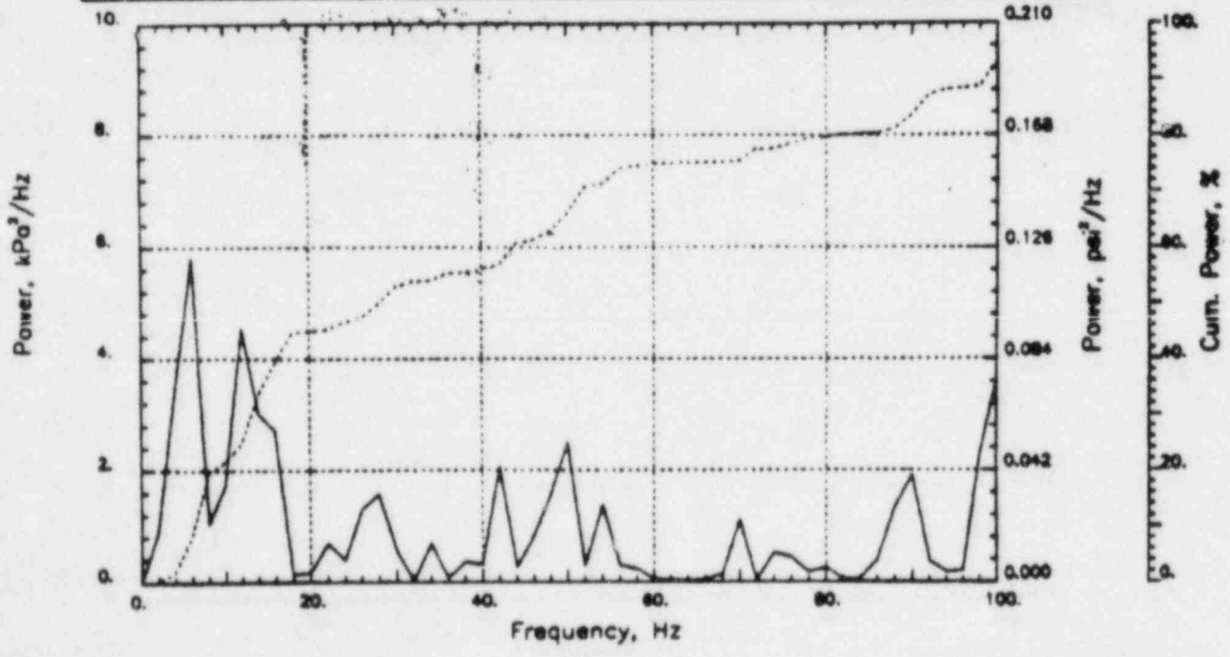

PERRY RHR CO

Output at point (15.77,28.00,0.00)

NAME - LEONG, TAI SENG
DATE - FEB 21, 1984
PROJECT NO. - 15026004

CHECKED _____
DATE _____
CALC NO. - AP-84-

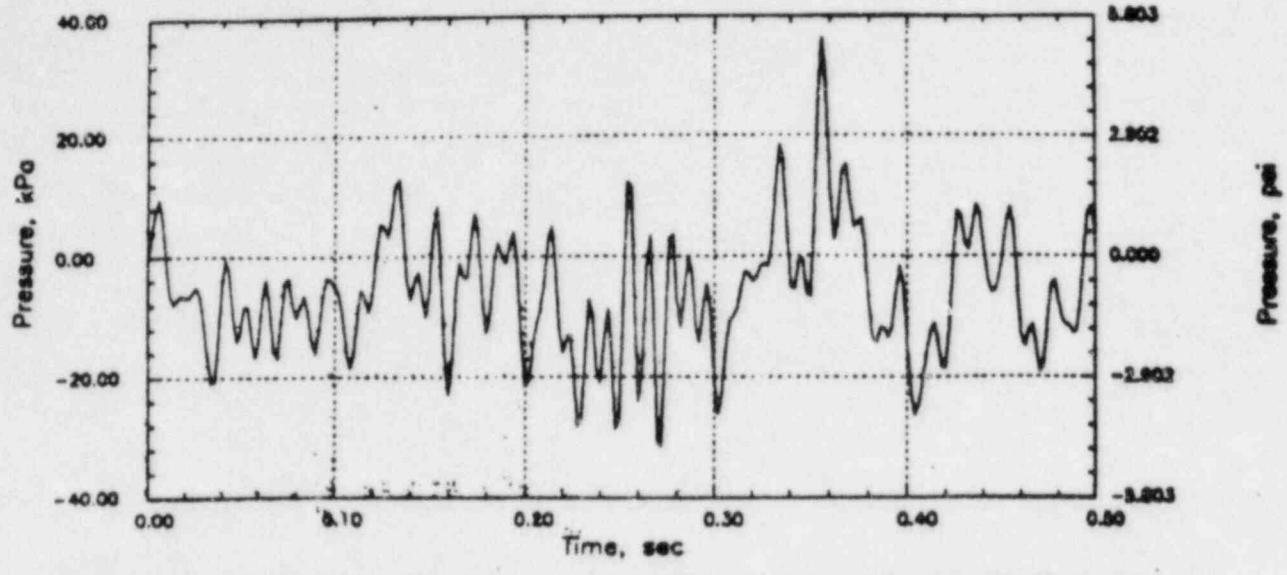

POP = 36.16 kPa PUP = -31.44 kPa MSP = 103.95 kPa²

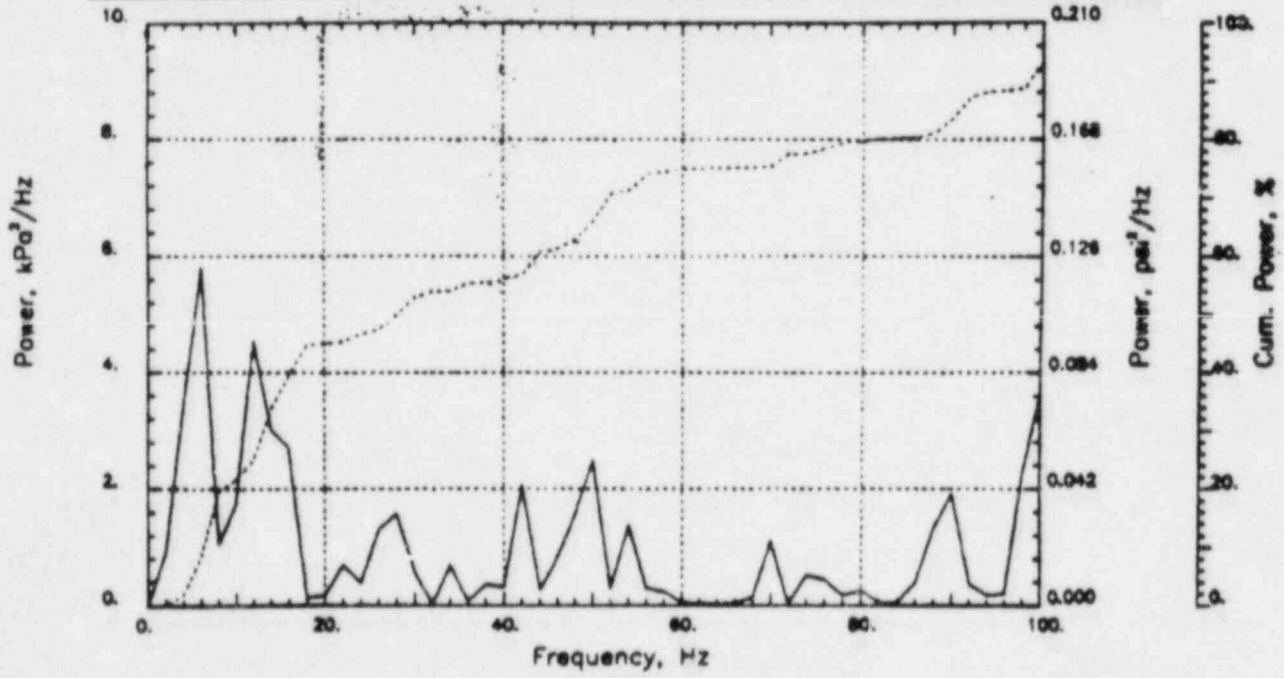

PERRY RHR CO

Output at point (14.21,28.00,0.00)

NAME - LEONG, TAI SENG
DATE - FEB 21, 1984
PROJECT NO. - 150260C4

CHECKED _____
DATE _____
CALC NO. - AP-84-

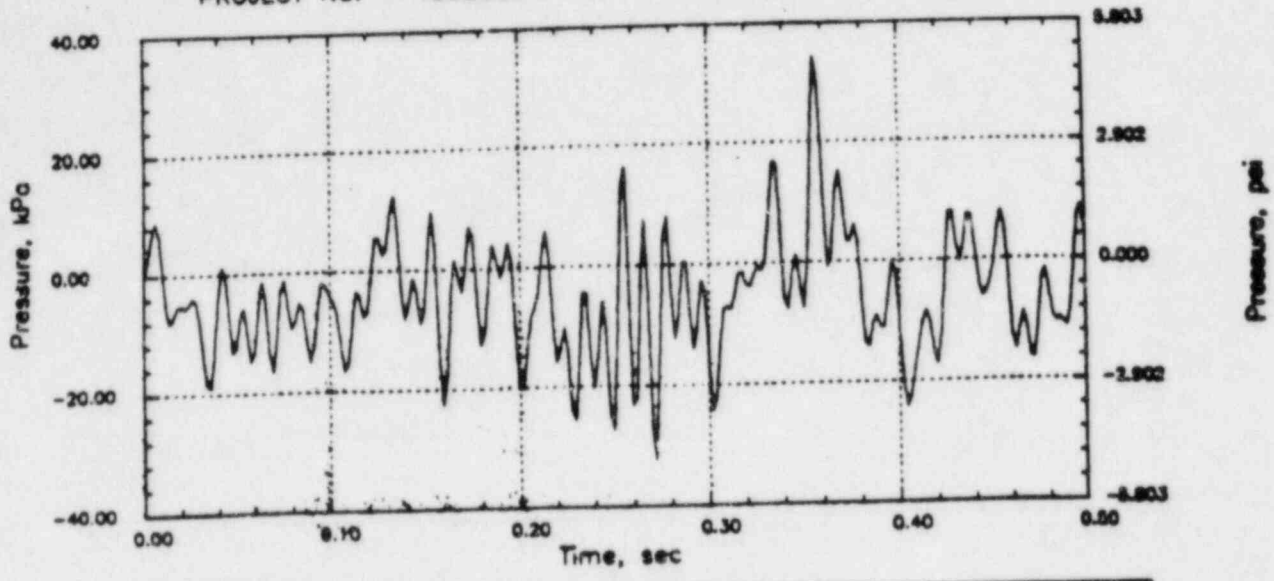

POP = 34.26 kPa PUP = -32.18 kPa MSP = 91.07 kPa²

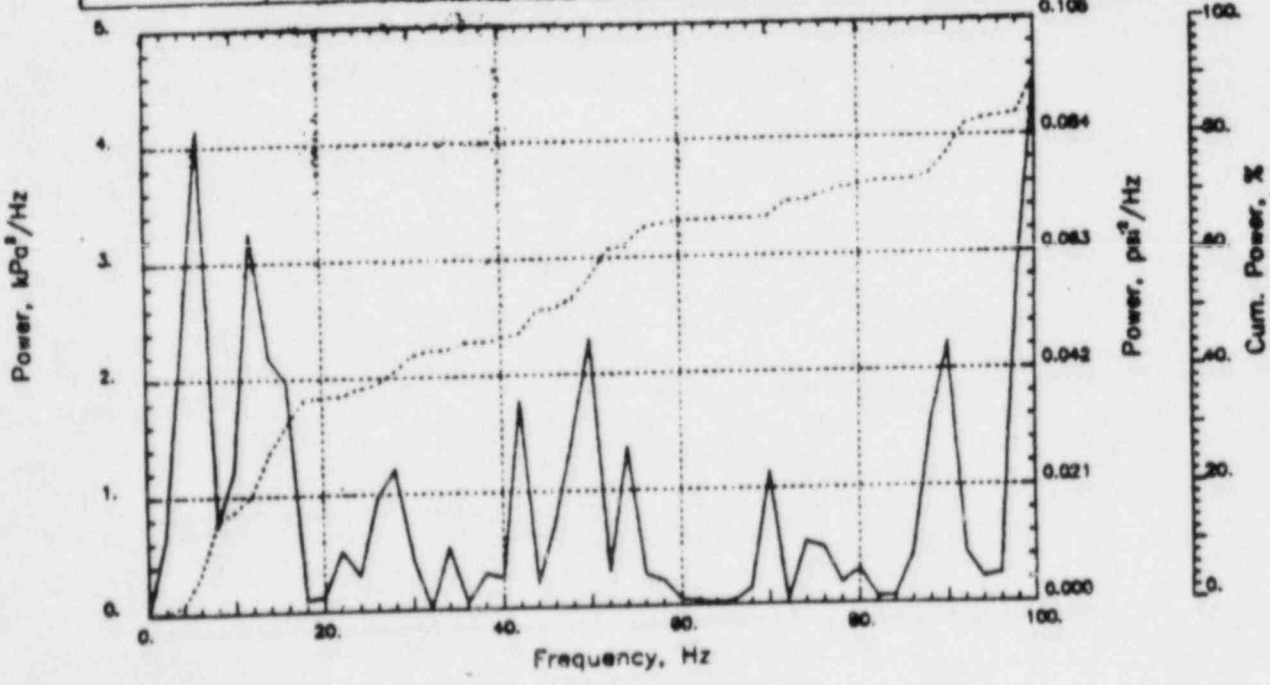

PERRY RHR CO

Output at point (12.65,28.00,0.46)

NAME - LEONG, TAI SENG
DATE - FEB 21, 1984
PROJECT NO. - 15026004

CHECKED _____
DATE _____
CALC NO. - AP-84-

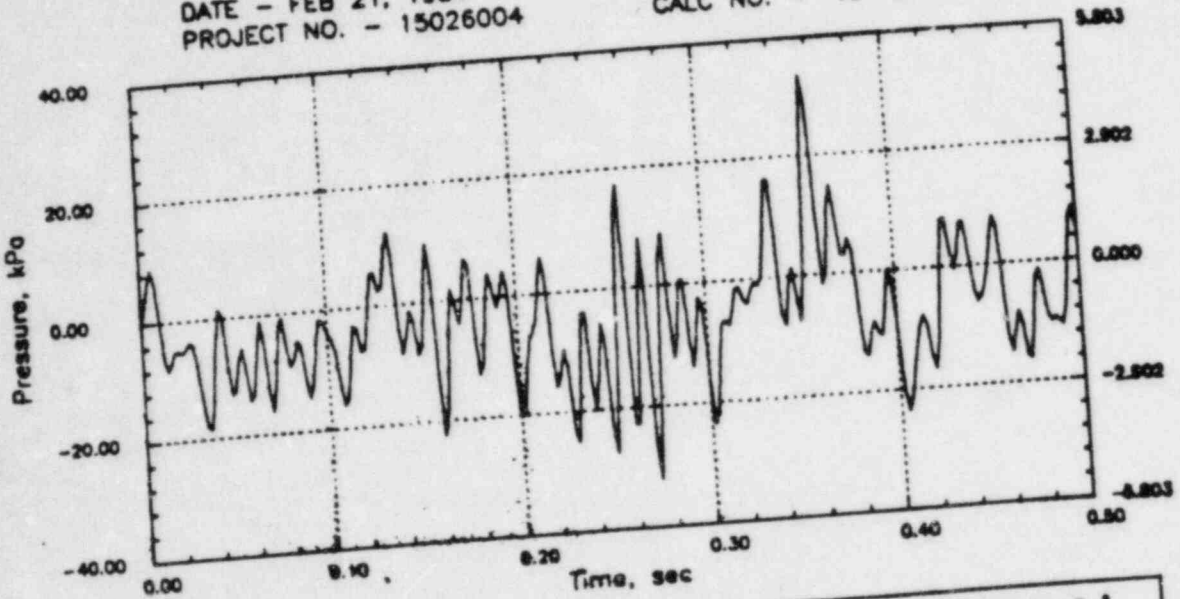

POP = 33.60 kPa PUP = -32.05 kPa MSP = 87.95 kPa²

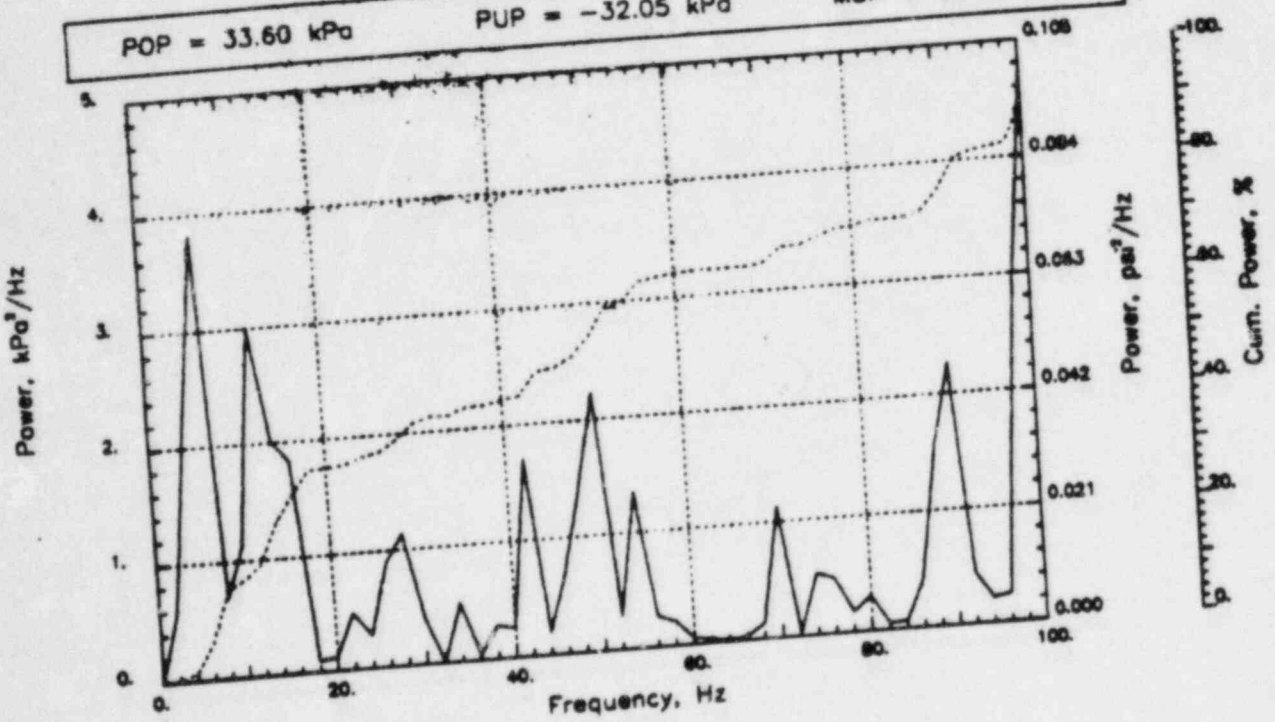

PERRY RHR CO

Output at point (12.65,28.00,0.00)

NAME - LEONG, TAI SENG
DATE - FEB 21, 1984
PROJECT NO. - 15026004

CHECKED _____
DATE _____
CALC NO. - AP-84-

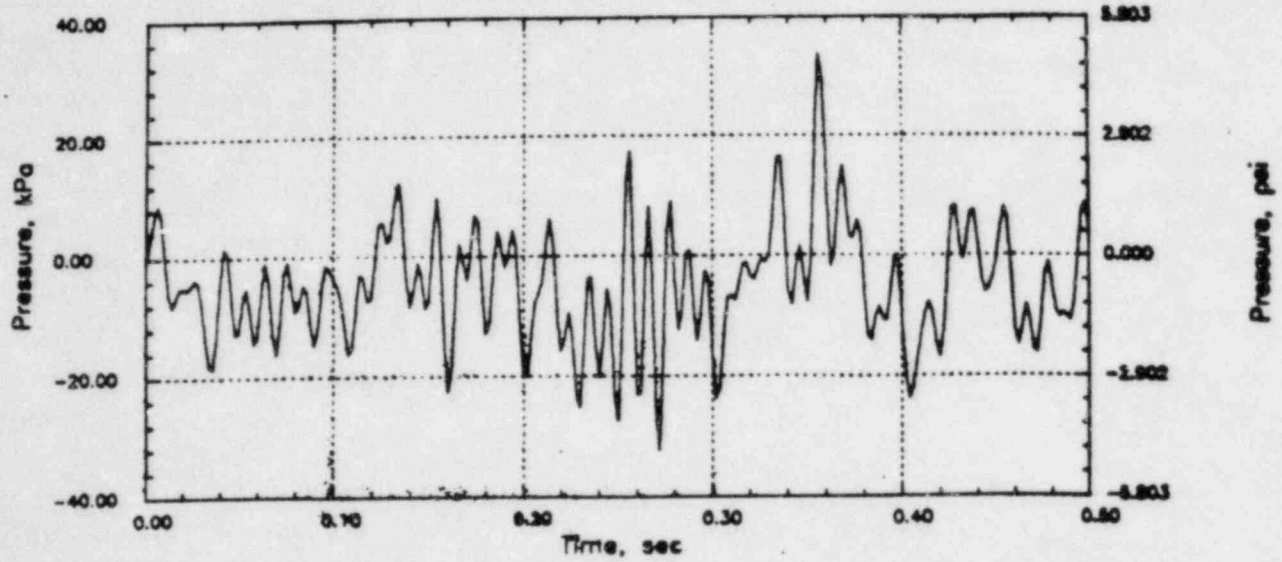

POP = 33.84 kPa PUP = -32.33 kPa MSP = 89.22 kPa²

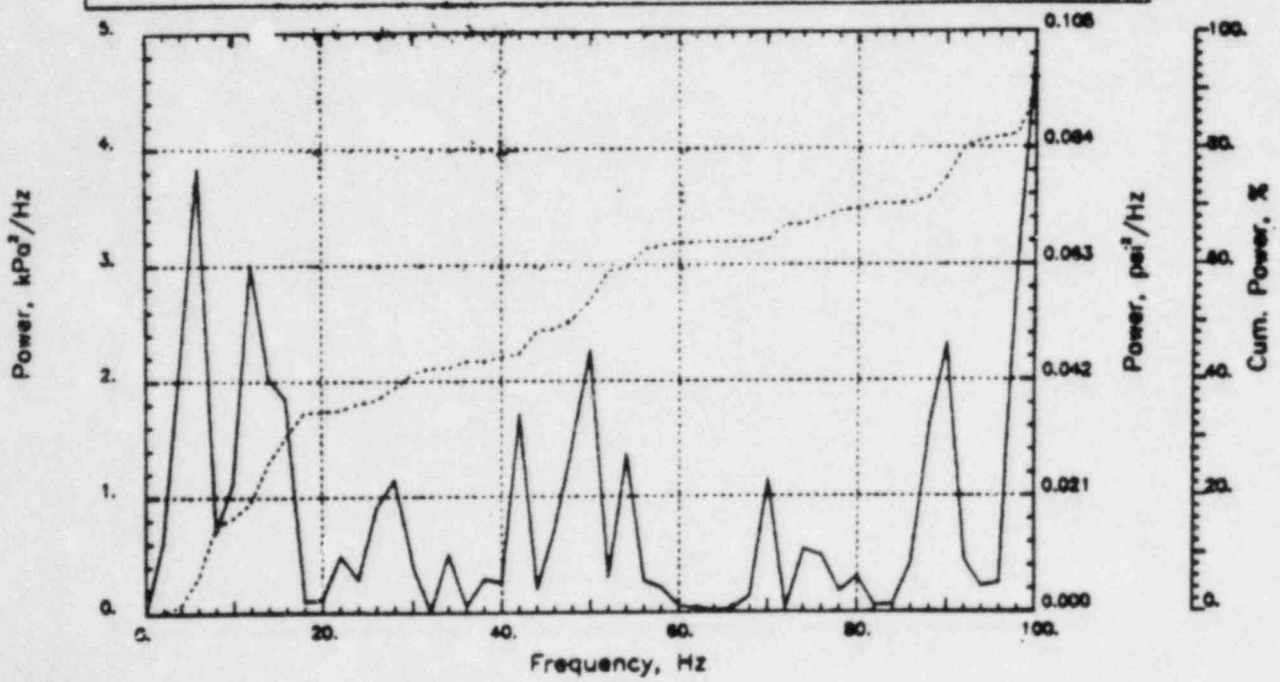

PERRY RHR CO

Output at point (12.65,28.00,1.55)

NAME - LEONG, TAI SENG
DATE - FEB 21, 1984
PROJECT NO. - 15026004

CHECKED _____
DATE _____
CALC NO. - AP-84-

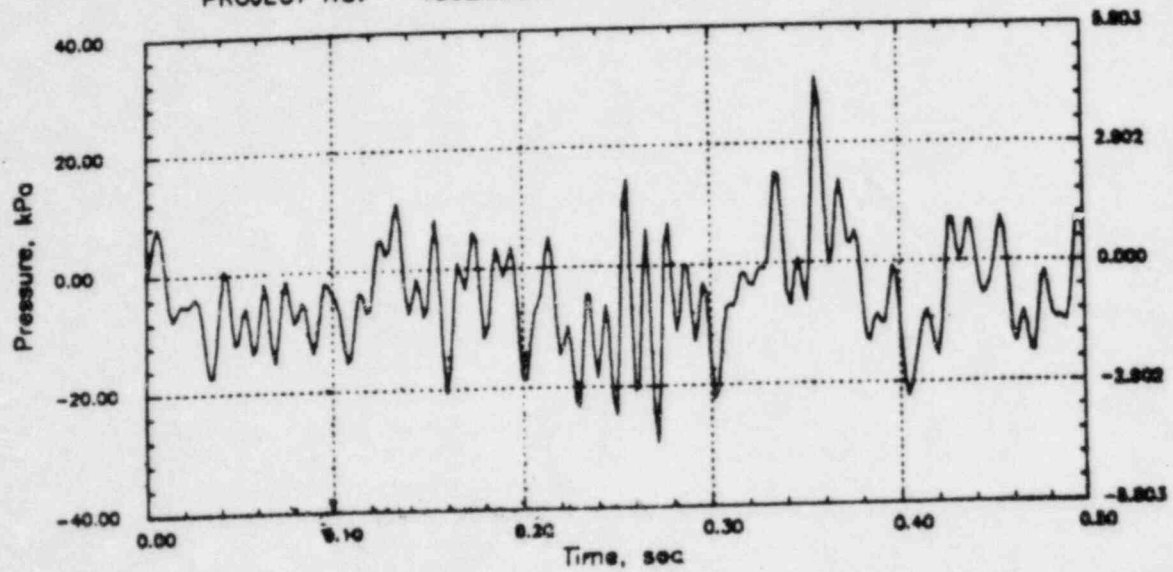

POP = 31.14 kPa PUP = -29.22 kPa MSP = 75.89 kPa²

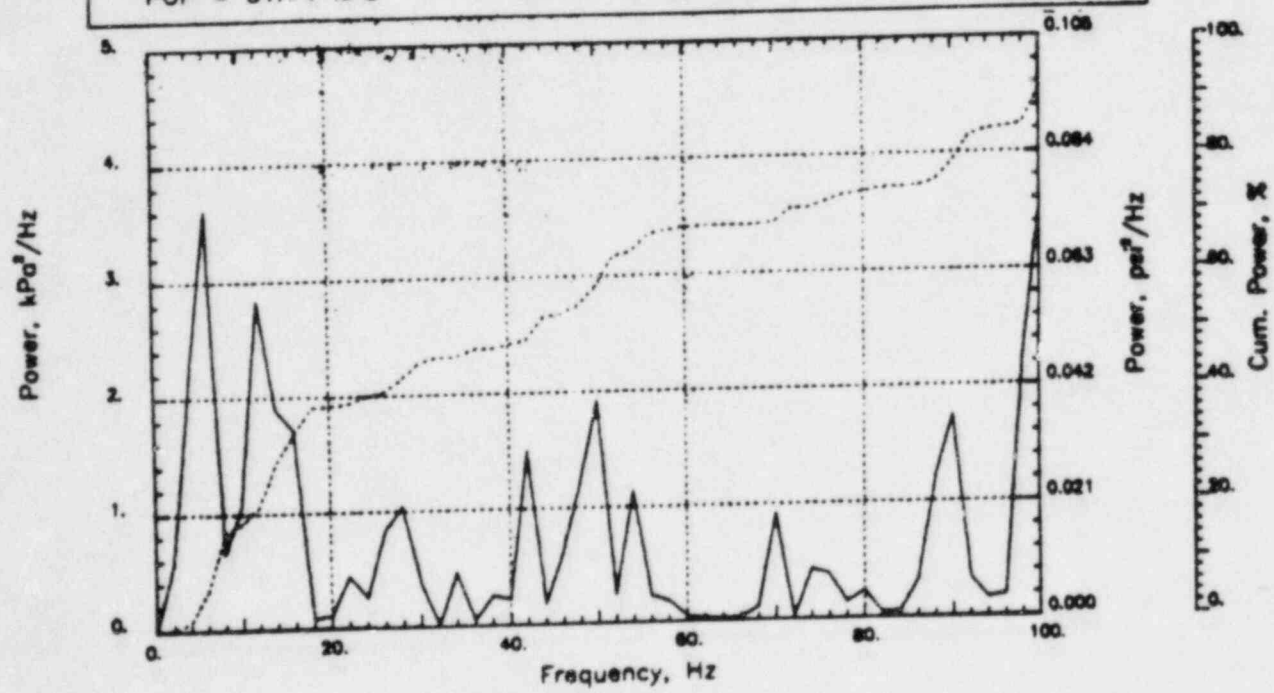

PERRY RHR CO

Output at point (12.65,28.00,2.18)

NAME - LEONG, TAI SENG
DATE - FEB 21, 1984
PROJECT NO. - 15026004

CHECKED _____
DATE _____
CALC NO. - AP-84-

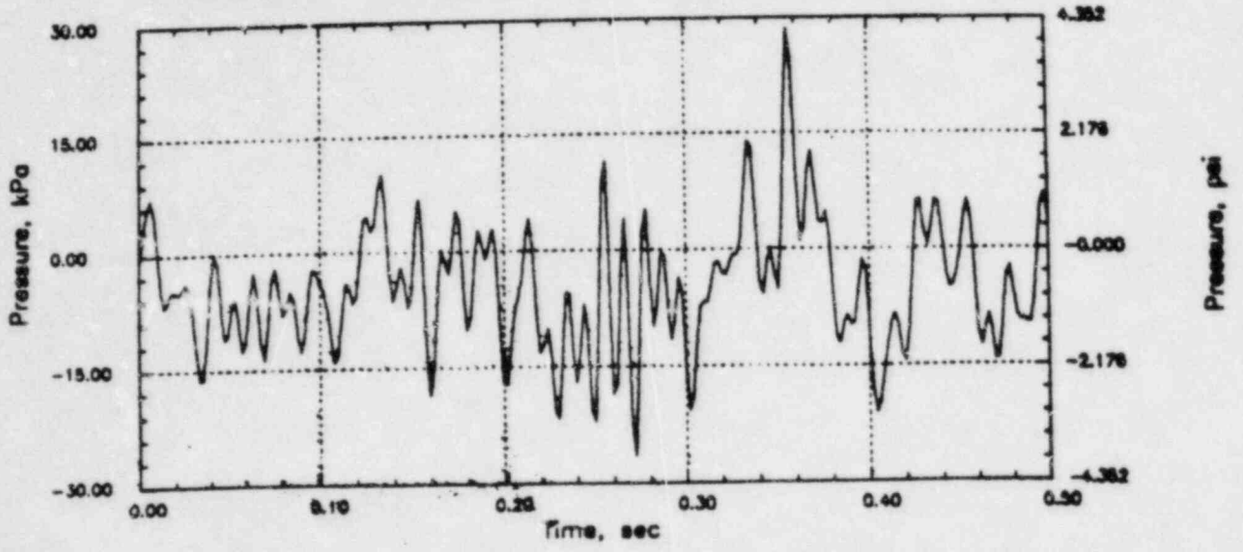

POP = 28.62 kPa PUP = -26.38 kPa MSP = 64.94 kPa²

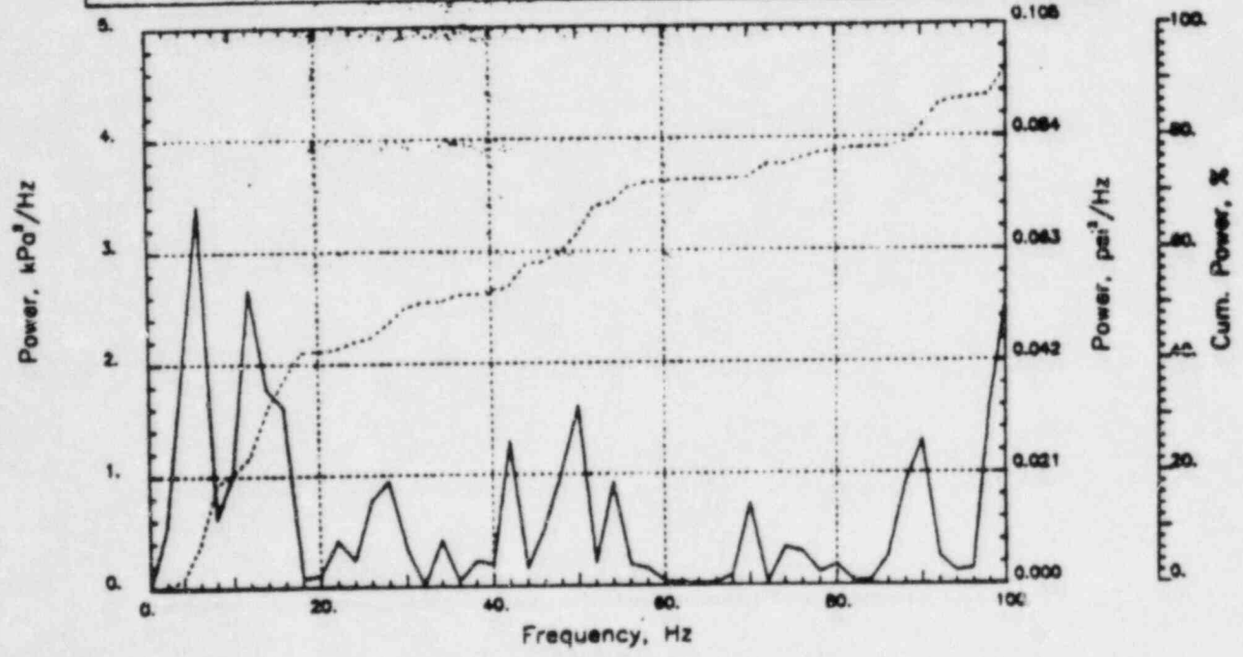

PERRY RHR CO

Output at point (12.65,28.00,2.82)

NAME - LEONG, TAI SENG
DATE - FEB 21, 1984
PROJECT NO. - 15026004

CHECKED _____
DATE _____
CALC NO. - AP-84-

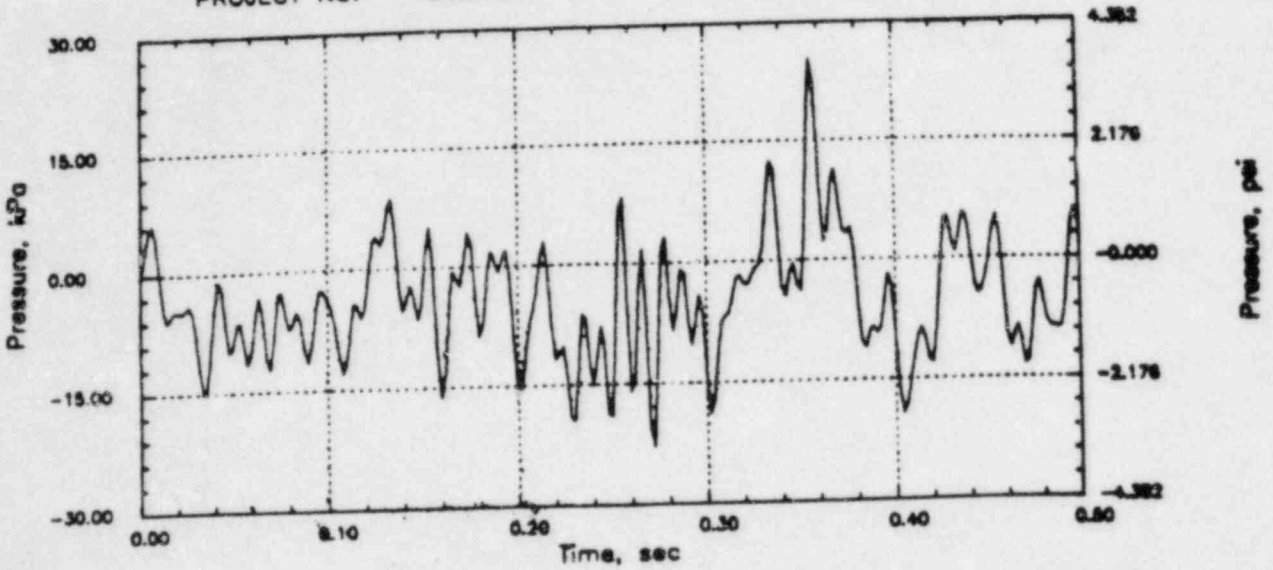

POP = 25.33 kPa PUP = -22.83 kPa MSP = 52.42 kPa²

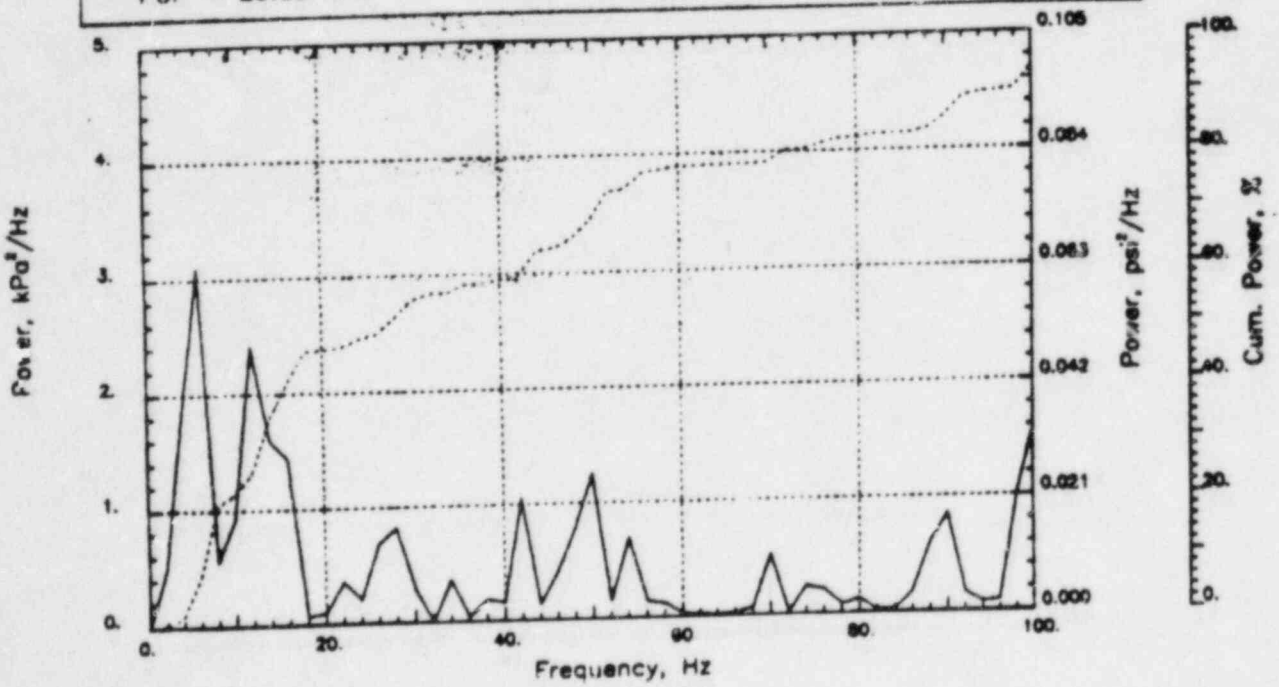

PERRY RHR CO

Output at point (12.65,28.00,3.45)

NAME - LEONG, TAI SENG
DATE - FEB 21, 1984
PROJECT NO. - 15026004

CHECKED _____
DATE _____
CALC NO. - AP-84-

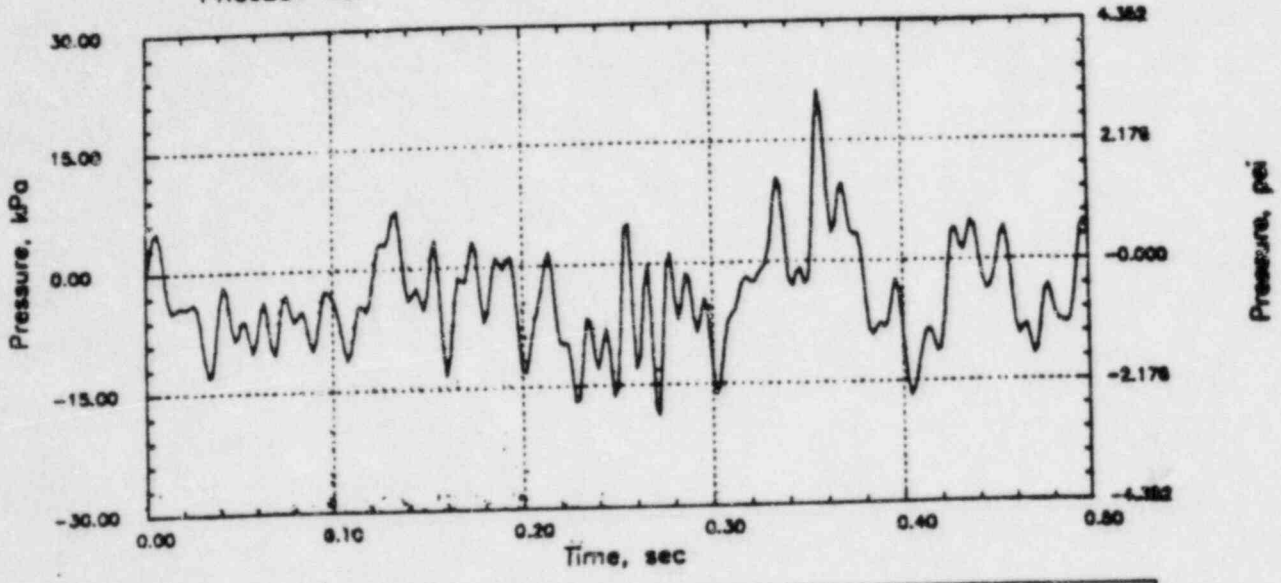

POP = 21.24 kPa PUP = -18.67 kPa MSP = 38.65 kPa²

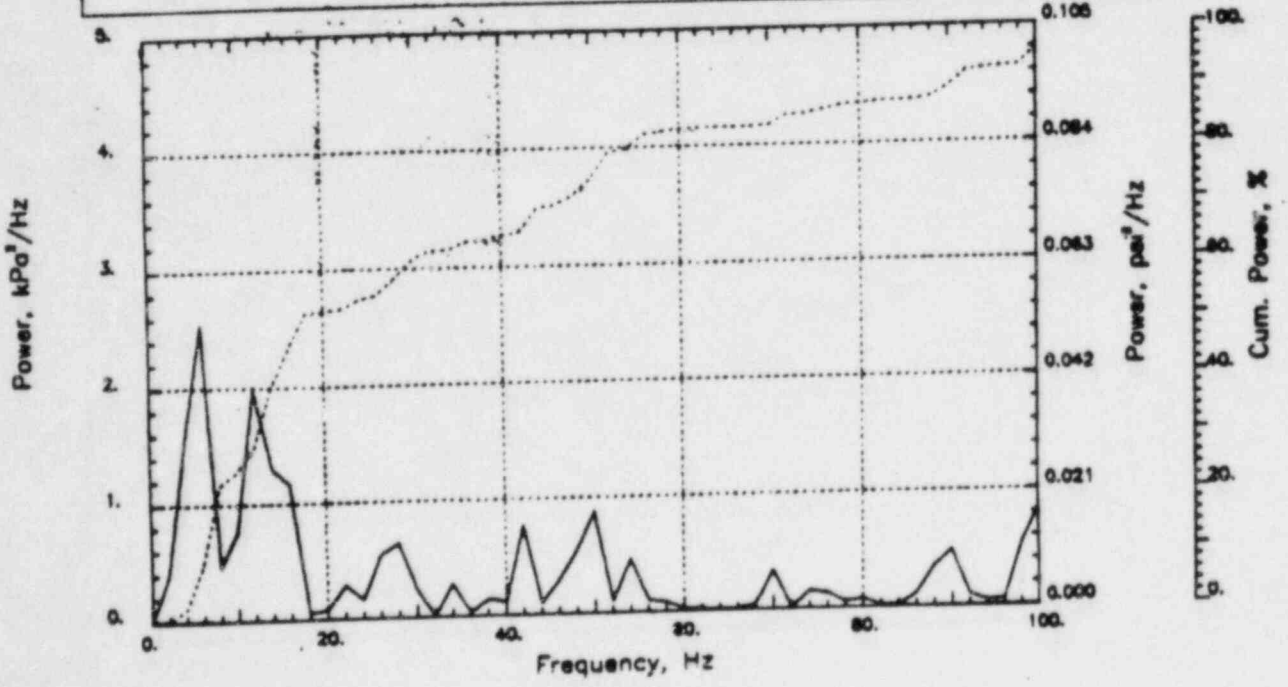

PERRY RHR CO

Output at point (12.65,28.00,4.09)

NAME - LEONG, TAI SENG
DATE - FEB 21, 1984
PROJECT NO. - 15026004

CHECKED _____
DATE _____
CALC NO. - AP-84-

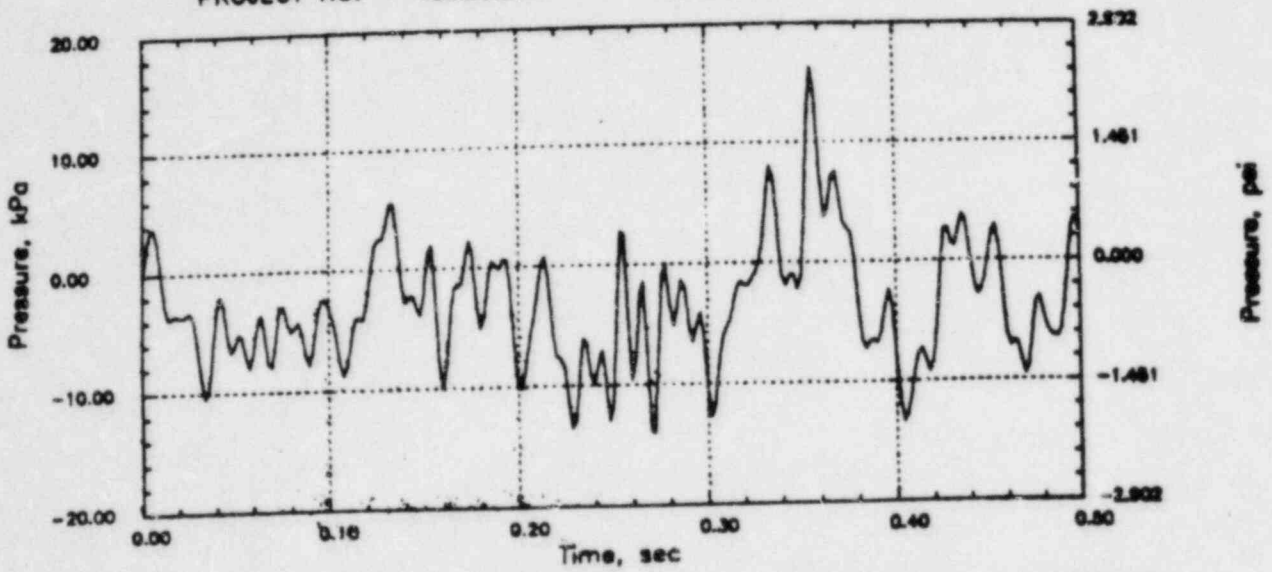

POP = 16.28 kPa PUP = -13.97 kPa MSP = 24.06 kPa²

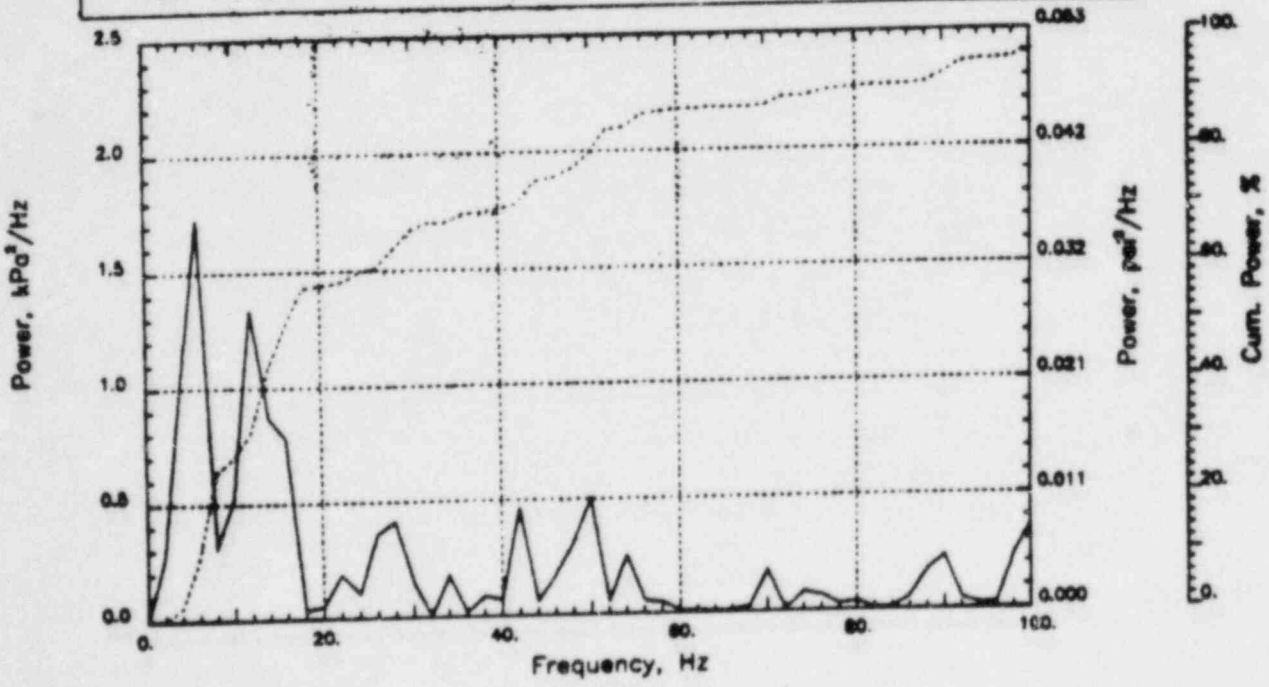

PERRY RHR CO

Output at point (12.65,28.00,4.91)

NAME - LEONG, TAI SENG
DATE - FEB 21, 1984
PROJECT NO. - 15026004

CHECKED _____
DATE _____
CALC NO. - AP-84-

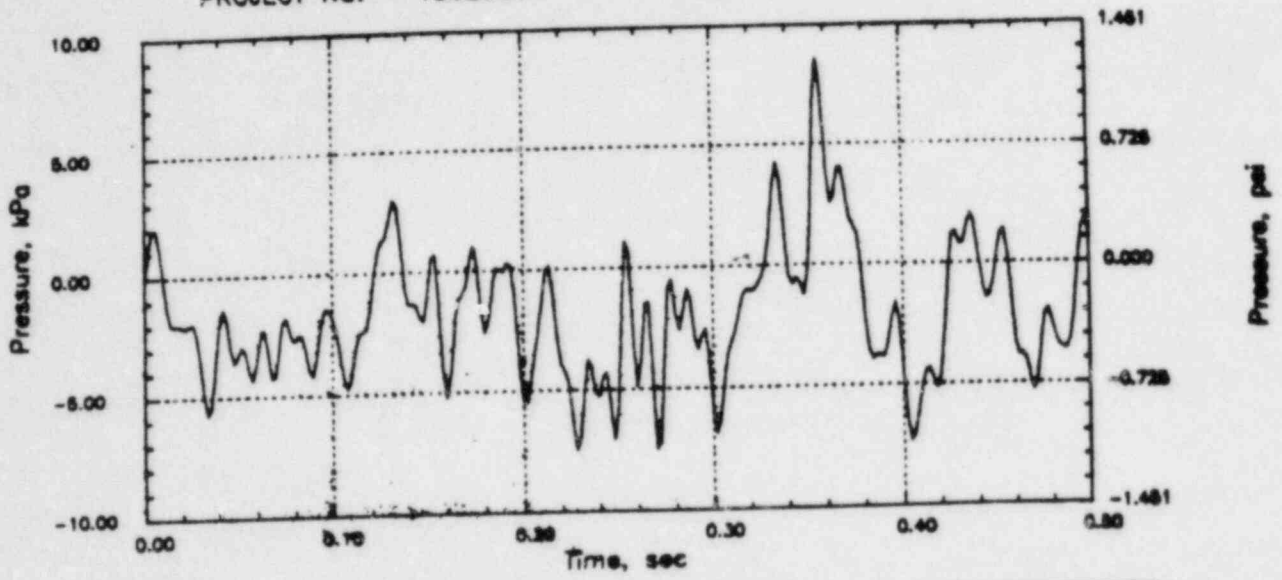

POP = 8.59 kPa PUP = -7.46 kPa MSP = 7.16 kPa²

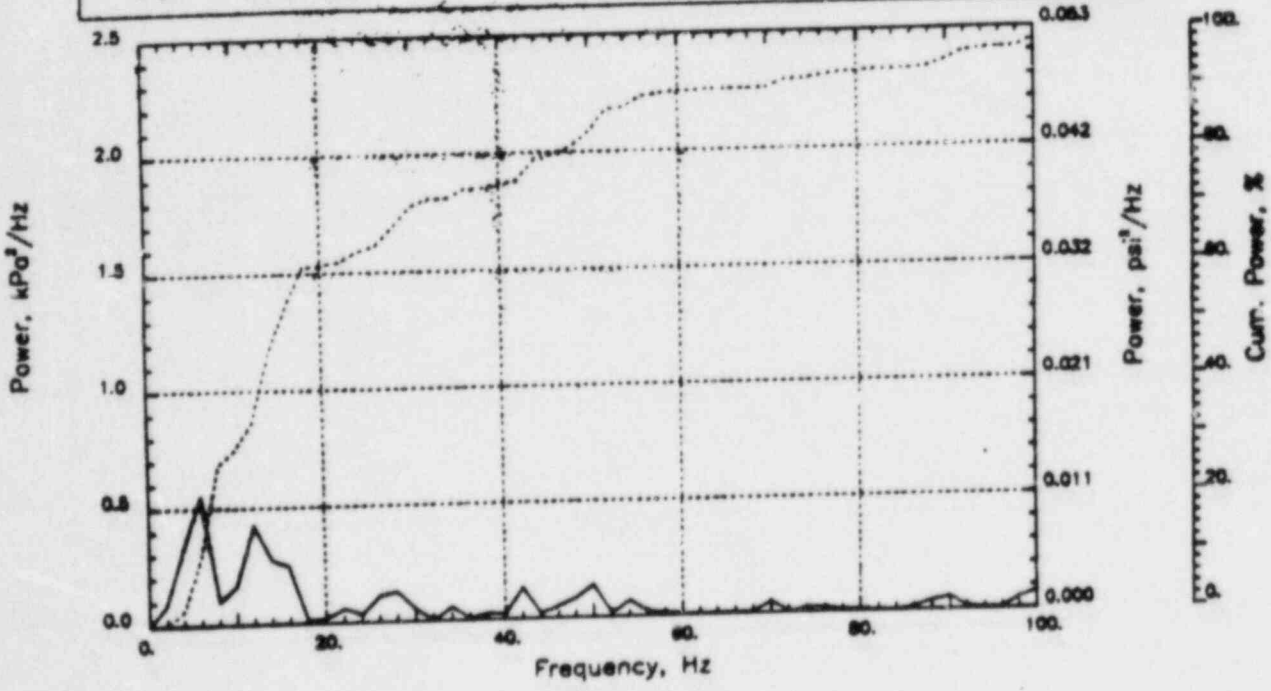

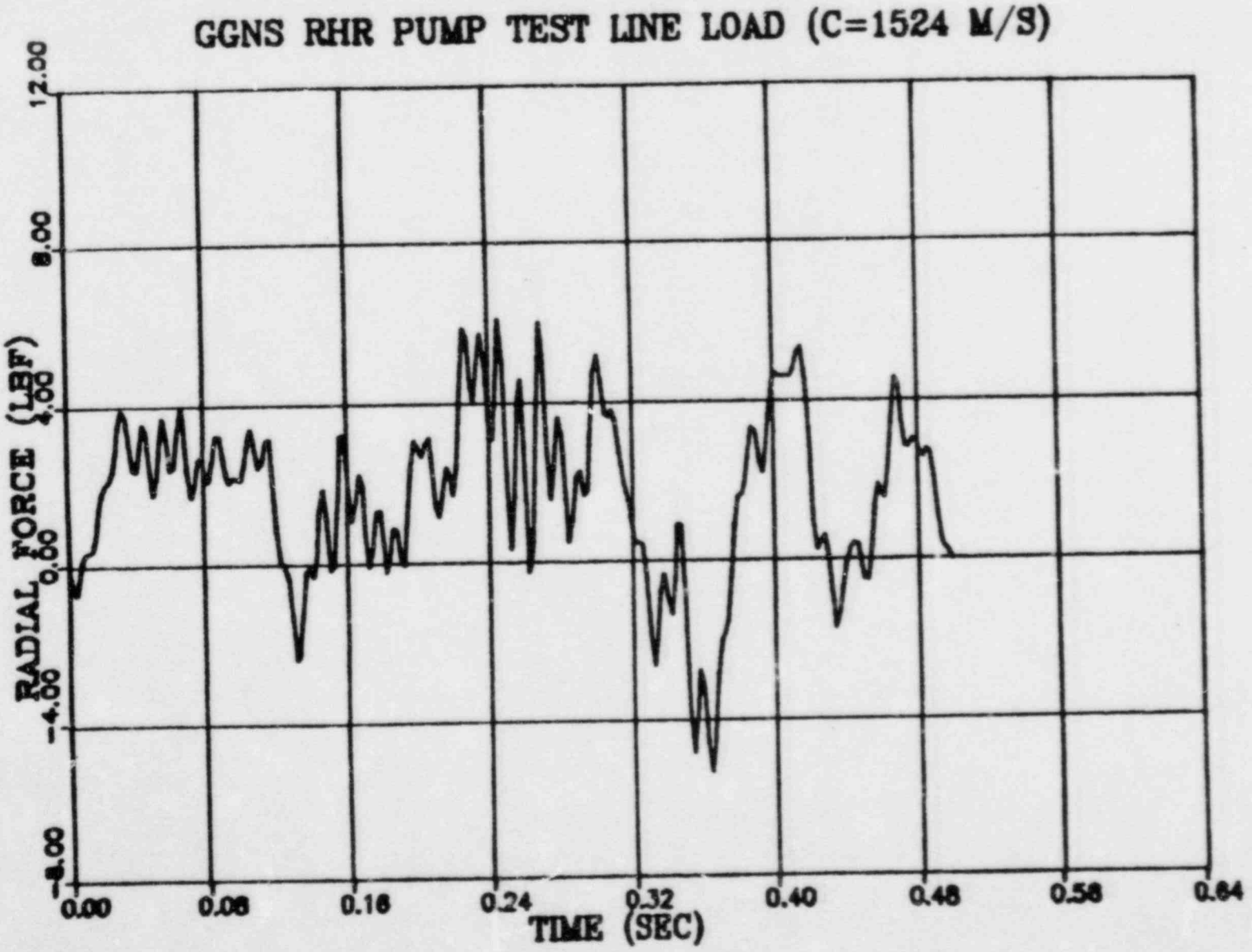
GGNS RHR PUMP TEST LINE LOAD (C=1524 M/S)
RADIAL FORCE (LBF)
12.00
8.00
4.00
0.00
-4.00
-8.00
0.00
0.08
0.16
0.24
0.32
0.40
0.48
0.56
0.64
TIME (SEC)

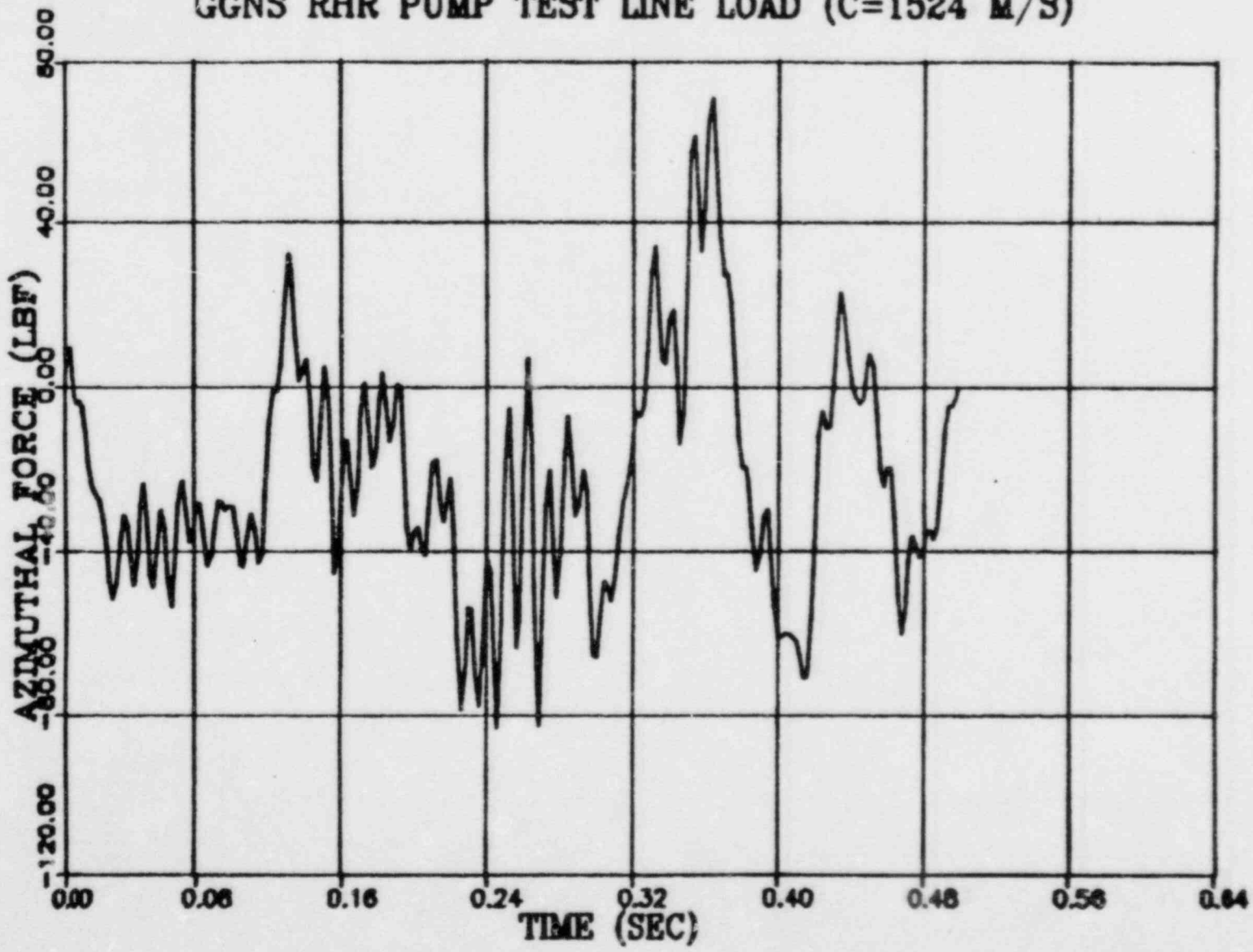
GGNS RHR PUMP TEST LINE LOAD (C=1524 M/S)
AZIMUTHAL FORCE (LBF)
80.00
40.00
0.00
-40.00
-80.00
-120.00
0.00
0.08
0.16
0.24
0.32
0.40
0.48
0.56
0.64
TIME (SEC)

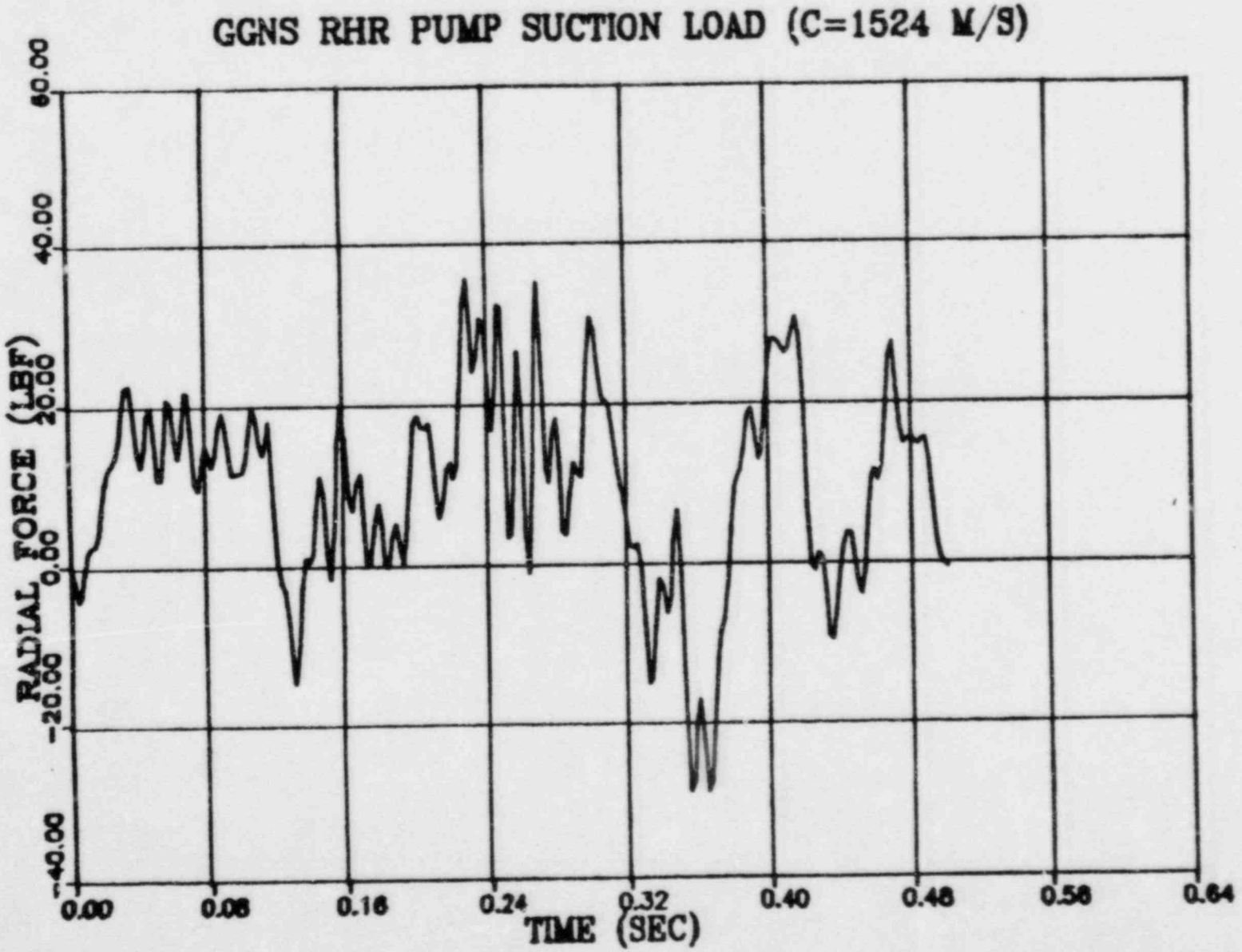
GGNS RHR PUMP SUCTION LOAD (C=1524 M/S)
RADIAL FORCE (LBF)
60.00
40.00
20.00
0.00
-20.00
-40.00
0.00
0.08
0.16
0.24
0.32
0.40
0.48
0.56
0.64
TIME (SEC)

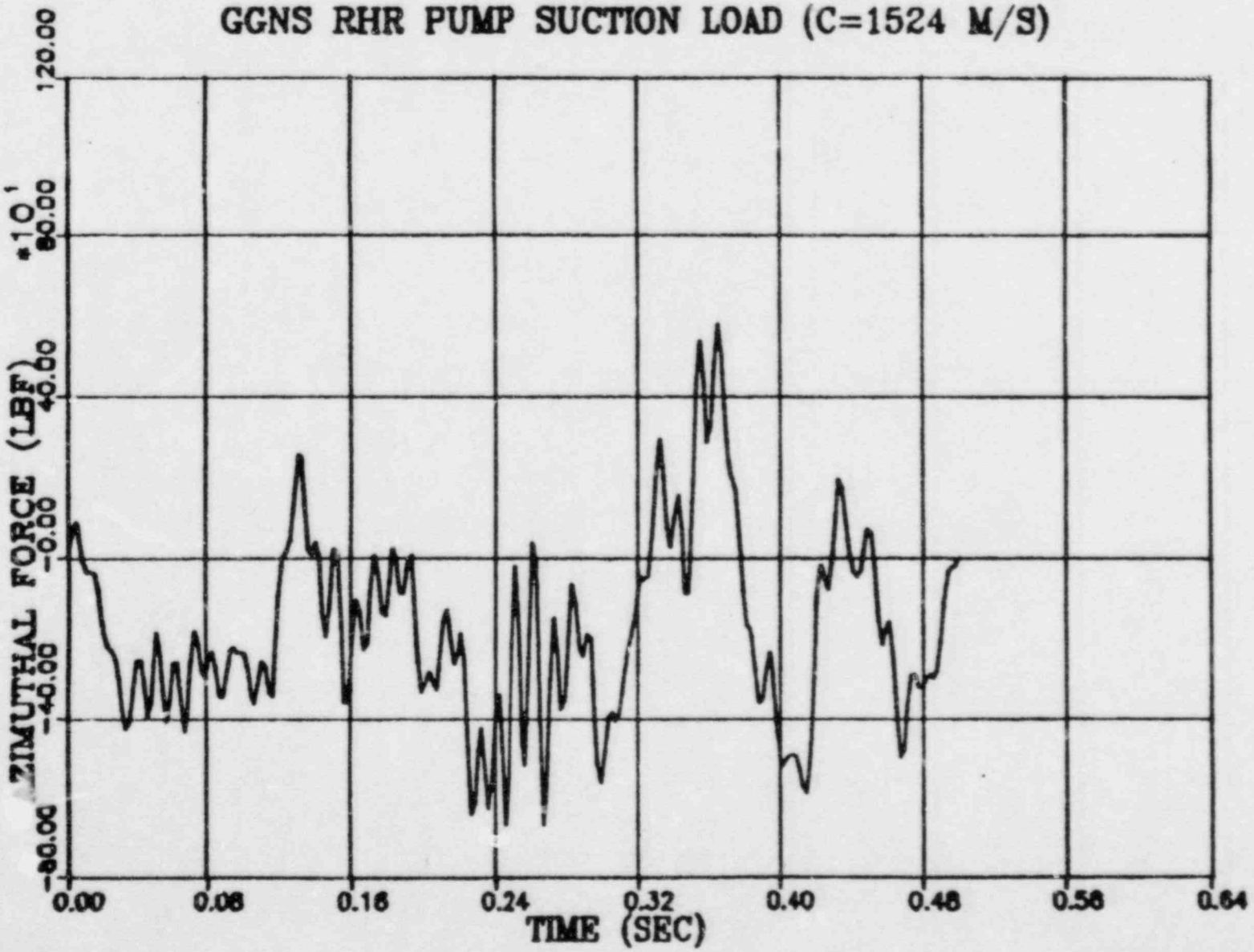
GGNS RHR PUMP SUCTION LOAD (C=1524 M/S)
AZIMUTHAL FORCE (LBF) *10^1
120.00
80.00
40.00
-0.00
-40.00
-80.00
0.00
0.08
0.16
0.24
0.32
0.40
0.48
0.56
0.64
TIME (SEC)

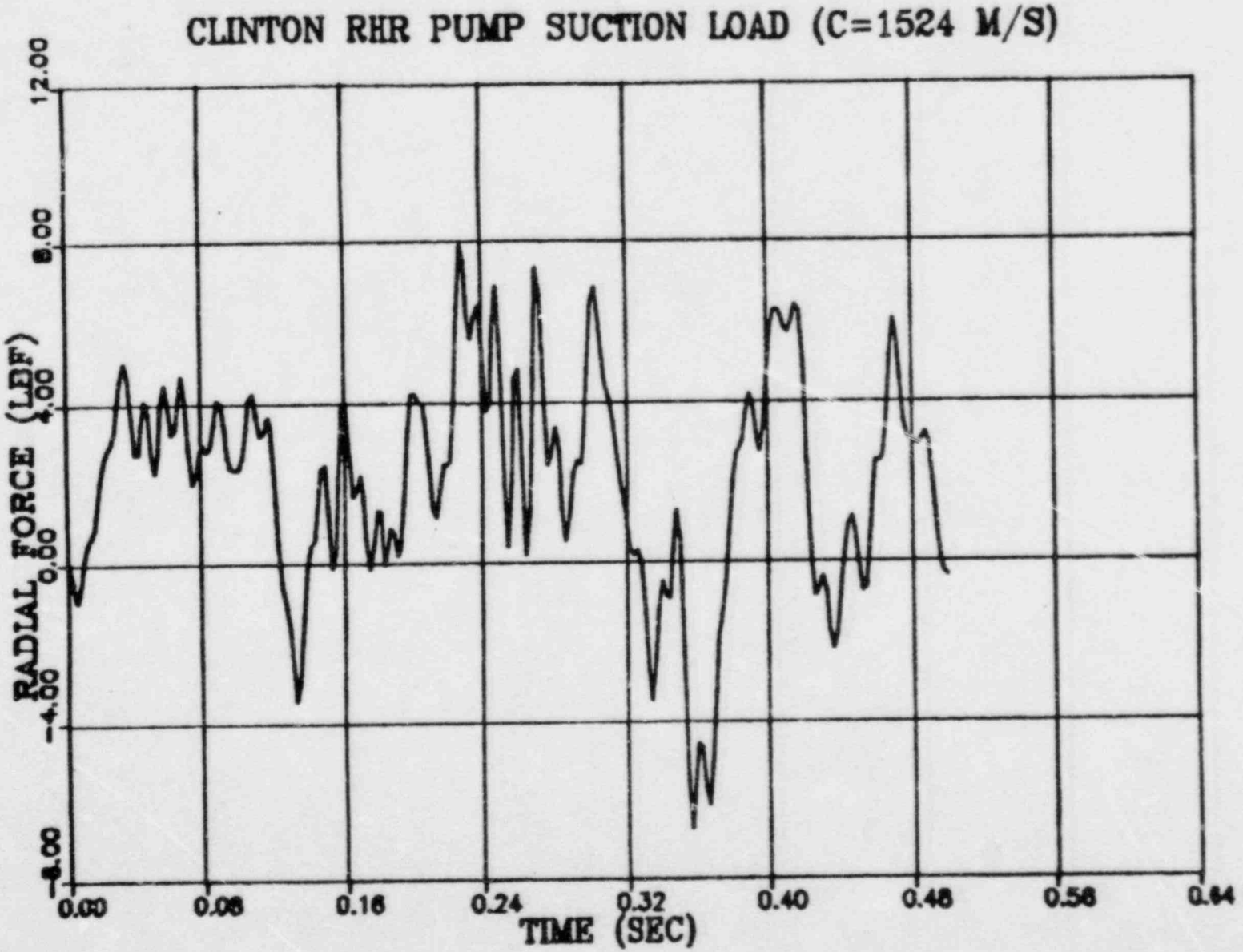
CLINTON RHR PUMP SUCTION LOAD (C=1524 M/S)
RADIAL FORCE (LBF)
12.00
8.00
4.00
0.00
-4.00
-8.00
0.00
0.08
0.16
0.24
0.32
0.40
0.48
0.56
0.64
TIME (SEC)

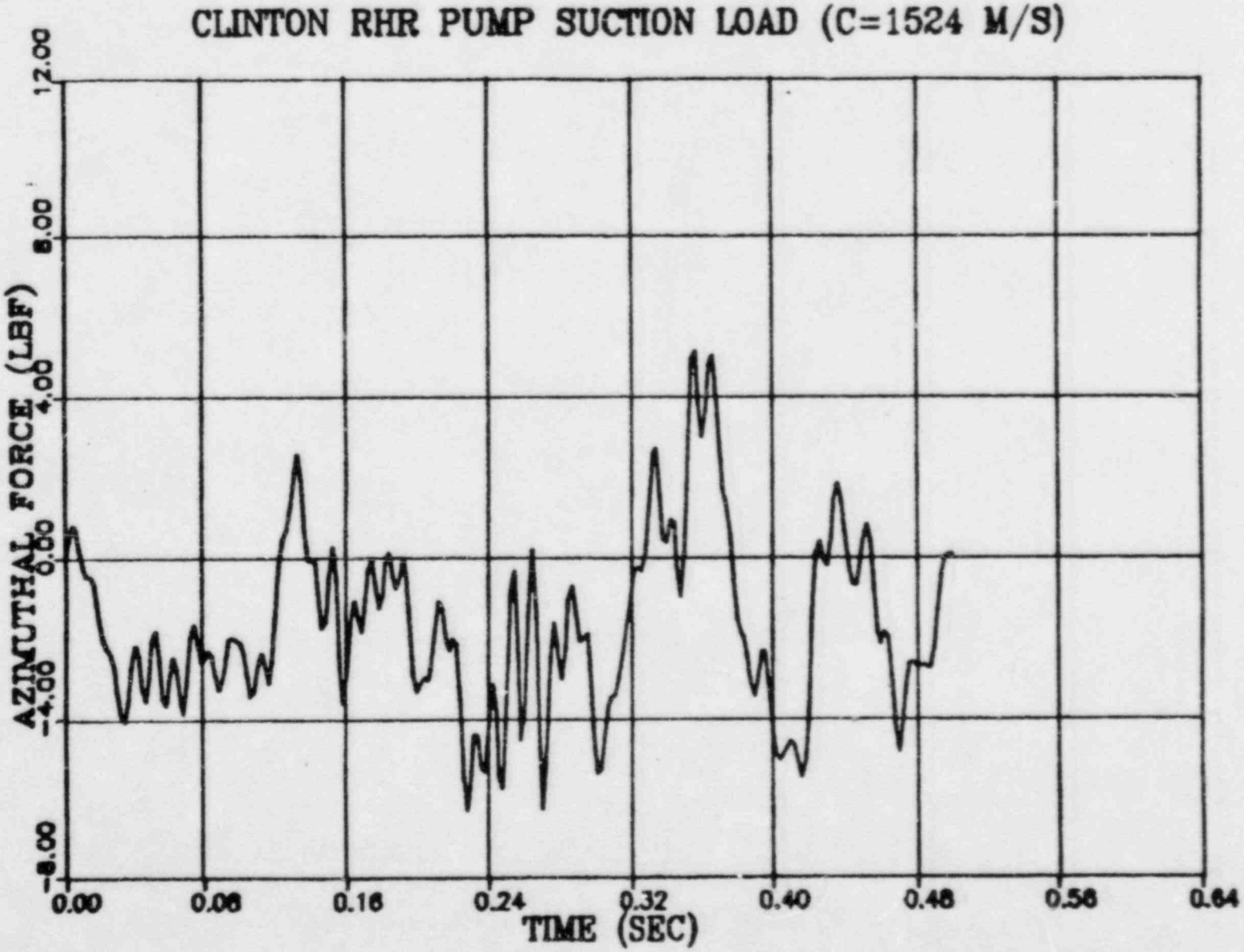
CLINTON RHR PUMP SUCTION LOAD (C=1524 M/S)
AZIMUTHAL FORCE (LBF)
12.00
8.00
4.00
0.00
-4.00
-8.00
0.00
0.08
0.16
0.24
0.32
0.40
0.48
0.56
0.64
TIME (SEC)

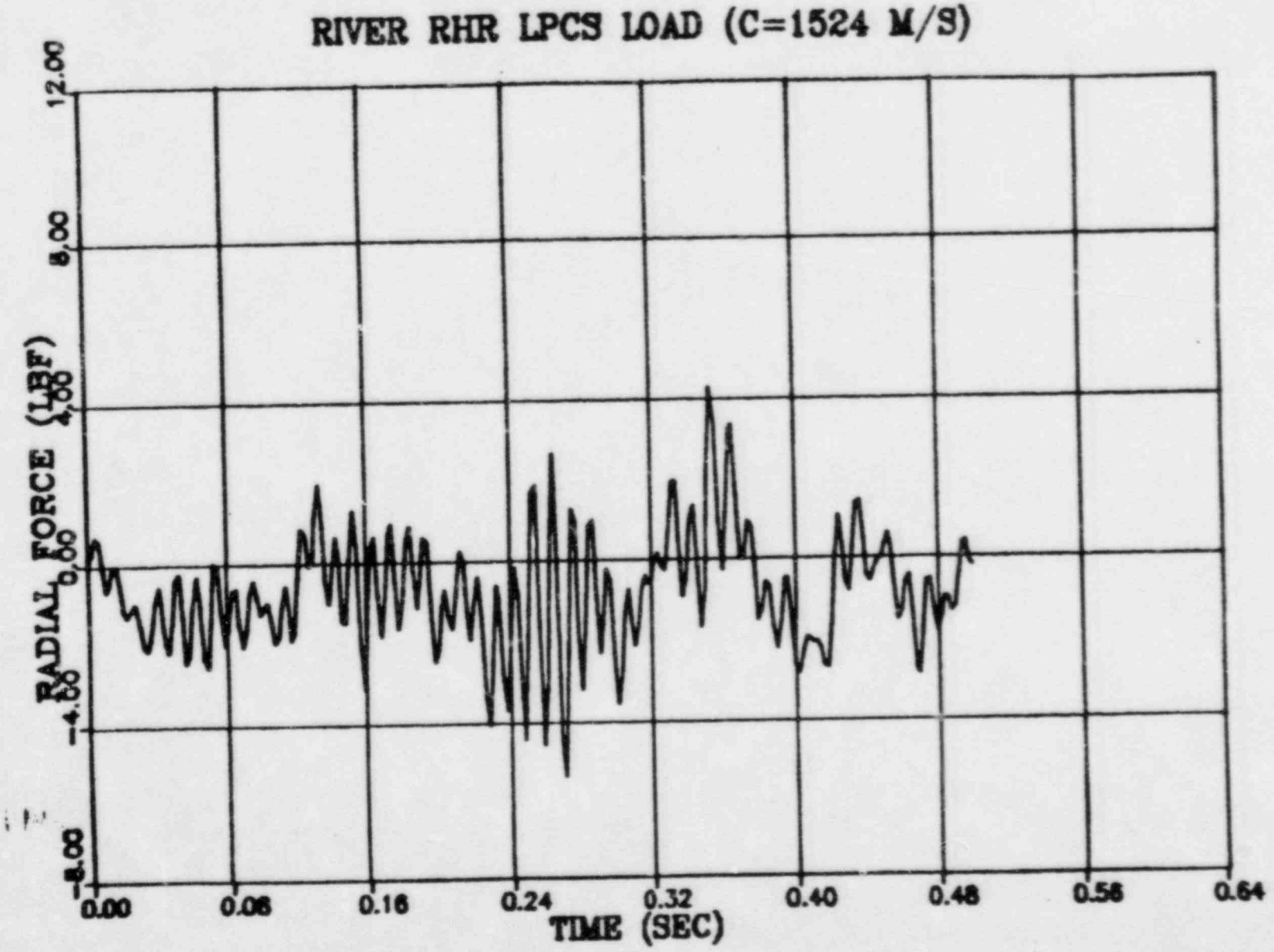
RIVER RHR LPCS LOAD (C=1524 M/S)
12.00
8.00
4.00
0.00
-4.00
-8.00
RADIAL FORCE (LBF)
0.00
0.08
0.16
0.24
0.32
0.40
0.48
0.56
0.64
TIME (SEC)

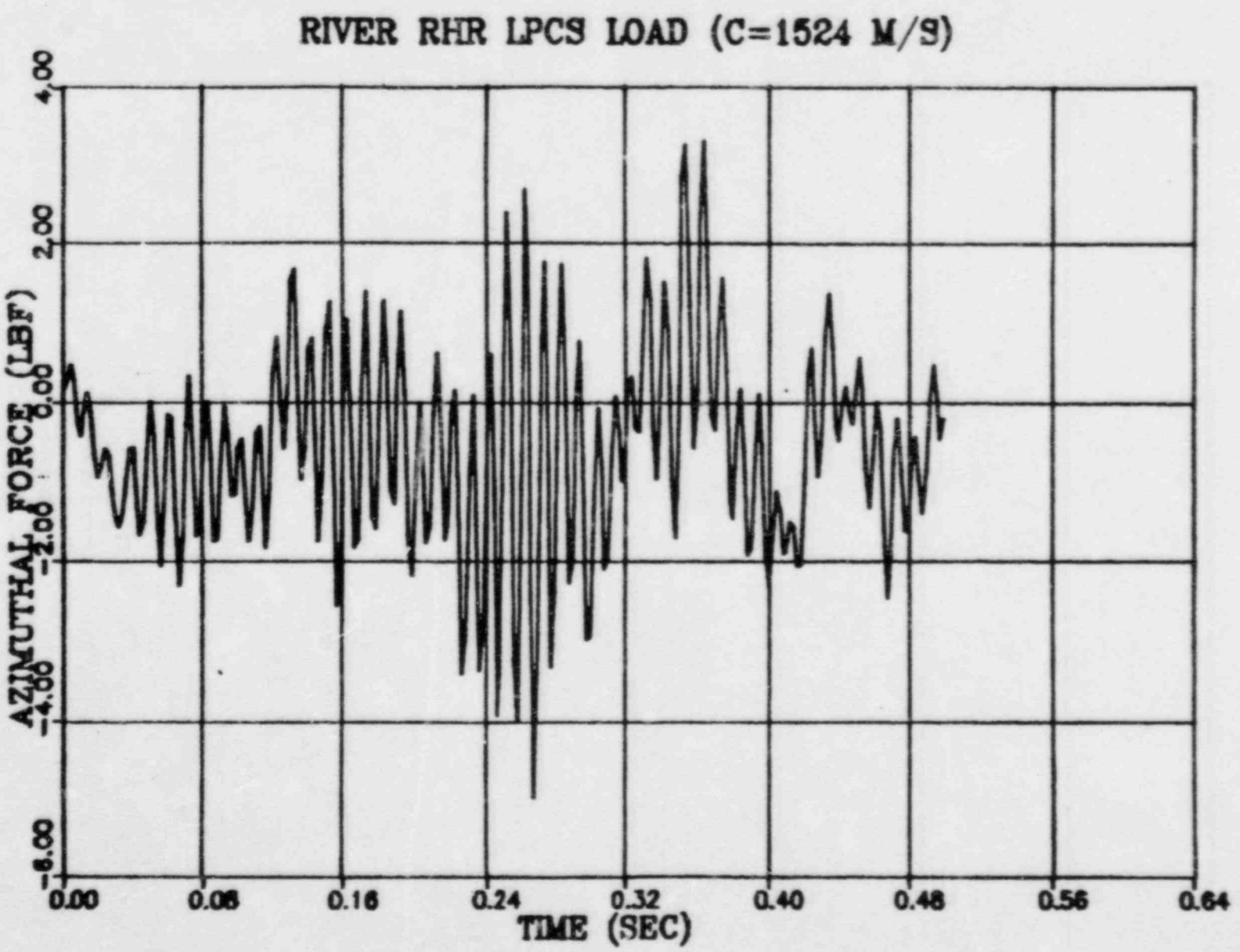
RIVER RHR LPCS LOAD (C=1524 M/S)
AZIMUTHAL FORCE (LBF)
4.00
2.00
0.00
-2.00
-4.00
-6.00
0.00
0.08
0.16
0.24
0.32
0.40
0.48
0.56
0.64
TIME (SEC)

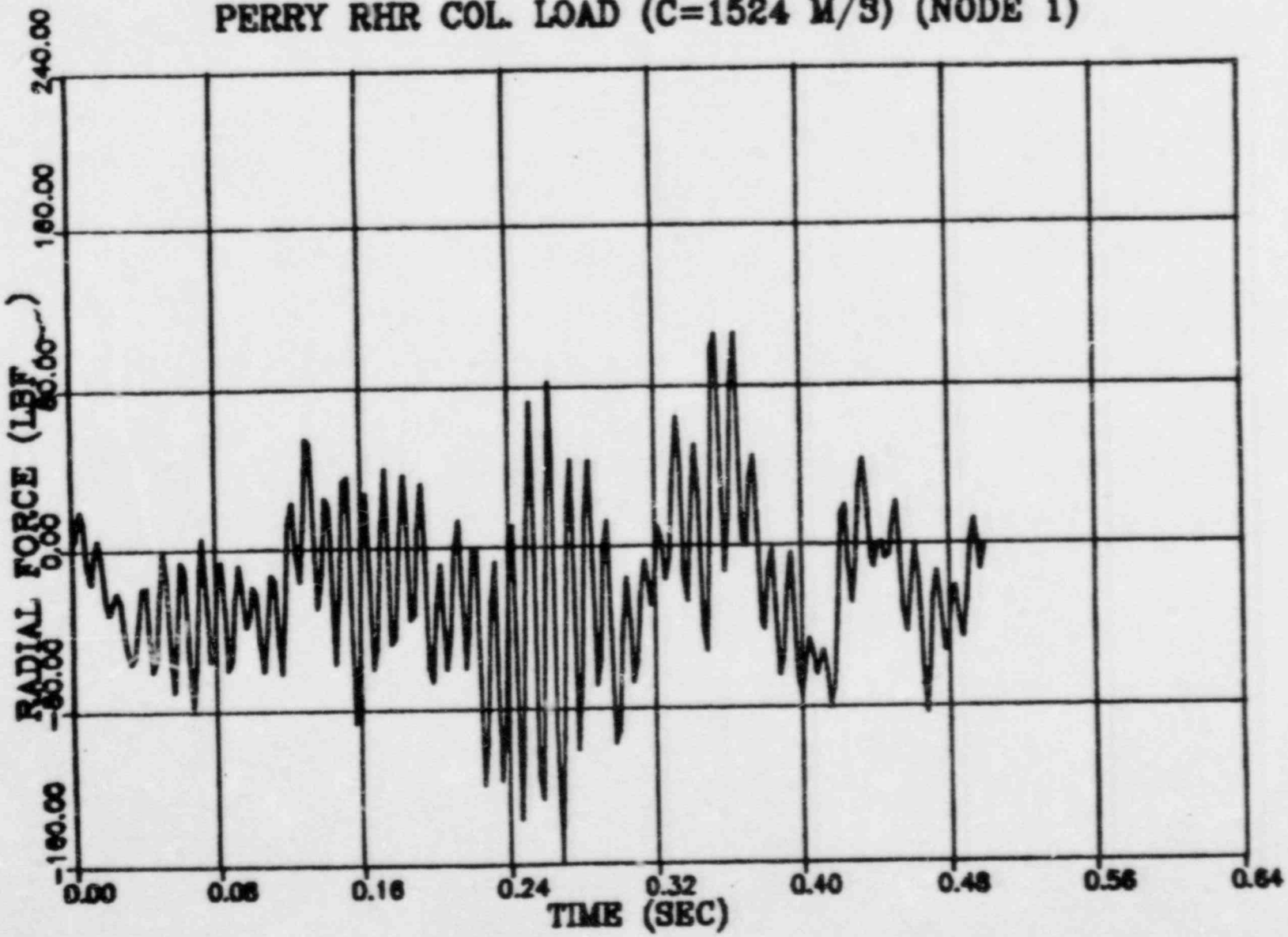
PERRY RHR COL. LOAD (C=1524 M/S) (NODE 1)
RADIAL FORCE (LBF)
240.00
160.00
80.00
0.00
-80.00
-160.00
0.00
0.08
0.16
0.24
0.32
0.40
0.48
0.56
0.64
TIME (SEC)

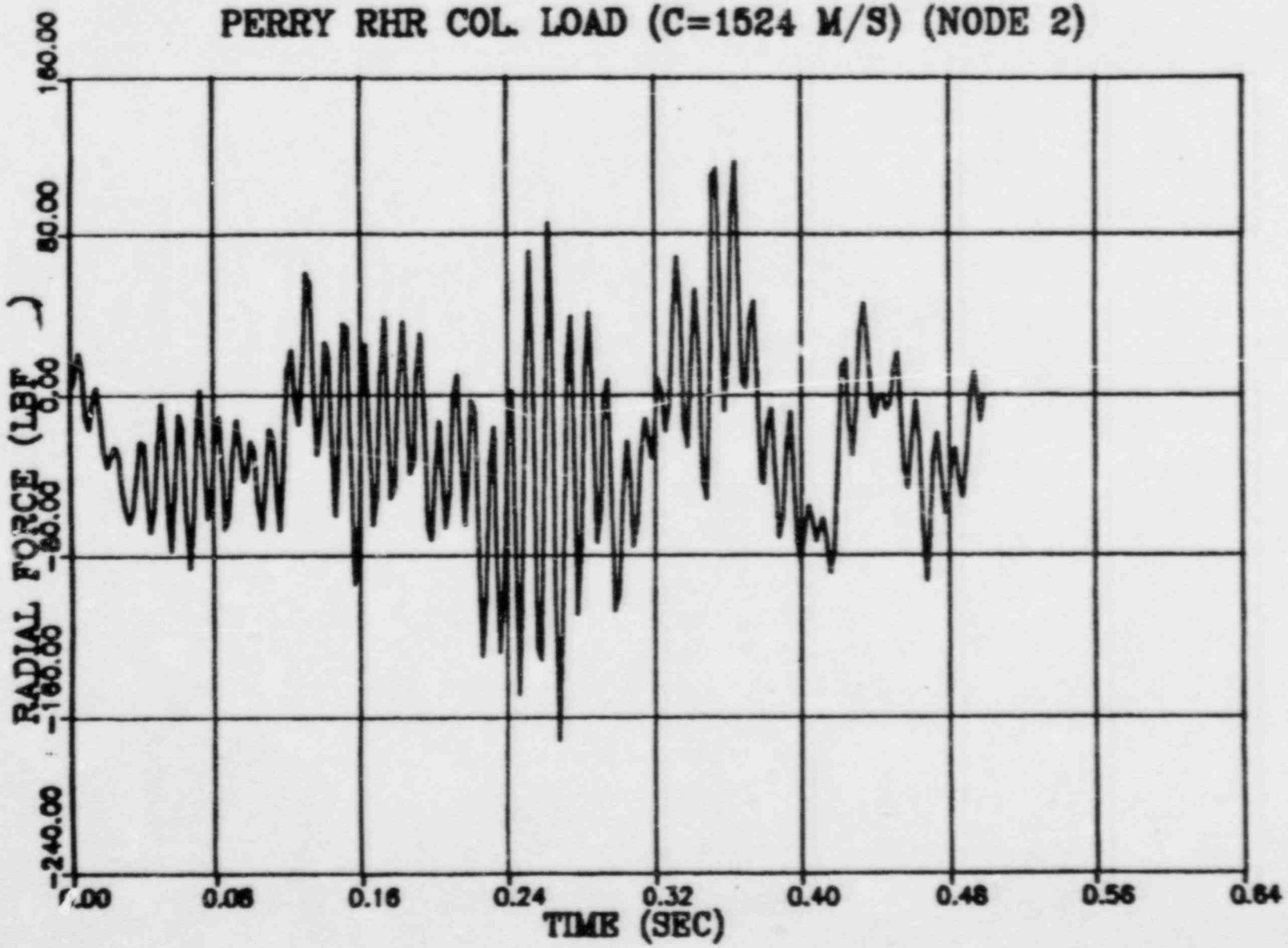
PERRY RHR COL. LOAD (C=1524 M/S) (NODE 2)
RADIAL FORCE (LBF)
160.00
80.00
0.00
-80.00
-160.00
-240.00
0.00
0.08
0.16
0.24
0.32
0.40
0.48
0.56
0.64
TIME (SEC)

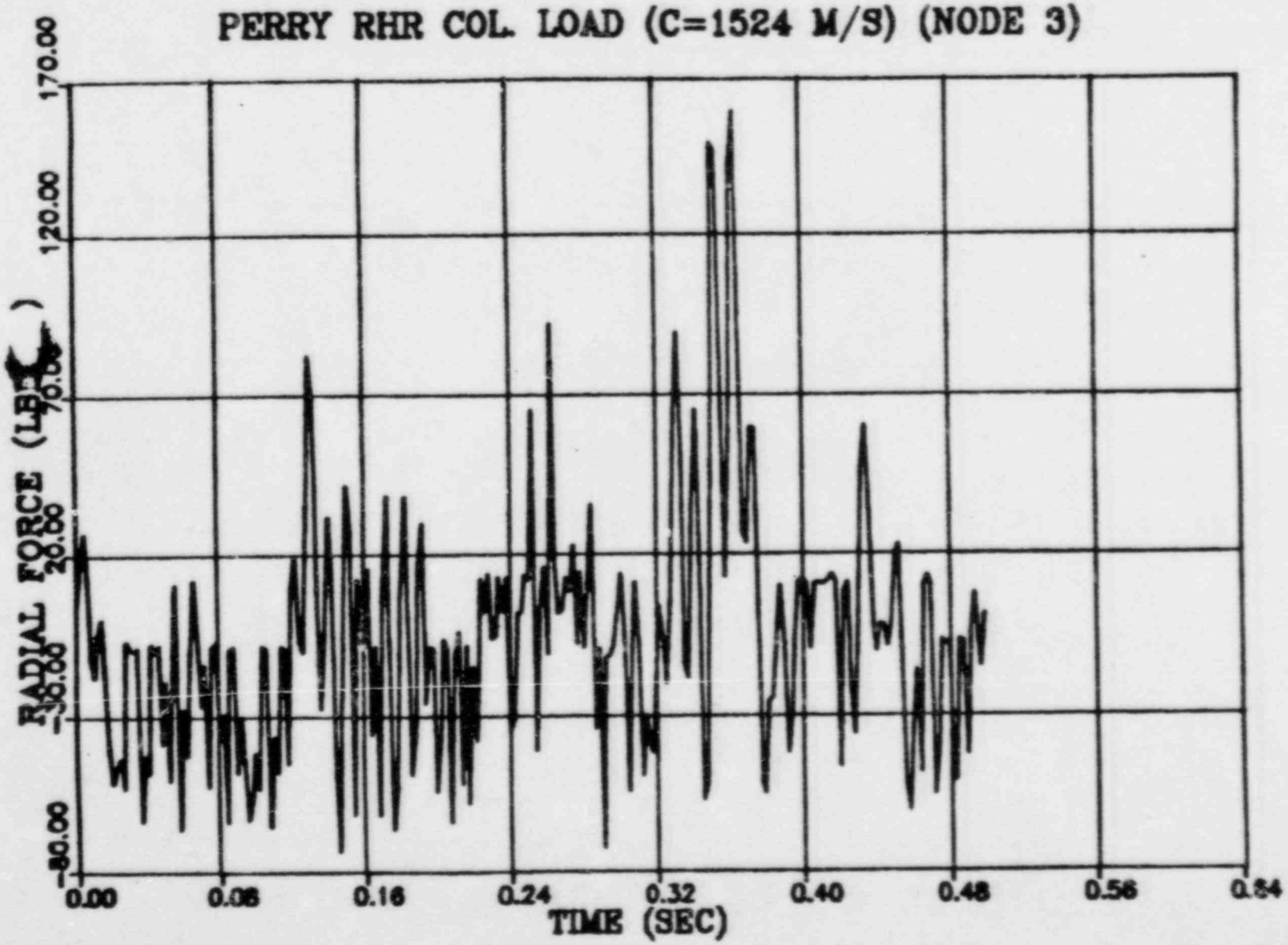
PERRY RHR COL. LOAD (C=1524 M/S) (NODE 3)
RADIAL FORCE (LBF)
170.00
120.00
70.00
20.00
-30.00
-80.00
0.00
0.08
0.16
0.24
0.32
0.40
0.48
0.56
0.64
TIME (SEC)

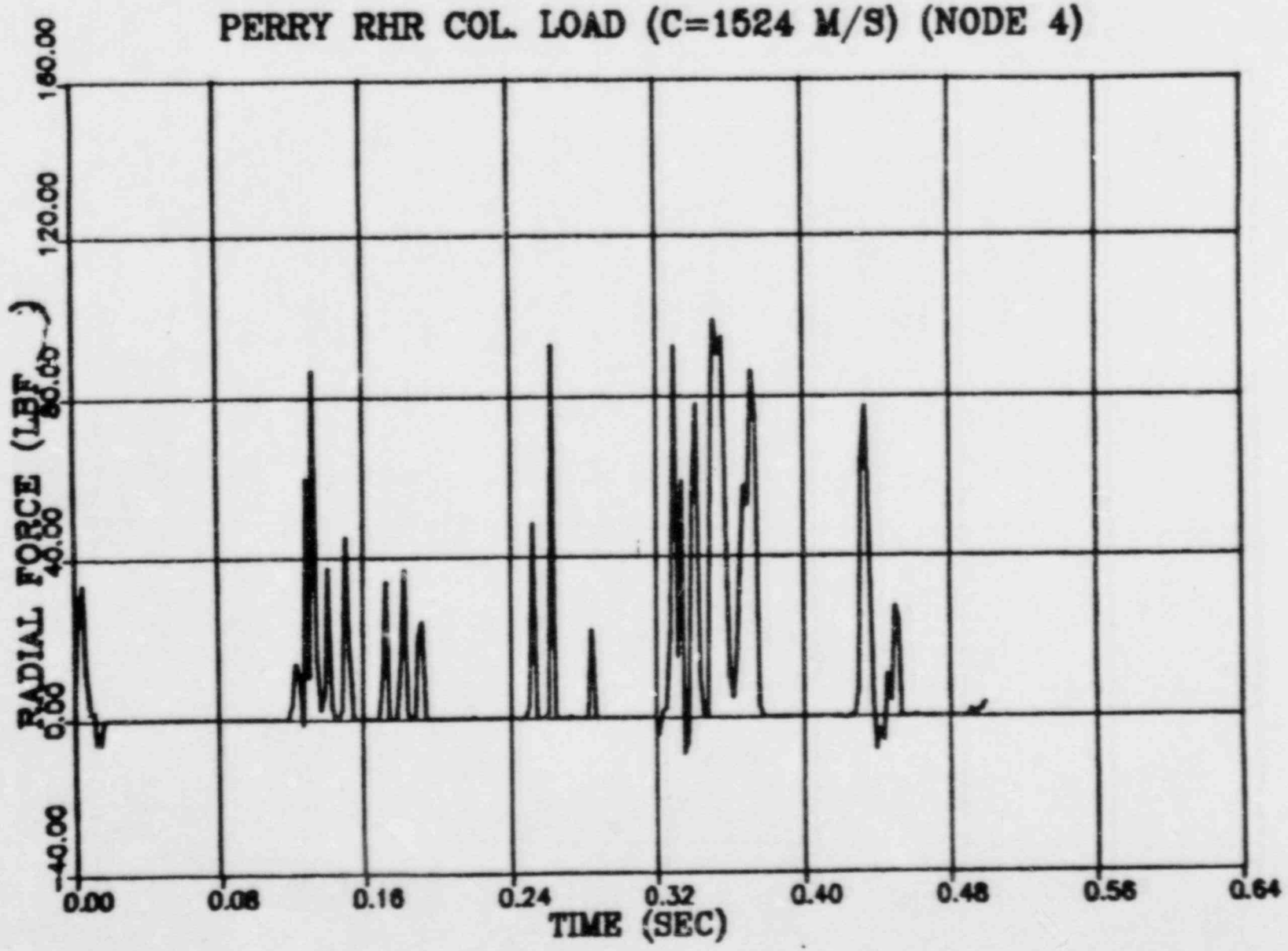
PERRY RHR COL. LOAD (C=1524 M/S) (NODE 4)
RADIAL FORCE (LBF)
160.00
120.00
80.00
40.00
0.00
-40.00
0.00
0.08
0.16
0.24
0.32
0.40
0.48
0.56
0.64
TIME (SEC)

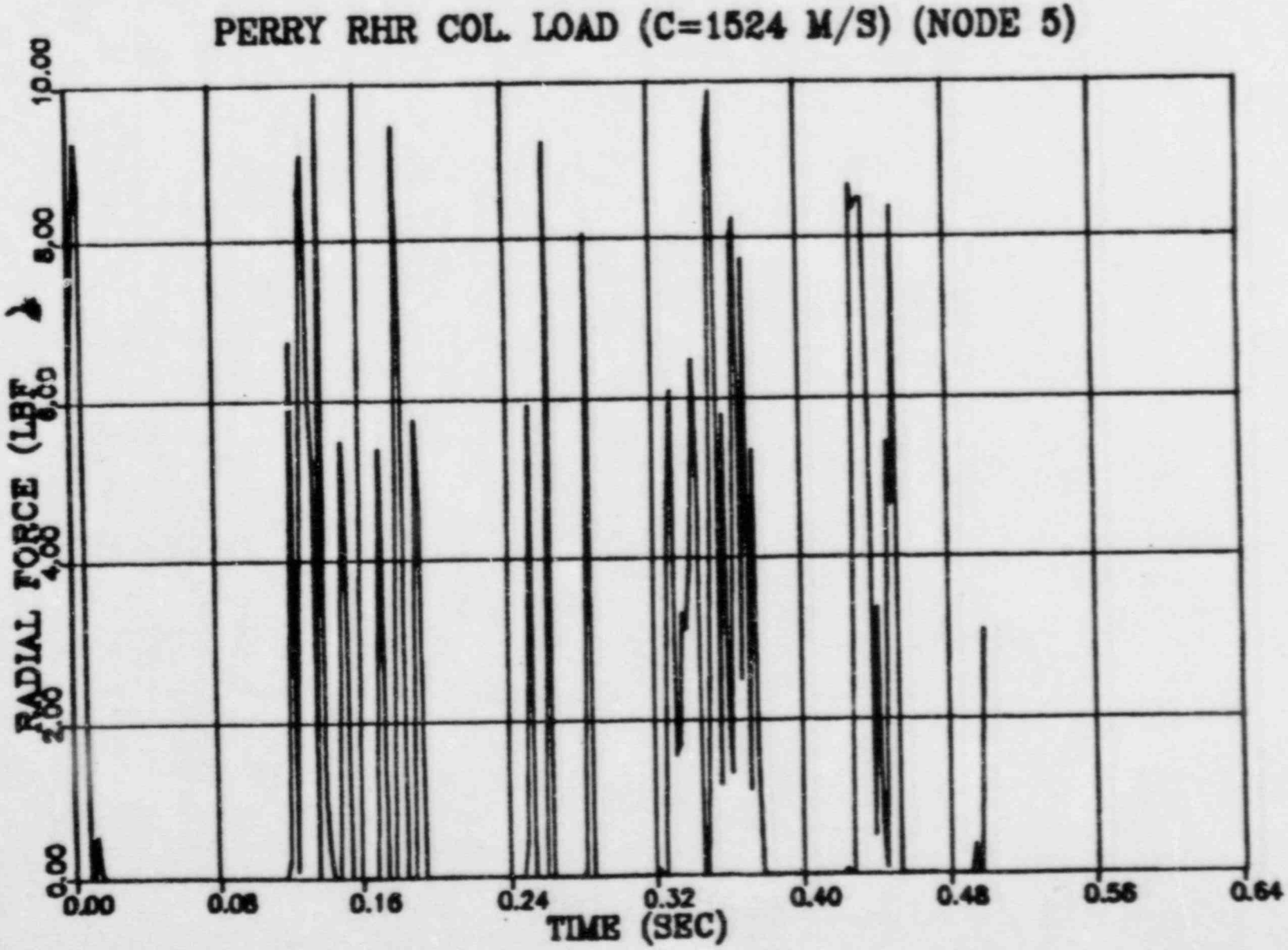
PERRY RHR COL. LOAD (C=1524 M/S) (NODE 5)
RADIAL FORCE (LBF
10.00
8.00
6.00
4.00
2.00
0.00
0.00
0.08
0.16
0.24
0.32
0.40
0.48
0.56
0.64
TIME (SEC)

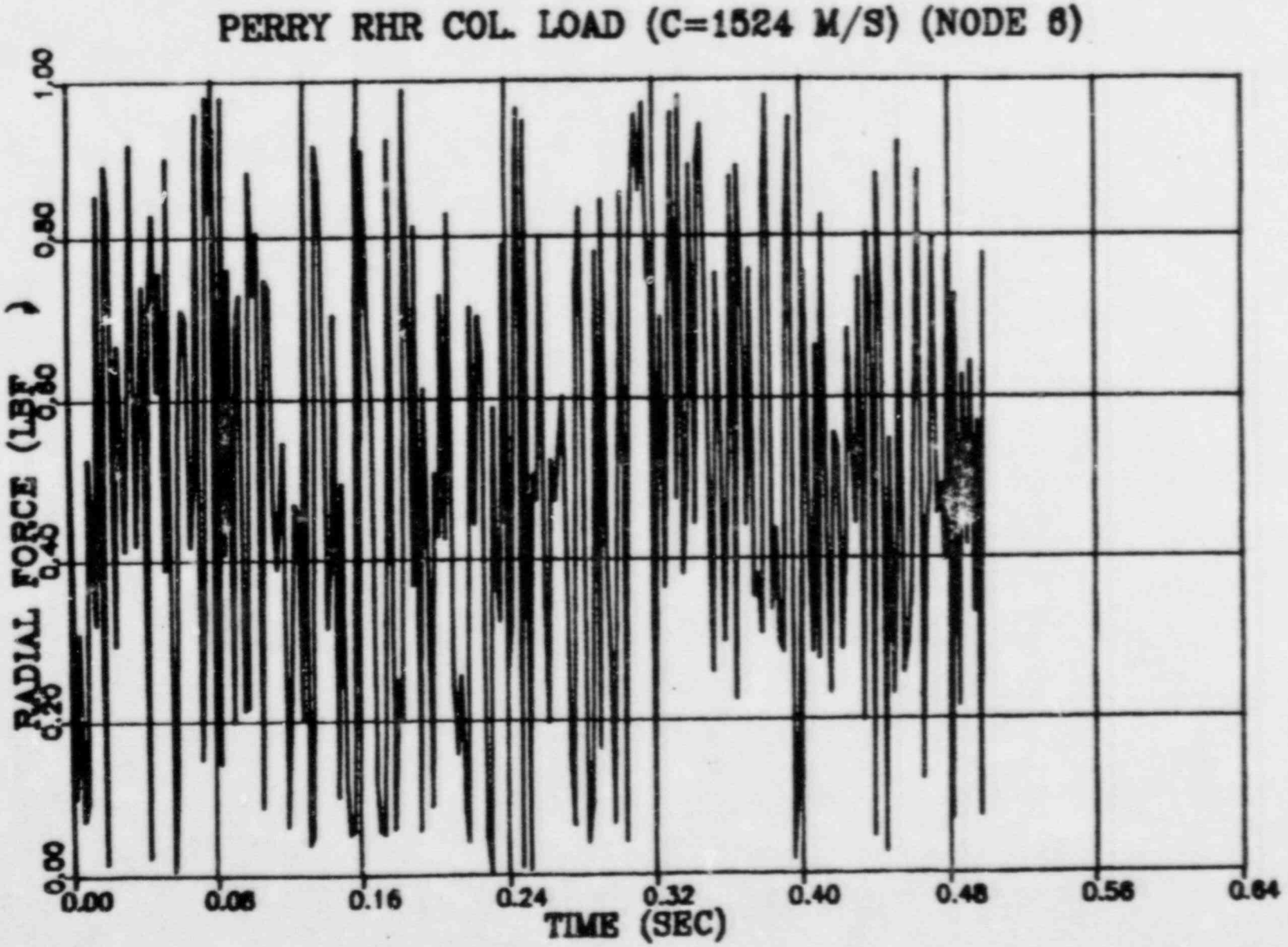
PERRY RHR COL. LOAD (C=1524 M/S) (NODE 6)
RADIAL FORCE (LBF)
1.00
0.80
0.60
0.40
0.20
0.00
0.00
0.08
0.16
0.24
0.32
0.40
0.48
0.56
0.64
TIME (SEC)

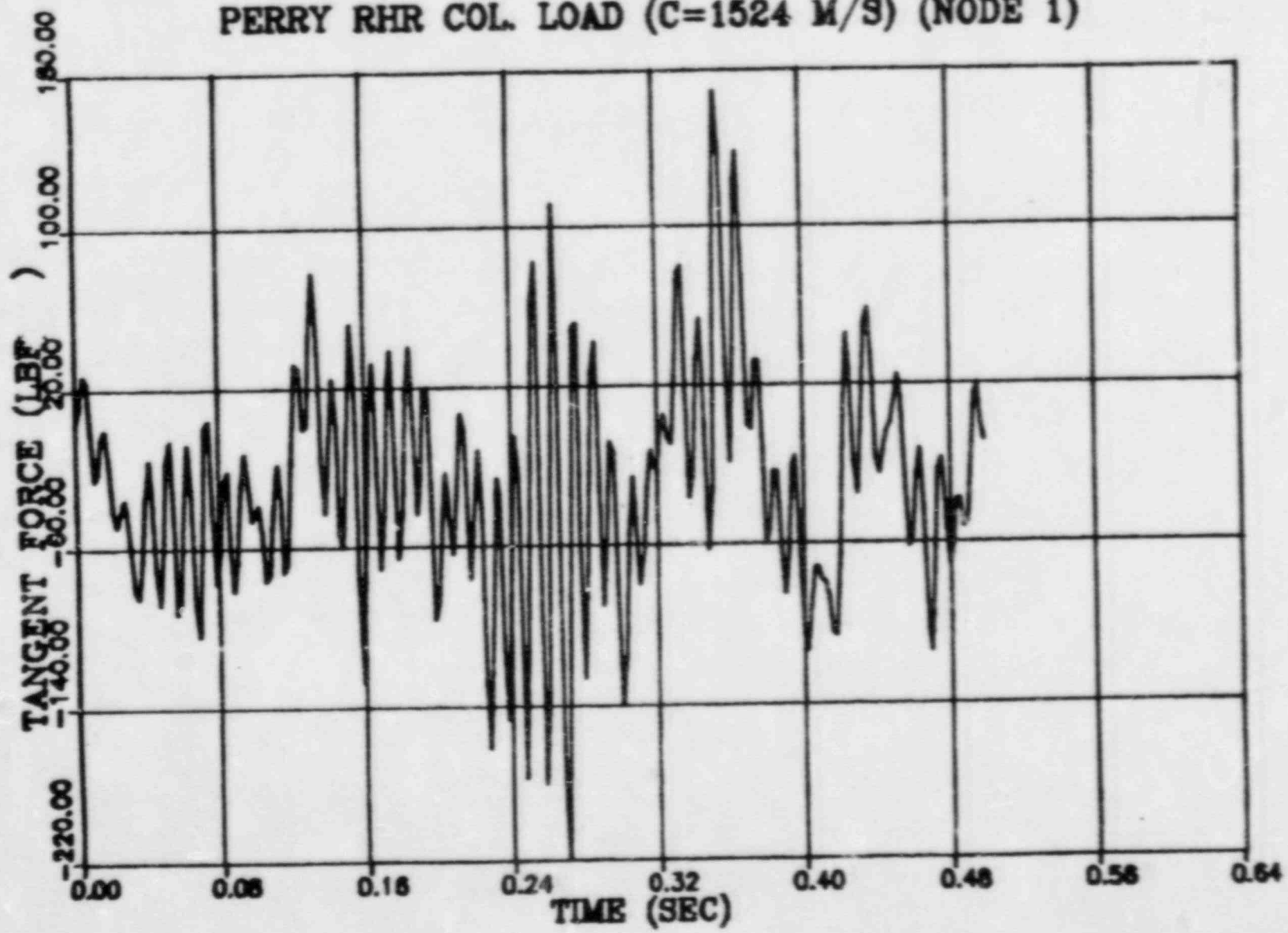
PERRY RHR COL. LOAD (C=1524 M/S) (NODE 1)
TANGENT FORCE (LBF)
180.00
100.00
20.00
-60.00
-140.00
-220.00
0.00
0.08
0.16
0.24
0.32
0.40
0.48
0.56
0.64
TIME (SEC)

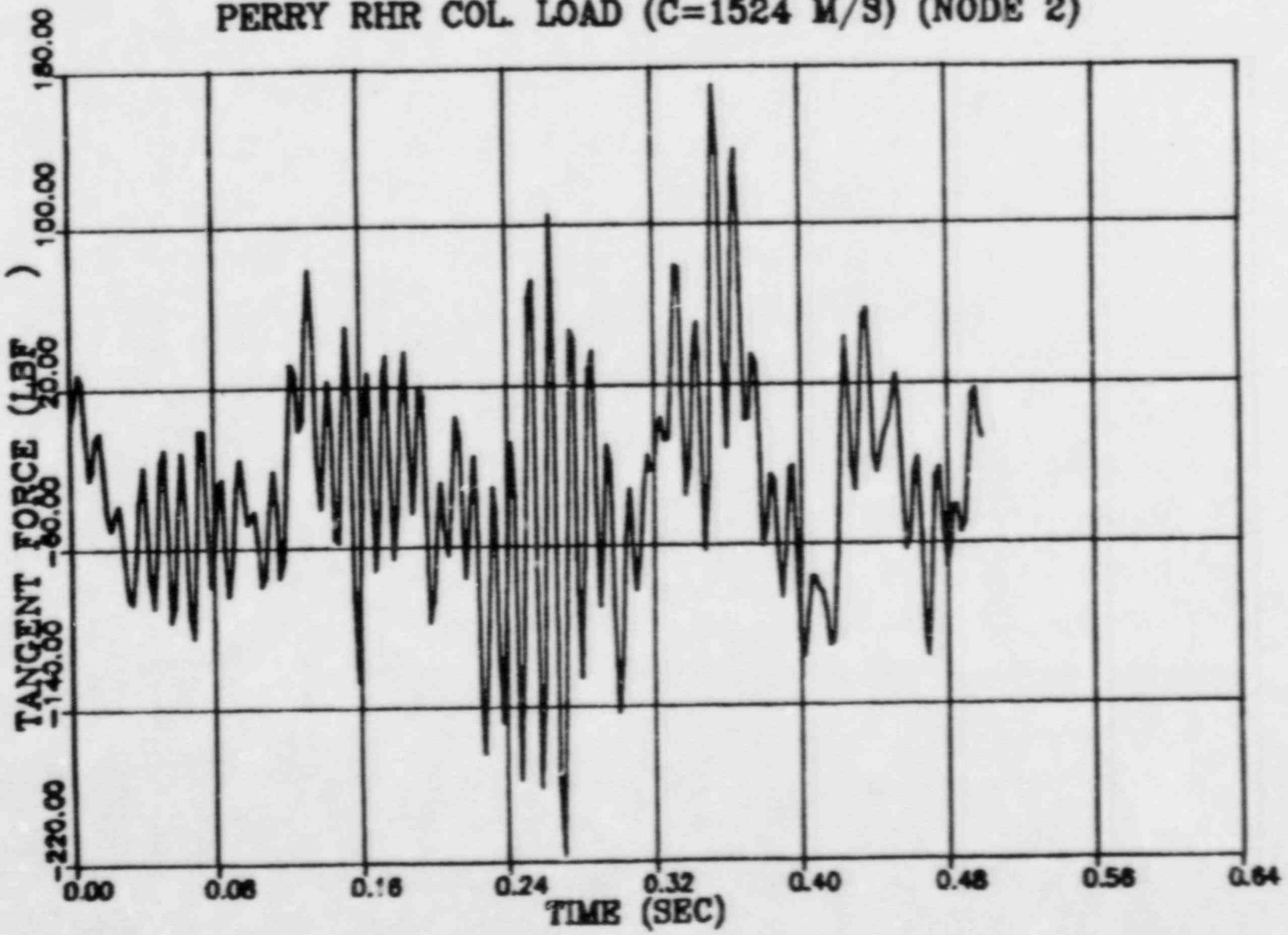
PERRY RHR COL. LOAD (C=1524 M/S) (NODE 2)
TANGENT FORCE (LBF)
180.00
100.00
20.00
-60.00
-140.00
-220.00
0.00
0.08
0.16
0.24
0.32
0.40
0.48
0.56
0.64
TIME (SEC)

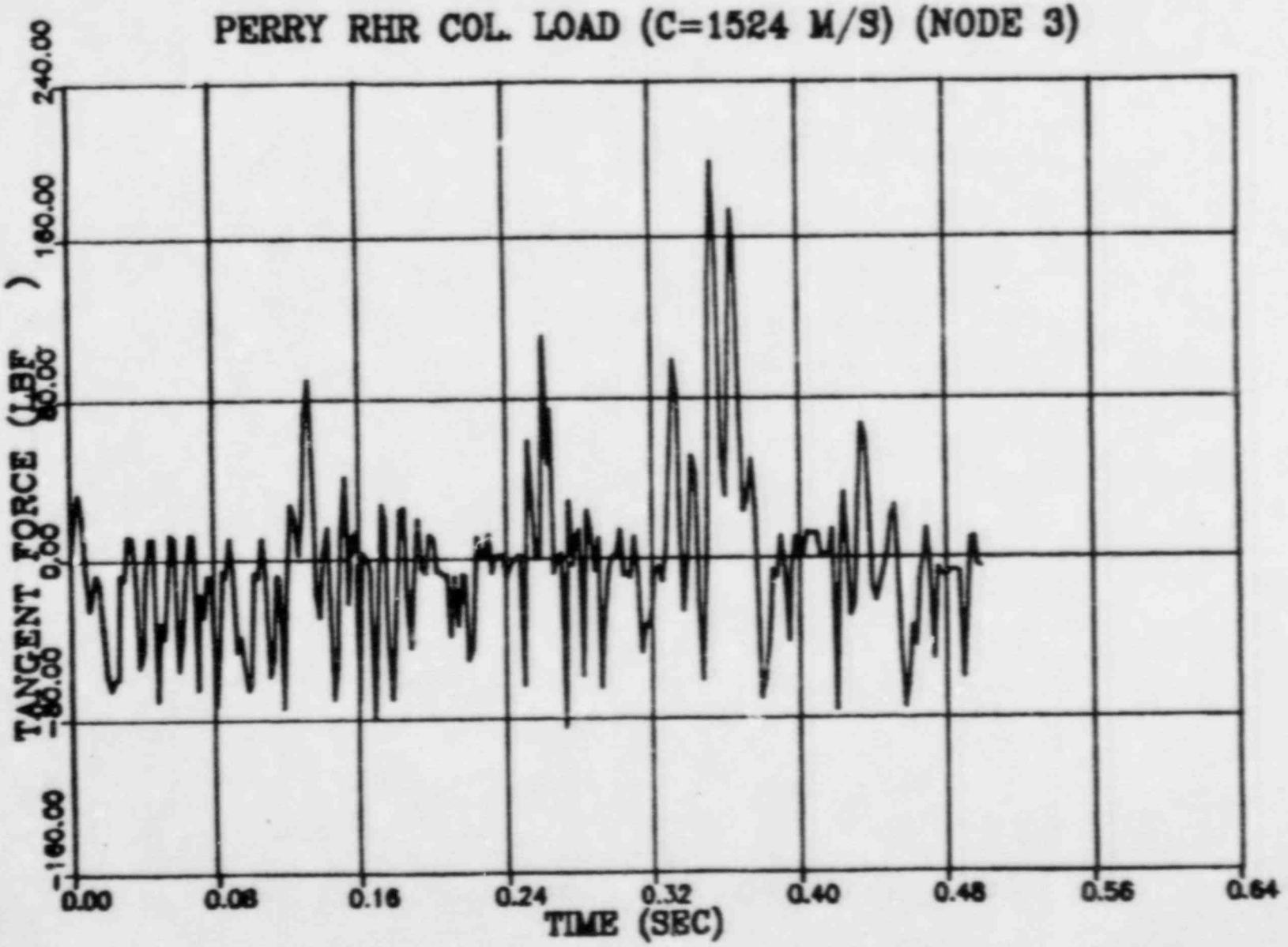
PERRY RHR COL. LOAD (C=1524 M/S) (NODE 3)
TANGENT FORCE (LBF)
240.00
160.00
80.00
0.00
-80.00
-160.00
0.00
0.08
0.16
0.24
0.32
0.40
0.48
0.56
0.64
TIME (SEC)

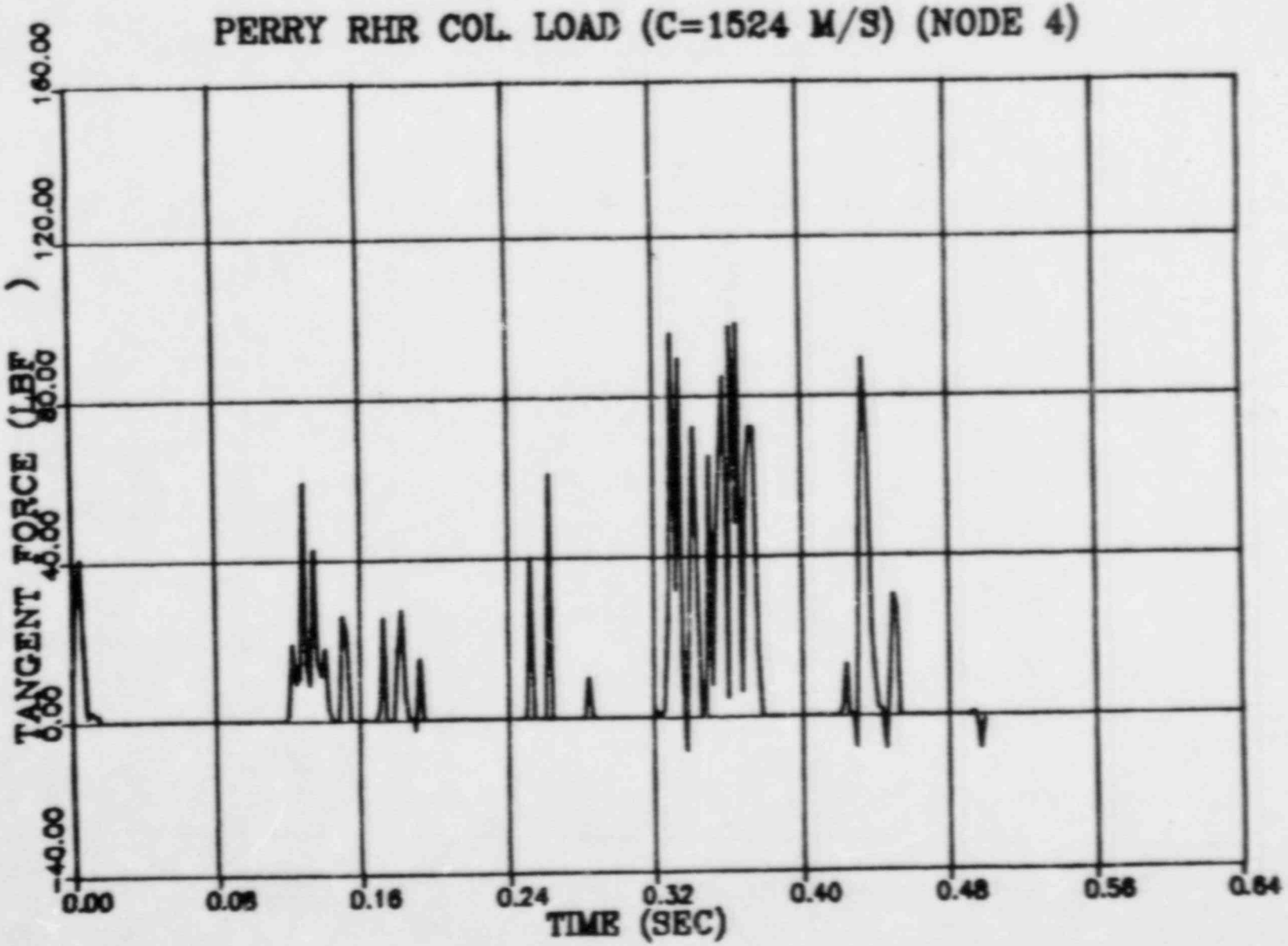
PERRY RHR COL. LOAD (C=1524 M/S) (NODE 4)
TANGENT FORCE (LBF)
160.00
120.00
80.00
40.00
0.00
-40.00
0.00
0.08
0.16
0.24
0.32
0.40
0.48
0.56
0.64
TIME (SEC)

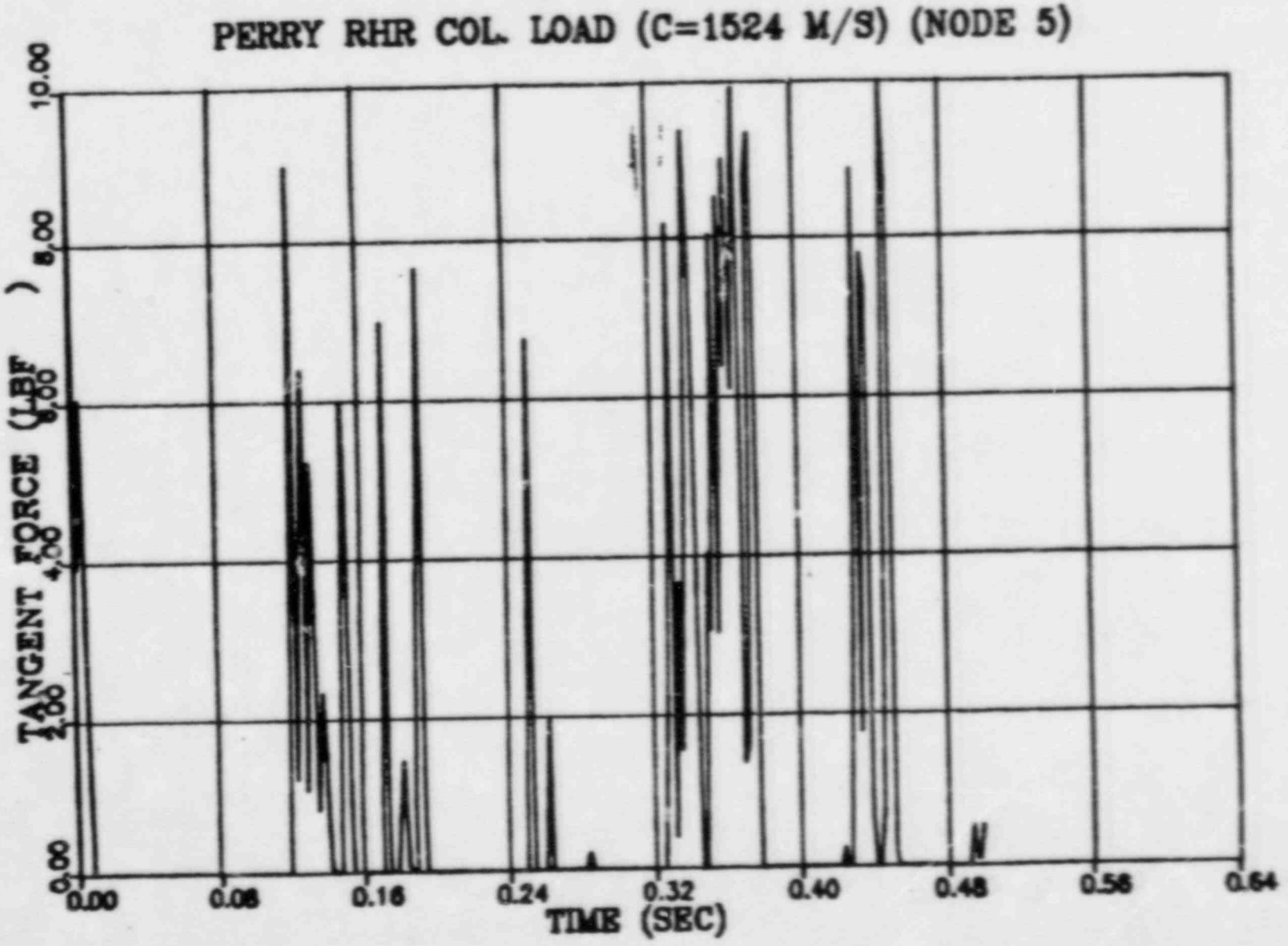
PERRY RHR COL. LOAD (C=1524 M/S) (NODE 5)
TANGENT FORCE (LBF)
10.00
8.00
6.00
4.00
2.00
0.00
0.00
0.08
0.16
0.24
0.32
0.40
0.48
0.56
0.64
TIME (SEC)

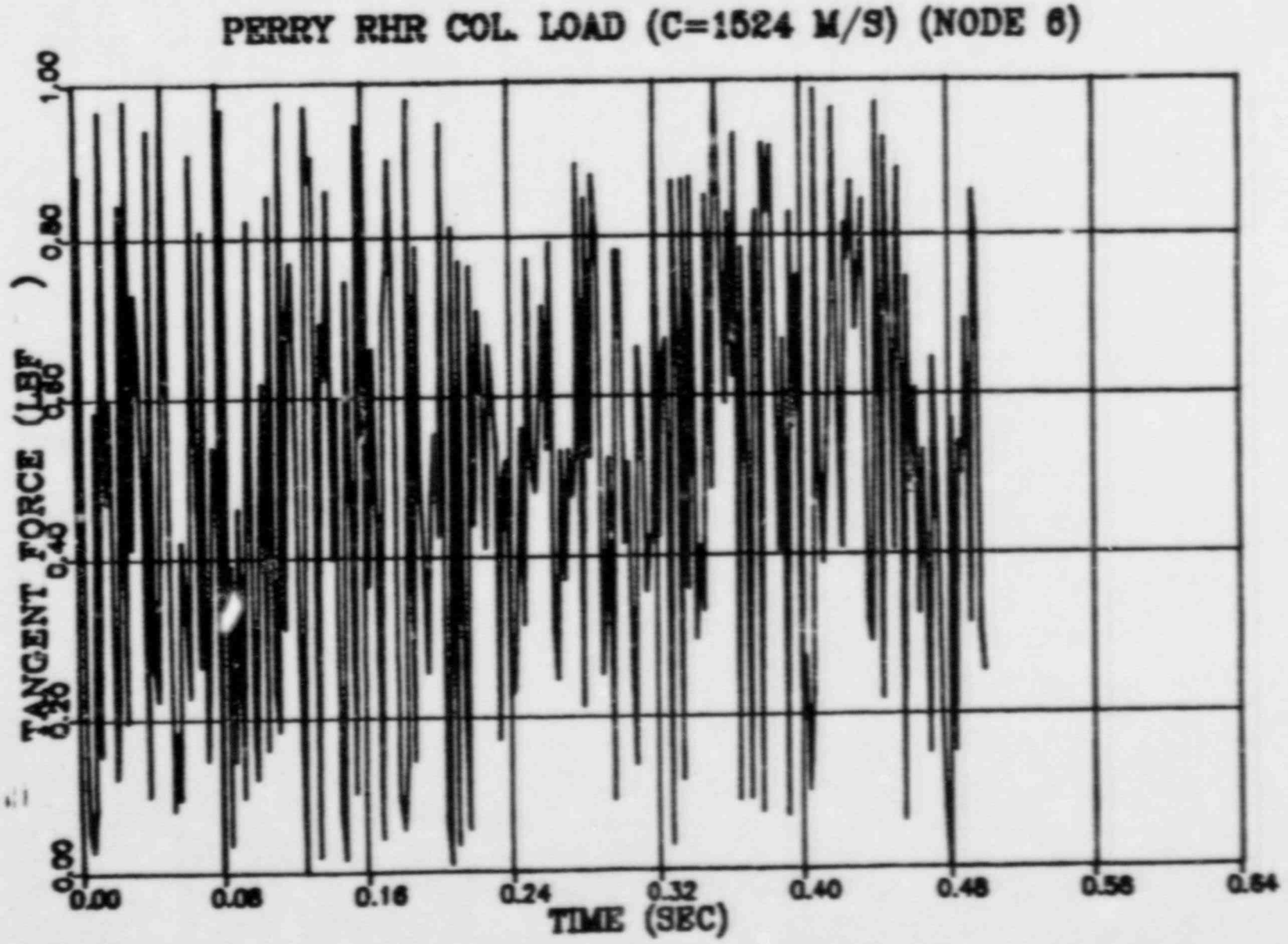
PERRY RHR COL. LOAD (C=1524 M/S) (NODE 6)
TANGENT FORCE (LBF)
1.00
0.80
0.60
0.40
0.20
0.00
0.00
0.08
0.16
0.24
0.32
0.40
0.48
0.56
0.64
TIME (SEC)